N. Bondaryuk, S. M. Il'yashenko

RAMJET ENGINES

Part 1 of 2 Parts

RAMJET ENGINES (Part 1 of 2 Parts)

By M. N. Bondaryuk and S. M. Il'yashenko

February 1960

431 Pages

M. N. Bondaryuk and S. M. Il'yashenko

Pryamotochnyye Vozdushno-Reaktivnyye Dvigateli

In this book the information on the theory, characteristics, construction, and design of subsonic and supersonic ramjet engines is based on domestic and foreign materials which have been published in the form of books and magazine articles. The theory of the basic elements of the engine -- diffusers, combustion chambers, and jet nozzles -- is considered, as well as the operation of the entire engine. Molecular and even atomic fuels are regarded as sources of energy. This book is intended for engineers who are specialists in aircraft engine construction, and for students in higher educational aviation institutions who are familiar with the fundamentals of thermodynamics and gas dynamics.

CONTENTS

5. Expanded diffusers in a supersonic flow........................ 113
6. Multiple shock wave diffusers.................................. 115
7. The calculation of a multiple-shock wave diffuser............. 121
8. The operation of a multi-shock wave diffuser at off-design
   point conditions. Additional resistance...................... 128

Bibliography.. 133

CHAPTER V. JET NOZZLES.. 135

1. The equation of a flow through a nozzle...................... 135
2. Subsonic and supersonic nozzle.............................. 136
3. Energy dissipation and losses during discharge from a nozzle.... 139
4. The impulse of gases exhausting from a nozzle. Impulse loss
   factor.. 142
5. Nozzle operation during off-design point conditions.......... 146
6. Variable area nozzles....................................... 149
7. Nozzle contouring and designing............................. 149

Bibliography.. 153

CHAPTER VI. BASIC PRINCIPLES OF MOLECULAR FUELS USED IN A RAMJET ENGINE,
            AND THEIR COMBUSTION............................... 154

1. The physico-chemical parameters of ramjet engine fuels........ 154
2. The calculation of the heating value of a fuel from its
   composition... 157
3. Calculation of the amount of air theoretically required, the
   composition and thermodynamic parameters of the combustion
   products.. 162
4. The concept of chemical equilibrium. The dissociation of
   combustion products... 168
5. The calculation of the composition of dissociated combustion
   products.. 172
6. Thermal /Mollier/ charts of combustion products.............. 177
7. The combustion of fuel - air mixtures....................... 182
8. Ignition limits of hydrocarbons. Ignition lag............... 192
9. Flame stabilization... 195
10. Combustion in ceramic tubes................................ 201

Bibliography.. 202

CHAPTER VII. CARBURETION.. 204

1. Direct-spray injectors...................................... 205
2. Centrifugal injectors....................................... 207
3. The break-down of liquid streams and drops.................. 212
4. Injector dispersion spectra................................. 217
5. Experimental research of dispersion spectra................. 221
6. The influence of the physical parameters of the liquid and
   the air on the dispersion and the form of the jet........... 224
7. Formulae for computing dispersion spectra................... 230
8. The evaporation of an atomized fuel......................... 234
9. The effect of the parameters of the fuel and air upon
   evaporation... 244
10. The experimental determination of local fuel concentrations..... 246

FOREWORD

At the present time, in the domestic and foreign literature much material is published concerning questions about the theory and research of the individual elements of ramjet engines, such as diffusers, combustion chambers, fuel injectors, flame holders, and jet nozzles. However, these enumerated questions have not been correlated in sufficient detail by ourselves or those abroad. This book proposes, for that reason, to be the first endeavour to summarize this cited information, which is indispensable for an understanding of the physical processes and for the gas dynamic and thru $_{,}$t computations of ramjet engines.

Monographs and magazine articles published by the domestic and foreign press, as well as the personal works of the authors, have served as the basic materials for the writing of this book.

In those cases where data about a numerical value or different parameters are absent in the literature, e.g., the combustion efficiency in the combustion chamber or the burner drag coefficient, the authors have confined themselves to resolving the problem in a basic form and drawing up qualitative characteristics.

Information about atomic aircraft engines has previously appeared in the literature. The authors have included a short review chapter devoted to atomic ramjet engines.

To facilitate comprehension, a large number of examples with detailed numerical solutions are included in the material set forth in this book.

The authors have sought to make use of the more widely used terms and designations. Unfortunately, this does not always work out, since in the various fields of science various terms and designations are used. For example, in aerodynamics the technical system of units is widely employed where mass is expressed as technical units of mass (not having a conventional name) with the dimension $kg\ sec^2/m$, and the density of a substance ρ is expressed in technical units of density with the dimension $kg\ sec^2/m^4$. In physics and thermodynamics the CGS system is accepted, in which mass is expressed in grams of mass g and density ρ in g/cm^3. In the tables of

such physical constants as density, specific heat c, heating value H, heat of reaction E, heat of fusion l, etc., grams of mass usually serve as units of mass (in this case calories serve as units of heat), or kilograms of mass (1 kg = 1,000 g). In this case large (kilo) calories serve as units of heat. The numerical meaning of the measured parameter is one and the same in both cases, for example: C_p = 0.24 cal/g = 0.24 kcal/kg. For this reason, when values and terms expressed in technical units of mass, and impossibly attributed to kilograms of mass, enter into the equations simultaneously, the constant of proportionality is eliminated. The authors have decided to make use only of individual units, namely, kilograms of mass, so that gas consumption is usually expressed in kilograms per second and not in technical units (kg sec^2/m). Therefore in all our equations of mechanics the proportional constant g $\approx$ 9.81 m/sec^2 is entered. We express density in equations of mechanics and in heat balance equations as kg/m^3, retaining the gravitational constant g in the first case. Density expressed in kg/m^3, in contrast to density expressed as kg sec^2/m^4, we designate as γ:

$$\gamma = g\rho.$$

Density expressed in kg/m^3 is numerically equal to specific weight in kg/m^3, measured at sea level and at a latitude of $45°$ (geographic). Thus "density γ in kg/m^3" may also be stated as "specific weight in kg/m^3."

The authors express their gratitude to Prof. Ye. S. Shchetnikov, Doctor of Technical Sciences, and to Engineer B. V. Makarov for their valuable observations made during the process of reviewing and editing this manuscript.

The authors request that all remarks and comments relative to the content and design of this book be directed to this address: Moscow, I-51; Petrovka 24, OBORONGIZ.

CONVENTIONAL SYMBOLS

(In alphabetical order)

a   - critical speed in m/sec

a   - molecular change coefficient

A   - geometric characteristic of the nozzle

A   - thermal equivalent of work

α - shock wave angle of the surface in degrees

α - excess air coefficient

α_{π} - angle of divergence of the diffuser (α_{c})

α_T - heat transfer coefficient

b   - width of the diffuser inlet slot in meters

B   - factor in the flow formula: $B = \sqrt{\dfrac{gk}{R}\left(\dfrac{2}{k+1}\right)^{\frac{k+1}{k-1}}}$

β - fuel transfer coefficient in $\dfrac{1}{sec}$

c   - speed of sound in m/sec

C   - concentration in kg/m^3

c_p - specific heat at constant pressure in kcal/kg deg

c_v - specific heat at constant volume in kcal/kg deg

c_R - thrust coefficient

c_x - drag coefficient

c_λ - Laval nozzle impulse expansion coefficient

d   - drop diameter in mm or μ

d   - diameter of the diffuser and chamber in meters

D_ς - diffusion coefficient, pressure gradient in m^2/sec

D_p - diffusion coefficient, concentration gradient in m/sec

δ - thickness of the associated film in microns

E   - heat of formation in kcal/kg mol

ε - nozzle expansion ratio $\varepsilon = \dfrac{S_i}{S_{icp}}$ $(S_{l;cr})$

f   - friction force in kg

φ_x - diffusion flow coefficient (φ_d)

φ - velocity coefficient

φ - injector nozzle cross section coefficient

φ cr   - combustion efficiency (φ_{sg})

g   - gravity acceleration at sea level and at a latitude of 45°

g_i - weight content

G_B - mass weight flow of air in kg/sec (G_v)

G   - mass weight flow of gas in kg/sec

G_r - mass weight flow of fuel in kg/sec (G_g)

γ - density (specific gravity) in kg/m^3

h   - slot height in meters

H   - flight altitude in meters

H_u - fuel heating value (net heating value) in kcal/kg

i   - enthalpy (heat content) in kcal/kg

I   - enthalpy in kcal

j   - acceleration in m/sec^2

k   - Poisson's ratio (using "x " for the injected air and "r " for the hot gases)

k   - aerodynamic quality (i.e. lift-to-drag ratio) $(\Gamma = g)$

k   - proportionality constant

K   - velocity (gas dynamic) coefficient of a ramjet engine, $K = \dfrac{\lambda_4}{\lambda_n}$ (λ_n)

ψ - absorptive shock factor

1   - length in meters

L   - the quantity of air theoretically necessary for the combustion of 1 kg of fuel

λ - relative velocity $\lambda = \dfrac{w}{a}$

λ - heat conductivity in kcal/m/sec

m   - mass in kilograms of mass

m   - degree of taper (geometric parameter) of a jet engine

n   -   degree of diffuser expansion

M   -   Mach number

μ -   molecular weight in kg

μ -   dynamic viscosity in $kg/sec/m^2$

η -   efficiency

n   -   number of drops

N   -   power in hp or kcal/sec

Nu   -   Nusselt's number

ν -   kinematic viscosity in m^2/sec

ν_T -   specific gravity of the fuel

ω -   rake angle in degrees

ω -   angular velocity in radians/sec

p   -   pressure in kg/m^2

p_o -   stagnation pressure in kg/m^2

p_n -   vapor pressure in kg/m^2 or in mm of a mercury column   (p_p)

P   -   weight in kg or t

P   -   reaction thrust of the exhaust gases in kg

P_r -   Prandtl's number

π -   pressure ratio in the nozzle in $\dfrac{p_{04}}{p_4}$

q   -   dynamic head in kg/m^2

q_T -   heat flow in $kcal/m^2/sec$

q_m -   flow of matter in $kg/m^2/sec$

Q   -   quantity of heat in kcal

$Q_{пот}$ -   heat loss in kcal   (Q_{pot})

r   -   drop radius in microns or meters

R   -   rotation radius in meters

r_i -   volume percentage of components

R_0 --   -   stream thrust (reaction of a stream on the sides of a duct in kg)

R --   -   thrust in kg

$R_{эф}$ — effective thrust in kg (R_{eff})

$R_м$ — frontal or maximum cross sectional thrust in kg/m^2

R — gas constant in kcal/kg/deg with the indices "в" for air and "г" for combustion products $(в = v)$ $(г = g)$

Re — Reynolds number

ρ — density in $kg/sec^2/m^4$

s — entropy in kcal/kg/deg

S — entropy in kcal/deg

S — cross section in m^2

δ — pressure ratio

$\sigma_д$ — over-all diffuser pressure ratio (σ_d)

$\sigma'_д$ — pressure ratio across the supersonic portion of the diffuser (σ'_d)

$\sigma''_д$ — pressure ratio across the subsonic portion of the diffuser (σ''_d)

$\sigma_м$ — pressure ratio across the flame-holder

$\sigma_{сг}$ — pressure ratio across the combustion chamber (σ_{sg})

$\sigma_с$ — over-all nozzle pressure ratio (σ_s)

$\sigma''_с$ — pressure ratio across the supersonic portion of the nozzle (σ''_s)

$\sigma'_с$ — pressure ratio across the subsonic portion of the nozzle (σ'_s)

$\sigma_{об}$ — pressure ratio across the entire engine (σ_{ob})

t — time in sec

t — temperature in degrees C

T — temperature in degrees K

T_0 — stagnation temperature in degrees K; for cold air with the index "х "; for the combustion products with the index "г " $(х = kh)$ $(г = g)$

θ — temperature ratio, $\theta = \dfrac{T_{0.г}}{T_{0.х}}$ $\left\{ \dfrac{T_{0.g.}}{T_{0.kh.}} \right\}$

u — circumferential velocity in m/sec

u — relative velocity of a drop in m/sec

u_n — normal flame propagation velocity in cm/sec

u — internal energy in kcal/kg

U — internal energy in kcal

v   -   absolute velocity of a drop in m/sec

v   -   specific volume in m^3/kg

V   -   volume in m^3

w   -   air velocity in m/sec

W   -   calorific value of the fuel in kcal per kg of combustion products

x   -   coordinate in meters

X   -   drag in kg

y   -   coordinate in meters

z   -   percentage of the evaporated substance

$$\left.\begin{array}{l} x = \sqrt{\dfrac{k_r}{k_x}\dfrac{k_x+1}{k_r+1}\dfrac{R_r}{R_x}} \\[2em] \mathfrak{t} = \sqrt{\dfrac{k_x}{k_r}\dfrac{k_r+1}{k_x+1}\dfrac{R_r}{R_x}} \\[3em] x = \sqrt{\dfrac{k_x}{k_r}\dfrac{R_r}{R_x}\dfrac{\left(\dfrac{2}{k_x+1}\right)^{\frac{k_x+1}{k_x-1}}}{\left(\dfrac{2}{k_r+1}\right)^{\frac{k_r+1}{k_r-1}}}} \end{array}\right\} \text{functions of } k$$

Russian	Transliteration		Meaning
акт	akt	(subscript)	active
ат	at	(subscript)	atmosphere; atmospheric
ата	ata	(abbreviation)	absolute atmosphere
атм	atm	(subscript)	atmosphere; atmospheric
бок	bok	(subscript)	oblique
в	v	(subscript)	air
вих	vikh	(subscript)	vortex
возд	vozd	(subscript)	air
вол	vol	(subscript)	wave
воспл	vospl	(subscript)	ignition
ВРД	VRD	(abbreviation)	air-breathing jet engine
всп	vsp	(subscript)	ignition
вх	vkh	(subscript)	inlet
вых	vykh	(subscript)	exit
г	g	(subscript)	gas; fuel; hot
гр	gr	(subscript)	boundary
д	d	(subscript)	pressure; diffuser
дав	dav	(subscript)	pressure
дел	del	(subscript)	· fission
дис	dis	(subscript)	dissipation
доп	dop	(subscript)	additional
ЖРД	ZhRD	(abbreviation)	liquid-fuel rocket engine
зат	zat	(subscript)	used (supplied, delivered)
защ	zashch	(subscript)	protective (shield)
иг	ig	(subscript)	spine (bullet)
ид	id	(subscript)	ideal

Russian	Transliteration		Meaning
изб	izb	(subscript)	excess, surplus
ист	ist	(subscript)	true, actual; discharge, exhaust
к	k	(subscript)	wedge
кам	kam	(subscript)	chamber
кип	kip	(subscript)	boiling
кольц	kol'ts	(subscript)	annular, ring-shaped
кон	kon	(subscript)	cone
корм	korm	(subscript)	stern, boat-tail
кр	kr	(subscript)	critical
КРДД	KRDD	(abbreviation)	winged long-range rocket
крит	krit	(subscript)	critical
к.сг	k.sg	(subscript)	combustion chamber
л	l	(subscript)	frontal
мест	mest	(subscript)	local
н	n	(subscript)	initial, starting; normal
нас	nas	(subscript)	saturated
об	ob	(subscript)	diffuser lip (shell)
общ	obshch	(subscript)	total
опт	opt	(subscript)	optimum
ось	os'	(subscript)	axis
отб	otb	(subscript)	abstracting (sampling)
отн	otn	(subscript)	relative
п	p	(subscript)	vapor
ПВРД	PVRD	(abbreviation)	ramjet engine
ПД	PD	(abbreviation)	piston engine
пл	pl	(subscript)	plane, flat
пол	pol	(subscript)	flight (take-off)
пот	pot	(subscript)	used (consumed, released); losses

Russian	Transliteration		Meaning
пр	pr	(subscript)	maximum, critical, terminal, limiting
пред	pred	(subscript)	maximum, critical, terminal, limiting
пр.сг	pr.sg	(subscript)	combustion products
пульс	pul's	(subscript)	pulse; pulsation
рав	rav	(subscript)	equilibrium
расч	rasch	(subscript)	rated, design, point
с	s	(subscript)	nozzle
сг	sg	(subscript)	combustion
соб	sob	(subscript)	proper, eigen (natural)
ср	sr	(subscript)	average, mean; medium; middle
сред	sred	(subscript)	average, mean; medium; middle
срыв	sryv	(subscript)	blow-out
ст	st	(subscript)	standard; flameholder; stabilization
стр	str	(subscript)	stream, jet
т	t	(subscript)	fuel
теп	tep	(subscript)	heat; heat-carrying agent
тр	tr	(subscript)	friction
ТРД	TRD	(abbreviation)	turbojet engine
ТРДФ	TRDF	(abbreviation)	turbojet engine with afterburner
тяг	tyag	(subscript)	thrust
уд	ud	(subscript)	shock, impact
ф	f	(subscript)	injector
чист	chist	(subscript)	net, pure
щ	shch	(subscript)	slot
эксп	eksp	(subscript)	experiment
эф	ef	(subscript)	effective

CHAPTER I

THE CLASSIFICATION OF JET PROPULSION ENGINES

AND THE FIELDS OF THEIR APPLICATION

Some contemporary flying machines, for example, the anti-aircraft guided missile and the long-range rocket, move several times faster than the speed of sound. With an increase in speed, aerodynamic drag quickly increases, and, therewith, the required thrust. For example, to propel a single-seater aircraft weighing nearly 3 t, at a speed of nearly 600 km/hr (equal to half the speed of sound), a thrust of almost 500 kg is necessary; to propel this same aircraft at the speed of sound would require a thrust of more than 4,000 kg. If it is accepted that at $M = 1$, the efficiency of the propeller is equal to 0.8, then the power of an engine developing a similar thrust will be:

$$N = \frac{Rw}{75\eta} > \frac{4000 \cdot 340}{75 \cdot 0,8} = 20\,000 \text{ h.p.}$$

Such a piston engine, without propeller or fuel, would weigh nearly 10 t. In reality, the required power for an engine-driven propeller would be still larger for a flight speed close to the speed of sound, since the efficiency of the propeller decreases rapidly.

Owing to the extraordinarily rapid growth of the required power and weight of the power plant of a propeller-driven aircraft, it was impossible to fly at a speed close to the speed of sound. The highest recorded speed of a propeller-driven aircraft -- 756 km/hr -- was set in 1939 by a German Messerschmidt aircraft without a radiator, fuel tanks, or equipment, and prepared for only this flight, which lasted only a few minutes. The previous record, set 6 years earlier by an Italian Macchi-Castoldi aircraft, was bettered by 7%.

For sonic and supersonic flight speeds it is necessary to have light-weight engines able to develop the necessary thrust at such high speeds. Only jet engines possess these qualities.

A unit which contains in itself a heat engine and an air-propelling device is

called a jet engine, wherein the thermal energy released is spent directly on increasing the kinetic energy of the gas stream whose reaction creates the useful thrust.

Section 1. The Classification of Jet Engines

There are two principal types of jet engines: rocket engines and air-breathing jet engines.

All that is necessary to create thrust is carried on board an aircraft having a rocket engine: an energy source and a working substance.. On board an aircraft with an air-breathing jet engine we find only the energy source taking air from the surrounding atmosphere to serve as the working substance.
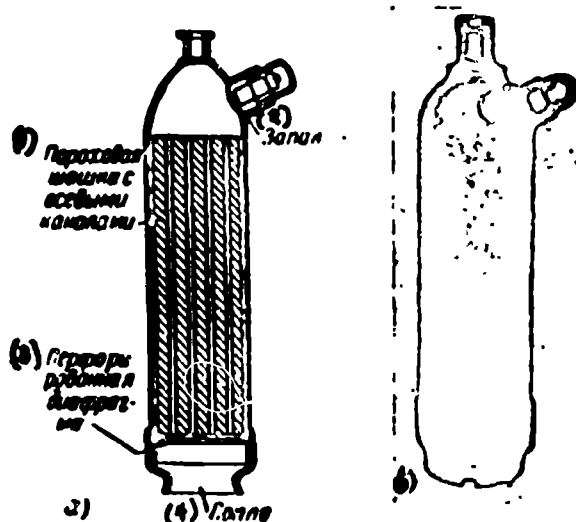
Fig. 1 A solid-fuel rocket engine. a -- schematic, b -- external view.
Legend: 1) powder charge with axial ducts; 2) igniter; 3) perforated diaphragm; 4) nozzle.

According to the physical state of the fuel, rocket engines are subdivided into PRDs /porokhovyye raketnyye dvigateli -- solid-fuel rocket engines/, Fig. 1, in which powder serves as the energy source, and the gases formed during combustion serve as the working substance; and ZhRDs /zhidkostnyye raketnyye dvigateli -- liquid-fuel rocket engines/, Fig. 2, in which a liquid propellant composed of a fuel and an oxidizer serves as the energy source, and the gaseous products of combustion serve as the working substance. In principle it is possible to create ARDs /atomnyye raketnyye dvigateli -- atomic rocket engines/ -- in which an atomic fuel serves as the energy source, and steam from a liquid with a light molecular weight, such as water, serves as the working substance.

Powder rockets were invented in China many centuries ago.

The theory of rocket propulsion -- a mass which changes with time -- was formulated during the years 1897-1904 by the outstanding Russian scientist, Academician I. V. Meshcherskiy. His labors laid the foundation of jet propulsion technology.

Rockets operating on liquid fuel were suggested by K. E. Tsiolkovskiy in 1903. He failed to bring his invention to life under the conditions of Tsarist Russia.

PRDs and ZhRDs consume 16 to 36 kg of fuel per hour for each kilogram of thrust. Fuel stored in a wingless rocket does not permit powered flights of more than 1.5-2 minutes.

Air-breathing jet engines (Fig. 3) which use air from the surrounding atmosphere as the working substance and as the oxidizer consume significantly less fuel per hour for each kilogram of thrust than a PRD or ZhRD (from 1.0 to 6 kg/hr per kilogram of thrust). The duration of the powered flight of a winged aircraft with a VRD[1] may be several hours (see Section 3 of this chapter). In contrast to rockets whose operation does not depend on the surrounding atmosphere, air-breathing jet engines may operate only within the limits of the earth's atmosphere.

All air-breathing jet engines have an inlet opening or a diffuser for the entrance of air and an exhaust or jet nozzle for the exhaust of the operating gases whose reaction creates useful thrust. This thrust is equal to the change in momentum of the exhausted gases and the incoming air that occurs every second.

Today three forms of air-breathing jet engines are prevalent: turbojet (abbreviated TRD /turboreaktivnyye7/), pulse-jet (PuVRD /pul'siruyushchiye7/), and ramjet (PVRD /pryamotochnyye7/).

We shall consider the principle of operation of each of these three forms of air-breathing jet engines.

A turbojet engine (TRD) is composed of an inlet diffuser, a compressor, a combustion chamber, turbines, and exhaust nozzle (Fig. 4a, in the diagram the diffuser is removed).

Air, compressed by the compressor, enters either a combustion chamber where

---

1. air-breathing jet engine.
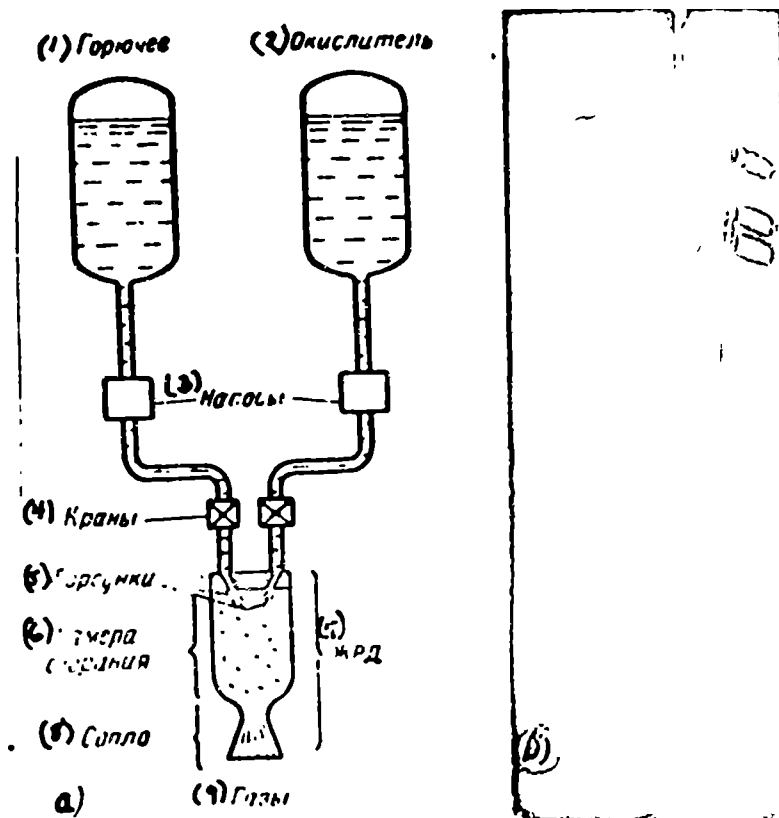
Fig. 2 A liquid-fuel rocket engine (ZhRD). a - schematic, b - external view.
Legend: 1) fuel; 2)oxidizer; 3) pumps; 4) valves; 5) injectors; 6) combustion chamber; 7) ZhRD; 8) nozzle; 9) gases.
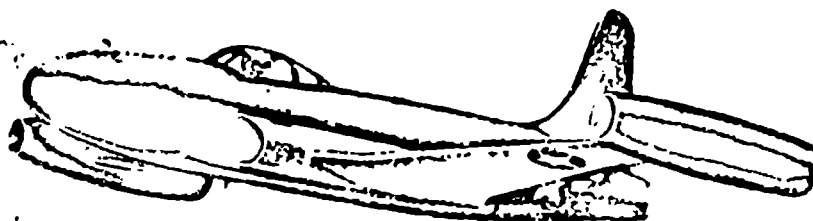
Fig. 3 VRD air-breathing jet engines on the wings of an aircraft.

fuel is injected, or into an atomic reactor. The enthalpy of the gas increases.
Compressed and burnt gases bring the operating wheel of the turbine into rotation
by giving up a portion of their energy, thus causing their temperature and pressure
to decrease. The gases, after operating in the turbine, flow out the exhaust nozzle
at a velocity which exceeds the velocity of the entering air stream, and act on the
engine with some reaction force. A TRD operates on energy liberated in a combustion
chamber or a reactor. If the heating of the gases is discontinued, the energy re-
leased by the gases in the turbine proves to be less than that used by the air
during compression in the compressor, and the rotation of the turbocompressor

rotor is stopped. The thrust of the turbojet engine is increased by increasing the number of compression stages for the air in the compressor and by an increase in the temperature of the gases which are exhausted from the combustion chamber or reactor. However, the temperature of the gases at the turbine entrance is limited by the heat-resistant qualities of its guide vanes and operating blades. During supersonic flight speeds, the temperature of the gases which leave the compressor becomes high, and the possible heating of the gases in the combustion chamber is negligible. Therefore turbojet engines are suitable only for flight speeds which do not exceed the speed of sound more than 3 times (see Fig. 11).

For an increase in the fields of application of turbojet engines they are equipped with afterburners for burning fuel in the gases which have passed through the turbine (Fig. 4b and Fig. 144, see page 258). Turbojet engines with afterburners are suitable for speeds which do not exceed the speed of sound more than 3 or 4 times.[1]

Turbojet engines are widely used in both subsonic and supersonic aviation.

Pulse-jet engines (PuVRD) consist of a short inlet diffusor, a flap valve assembly, a combustion chamber, and a long cylindrical exhaust nozzle (Fig. 5). Fuel is injected into the combustion chamber. An electric igniter, a "spark plug," ignites the mixture which is formed. Burning occurs in a partially enclosed area, since the column of gases in the long cylindrical nozzle, due to its inertia prevents the rapid expansion of the combustion products. Therefore the pressure in the combustion chamber rises, the inlet valves automatically close, and the gases are being expelled from the nozzle with increased velocity, which acts upon the engine with some reaction force. Owing to the inertia of the column of gases which move through the exhaust nozzle, the pressure in the combustion chamber falls below that of the atmosphere and fresh air enters the chamber through the valves which open automatically. Then the entire cycle is repeated.

---

[1]Roy Marquardt, "Future of Ramjet Engines," American Aviation, I-II, 1954, 24-28.

During the period when the valves are closed, the engine has great aerodynamic drag, especially noticeable during transsonic flights. Therefore a PVRD is suitable only for aircraft whose speed is less than that of sound.

Ramjet engines (PVRD) have an inlet diffuser, a combustion chamber with nozzles for feeding fuel, an ignition device, a flame holder, and an exhaust nozzle (Fig. 6). The compression of air occurs in the diffusor of the PVRD at the expense of its kinetic energy. Therefore a PVRD may operate only in an air stream. The oncoming air enters the expanding diffuser and partially loses its speed; because of this its pressure, density, and temperature are raised in proportion to the initial velocity of the air stream. The air, compressed by the diffuser, enters the combustion chamber and is mixed with fuel. During the burning of the mixture that is formed, the enthalpy of the gas increases, while the pressure decreases insignificantly. The combustion products are forced out the exhaust nozzle with a speed greater than that of the entering air stream.

During speeds of 3 times the speed of sound, the pressure in the combustion chamber of a PVRD may be raised approximately 25 times. Because of this, a device that raises the pressure, similar to a turbine or a compressor in a turbojet engine, becomes unnecessary.

At speeds which are approximately lower than half the speed of sound, the increase of pressure attributable to the velocity on the free stream air, is insignificant (less than 20%). The energy liberated by the burning of the fuel is low, and only a small portion of the enthalpy of the combustion products is transformed into kinetic energy. Therefore a PVRD is not used at low speeds ($M<0.5$).

The air pressure in a ramjet engine is noticeably sustained only during heating. In the absence of heating, the air flows through the engine duct without slowing and the pressure remains low. At the same time, the speed of the exhaust is less than that of the incoming air, because of the energy loss due to friction and shock waves, and only the force of aerodynamic drag acts on the engine.

At flight speeds greater than 3 times the speed of sound, ramjet engines prove

(1) Электро-стартер
(1) 13-ступенчатый компрессор
(3) Камера сгорания
(4) Двухступенчатая турбина
(5) Сопло

a)

(6) Сопло ТРД
(7) Термопары
(3) Камера сгорания
(8) Регулируемое сопло
(9) Диффузор
(10) Пневмопривод сопла

b)
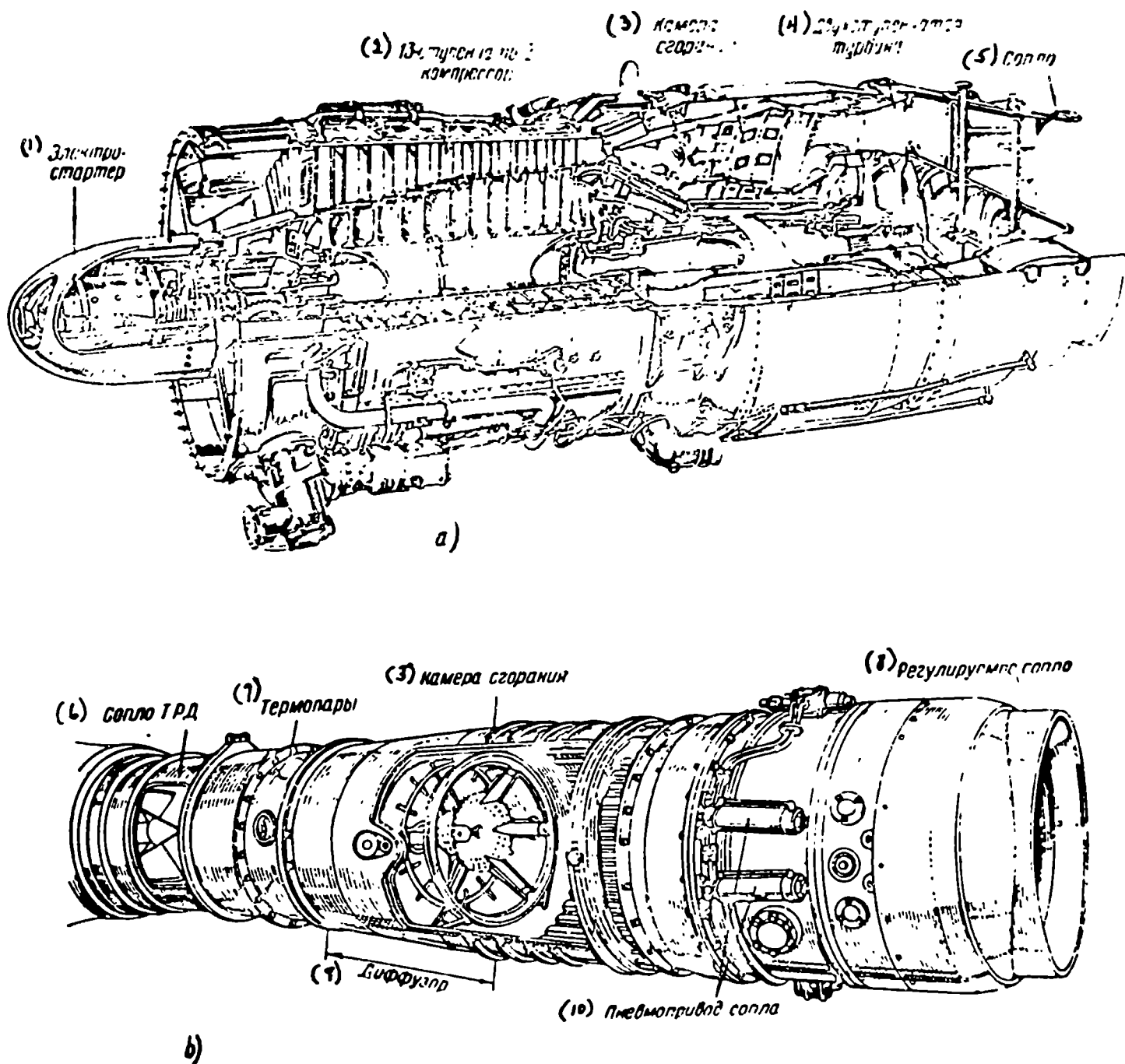
Fig. 4   Diagram of a gas turbine engine.   a -- turbojet engine, b -- afterburner
of a turbojet engine.
Legend: 1) electric starter; 2) 13-stage compressor; 3) combustion cham-
ber; 4) two-stage turbine; 5) nozzle; 6) turbojet engine nozzle; 7) ther-
mocouples; 8) variable-area nozzle; 9) diffuser; 10) pneumatic nozzle
instrument.

a)

б)
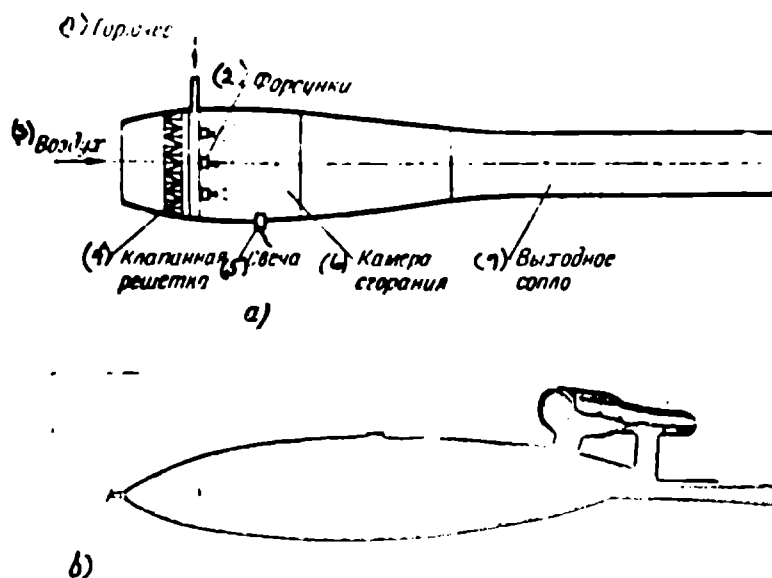
Fig. 5 A pulse-jet engine (PuVRD). a -- schematic, b -- installed on a missile.
Legend: 1) fuel; 2) injectors; 3) air; 4) flap valve assembly; 5) igniter; 6) combustion chamber; 7) exhaust nozzle.

a)   б)

c)
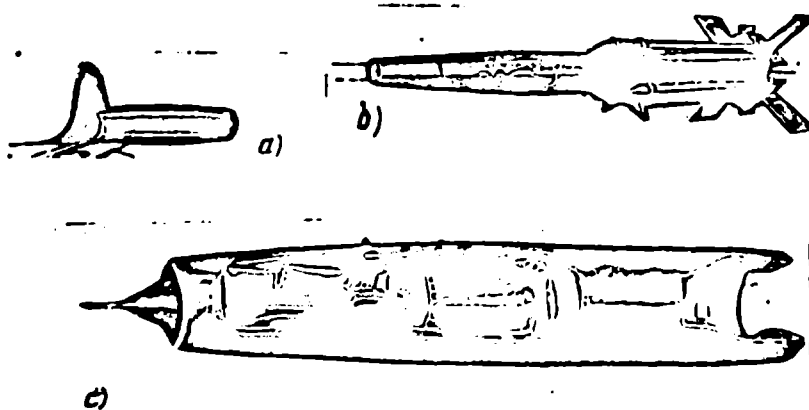
Fig. 6 A ramjet engine (PVRD). a -- subsonic PVRD, b and c -- supersonic PVRDs
at $M_n < 2$ and at $M_n > 2$.

to be more economical than any other sort of power plant.

The idea of a ramjet engine was advanced in 1913 by the French engineer René Loren, who described his invention in an article published in the magazine Aerofile in 1913. He did not have a clear-cut idea of high-speed flight and therefore believed that the engine efficiency would always be low. Loren apparently did not undertake any attempts to bring his invention to reality.
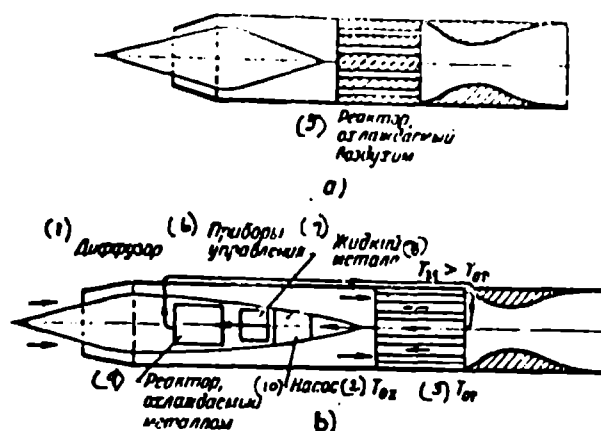
Fig. 7 Basic schematic of an atomic air-breathing engine. a -- engine with direct air heating; b -- engine with intermediate heat conductor.
Legend: 1) diffuser; 2) T_{okh}; 3) T_{og}; 4) nozzle; 5) air-cooled reactor; 6) control instruments; 7) liquid metal; 8) $T_M > T_{og}$; 9) metal-cooled reactor; 10) pump.

In 1926, the Englishman Benjamin Carter took out a patent on a ramjet engine for artillery shells. He specified the necessary units for the flameholders, and for flight speeds in the order of 100 m/sec he suggested injecting the fuel against the air stream to increase its spray and vaporization. Information about the tests of his invention is not to be found.

In 1929 the Russian scientist B. S. Stechkin published the article "The Theory of Air-Breathing Jet Engines," which served as the foundation for the furthering of theoretical development.

In 1934 the French engineer Rene Leduc took out a patent on an aircraft with a ramjet engine. Leduc began the development of ramjet engines in 1933, and in 1935 began static tests of a model PVRD which, for that time, had the high speed of 1,000 km/hr, and which proved its practicability over any other type engine. Leduc's model of an aircraft with a PVRD was exhibited at the Paris air exhibition in 1938, and during the same year the construction of an experimental aircraft was begun at the Brega plant.

At the time of the German invasion of France, this experimental aircraft was not finished. The interrupted work was resumed in 1945, and at the end of that year the experimental aircraft Leduc-010 was finished. However, until the end of 1956, no tests were conducted of the modified forms of this aircraft at supersonic speeds.

In 1939 the Soviet engineer I. A. Merkulov built and flight-tested a subsonic ramjet engine which was intended as an auxiliary engine for propeller-driven aircraft.

During the Second World War, work on ramjet engines was carried out in Germany, England, the USA, and the USSR. Reference to the progress made in this work will be found further in the text dealing with the development of the individual parts of the ramjet engines.

PVRDs, just as TRDs, are able to operate on both molecular fuel and atomic fuel (Fig. 7).

Section 2. Parameters of Jet-Propelled Engines

The operation of jet-propelled engines is characterized by a number of parameters. By comparing the numerical significance of the various systems of jet-propelled engine parameters with one another, their comparative advantages and disadvantages may be brought out.

The thrust-weight ratio of an engine is characterized by the frontal or midship thrust R_{ℓ}. Frontal thrust is equal to thrust R, which is attributed to the frontal area of the engine S_M, that is, to the unit of area of its maximum cross section.

$$R_a = \frac{R}{S_u}.$$ (1.1)

The frontal thrust of a rocket engine depends on the nature of the propellants, the pressure in the combustion chamber, and on the construction of the chamber and nozzle.

Knowing the nature of the fuel, the oxidizer, and the pressure in the combustion chamber, it is possible to calculate the frontal thrust and the fuel comsumption of a rocket engine. Similar computations indicate that solid-fuel rocket engines usually possess higher frontal thrust, but always at lower economy than liquid-fuel rocket engines.

The parameters of air-breathing reaction engines depend on the speed and altitude of the flight, and on the temperature and pressure of the combustion products

before the exhaust. The temperature is determined by the nature of the fuel and the composition of the mixture: the pressure by the speed of flight, the construction of the diffuser, and the operation of the compressor. The parameters of turbojet engines depend on the gas temperature before the turbine and the heat-resistance limits of the material from which the turbine blades are made. The use of new heat-resistant alloys and cermets affords the possibility of raising the temperature of the turbine blades, which will improve the parameters of the engine.

The parameters of supersonic ramjet engines, apart from the nature of the fuel and the composition of the fuel mixture, depend mainly on the perfection of the diffuser, in which the compression of the entering air stream occurs.

In order to give an idea of the comparative advantages and disadvantages of various aircraft engines, Fig. 8, 9, and 10 indicate the parameters computed with the high heat resistance and coefficient of pressure recovery which were reached in 1953. (These diagrams are borrowed from an article by Marquardt.[1]) With an increase in permissible temperature and the perfection of diffusers, the parameters of jet engines improved and the field of their application were broadened, but the comparative evaluation of various types of engines was not significantly altered.

The thrust of a jet engine, stated in units of weight of the engine construction P_{VRD}, is called the specific weight impulse.

$$I_p = \frac{R}{P_{BPД}} .$$ (1.2)

With a higher specific weight impulse, the relative weight of construction is less (Fig. 8).

The relation of frontal thrust to the dynamic head of the free air stream $q = \frac{\gamma w^2}{2g}$ is called the thrust coefficient c_R:

$$c_R = \frac{R_4}{q} .$$ (1.3)

---

[1]Roy Marquardt, "Future of Ram-jet Engines," American Aviation, I-II, 1954, 24-28.
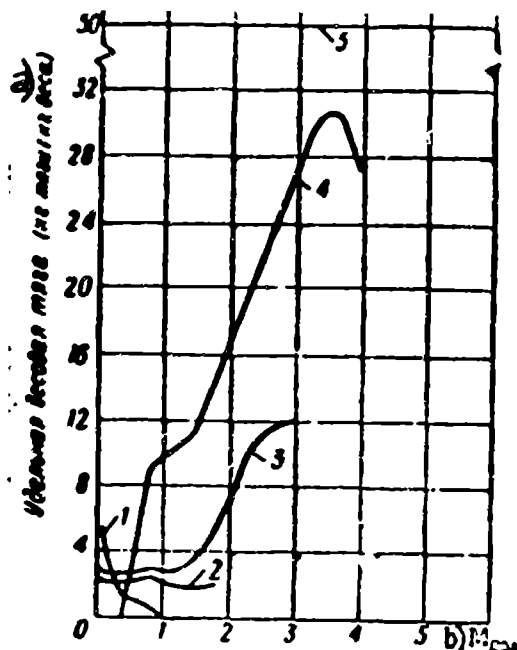
Fig. 8 Specific weight impulses of various engines.
1. Piston engine (PD). 2. Turbojet engine (TRD). 3. Turbojet engine with afterburner (TRDF). 4. Ramjet engine (PVRD). 5. Liquid-fuel rocket engine (ZhRD)
Legend: a) Specific weight impulse (kg thrust/kg weight); b) Mach.

From (1.1) and (1.3) we get

$$R = c_R S_u \frac{\gamma w^2}{2g},$$
(1.4)

where w is the flight speed in m/sec;

γ is the density of the free air stream in kg/m^3.

As seen from the formula (1.4), the thrust coefficient is determined by such expressions as the drag coefficient c_r:

$$x = c_x S_u \frac{\gamma w^2}{2g}.$$
(1.5)

The thrust of the engine R during stable horizontal flight is equal to the total aerodynamic drag of the aircraft X: $R = X$.

For an increase in speed or altitude $R > X$.

Therefore, in order for a jet engine to be suitable for use in an aircraft, the thrust coefficient must be not less than the drag coefficient $c_R \geqslant c_x$. If the drag coefficient of the aircraft is known, then by the magnitude of the thrust coefficient it becomes possible to judge the suitability of a jet engine for flights at some given speed (since c_R and c_x depend on the flight speed in various forms).

The operation of rocket engines does not depend on the speed of the free airstream; therefore, the conception of thrust coefficient does not usually apply for liquid-fuel rocket engines.

12

The economy of an engine which develops thrust at the expense of heat liberated during propellant combustion is expressed by the specific impulse I or specific fuel consumption C_e.

The thrust obtained in burning 1 kg of fuel in 1 second is called the specific impulse. If during fuel consumption G kg/sec the engine develops a thrust of R , then the specific impulse is:

$$I = \frac{R}{G} \cdot$$
(1.6)

The dimension of specific impulse is

$$[I] = \left[\frac{R}{G}\right] = \left[\frac{\text{kg of thrust}}{\text{kg of fuel/sec}}\right] = [\text{sec}]$$

The greater the specific impulse, the more economical the engine operates.

The fuel consumption per hour necessary to develop 1 kg of thrust is called the specific fuel consumption. If an engine consuming G kg/sec of fuel develops a thrust of R kg, the specific fuel consumption C_e will be equal to:

$$C_e = \frac{3600 G}{R} = \frac{3600}{I} \cdot$$
(1.7)

The dimension $\left[C_e\right] = \left[\frac{\text{kg of fuel}}{\text{kg of thrust/hr}}\right] = \left[\frac{1}{\text{hr}}\right]$

The specific fuel consumption or specific impulse of a rocket engine depends on the nature of the propellants, the pressure in the combustion chamber, and the construction of the engine. The specific fuel consumption or the specific impulse of an air-breathing jet engine depends on the nature of the fuel, the construction of the engine, and the speed and altitude of flight (Fig. 9).

From Fig. 9 we see that at $M < 0.7$ piston engines with propellers possess the most economical specific weight impulses. At M from 0.7 to 2.0 turbojet engines have the best economy. At $M \approx 2$ turbojet engines with afterburners (TRDF) have the best economy.[1] At $M > 2$ ramjet engines have the best economy and highest frontal thrust. With the improvement of heat-resistant materials, the field of application of a turbojet engine will be broadened.

---

[1]TRDF -- Turboreaktivnyy ovigatel's forsazhnoy kameroy -- Turbojet engine with afterburner. A turbojet engine which burns additional fuel after the turbine, or a turbojet with an afterburner.

For the final elucidation of the question of the fields of application of the same or different types of engines, it is necessary to compute the duration and length of flight.
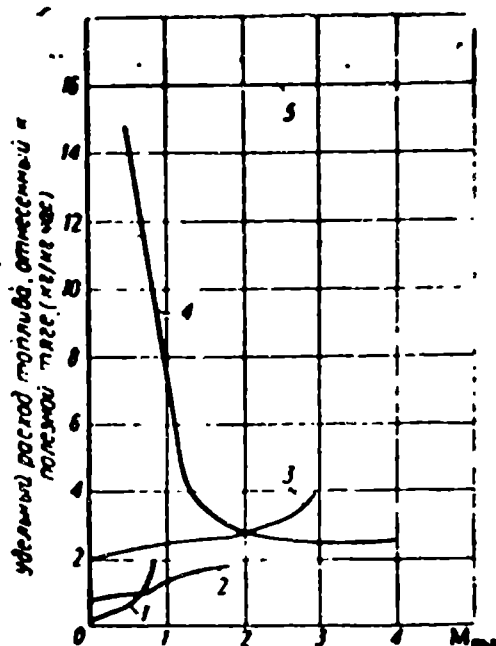
Legend:
a) Specific fuel consumption attributed to useful thrust, kg/kg hr.
b) Mach

Fig. 9 Specific fuel consumption of various types of engines. Designation same as in Fig. 8.

Section 3. Duration of Operation and Range

The duration of the cruising flight of an aircraft (the duration of flight with an operating engine) is determined by the relative fuel capacity on board $\mathcal{V}$ and the fuel consumption per second G.

The ratio of a full load of fuel P_g to the take-off weight of the device P_n is called the relative fuel capacity (fuel to gross weight ratio).

$$\nu = \frac{P_r}{P_s} \, . \tag{1.8}$$

The relative fuel capacity of a long-range rocket of the V-2 type reached 0.68. In essence, it is possible to increase somewhat this value. The relative fuel capacity of an aircraft is usually less than that of a wingless rocket.

The thrust R required for a flight depends on the angle of the flight trajectory to the horizon, on the aerodynamics of the aircraft, and on the flight speed.

The ratio of lift to drag or the ratio of weight to thrust during horizontal flight with a constant speed is called the aerodynamic quality of an aircraft k:

$$k = \frac{P}{R} \, . \tag{1.9}$$

The fuel consumption is determined by the required thrust R and the specific thrust I or the specific fuel consumption C_e

$$G = \frac{R}{I} = \frac{RC_e}{3600} \, \text{kg/sec} = RC_e \, \text{kg/hr.} \tag{1.10}$$

The duration of flight during constant thrust R = const is equal to the ratio of fuel load P_T to the fuel consumption G:

$$t = \frac{P_t}{G} = \frac{vP_n I}{R} = vkI. \tag{1.11}$$

By the combustion of the fuel, the gross weight of an aircraft $P = P_T + P_s$ is decreased, and therewith the required thrust.

$$R = \frac{P}{k} = \frac{P_c + P_t}{k}. \tag{1.12}$$

Here P_s is the empty weight of the device. The reduction of weight for the time dt is equal to the weight of the burned fuel:

$$-dP = G \quad dt = \frac{R}{I} \quad dt = \frac{P}{kI} \, dt$$

Hence

$$dt = - kI \, \frac{dP}{P}$$

Integrating to the limit from P_n to P_s, we find that the duration of flight at a constant speed (w = const), constant quality k, and varying thrust $R = \frac{P}{k}$

$$t = -\int_{P_n}^{P_c} kI \, \frac{dP}{P} = -kI \left| \ln P \right|_{P_n}^{P_c};$$

$$t = kI \ln \frac{P_n}{P_c} = kI \ln \frac{1}{1-v}. \tag{1.13}$$

Comparing the expressions 1.11 and 1.13, we see that the duration of flight during variable thrust is greater than with constant thrust by $\dfrac{\ln \frac{1}{1-v}}{v}$ times. If $V \approx 0.70$, then

$$\frac{\ln \frac{1}{1-v}}{v} = \frac{2.3}{0.7} \lg \frac{1}{1-0.7} = 1.725.$$

The range of flight depends on the duration and speed of flight

$$l = wt = cMt. \tag{1.14}$$

Here $M = \frac{w}{c}$ is the Mach number (see Chapter II, Section 7); c is the speed of sound in m/sec or km/sec.

Having used 1.13, we finally obtain

$$l = cM/k \ln \frac{1}{1-v},$$

(1.15)

; expressed in the same units of length used in defining the velocity.

The last formula is called Tsiolkovskiy's formula, or

$$l = \frac{w}{C_e} k \ln \frac{1}{1-v} \text{ km.}$$

(1.16)

The speed w in the formula (1.16) is expressed in km/hr.

The product $cMI = \frac{w}{C_e} = wI$ is called the range parameter. It is expressed in

The value of the range parameter $\frac{w}{C_e}$ depends on the type of engine and the

ght speed (Fig. 10). At subsonic flight speeds a longer flight range may be ob-

ned through the use of piston engines; at transsonic flight, by the use of turbo-

engines; at speeds of $M = 1.6$ to $M = 2.5$, by the use of turbojet engines with

erburners; and at $M > 2.5$ and greater, the longest powered guided flight is by

ns of ramjet engines. With increased permissible temperatures at the turbine

rance, the field of application of a turbojet engine for long flights is widened

include higher speeds.
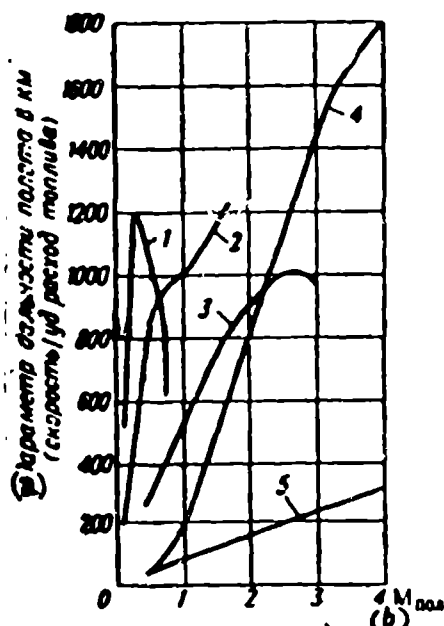
g. 10 Range factors of various engines. Designations same as in Fig. 8.
Legend: a) Flight range parameter in km (speed/specific fuel consumption); b)Mach.

Example 1. Let us find the duration of flight of an aircraft with a turbojet

gine when $M = 1$; $V = 0.4$; $k = 8$; $C_e = 1.2 \frac{1}{hr}$:

$$t = \frac{k}{C_e} \ln \frac{1}{1-V} = \frac{8}{1.2} \ln \frac{1}{0.6} = 3.4 \text{ hours}$$

Example 2. Let us find the duration of vertical flight of a rocket with a

liquid-fuel rocket engine when $\nu = 0.68$; $C_e = 16 \frac{1}{hr}$, if the ratio of take-off weight

to thrust is $\frac{P_n}{R} = 0.5$ and thrust tends to be constant in flight:

$$t = \frac{\nu P_n}{C_e R} = \frac{0.68 \cdot 0.5}{16} = 0.021 \text{ hr.} = 76 \text{ sec.}$$

Example 3. Let us find the range of powered horizontal flight of a winged

stratosphere missile of the "Navaho" type (see page 21), with a ramjet engine at

speeds of M = 2.5, if the quality of the missile k = 5 and the relative fuel weight

$\nu = 0.7$.

The speed of sound in the stratosphere is c = 295 m/sec. The specific fuel

consumption of a ramjet engine at M = 2.5 is $C_e = 2.6$ kg/hr kg. The range is

$$t = \frac{cMk}{C_e} \ln \frac{1}{1-\nu} = -\frac{295 \cdot 3.6 \cdot 2.5 \cdot 5}{2.6} \ln \frac{1}{1-0.7} = 6240 \text{ km.}$$

Section 4. The Fields of Application of Various Types of Jet Engines

The brief information about jet engine parameters in the foregoing paragraphs

permits determination of the areas of speed and altitude at which the engines of one

or another type may be most effectively used (Fig. 11)[1].
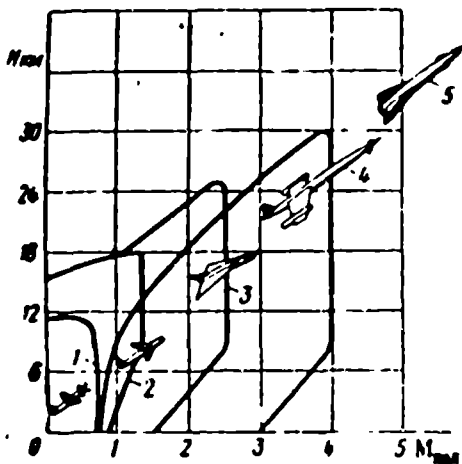
Fig. 11. Areas of operation of various types of jet engines. (Designations same as in Fig. 8).
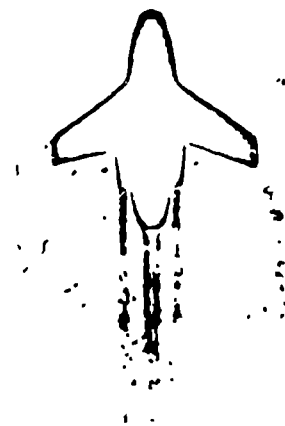
Fig. 12. The take-off of a missile with assist rockets.

---

[1] "Guided Missiles" (review), Voprosy raketnoy tekhniki /Questions of Rocket Technics/, No 1, 1956; G.W. Gardner, "Guided Missiles," Chartered Mech. Engineers, 1955, No 1, page 2.

Rocket engines operating on solid fuels (PRD) and those operating on liquid fuels (ZhRD) may be used at any speed and at any altitude. The altitudes are limited by the aerodynamics of the aircraft and not by the peculiarities of the rocket engine.

Rocket engines are used as take-off boosters to cut down runway lengths and time during the take-off of aircraft with piston, turboprop, or air-breathing jet engines; on guided missiles; on antiaircraft rockets; and on long-range rockets (Figures 12, 13 and 14). At the end of the Second World War, rockets had a range of 300 km. This range was increased by increasing the specific thrust, the takeoff weight, and the relative fuel supply.

The intercontinental ballistic missile has been successfully tested in the USSR; it is able to hit any point on the earth's surface. The speed of the missile is many times greater than that of sound at the end of the operation of the missile's engine. The missile is propelled by inertia for the greater portion of its flight at enormous altitudes and in very rarefied atmosphere. This portion of flight is practically unguided.
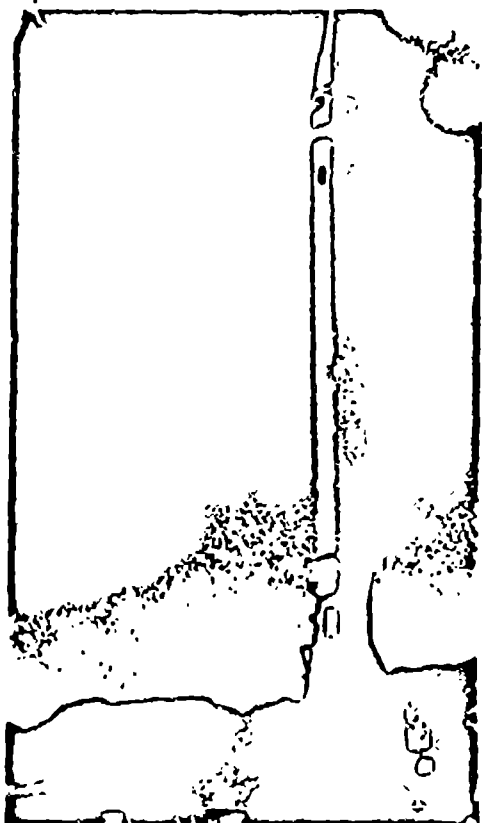
Fig. 13. The "Viking" high-altitude rocket.

Fig. 14. The "Nike" antiaircraft guided missile.

During powered flight, the long-range missile is directed by means of internal

rudders located in the exhaust gas stream and receiving signals from the autopilot or by radio.

High-altitude rockets with ZhRDs are also used for scientific purposes: for research of the upper layers of the atmosphere, solar radiation, cosmic rays, etc. Data about the layers of the atmosphere at altitudes of more than 40 km (Table 1.1) are obtained by high-altitude rockets (V-2s and "Vikings") which have instrument compartments in place of warheads in their upper portions.

TABLE 1.1

PHYSICAL DATA OF THE ATMOSPHERE

(Obtained by High-Altitude Rockets)

Altitude H, km.	Temperature T_H K	Pressure P_H, mm Hg	Density γ_H kg/m³
0	288.0	760	1.1
10	230.8	210	$4.2 \cdot 10^{-1}$
20	212.8	42	$9.3 \cdot 10^{-2}$
30	231.7	9.5	$1.9 \cdot 10^{-2}$
40	262.5	2.4	$4.2 \cdot 10^{-3}$
50	270.8	$7.6 \cdot 10^{-1}$	$1.2 \cdot 10^{-3}$
60	252.8	$2.2 \cdot 10^{-1}$	$3.5 \cdot 10^{-4}$
70	218.0	$5.5 \cdot 10^{-2}$	$9.7 \cdot 10^{-5}$
80	205.0	$1.1 \cdot 10^{-2}$	$2.1 \cdot 10^{-5}$
90	217.0	$2.0 \cdot 10^{-3}$	$4.1 \cdot 10^{-6}$
100	240.0	$6.0 \cdot 10^{-4}$	$8.6 \cdot 10^{-7}$
110	270.0	$2.0 \cdot 10^{-4}$	$2.0 \cdot 10^{-7}$
120	330.0	$6.0 \cdot 10^{-5}$	$5.6 \cdot 10^{-8}$
130	390.0	$2.0 \cdot 10^{-5}$	$1.9 \cdot 10^{-8}$
140	447.0	$7.0 \cdot 10^{-6}$	$7.6 \cdot 10^{-9}$
150	503.0	$3.7 \cdot 10^{-6}$	$3.4 \cdot 10^{-9}$
160	560.0	$2.0 \cdot 10^{-6}$	$1.6 \cdot 10^{-9}$
180	676.9	$7.0 \cdot 10^{-7}$	$4.8 \cdot 10^{-10}$
200	792.5	$3.0 \cdot 10^{-7}$	$1.7 \cdot 10^{-10}$
220	906.6	$1.4 \cdot 10^{-7}$	$7.0 \cdot 10^{-11}$

On 4 October 1957 the Soviet Union launched the first earth satellite vehicle by means of a rocket carrier. The satellite had a diameter of 58 cm, a weight of 83.6 kg, and carried instruments and transmitters. A month ater, 3 November 1957, the second satellite was launched, carrying more complicated equipment and weighing 6 times as much.

ZhRDs are used as the primary engines also for planes designed for the study of supersonic flights(Fig. 15).

Turbojet engines (TRD) are used on high-speed civil and military aircraft of various types (Fig. 16). Heavy aircraft with TRDs are able to fly 8,000 km with a speed of more than 1,000 km/hr. Modern aircraft with TRDs develop supersonic speeds.

TRDs with afterburners and dual cycle TRDs are intended for flights at speeds reaching 3 times that of sound (see Fig. 11). Augmented TRDs are installed in light as well as heavy aircraft.

The broadest application in regard to speed and altitude is that of ramjet engines (see Fig. 11).

With an increase in flight altitude the atmospheric pressure falls (see Table 1.1) and conditions for carburetion and fuel ignition in the combustion chamber of a VRD worsen (see Chapter VIII). On the other hand, with an increase in flight velocity, the pressure in the chamber increases in proportion to the free stream dynamic
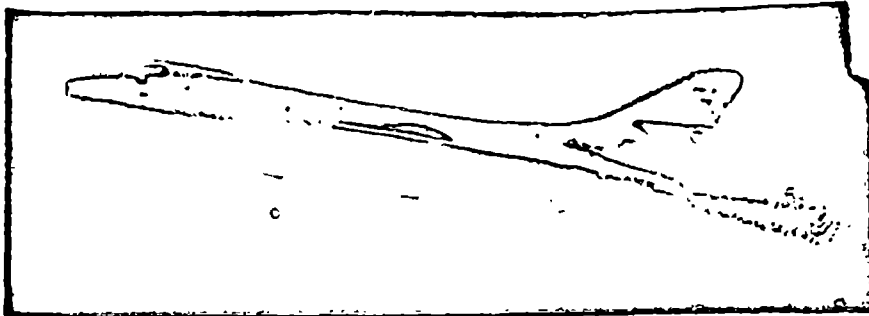
Fig. 15. A supersonic aircraft with ZhRDs (Mach 2.6, ceiling 20 km).

head. Therefore, the greater the flight speed, the greater the altitude up to which burning in the combustion chamber of a VRD will occur under satisfactory conditions. Ramjet engines are able to develop the greatest speeds. Therefore they can operate at greater altitudes than any other air-breathing jet engine. Supersonic PVRDs possess greater altitude capabilities than subsonic ones. The altitude capability of a subsonic PVRD operating on hydrocarbon fuel is almost 10 km.

Subsonic PVRDs are used in target drones, aircraft-type missiles, and helicopters.

Target drones are used for training antiaircraft-artillery and fighter pilots, and for testing various means of antiaircraft defense, replacing costly aircraft. The target drone is carried to the required altitude by a control aircraft, the ramjet

engine is started, and the target is released from the control aircraft. It flies independently, controlled by an autopilot or by radio command (Fig. 17).

Subsonic PVRDs installed in helicopters are located at the ends of the rotor blades (Fig. 18). A helicopter with a PVRD is simple, reliable, cheap, and does not need any additional means to counteract body torque since the engines are on the rotor itself.

Supersonic ramjet engines are used in antiaircraft missiles, on supersonic aircraft, and in winged long-range missiles.

Antiaircraft rockets with ramjet engines take off with the aid of starting rockets, gaining altitude and following thei selected target through the operation of the ramjet engine (Fig. 19).

A fighter aircraft with a ramjet engine, a prototype of which is the Leduc aircraft, starts with the aid of rockets or a turbojet engine and continues its flight through the operation of a ramjet engine (Fig. 20).

A winged long-range missile, an example of which is the "Navaho," designed in the USA, starts with the aid of a liquid-fuel rocket engine and then completes its planned flight through the operation of two ramjet engines located under the fuselage. The computed range of this missile, which is intended for intercontinental flights with a hydrogen bomb at speeds 2.5 - 3.0 times greater than that of sound, is 8,000 km at an altitude of 20 km. The most effective means of defense against winged long-range rockets would probably be supersonic fighters with ramjet engines, carried into the air by control aircraft, forming barrages near the defensive object and supersonic missiles supplied with a radio control and an internal guidance system (see Fig. 14 and 19).

In summary, we may say that the primary characteristics of ramjet engines are their ability to operate at very high flight speeds and at greater altitudes than turbojet engines; greater economy and lighter weight as compared with liquid-fuel engines; absence of moving parts and simplicity of construction. Basically, their shortcomings are the absence of static thrust, their need for a positive start, and low economy at subsonic flight speeds. Ramjet engines are the most effective engines for great supersonic speeds in aviation.
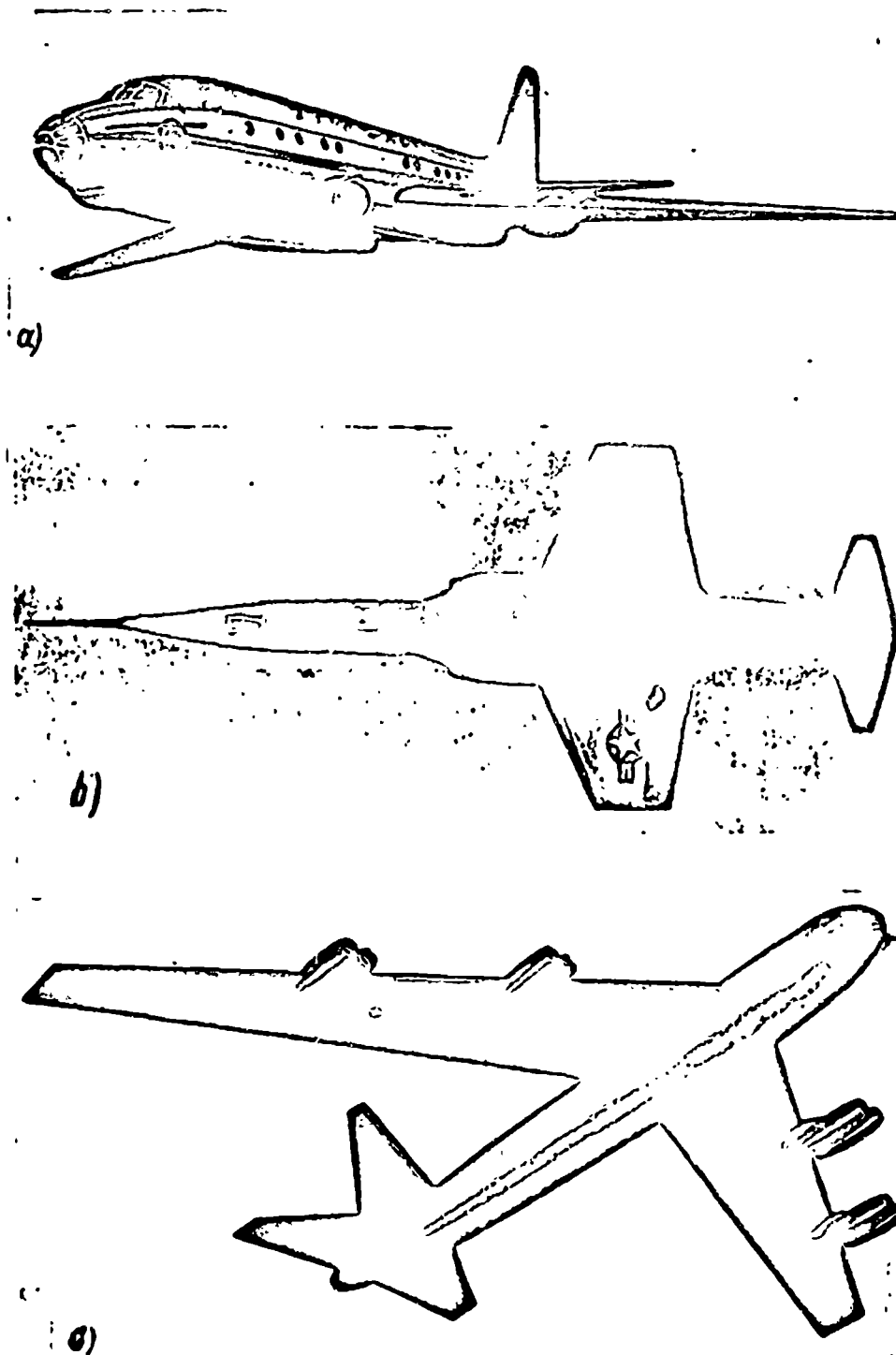
Fig. 16. Aircraft with turbojet engines.
a -- Passenger aircraft Tu-104; b -- fighter; c -- heavy bomber.
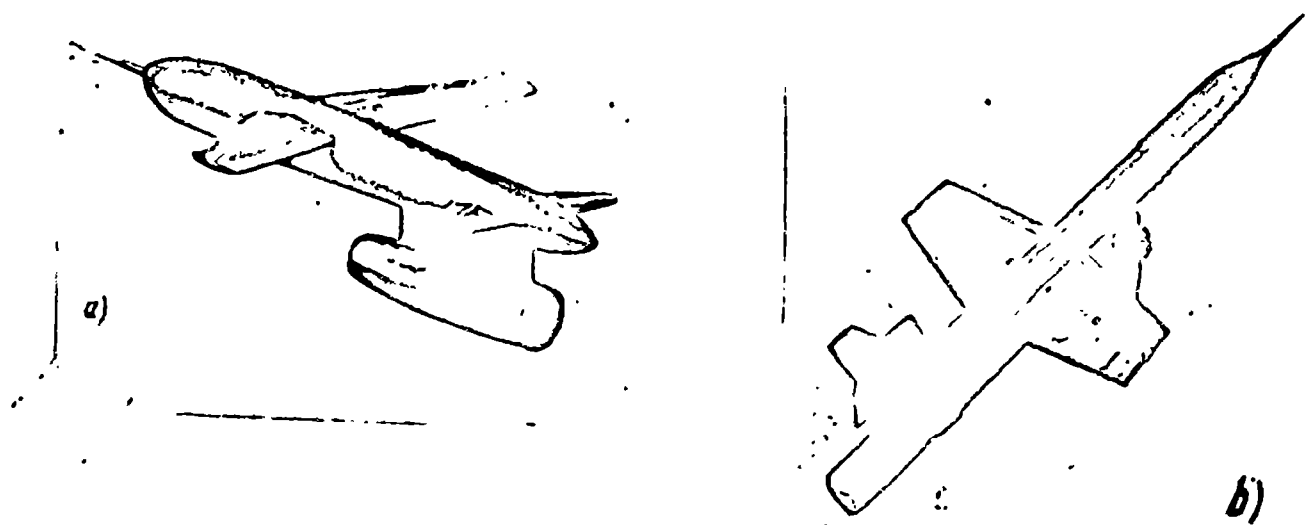
Fig. 17. Application and testing of PVRDs.   a -- Gorgon IV target drone;
b -- American Lockheed X-7 test missile used for testing supersonic
ramjet engines.
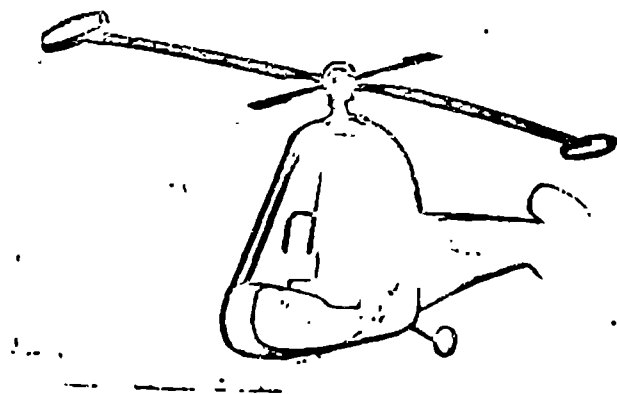
Fig. 18. A helicopter with ramjet engines at the ends of the rotor blades.
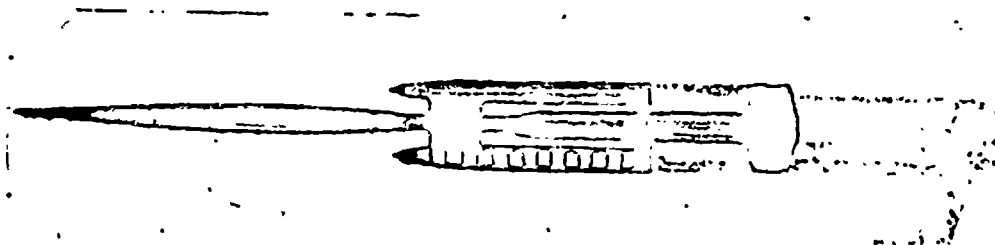
Fig. 19. Bristol-Boeing antiaircraft rocket with two supersonic ramjet engines.
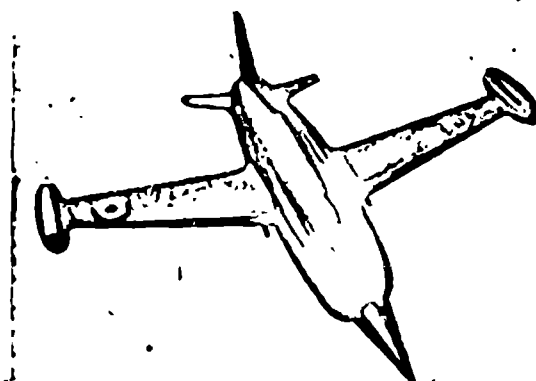
Fig. 20. Interceptor with a ramjet engine.
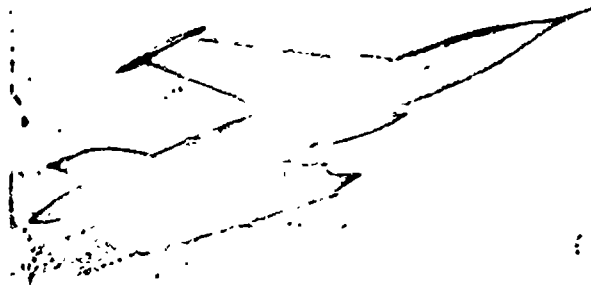
Fig. 21. Winged long-range rocket of the "Navaho" type with supersonic ramjet engines.

BIBLIOGRAPHY

1. Sanger, E. and Bredt, I. Dal'niy bombardirovshchik s raketnym dvigatelem /Long-Range Bomber with a Rocket Engine/, Voyenizdat, Moscow, 1946.

2. Seifert, H.S., Mills, M.M., and Summerfield, M., "Rocket Physics," Uspekhi fizicheskikh nauk /Advances in the Physical Sciences/, Vol XXXIV, No 4, 1948, 580-591.

3. Merkulov, I.A., Vestnik vozdushnogo flota /Herald of the Air Fleet/, 1953, No 12.

4. Murray, R., Vvedeniye v yadernuyu energetiku /Introduction to Atomic Energy/, State Publishing House for Foreign Literature, 1955.

5. Meshcherskiy, I.V., Raboty po dinamike tel peremennoy massy /Work on the Dynamics of Bodies with Variable Masses/, Gostekhizdat, 1950.

6. Namias, M., Yadernaya energiya /Atomic Energy/, State Publishing House for Foreign Literature, 1955.

7. Sutton, G., Raketnyye dvigateli /Rocket Engines/, State Publishing House for Foreign Literature, 1952.

8. Stechkin, B.S., "Theory of Ramjet Engines," Tekhnika Vozdushnogo Flota, 1929, No 2.

9. "Guided Missiles" (review), Voprosy raketnoy tekhniki /Problems of Rocket Technology/, No 1, 1956.

10. Tsiolkovskiy, K.E., Nauchnoye obozreniye /Scientific Review/, 1903.

11. Avery, W.H., "Twenty-Five Years of Ramjet Development," Jet Propulsion, Vol 25, XI, 1955.

12. Kalitinsky, A., Society of Automotive Engin., Transactions, 1949, p. 1.

13. Gardner, G.W., "Guided Missiles," Chartered Mech. Engineer, 1955, No 1, p. 2.

14. Leduc, Rene, Brevet dinvention, France, No 770326, 1933; No 779655, 1934.

15. Lorin, Rene, "De la turbine a gaz au propulseur a reaction," Aerophile,

1913, No 10. "Une experience relative au propulseur a reaction directe," *Aerophile* 1913, No 22.

16. Carter, B.C., British Patent, No 293594, 1926.

17. Marquardt, R., "Future of Ramjet Engines," *American Aviation*, I-II, 1954, 24-28.

18. Hill, P.R., "Parameters Determining Performance of Supersonic Pilotless Airplanes Powered by Ram-Compression Power Plants," *NACA Wartime Rep.* L. 755, VI, 1946.

19. Sanders, N.D., "Performance Parameters for Jet Propulsion Engines," *NACA TN*, 1106, 1946.

CHAPTER II

THE FUNDAMENTALS OF GAS DYNAMICS

The velocity of gases relative to the walls of a jet engine is so great that in investigating the flow it is necessary to consider the compressibility of the gas. The temperature and pressure c° a compressed gas fluctuate. The changes in the state of a gas which exchanges energy with the surrounding medium are expressed in terms of the laws of thermodynamics. The motion of a gas which is considered an incompressible fluid is described in terms of the law of aerodynamics. The laws of the flow of a compressed gas are a combination of aerodynamic and thermodynamic laws. The science of the motion of a compressed gas is called <u>gas dynamics</u>. Generally, aerodynamics may be considered as a particular case of gas dynamics.

Valuable conclusions about the characteristics of a flow of compressed gas may be made from the laws of the conservation of matter and energy.

Section.1. The Law of Flow Continuity

We shall consider a gas flow which flows through the cross-section of a tube (Fig. 22). In the section S_1 the gas has a speed of w_1, a density of γ_1, a temperature of T_1, and a pressure of p_1. The gas parameters in section S_2 are marked with the index "2".

The volume which flows through this tube section every second is called the volumetric discharge Q:

$$Q = \frac{dV}{dt} = \frac{S\,dx}{dt} = Sw \tag{2.1}$$
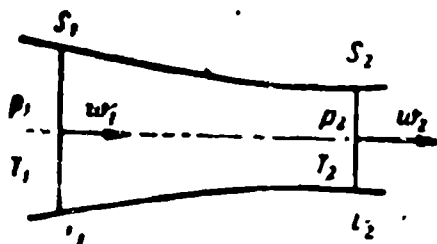
Fig. 22 For the solution of the basic flow equation.

The volumetric discharge equal to the time derivitive of the incoming volume is measured by the product of the speed of the flow w and the flow section S. In the computation of the volumetric discharge, the same units of length are used in the expression of speed and cross section: if, for example, speed is expressed in m/sec and the cross section in m^2, then the volumetric discharge is obtained in m^3/sec.

The quantity of kilograms of gas which flow through the section under consideration, per unit of time, is called the <u>mass flow rate</u> G:

$$G = \frac{dm}{dt} = \gamma S w.\tag{2.2}$$

The mass flow rate equal to the time derivative of the mass of the flowing substance is measured by the product of the flow section S, speed w, and density .

If, along the length of the tube, mass exchange with the surrounding medium is absent, then, according to the law of the conservation of matter, the amounts of substance which flow every second through any section of a pipe are equal to one another.

Sections 1 and 2 may be described by $\qquad$ (2.3)

$$G_1 = G_2 ;$$

or

$$G = w_1 S_1 \gamma_1 = w_2 S_2 \gamma_2.\tag{2.4}$$

In the absence of sources and sinks, the product of the pipe's cross-section, the flow speed, and the density is of constant value. The law expressed by equation (2.4) is called the <u>law of the continuity of flow.</u>

The law of the continuity of flow is a result of the law of the conservation of matter.

Density is written in the same units of volume as is volumetric discharge. If, for example, speed is expressed in m/sec, cross-section in m^2, then density will be expressed as kg/m^3 or t/m^3. The discharge by weight will then be expressed in kg/sec. or t/sec.

The law of flow continuity is widely used in the gas dynamics of reaction engines.

Section 2. The Law of Conservation of Energy for a Gas Stream

The law of the conservation of energy is also widely used in gas dynamics. Let us assume a gas is allowed to flow along the cross-section of a tube (see Fig. 22). During time dt, dm_1 kg of gas will enter the tube. The speed of the movement of the gas is equal to w_1. The kinetic energy of the gas entering the tube in time dt is equal to

$$dK_1 = \frac{w_1^2 \, dm_1}{2g} \, .$$

(2.5)

The sum of the kinetic and potential energies of the atoms, molecules, and other particles is called the _internal energy of the body_. The internal energy of an ideal gas is proportionate to its temperature.

If the temperature of a gas is T_1, then the internal energy of the gas, which enters the tube in time dt, is equal to

$$dE_1 = c_v T_1 \, dm_1.$$

(2.6)

The gas pressure is equal to p_1. The section S_1 may be considered as a rigid piston. The work which this hypothetical piston accomplishes on the gas in the tube is equal to

$$dU_1 = p_1 S_1 \, dx = p_1 \, dV_1.$$

(2.7)

The energy brought in by the gas in the tube through section S_1, is equal to the sum

$$A \, dK_1 + A \, dU_1 + dE_1 = \frac{A w_1^2 \, dm_1}{2g} + c_v T_1 \, dm_1 + A p_1 \, dV_1.$$

(2.8)

$A = \frac{1}{427}$ is the thermal equivalent of work.

The energy carried away by the quantity of gas dm_2 flowing out through section S_2 in time dt is equal to

$$A \, dK_2 + A \, dU_2 + dE_2 = \frac{A w_2^2 \, dm_2}{2g} + c_v T_2 \, dm_2 + A p_2 \, dV_2.$$

The energy released in the tube is designated by dH. The heat which goes through the walls of the tube and is dissipated into the surrounding atmosphere is designated by δq.

According to the law of the conservation of energy

$$A \, dK_1 + dE_1 + A \, dU_1 + dH = A \, dK_2 + dE_2 + A \, dU_2 + \delta q.$$

(2.9)

If liberation of energy does not occur in the flow, then

$$dH = 0$$

If the flow is adiabatic, i.e. if it occurs without exchange of energy with the ambient atmosphere, then

$$\delta q = 0.$$

In this case

$$\frac{A w_1^2\, dm_1}{2g} + c_v T_1\, dm_1 + A p_1\, dV_1 = \frac{A w_2^2\, dm_2}{2g} + c_v T_2\, dm_2 + A p_2\, dV_2. \qquad (2.10)$$

According to the law of the conservation of matter

$$dm_1 = dm_2$$

Dividing both sides of the last equation by dm and noting that $\frac{dV}{dm}$ is equal to the specific volume of the gas v, we obtain

$$\frac{A w_1^2}{2g} + c_v T_1 + A p_1 v_1 = \frac{A w_2^2}{2g} + c_v T_2 + A p_2 v_2. \qquad (2.11)$$

The sum of the internal energy of 1 kg of gas $c_v T$ and the work of gas displacement under the action of internal pressure p is called <u>enthalpy</u>, or <u>heat content</u> i:

$$i = c_v T + A p v. \qquad (2.12)$$

According to the equation, the composition of an ideal gas is

$$p v = R T, \qquad (2.13)$$

consequently,

$$i = (c_v + A R) T = c_p T, \qquad (2.14)$$

since, according to Mayer's equation,

$$c_p = c_v + A R. \qquad (2.15)$$

Substituting (2.15) in (2.11) we obtain the basic equation of adiabatic flow:

$$\frac{w_1^2}{2g} + \frac{i_1}{A} = \frac{w_2^2}{2g} + \frac{i_2}{A} \qquad (2.16)$$

or

$$\frac{A w_1^2}{2g} + c_p T_1 = \frac{A w_2^2}{2g} + c_p T_2. \qquad (2.17)$$

During adiabatic flow the sum of the kinetic energy and the enthalpy of the gas is a constant value.

The variation in density of liquids during changes of flow speeds is practically immeasurable. If changes in gas speeds are small in comparison with the speed of sound ($\frac{u}{c} < 0.5$), then the gas density remains practically constant: γ = const. If the gas density is a constant, if friction losses are negligibly small, and if energy exchange with the surrounding medium is absent, then the internal energy and temperature of the flow will remain constant:

$$T_1 = T_2 = \text{const} \text{ and } c_v T_1 = c_v T_2 = \text{const.} \tag{2.18}$$

In this case the terms $c_v T_1$ and $c_v T_2$ in the equation (2.11), expressing the law of conservation of energy for the flowing gas, cancel each other out.

Then,

$$\frac{w_1^2}{2g} + p_1 v = \frac{w_2^2}{2g} + p_2 v. \tag{2.19}$$

After multiplying both parts of the equation (2.19) by the density of the flow γ, then noting that γv × 1, we obtain the so-called <u>Bernoulli equation</u>, which relates the speed and pressure of an incompressible fluid with each other:

$$\frac{\gamma w_1^2}{2g} + p_1 = \frac{\gamma w_2^2}{2g} + p_2. \tag{2.20}$$

The equation $\frac{\gamma w^2}{2g}$ has the dimension of pressure

$$\left[\frac{\gamma w^2}{2g} \right] = \left[\frac{\text{kg}}{\text{m}^3} \frac{\text{m}^2}{\text{sec}^2} \frac{\text{sec}^2}{\text{m}} \right] = \left[\frac{\text{kg}}{\text{m}^2} \right]$$

which is called the <u>impact pressure</u>; p is called the <u>static pressure</u>.

The sum of the static pressure p and the impact pressure $\frac{\gamma w^2}{2g}$ is called the <u>total pressure</u>. If the flow is totally decelerated (when w_2 = 0) the static pressure becomes equal to total pressure: $p_2 = p_1 + \frac{\gamma w_1^2}{2g}$.

Pressure is expressed in kg/m^2, speed in m/sec, density in kg/m^3, and g in m/sec^2.

Static pressure is measured by means of a manometer stationary in relation to the flow or by means of a manometer whose intake opening is parallel to the current (Fig. '3a). The total pressure of a flow is measured by a tube fixed to the side of the duct, with an opening directed against the stream so that its face is perpendicular
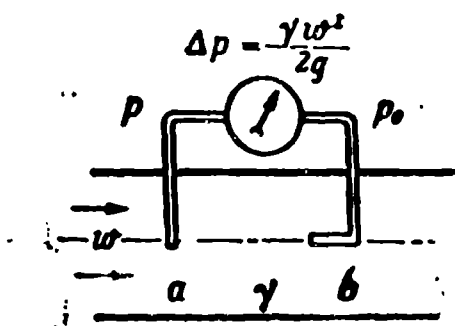
Fig. 23. Measuring the pressure of a stream.
a -- static tube; b -- Pitot tube.
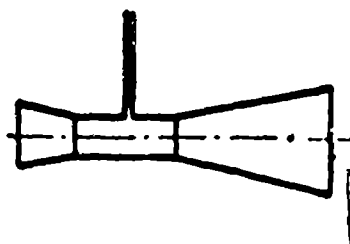
Fig. 24. A Venturi tube.

to the direction of the current (Fig. 23b). The impact pressure and the speed of the fluid's current `w` may be calculated from the manometer measurements of static and total pressure,

A manometer tube serving to measure total pressure is called a _Pitot tube_ (Fig. 23b).

The equation of continuity (2.4) for an incompressible fluid is:

$$w_1 S_1 = w_2 S_2 \qquad (2.21)$$

or

$$\frac{w_1}{w_2} = \frac{S_2}{S_1}.$$

The stream speed of an incompressible fluid is inversely proportional to the cross-section of the tube: the smaller the tube's cross-section, the greater the stream speed of the incompressible fluid. Thus, according to Bernoulli's equation, the less the static pressure:

$$p_2 - p_1 = \frac{\gamma w_1^2}{2g} - \frac{\gamma w_2^2}{2g} = \frac{\gamma w_1^2}{2g}\left(1 - \frac{S_1^2}{S_2^2}\right). \qquad (2.22)$$

Measuring the static pressure p_1 and p_2 and knowing the ratio of the cross sections $\frac{S_1}{S_2}$, it is possible to determine by means of formula (2.22) the flow velocity w_1 and the fluid mass flow $G = \gamma w_1 S_1$.

A variable section tube which serves for the computation of the local value of velocity or fluid flow is called a _Venturi tube_ (Fig. 24).

Bernoulli's equation is used, for example, in the design of fuel injectors, for the computation of fluid flow, and in the design of fuel supply lines.

A flow of real liquids and gases is accompanied by various losses; therefore, ·ring velocity or flow calculations involving either Pitot or Venturi tubes, the

correction coefficient φ, determined by test, enters Bernoulli's equation:

$$w = \varphi \sqrt{2g \frac{p_2 - p_1}{\gamma}}.$$ (2.23)

Density is expressed in kg/m^3 and pressure in kg/m^2. The value of φ, which takes into account the flow and shock losses, is called the __tube__ __coefficient__.

__Example.__ Let us determine the discharge of a stream of gasoline from an ideal injector, if the excess pressure in the fuel supply line is 25 kg/cm^2 and the density of the gasoline is $\gamma = 0.74$ $kg/l = 740$ kg/m^3. Its velocity before discharge is considered as zero: $w_2 = 0$

Then, using the equation (2.20), we may note:

$$w = \sqrt{\frac{2g\Delta p}{\gamma}} = \sqrt{\frac{2 \cdot 9.8 \cdot 25 \cdot 10^4}{740}} = 81.3 \text{ m/sec.}$$

Section 4. The Law of the Conservation of Impulse. Euler's Equation

The product of a mass of gas m and its velocity w, equal to mw, is called momentum.

If there are no forces acting upon a stream of gas, then according to the third law of mechanics, the momentum of the gas will remain constant.

During flow through a tube having a variable cross-section, or during air flow round various bodies, the velocity and pressure of a gas stream τ as.

According to a well-known theorem of mechanics, the fluctuation of momentum, (mw), is equal to the impulse of the effective force.

$$d(mw) = f\,dt,$$ (2.24)

where f is the effective force,

dt is the elementary small time interval of the effective force.

We shall divide the gas stream into a segment having the width dx (Fig. 25). The gas pressure on one side of the isolated layer is designated by p, and on the other side by p':

$$p' = p + dp;$$ (2.25)

The mass of the isolated segment is

$$dm = \frac{1}{g} S dx = \rho S dx,$$ (2.26)

where $\rho = \frac{1}{g}$ is the gas density in technical units of mass.

The force f, which acts on the segment whose mass is dm, is created by an increase of pressure dp:

$$f = S\,dp. \qquad (2.27)$$

For the time dt, the speed of the gas mass under consideration will change by quantity dw.

The fluctuation of momentum is equal to the impulse of the force:

$$\rho S\,dx\,dw = -S\,dp\,dt. \qquad (2.28)$$

The differentials dw and dp have different signs, since an increase of velocity normal to the sides of the segment decreases the pressure. Consequently,

$$\rho \frac{d\dot{w}}{dt} = -\frac{dp}{dx}. \qquad (2.29)$$
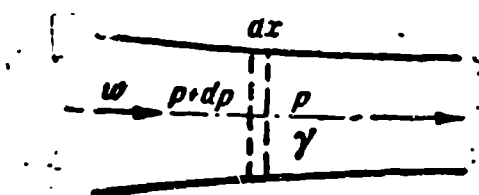
Fig. 25. Developing the equation of the conservation of impulse.

The product of density and the acceleration of a gas $\frac{dw}{dt}$ is equal to the negative pressure gradient $\frac{dp}{dx}$.

The equation (2.29) expressed as a law of the conservation of momentum for the stream of a gas is called Euler's equation for a one-dimensional flow.

During the acceleration of a flow of gas along a cylindrical pipe having the cross-section S, the law of the conservation of impulse may be written as

$$w_1\,dm - w_2\,dm = S(p_2 - p_1)dt, \qquad (2.30)$$

where w_1 and p_1 are the velocity and pressure of the flow at the beginning of the pipe; w_2 and p_2 are the velocity and pressure at the end of the pipe; dm is the mass of the gas which flows through a cross-section of the pipe for time dt.

Noting that $\frac{dm}{dt} = G$ kg/sec, we obtain

$$\frac{1}{g}(w_1 G - w_2 G) = S(p_2 - p_1). \qquad (2.31)$$

We substitute (2.4) in (2.3) and reduce it by S:

$$\frac{\gamma_1 w_1^2}{g} - \frac{w_2^2}{g} = p_2 - p_1.$$

(2.32)

The ratio (2.32) occurs, for example, during the flow of heated gases in a cylindrical combustion chamber of a jet engine or during a sudden variation of pressure in a normal shock wave.

The laws of flow continuity (2.4), conservation of energy (2.16), and conservation of impulse (2.29 or 2.32) are used to resolve problems which crop up in jet-engine research.

We notice that, according to Bernoulli's equation, the variation of pressure is proportional to $\frac{\gamma_w^2}{2g}$, and, according to the impulse equation, proportional to $\frac{\gamma w^2}{g}$. This apparent disparity may be clarified: the impulse equation in the form of (2.32) is only suitable for a cylindrical tube, when according to Bernoulli's equation for an incompressible fluid, the flow velocity is constant and the pressure variation $\Delta p = 0$. To omit consideration of S during a flow through a tube having a variable cross-section is not permitted, and the impulse equation in the form (2.32) is not correct. In the case of an incompressible liquid (γ = const) flowing along a pipe which has a variable cross-section between S_1 and S_2, Bernoulli's equation will be obtained during the integration of the impulse equation in the form (2.29).

Example: The speed of a gas heated in a cylindrical combustion chamber increases from 80 to 320 m/sec. Find the drop in pressure if the starting density of the gas γ_1 = 2 kg/m^3.

To find the variation of the gas density according to the law of continuity

$$\gamma_2 = \gamma_1 \frac{w_1}{w_2} \frac{S_1}{S_2} = \gamma_1 \frac{w_1}{w_2}.$$

According to the law of the conservation of impulse

$$p_1 - p_2 = \frac{\gamma_2 w_2^2}{g} - \frac{\gamma_1 w_1^2}{g} = \frac{\gamma_1 w_1 w_2}{g} - \frac{\gamma_1 w_1^2}{g} =$$

$$= \frac{\gamma_1 w_1^2}{g}\left(\frac{w_2}{w_1} - 1\right) = \frac{2 \cdot 80^2}{9.81}\left(\frac{320}{80} - 1\right) = 3920 \, \text{kg/m}^2 = 0.392 \, \text{kg/cm}^2.$$

Section 5. An Accelerated Flow

An accelerated flow occurs during the motion of a gas from an area of higher pressure to an area of lower pressure, for example, during discharge from containers, boilers, combustion chambers, etc. (Fig. 26).

The flow parameters in section S_1 are marked by w_1, p_1, T_1, and γ_1. The gas parameters in section S_2 are marked by w_2, p_2, T_2, and γ_2. Pressure is $p_1 > p_2$.

We find the increase of the kinetic energy of a gas by the law of conservation of energy for a gas stream:

$$\frac{Aw_2^2}{2g} - \frac{Aw_1^2}{2g} = i_1 - i_2 = c_{p_1}T_1 - c_{p_2}T_2.$$

The decrease in the enthalpy of a flowing gas is called the <u>heat</u> <u>drop</u> h.

If the heat capacity of a gas is constant through the entire possible range of temperature variation: c_p = const, then

$$h = i_1 - i_2 = c_p T_1 \left(1 - \frac{T_2}{T_1}\right) = \frac{Aw_2^2}{2g} - \frac{Aw_1^2}{2g}. \qquad (2.33)$$

If the flow is reversible, i.e., not accompanied by the dissipation of energy in the presence of friction or shock, then the lowering of the temperature $\frac{T_2}{T_1}$ may be expressed by the lowering of the temperature, taking advantage of Poisson's ratio for the reversible adiabatic expansion of gases:

$$\frac{p_2}{p_1} = \left(\frac{v_1}{v_2}\right)^k = \left(\frac{\gamma_2}{\gamma_1}\right)^k. \qquad (2.34)$$

where v is the specific volume of the gas: $v = \frac{1}{\gamma}$,

k is Poisson's index, equal to the ratio of specific heat during constant pressure c_p to the specific heat during constant volume c_v:

$$k = \frac{c_p}{c_v}. \qquad (2.35)$$

According to the equation of a gaseous state:

$$\frac{p_1 v_1}{p_2 v_2} = \frac{T_1}{T_2} \qquad (2.36)$$

Raising (2.34) to the degree of $\frac{1}{k}$ and multiplying by (2.36), we obtain

$$\frac{T_2}{T_1} = \left(\frac{p_2}{p_1}\right)^{\frac{k-1}{k}}. \qquad (2.37)$$

This last ratio is correct only for the reversible change of a gas. Substituting (2.37) in (2.33), we obtain

$$h := c_p T_1 \left[1 - \left(\frac{p_2}{p_1} \right)^{\frac{k-1}{k}} \right].$$

(2.38)
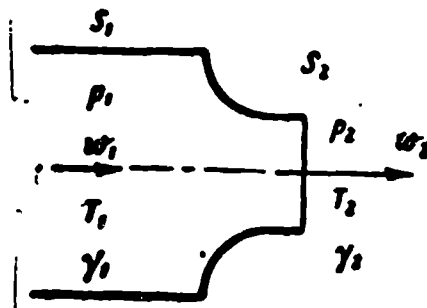
Fig. 26 An accelerated flow.

Heat content change, i.e., the enthalpy variation of 1 kg of gas, depends on the temperature T_1 and on the relative variation of pressure $\frac{p_1}{p_2}$, not on the absolute value of the pressure.

We find the speed of the gas in the S_2 section from the law of the conservation of energy for a gaseous flow (2.33):

$$w_2 = \sqrt{\frac{2g}{A} h + w_1^2}.$$

(2.39)

The decrease in the enthalpy of the gas, the initial rate of which is equal to zero ($w_1 = 0$), is designated by h_0. The temperature and pressure of a retarded flow of gas (the speed of which is equal to zero) are called the <u>stagnation temperature and pressure</u> T_{01} and p_{01}

$$h_0 = \frac{A w_2^2}{2g} = c_p T_{01} \left[1 - \left(\frac{p_2}{p_{01}} \right)^{\frac{k-1}{k}} \right].$$

(2.40)

The velocity of the gas in section S_2 may be expressed by the original parameter of the gas by substituting (2.38) in (2.39)

$$w_2 = \sqrt{\frac{2g c_p}{A} T_1 \left[1 - \left(\frac{p_2}{p_1} \right)^{\frac{k-1}{k}} \right] + w_1^2}.$$

(2.41)

The terminal velocity of the gas may be expressed by the stagnation parameters:

$$w_2 = \sqrt{\frac{2g}{A} c_p T_{01} \left[1 - \left(\frac{p_2}{p_{01}} \right)^{\frac{k-1}{k}} \right]}.$$

(2.42)

Using equations (2.15) and (2.35), we express specific heat by the gas constant and Poisson's index k:

$$c_p = c_v + AR = \frac{AkR}{k-1}.$$

(2.43)

Substituting (2.43) in (2.42), we obtain

$$w_a = \sqrt{\frac{2gk}{k-1} R T_{01} \left[1 - \left(\frac{p_2}{p_{01}}\right)^{\frac{k-1}{k}}\right]}. \qquad (2.44)$$

The last formula is often used in computations of the discharge speeds of gases from jet engines.

With an infinitely large initial pressure ($p_1 \to \infty$), or with an infinitely small terminal pressure ($p_2 \to 0$), the speed of the discharge reaches the maximum possible value w_{max}:

$$w_{max} = \sqrt{\frac{2gk}{k-1} R T_{01}} = \sqrt{\frac{2g}{A} i_{01}}. \qquad (2.45)$$

Moreover, the temperature and enthalpy of the gases falls to zero:

$$T_a = T_1 \left(\frac{p_2}{p_1}\right)^{\frac{k-1}{k}} \to 0.$$

The energy of the chaotic movement of the molecules changes entirely to the energy of the organized motion of a gas flow. A maximum discharge speed is unattainable in practice, because the pressure and temperature of the gases are always finite quantities.

The relationship of the increase in kinetic energy of gas to the enthalpy of deceleration is called the _efficiency_ of the _discharge_ process η_t:

$$\eta_t = \frac{A w_2^2}{2 g i_{01}} = \frac{i_{01} - i_2}{i_{01}} = 1 - \frac{T_2}{T_{01}}. \qquad (2.46)$$

During a reversible discharge

$$\eta_t = 1 - \left(\frac{p_2}{p_{01}}\right)^{\frac{k-1}{k}}. \qquad (2.47)$$

With an increase in the relative pressure drop during discharge, $\dfrac{p_{01}}{p_2}$, the thermal efficiency of the discharge process increases (Fig. 27). With an increase in the relative drop $\dfrac{p_{01}}{p_2}$ of one or more units, the thermal efficiency rapidly increases, but after exceeding $\dfrac{p_{01}}{p_2}$ by several tens of units, the rate of growth η_t is retarded, because η_t asymptotically approaches one. Therefore, it is impracticable to increase the relative pressure drop in order to achieve greater discharge speeds, up to 100 or more.

With the increase in the relative pressure drop $\dfrac{p_{01}}{p_2}$ the density of the dis-

charging gases γ_2 decreases:

$$\gamma_2 = \gamma_{01}\left(\frac{p_2}{p_{01}}\right)^{\frac{1}{k}} = \frac{p_{01}}{RT_{01}}\left(\frac{p_2}{p_{01}}\right)^{\frac{1}{k}}. \qquad (2.48)$$

The gas discharge through section S_2 is determined by the continuity equation (2.4) with consideration of (2.44) and (2.48).

$$G = w_2\gamma_2 S_2 = S_2 p_{01}\sqrt{\frac{2gk}{(k-1)RT_{01}}\left[\left(\frac{p_2}{p_{01}}\right)^{\frac{2}{k}} - \left(\frac{p_2}{p_{01}}\right)^{\frac{k+1}{k}}\right]}. \qquad (2.49)$$
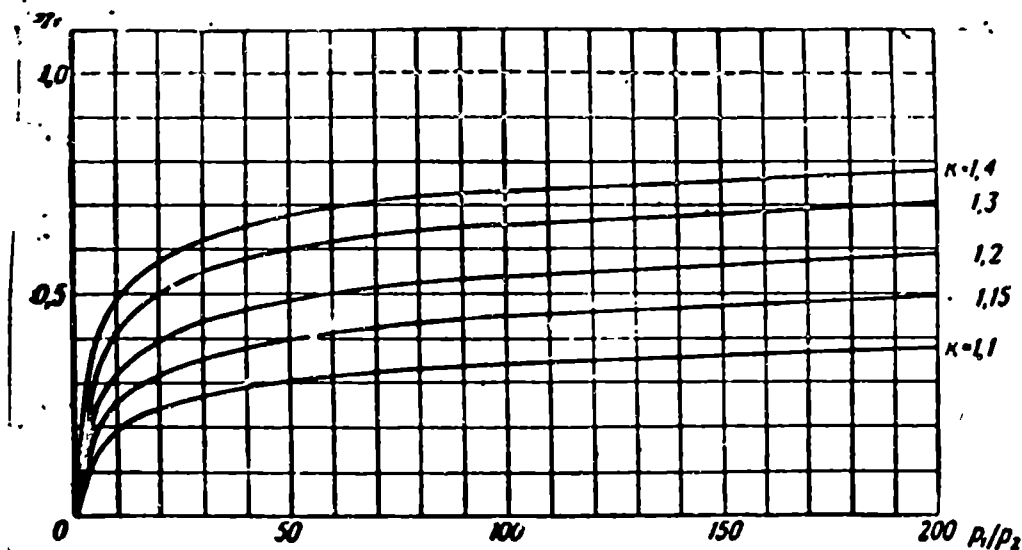
Fig. 27. The dependence of thermal efficiency on relative pressure drop.

The gas constant R is expressed in $\frac{kg\ m}{kg\ deg}$, w_2 in m/sec, T_{01} in degrees Kelvin, p_{01} in kg/m^2, and S_2 in m^2. Discharge is measured in kg/sec.

When the pressure before the discharge p_{01} increases, the gas density γ_2 mounts and the discharge G grows. With an increase in temperature T_{01}, the density γ_2 decreases and the velocity w_2 increases proportionally to $\sqrt{T_{01}}$. Therefore the discharge varies in inverse proportion to $\sqrt{T_{01}}$.

Example. The pressure and temperature of the air before the discharge: $p_{01} = 16\ kg/cm^2$; $T_{01} = 600°\ K$; $w_1 = 0$; $g = 9.8\ m/sec^2$; $k = 1.4$; $R = 29.3\ kg\ m/kg\ deg$. Find the velocity, density, temperature, and discharge of the gas for two cases: when the pressure at the outlet $p_2 = 10\ kg/cm^2$ and when $p_2 = 2\ kg/cm^2$.

a) The relative drop $\frac{p_{01}}{p_2} = \frac{16}{10} = 1.6$

The discharge velocity is in accordance with (2.44)

$$w_2 = \sqrt{\frac{19.6 \cdot 1.4 \cdot 29.3 \cdot 600}{(1.4-1)} \left[1 - \left(\frac{1}{1.6}\right)^{\frac{0.4}{1.4}} \right]} =$$

$$= 44.7 \sqrt{600 \cdot 0.306} = 604 \ \text{m/sec.}$$

Density

$$\gamma_2 = \frac{p_1}{RT_1} \left(\frac{p_2}{p_1}\right)^{\frac{1}{k}} = \frac{160\,000}{29.3 \cdot 600} \left(\frac{1}{1.6}\right)^{\frac{1}{1.4}} = \frac{9.1}{1.488} = 6.11 \ \text{kg/m}^3.$$

The discharge through a unit of a section

$$\frac{G}{S} = w_2 \gamma_2 = 604 \cdot 6.11 \approx 3700 \ \text{kg/sec-m}^2.$$

b) If the pressure were to be reduced to $p_2 = 2$, then the discharge velocity would increase

$$w_2 = 44.7 \sqrt{600 \left[1 - \left(\frac{2}{16}\right)^{\frac{0.4}{1.4}} \right]} = 44.7 \sqrt{600 \cdot 0.449} = 733 \ \text{m/sec.}$$

The density of the exhausted air would then decrease:

$$\gamma_2 = \frac{p_1}{RT_1} \left(\frac{p_2}{p_1}\right)^{\frac{1}{k}} = \frac{9.1}{8^{\frac{1}{1.4}}} = \frac{9.1}{4.42} = 2.06 \ \text{kg/m}^3.$$

The discharge per exhaust cross-section unit would not increase but decrease:

$$\frac{G}{S} = 733 \cdot 2.06 = 1510 \ \text{kg/sec.m}^2.$$

It is clear that with a decrease in back pressure, the discharge of gas cannot, in fact, decrease. The solution of this contradiction is set forth in paragraph "e."

Section 6. Critical Flow. Reduced Velocity

Let us consider a flow of gas from a reservoir, where—when $w_1 = 0$—the stagnation pressure is equal to p_{01}, into a container where the static pressure is equal to p_2 (Fig. 28). Let us assume the parameters of the gas before the discharge p_{01}, T_{01}, and γ_{01} remain constant and the back pressure p_2 decreases. (This may take place if the gas is evacuated from the receiving container):

If $p_2 = p_{01}$, the discharge of the gas $G = 0$.

With a decrease in pressure p_2, the discharge first increases in accordance with equation (2.49). This discharge increase during large pressure drops depends on the

increase of the discharge velocity w_2 (2.44). The change in density of the gases during minor pressure drops is insignificant.

If the pressure of a discharging flow were to decrease lower than a certain limit, the decrease in the density would seem to be greater than the increase in velocity and the discharge of the gases $G = w_2 \gamma_2 S_2$ would begin to decrease. In fact, with a decrease in back pressure, the discharge of the gases cannot diminish; a certain maximum pressure is established in a discharging flow.
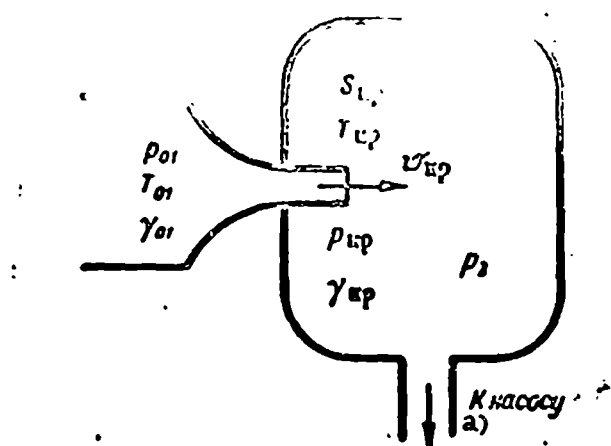
Fig. 28. Solving the formula of a critical discharge.
Legend: a) to the pump.

The pressure in a flow in which the discharge of the gases turns out to be the greatest is called the <u>critical pressure</u> p_{cr}.

We identify the relative pressure of the discharging gases by x:

$$x = \frac{p_2}{p_{01}}.$$

We find the relative pressure drop x_{cr}, at which the discharge of the gases will be maximum, by equating to zero the first derivative from the radicand of the expression in the discharge formula by x.

$$\frac{d}{dx}\left[\frac{2gk}{(k-1)RT}\left(x^{\frac{2}{k}} - x^{\frac{k+1}{k}}\right)\right] = 0.$$

Differentiating, we obtain

$$\frac{2}{k}x_{\kappa p}^{\frac{2}{k}-1} - \frac{k+1}{k}x_{\kappa p}^{\frac{1}{k}-1} = 0.$$

From this

(2.50)

$$x_{\kappa p} = \frac{p_{\kappa p}}{p_{01}} = \left(\frac{2}{k+1}\right)^{\frac{k}{k-1}}.$$

The pressure of the gases in the discharging flow cannot be lowered more than $\left(\dfrac{k+1}{2}\right)^{\frac{k}{k-1}}$ times.

The lower the Poisson's index k, the lower the critical pressure drop (see Table 2.1). Thus, when k = 1.4

$$\frac{p_{01}}{p_{\text{кр}}} = \left(\frac{1,4+1}{2}\right)^{\frac{1,4}{0,4}} = 1,89;$$

when k = 1.2

$$\frac{p_{01}}{p_{\text{кр}}} = \left(\frac{1,2+1}{2}\right)^{\frac{1,2}{0,2}} = 1,77.$$

Critical temperature drop:

$$\frac{T_{01}}{T_{\text{кр}}} = \left(\frac{p_{01}}{p_{\text{кр}}}\right)^{\frac{k-1}{k}} = \frac{k+1}{2}. \tag{2.51}$$

Critical density drop:

$$\frac{\gamma_{01}}{\gamma_{\text{кр}}} = \left(\frac{p_{01}}{p_{\text{кр}}}\right)^{\frac{1}{k}} = \left(\frac{k+1}{2}\right)^{\frac{1}{k-1}}. \tag{2.52}$$

If the back pressure is less than the critical pressure: $p_2 < p_{cr}$, then the pressure in the flow will be equal to the critical value of p_{cr}.

The discharge of the gases will have a maximum value. Substituting (2.50) in (2.49) we obtain

$$G_{\text{кр}} = p_{01} S_{\text{кр}} \sqrt{\frac{2gk}{(k-1)RT_{01}}\left[\left(\frac{2}{k+1}\right)^{\frac{2}{k-1}} - \left(\frac{2}{k+1}\right)^{\frac{k+1}{k-1}}\right]},$$

but

$$\frac{2}{k-1}\left[\left(\frac{2}{k+1}\right)^{\frac{2}{k-1}} - \left(\frac{2}{k+1}\right)^{\frac{k+1}{k-1}}\right] = \frac{2}{k-1}\left(\frac{2}{k+1}\right)^{\frac{2}{k-1}}\left[1 - \frac{2}{k+1}\right] = \left(\frac{2}{k+1}\right)^{\frac{k+1}{k-1}};$$

Consequently,

$$G_{\text{кр}} = \sqrt{\frac{gk}{R}\left(\frac{2}{k+1}\right)^{\frac{k+1}{k-1}}} \frac{p_{01} S_{\text{кр}}}{\sqrt{T_{01}}} = B\frac{p_{01} S_{\text{кр}}}{\sqrt{T_{01}}}. \tag{2.53}$$

The coefficient B depends on the index k (see Table 2.1 in which it is calculated for R = 29.5 kg m/kg deg C).

The velocity in the critical section S_{cr} is in accordance with (2.44) and (2.51):

$$w_{\text{кр}} = \sqrt{\frac{2gkRT_{01}}{k-1}\left(1 - \frac{2}{k+1}\right)},$$

$$w_{\text{кр}} = \sqrt{\frac{2gkRT_{01}}{k+1}} = \sqrt{gkRT_{\text{кр}}} = a,$$

(2.54)

since

$$\frac{2}{k+1} T_{01} = T_{\text{кр}}.$$

The equation $\sqrt{gkRT_{\text{кр}}} = a$ represents the speed of sound at temperature T_{cr}.

The critical velocity of the discharge is equal to the speed of the local speed of sound.

During the decrease of back pressure p_2 the velocity of the discharge increases until it is not equal to the local speed of sound.

The changes of pressure widen in a gas at the speed of sound. If the velocity of the discharge reaches a sonic value, then the subsequent variations of back pressure, whose impulses travel upstream against the flow with the speed of sound, do not reach the internal area of the reservoir, and the discharge of the gas ceases to depend on the subsequent pressure drops. If the pressure before the discharge is larger than critical: $\dfrac{p_{01}}{p_2} > \left(\dfrac{k+1}{2}\right)^{\frac{k}{k-1}}$, then the pressure in the flow p_{cr} proves to be greater than the back pressure p_2; $p_{\text{cr}} > p_2$. At the nozzle outlet the stream of gases suddenly expands. The expansion of the flow during a supercritical discharge is clearly seen, for example, as in the form of a smoke cloud formed during firing guns.

These supercritical phenomena are observed during the discharge of exhaust gases from the cylinders of a piston engine, during firing guns, during the discharge of gases from containers, and during the operation of jet engines, if the pressure exceeds that of the atmosphere more than 1.89 times.

If after the critical section S_{cr} the pipe widens, then the gas pressure will continue to fall, the density will decrease, and the velocity will increase and become greater than the local speed of sound (see Chapter V). The acceleration of a subsonic flow occurs in tapering pipes; that of a supersonic flow in widening pipes. The greater the ratio of the section under consideration to the one that is critical,

the greater the decrease in pressure $\dfrac{p}{p_{cr}}$ and the greater the relative increase in the velocity of the flow.

The ratio of the flow velocity w to the critical velocity a is called the relative velocity λ:

$$\lambda = \frac{w}{a} = \frac{w}{\sqrt{\dfrac{2gk}{k+1}RT_0}} .$$

(2.55)

Utilizing (2.44) and (2.55) we can express the relative velocity by the ratio of static pressure p to the stagnation pressure p_0:

$$\lambda = \sqrt{\frac{k+1}{k-1}\left[1 - \left(\frac{p}{p_0}\right)^{\frac{k-1}{k}}\right]} .$$

(2.56)

During the decrease in pressure to vacuum the velocity will attain the maximum possible value λ_{max}.

$$\lambda_{max} = \sqrt{\frac{k+1}{k-1}} .$$

(2.57)

The maximum possible value of the relative velocity depends only on Poisson's index (k). When k = 1.4, $\lambda_{max} \approx 2.45$. With a decrease in k, the maximum relative velocity increases. Listed in Table 2.1 are the functions of Poisson's index (k) which are encountered during gas dynamic computations.

TABLE 2.1

FUNCTIONS OF POISSON'S INDEX k

k	1,40	1,35	1,30	1,25	1,20	1,15	1,10
$\dfrac{k+1}{2}$	1,200	1,175	1,150	1,125	1,100	1,075	1,050
$\left(\dfrac{k+1}{2}\right)^{\frac{k}{k-1}}$	1,89	1,863	1,83	1,80	1,77	1,725	1,70
$\left(\dfrac{k+1}{2}\right)^{\frac{1}{k-1}}$	1,575	1,585	1,592	1,600	1,610	1,615	1,62
$\dfrac{k}{k-1}$	3,50	3,86	4,33	5,00	6,00	7,67	11,0
$\dfrac{k+1}{k-1}$	6,00	6,72	7,67	9,00	11,00	14,35	21,0
$\sqrt{\dfrac{k+1}{k-1}}$	2,45	2,59	2,767	3,00	3,31	3,79	4,58
$\sqrt{gk\left(\dfrac{2}{k+1}\right)^{\frac{k+1}{k-1}}}$	2,14	2,11	2,08	2,06	2,03	2,00	1,98
$B\ (R=29,5)$	0,394	0,389	0,383	0,379	0,374	0,368	0,364
$\sqrt{\dfrac{2g}{R}\dfrac{k}{k+1}}$	0,623	0,617	0,613	0,609	0,603	0,598	0,59

Example: The pressure in a jet-engine combustion chamber is $p_0 = 5$ absolute atmospheres (ata), the temperature T_0 is 2,200° K. Find the critical pressure, temperature, velocity, and discharge through a unit of a section, if k = 1.25 and the gas constant is

$$R = 30 \text{ kgm/kg deg.}$$

The critical pressure

$$p_{\text{кр}} = \left(\frac{2}{k+1}\right)^{\frac{k}{k-1}} p_0 = \frac{5}{1.8} = 2.78 \text{ ata.}$$

The critical temperature

$$T_{\text{кр}} = \frac{2}{k+1} T_0 = \frac{2200}{1.125} = 1960° \text{ K.}$$

The critical velocity

$$a = \sqrt{gkRT_{\text{кр}}} = \sqrt{9.81 \cdot 1.25 \cdot 30 \cdot 1960} = 846 \text{ m/sec.}$$

The critical density

$$\gamma_{\text{к}} = \left(\frac{2}{k+1}\right)^{\frac{1}{k-1}} \gamma_0 = \left(\frac{2}{k+1}\right)^{\frac{1}{k-1}} \frac{p_0}{RT_0} = \frac{5 \cdot 10^4}{1.6 \cdot 30 \cdot 2200} = 0.473 \text{ kg/m}^3.$$

The discharge per unit of a critical section

$$\frac{G}{S_{\text{кр}}} = B \frac{p_0}{\sqrt{T_0}} \approx \frac{0.376 \cdot 5 \cdot 10^4}{\sqrt{2200}} = 400 \text{ kg/sec.m}^2.$$

The discharge may also be determined by the continuity equation

$$\frac{G}{S_{\text{кр}}} = a\gamma_{\text{кр}} = 846 \cdot 0.473 = 400 \text{ kg/sec.m}^2.$$

Section 7. Adiabatic Flow with Deceleration. Mach Numbers. Gas Dynamic Functions

The velocity of the air entering the diffuser of an air-breathing reaction engine is diminished. We shall investigate how to compute the change in the parameters of an air flow during a decelerated adiabatic flow (Fig. 29).

The parameters of the flow in section S_1 are identified by p_1, T_1, γ_1, and w_1; the parameters in section S_2 are identified by p_2, T_2, γ_2, and w_2.

Decrease of velocity occurs under the action of a force opposing the motion. Therefore the gas will move slowly only in the event that the pressure in the stream increases: $p_2 > p_1$.

According to the law of the conservation of energy, the decrease in velocity is accompanied by an increase in enthalpy and in the temperature of the gas:
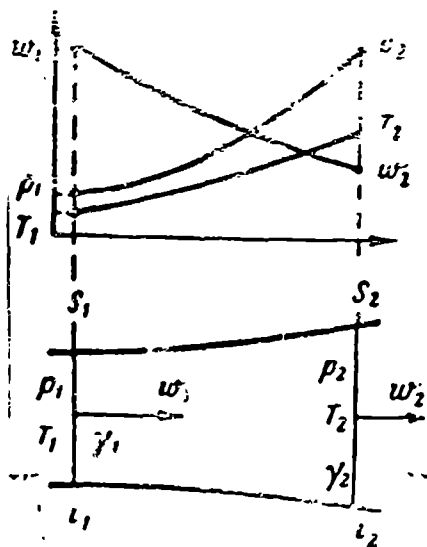
Fig. 29. A flow with deceleration.

$$i_2 - i_1 = c_{p_2} T_2 - c_{p_1} T_1 = \frac{A w_1^2}{2g} - \frac{A w_2^2}{2g} \qquad (2.58)$$

Assuming that the specific heat of the gas c_p is constant in the entire range of temperature

$$\frac{T_2}{T_1} = 1 + \frac{A(w_1^2 - w_2^2)}{2g c_p T_1} = 1 + \frac{w_1^2 - w_2^2}{2g \frac{kR}{k-1} T_1} . \qquad (2.59)$$

When the gas is completely decelerated; $w_2 = 0$, its temperature increases to the stagnation temperature:

$$\frac{T_{02}}{T_1} = 1 + \frac{k-1}{2} \frac{w_1^2}{gkRT_1} . \qquad (2.60)$$

When $k = 1.4$ and $R = 29.3$ kg m/kg deg

$$\Delta T = T_{02} - T_1 = \frac{k-1}{2} \frac{w_1^2}{gkR} \approx \frac{w_1^2}{2000} . \qquad (2.61)$$

Equations (2.59-2.61) correctly express the increase in flow temperature only in the event that its initial velocity is not too high. When $w_1 > 1,5000$ m/sec, the stagnation temperature becomes so great that to disregard the variations of specific heat appears to be impossible, and the equations obtained with the assumption that $c_{p1} = c_{p2}$ become incorrect (see Chapter VI, Section 6).

The product $gkRT_1$, which enters formula (2.59), represents the square of the speed of sound at temperature T_1

$$c = \sqrt{gkRT_1}. \qquad (2.62)$$

The ratio of the velocity of the stream w to the local speed of sound c, is

called the _Mach_ _number_ and is denoted by the symbol M:

$$M = \frac{w}{c} = \frac{w}{\sqrt{gkRT}}.$$ (2.63)

The increase in temperature during deceleration, as indicated in the equation (2.60), is proportional to the square of the Mach number:

$$\frac{T_0}{T} = 1 + \frac{k-1}{2}M^2.$$ (2.64)

If there is an adiabatic reversible flow process, e.g., is not accompanied by a dissipation of energy, the increase in pressure during deceleration may be found according to the increase in temperature, using Poisson's equation (2.37):

$$\frac{p_0}{p} = \left(\frac{T_0}{T}\right)^{\frac{k}{k-1}} = \left(1 + \frac{k-1}{2}M^2\right)^{\frac{k}{k-1}}.$$ (2.65)

The last equation expresses the increase in pressure during the reversible process of a compressible fluid. Expanding the equation (2.65) in series and limiting the first two terms of the expansion, it is possible to bring it to Bernoulli's equation (2.20), which is correct for the deceleration of an incompressible fluid:

$$\left(\frac{p_0}{p}\right)_{acc.} = \left(1 + \frac{k-1}{2}M^2\right)^{\frac{k}{k-1}} = 1 + \frac{k}{2}M^2 = 1 + \frac{w^2}{2gRT} = 1 + \frac{\gamma w^2}{2gp}.$$

When the initial flow velocity is given, the increase in pressure during deceleration of a compressible fluid has a greater value than that of an incompressible fluid (Table 2.2).

TABLE 2.2

DECELERATION PARAMETERS FOR REVERSIBLE FLOW k = 1.4

M	0,5	1,0	2,0	3,0	4,0	5,0
$\frac{T_0}{T}$	1,05	1,2	1,8	2,8	4,2	6,0
$\frac{p_0}{p}$	1,19	1,89	7,8	37	150	528
$\left(\frac{p_0}{p_{acc.}}\right)$	1,175	1,70	3,8	7,3	12,2	18,5
$\frac{\gamma_0}{\gamma}$	1,13	1,575	4,31	13,2	36	88

During M > 1 deceleration of the flow occurs in a tapering pipe, because the relative density increase $\frac{\gamma_2}{\gamma_1}$ is more significant than the relative decrease in velocity $\frac{w_2}{w_1}$.

$$\frac{S}{S_1} = \frac{w_1}{w_2} \frac{T_1}{T_2} < 1.$$ (2.66)

In the narrowest section, the velocity of the flow is equal to the critical value, e.g., the local speed of sound (Fig. 30).

$$w_{\text{кр}} = a = \sqrt{\frac{2gkR}{k+1}T_0} = \sqrt{\frac{2gkR}{k+1}T\left(1+\frac{k-1}{2}M^2\right)}.$$ (2.67)

The critical velocity resulting from the last equation grows with an increase in the initial Mach number.

If the pressure at a critical section (throat) continues to increase: $p_2 > p_c$, then the flow will be accompanied by a subsequent deceleration and increase in static pressure. If the pressure p_2 is less than that in the critical section: $p_2 < p_{cr}$, then the flow will be accompanied by an increase in velocity and the temperature and static pressure will fall.
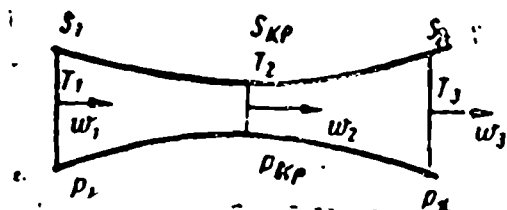
Fig. 30. Illustrating the concept of reversibility of flow.

During adiabatic flow the stagnation temperature along the entire pipe is constant:

$$c_p T_0 = i_1 + \frac{Aw_1^2}{2g} = i_2 + \frac{Aw_2^2}{2g} = \text{const};$$

$$T_0 = T_1\left(1+\frac{k-1}{2}M_1^2\right) = T_2\left(1+\frac{k-1}{2}M_2^2\right).$$

During a reversible flow process, the stagnation pressure along the entire pipe is also constant:

$$p_0 = p_1\left(1+\frac{k-1}{2}M_1^2\right)^{\frac{k}{k-1}} = p_2\left(1+\frac{k-1}{2}M_2^2\right)^{\frac{k}{k-1}}.$$

If the static pressures in the sections S_1 and S_2 are equal: $p_1 = p_2$, then during a reversible flow process, the velocities in the sections S_1 and S_2 are equal: $w_1 = w_2$.

In the presence of friction and shocks, the velocity after the diffusion of the flow up to the initial static pressure $p_2 = p_1$ will be less than the initial velocity:

$w_2 < w_1$; the kinetic energy of the gas will dissipate. The ratio of the decrease of the kinetic energy to its original value serves as a measure of the irreversibility of process. During irreversible flow the entropy of the gas increases.

The greater the static temperature in a given section of pipe T_i and the local speed of sound $c_i = \sqrt{gkRT_i}$, the less the local value of the velocity w_i, if the initial velocity is constant: w_1 = const. Therefore, in order to find the local value of the Mach number, M_i one must first find the local temperature T_i. The stagnation temperature is constant for the entire flow: T_0 = const; consequently the critical velocity is also constant for all sections. Therefore, in some cases it is more convenient to use the relative velocity λ than the Mach number M.

The relative velocity and the Mach number are uniquely related to each other. Utilizing (2.62 and 2.67) we obtain

$$\lambda = \frac{w}{a} = \frac{Mc}{a} = \frac{M\sqrt{gkRT}}{\sqrt{2\dfrac{gk}{k+1}RT\left(1+\dfrac{k-1}{2}M^2\right)}}.$$

From this

$$\lambda = \sqrt{\frac{k+1}{k-1+\dfrac{2}{M^2}}} = \sqrt{\frac{k+1}{k-1}\left[1-\left(\frac{p}{p_0}\right)^{\frac{k-1}{k}}\right]}, \tag{2.68}$$

or

$$M = \lambda\sqrt{\frac{2}{k+1-(k-1)\lambda^2}}. \tag{2.69}$$

When M = 1, λ = 1. When $M \to \infty$ $\lambda \to \lambda_{max} = \sqrt{\dfrac{k+1}{k-1}}$.

The dependence of the relative velocity on the Mach number for various values of Poisson index k is shown in Fig. 31.

The velocity head q may be expressed by the Mach number or by the relative velocity and atmospheric pressure P_n :

$$q = \frac{\gamma_n w_n^2}{2g} = \frac{p_n w_n^2}{2gRT_n}.$$

Using (2.63) or (2.55) we obtain:

$$q = \frac{k}{2}p_n M_n^2 = \frac{k}{k+1}\frac{\lambda_n^2}{1-\dfrac{k-1}{k+1}\lambda_n^2}p_n. \tag{2.70}$$
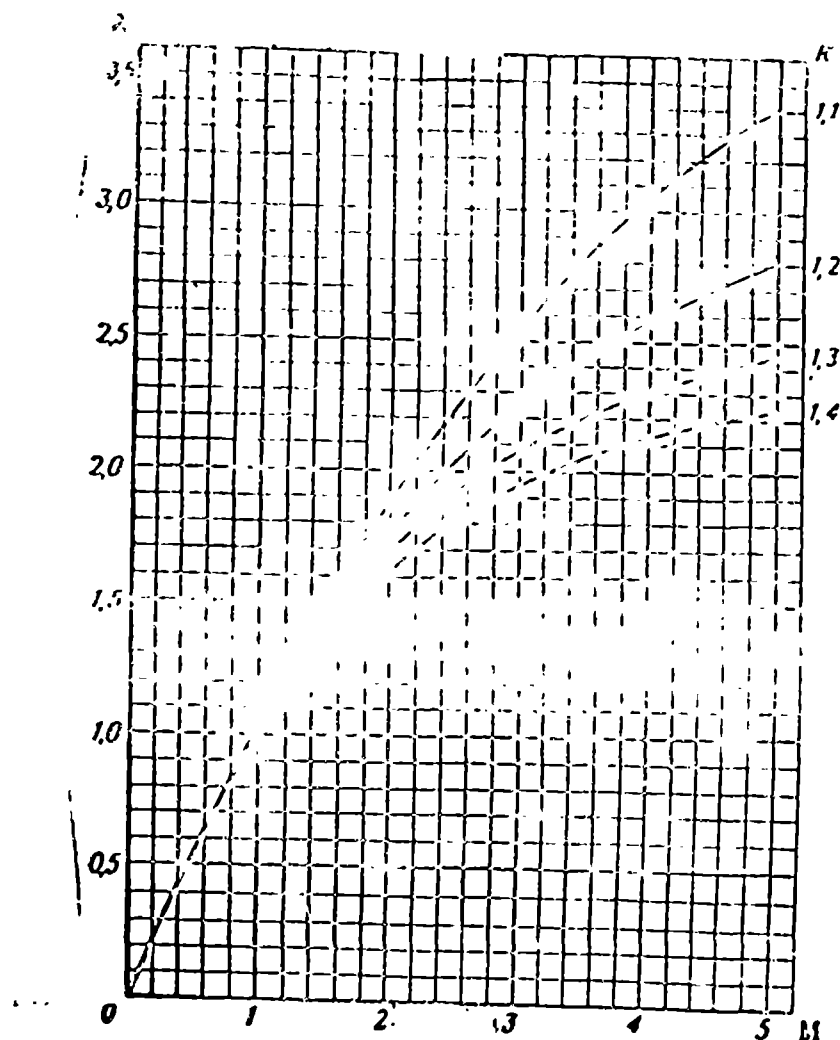
Fig. 31. The Dependence of λ on M for various K.

In making use of the basic flow equation, it ... to ... (... ? tion parameters in terms of relative velocity.

$$c_p T_0 - c_p T = \frac{A w^2}{2g}.$$

From this

$$\frac{T}{T_0} = 1 - \frac{A w^2}{2g c_p T_0} = 1 - \frac{w^2}{\frac{2gkR}{k-1} T_0} = 1 - \frac{k-1}{k+1} \lambda^2$$

The relative variations of temperature, pressure, and density during a decelerating reversible flow process are dependent only on the relative velocity of the advancing flow and the k index, and are called gas dynamic functions.

$$\tau(\lambda) = \frac{T}{T_0} = 1 - \frac{k-1}{k+1} \lambda^2, \qquad (2.71)$$

$$\pi(\lambda) = \frac{p}{p_0} = \left(\frac{T}{T_0}\right)^{\frac{k}{k-1}} = [\tau(\lambda)]^{\frac{k}{k-1}}, \qquad (2.72)$$

$$\varepsilon(\lambda) = \frac{\gamma}{\gamma_0} = \left(\frac{p}{p_0}\right)^{\frac{1}{k}} = [\tau(\lambda)]^{\frac{1}{k-1}}. \qquad (2.73)$$

The discharge of gases through section S, in which the relative velocity is equal to λ, may also be expressed by gas dynamic functions:

$$G = \gamma S w = \frac{p}{RT} S a \lambda = \sqrt{\frac{2gk}{(k+1)RT_0}} S p_0 \lambda \varepsilon(\lambda) =$$

$$= \sqrt{\frac{2gk}{(k+1)RT_0}} S p_0 q(\lambda). \tag{2.74}$$

Here

$$q(\lambda) = \lambda \varepsilon(\lambda) = \lambda \left(1 - \frac{k-1}{k+1} \lambda^2\right)^{\frac{1}{k-1}}. \tag{2.75}$$

When $\lambda > 2.3$, and $T_0 > 2,500°K$ a significant dissociation of the gases occurs; the k index may not be considered as constant, and the formulas of gas dynamic functions cease to be accurate.

Graphs of gas dynamic functions at various values of k are included at the end of the book (Fig. 204-208).

Section 6. The Reaction of a Flow on the Side of a Pipe. Jet Thrust and Additional Drag

The air-gas flow in any ramjet engine flows through a tube of variable cross-section area (Fig. 32). The amount of flow of a gas per second through the section S is equal to

$$\frac{Gw}{g} = \frac{S\gamma w^2}{g}.$$

This amount of movement, or impulse per second (impulse for short), is equal to the force with which the gas will act on the tube from deceleration to a complete stop.

If the flow's static pressure in section S is equal to p, then the pressure force which acts parallel to the flow upon the section in question is equal to pS. The total impulse of the gas flowing through section S is equal to the sum of

$$F = \frac{Gw}{g} + pS. \tag{2.76}$$

If the flow did not exist, then the force of the atmospheric pressure $p_n S$ would act on the section in question.

The difference between the deceleration force of the flow F and the force of the atmospheric pressure $p_n S$ is called the excess impulse F_{izb}:

$$F_{из6} = \frac{Gw}{g} + S(p - p_{н}).$$

(2.77)
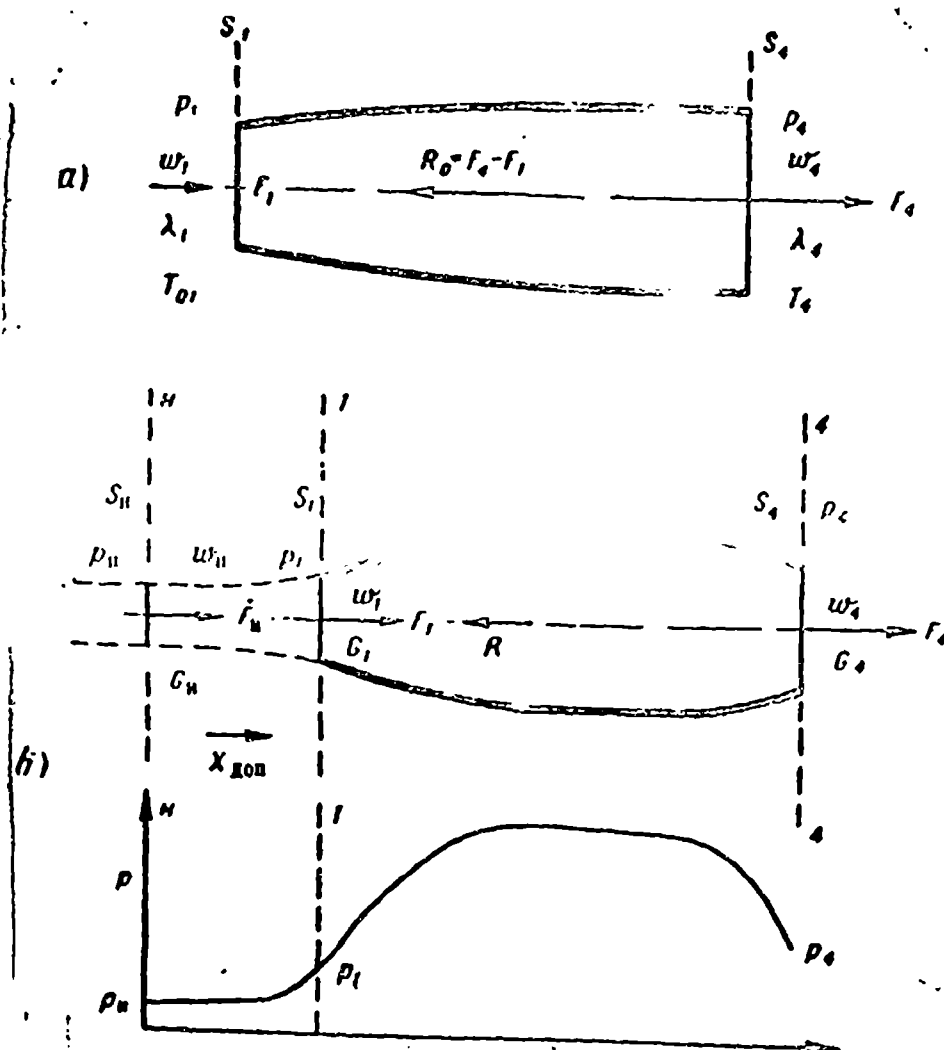
Fig. 32. Graphs for flow reaction calculation.

The gas impulse varies if the flow takes place in a pipe of variable cross-section, and also in the event of increase of dissipation of energy. The variation of the impulse is equal to the force with which the sides of the pipe act on the gas. According to Newton's third law, a flow acts on the sides of a pipe with a force equal in value, but opposite in direction, to the force of the reaction R_0.

The reaction of the flow on the sides of a tube between sections S_1 and S_4 is equal to the differences of the impulses:

$$R_0 = F_4 - F_1 = \left(\frac{Gw}{g} + pS\right)_4 - \left(\frac{Gw}{g} + pS\right)_1.$$

(2.78)

The reaction of the flow, as B.M. Kiselev first indicated, may be expressed by the relative velocities λ_1 and λ_4.

The total impulse of a flow in any section of a tube is equal to

$$F = \frac{Gw}{g} + pS = \frac{G}{g}\left(w + \frac{gp}{\gamma w}\right).$$

(2.79)

Utilizing the equations of composition and ratio (2.71) and (2.54), we obtain

$$\frac{p}{\gamma} = RT = RT_0\left(1 - \frac{k-1}{k+1}\lambda^2\right) = \frac{k+1}{2gk}a^2\left(1 - \frac{k-1}{k+1}\lambda^2\right).$$

(2.80)

Consequently,

$$F = \frac{G}{g}\left[w + \frac{k+1}{2k}\frac{a^2}{w}\left(1 - \frac{k-1}{k+1}\lambda^2\right)\right],$$

whence, using (2.55), we obtain

$$F = \frac{k+1}{2k}\frac{Ga}{g}\left(\lambda + \frac{1}{\lambda}\right).$$

(2.81)

The reaction of the flow is

$$R_0 = F_4 - F_1.$$

(2.82)

Using the ratio (2.81) we express the reaction of the flow on the sides of the tube by λ:

$$R_0 = \left[\frac{k+1}{2gk}aG\left(\lambda + \frac{1}{\lambda}\right)\right]_4 - \left[\frac{k+1}{2gk}aG\left(\lambda + \frac{1}{\lambda}\right)\right]_1.$$

(2.83)

The last equation was developed by B.M. Kiselev.

The temperatures of the flow and the masses of the gas in sections 1 and 4, generally speaking, are different. Therefore, the stream parameters, a, λ, G, and k in the various sections are not the same. The indexes "1" and "4" refer to all the parameters of the gas which depend on the temperature.

Relative velocities at the inlet of the duct and at the exhaust depend on the geometry of the duct.

In some cases the parameters at the inlet to the duct are equal to the parameters of an undisturbed flow. Then the index "1" in the second term of Kiselev's formula is replaced by "H."

The critical velocity, a, depends on the stagnation temperature. Substituting a for its value, we obtain

$$R_0 = \left[G\sqrt{\frac{k+1}{2gk}RT_0}\left(\lambda + \frac{1}{\lambda}\right)\right]_4 - \left[G\sqrt{\frac{k+1}{2gk}RT_0}\left(\lambda + \frac{1}{\lambda}\right)\right]_1.$$

(2.84)

Let us compare the differences of the right and left portions.

$$[R_0] = \left[\frac{kg}{sec}\sqrt{\frac{kg\,m\,deg\,sec^2}{kg\,deg\,m}}\right] = [kg].$$

The calculation of any jet engine is reduced to the calculation of the discharges, velocities, pressure, and stagnation temperature at the inlet and exhaust sections.

The impulse of gas, flowing at the speed of sound, i.e., during $\lambda = 1$, is called the critical impulse F_{cr}. On the basis of (2.81) it may be described as

$$F_{\kappa p} = \frac{k+1}{k} \frac{Ga}{g};$$
(2.85)

The ratio of the impulse during a flow of supersonic velocity $\lambda > 1$ to the critical impulse F_{cr} is called the coefficient of impulse increase c_λ. From (2.81) and (2.85) we find

$$c_\lambda = \frac{F}{F_{\kappa p}} = \frac{1}{2}\left(\lambda + \frac{1}{\lambda}\right) = \frac{z(\lambda)}{2};$$
(2.86)

The coefficient of impulse increase reaches its maximum possible value when

$$\left| \lambda = \lambda_{max} = \sqrt{\frac{k+1}{k-1}} \right.$$

$$c_{\lambda\,max} = \frac{k}{\sqrt{k^2-1}}.$$

Knowing the impulse of the flow, one may find the thrust of an air-breathing jet engine which operates on an internal stream of air (see Fig. 32,b).

Let us assume that the bounding surfaces pass in front of the engine at a distance at which its disturbing action is insignificant (surface H -H), and in the plane of the exhaust nozzle (surface 4 - 4). The section of the tube through which the air-flow penetrates into the engine we shall denote by S_n.

The impulse of the flowing air acting in the section S_n in conformance with (2.76) is equal to

$$F_n = \frac{G_n w_n}{g} + p_n S_n.$$
(2.87)

This impulse is parallel to and in the direction of the moving air.

The impulse of the exhausting gases in section S_4 is equal to

$$F_4 = \frac{G_4 w_4}{g} + p_4 S_4;$$
(2.88)

This impulse is also directed in the direction of the moving air.

The force of atmospheric pressure acts on the contour H-4-4-H.

The integral of the atmospheric pressure forces on a closed surface is equal to zero:

$$\oint_s p_{\text{н}} dS = 0.$$

The contour under our consideration has gaps in the inlet and exhaust areas of the tubes of flow, the sections of which are equal to S_n and $S_{\text{ц}}$. The integral of the force of atmospheric pressure on the external surface of the contour in question is equal to

$$\int_s p_{\text{н}} dS = p_{\text{н}} (S_{\text{ц}} - S_{\text{н}}).$$

(2.89)

The force of the atmospheric pressure acts in a direction from that side of the contour which has the lesser opening S_n, to that side which has the larger opening $S_{\text{ц}}$. This force is directed from S_n to $S_{\text{ц}}$, that is, with the air movement.

The growth of the total impulse of the flow together with allowance for the pressure forces is equal to the force of the reaction or the jet thrust R :

$$R = F_{\text{ц}} - F_{\text{н}} - \int_s p_{\text{н}} dS.$$

(2.90)

Using (2.87), (2.88), and (2.89) we obtain

$$R = \frac{G_{\text{ц}} w_{\text{ц}}}{g} + p_{\text{ц}} S_{\text{ц}} - \frac{G_{\text{н}} w_{\text{н}}}{g} - p_{\text{н}} S_{\text{н}} - p_{\text{н}} (S_{\text{ц}} - S_{\text{н}}).$$

After opening the parentheses and reducing the similar terms, the last formula becomes simplified:

$$R = \frac{G_{\text{ц}} w_{\text{ц}}}{g} - \frac{G_{\text{н}} w_{\text{н}}}{g} + S_{\text{ц}} (p_{\text{ц}} - p_{\text{н}}).$$

(2.91)

In the particular case, when the exhausting gases accelerate until the back pressure $p_{\text{ц}} = p_n$, the jet thrust is equal to:

$$R = \frac{G_{\text{ц}} w_{\text{ц}}}{g} - \frac{G_{\text{н}} w_{\text{н}}}{g}.$$

(2.92)

During the movement of air through a diffusing stream tube, its momentum between the sections S_n and S_1 diminishes. The loss of air impulse produces a rise in drag force X_{dop}. The force of additive drag which appears during deceleration of the air ahead of the inlet in an air-breathing jet engine, is equal to the difference between the surplus impulses at the inlet section $(F_1)_{izb}$ and in the undisturbed stream $(F_n)_{izb}$

$$X_{\text{доп}} = (F_1)_{\text{изб}} - (F_{\text{н}})_{\text{изб}} = \frac{G_1 w_1}{g} + S_1 (p_1 - p_{\text{н}}) - \frac{G_{\text{н}} w_{\text{н}}}{g}.$$

(2.93)

Utilizing the equations (2.76) and (2.77), one may change the surplus impulses

to total impulses:

$$X_{\text{доп}}=F_1-F_{\text{н}}'-p_{\text{н}}(S_1-S_{\text{н}}).$$ (2.94)

Additive drag is measured experimentally (see Chapter IV, Section 2).

The difference between jet thrust and additive drag is called the effective thrust R_{eff}:

$$R_{\text{эф}}=R-X_{\text{доп}}=F_4-F_{\text{н}}'-p_{\text{н}}(S_4-S_{\text{н}})-X_{\text{доп}}=$$
$$=F_4-F_1-p_{\text{н}}(S_4-S_1)=R_0-p_{\text{н}}(S_4-S_1).$$ (2.95)

The force of aerodynamic thrust X acts on the skin of an uncooled engine.

The difference between the effective thrust and the force of the aerodynamic drag on the skin is called the net thrust of an uncooled engine $R_{\text{чист}}$:

$$R_{\text{чист}}=R-X_{\text{доп}}-X.$$ (2.96)

Aerodynamic skin drag is determined by experimental wind-tunnel tests.

<u>Example</u>: Let us find the reaction on the walls of an engine duct when the speed v_n = 3,600 km/hr, if the cross section of the enclosed stream S_1 = 1 m^2, the flight altitude H = 20 km, the stagnation temperature before the discharge T_{03} = 2,400° K; during this temperature k = 1.25, the relative velocity at the exhaust is equal to 96% of the relative velocity at the inlet.

At the given altitude the temperature is equal to T_n = 216.5° K, the density γ_n = 0.088 kg/m^3, the pressure p_n = 41 mm merc.col. = 41 · 31.6 = 554 kg/m^2. The velocity w_n = 3,600 km/hr = 1,000 m/sec.

The stagnation temperature of the advancing flow

$$T_{0\text{н}}=T_{\text{н}}+\frac{w_{\text{н}}^2}{2000}=216,5+\frac{1000^2}{2000}=716,5° \text{K}.$$

The critical velocity

$$a=\sqrt{\frac{2gkRT_{0\text{н}}}{k+1}}=\sqrt{\frac{19,6\cdot 1,4\cdot 29,3}{2,4}716,5}=18,3\sqrt{716,5}=490 \text{ r/sec}.$$

The relative velocity at the inlet

$$\lambda_{\text{н}}=\frac{w_{\text{н}}}{a_{\text{кр}}}=\frac{1000}{490}=2,04.$$

The discharge of gases (disregarding additional fuel)

$$G_4=G_1=w_{\text{н}}\gamma_{\text{н}}S_1=1000\cdot 0,088\cdot 1=88 \text{ kg/sec}.$$

The relative velocity at the exhaust

$$\lambda_4=0,96\lambda_{\text{н}}=0,96\cdot 2,04=1,96.$$

The reaction on the sides of the engine duct we determine by the formula (2.84)

$$R_0 = 83 \left\{ \sqrt{\frac{2.25 \cdot 29.3}{19.6 \cdot 1.25} \, 2400 \left(1.95 + \frac{1}{1.95}\right)} - \sqrt{\frac{2.4 \cdot 29.3}{19.6 \cdot 1.4} \, 716.5 \times} \right.$$
$$\left. \times \left(2.04 + \frac{1}{2.04}\right) \right\} = 6080 \, kg.$$

Section 9. Compression Waves. Shock Waves

In practice, the deceleration of a supersonic flow is not reversible. If the velocity of the oncoming gas flowing around some or another body is greater than the speed of sound ($w_n > C$, $M > 1$), then, during the interaction of the flow with stream-lined body, the velocity does not change gradually, with a jump (Fig. 33 b). The pressure density, and temperature also increase as suddenly.

This sudden change of the parameters of a supersonic flow is called a compression wave. The size of the shock layer in which the change of the gas parameters occurs is not large; it has the length of a molecular free path.

The area of compressed air following behind the jump is called a shock wave. Even at transsonic speeds of a flow, the density difference of a shock wave in an undisturbed stream is large enough so that the surface of the wave can be registered in a shadow picture or by Schlieron photography (Fig. 34).

The reason for the origin of shock waves follows: The comparative velocity of a flow of gas in front of the nose of a body is small; the pressure of the flow increases. The gas approaching the nose of the body moves slowly. An impulse transmitted by the body to the advancing gas radiates along the top of the stream at the speed of sound. If the velocity of the motion is subsonic, the masses of the oncoming gas have time to obtain the "news" beforehand about the approaching body in the form of a pressure impulse, and the velocity of the gas begins to change in value and in direction. The stream lines of the flow warp, and the gas flows smoothly around the frontal surface of the body (Fig. 33a). If the approach velocity is greater than the speed of sound ($M > 1$), the pressure impulse, moving at the speed of sound, does not have time to reach the oncoming gas masses. Therefore, while meeting the frontal surface of the body, the gas decelerates suddenly, within the span
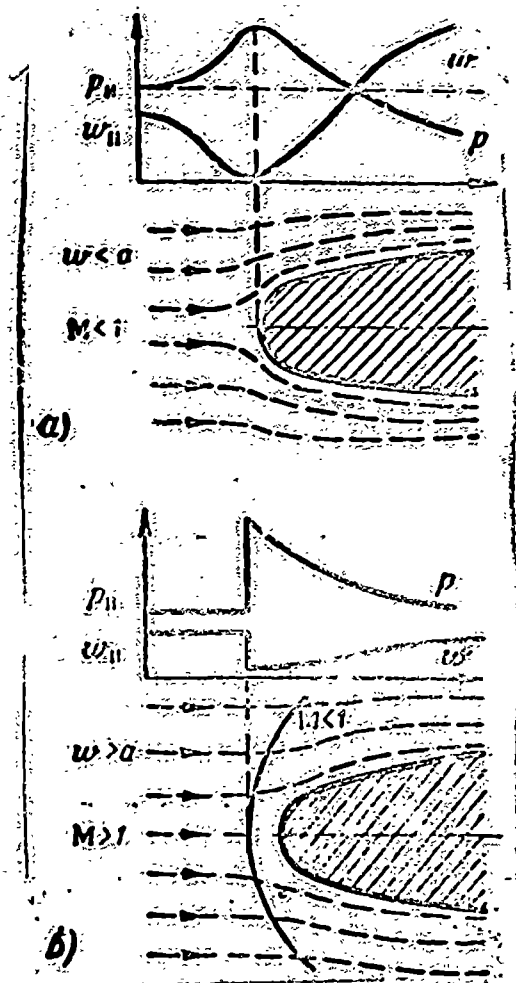
Fig. 33. Pressure variation in front of the nose of a body.
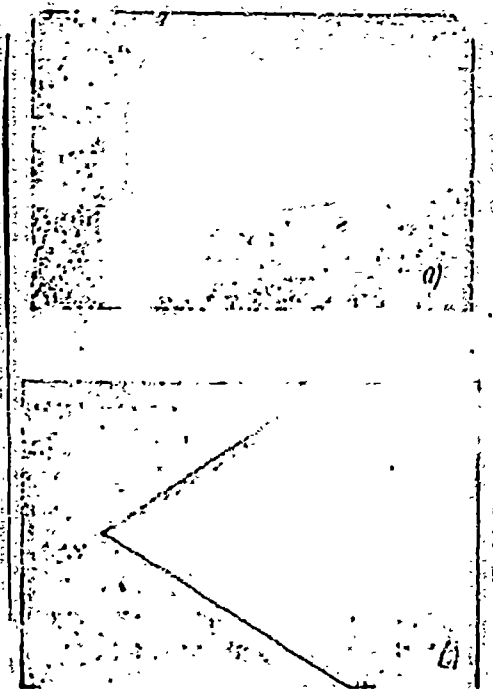
Fig. 34. Photographs of shock waves.
a -- normal shock, M = 1.5;
b -- oblique shock, M = 3.0

of the average molecular free path. At the same time, a surface of continuous disruption or a shock wave is formed. The velocity of the gas flow as a whole (macroscopic velocity) decreases, and the speed of the irregular thermal movement of molecules during passage through the area of the shock wave increases, owing to the collision of the molecules of the oncoming gas with the molecules of ~~~~~ ~~~~~~ ~~~~~~~ ~~~~~~~~~. Thus the energy of the flow is dissipated.

The variation of the gas parameters in a shock wave depends upon the Mach number of the oncoming flow and upon the form of the streamlined body (see Fig. 34). During the approach of a supersonic flow to the surface that is placed normal to the flow (Fig. 34a), a normal shock wave appears. During the approach to a surface, located at an angle to the flow, oblique shock waves appear (Fig. 34b).

The larger the Mach number of the advancing flow, the greater the relative variations of speed, temperature, and density, and the more intensive is the jump.

The deceleration of a gas in the jump, accompanied by the shock of the advancing

gas on the already decelerated gas and the dissipation of energy, is irreversible. Therefore, during the computation of pressure variation in a jump, Poisson's equation, which by right is only valid for a reversible process, cannot be used. The variation of the parameters of a gas in a jump is calculated by the equation of the continuity of flow and by the laws of the conservation of impulse and energy.

The more simple relationships have application in describing normal shock waves.

Section 10. A Normal Shock Wave.

The parameters of the air in front of a normal shock wave are denoted by index "H"; the parameters of the air behind the shock wave are denoted by index "1."

The impulses of the flow in front of the shock wave and behind it are equal to each other, because the reaction of a flow on the cylindrical walls of a tube of flow is equal to zero (Fig. 35).

$$F_{\mu} = F_1. \qquad (2.97)$$

Utilizing Kiselev's formula (2.81), we find the ratio between the relative velocity in front of the shock wave and behind it, noting that the stagnation temperatures and, consequently, the critical velocities in the shock wave do not vary $T_{0\text{H}} = T_{01}$; $a_{\text{H}} = a_1$ and the discharge of the air is constant $G_1 = G_{\text{H}}$:

$$\sqrt{\frac{k+1}{2k}} \frac{aG}{g} \left(\lambda_{\mu} + \frac{1}{\lambda_{\mu}} \right) = \frac{k+1}{2k} \frac{aG}{g} \left(\lambda_1 + \frac{1}{\lambda_1} \right).$$

Whence

$$\lambda_{\mu} + \frac{1}{\lambda_{\mu}} = \lambda_1 + \frac{1}{\lambda_1} \qquad (2.98)$$

or

$$(\lambda_1 - \lambda_{\mu})(\lambda_{\mu}\lambda_1 - 1) = 0. \qquad (2.99)$$

The last quadratic equation has two roots: $\lambda_1 = \lambda_{\mu}$; the flow occurs with a constant velocity, the shock wave is absent, and

$$\lambda_{\mu}\lambda_1 = 1, \quad \lambda_1 = \frac{1}{\lambda_{\mu}}. \qquad (2.100)$$

The greater the relative velocity of the advancing flow λ_{μ}, the less the relative velocity behind the shock wave λ_1. The shock wave appears only during a supersonic flow: $\lambda_{\mu} > 1$. Consequently, the flow behind a normal shock wave is

always subsonic: $\lambda_1 < 1.$

The absolute flow speed behind a normal shock wave

$$w_1 = a\lambda_1 = \frac{a}{\lambda_{\text{м}}} = \frac{a^2}{w_{\text{м}}} = \frac{2gkR}{k+1}\frac{T_{01}}{w_{\text{м}}} \tag{2.101}$$

With an increase in velocity, the stagnation temperature $T_{0\text{п}}$ grows. The temperature behind a normal shock wave T_1 is:

$$T_1 = T_0 \tau(\lambda_1) = T_{\text{м}}\frac{\tau(\lambda_1)}{\tau(\lambda_{\text{м}})} \tag{2.102}$$

$$\frac{T_1}{T_{\text{м}}} = \frac{1 - \dfrac{k-1}{k+1}\dfrac{1}{\lambda_{\text{м}}^2}}{1 - \dfrac{k-1}{k+1}\lambda_{\text{м}}^2}. \tag{2.103}$$
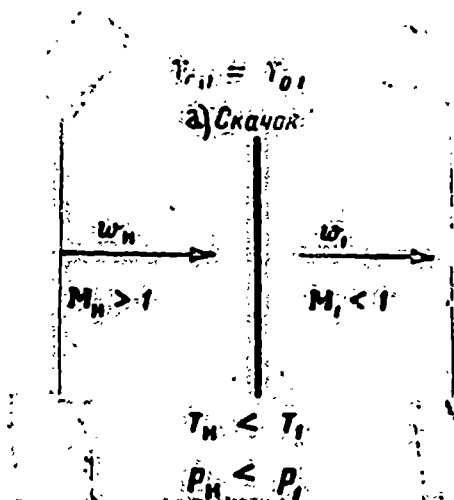
Fig. 35. Diagram of a normal shock wave.
Legend: a) shock wave

We find the stagnation pressure behind a normal shock wave by the discharge formula (2.74)

$$Q = Sp_{0\text{м}}\sqrt{\frac{2gk}{(k+1)RT_0}}\, q(\lambda_{\text{м}}) = Sp_{01}\sqrt{\frac{2gk}{(k+1)RT_0}}\, q(\lambda_1);$$

Whence

$$p_{01} = p_{\text{м}}\frac{q(\lambda_{\text{м}})}{q(\lambda_1)} = p_{\text{м}}\frac{\lambda_{\text{м}}\varepsilon(\lambda_{\text{м}})}{\pi(\lambda_{\text{м}})\lambda_1\varepsilon(\lambda_1)} = p_{\text{м}}\frac{\lambda_{\text{м}}^2\varepsilon(\lambda_{\text{м}})}{\pi(\lambda_{\text{м}})\varepsilon(\lambda_1)} = p_{\text{м}}\frac{\lambda_{\text{м}}^2}{\tau(\lambda_{\text{м}})\varepsilon(\lambda_1)};$$

and

$$\frac{p_{01}}{p_{\text{м}}} = \frac{\lambda_{\text{м}}^2}{\left(1 - \dfrac{k-1}{k+1}\lambda_{\text{м}}^2\right)\left(1 - \dfrac{k-1}{k+1}\dfrac{1}{\lambda_{\text{м}}^2}\right)^{\frac{1}{k-1}}}. \tag{2.104}$$

The last formula is called <u>Rayleigh's formula</u>.

The ratio of the stagnation pressure behind a normal shock wave to the stagna-

tion pressure of the advancing flow p_{0n} is called the recovery of pressure in a normal shock wave σ_{pr}.

$$\sigma_{np} = \frac{p_{01}}{p_{0n}} = \frac{q(\lambda_n)}{q(\lambda_1)} = \lambda_n^2 \left[\frac{1 - \frac{k-1}{k+1}\lambda_n^2}{1 - \frac{k-1}{k+1}\frac{1}{\lambda_n^2}} \right]^{\frac{1}{k-1}} \cdot \tag{2.105}$$

Static pressure behind a normal shock wave is

$$p_1 = p_{01}\pi(\lambda_1) = p_n \frac{\lambda_n^2 \varepsilon(\lambda_n)\pi(\lambda_1)}{\pi(\lambda_n)\varepsilon(\lambda_1)},$$

$$\frac{p_1}{p_n} = \lambda_n^2 \frac{\tau(\lambda_1)}{\tau(\lambda_n)} = \frac{\lambda_n^2 - \frac{k-1}{k+1}}{1 - \frac{k-1}{k+1}\lambda_n^2} \cdot \tag{2.106}$$

Substituting M_n in the place of λ_n, according to formula (2.70), we obtain, after some modifications

$$\frac{p_1}{p_n} = \frac{2k}{k+1}M_n^2 - \frac{k-1}{k+1} \cdot \tag{2.107}$$

We find the relative density increase in a normal shock wave from equation

$$\frac{\gamma_1}{\gamma_n} = \frac{Sw_n}{Sw_1} = \frac{a\lambda_n}{a\lambda_1} = \frac{\lambda_n}{\lambda_1} = \lambda_n^2. \tag{2.108}$$

When the maximum possible value of the relative velocity of an advancing flow is $(\lambda_n^2)_{max} = \frac{k+1}{k-1}$,

$$\left(\frac{\gamma_1}{\gamma_n}\right)_{max} = \frac{k+1}{k-1} \cdot \tag{2.109}$$

The density in a normal shock wave may be increased not more than $\frac{k+1}{k-1}$ times. When k = 1.4, the maximum possible density increase is equal to six.

The velocity in a normal shock wave may vary not more than $\frac{k-1}{k+1}$ times.

The parameters of the air behind a normal shock wave plotted as function of Mach number are shown in the graph of Fig. 36.

If the Pitot tube be placed in a supersonic flow, then a normal shock wave will appead in front of its inlet opening. The relative perssure increase in the tube will be expressed by Rayleigh's formula (2.104). The Mach number of the flow may be calculated from the pressure increase. A Pitot tube with a metallic manometer whose scale is graduated in Mach numbers is called a machmeter. Machmeters are installed in wind
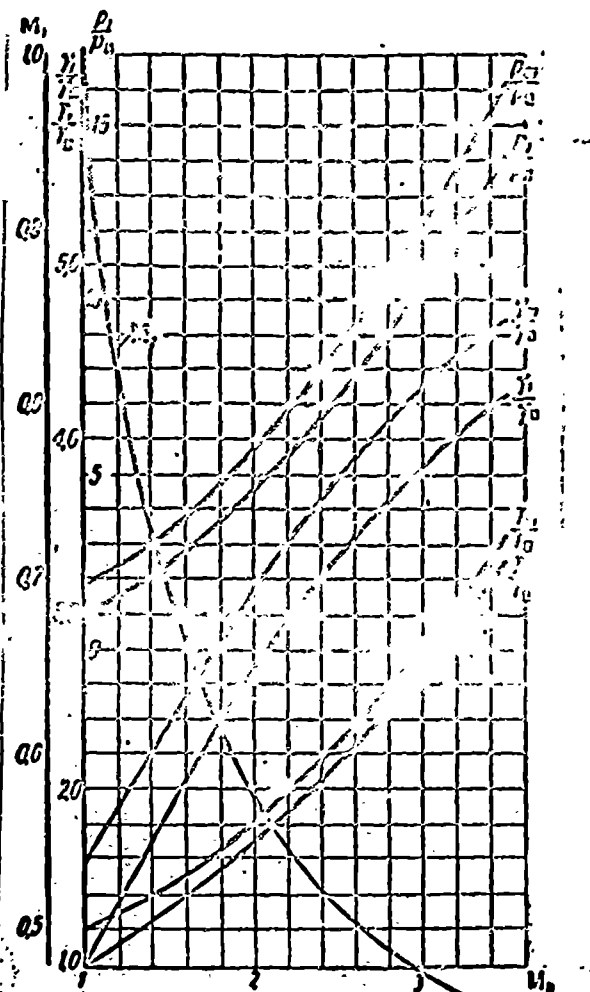
Fig. 36. The variation of air parameters in a normal shock wave.

tunnels and in aircraft.

The dissipation of energy has the greatest value in a normal shock wave. Therefore the deceleration of the air through a normal shock wave is the least advantageous. Energy losses are significantly less in oblique shock waves.

Section 11. Oblique Shock Waves

Oblique shock waves appear during the approach of a supersonic flow to wedges, cones, and other bodies that have a surface located at an angle to the direction of the velocity (see Fig. 34). A schematic of an oblique shock wave is represented in Fig. 37.

During the approach of a supersonic flow to an inclined plate or a wedge, a two dimensional oblique shock wave appears. During the air flow around the cone, the front of a shock wave has a cone-shaped surface.

We shall first consider two dimensional shock waves. We identify the angle between the surface of a wedge and the direction of an undisturbed flow -- the rake
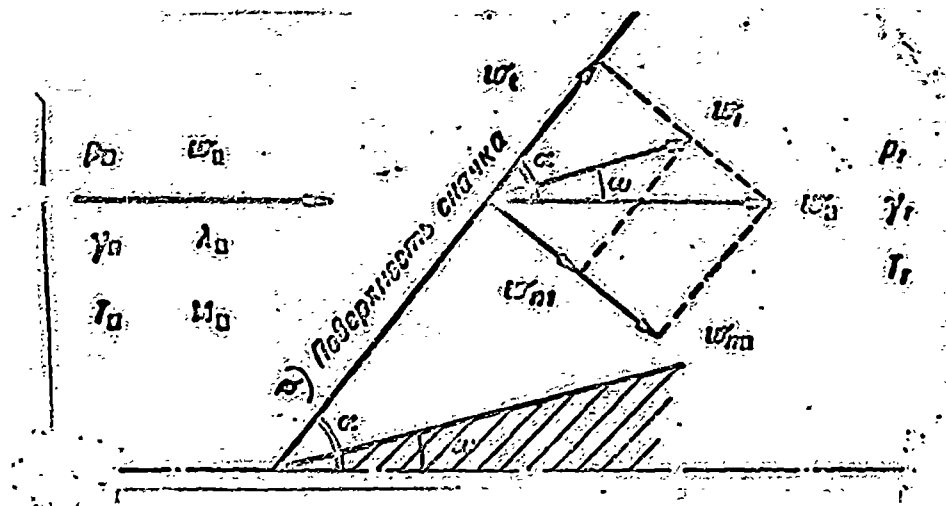
Fig. 37 Schematic of a two dimensional oblique shock wave.
Legend: a) Surface of shock wave.

angle -- by $\tilde{\omega}$ (Fig. 37). The angle between the front of the shock wave and the direction of an undisturbed flow -- the incidence angle of the shock wave -- is designated by α. This angle is unknown; it will be [~~~~~~~~~~~~] /see (2.124)7.

The velocity of an undisturbed flow w_n may be divided into two components: w_{tn} and w_{nn}, the first of which is parallel to, and the second perpendicular to, the surface of the shock wave.

$$w_{tn} = w_n \cos \alpha;$$ (2.110)

$$w_{nn} = w_n \sin \alpha.$$ (2.111)

Only the normal component of velocity varies when crossing the surface of a shock wave; the tangential component remains constant:

$$w_{t1} = w_{t\,n} = w_t.$$

The normal component of velocity experiences a normal shock wave, for which all the relationships obtained in the foregoing paragraph are valid.

The stagnation temperature ratio of the normal component w_{nn}:

$$\frac{T_{0n}}{T_n} = 1 + \frac{w_{n\,n}^2}{2g \frac{kR}{k-1} T_n} = 1 + \frac{w_n^2 \sin^2 \alpha}{2g \frac{kR}{k-1} T_n};$$

$$\frac{T_{0n}}{T_n} = 1 + \frac{k-1}{2} M_n^2 \sin^2 \alpha.$$ (2.112)

The critical velocity for the normal component is identical in front of and behind the shock wave:

$$a_n = \sqrt{\frac{2gkR}{k+1} T_{0n}} = \sqrt{\frac{2gkR}{k+1} T_n \left(1 + \frac{k-1}{2} M_n^2 \cos^2 c\right)} \tag{2.113}$$

The relative normal velocity in a shock wave is determined by the continuity equation

$$\frac{w_{n1}}{w_{nu}} = \frac{T_n}{T_1} = \frac{a_n \lambda_{n1}}{a_n \lambda_{nu}} = \frac{\lambda_{n1}}{\lambda_{nu}} = \frac{1}{\lambda_{nu}^2} \tag{2.114}$$

since in a normal shock wave

$$\lambda_{n1} = \frac{1}{\lambda_{nu}} \tag{2.115}$$

The relative velocity λ_{nu} is

$$\lambda_{nu}^2 = \frac{w_{nu}^2}{a_n^2} = \frac{a_u^2 \sin^2 c}{\frac{2gk}{k+1} T_n \left(1 + \frac{k-1}{2} M_u^2 \sin^2 \alpha\right)} \tag{2.116}$$

Substituting $a_u = \sqrt{gkRT_u} M_u$, to obtain

$$\lambda_{nu}^2 = \frac{1}{\frac{2}{k+1} \frac{1}{M_u^2 \sin^2 \alpha} + \frac{k-1}{k+1}} \tag{2.117}$$

The density ratio in an oblique shock wave is

$$\frac{T_u}{T_1} = \frac{1}{\lambda_{nu}^2} = \frac{2}{k+1} \frac{1}{M_u^2 \sin^2 \alpha} + \frac{k-1}{k+1} \tag{2.118}$$

The pressure ratio in an oblique shock wave, in accordance with the formula (2.107), will be

$$\frac{p_1}{p_u} = \frac{2k}{k+1} M_u^2 \sin^2 \alpha - \frac{k-1}{k+1} \tag{2.119}$$

The normal velocity behind the shock wave, according to the continuity equation:

$$w_{n1} = w_{nu} \frac{T_u}{T_1} = w_u \sin \alpha \left[\frac{k-1}{k+1} + \frac{2}{k+1} \frac{1}{M_u^2 \sin^2 \alpha}\right] \tag{2.120}$$

The total velocity behind a shock wave from a triangle of velocities (Fig. 37):

$$w_1^2 = w_t^2 + w_{n1}^2 \tag{}$$

Utilizing (2.111) and (2.120), we obtain

$$w_1^2 = w_u^2 \left\{\cos^2 \alpha + \sin^2 \alpha \left[\frac{k-1}{k+1} + \frac{2}{k+1} \frac{1}{M_u^2 \sin^2 \alpha}\right]^2\right\} \tag{2.121}$$

On the basis of (2.118) and (2.119), the static temperature behind an oblique shock wave is

$$\frac{T_1}{T_н} = \frac{T_н}{T_1}\frac{p_1}{p_н} = \left(\frac{2}{k+1}\frac{1}{M_н^2 \sin^2\alpha} + \frac{k-1}{k+1}\right)\left(\frac{2k}{k+1}M_н^2\sin^2\alpha - \frac{k-1}{k+1}\right).$$

(2.122)

We obtain the Mach number behind an oblique shock wave by the equation

$$\frac{M_1}{M_н} = \frac{v_1}{c_1} : \frac{v_н}{c_н} = \frac{v_1}{v_н}\sqrt{\frac{T_н}{T_1}}.$$

Noting (2.121) and (2.122), we obtain

$$M_1 = M_н\sqrt{\frac{T_н}{T_1}\left\{\cos^2\alpha + \sin^2\alpha\left[\frac{k-1}{k+1} + \frac{2}{k+1}\frac{1}{M_н^2\sin^2\alpha}\right]^2\right\}}$$

$$M_1 = M_н\sqrt{\frac{(k+1)^2\cos^2\alpha + \sin^2\alpha\left[k-1+\dfrac{2}{M_н^2\sin^2\alpha}\right]^2}{(k-1)\left[2kM_н^2\sin^2\alpha - \dfrac{2}{M_н^2\sin^2\alpha} + \dfrac{4k}{k-1} - k+1\right]}}$$

(2.123)

The angle of incidence of an oblique shock wave to the direction of an undisturbed flow is found from the triangle of the velocity (see Fig. 34).

$$\operatorname{tg}(\alpha - \omega) = \frac{v_{н1}}{v_1} = \left[\frac{k-1}{k+1} + \frac{2}{k+1}\frac{1}{M_н^2\sin^2\alpha}\right]\operatorname{tg}\alpha.$$

(2.124)

For the solution of the above equation given values are set for the Mach number $M_н$, and the incidence angle of the shock wave α, and the rake angle ω is determined. At a given Mach number one value for the rake angle ω corresponds to two values of the shock wave incident angle α.

One value of the incidence angle α conforms to deceleration of less than supersonic speed. This usually takes place during the beginning of oblique shock waves. The other, the greater value of α, conforms to deceleration of less than subsonic speed, which may occur in an oblique shock wave accompanied by additive aerodynamic drag.

The dependence of a shock wave's angle of incidence α upon the Mach number of an advancing flow at various rake angles is shown in Fig. 43. Only such α values are plotted here which correspond to the supersonic velocity behind a shock wave, since this is precisely what happens when an aircraft is in flight.

A certain critical value of the rake angle ω_{pred} corresponds to each Mach num at which the roots of the equation become imaginary. If the rake angle is larger t the critical angle $\omega > \omega_{pred}$, then the oblique shock wave changes into normal.

The dependence of the critical rake angle on the Mach number is shown in Fig.

It also shows the curve of flow velocity behind an oblique shock wave at critical rake angle. It is seen from the graph that it the Mach number = 3, the critical rake angle is
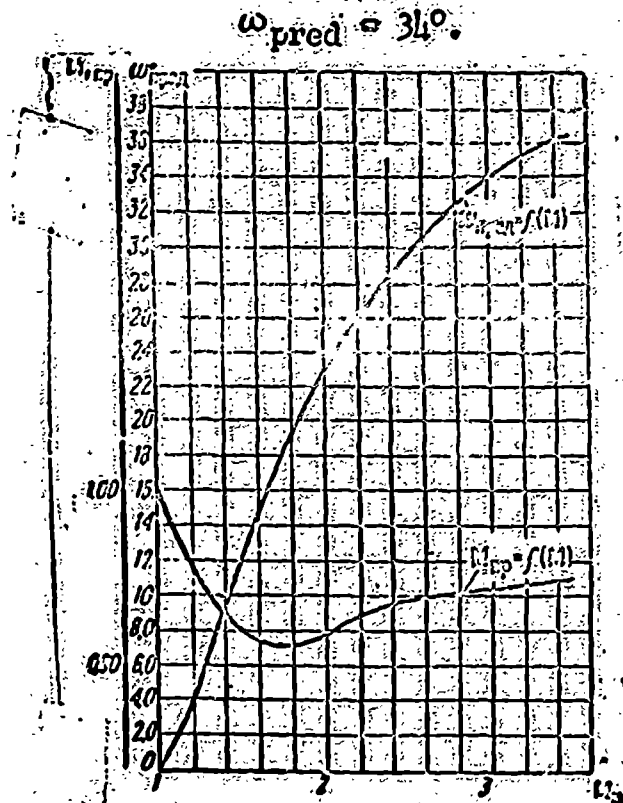
Fig. 38. Critical rake angle as function of the Mach number.

From the quadratic equation (2.123) it is apparent that at a given M_n two values of the Mach number behind the shock wave, $M_1 < 1$ and $M_1 > 1$, correspond to each value of the incidence angle α of the shock wave. Fig. 39 shows the relation of the velocity behind an oblique shock wave to the velocity of an advancing flow. Here only $M_1 > 1$ is presented, the condition usually observed during free flow.

The lesser the rake angle ω, the lesser the incidence angle α of the shock wave, the weaker the shock wave, and the more similar M_1 to M_n. When $\omega = 0$, $M_1 = M_n$.

The relation of the relative variations in pressure, density, and temperature to M_n is shown in Fig. 40, 41, and 42. The incidence angles of shock waves are shown in Fig. 43.

Oblique shock waves at equal Mach numbers of the flow are less intensive than normal shock waves. Irreversible losses of energy in oblique shock waves are
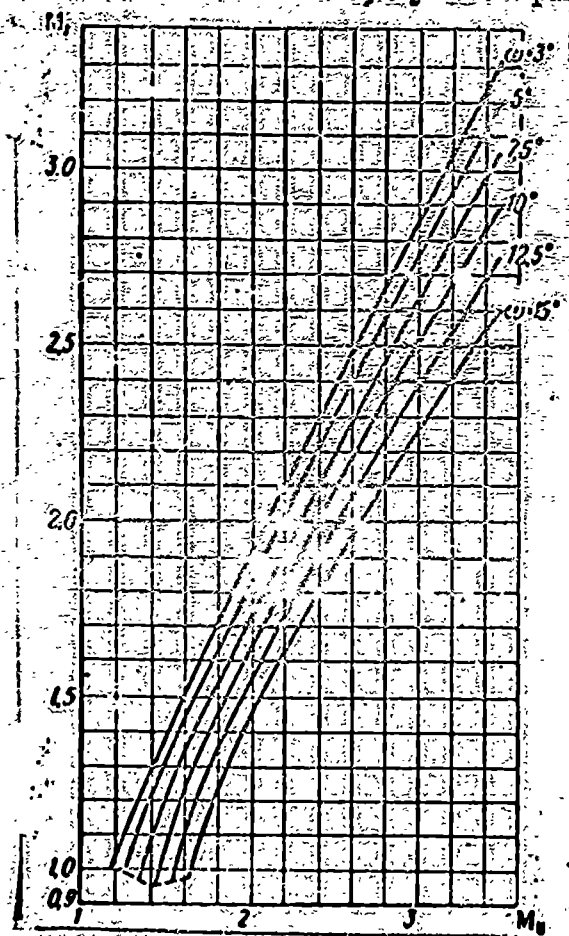
Fig. 39. The relation of the velocity behind an oblique shock wave to the velocity of the advancing flow.
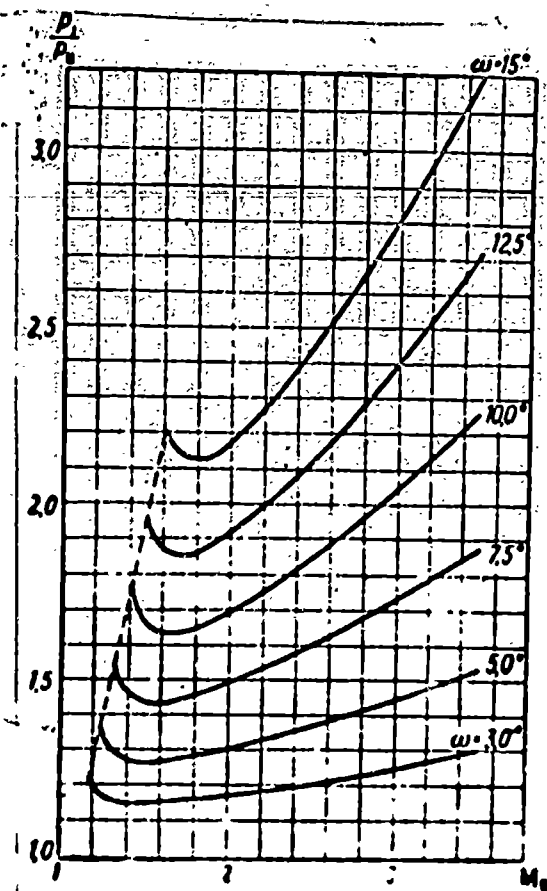
ig. 40. The relation of pressure behind an oblique shock wave to the velocity of the advancing flow.

through several oblique shock waves following one another, one may obtain less

energy losses and a higher stagnation pressure than with a single normal shock wave.

Compression by means of a number of oblique shock waves is used in supersonic

diffusers.
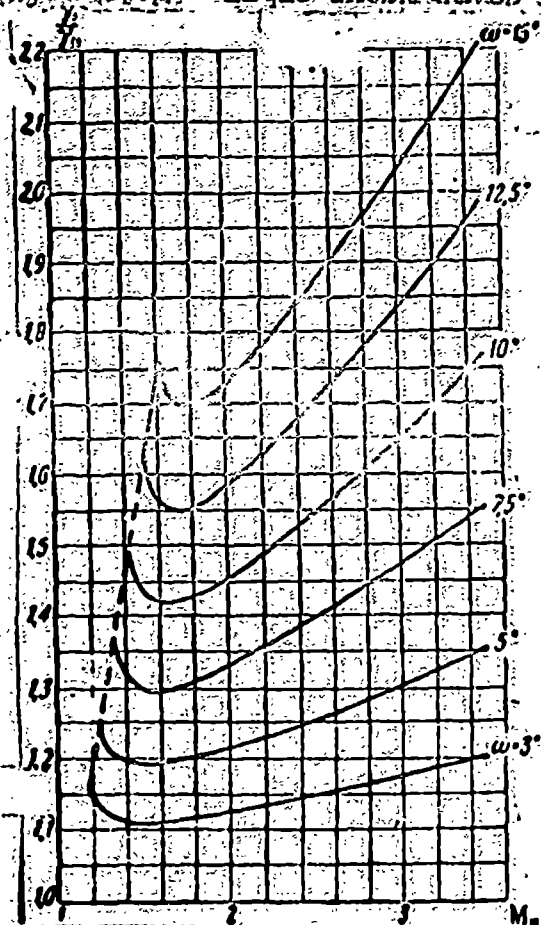
Fig. 41.   Relation of the density behind an oblique shock wave to the velocity
of the advancing flow.

At a very small rake angle, $\omega \to 0$, the increase of pressure, temperature, and

density in an oblique shock wave remains infinitely small. When $\omega = 0$, $M_{u} \sin \alpha = 1$,

$\dfrac{p_1}{p_u} = 1$;

$$\frac{\gamma_1}{\gamma_u} = 1; \quad \frac{T_1}{T_u} = 1; \quad M_1 = M_u.$$

The incidence angle of an infinitely weak shock wave, e.g., at which $\left(\dfrac{p_1}{p_u} \to 1\right)$,

as seen from equation (2.119), is equal to

$$\sin \alpha_0 = \frac{1}{M_u} \tag{2.125}$$

An infinitely weak shock wave constitutes a sound wave propagating at velocity

c (Fig. 44).

For the time interval t, a body traverses the path $w_n t$, and the sound wave

spreads out over a distance ct.
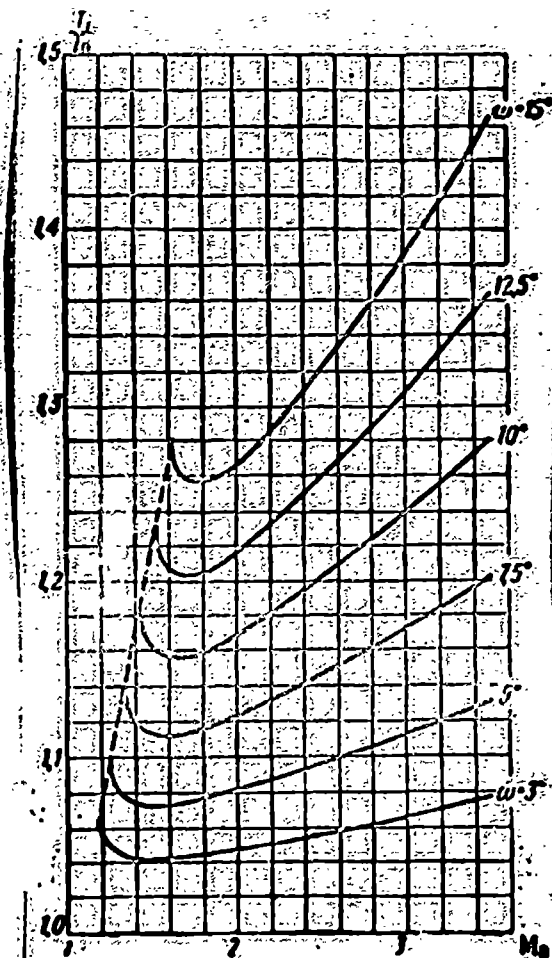
Fig. 42. Relation of the temperature behind an oblique shock wave to the velocity of the advancing flow.

The envelope of all spherical sound waves represents the surface of a sound wave. The half-angle at the apex of a sound wave -- the Mach angle -- α_0 is deter-mined by equation

$$\sin \alpha_0 = \frac{ct}{w_n t} = \frac{c}{w_n} = \frac{1}{M_n}$$

Thus the angle at the apex of a sound wave is equal to the incidence angle of an infinitely weak shock wave, which appears as the rake angle ω approaches zero. With growing rake angle, the incidence angle of the shock wave increases until it, finally, reaches the critical value of ω_{pred}, at a certain critical value of the rake angle ω_{pred} (see Fig. 38). During subsequent increase of ω the oblique shock wave suddenly becomes a normal one.

Example: Find the parameters of the air behind a plane oblique shock wave when the incidence angle ω_{p1} /apex angle of wedge/ = 12.5° and M = 3.5.

The incidence angle of the shock wave (see Fig. 43) α = 27°. The velocity behind the shock wave (according to Fig. 39) M_1 = 2.76. We find the increase in pressure, temperature, and density in the shock wave according to Fig. 40, 41, and 42.

$$\frac{p_1}{p_n} = 2.71; \quad \frac{T_1}{T_n} = 1.366; \quad \frac{\gamma_1}{\gamma_n} = 1.98.$$
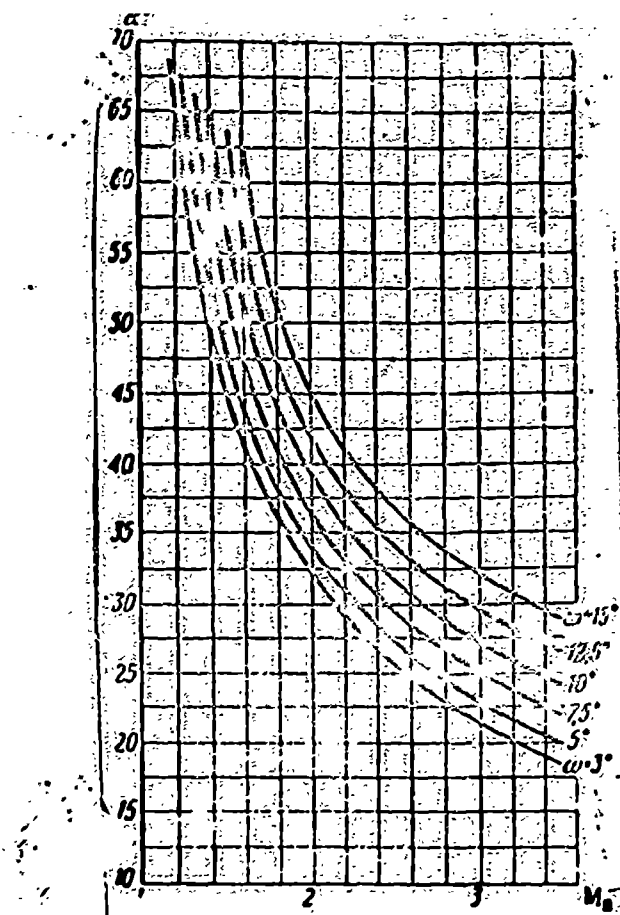
Fig. 43. Relation of the incidence angle of the shock wave to the Mach number of the advancing flow.
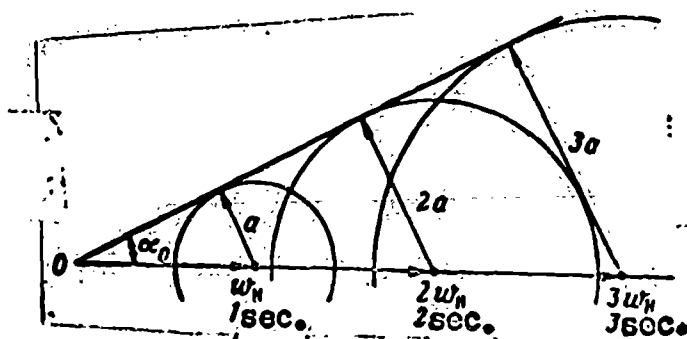
Fig. 44. Formation of a wave of weak disturbances.

Section 12. Supersonic Airflow over a Cone

At the approach of a supersonic flow to the point of a cone, cone-shaped shock waves are formed. Let us examine the symmetrical air flow over a cone (Fig. 45).

If the direction of a supersonic flow coincides with the axis of a cone, then a cone-shaped shock wave appears at the apex of the cone, whose generatrix forms an angle α with the undisturbed flow axis.

The direction of the flow behind the shock wave will be approximately the same as in the case of a plane oblique shock wave. The turn angle of the flow behind the

shock wave is less than the half angle at the apex of the cone (see Fig. 45). As they approach the surface of the cone, the stream lines warp asymptotically to the surface of the generatrix. For a given Mach number of an advancing flow and a given angle of conical shock wave α, the parameters of the air behind the shock wave may be found by the formulas and graphs for a plane oblique shock wave.
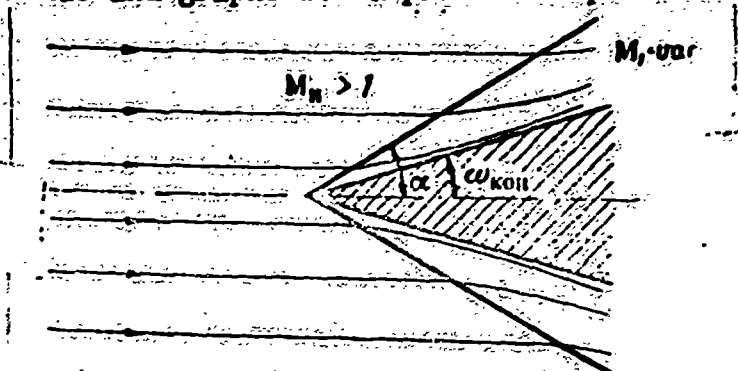
Fig. 45. The flow behind a conical shock wave is heterogeneous.

A cone produces significantly less disturbance in a supersonic stream than a wedge. Therefore, in order to obtain a shock wave of the same intensity at the apex of a cone as at the apex of a wedge, one should take a cone having a greater angle at the apex than that of the wedge. The relation of the angles at the apex of a cone to the angles at the apex of a wedge at various M_n numbers of an advancing flow is shown in Fig. 46. If the angle at the apex of the cone ω_{kon} is replaced by the angle at the apex of the wedge ω_{kl}, the intensity of a shock wave at a given M_n will not vary. As one goes from the surface of the shock wave to the cone surface, the velocity M_1 decreases, and the pressure, density, and temperature are increased, reaching maximum value at the surface of the cone. The relation of the Mach number immediately behind the shock wave and on the surface of the cone to the half-angle of its apex for various flow velocities is shown in Fig. 47. The figures in the graph are average values, since the velocity distribution behind a cone-shaped shock wave is not uniform. The pressure of the flow at various portions of the cone's surface has different values. The average pressure on the cone's surface following a shock wave of a certain intensity has a larger value than that on the surface of a wedge. When the apex angles of a wedge and cone are equal: $\omega_{kl} = \omega_{kon}$, the wedge produces a more disturbed flow than does a cone. The shock wave proves to be more intensive,

and the pressure on the surface of the wedge is greater than on the surface of the cone.

At the point where the surface of a streamlined body changes from a conical to a cylindrical form, a weak disturbance appears, which ⸻⸻⸻⸻⸻⸻⸻⸻⸻⸻ sloped ⸻⸻⸻⸻⸻⸻⸻⸻⸻ then angle determined ⸻ equation ⸻

$$\sin \alpha_0 = \frac{1}{M_1}$$

With supersonic flow around the obtuse angle ABC, the gas spreads out and increases in velocity. The stream lines warp and become parallel to the cylinder generatrix BC. The velocity of the flow near the surface of the cylinder increases approximately to the value which it had before the oblique shock wave.
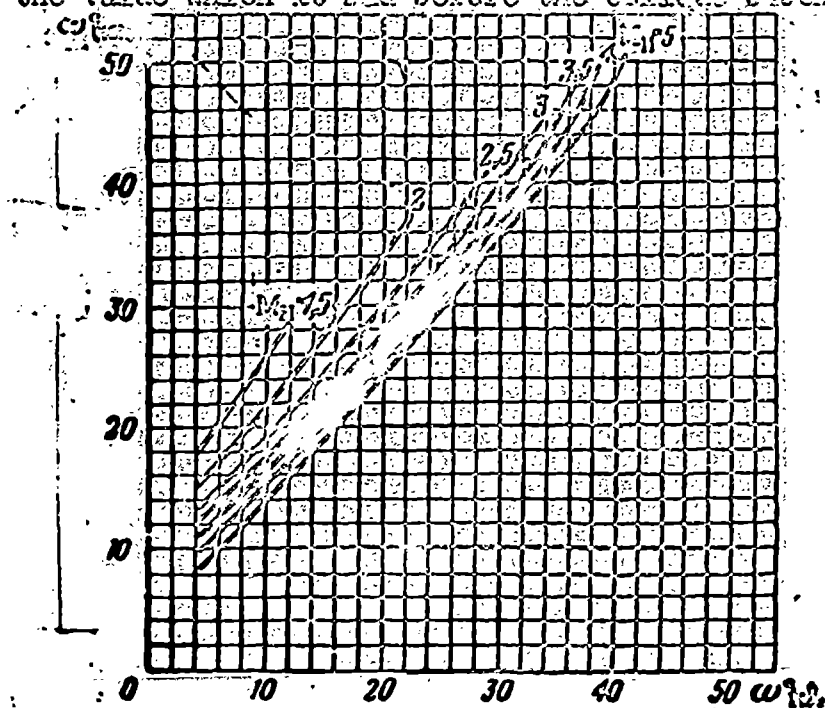
Fig. 46. Incidence angles of shock waves of equal intensities, for airflows around a wedge and a cone.

If the velocity of the flow which approaches the cone is less than the critical value M_{pred}, the shock wave breaks contact from its point at the apex of the cone and changes to a normal shock wave. The value of the maximum velocity or the critical angle ω_{pr} may be found in Fig. 38, by substituting the cone-shaped angle for a two dimensional one which produces an equally disturbed flow.

Example: The angle at the apex of a wedge $2\omega_{k\ell} = 40°$, Find the maximum velocity M_{pr} and the equivalent angle of a cone at maximum velocity.

The maximum velocity is found on the graph shown in Fig. 38; $M_{pred} = 1.84$. The cone angle we find on the graph pictured in Fig. 46: · $2\omega_{kou} = 72°$.
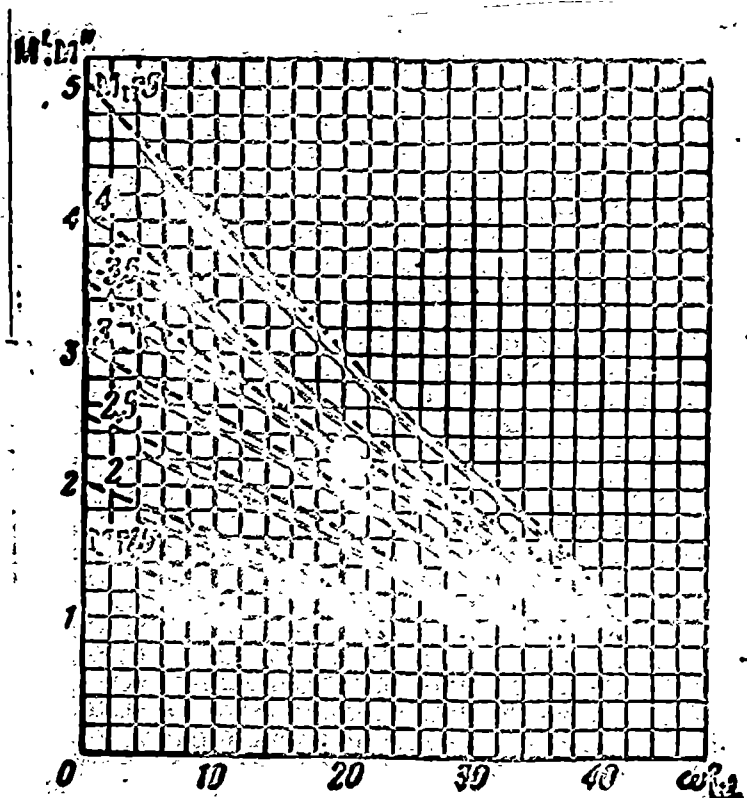
Fig. 47 The relation of the Mach number behind the shock wave (dotted line) and on the surface of a cone (solid line) vs the rake angle ω at various Mach numbers of a flow.

Section 13. Drag

Shock waves appear in the interaction of a body moving at supersonic speed and the surrounding air. The pressure in a shock wave is increased. This increased pressure acting on the frontal surface of the body creates additional drag, which is called wave drag. The energy spent on overcoming wave drag is transformed into the energy of shock waves. With damping waves this energy is dissipated.

The drag of a body may be expressed by the following conventional formula:

$$X = c_x S_M \frac{\gamma_H w_H^2}{2g} \qquad (2.126)$$

Usually the drag of a body is referenced to a unit of its cross-section S_M.

The velocity head:

$$q = \frac{\gamma_H w_H^2}{2g} = \frac{k}{2} p_H M_H^2 = \frac{k}{k+1} \frac{\lambda_H^2}{\tau(\lambda_H)} \qquad (2.127)$$

At supersonic speeds the velocity head q has only the conventional meaning, since the actual increase in pressure during deceleration of the compressed supersonic flow depends on the manner of deceleration, and, generally speaking, is not equal to q.

The factor c_x is called the <u>drag coefficient</u>. This c_x depends on the shape of the body and on the Mach and Reynolds numbers of the advancing flow.

Usually c_x is determined by experiment, by placing a model in a wind tunnel and measuring the forces acting on it. In some cases the aerodynamic drag may be calculated.

At supersonic speed aerodynamic drag is made up of three forms of resistance, caused by physical processes: friction, vortex formations, and shock waves.

<u>Friction drag</u> depends on the size of the lateral face of the body S_{bok} and on the Reynolds number Re of the advancing flow.

The force of friction:

$$X_{тр} = c_f S_{бок} \frac{\gamma_н w_н^2}{2g} .$$ (2.128)

With turbulence the friction coefficient c_f, may be expressed by these empirical formulas:

When Re $<$ 10^6

$$c_f = \frac{0,074}{Re^{1/5}} ;$$ (2.129a)

When Re $>$ 10^6

$$\sqrt{c_f} = \frac{0,242}{\lg Re} .$$ (2.129b)

The coefficient of friction resistance is:

$$c_{x тр} = \frac{X_{тр}}{q S_м} = c_f \frac{S_{бок}}{S_м} .$$ (2.130)

The <u>force of wave drag</u> may be expressed by the pressure appearing in the leading wave:

$$X_{вол} = \int_0^s \Delta p \, dS \sin \omega = S_л \Delta p_{сред} .$$ (2.131)

where $S_л$ -- is the frontal surface (for shapes which do not have a duct for the passage of air, $S_л$ is represented by the area of maximum cross-section $S_м$).

Δp is the surplus pressure in the leading wave, $\Delta p = p - p_n$;

p is the pressure along the surface of the body;

p_n is the pressure of an undisturbed flow.

In the case of airflow around axially symmetric bodies, the surplus pressure at various points of the surface has an unequal value. Therefore, the theoretical compu-

tation of the pressure presents great difficulties. The wave-drag coefficients of bodies are usually determined experimentally.

In the case of airflow around a wedge, the pressure on the surface, equal to the pressure behind jump p_1, is equal at all points on the surface; therefore the computation of the drag coefficient does not present any difficulty:

$$X_{\text{вол}} = p_{\text{н}} S_{\text{м}} \left(\frac{p_1}{p_{\text{н}}} - 1 \right);$$

$$c_{x\,\text{вол}} = \frac{X_{\text{вол}}}{S_{\text{м}} q} = \frac{2}{k M_{\text{н}}^2} \left(\frac{p_1}{p_{\text{н}}} - 1 \right). \qquad (2.132)$$

The pressure ratio $\dfrac{p_1}{p_n}$ is determined by formula (2.119).

The coefficient of wave drag of a wedge is

$$c_{x\,\text{вол}} = \frac{4}{k+1} \left(\sin^2 \alpha - \frac{1}{M_{\text{н}}^2} \right). \qquad (2.133)$$

With an increase of the number M_n or a decrease in the rake angle ω, the angularity of jump α diminishes and c_x decreases. The wave-drag versus Mach number curve at various rake angles of a wedge is shown in Fig. 48.

If the angle at the apex of a cone is such that the jump has the same intensity as during the airflow over a wedge, the wave drags of the wedge and cone are similar. At supersonic velocities of a flow, pointed bodies create weaker jumps; therefore they have less wave drag than blunt ones. A normal shock wave appears before the nose of a body which has the most wave drag (Fig. 49). During the transition of the rake angle to a critical value, an oblique shock wave changes into a normal one and the wave drag increases abruptly.

During supersonic airflow at an obtuse angle to an axial supersonic flow or during supersonic flow past the transition from the conical to the cylindrical portions of a body, the pressure falls and the flow turns. The pressure on the cylindrical portion of the surface of a cylindrical-conical body is similar to the pressure of undisturbed flow p_n; The pressure behind the stern (boat tail) portion of a body is lower than that of the atmosphere. This area behind the stern portion of a body represents a turbulent zone full of vortexes which increase following a moving body. The greater the Mach number of the advancing flow, the lower the relative pres-

boat tail drag:

$$X_{\text{корм}} = p_н S_н \left(1 - \frac{p_{к,он}}{p_н}\right).$$ (2.134)

The boat tail drag coefficient is

$$c_{x\,\text{корм}} = \frac{2}{kM_н^2}\left(1 - \frac{p_{\text{корм}}}{p_н}\right).$$ (2.135)

The lowered pressure behind the stern at supersonic velocities of a flow is usually less than the increased pressure before the frontal surface of the body. Therefore, the wave drag of the stern is less than the wave resistance of the nose (Fig. 50).
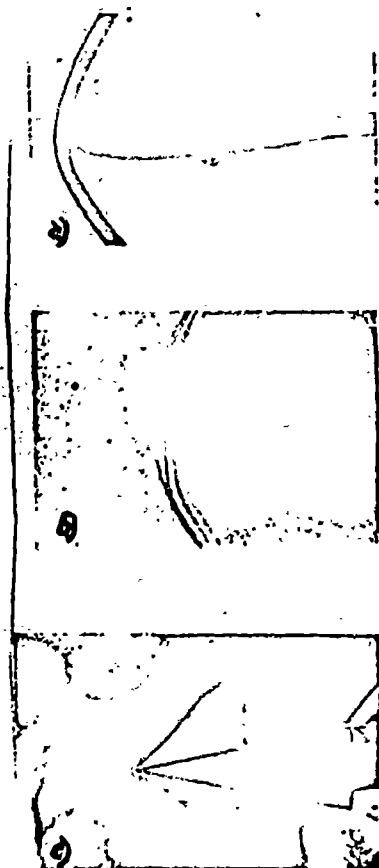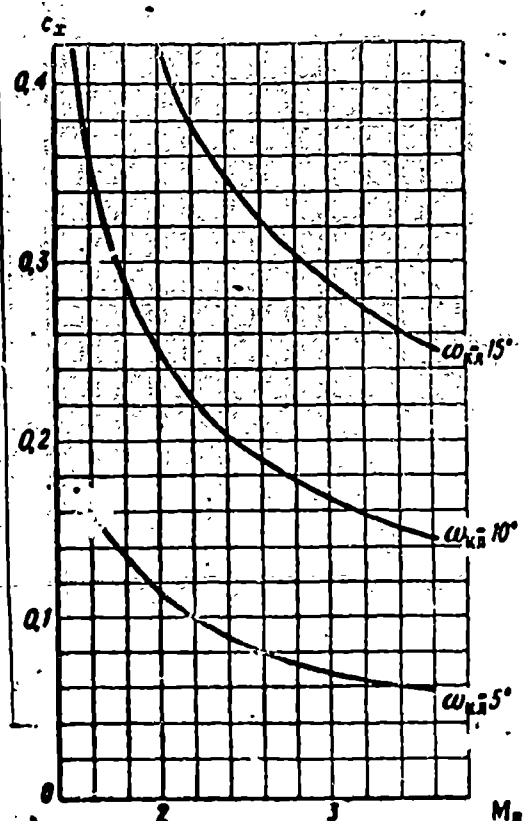
Fig. 48. Wave-Drag coefficients of wedges.

Fig. 49. Waves appearing during supersonic airflow.
a -- rounded body;
b -- blunt body;
c -- pointed body.

Example: When M = 3, if the angle at the apex of a cone ω_{kon} = 30°, then the corresponding angle of a wedge ω_{kl} = 22° (see Fig. 46). Rake angle ω is equal to half of the angle at the apex of the wedge, ω = 11°; then the relative increase in pressure in front of the nose $\frac{p_1}{p_n}$ = 2.2 (see Fig. 40). The relative lowered pressure behind the stern $\frac{p_{korm}}{p_n}$ = 0.45.

Boat tail drag X_{korm} = $p_n S_n (1-0.45)$. The boat tail drag coefficient is

$$c_{x\;\text{кори}}=\frac{2}{kM_{\text{в}}^2}\left(1-\frac{p_{\text{кори}}}{p_{\text{в}}}\right)=\frac{2\cdot0,55}{1,4\cdot3^2}=0,087$$ (see Fig. 50)
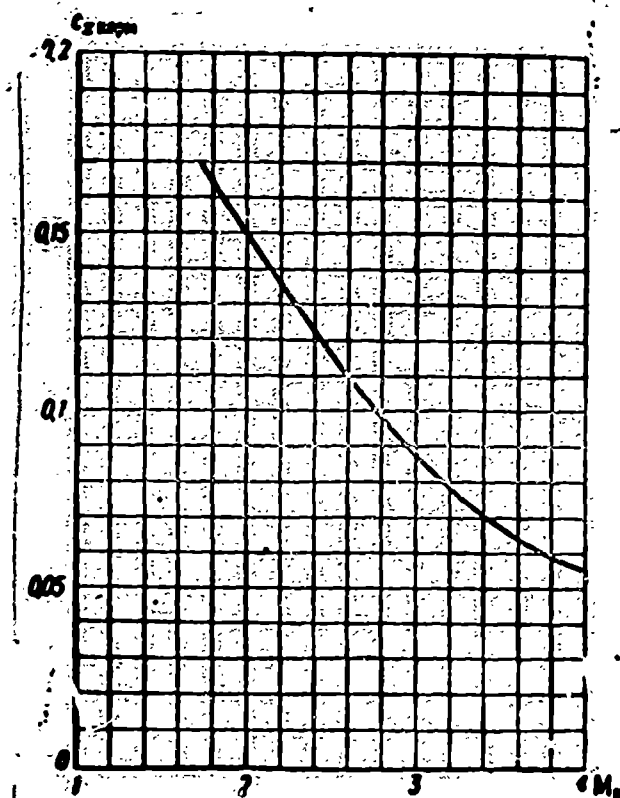
Fig. 50 Boat tail drag coefficient when $M_n > 1$.

The wave drag of the cone is

$$X_{\text{кон}}=p_{\text{в}}S_{\text{м}}\left(\frac{p_1}{p_{\text{в}}}-1\right).$$

The wave-drag coefficient of the cone is

$$c_{x\;\text{кон}}=\frac{2}{kM_{\text{в}}^2}\left(\frac{p_1}{p_{\text{в}}}-1\right)=\frac{2(2,2-1)}{1,4\cdot3^2}=0,175.$$

With allowance for the friction coefficient, the overall drag coefficient of a cylindrical-conical body at M = 3 is

$$c_x=c_{x\;\text{тр}}+c_{x\;\text{кон}}+c_{x\;\text{кор}}\approx0,3$$

(compare with Fig. 184).

BIBLIOGRAPHY

1. Abramovich, G.N., Prikladnaya gazovaya dinamika /Applied Gas Dynamics7, Gostekhiz-dat, Moscow-Leningrad, 1951.

2. Arzhanikov, N.S. and Mal'tsev, V.N., Aerodinamika /Aerodynamics7, Oborongiz, 1956.

3. Vulis, L.A., Termodinamika gazovykh potokov /Thermodynamics of Gas Flows7, Energoizdat, Moscow-Leningrad, 1950.

4. Karman, T., Sverkhzvukovaya aerodinamika /Supersonic Aerodynamics7, Foreign-Literature Press, 1948.

5. Kibel', I.A., Kochin, N.Ye., Roze, N.V., Teoreticheskaya gidromekhanika /Theoretical Fluid Mechanics/, Moscow-Leningrad, 1948.

6. Kiselev, B.M., "Computing Uniform Gas Flows," Prikladnaya matematika i mekhanika /Applied Mathematics and Mechanics/, 1947, Vol 11, No 1.

7. Landau, L.D. and Livshits, Ye.M., Mekhanika sploshnykh sred /Mechanics of Continua_/, GITTL, Moscow-Leningrad, 1953.

8. Prandtl', L., Gidromekhanika /Fluid Mechanics/, Foreign-Literature Press, 1951.

9. Sedov, L.I., Ploskiye zadachi gidrodinamiki i aerodinamiki /Two Dimensional Problems of Fluid Dynamics and Aerodynamics/, GITTL, Moscow-Leningrad, 1950.

10. Sovremennoye sostoyaniye aerodinamiki bol'shikh skorostey /Contemporary State of High-Speed Aerodynamic_/, Foreign-Literature Press, edited by L. Khouart, 1955.

11. Khristianovich, S.A., Gal'perin, V.G., Millionshchikov, M.D., Simonov, L.A., Prikladnaya gazovaya dinamika, 1948.

CHAPTER III

IDEAL RAMJET ENGINES

We call _ideal_ those imaginary ramjet engines in which the dissipation of kinetic energy does not occur and heat losses are absent. Such idealization presents the possibility of obtaining very simple formulas for the computation of gas dynamic and thrust parameters of a ramjet engine. Those values, found by the formulas of an ideal ramjet engine, are the upper limits which the parameters of actual engines strive for in the presence of mechanical and thermal losses.

Section 1. Fundamental Definitions and Assumptions

A schematic of an ideal ramjet engine is presented in Fig. 51. The engine consists of a diffuser, a combustion chamber (or heat exchanger), and an exhaust nozzle. The engine operates on a stream of air which is considered to be an ideal gas. We designate by the index ("H") the parameters of the air in front of the engine, i.e., the parameters of an undisturbed flow. A reversible deceleration of the flow occurs in the diffuser of an ideal ramjet engine regardless of whether the flow enters the engine at subsonic or supersonic velocity. The static pressure increases thereby from p_n to p_2. The stagnation pressure remains constant: $p_{02} = p_{0n}$. The p-v diagram of an ideal ramjet engine is presented in Fig. 52. The compressed air increases in temperature from T_{02} to T_{03}. The stagnation pressure remains constant: $p_{03} = p_{02}$. The compressed heated gas discharges through the exhaust nozzle. The static pressure diminishes until back pressure $p_4 = p_n$. The stagnation pressure remains constant during the flow: $p_{04} = p_{03}$. The flow occurs without any thermal losses; hence stagnation temperature does not vary: $T_{04} = T_{03}$.

The stagnation pressure of the gases exhausted from an ideal ramjet engine is equal to the stagnation pressure of the incoming flow: $p_{0n} = p_{02} = p_{03} = p_{04}$.

The velocity and, consequently, the momentum of the discharging gases are greater than those of the incoming flow: $w_4 > w_n$.

Due to the increase in momentum, jet thrust R appears:

$$R = \frac{G_4 w_4}{g} - \frac{G_u w_u}{g}.$$

The thermodynamic cycle described by the operating substance flowing through a ramjet engine (Fig. 52) is called the <u>Brayton</u> <u>cycle</u>. Adiabatic curve H-2 shows the
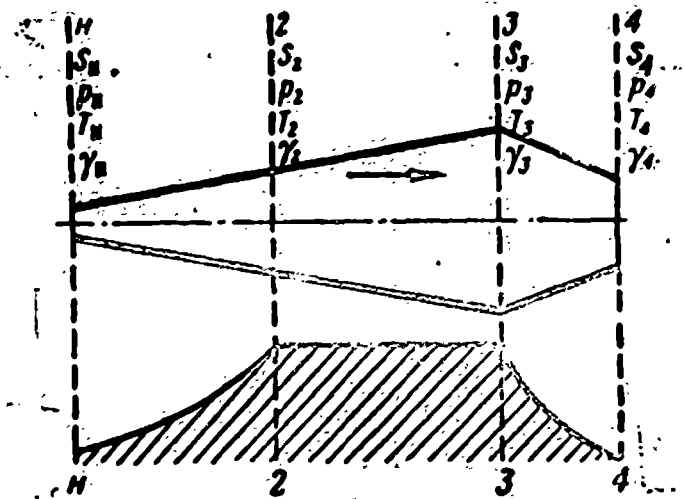
Fig. 51. Schematic of an ideal ramjet engine.

reversible compression of the inflowing air in an ideal diffuser. Constant-pressure line 2-3 represents the heating of the compressed air from temperature T_{02} to T_{03} at constant pressure. Adiabatic curve 3-4 shows the reversible expansion of the hot gas, during which its enthalpy is partially transformed into kinetic energy. Constant-pressure line 4-H shows the cooling of the discharge gases to the temperature of the surrounding medium. This process obviously occurs outside the engine.
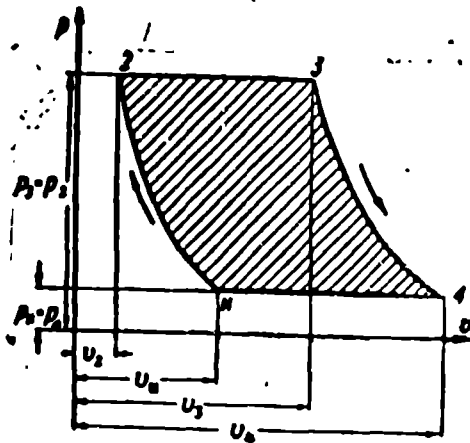
Fig. 52. P-v diagram of the operating process of an ideal ramjet engine.

The area of the p-v diagram H234, in a certain conventional scale, expresses the amount of enthalpy transformed into kinetic discharge energy.

In analyzing the processes which occur in an ideal ramjet engine, the following assumptions should be made:

1. The dissipation of kinetic energy and thermal losses are absent.

2. The pressures in the inlet and in the exhaust sections are equal to the back pressure: $p_1 = p_n$ and $p_4 = p_n$.

3. The stagnation pressure does not vary during heating: $p_{03} = p_{02}$.

4. The working substance is an ideal gas the specific heat of which is constant: $c_p = $ const; $k = $ const.

5. At any point of the engine the gas parameters are constant throughout the entire cross-section (radial gradients are absent):

$$\frac{\partial p}{\partial r} = 0; \quad \frac{\partial T}{\partial r} = 0 \text{ and } \frac{\partial w}{\partial r} = 0.$$

Section 2. Gas Dynamics of an Ideal Ramjet Engine

The velocity of a flow through the diffuser of a ramjet engine decreases; the temperature, pressure, and density increase (see Chapter II, Section 7).

Let us designate by w_n, T_n, p_n, and γ_n the parameters of an undisturbed flow flowing into an engine.

The parameters of a flow which is partially decelerated in a diffuser may be expressed either as a function of a Mach number or of relative velocity λ.

The Mach number of free stream flow (2.63) is

$$M_n = \frac{w_n}{c_n} = \frac{w_n}{\sqrt{gkRT_n}}.$$ (3.1)

The relative velocity of a free stream flow (2.55) is

$$\lambda_n = \frac{w_n}{c_n} = \frac{w_n}{\sqrt{\frac{2gkR}{k+1}T_{0n}}}.$$ (3.2)

The stagnation ratios of a free stream flow, as mentioned earlier (Chapter II, Section 7), are equal to

$$\frac{T_{0n}}{T_n} = 1 + \frac{k-1}{2}M_n^2 = \frac{1}{\tau(\lambda_n)};$$ (3.3)

$$\frac{p_{0n}}{p_n} = \left[1 + \frac{k-1}{2}M_n^2\right]^{\frac{k}{k-1}} = \frac{1}{\pi(\lambda_n)};$$ (3.4)

$$\frac{\gamma_{0n}}{\gamma_n} = \left[1 + \frac{k-1}{2}M_n^2\right]^{\frac{1}{k-1}} = \frac{1}{\varepsilon(\lambda_n)}.$$ (3.5)

By definition, the pressure at the inlet section of an ideal ramjet engine is equal to the pressure of a free stream flow: $p_1 = p_n$. Consequently, according to

Bernoulli's equation

$$w_1 = w_a; \quad M_1 = M_a \quad \text{and} \quad \lambda_1 = \lambda_a.$$

Air flow through the inlet section S_1 is

$$G_1 = w_1 \gamma_1 S_1 = w_a \gamma_a S_a = \sqrt{\frac{gk}{R}} \cdot \frac{p_a S_1 M_a}{\sqrt{T_a}},$$ (3.6)

The flow may be expressed by the relative velocity λ_n (see Chapter II, Section 7)

$$G_1 = \sqrt{\frac{2gk}{(k+1)RT_{0n}}} \, p_{0n} S_1 \lambda_n \varepsilon (\lambda_n).$$ (3.7)

Stagnation temperature remains constant along the entire engine as long as a heat supply is not added.

$$T_{0n} = T_{01} = T_{02} = T_{0x}.$$ (3.8)

The compression of a flow in an ideal engine occurs without losses; therefore the stagnation pressure at the outlet of the diffuser is equal to the stagnation pressure of the incoming flow:

$$p_{02} = p_{01} = p_{0n} = \frac{p_n}{\pi (\lambda_n)}.$$ (3.9)

The velocity of the flow in section S_2 decreases to value w_2. The Mach number and the relative velocity M_2 and λ_2 remain equal.

Air flow through section S_2 is

$$G_2 = \sqrt{\frac{2gk}{(k+1)RT_{02}}} \, p_{02} S_2 \lambda_2 \varepsilon (\lambda_2).$$ (3.10)

Since the air does not escape and then appear again in the diffuser, the right-hand portions of equations (3.7) and (3.10) may be equated. Considering that $T_{02} = T_{0n}$ and $p_{02} = p_{0n}$ for an ideal ramjet engine, we shall find the ratio between the cross-sections and relative velocities:

$$\frac{S_2}{S_1} = \frac{\lambda_n \varepsilon (\lambda_n)}{\lambda_2 \varepsilon (\lambda_2)} = \frac{\lambda_n}{\lambda_2} \left[\frac{1 - \frac{k-1}{k+1}\lambda_n^2}{1 - \frac{k-1}{k+1}\lambda_2^2} \right]^{\frac{1}{k-1}}.$$ (3.11)

Expressing λ by M, after simple reorganizations we obtain

$$\frac{S_2}{S_1} = \frac{M_n}{M_2} \left[\frac{1 + \frac{k-1}{2}M_2^2}{1 + \frac{k-1}{2}M_n^2} \right]^{\frac{k+1}{2(k-1)}}.$$ (3.12)

The relation between Mach numbers and the cross-sections is shown in Fig. 53.

If $M_n < 1$ or $\lambda_n < 1$, then the deceleration of the flow will occur in a widening diffuser; the increase of S corresponds to the decrease of M. (If, for example, $M_1 = 0.5$, and $M_2 = 0.2$, then by plotting the Mach number S on the vertical axis of the graph in Fig. 53, on the basis of curve II we find:

$$\frac{S_1}{S_{\kappa p}} = 1.4; \quad \frac{S_2}{S_{\kappa p}} = 3; \quad \frac{S_2}{S_1} = \frac{3}{1.4} = 2.14 \Big).$$

When $M_n < 0.5$, density variations are insignificant and flow velocities are approximately inversely proportional to the cross-sections.

If $M > 1$ or $\lambda > 1$, then the stagnation of the flow will occur in a tapering tube until the velocity of the flow becomes equal to the local speed of sound:

$$w = w_{\kappa p} = a = \sqrt{\frac{2gkR}{k+1} T_{0n}}.$$

The section in which $M = 1$ and $\lambda = 1$ is called the **critical** **section** S_{cr} (Fig. 53). Subsequent retardation occurs in a widening tube.
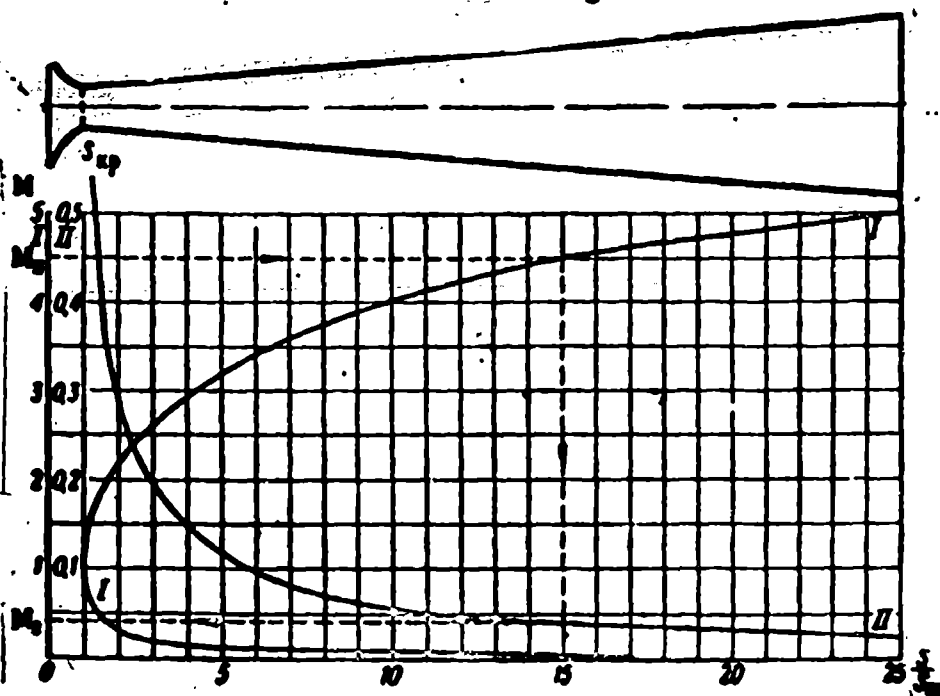
Fig. 53. The relation of the local values of the Mach number during a flow along a tube of variable cross-section to the ratio of the cross sections $\dfrac{S_i}{S_{cr}}$.

We find the ratio between an arbitrary section of the tube and the critical section S_{cr} from equation (3.11 or 12), substituting $M_2 = 1$ or $\lambda_2 = 1$ therein:

$$\frac{S_i}{S_{\kappa p}} = \frac{1}{\lambda} \frac{\left(\frac{2}{k+1}\right)^{\frac{1}{k-1}}}{\left(1 - \frac{k-1}{k+1}\lambda^2\right)^{\frac{1}{k-1}}}. \tag{3.13}$$

The velocity in the exhaust section of diffuser S_2 is equal to

$$w_4 = a\lambda_4 = \lambda_4 \sqrt{\frac{2gkR}{k+1} T_{0\pi}}. \tag{3.14}$$

The static temperature, pressure, and density in section "2"

$$\frac{T_2}{T_\pi} = \frac{T_{0\pi}}{T_\pi} \frac{T_2}{T_{02}} = \frac{\tau(\lambda_2)}{\tau(\lambda_\pi)} = \frac{1 + \frac{k-1}{2} M_\pi^2}{1 + \frac{k-1}{2} M_2^2}; \tag{3.15}$$

$$\frac{p_2}{p_\pi} = \frac{\pi(\lambda_2)}{\pi(\lambda_\pi)}; \tag{3.16}$$

$$\frac{\gamma_2}{\gamma_\pi} = \frac{\varepsilon(\lambda_2)}{\varepsilon(\lambda_\pi)}. \tag{3.17}$$

The air, compressed in the diffuser, enters either a chamber where a molecular fuel is burned, or the heat exchanger of a reactor in which atomic energy is released The stagnation temperature in a heat exchanger increases; the stagnation pressure, by definition, remains constant $p_{03} = p_{02}$.

The ratio of the stagnation temperature of the heated gases T_{03} to the stagnation temperature of the incoming flow $T_{0\pi}$ is called temperature ratio θ :

$$\theta = \frac{T_{03}}{T_{0\pi}} = \frac{T_{03}}{T_{02}}. \tag{3.18}$$

According to the equation of continuity (3.7) for sections S_2 and S_3:

$$\frac{G_3}{G_2} = \frac{p_{03} S_3 q(\lambda_3)}{p_{02} S_2 q(\lambda_2)} \sqrt{\frac{T_{02}}{T_{03}}}. \tag{3.19}$$

Whence

$$\frac{S_3}{S_2} = \beta \sqrt{\theta} \frac{q(\lambda_2)}{q(\lambda_3)}, \tag{3.20}$$

where

$$\beta = \frac{G_3}{G_2} = \frac{G_4}{G_1}. \tag{3.21}$$

The relation of the calculated sections to velocity and temperature ratio is presented in Fig. 54.

The hot gases discharge through the exhaust nozzle. Their velocity increases to value w_4, and the pressure falls to that of the back pressure:

$$p_4 = p_\pi. \tag{3.22}$$

The drop in pressure during the discharge from an ideal ramjet engine is equal to the increase in pressure during the retardation of the incoming flow

$$\frac{p_{04}}{p_4} = \frac{p_{0\pi}}{p_\pi}.$$

Since

$$p_{04} = p_{03} = p_{02} = p_{01} \text{ and } p_4 = p_{\text{н}}$$
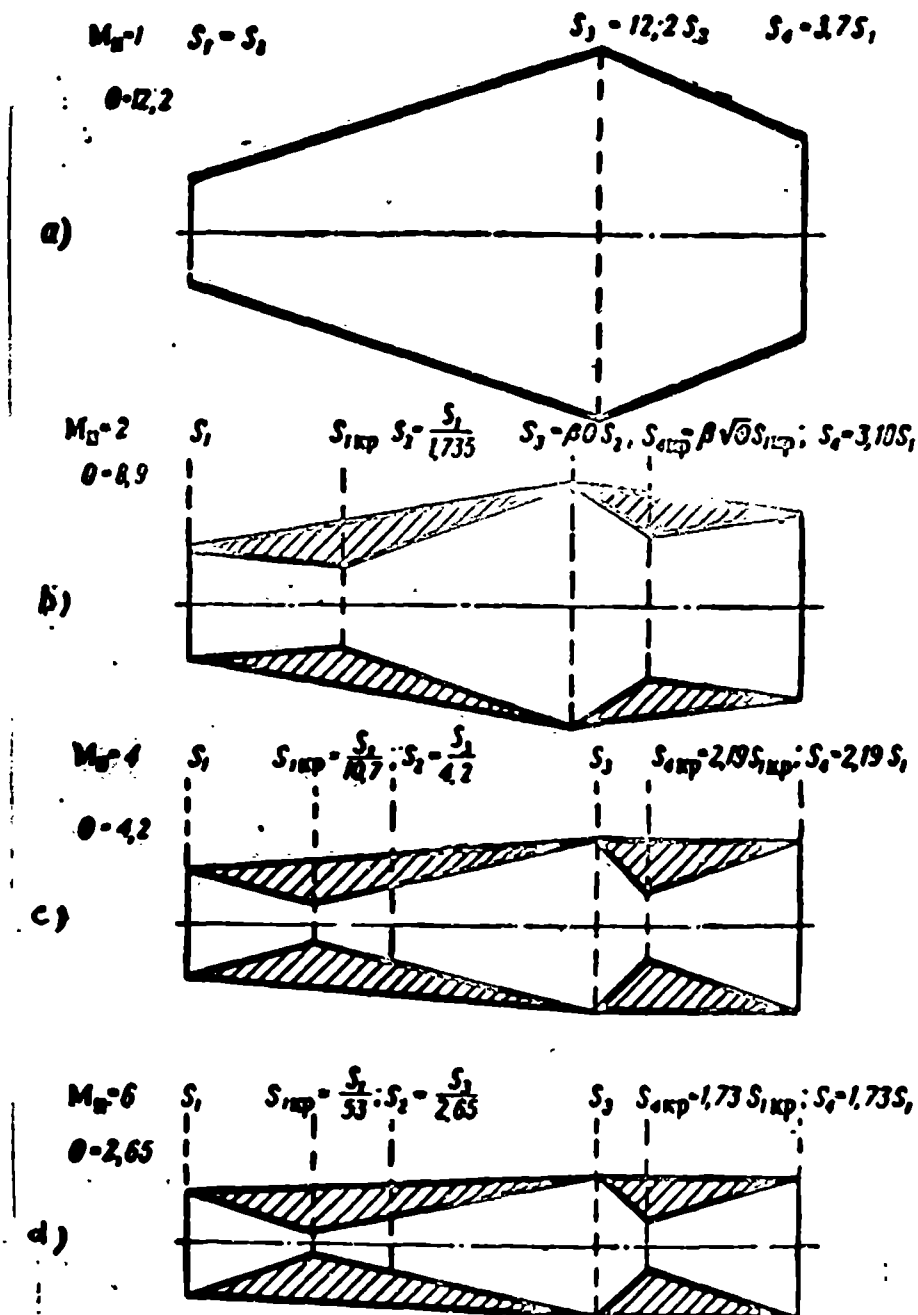
Fig. 54. Variation of the computed form of an ideal ramjet engine during the variation of flight speed when $\alpha = 1$.
a) $M_n = 1$; b) $M_n = 2$; c) $M_n = 4$; d) $M_n = 6$
Note: According to schematic a), the heating process begins at the inlet section of the diffuser and proceeds simultaneously with the compression process.

consequently,

$$\frac{p_{03}}{p_{\text{н}}} = \frac{p_{04}}{p_4} = \left(1 + \frac{k-1}{2} M_{\text{н}}^2\right)^{\frac{k}{k-1}} = \left(1 + \frac{k-1}{2} M_4^2\right)^{\frac{k}{k-1}} \cdot$$

or

$$\left(1 - \frac{k-1}{k+1} \lambda_{\text{н}}^2\right)^{\frac{k}{k-1}} = \left(1 - \frac{k-1}{k+1} \lambda_4^2\right)^{\frac{k}{k-1}}.$$

Hence

$$M_4 = M_u; \quad \lambda_4 = \lambda_u.$$
(3.23)

The Mach numbers or the relative velocities at the inlet to an ideal ramjet engine and at its exhaust are equal to each other.

The sections of the exhaust nozzle are also related to local velocities by equations (3.11), (3.12), and (3.13), in which the indices "n" and "2" are correspondingly replaced by "4" and "3."

We find the relationship of the terminal sections from the flow equation, noting that $\lambda_1 = \lambda_4$; $\frac{G_4}{G_1} = \beta$ and $\frac{T_{04}}{T_{0n}} = \theta$:

$$\frac{S_4}{S_1} = \beta \sqrt{\theta}.$$
(3.24)

Temperature ratio θ depends on the increase in temperature in heat exchanger ΔT, on the temperature of the surrounding atmosphere T_n, and on the flight velocity M_n:

$$\theta = \frac{T_{04}}{T_{0n}} = \frac{T_{03}}{T_{0x}} = \frac{T_{0x} + \Delta T}{T_{0x}} = 1 + \frac{\Delta T}{T_{0x}}.$$

$$\theta = \frac{T_{03}}{T_{0x}} = 1 + \frac{\Delta T \tau(\lambda_n)}{T_n}.$$
(3.25)

With an increase in flight speed, the stagnation temperature of the incoming flow T_{0x} increases and the temperature ratio θ decreases.

The increase in the temperature of a heated gas ΔT during the compression of a molecular fuel is determined by the lower heating value and the excess air coefficient α :

$$\Delta T = \frac{H_u}{c_p (1 + \alpha L)},$$
(3.26)

where c_p is the specific heat of the combustion products;

L is the quantity of air theoretically required for the combustion of 1 kg of fuel.

For hydrocarbon fuels $H_u \approx 10,000$ kcal/kg and $L \approx 15$. The specific heat of the combustion products increases with the increase in temperature; however, for the analysis of the ideal ramjet engine, we agreed to consider specific heat as constant: $c_p = 0.24$ kcal/kg deg. The relation of the temperature rise to α during operation with a hydrocarbon fuel is shown in Table 3.1.

TABLE 3.1

THE RELATION OF AIR HEATING DURING OPERATION WITH A HYDRO-

CARBON FUEL TO THE COMPOSITION OF THE MIXTURE

α	1	1,5	2,0	3,0	4,0
$\Delta T^\circ K$	2800	1770	1350	910	685

If the temperature of the atmospheric air $T_n = 216.5^\circ$ K, the stagnation tem-

perature ratio $\dfrac{T_{On}}{T_n}$ is equal to 1.2, and $\alpha = 1$, then the maximum possible temperature

rati J is equal to 12.2 when operating with a hydrocarbon fuel. With an increase

in flight speed, temperature ratio decreases (see Table 3.2).

TABLE 3.2

THE RELATION OF MAXIMUM COMBUSTION TEMPERATURE RATIO TO

VELOCITY WHEN $\dfrac{T}{T_n} = 10$

M_u	0,5	1,0	2	4	6	8	10
θ	10,5	9,3	6,55	3,38	2,23	1,72	1,48

With a sufficient increase in flight speed, the "thermal death" of an air-

breathing jet engine sets in, since combustion temperature ratio approaches to unity.

The increase in temperature during operation on atomic fuel is determined by

thermal power of the reactor N_Q, which is expressed in kilocalories per second, and

in air consumption G:

$$\Delta T = \frac{N_Q}{c_p G}.$$ (3.27)

The maximum increase in air temperature in a reactor is limited only by the

heat-resistance capability of the materials used.

Section 3. Thrust Parameters of an Ideal Ramjet Engine

The Mach numbers or the relative velocities at the inlet to an ideal engine and at

its outlet, as shown in the previous paragraph, are equal: $M_4 = M_n$; $\lambda_4 = \lambda_n$. The

stagnation temperature of the exhausting gases is higher than the stagnation tempera-

ture of the incoming flow:

$$T_{04} = T_{03} = \theta T_{02} = \theta T_{01} = \theta T_{0n}.$$ (3.28)

The critical velocity in the flow of exhausting gases is greater than the critical velocity of the incoming flow:

$$a_{\kappa} = \sqrt{\frac{2gkR}{k+1} T_{03}} = \sqrt{\frac{2gkR}{k+1} T_{0\kappa} \theta} = a_{\kappa} \sqrt{\theta}.$$ (3.29)

The velocity of the discharge is greater than the velocity of the influx:

$$\frac{w_4}{w_{\kappa}} = \frac{a_2 \lambda_4}{a_{\kappa} \lambda_{\kappa}} = \sqrt{\theta}.$$ (3.30)

Owing to an increase in the momentum of the gases, jet thrust R appears when $p_1 = p_n$ and $p_4 = p_n$; according to (2.92) it is equal to

$$R = \frac{G_4 w_4}{g} - \frac{G_{\kappa} w_{\kappa}}{g}.$$ (3.30a)

Noting (3.21) and (3.30), we obtain

$$R = \frac{G_{\kappa} w_{\kappa}}{g} \left(\beta \frac{w_4}{w_{\kappa}} - 1 \right) = \frac{\gamma_{\kappa} w_{\kappa}^2}{g} S_1 (\beta \sqrt{\theta} - 1).$$ (3.31)

The fraction $\frac{\gamma_{\kappa} w_{\kappa}^2}{g}$ is equal to twice the velocity head, q, of the free stream flow (2.70):

$$q = \frac{\gamma_{\kappa} w_{\kappa}^2}{2g} = \frac{k}{2} p_{\kappa} M_{\kappa}^2.$$

Noting (3.24), we obtain

$$R = 2qS_1 (\beta \sqrt{\theta} - 1) = kp_{\kappa} M_{\kappa}^2 S_4 \left(1 - \frac{1}{\beta \sqrt{\theta}} \right)$$ (3.32)

The frontal or maximum cross sectional thrust of an ideal ramjet engine is

$$R_{\kappa} = \frac{R}{S_{M}} = kp_{\kappa} M_{\kappa}^2 \frac{S_4}{S_{M}} \left(1 - \frac{1}{\beta \sqrt{\theta}} \right).$$ (3.33)

The ratio of the exhaust cross-sectional area to the maximum cross-sectional area is called the <u>relative</u> <u>exit</u> <u>ratio</u> $s_4 = \frac{S_4}{S_M}$. For subsonic ramjet engines $s_4 = 0.5$-1. For supersonic ramjet engines s_4 usually equals 1.

The thrust coefficient of an ideal ramjet engine is

$$c_R = \frac{R_{\kappa}}{q} = 2s_4 \left(1 - \frac{1}{\beta \sqrt{\theta}} \right).$$ (3.34)

It is seen from the last equation that when $s_4 = 1$, the thrust coefficient with an increase in heating, approaches the maximum value $c_{Rmax} = 2$.

With an increase in velocity the thrust coefficient decreases, owing to the decrease in combustion temperature ratio $\theta = \frac{T_{03}}{T_{0n}}$.

The specific thrust of an ideal ramjet engine operating on a molecular fuel is

$$I = \frac{R}{G_r} = \frac{\alpha L R}{G_\pi} = \frac{\alpha L c_R \, w_\pi}{2 g s_1} \, . \tag{3.35}$$

since the fuel consumption $\quad G_g = \dfrac{G_n}{L}$

Utilizing (3.31), we obtain

$$I = \frac{\alpha L w_\pi}{g}(\beta\sqrt{\theta}-1) = \frac{\alpha L c_\pi M_\pi}{g}(\beta\sqrt{\theta}-1). \tag{3.36}$$

With an increase in flight speed w_n or M_n, the specific thrust increases at first rapidly, passes the maximum, which lies near $M_n = 3$, and then begins to decrease, owing to the decrease in combustion temperature ratio θ .

Specific fuel consumption has the minimum value at the velocity w_n, at which the specific thrust reaches the maximum.

With an increase in excess air coefficient α the specific thrust increases, asymptotically approaching a certain limit.

Utilizing the equation (3.26), it is possible to write:

$$I = \frac{\alpha L w_\pi}{g}\left[\left(1+\frac{1}{\alpha L}\right)\sqrt{1+\frac{H_s}{c_p T_{0x}(1+\alpha L)}} - 1\right];$$

$$I = \frac{w_\pi}{g}\left[\sqrt{(1+\alpha L)^2 + \frac{H_s(1+\alpha L)}{c_p T_{0x}}} - \alpha L\right]. \tag{3.37}$$

This conception of specific thrust is not applicable in the case of an engine operating on nuclear energy, since the consumption of atomic fuel is insignificantly small.

The economy of an engine both during operation on a molecular and during operation on a nuclear fuel may be characterized by its efficiency.

Section 4. Thermal Efficiency of an Ideal Ramjet Engine

The gases which flow through an ideal ramjet engine describe an operating cycle which is depicted in Fig. 52. The increase in the kinetic energy of the gases describing this cycle may be expressed by the equation

$$A\frac{G_4 w_4^2 - G_\pi w_\pi^2}{2g} = G_4 c_p T_{04} - G_\pi c_p T_{02} - G_4 c_p T_4 + G_\pi c_p T_\pi. \tag{3.38}$$

The thermal power input $N_{Qzat} = G_4 c_p T_{04} - G_n c_p T_{02}$.

The thermal power lost to the surrounding space is

$$N_{\text{пот}} = G_4 c_p T_4 - G_\pi c_p T_\pi.$$

The ratio of the heat converted to kinetic energy, to the heat supplied is called the thermal efficiency of the η_t cycle:

$$\eta_t = \frac{G_4 c_p T_{04} - G_H c_p T_{02} - G_4 c_p T_4 + G_H c_p T_H}{G_4 c_p T_{04} - G_H c_p T_{02}} \qquad (3.39)$$

If the consumption of the working substance does not decrease during heating: $G_4 = G_n$, we obtain

$$\eta_t = 1 - \frac{T_4 - T_H}{T_{04} - T_{02}} . \qquad (3.40)$$

For an ideal ramjet engine $p_{04} = p_{02}$ and $p_4 = p_n$; consequently,

$$\frac{T_H}{T_{02}} = \left(\frac{p_H}{p_{02}}\right)^{\frac{k-1}{k}} = \frac{T_4}{T_{04}} = \left(\frac{p_4}{p_{04}}\right)^{\frac{k-1}{k}} . \qquad (3.41)$$

Substituting (3.41) in (3.40), we obtain

$$\eta_t = 1 - \frac{T_H\left(\frac{T_{04}}{T_{02}} - 1\right)}{T_{0H}\left(\frac{T_{04}}{T_{02}} - 1\right)} = 1 - \frac{T_H}{T_{0H}} \qquad (3.42)$$

or

$$\eta_t = 1 - \left(\frac{p_H}{p_{02}}\right)^{\frac{k-1}{k}} . \qquad (3.43)$$

The thermal efficiency of an ideal ramjet engine depends only on the ratio of the stagnation pressure of the incoming flow p_{0n} to the static pressure p_n. This ratio depends on the relative flight speed or Mach number. Utilizing (3.43) and (3.4), we obtain

$$\eta_t = 1 - \frac{1}{1 + \frac{k-1}{2} M_H^2} = \frac{k-1}{k+1} \lambda_H^2 . \qquad (3.44)$$

The thermal efficiency of an ideal ramjet engine is directly proportional to the square of the relative flight speed. When $\lambda_n = 0$, $\eta_t = 0$; when

$$\lambda_H = \lambda_{max} = \sqrt{\frac{k+1}{k-1}} \ (M_H = \infty), \ \eta_t = 1$$

The rapid growth in thermal efficiency with increasing velocity is one of the important features of a ramjet engine (Table 3.3).

TABLE 3.3

THE RELATION OF THE THERMAL EFFICIENCY OF AN IDEAL RAMJET ENGINE TO THE MACH NUMBER

M_H	1	2	3	4	6	10
η_t %	16,7	44,4	64,2	76,2	83	99

The temperature increase of the working substance in an engine operating on

a molecular fuel occurs due to the heat released in the combustion chamber:

$$c_p(T_{04} - T_{02}) = \frac{H_u}{1 + \alpha L}.$$ (3.45)

Consequently,

$$\eta = A \frac{G_4 w_4^2 - G_u w_u^2}{2 g c_p G_4 (T_{04} - T_{0u})} = \frac{A_2 L}{H_u} \frac{\beta w_4^2 - w_u^2}{2 g}.$$ (3.46)

The thermal efficiency characterizes the completeness of the transformation of the supplied heat to the kinetic energy of the gas stream.

Section 5. Thrust Efficiency of an Ideal Ramjet Engine

The useful or thrust power of an engine N_{tyag} is equal to the product of the force of thrust R and the flight speed w_n:

$$N_{tyag} = R w_n.$$ (3.47)

Substituting (3.30a) in (3.47), we obtain

$$N_{tyag} = \frac{G w_u^2}{g} \left(\beta \frac{w_4}{w_u} - 1 \right).$$ (3.48)

The ratio of the thrust power N_{tyag} to the increase in the kinetic energy of gases, whose discharge creates jet thrust R, is called the <u>thrust efficiency of the engine</u> η_{tyag}:

$$\eta_{tyag} = \frac{R w_u}{G \dfrac{\beta w_4^2 - w_u^2}{2g}} = \frac{2 w_u (\beta w_4 - w_u)}{\beta w_4^2 - w_u^2}.$$ (3.49)

The conception of thrust efficiency was introduced to science by N. Ye. Zhukovskiy for the case of ship's movement. This conception of thrust efficiency was first used by B.S. Stechkin in relation to ramjet engines.

The formula for thrust efficiency may appear very simple, if the heating occurs without an increase of the mass of the working substance $\beta = 1$.

$$\eta_{tyag} = \frac{2 w_u}{w_4 + w_u} = \frac{2}{\sqrt{\theta} + 1}.$$ (3.50)

If the device flies at velocity w_n and the gases discharge from the nozzle at speed w_4, then the speed of the gases relative to the surrounding air is equal to the difference of $w_4 - w_n$. The kinetic energy of the exhausting gases in relation to the surrounding air is equal to $G \dfrac{w_4^2 - w_u^2}{2g}$.

Thrust efficiency is equal to the ratio of useful thrust power to the sum of

useful power and the gases' kinetic energy due to their motion

$$\eta_{\text{тяг}} = \frac{\mathfrak{k}w_{\text{и}}}{\mathfrak{k}w_{\text{и}} + G\frac{(w_4 - w_{\text{и}})^2}{2g}} = \frac{\mathfrak{k}w_{\text{и}}}{G\frac{w_4^2 - w_{\text{и}}^2}{2g}} .$$ (3.51)

For an increase in thrust efficiency, the difference between the discharge velocity and the free stream velocity, i.e., combustion temperature ratio $\sqrt{\bar{\theta}} = \frac{w_4}{w_{\text{и}}}$. must be decreased.

It is seen from equation (3.50) that thrust efficiency depends only on the combustion temperature ratio θ. A given thrust may be obtained either by increasing the discharge velocity or by increasing the air input G. The second way is advantageous, since it gives the greater thrust efficiency (Table 3.4).

TABLE 3.4

THRUST EFFICIENCY OF AN IDEAL RAMJET ENGINE η_{tyag} %

VERSUS THE MACH NUMBER AND THE EXCESS AIR

COEFFICIENT α.

$M_{\text{и}}$ / $\bullet$	1	2	3	4	6	10
1.0	43	50	57	64	74	85
3.0	62	69	75	81	88	93
5.0	71	77	83	87	92	96

Section 6. General or Total Efficiency of an Ideal Ramjet Engine

The general or total efficiency of an ideal ramjet engine is equal to the ratio of the useful thrust power to the thermal power input

$$\eta = \frac{N_{\text{тяг}}}{N_Q} = \frac{\mathfrak{k}w_{\text{и}}}{c_p G (T_{04} - T_{0\text{и}})} .$$ (3.52)

Total efficiency may be conceived as the product of multiplication of the thermal efficiency, characterizing the ramjet engine as a heat engine, by the thrust efficiency, characterizing an air-breathing jet engine as propelling agent. In the case of a power plant with a propeller, both of these coefficients are clearly limited: the engine is characterized by thermal efficiency and the propeller by thrust efficiency. In the case of a jet engine both of these coefficents are characterized by the action of a single unit and are organically related to each other.

The expression (3.52) may be transformed in the following manner:

$$\eta = A \frac{w_4^2 - w_n^2}{2gc_p(T_{04}-T_{0n})} \frac{Rw}{\frac{G}{2g}(w_4^2 - w_n^2)}$$

The first factor according to (3.46) represents thermal efficiency η_t, the second factor according to (3.49) represents thrust efficiency η_{tyag}. Consequently,

$$\eta = \eta_t \eta_{tyag}.$$ (3.53)

Utilizing (3.44) and (3.50), we obtain

$$\eta = \frac{k-1}{k+1}\lambda_n^2 \frac{2}{\sqrt{\theta}+1}.$$ (3.54)

Total efficiency is directly proportional to the square of the relative flight speed λ_n. With an increase in temperature ratio $\theta = \frac{T_4}{T_{0n}}$, total efficiency decreases. If heating of the gases is absent: $\theta = 1$, then $w_4 = w_n$ and $\eta_{tyag} = 1$. But the flow momentum does not increase thereby, and the thrust is equal to zero. With an increase in temperature ratio θ, the kinetic energy of the exhausting gases $\frac{G}{2g}(w_4^2 - w_n^2)$ increases and the thrust and total efficiency diminish. With moderate heating $\theta = 3$-4 and supersonic flight velocities, the total efficiency of ideal ram jet engines is very high (Table 3.5). Thus, when $M_n = 3$ and $\theta = 3$ $\eta = 49\%$, i.e., greater than that of any other thermal power plant.

TABLE 3.5

TOTAL EFFICIENCY OF AN IDEAL RAMJET ENGINE

$\eta\%$ VS. THE FLIGHT SPEED AND

AIR COEFFICIENT α WHEN $H_u = 10,500$ AND L = 15

M_n / α	1	2	3	4	6	10
1,0	7,3	22	37	49	65	84
2,0	10,4	30,5	49	62	77	92
3,0	11,9	34	54	66	81	95

With decreasing heating η grows, but the thrust coefficient becomes smaller than the drag coefficient of the aircraft and the engine becomes useless for flight.

Section 7. Characteristics of an Ideal Ramjet Engine

The thrust parameters of an ideal ramjet engine depend on the velocity, temper

ture, and pressure of the air, on the temperature ratio of the gases, and on a number of other parameters.

The dependence of the thrust coefficient c_R, the specific thrust I, frontal thrust R_H, the calculated cross sections $\frac{S_4}{S_1}$ and $\frac{S_{4cr}}{S_{1cr}}$ and other parameters on the speed and altitude of flight, as well as on the heating of the gases in the combustion chamber are called the engine characteristics. Speed, altitude, and control characteristics have the greatest values.

The speed characteristics of an ideal ramjet engine (Fig. 55 a, b, c, d) represent the relation of the engine parameters vs. the relative flight velocity λ_n or the Mach number M_n at a given flight altitude H and combustion temperature ratio θ or excess air coefficient α.

The stagnation temperature increases with an increase in flight speed (3.3). The combustion temperature ratio at a constant excess air coefficient α = const decreases with an increase in speed:

$$\theta = \frac{T_{04}}{T_{0H}} = 1 + \frac{H_a \tau (\lambda_4)}{c_p T_H (1 + \alpha L)}$$

The relative discharge velocity $\frac{w_4}{w_n}$ and the ratio of the terminal and throat sections $\frac{S_4}{S_1}$ and $\frac{S_{4cr}}{S_{1cr}}$ decrease with an increase in speed, owing to the decrease in combustion temperature ratio:

$$\frac{S_4}{S_1} = \frac{S_{4\,cr}}{S_{1\,cr}} = \beta \frac{w_4}{w_1} = \beta \sqrt{\theta}.$$

When

$$\lambda_n \to \sqrt{\frac{k+1}{k-1}} \qquad \tau \to 1 \qquad \left(\frac{S_4}{S_1}\right) \to 1,$$

i.e., the engine becomes cylindrical.

The thrust coefficient decreases with an increase of M, owing to the decrease in the relative exhaust velocity $\frac{w_4}{w_n} = \sqrt{\theta}$.

When $\sqrt{\theta} \to 1$, according to (3.34) $c_R \to 0$.

The specific thrust, according to (3.36), first grows with an increase in flight speed, owing to the increased pressure in the chamber and the increase of thermal efficiency; then passes over maximum, which lies near $M \approx 3$; and begins to diminish, owing to the decrease in the relative exit velocity $\frac{w_4}{w_n} = \sqrt{\theta}$ (see Fig. 55, c).
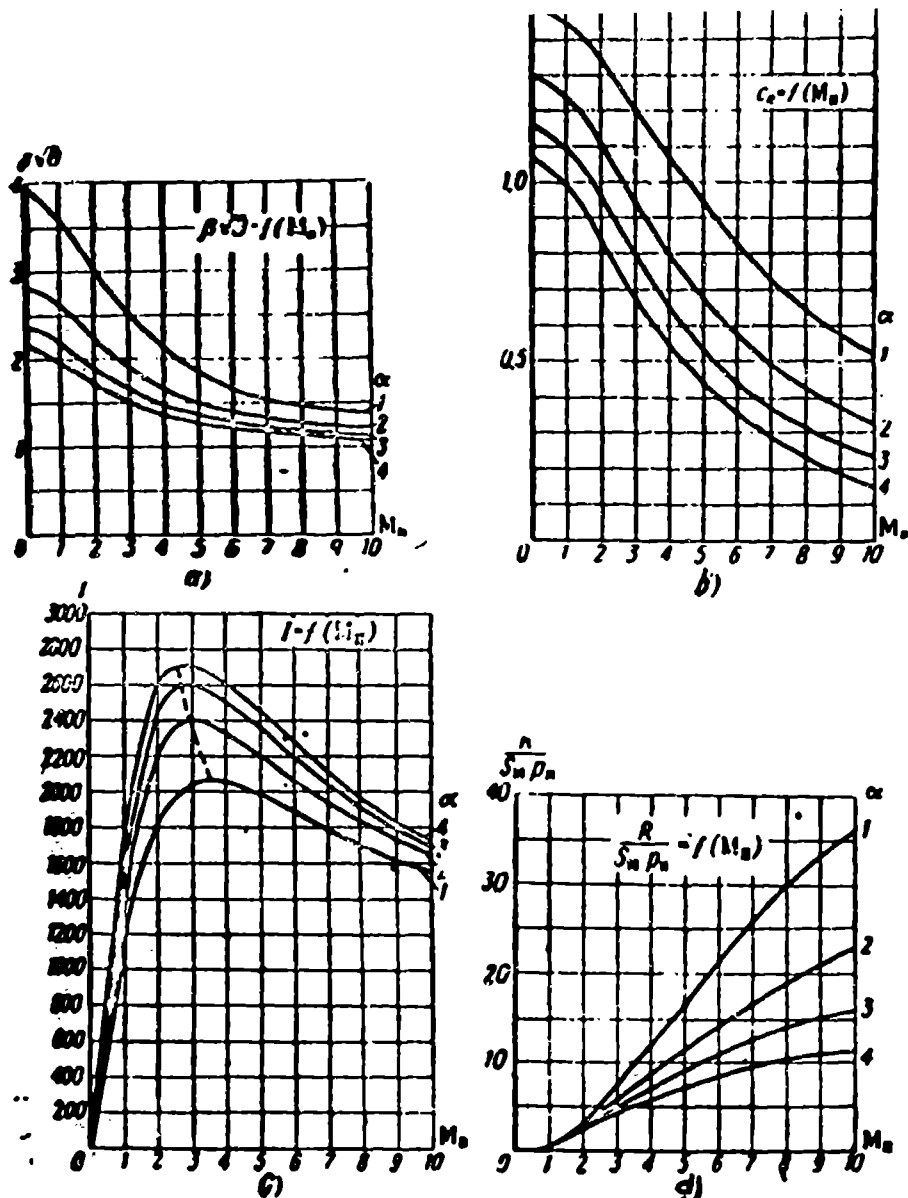
Fig.55. Velocity characteristics of an ideal ramjet engine.

a) $\beta \sqrt{\theta} = f(M_n)$; b) $c_R = f(M_n)$; c) $I = f(M_n)$; d) $\dfrac{R}{S_M P_n} = f(M_n)$.

The relative frontal thrust $\dfrac{R}{p_n}$ at $M < 1$, when c_R varies insignificantly, is directly proportional to M_n^2. With the subsequent increase in M, the frontal thrust goes past the maximum, which lies near very high Mach numbers (see Fig. 55, d).

With an increase in M, the density and pressure of the flow in the throat section increases and the calculated ratio of the throat section diminishes (see 3.12 and Fig. 54).

For this reason, an ideal ramjet engine, which fundamentally is a single-speed engine, suitable for one flight speed $M_n = M_{rasch}$ and for a single value of combustion temperature ratio $\theta = \theta_{rasch}$. With a deviation from the rated operating conditions, compression and discharge cease to be reversible, and the parameters of the ramjet engine cease to comply with Poisson's equation. However, achieving the reversible compres-

sion of a supersonic flow in a tapering diffuser is difficult even at rated operating conditions (see Chapter IV, Section 6).

An ideal ramjet engine, suitable for flight at various Mach numbers, would have to possess controllable cross sections and a variable area diffuser and nozzle.

The **altitude** **characteristics** of an ideal ramjet engine are shown in Fig. 56. With a variation in flight altitude, the pressure and temperature of the surrounding air change and, together with them, the parameters which depend on T_n and p_n.

Combustion temperature ratio θ increases with an increase in altitude, owing to the decrease in air temperature T_n: $\qquad \theta = 1 + \dfrac{H_u \tau (\lambda_u)}{c_p (1 + \varkappa L) T_u}.$
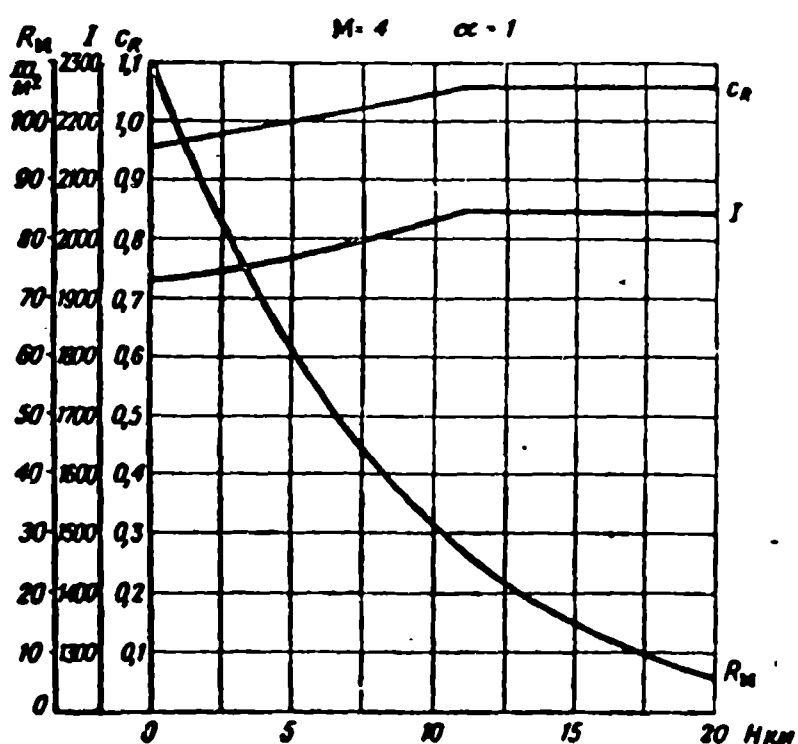
Fig. 56 Altitude characteristics of an ideal ramjet engine.

After crossing the limits of the troposphere ($H > 11$ km), the air temperature remains constant, and the combustion temperature ratio ceases to vary. Beyond the limits of the stratosphere, the temperature ceases to be constant (see Table 1.1).

Together with the change in combustion temperature ratio θ the relative exit velocity and ratio of the exit nozzle sections change:

$$\frac{S_4}{S_n} = \beta \frac{w_4}{w_n} = \beta \sqrt{\theta}.$$

With an increase in altitude from 0 to the beginning of the stratosphere,

θ **increases** along with an increasing thrust coefficient c_R (see Fig. 5c)

$$c_R = 2\left(1 - \frac{1}{\beta\sqrt{\theta}}\right).$$

The specific thrust I grows insignificantly with an increase in altitude, owing to the increase of temperature ratio across the combustion chamber:

$$I = \frac{\alpha L}{g} w_{\scriptscriptstyle \rm H}\left(\beta\frac{w_4}{w_{\scriptscriptstyle \rm H}} - 1\right) = $$
$$= \frac{\alpha L}{g} M_{\scriptscriptstyle \rm H}\sqrt{gkRT_{\scriptscriptstyle \rm H}}\left[\beta\sqrt{1 + \frac{H_u\tau(\lambda_{\scriptscriptstyle \rm H})}{(1+\alpha L)c_p T_{\scriptscriptstyle \rm H}}} - 1\right].$$

Maximum cross sectional thrust diminishes with an increase in altitude, due to the decrease in air pressure $p_{\scriptscriptstyle \rm H}$:

$$R_{\scriptscriptstyle \rm H} = kp_{\scriptscriptstyle \rm H}M_{\scriptscriptstyle \rm H}^2\left(1 - \frac{1}{\beta\sqrt{\theta}}\right).$$

In the troposphere, the loss of maximum cross sectional thrust is somewhat reduced by the increase in temperature ratio θ .

The decrease in thrust does not prevent a ramjet engine from being used at various altitudes, since the aerodynamic drag of the aircraft X also varies proportionally to the pressure of the surrounding medium:

$$X = c_x S_{\scriptscriptstyle \rm H}\frac{\gamma_{\scriptscriptstyle \rm H}w_{\scriptscriptstyle \rm H}^2}{2g} = \frac{1}{2}c_x S_{\scriptscriptstyle \rm H}kp_{\scriptscriptstyle \rm H}M_{\scriptscriptstyle \rm H}^2.$$

The <u>control</u> (<u>throttle</u>) <u>characteristics</u> of a ramjet engine **represent** the dependence of the engine parameters on the excess air coefficient α or on the fuel supply factor $\frac{1}{\alpha}$ at a given Mach number for the free stream flow $M_{\scriptscriptstyle \rm H}$ = const and a given flight altitude H = const (Fig. 57).

The discharge of air through an ideal ramjet engine does not depend on the fuel supply

$$G = w_{\scriptscriptstyle \rm H}\gamma_{\scriptscriptstyle \rm H}S_1 = \sqrt{gkRT_{\scriptscriptstyle \rm H}}\ \frac{p_{\scriptscriptstyle \rm H}M_{\scriptscriptstyle \rm H}}{RT_{\scriptscriptstyle \rm H}}\ S_1 = \sqrt{\frac{gk}{R}}\ \frac{p_{\scriptscriptstyle \rm H}S_1}{\sqrt{T_{\scriptscriptstyle \rm H}}}\ M_{\scriptscriptstyle \rm H}.$$

Therefore the fuel supply factor $\frac{1}{\alpha}$ is directly proportional to the fuel weight flow G_g:

$$\frac{1}{\alpha} = \frac{LG_r}{G}\ .$$

When the fuel supply is cut off, $G_g = 0$, $\frac{1}{\alpha} = 0$, $\alpha = \infty$, temperature ratio $\theta = 1$, and relative exit velocity $\frac{w_4}{w_{\scriptscriptstyle \rm H}} = \sqrt{\theta} = 1$. At the same time,

$$\left(1 - \frac{1}{\beta\sqrt{\theta}}\right) = 0, \quad S_4 = S_1, \quad c_R = 0, \quad I = I_{max}.$$

With an increase in fuel flow G_g, temperature ratio θ increases, and, together with it, the relative exit velocity $\frac{w_4}{w_n}$, the ratio of $\frac{S_4}{S_n}$, the thrust coefficient $c_R = 2 \left(1 - \frac{1}{\beta\sqrt{\theta}}\right)$, and the frontal thrust $R_\ell = c_R c$ increase.too.

Impulse, I, decreases from the maximum value I_{max} to I_{min} when $\alpha = 1$. An engine intended for maximum thrust must operate when $\alpha = 1$.
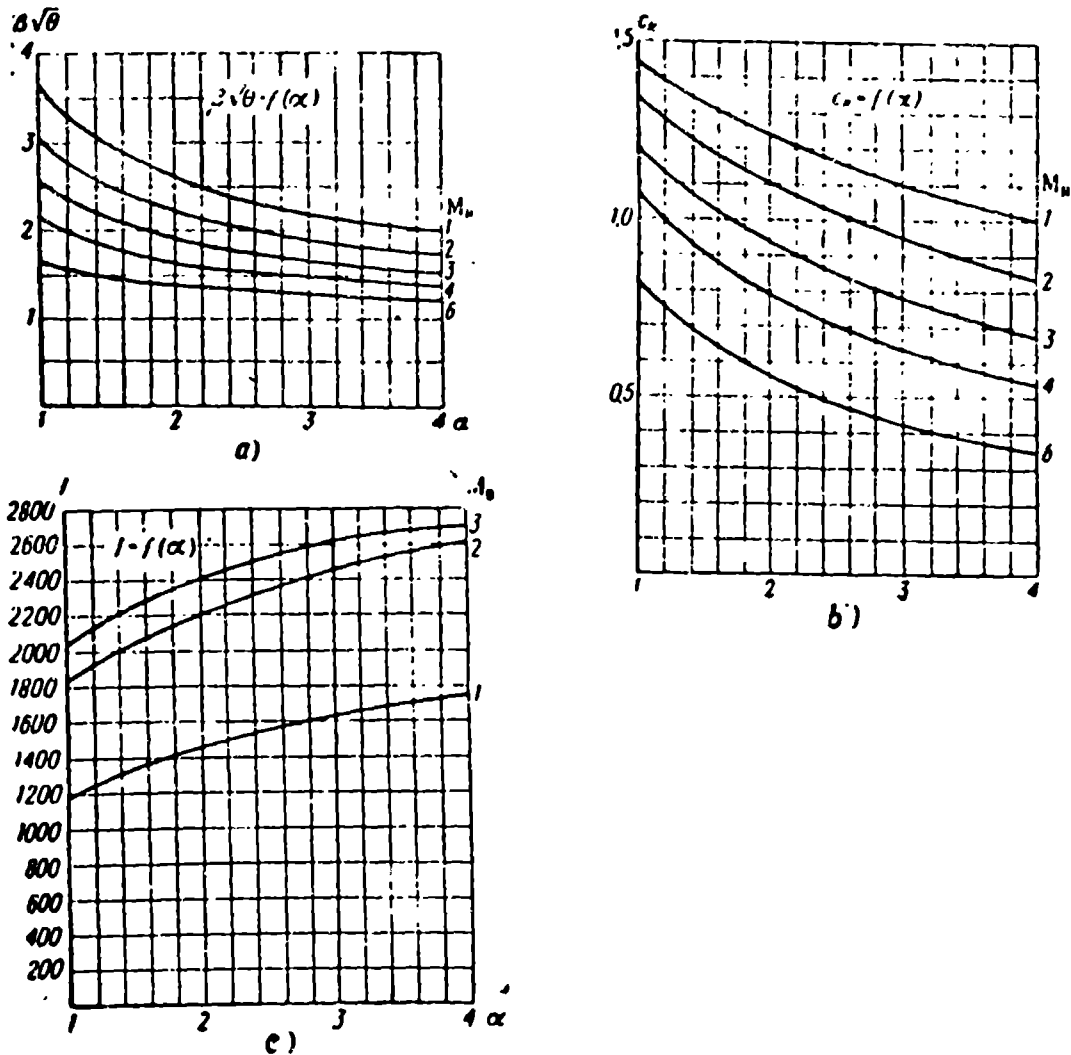
Fig. 57. Control characteristics of an ideal ramjet engine.
a) $\beta\sqrt{\theta} = f(\alpha)$; b) $c_R = f(\alpha)$; c) $J = f(\alpha)$.

The dependence of the calculated cross sections of an ideal ramjet engine upon the mixture ratio is shown in Fig. 58.

An engine intended for long range must operate at the least possible fuel flow, since with a decrease in $\frac{1}{\alpha}$, the range factor I^k (1.15) increases.

The decrease in fuel flow is limited only by the drag coefficient c_x of an aircraft, since during horizontal flight $c_R \geqslant c_x$. (Both coefficients are usually based upon the midship or maximum cross section of an engine.)
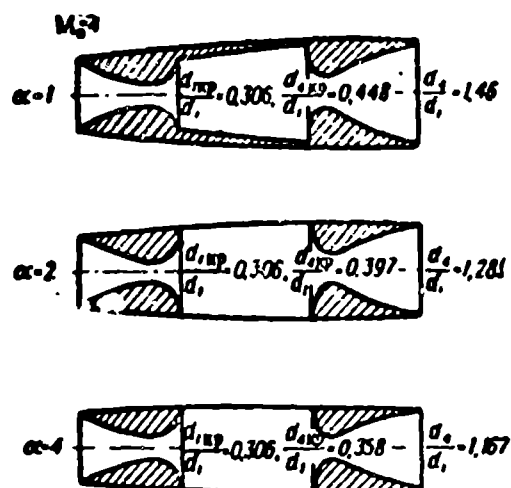
Fig. 50 The computed values of the through sections of an ideal ramjet engine.

BIBLIOGRAPHY

1. Zhukovskiy, N. Ye., Sobraniye sochineniy /Collected Works/, Vol II, Gostekhizdat, Moscow-Leningrad, 1948.

2. Stechkin, B. S., Teoriya vozdushnogo reaktivnogo dvigatelya /Theory of Air-Breathing Jet Engines/, TVF, 1929, No 2.

3. Stechkin, B. S., Teoriya Vozdushno-Reaktivnikh Dvigateley /Theory of Air-Breathing Jet Engines/, A Synopsis of Lectures, VIA imeni Zhukovskiy, 1945.

4. Sänger, F. and Bredt, I., Pryamotochnyye VRD dlya istrebiteley /Ramjet Engines for Pursuit Aircraft/. NACA Techn. Memo 1106, Oct. 1947.

5. Ackeret, J., "Probleme des Flugzeugantriebes in Gegenwart und Zukunft," NACA TN, No 976, May, 1941.

6. Leduc, R. et Viley, U. I., "Sur les tuyeres thermopropulsive," C. R. Acad. Sc., Paris, vol. 202, 1936.

7. Leduc, R. et Viley, U. I., "Le rendement des tuyeres propulsives," C. R. Acad. Sc., Paris, vol. 202, 1936.

8. Becker, I. V. and D. D. Baals, "Analysis of Heat and Compressibility Effects in Internal Flow Systems and High-Speed Tests of a Ramjet System," NACA Rep. No 773, 1942.

Diffusers transform the velocity head of an incoming flow to static pressure. The diffusers of ramjet engines have the same function as compressors of gas turbine engines. The greater the pressure increases in a diffuser $\frac{P_{02}}{P_n}$, the less the entropy of the compressed gas s, the greater its potential energy and the greater the thermal efficiency η_t of the engine.

Pressure recovery in a diffuser has a decisive significance for the operation of the engine as a whole.

The geometrical form of the diffuser at which the relative pressure increase will be the greatest is determined by the Mach number of the free stream flow M_n. The structure of subsonic diffusers ($M_n < 1$), transsonic diffusers ($M_n = 1-2$), and supersonic diffusers ($M_n > 2$) differs essentially from one another.

The action of diffusers may be characterized by the following coefficients: efficiency η_d, pressure recovery σ_d, additive drag c_{xd}, local losses ζ, and air flow ratio φ.

Section 1. Efficiency, Pressure Recovery, and Mass Flow Factors

The operation of actual diffusers is accompanied by energy losses from friction and shocks, due to which a portion of the kinetic energy of the flow is dissipated and the free energy of the gas decreases. The utilization of a flow's kinetic energy in a diffuser is characterized by the efficiency η_d.

The ratio of the increase in free energy of the compressed air Δu to the kinetic energy of the flow $\frac{w^2}{2g}$ is called diffuser efficiency:

$$\eta_A = \frac{\Delta u}{\frac{w_n^2}{2g}}.$$

(4.1)

With a reversible discharge from the nozzle which is joined to the exhaust section of the diffuser (Fig. 59), the free energy of the compressed air is turned into the kinetic energy of the stream:

$$\Delta u = \frac{v_{\text{ист}}^2}{2g}.$$ (4.2)

Consolidating (4.1) and (4.2), we find that the efficiency of the diffuser is

asured by the ratio of the kinetic energy of gas after a reversible discharge $\frac{w_{\text{ist}}^2}{2g}$

the kinetic energy of the incoming flow $\frac{w_{\text{н}}^2}{2g}$:

$$\eta_{\text{д}} = \frac{w_{\text{ист}}^2}{w_{\text{н}}^2}.$$ (4.3)
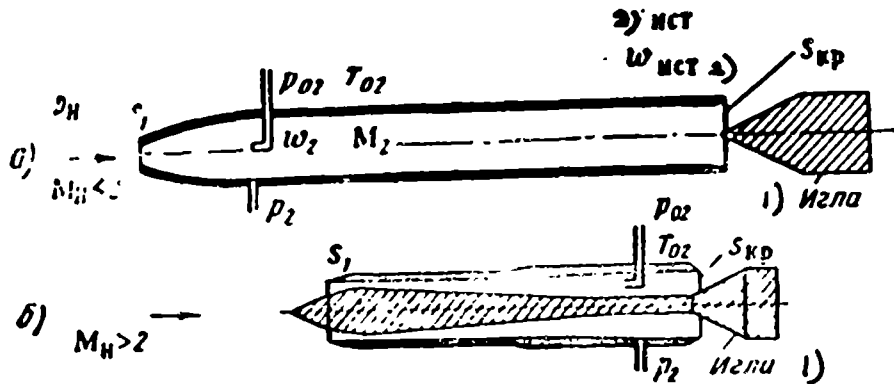
. 59. Diagram of diffuser tests.   Legend: 1) spike; 2) discharge
      a -- subsonic; b -- supersonic.

If heat exchange with the surrounding air is absent, then the stagnation temp-

ature $T_{0\text{н}}$ does not change during a flow through the diffuser:

$$T_{0\text{н}} = T_{\text{н}} + \frac{w_{\text{н}}^2}{2g\frac{kR}{k-1}} = T_{\text{ист}} + \frac{w_{\text{н}}^2 \tau_{\text{д}}}{2g\frac{kR}{k-1}}.$$ (4.4)

The greater the dissipation of energy, i.e., the lesser the efficiency of the

fuser η_{d}, the higher the static pressure of gases after a reversible discharge

t.

From (4.4) we find

$$\frac{T_{\text{ист}}}{T_{\text{н}}} = 1 + \frac{k-1}{2} M_{\text{н}}^2 (1 - \tau_{\text{д}}).$$ (4.5)

We find the increase in flow entropy when p = const by using (4.5)

$$\Delta s = \frac{\Delta u_{\text{ямс}}}{T_{\text{н}}} = \frac{c_p (T_{\text{ист}} - T_{\text{н}})}{T_{\text{н}}} = \frac{k-1}{2} c_p M_{\text{н}}^2 (1 - \tau_{\text{д}}).$$ (4.6)

The stagnation pressure of the discharging air is ecual to the stagnation pres-

e of an actual diffuser, since the exhaust actually occurs under the action of

s pressure:

$$\frac{p_{02}}{p_{\text{н}}} = \left(1 + \frac{w_{\text{н}}^2 \eta_{\text{д}}}{2k\frac{kR}{k-1}T_{\text{ист}}}\right)^{\frac{k}{k-1}}.$$ (4.7)

After substituting here T_{ist} from (4.6), we obtain an equation which expresses

stagnation pressure in terms of the velocity of the incoming flow and of the efficiency of the diffuser

$$\frac{p_{02}}{p_{\text{H}}} = \left[1 + \frac{w_{\text{H}}^2 \eta_{\text{A}}}{2g \frac{kR}{k-1} T_{\text{H}} + w_{\text{H}}^2 (1-\eta_{\text{A}})} \right]^{\frac{k}{k-1}} =$$

$$= \left[1 + \frac{\eta_{\text{A}}}{\frac{2}{k-1} \frac{1}{M_{\text{H}}^2} + 1 - \eta_{\text{A}}} \right]^{\frac{k}{k-1}} . \qquad (4.8)$$

When $\eta_d = 1$ the equation (4.8) turns into a well-known equation for reversible stagnation pressure; when $\eta_d = 0$, $\frac{p_{02}}{p_{\text{H}}} = 1$.

Equation (4.8), which expresses the stagnation pressure in an actual diffuser diffuser in terms of efficiency η_d, is involved and unsuitable for practical computations; diffuser efficiency η_d is difficult to measure in practice. Therefore, although the value η_d has a clear-cut physical meaning, it is seldom used.

The quality of an actual diffuser is usually evaluated b_ <u>pressure recover</u>_ <u>factor</u> σ_d.

The ra_io of the stagnation pressure of the flow which passes through a diffuser, to the reversible stagnation pressure of the incoming flow is called the <u>pressure recovery factor</u> σ_d.

$$\sigma_{\text{A}} = \frac{p_{02}}{p_{0\text{H}}} = \frac{p_{02}}{p_{\text{H}} \left(1 + \frac{k-1}{2} M_{\text{H}}^2 \right)^{\frac{k}{k-1}}} = \frac{p_{02} \pi (\lambda_{\text{H}})}{p_{\text{H}}} . \qquad (4.9)$$

The greater the kinetic-energy losses occasioned by friction and shocks as the flow enters the diffuser, i.e., the greater the dissipation of energy, the lesser the pressure recover_ factor σ_d. For total dissipation of kinetic energy, the pressure does not increase during the flow deceleration: $p_{02} = p_{\text{H}}$. In this case the diffuser pressure recovery factor has the minimum possible value σ_{min}:

$$\sigma_{\text{min}} = \frac{p_{02}}{p_{0\text{H}}} = \frac{p_{\text{H}}}{p_{0\text{H}}} = \pi (\lambda_{\text{H}}).$$

With an increase in velocity of the incoming flow λ_n or M_n, the minimum possible value of the pressure recovery factor σ_{min} decreases (see Fig. 70). The pressure recover_ factor of an actual diffuser σ_d lies between unity and σ_{min}:

$$\pi(\lambda_H) < \sigma_\lambda < 1.$$

The pressure recovery factor is easily measured in practice: diffuser stagnation pressure is measured by means of a Pitot tube; the Mach number of the incoming flow is measured, for example, by means of a machmeter or by the incidence angle of an oblique shock wave which appears in the presence of the airflow around a wedge or a cone (these shock waves are distinctly visible in a Tepler instrument or in shadow photographs).

The dependence of the pressure recovery factor upon the Mach number of the free stream flow is called the diffuser characteristic (see Fig. 72).

Air input through the diffuser depends upon the cross-sectional area of the tube's exhaust opening which is joined to the diffuser (see Fig. 59), and upon stagnation parameters p_{02} and T_{02}.

The ratio of the diffuser's inlet section S_1 to the area of its exhaust opening section S_2 is called the diffuser area ratio f:

$$f = \frac{S_1}{S_2}. \tag{4.10}$$

The ratio of the weight flow rate of air G_1 through a diffuser to that weight flow rate at which the velocity at the inlet is equal to the velocity of the undisturbed flow, is called the weight flow ratio φ:

$$\varphi = \frac{G_1}{\gamma_H w_H S_1} = \frac{\gamma_1 w_1}{\gamma_H w_H} = \frac{S_H}{S_1}. \tag{4.11}$$

For subsonic diffusers, the weight flow ratio may be either lesser or greater than one: $\varphi \lessgtr 1$. For supersonic diffusers (see Section 5 and those following) $\varphi \leqslant 1$.

Section 2. Additive Drag of Diffusers. Local Resistance Factor

Let us examine the flow that enters a diffuser (Fig. 60). Its velocity at the inlet section of diffuser w_1 is not equal to the velocity of the free stream flow w_H.

This surplus air impulse which passes through the diffuser is expressed by equation (2.77)

$$(F_H)_{area} = \frac{G_H w_H}{g}. \tag{4.12}$$

According to the theorem of impulses, this surplus impulse, acting in inlet section S_1, is equal to

$$(F_1)_{изб} = \frac{G_0 w_1}{g} + (p_1 - p_н) S_1. \qquad (4.13)$$

The difference between the decelerating force of the flow acting in section S_1 and the momentum of the enclosed air is called the <u>additive diffuser drag</u> X_d:

$$X_д = (F_1)_{изб} - (F_н)_{изб} = \frac{G_н w_1}{g} + (p_1 - p_н) S_1 - \frac{G_0 w_н}{g}. \qquad \lfloor изб = surplus \rfloor \quad (4.14)$$

The air which moves from section $S_н$ to section S_1 varies in its velocity from value $w_н$ to w_1. At the same time, the pressure varies from $p_н$ to p_1.

Additive drag is represented by a force which would act on the external surface of a solid flow tube H-1 (see Fig. 60). The force which acts upon the surface of the flow entering the diffuser, i.e., the enclosed air, varies its momentum. According to the law of the equality of motion and countermotion, the flow acts upon the diffuser with a counteracting force X_d equal in magnitude but opposite in direction.

Additive drag may be calculated theoretically by determining the velocity w_1 and the pressure p_1, or may be measured experimentally.
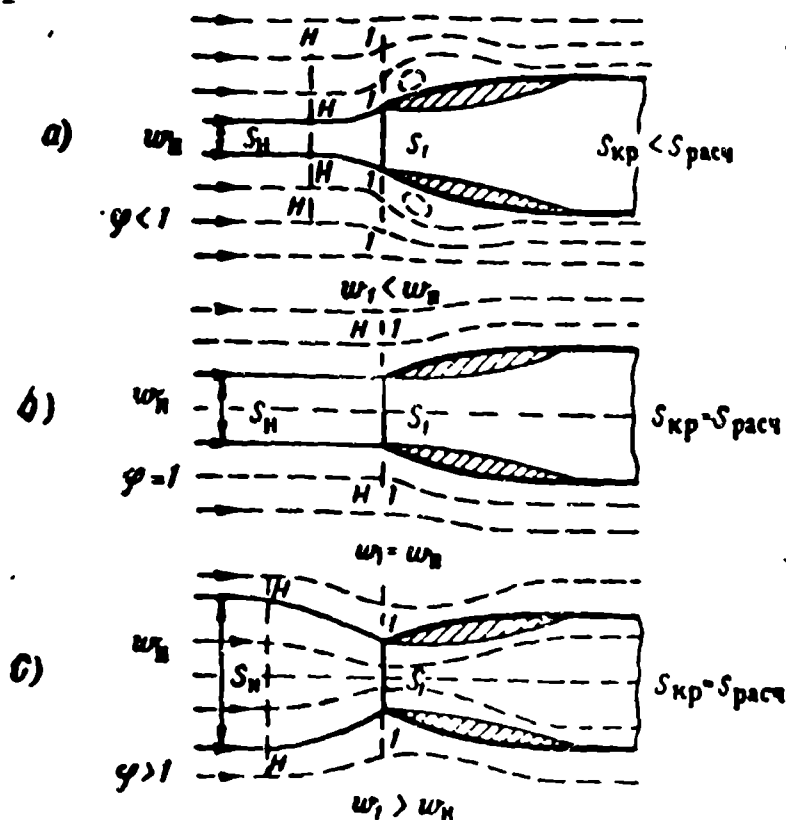
Fig. 60 Stream lines at the inlet to a subsonic diffuser.
a) $\varphi < 1$; b) $\varphi = 1$; c) $\varphi > 1$

During the operation of the diffuser under design point conditions $w_1 = w_н$,

$\varphi = 1$, $S_n = S_1$, additive drag is about $X_a = 0$.

Additive diffuser drag reaches its highest value when the exhaust opening is completely closed, i.e., when $\varphi = 0$.

The ratio of additive drag to the dynamic head at midship cross section S_M of an engine is called the additive drag coefficient c_d:

$$c_A = \frac{X_A}{q S_M}. \qquad (4.15)$$

Additive drag coefficients of supersonic diffusers are shown in Fig. 73.

The flow around the external surface of a diffuser acts upon it with a certain force. The nacelle's aerodynamic drag coefficient depends upon the Mach number of the oncoming flow, upon the relative inlet area ratio $f = \dfrac{S_1}{S_2}$, upon the mass flow ratio φ, and upon Reynolds number Re.

During a flow through the internal duct of the engine, friction and shocks occur, and as a result the pressure decreases.

Pressure losses from shocks during a sudden expansion of the flow are expressed by the Borda-Carnot formula

$$\Delta p_{ya} = \frac{1}{2g}(w_1 - w_2)^2 = \frac{\gamma w_2^2}{2g}\left(\frac{S_2}{S_1} - 1\right)^2, \qquad \underline{/}\,ya = \text{shock}\,\underline{/} \quad (4.16)$$

where γ is the air density, which is considered to be a constant;

w_1 and w_2 are the velocities of the flow before and after the shock.

The pressure losses in the diffuser are less than those during a sudden expansion. The ratio of pressure losses in the diffuser Δp_d to the pressure losses during a sudden expansion Δp_{ud} is called the absorptive shock coefficient ψ:

$$\psi = \frac{\Delta p_A}{\Delta p_{ya}}. \qquad (4.17)$$

During a subsonic flow through the expanding portion of the diffuser the absorptive shock coefficient ψ depends only on the angle of the diffuser opening α_a (Fig. 61, b).

Pressure losses in the diffuser duct may be expressed by the so-called loss factor or drag factor ζ, which is measured by the ratio of the pressure losses to the local value of the dynamic head q_2 (Fig. 61, b)

$$\zeta = \frac{\Delta p}{q_2}.$$

(4.1c)

The loss of total pressure during a flow through the diffuser duct is equal to

$$\Delta p = p_{01} - p_{02} = \zeta q_2 = \zeta \frac{\gamma_2 w_2^2}{2g}.$$

(4.19)
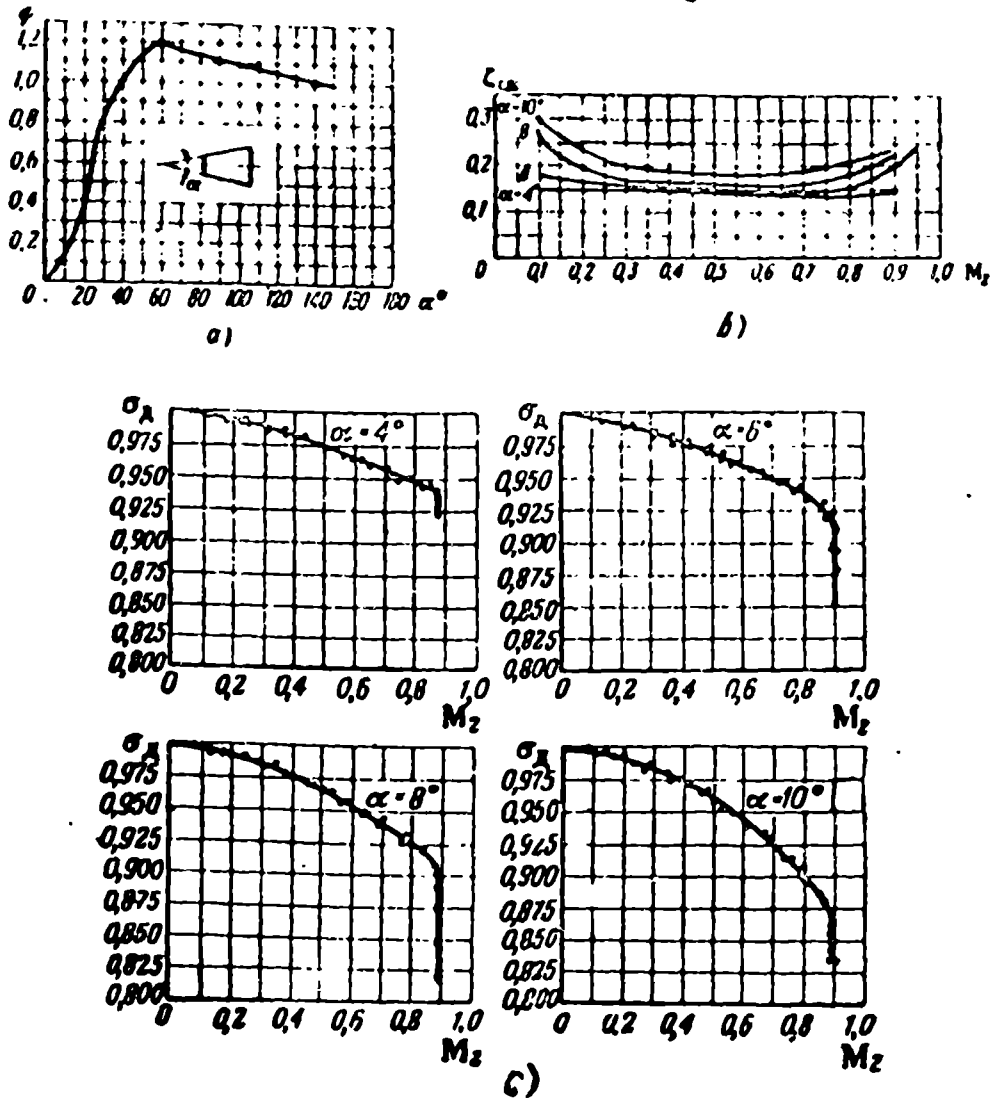
Fig. 61 The characteristics of a subsonic diffuser.
a -- relation of absorptive shock coefficient ψ to the angle of the diffuser opening α_d; b -- dependence of drag factor ζ upon the Reynolds number Re; c -- relation of pressure recovery σ_d'' to the Mach number as a function of various opening angles α_d.

The pressure recovery factor σ_d'' in the duct of a subsonic diffuser is

$$\sigma_\Lambda^* = \frac{p_{02}}{p_{01}} = \frac{1}{1 + \zeta \frac{\gamma_2 w_2^2}{2g p_{02}}} = \frac{1}{1 + \zeta \frac{\gamma_{02} w_2^2}{2g p_{02}} \varepsilon(\lambda_2)}.$$

Utilizing the state formula $\frac{p_{02}}{\gamma_{02}} = R T_{02}$ and noting that $\frac{w_2^2}{2g R T_{02}} = \frac{k}{k+1}\lambda_2^2$,

we obtain

$$\sigma_\Lambda^* = \frac{1}{1 + \frac{k\zeta}{k+1}\lambda_2^2 \varepsilon(\lambda_2)}.$$

(4.20)

At a low velocity of λ_2 the dependence of density upon velocity may be disregarded. Then, from equation (4.19), noting that $\gamma_2 = \gamma_{01}$, we find

$$\sigma_{\Delta} = \frac{p_{02}}{p_{01}} = \frac{p_{01} - \Delta p}{p_{01}} = 1 - \zeta \frac{\gamma_2 w_2^2}{2g p_{01}} = 1 - \zeta \frac{k}{k+1} \lambda_2^2. \qquad (4.21)$$

The last equation is used for the determination of pressure recovery in the duct of a diffuser when $\lambda_2 < 0.3$.

Assuming that pressure losses in a diffuser are determined by the absorptive shock, we express the drag factor as a function of absorptive shock factor ψ:

$$\Delta p = \psi \Delta p_{y\lambda} = \zeta \cdot \frac{\gamma_2 w_2^2}{2g},$$

$$\zeta = \psi \left(\frac{S_2}{S_1} - 1 \right)^2. \qquad (4.22)$$

Section 3. Subsonic Diffusers

A subsonic diffuser is represented by an expanding tube whose forward edge has smooth outlines. To prevent disruption of the stream, a special aerodynamic form has been imparted to the diffuser lip (Fig. 62). The relative inlet area ratio of subsonic diffusers is always less than one: $\frac{S_1}{S_2} = f < 1$.

Air flow through the operating system of an engine, to which the diffuser is connected, depends upon the total hydraulic resistance of the duct and also upon the stagnation temperature and pressure of the exhaust gases. The hydraulic resistance of the air duct is basically determined by the cross-sectional area of the exhaust nozzle (see Fig. 59).

Velocity w_1 in the inlet section of subsonic diffuser S_1 is not equal to the velocity of the free stream flow: $w_1 \lessgtr w_n$.

In the presence of great hydraulic resistance or a large temperature ratio $-\frac{T_{0g}}{T_{0x}}$ the mass flow factor φ is small and the velocity at inlet section S_1 is less than that of the free stream flow: $w_1 < w_n$. The deceleration of the air begins in front of inlet section S_1; the static pressure of the flow, in accordance with Bernoulli's equation, increases and becomes greater than the atmospheric pressure: $p_1 > p_n$. The deceleration of the flow in front of the diffuser is not accompanied by any losses. Therefore, during operation with external compression the pressure recovery factor σ_d

increases. However, the diffuser's additive drag coefficient c_c also increases with an increase of external compression.
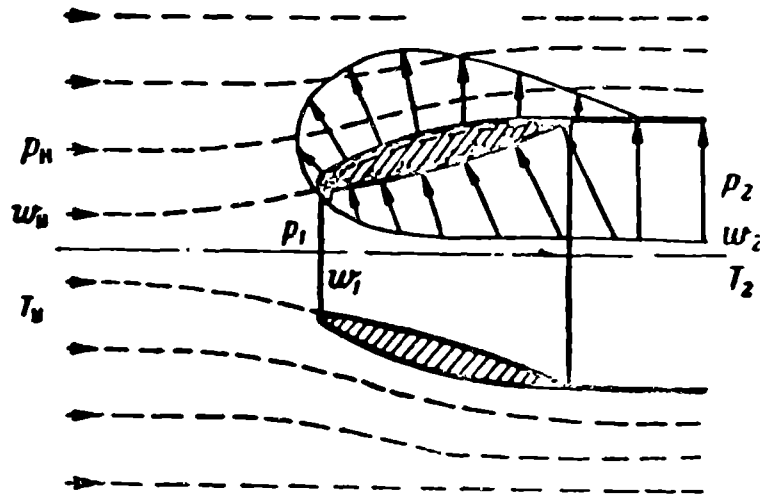
Fig. 62 The aerodynamic forces which act on a diffuser lip.

When the duct's drag decreases, the mass flow through the diffuser grows, and the velocity of the gases w_1 in inlet section S_1 increases and may become greater than the velocity of the free stream flow w_H, but may not become greater than the speed of sound: $w_1 < c_1$. With an increase in velocity w_1, the static pressure at inlet p_1 decreases and may become less than the atmospheric pressure p_n, but by not more than 1.89 times:

$$p_1 > \left(\frac{2}{k+1}\right)^{\frac{k}{k-1}} p_H = \frac{p_H}{1.89}.$$

Stream lines at the inlet to a subsonic diffuser at various velocities at the inlet are shown in Fig. 60. During operation when the air stream that enters the diffuser is rarefied at the inlet, the air moves in a direction toward the diffuser axis at an angle comparable to the degree of rarefaction at the inlet, i.e., the greater the rarefaction, the greater the angle (Fig. 60, c). At the same time, the flow detaches from the internal walls of the diffuser, and vortex formation accom-panied by an increased dissipation of the air's kinetic energy occur: pressure re-covery in the diffuser diminishes. Rarefaction at the inlet to the diffuser is un-desirable. The relative cross sections of the diffuser are so selected that mass flow factor φ increases to reach unity only at the least of the expected hydraulic resistances or at the minimum combustion temperature ratio θ_{min}.

Subsonic diffusers usually operate with external compression (Fig. 60, a).

The air velocity w_2 in the diffuser's exhaust (wide) section S_2, just as velocity w_1 in the inlet section, depends upon the area of sections S_1 and S_2, upon λ_n, T_n, p_n, and upon the air flow G_v. On the basis of equation (2.4) it may be described as

$$w_1 = \frac{f\,(G_v)_{max}}{\gamma_1 S_1} = a\lambda_1; \quad w_2 = \frac{f\,(G_v)_{max}}{\gamma_2 S_2} = a\lambda_2. \tag{4.23}$$

The critical flow velocity **a** and the stagnation temperature T_{ox} are constant along the entire duct of the diffuser:

$$T_{ox} = \frac{T_{_H}}{1 - \frac{k-1}{k+1}\lambda_{_H}^2}; \quad a = \sqrt{\frac{2gk}{k+1} RT_{ox}}. \tag{4.24}$$

The relative velocity may be found by the ratio of the total pressure to the static pressure:

$$\lambda = \sqrt{\frac{k+1}{k-1}\left[1 - \left(\frac{p}{p_0}\right)^{\frac{k-1}{k}}\right]}. \tag{4.25}$$

With an increase of the mass flow ratio $\varphi = \dfrac{G_v}{w_{_H}\gamma_{_H}S_1}$, the relative velocities λ_1 and λ_2 increase, the dissipation of kinetic energy increases, and pressure recovery factor σ_d decreases (see 4.20 and 4.21). The dependence of the pressure recovery factor upon mass flow ratio is called the off-design point characteristic of the diffuser σ_d = f (φ).

In the selection of a diffuser for an air-breathing jet engine, the maximum possible air mass flow G_{max} should be set and, the cross-sectional area of inlet S_1 determined in the assumption that φ = 1 for the maximum possible mass flow. From equation (4.11) we find

$$S_1 = \frac{G_{max}}{w_{_H}\gamma_{_H}}. \tag{4.26}$$

Section S_2 is found from mass flow (2.74), in setting a given value for the relative velocity λ_2. (The relative velocity at the diffuser exhaust λ_2 is a function of the operating process of the engine.)

$$S_2 = \sqrt{\frac{k+1}{2gk} RT_{_{0H}}} \frac{G_{max}}{e_2 p_{0H}' z^2 (\lambda_2)}. \tag{4.27}$$

Example: Let us find diffuser cross sections S_1 and S_2 if the maximum air flow

through the diffuser G_{max} = 100 kg/sec, the relative flight velocity λ_n = 0.9, the result velocity at the diffuser exhaust at maximum flow is

$$\lambda_2 = 0.2, \quad T_n = 216.5°K \text{ and } p_n = 2310 \text{ kg/m}^2$$

The stagnation temperature of the free stream flow is

$$T_{0H}=\frac{T_u}{\tau(\lambda_u)}=\frac{216.5}{1-\frac{0.9^2}{6}}=\frac{216.5}{0.865}=250° \text{ K.}$$

The flow velocity is

$$S_1=\lambda_u a=\lambda_u \sqrt{\frac{2gkR}{k+1}T_{0H}}=0.9\cdot18.3\sqrt{250}=260 \text{ м/сек.}$$

The diffuser inlet cross-section is

$$p_1=\frac{G_{max}}{w_u\gamma_u}=\frac{G_{max}}{w_u p_u}RT_u=\frac{100\cdot29.3\cdot216.5}{260\cdot2310}=1.06 \text{ м}^2.$$

The stagnation pressure of the free stream flow p_{0n} is

$$p_{0u}=\frac{p_u}{\tau(\lambda_u)^{\frac{k}{k-1}}}=\frac{2310}{0.865^{3.5}}=3850 \text{ кг/м}^2.$$

The diffuser exhaust cross section is

$$S_2=\sqrt{\frac{k+1}{2gk}RT_{0H}}\frac{G_{max}}{\sigma_\lambda p_{0H}\lambda_2\tau(\lambda_2)}=$$
$$=S_1\frac{\gamma_u w_u}{\gamma_2 w_2}\approx S_1\frac{\lambda_u}{\lambda_2}\frac{\varepsilon(\lambda_u)}{\varepsilon(\lambda_2)}=\frac{1.06\cdot0.9}{0.2}0.692=3.3 \text{ м}^2.$$

$$(T_{0H}\approx T_2; \quad \sigma_\lambda\approx 1; \quad \varepsilon(\lambda_2)\approx 1).$$

Section 4. Various Forms of Subsonic Diffusers

The inlet section of a subsonic diffuser, as already stated in the foregoing paragraph, is so chosen that through the entire operating range of the engine, the diffuser operates with the flow being compressed externally.

In those cases where the deceleration of the flow begins in front of the diffuser inlet ($\varphi < 1$), streams of the enclosed air approach the edge at large angles. Because of this, disruption may occur (see Fig. 60). To decrease vortex formations, the walls of the diffuser have a smoothly formed profile of the longitudinal section (see Fig. 62). The velocity of the air which flows around the diffuser lip and the pressure on the outside wall change. If the lip shape is correctly selected, rarefication will occur on it (ig. 62) as a result of which thrust may arise -- as initially shown by Ye. S. Shcherbakov -- even when the inlet is totally open, i. e.,

when $f_1 = \dfrac{S_1}{S_2} = 1.$

The thrust of a jet engine acts on the internal and external surfaces of the diffuser.

The internal duct of a diffuser may have any of various outlines. The most prevalent of these are conical and isogradient diffusers.

The conical diffuser. The geometry of a conical diffuser is determined by two parameters: the expansion angle α_d and the inlet cross section ratio $f_1 = \dfrac{S_1}{S_2}$ (Fig. 63, a). The length of the diffuser, as seen in Fig. 63, a, is expressed as a function of the ratio $\dfrac{1}{d_2}$; the greater it is, the smaller the expansion angle α_c and
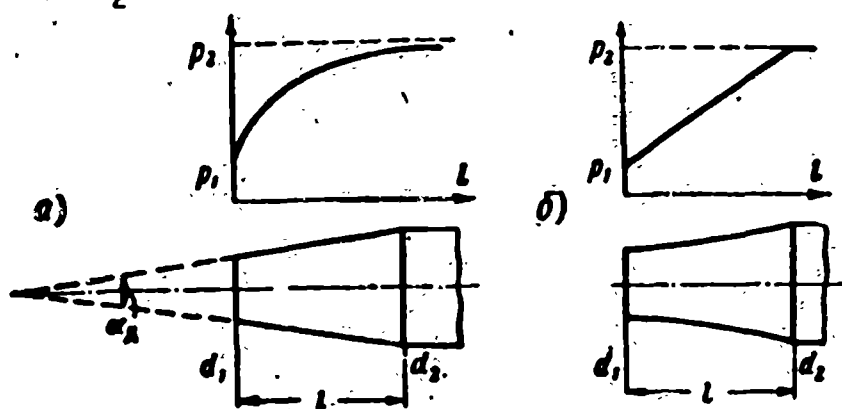
Fig. 63 Various forms of subsonic diffusers.
   a -- conical diffuser; b -- isogradient diffuser.

the inlet area ratio f_1:

$$\frac{l}{d_2} = \frac{d_2 - d_1}{2d_2 \, \text{tg} \, \frac{\alpha_l}{2}} = \frac{1 - \sqrt{f_1}}{2 \, \text{tg} \, \frac{\alpha_l}{2}}.$$

(4.28)

With a decrease in the expansion angle α'_d, the length of the diffuser increases and, therewith, its internal surface and friction losses. The pressure recovery factor σ_d decreases; in addition, the construction weight of the diffuser increases, but with small expansion angles, the flow does not separate from the sides.

With an increase in the diffuser expansion angle α_d, friction losses decrease and the diffuser's construction weight diminishes; whereas with a sufficiently large expansion angle, separation of the flow occurs and the pressure recovery quickly falls. The most advantageous expansion angle is on the order of 10-15°.

The selection of the inlet area ratio f is accomplished on the basis of an analysis of the engine's operation as a whole. The velocity of the flow moving

through an expanding diffuser diminishes. The static pressure grows in proportion to the lessening of the velocity. If the air density is taken as a constant, and losses are disregarded in the first approximation, it is not difficult to find the dependence between the increase in static pressure and the length of the diffuser by means of Bernoulli's equation:

$$p_i - p_1 = \frac{\gamma}{2g}(w_1^2 - w_i^2) = \frac{\gamma w_1^2}{2g}\left(1 - \frac{S_1^2}{S_i^2}\right).$$

$$p_i - p_1 = \frac{\gamma w_1^2}{2g}\left(1 - \frac{d_1^4}{d_i^4}\right) = \frac{k}{2}p_1 M_1^2\left[1 - \frac{1}{\left(1 + 2\frac{l_i}{d_1}\,\mathrm{tg}\,\frac{a_s}{2}\right)^4}\right].$$ (4.29)

The "i" indices belong to the local values of velocity, pressure, and diameter As is seen from equation (4.29), the pressure recovery occurs basically in the forward portions of the diffuser.

Isogradient diffusers. The deceleration of the flow in an isogradient diffuser occurs in such a manner that the rise in pressure is uniform along the entire length (Fig. 63, b):

$$\frac{dp}{dl} = \mathrm{grad}\,p = \mathrm{const.}$$ (4.30)

The relation between the acceleration of the flow j and the pressure gradient $\frac{dp}{dl}$ is expressed by Euler's equation (2.29) $\frac{dp}{dl} = -\frac{\gamma}{g}\,j$. The minus sign indicates that the direction of the acceleration is towards decreasing pressure. In an isogradient diffuser the product of the acceleration and density is constant along the length of the diffuser

$$\frac{\gamma}{g}j = \mathrm{const.}$$

Assuming that the density of the flow is constant, we find the relation between the length of the diffuser and its diameter, at which the deceleration of the flow is constant: j = const.

The distance traveled during uniform deceleration, as is known from kinematics, may be expressed by initial and terminal velocities w_1 and w_i

$$l_i = \frac{w_1^2 - w_i^2}{2j}.$$

According to the continuity equation

$$w_i = w_1\frac{S_1}{S_i} = w_1\frac{d_1^2}{d_i^2}.$$

From here we obtain the equation of the profile of an isogradient diffuser without considering the compressibility of the air

$$l_i = \frac{w_i^2}{2j}\left(1 - \frac{d_i^4}{d^4}\right).$$

(4.31)

For the inlet section $d_i = d_j$ and $l_i = 0$. The length, which corresponds to the total deceleration of the flow ($d_i \rightarrow \infty$)

$$l = \frac{w_i^2}{2j}.$$

At high velocities of free stream flow $0.5 < M_n < 1.0$, one must consider the compressibility of the air for the design of the outlines of an isogradient diffuser.

As the diffuser cross section increases, the velocity decreases and the pressure and density of the flow increase. Thanks to the density increase, the velocity decreases several times more than the cross section increases.

In a conical diffuser, where the velocity quickly decreases as the distance from the inlet increases, pressure recovery occurs basically in the forward portions of the diffuser (see Fig. 63, a), and the pressure gradient is great. A large pressure gradient contributes to the separation of the flow from the walls and increases the losses from vortex formations. To decrease the pressure gradient, the length of conical diffusers is increased and the expansion angle α is decreased. At greater distances from the inlet section, the pressure gradient in a conical diffuser is decreased. Thus a conical diffuser may be likened to an axial compressor, the subsequent stages of which increase the pressure less than does the first.

Pressure in an isogradient diffuser rises uniformly along its entire length. The probability of the boundary layer separation is equally low in all sections of the diffuser. An isogradient diffuser may be likened to an axial compressor the subsequent stages of which produce an equal increase in pressure.

For the same initial and terminal diameters and the same pressure recovery factors, isogradient diffusers are shorter than are the conical diffusers. For the same length, the pressure recovery factor of an isogradient diffuser is higher than that of a conical one.

Section 5. Expanded Diffusers in a Supersonic Flow

At low supersonic velocities of a flow ($1.0 < M < 2$) expanded diffusers are used (Fig. 64). To decrease drag, the forward edge of a diffuser is made sharp and its external surface is conical with a small incidence angle.

The air flow through the diffuser is determined by the exhaust section of the tube which is connected with the diffuser (see Fig. 59). If the throttle valve is completely closed, the mass flow through the diffuser is equal to zero: $G = 0$; $\varphi = 0$. When this happens, a normal shock wave (Fig. 64, a) appears in front of the diffuser inlet. The flow behind the shock wave remains subsonic ($M < 1$) and the air flows around the side of the diffuser. The additive "wave" drag X_d is at maximum. The pressure in the tube, equal to the stagnation pressure behind the normal shock wave, is determined by Rayleigh's formula (2.104).

As the tube's inlet section is gradually increased, the air flow G_v through the diffuser will increase, the normal shock wave will approach section S_1 and will finally "sit" at the inlet rake (see Fig. 64, b). At this time, the air flow through the diffuser will become the greatest:

$$G_{max} = w_n \gamma_n S_1 = w_1 \gamma_1 S_1. \tag{4.32}$$

The cross section of the stream tube will be equal to the inlet cross section: $S_n = S_1$. The mass flow ratio will be equal to one: $\varphi = 1$.
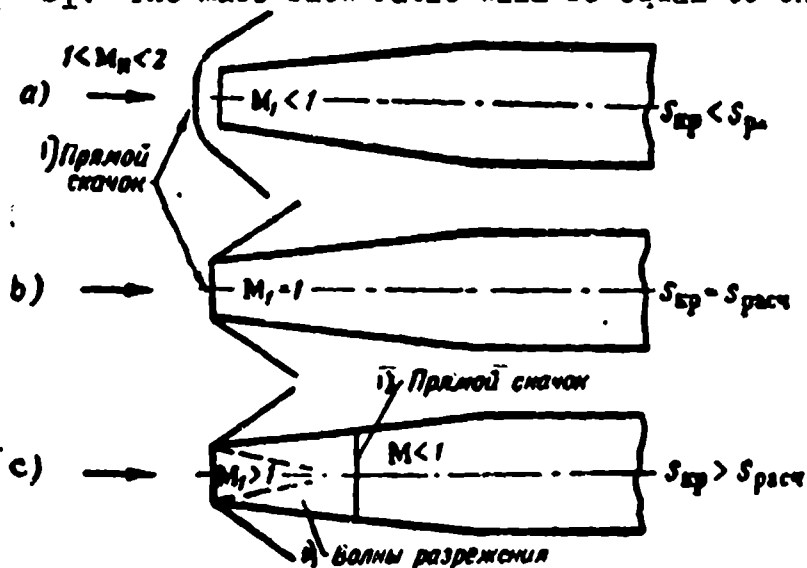
Legend:

1) Normal shock waves
2) Rarefication waves

Fig. 64. An expanded diffuser in a supersonic flow.
a) $S_{кp} < S_{расч}$; b) $S_{кp} = S_{расч}$; c) $S_{кp} > S_{расч}$.

The maximum possible flow through the diffuser during a supersonic flow is equal to the product of the velocity of the undisturbed flow, its density, and the area of the inlet opening cross section: $G_{max} = w_n \gamma_n S_1$.

For increases in the exhaust cross section, the flow rate will remain constant, since pressure disturbances during a supersonic condition cannot spread upstream in the flow and the signal reflecting the variation of back pressure will not be registered beyond the inlet section. The mass flow ratio during a supersonic flow cannot be more that one: if $M_n \geq 1$, then $\varphi \leq 1$.

If one continues to increase the exhaust opening of the tube even after a normal shock wave approaches the diffuser inlet opening, then there will occur an expansion of the supersonic flow similar to that as manifested during the flow around an obtuse angle. A supersonic flow through the expanding duct of the diffuser ends with a powerful normal shock wave (see Fig. 64 c), the losses increase, and the pressure in the tube p_{02} acquires a value sufficient enough to force out $G = w_n \gamma_n S_1$ kg of air through the exhaust section of tube $\overline{S}_{cr}$ every second. The pressure before the exhaust p_{02} may be found from critical flow formule (2.53)

$$p_{02} = \frac{G \cdot \sqrt{T_{02}}}{B S_{cp}}.$$ (4.33)

The function B, which is dependent on k and R_g, is shown in Table 2.1.

The pressure recovery factor of a simple expanding diffuser σ_d in a supersonic flow is equal to the product of the pressure recovery factor in a normal shock wave σ_{pr} and the pressure recovery factor of an expanded diffuser σ_d'' (when $M_H = M_1$):

$$(\sigma_d)_{max} = \sigma_{pr} \sigma_d''.$$ (4.34)

The pressure recovery factor in a normal shock wave σ_{pr} is expressed by Rayleigh's formula (2.105). The pressure recovery factor of the expanded portion, if the normal shock wave is located at or in front of the inlet section, is determined as indicated previously in Sections 3 and 4.

If supersonic flow continues into the expanded portion of a diffuser, losses in the terminal shock wave increase, and the diffuser pressure recovery factor becomes less than the maximum possible.

With an increase in flight speed, losses in the normal shock wave increase. Therefore, when $M_n > 2$, simple expanded diffusers are not utilized.

At high supersonic flight velocities ($M_n > 2$) energy losses in a diffuser with a normal shock wave at the inlet become large, and the pressure recovery factor becomes small: when $M = 2.5$ $\sigma_{pr} \approx 0.5$. To decrease the losses during the deceleration of the flow, it is advisable to replace the powerful normal shock wave at the diffuser inlet by a system of weaker oblique shock waves, concluding with a weak normal shock wave, since energy losses in a system of successive weak shock waves, which lead to subsonic velocity, are less than in a single normal shock wave.

To form oblique shock waves, the diffuser is supplied with a spike which projects from the inlet opening (Fig. 65). If several oblique shock waves are required, the spike or "bullet" has multiple steps (Fig. 65, a). Sometimes the subsequent oblique shock waves are created by the supersonic flow intersecting the shell (Fig. 65, b). Usually the deflection spike is cone-shaped. During the approach of a supersonic flow to the point of the cone, a shock wave appears, forming angle α_1 with the direction of the undisturbed flow. The velocity profiles during the flow around the cone are not uniform, therefore the problem of an exact gas-dynamic computation of the flow around a cone by a supersonic flow entails considerable difficulties. These may be significantly facilitated, if one solves the two-dimensional problem and finds the parameters of the flow behind the two-dimensional shock waves which are formed during the flow around a wedge whose incidence angles are so selected as to assure that the arising shock waves should be the same as those registered during the flow around a cone. A wedge produces greater disturbance of a flow than does a cone; therefore, in order to give rise to identical shock waves, the angle of the wedge must be less than the angle of the cone. If the angle of the cone ω_{kon} is given, the required angle of the wedge ω_{kl} may be found by means of the graph plotted in Fig. 46. The transition from a multiple shock-wave cone to a wedge is shown in Fig. 66.

The inlet slot, measured by the normal to the flow, has a ring-shaped cross section along the conical spike, with area

$$S_{\text{щ}} = \frac{\pi}{4}(d_1^2 - d_{\text{шп}}^2)\cos\omega_{\text{общ}}.$$

$$\begin{cases} \text{щ} = slot \underline{7} \\ \text{шп} = spike\underline{/} \\ \text{общ} = total\underline{/} \end{cases} \quad (4.35)$$

where d_1 and $d_{\text{шп}}$ are the diameters of the inlet and spike in the plane of the

inlet cross section;

$\omega_{\text{общч}}$ is the total rake angle of the flow.
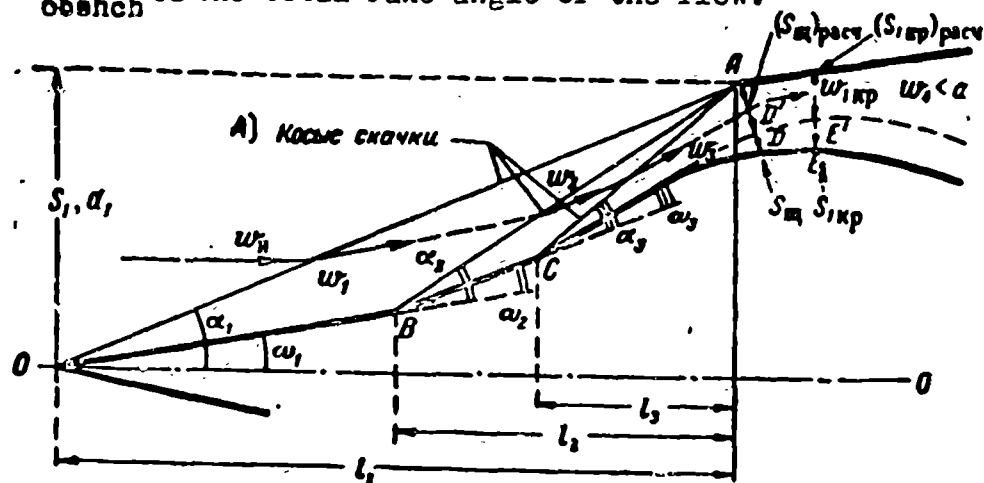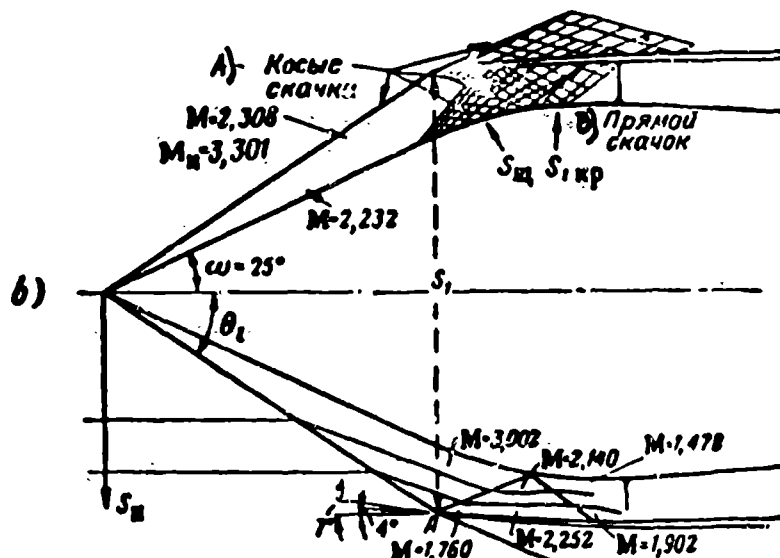
Fig. 65. Schematic of shock waves at the inlet to a multi-shock-wave supersonic
diffuser.
a -- diffuser with a multi-step bullet;
b -- diffuser with reflected shock waves.
Legend: A) oblique shock waves; B) normal shock wave.

The inlet slot corresponding to a wedge-shaped spike has the form of two

rectangles (see Fig. 66);

$$S_{\text{щ}}' = 2(a_{\text{вх}} - a_{\text{кл}})\,b\cos\omega_{\text{общ}}. \quad (4.36)$$

Here a_{vkh} is half of the "height" of the inlet slot (see Fig. 66);

$a_{\text{кл}}$ is half of the "height" of the wedge;

b is the width of the slot.

If the shock waves on a wedge and a cone have a similar intensity, then the

Legend:
1) cone
2) wedge
3) rectangular slot
4) ring-shaped slot
5) ω' cone
6) ω wedge
7) S slot
8) S plane
9) a inlet
10) S ring
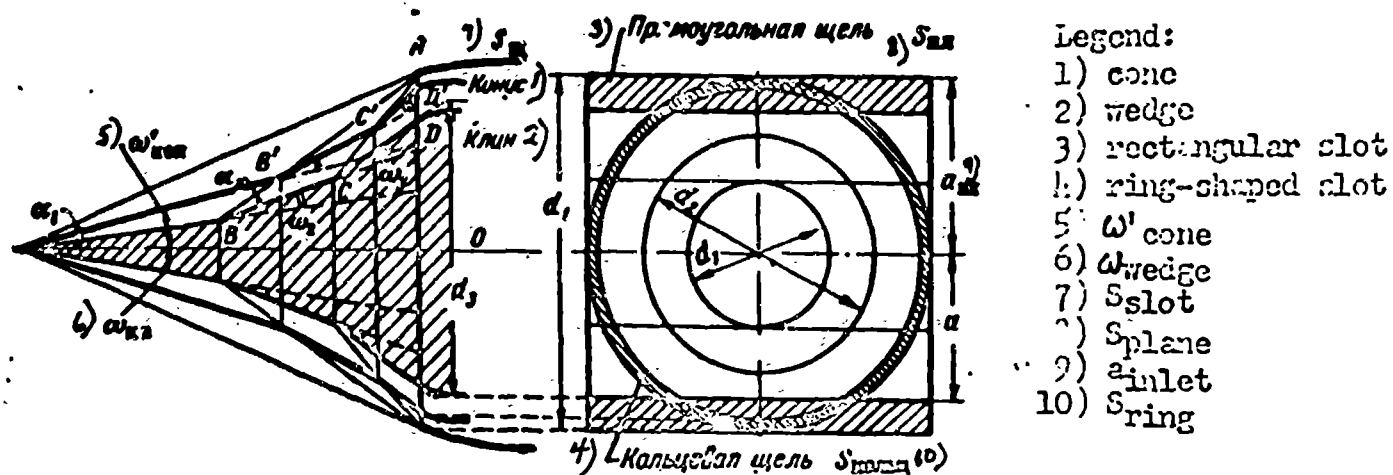
Fig. 66 The transformation of a computed two-dimensional (wedge-shaped) diffuser to a conical one.

Let us examine, first, a two dimensional multiple shock-wave diffuser.

Let us designate by ω_1, ω_2, ω_3, etc., the rake angles of the flow on the first, second, third, and other stages, which are equal to the wedge angles, (see Fig. 65). Let us designate by α_1, α_2, α_3, etc., the incidence angles of the shock wave with the flow direction behind the previous step. The distance from the apex of the angle of the first, second, and other stages to the plane of the inlet slot we designate by l_1, l_2, l_3, etc.

The angles of the wedge ω_1, ω_2, ω_3 are so selected that during a given flow velocity M_n one may obtain the highest pressure recovery corresponding to the least wave drag. The most advantageous flow rake angles are those by which the total growth of air entropy in a series of oblique shock waves seems to be the least. The calculations are confirmed in supersonic wind tunnels. This problem was solved by G. I. Petrov and Ye. P. Ukhov in the USSR and by Oswatich in Germany.

The incidence angles of the shock waves α_i depend upon the flow velocity before the shock wave and upon the flow rake angle ω_i. Thus, for example, the incidence angle of the second shock wave α_2 depends upon the flow rake angle ω_2 and upon the flow velocity M_1 ahead of the second shock wave.

The distances l_1, l_2, l_3 ... are such that as the flow proceeds along the external diffuser, the surfaces of all the shock waves intersect the edges of the inlet slot (see Fig. 65, a).

It is seen from the formula that

$$l_1 = \frac{d_1}{2 \lg \alpha_1} .$$

(4.37)

The distances l_2, l_3 etc., may be found either by trigonometric computations or by construction.

After passing through the first shock wave, which appears when the flow passes the apex of the wedge, the supersonic flow behind the shock wave deviates from its original direction and begins to move parallel to the surface of the first step of the wedge (the directions of the flow are indicated in Fig. 65 by arrows). The density and pressure increase; the flow velocity remains supersonic: $M_1 > 1$. After passing through the second shock wave, which appears at the junction line of the first step with the second, the flow again turns and moves parallel to the second step; the velocity remains supersonic: $M_2 > 1$, and the density and pressure increase. Behind the third shock wave, the flow moves parallel to the surface of the third step, the velocity continues to be greater than the speed of sound: $M_3 > 1$, and the density increases still more. For this reason, a strongly compressed flow appears in the engine inlet slot which has an area S_{shch}. The original cross-section of this flow is equal to the total inlet cross-section $S_n = S_1$. A normal shock wave appears in the inlet slot or behind it and the flow velocity becomes subsonic: $M_4 < 1$.

A multi-shock-wave diffuser operates similarly to the tapering duct of an ideal ramjet engine (see Fig. 58).

The air flow through the diffuser is determined by the continuity equation. For design point condition, when the shock waves are focused on the inlet edge, $\varphi = 1$:

$$G_s = w_n \gamma_n S_1 = w_n \gamma_n S_{sh} = w_{inp} \gamma_{inp} S_{inp} .$$

(4.38)

The flow parameters at the plane of this slot are marked by the index "shch". In this case the cross section of a free stream flow entering the diffuser is equal to the total area of the inlet, including the cross section of the inlet spike:

$S_1 = \frac{\pi}{4} d_1^2$, where d_1 is the inlet diameter.

For the given engine internal hydraulic resistance, the terminal normal shock

wave is located in the inlet section (see Fig. 65). The flow velocity behind the

normal shock wave becomes subsonic. During subsequent flow through the tapering duct

of the diffuser, the velocity may at first grow and reach the speed of sound in the

critical section of the throat: $w_{1cr} = a$, $M_{1cr} = 1$. The deceleration of the flow

$\lambda_2 < 1$ occurs in the expanding subsonic portion of the diffuser during operation

at the design point.

So that the flow velocity through the engine duct and the local pressure losses

do not become excessively large, the inlet diameter d_1 must be less than the maximum

cross sectional diameter: $d_1 < d_{\text{M}}$.

An oblique shock wave appears as the supersonic flow intersects the conical

diffuser shell (Fig. 67). The stream lines are distorted, and the static pressure of

the air increases. The ratio of the increase in static pressure to the dynamic head

of the free stream flow is called the pressure increase coefficient P_{dav}:

$$P_{\text{дав}} = \frac{p_1 - p_{\text{н}}}{q} = \frac{2}{k} \frac{\frac{p_1}{p_{\text{н}}} - 1}{M_{\text{н}}^2}.$$ (4.39)

As the distance from the inlet edge is increased, this pressure coefficient

gradually decreases to zero (Fig. 67).

The increased pressure acts upon the shell's surface, creating external wave

drag of the diffuser.
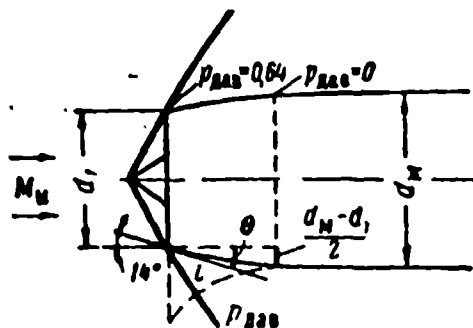
Fig. 67. The oblique shock waves which appear at the intersection of a supersonic
flow with the shell of a diffuser.
The relative pressure increase is shown by a dotted line.

The external drag of the diffuser is equal to the product of the average pres-

sure increase $\Delta p_{sr} = \bar{P}_{dav}q$ and the frontal area of that portion of the shell defined

as $S_{ob} = S_{\text{M}} - S_1$ plus the friction forces $X_{tr} = S_{bok}q$

$$X_{o\delta}=S_{o\delta}qP_{\text{м.в}}+S_{\delta o \kappa}qc_f=S_{\text{м}}q\left[P_{\text{м.в}}\frac{S_{o\delta}}{S_{\text{м}}}+c_f\frac{S_{\delta o \kappa}}{S_{\text{м}}}\right],$$ (4.40)

here c_f is the friction factor which is dependent on the Reynolds number (see Fig. 3).

The ratio of the external drag X_{ob} to the product of the dynamic head and the ~~maximum cross-sectional area~~ of the engine is called the diffuser-lip external-drag coefficient c_{xob}.

$$c_{x o\delta}=\left(P_{\text{м.в}}+\frac{c_f}{\sin\theta}\right)(1-f_1).$$ (4.41)

~~ωεn~~

$$f_1=\frac{S_1}{S_{\text{м}}}=1, \quad X_{o\delta}=0; \quad c_{x o\delta}=0.$$

With a decrease of the inlet area ratio $f_1 = \dfrac{S_1}{S_M}$ the external drag grows, th a decrease of the incidence angle of the shell's internal surface θ at constant inlet area ratio f = const, the shell's external surface $S_{\delta o \kappa}=\dfrac{S_{\text{м}}}{\sin\theta}(1-f)$ increases, due to the increase in its length $l=\dfrac{d_{\text{м}}-d_1}{2\sin\theta}$. The force of friction X_{fr} also increases erewith; whereas the oblique shock wave, which appears by the inlet edge, becomes ss powerful and the increase in static pressure diminishes. Calculations corroborated by test indicate that the most suitable lip incidence angle, the one at ich additive external drag seems to be lowest (when $M = 3.3$), is equal to $4°$.

A Schlieren photograph of oblique shock waves which appeared at a diffuser inlet at the design point condition, is shown in Fig. 69.
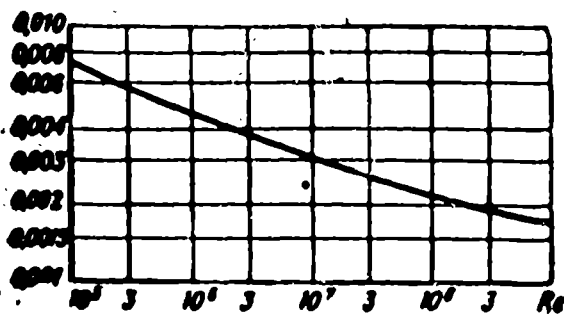
g. 68. The dependence of friction coefficient c_f upon Reynolds number R.

Fig. 69. A photograph of shock waves at a diffuser inlet at the design point conditions.

With an increase in flight velocity M_n or λ_n, the compression of the flow in lique shock waves grows, and the computed cross section of the inlet slot S_{shch}

and the diffuser throat S_{1cr} decrease.

The necessary diffuser cross sections are determined by means of a gas-dynamic calculation.

Section 7. The Calculation of a Multiple-Shock-Wave Diffuser

The calculation of a multi-shock-wave diffuser includes the following stages:

1. Calculation of pressure recovery.

2. Construction of the diffuser geometry.

3. Determination of the critical cross section of the diffuser.

4. Determination of the stagnation impulse.

The calculation of pressure recovery. We shall assume the calculated flight speed M_n, the number of steps, and the flow rake angles ω_1, ω_2, ω_3, etc.

We shall find the first step's incidence angle $\alpha_1 = f(M_n, \omega_1)$ by formula (2.124) or by the graph in Fig. 43. The velocity M_1, the pressure ratio $\frac{p_1}{p_n}$, the density ratio $\frac{\gamma_1}{\gamma_n}$, and the temperature ratio $\frac{T_1}{T_n}$ behind the first shock wave after 41 and 42, on the basis of velocity M_n and the flow rake angle ω_1 are found by formulas (2.118), (2.119), (2.122), and (2.123) or by the graphs in Fig. 39, 40, 41, and 42.

Subsequently, by formula (2.124) or by the graph in Fig. 43 we find the incidence angle of the second shock wave α_2 on the basis of velocity M_1 behind the first shock wave, and the flow rake angle at the second step ω_2: $\alpha'_2 = f(M_1, \omega_2)$. The velocity M_2, the pressure ratio $\frac{p_2}{p_1}$, the density ratio $\frac{\gamma_2}{\gamma_1}$, and the temperature ratio $\frac{T_2}{T_1}$ behind the second shock wave are found by the formulas or graphs indicated above.

We determine the third step's incidence angle α'_3 on the basis of velocity M_2 of the flow behind the second step and the flow rake angle on the third step ω_3; and then, on the basis of the same quantities, we find the relative air parameters behind the third shock wave

$$\frac{p_3}{p_2}, \frac{\gamma_3}{\gamma_2}, \frac{T_3}{T_2} \text{ and } M_3$$

The pressure, density, and temperature behind the last shock wave, expressed as ratios to the parameters of an undisturbed flow, are equal to

$$\frac{p_3}{p_н} = \frac{p_1}{p_н} \frac{p_2}{p_1} \frac{p_3}{p_2};$$

$$\frac{\gamma_3}{\gamma_н} = \frac{\gamma_1}{\gamma_н} \frac{\gamma_2}{\gamma_1} \frac{\gamma_3}{\gamma_2};$$

$$\frac{T_3}{T_н} = \frac{T_1}{T_н} \frac{T_2}{T_1} \frac{T_3}{T_2}.$$

Flow parameters behind the terminal normal shock wave, expressed as a ratio to the parameters of the flow behind the preceding shock wave $\frac{p_4}{p_3}$, $\frac{\gamma_4}{\gamma_3}$, $\frac{T_4}{T_3}$, are found by the graph in Fig. 36 or by formulas (2.101), (2.103), (2.106), and (2.108).

The stagnation parameters behind the normal shock wave as a ratio to the parameters of an undisturbed flow:

$$\frac{p_{04}}{p_н} = \frac{p_3}{p_н} \frac{p_{04}}{p_3}; \quad \frac{\gamma_{04}}{\gamma_н} = \frac{\gamma_3}{\gamma_н} \frac{\gamma_{04}}{\gamma_3}; \quad \frac{T_{04}}{T_4} = \frac{T_3}{T_4} \frac{T_{04}}{T_3}.$$

We carry out the verification:

$$\frac{T_{04}}{T_н} = 1 + \frac{k-1}{2} M_н^2; \quad \frac{p_{04}}{p_н} = \frac{\gamma_{04}}{\gamma_н} \frac{T_{04}}{T_н}.$$

The pressure recovery factor of a multi-shock-wave diffuser is

$$\sigma_д = \frac{p_{04}}{p_н \left(1 + \frac{k-1}{2} M_н^2\right)^{\frac{k}{k-1}}} = \frac{p_{04}}{p_н} \pi(\lambda_н).$$

The calculations of various diffuser systems, which are corroborated by experiments, show that the pressure recovery in multi-shock-wave diffusers is great, if the flow rake angles are correctly chosen.

Thus, with three oblique and one normal shock wave, if $K = 3$, then $\sigma_д > 0.6$. The pressure recovery factor diminishes with an increase in the Mach number. The velocity characteristic of the diffuser, which is found by an experimental method, is depicted in Fig. 70.

The construction of a diffuser geometry. After the incidence angles of the shock waves on the individual steps of the spike are found, it is not difficult to construct the geometry of a diffuser. For this, it is necessary that the surfaces of all the shock waves intersect the diffuser inlet edge at the design point velocity of the free stream flow $M_n = M_{rasch}$.

Let us take the surface of the first shock wave AO (see Fig. 65) at angle α_1

from point A to the axis of the engine OO. The point of intersection of line AO with the axis forms the apex of spike O. Let us take the surface of the first step of wedge OB at angle ω_1 from point O to the axis of the engine. We take the surface of the second shock wave AB at an angle of α_2 from point A to the surface of the first step OB. Point B forms the apex of the second step. We take the surface of the second step BC at angle ω_2 to the surface of the first step OB. We take the surface of the third shock wave AC at angle α_3 from point A to the second step BC. Point C forms the apex of the third step. We take the surface of the third step CD at angle ω_3 to step BC. In this way one may construct the remaining steps if their number is greater than three. We find the direction of the terminal normal shock wave by dropping a perpendicular AD from point A to the direction of the last step CD. The flow behind the normal shock wave becomes subsonic: $M_4 < 1$; the diffuser duct in the subsonic area must be expanded. The expansion of the duct is accomplished at the expense of the expansion of the outer shell and the narrowing of the rear portion of the deflecting spike. The form of the expanded portion of a supersonic multi-shock-wave diffuser is selected in the same way as for a subsonic diffuser.

After the geometry of a two-dimensional diffuser is constructed, one must proceed to the axially symmetrical diffuser with a wedge-shaped /sic/ spike. The directions of the oblique shock waves α_1, α_2, α_3, etc., remain as before. The rake angle of wedge ω'_{kl} we change to the greater rake angle of a cone ω'_{kon} (see Fig. 66) by making use of the graph in Fig. 46: $\omega'_{kon} > \omega'_{kl}$. The point of intersections B' of the cone's surface OB' with the surface of the second shock wave forms the apex of the cone's second step. The angle of the cone's second step we leave unvariable, since the curvature of the surface is small and the second terminal step produces almost the same flow disturbance as does a two-dimensional: $\omega''_{kon} = \omega''_{kl}$

We take the surface of the cone's second step at angle ω^2 to the surface of the cone's first step OB' (see Fig. 66). The point of intersection of the surface of the second step with the surface of the third shock wave C' forms the apex of the third step. We take the surface of the third step at angle ω_3 to the surface of the

second step. Thus the transition from a wedge-shaped spike to a conical one produces
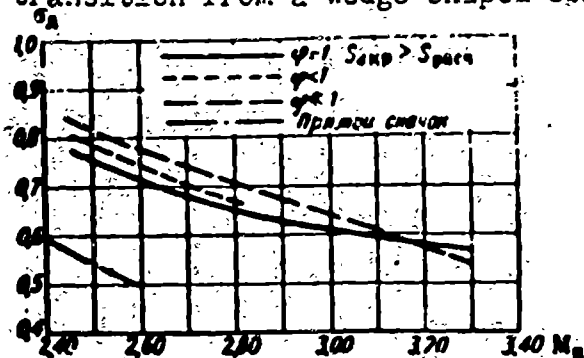
Fig. 70 The Dependence of the Pressure Recovery Factor in a Diffuser σ_D upon the Mach Number For Various Stagnation Methods and For Various Systems of Shock Waves

a substitution of only the first angle $\omega'_{k\ell}$ for the angle of a cone ω'_{kon}, and the rake angles of the second, third, and other cone steps remain equal to the angles of the wedge. This is natural, since the lesser the curvature of the step, the further it lies from the apex of the cone (see Fig. 65).

The cross sections of the spike steps are, correspondingly,

$$S_1 = \frac{\pi}{4} d_1^2;$$

$$S_2 = \frac{\pi}{4}(d_2^2 - d_1^2);$$

$$S_3 = \frac{\pi}{4}(d_3^2 - d_2^2).$$

Determination of the Critical Cross Section of a Diffuser. The cross section of the slot S_{shch} may be found from the continuity equation, when one knows the velocity and density behind the normal shock wave ω_4 and γ_4, or behind the previous oblique shock wave ω_3 and γ_3.

The absolute velocity behind the last oblique shock wave is

$$w_3 = M_3 \sqrt{g k \kappa T_3}.$$

The slot's cross section, which is measured along a normal to the flow behind the last oblique shock wave (see Fig. 65), is found by the continuity equation

$$\frac{S_{cr}}{S_{cz}} = \frac{w_n \gamma_n}{w_3 \gamma_3} = \frac{M_n}{M_3} \frac{\gamma_n}{\gamma_3} \sqrt{\frac{T_n}{T_3}}.$$

The equality of the values of S_{shch}, found from the above equation and by means of a geometric construction, is excellent proof of the exactness of the computations.

The normal shock wave will be located at the diffuser inlet only in case the tube's exhaust section S_{cr} is equal to the computed value (4.34). The following

paragraph discusses the operation of a multi-shock-wave diffuser at off design point conditions.

The calculations performed above are somewhat idealized. In actuality, the velocity profiles behind the shock waves are not uniform. Due to friction on the surface of the spike, a boundary layer develops, and the velocity of the flow falls; in order to admit all of the oncoming flow, the inlet slot is made larger than the calculated design value. A computed slot is indicated in Fig. 65 by a dotted line, and an actual one by a solid line.

The air velocity behind the inlet slot of the diffuser increases and becomes equal to the critical velocity

$$w_{\text{кр}} = \sqrt{\frac{2gkRT_{0\text{н}}}{k+1}}.$$

The density approaches the critical density

$$\gamma_{\text{t}} \approx \gamma_{\text{кр}} = \frac{p_{0\text{н}}}{RT_{0\text{н}}} \left(\frac{2}{k+1}\right)^{\frac{1}{k-1}},$$

where $p_{0\text{H}}$ is the stagnation pressure in the case of a given system of shock waves.

The critical section of the diffuser throat is found from the ratio

$$S_{1\text{кр}} = \frac{w_{\text{н}}\gamma_{\text{н}}S_{\text{вх}}}{w_{\text{кр}}\gamma_{\text{кр}}} = \frac{S_{\text{вх}}}{\lambda_{\text{н}}} \frac{\left(\frac{2}{k+1}\right)^{\frac{1}{k-1}}}{\varepsilon(\lambda_{\text{н}})\sigma'_{\text{д}}}.$$

Determination of the stagnation impulse. During operation at design conditions, the surfaces of the oblique shock waves intersect the diffuser inlet edge (see Fig. 65). The cross section of the stream tube S_n is equal to the cross section of the inlet S_1 (not to be confused with the cross section of the inlet slot S_{shch}). The mass flow ratio $\varphi = 1$ and additive drag is absent: $X_d = 0$. This means that the surplus stagnation impulse of the free stream $(F_1)_{\text{izb}}$, acting in section S_1, is equal to the momentum of the stream tube $(F_H)_{\text{izb}}$:

$$(F_1)_{\text{изб}} = \frac{Gw_{\text{н}}}{g} = \frac{\gamma_{\text{н}}S_1 w_{\text{н}}^2}{g}.$$

On the other hand, the stagnation impulse of the flow in section S_1 is equal to the pressure integral acting upon the spike, plus the momentum and the unbalanced pressure forces at the inlet slot. Projecting the acting forces onto the diffuser

axis, we obtain

$$(F_i)_{\text{int}} = \Delta p_1 S_1 + \Delta p_2 (S_2 + S_1) + \cdots \left(\frac{w_i G}{g} + S_{\text{in}} \Delta p_i\right) \cos \omega_{ob};$$

Here S_1, S_2, S_3 are the maximum cross-sections of the spike behind the first, second, third, and other steps;

Δp_1, Δp_2, Δp_3 are the average surplus pressures which act on the individual steps.

In the case of a two dimensional bullet these pressures are constant;

ω_{ob} is the total or general deviation angle of the flow:

$$\omega_{ob} = \omega_1 + \omega_2 + \omega_3 + \ldots;$$

S_{shch} is the slot's cross section, measured by a normal to the stream lines;

Δp_i is the surplus pressure in the inlet slot, equal to the pressure behind the last oblique shock wave;

w_i is the velocity in the inlet slot, equal to the velocity behind the last oblique shock wave.

The equality of the momentum of the free stream flow $\dfrac{G w_n}{g}$ and the stagnation forces acting in the inlet section is excellent proof of the exactness of the computations.

Example: Calculate the pressure recovery factor of a four-shock-wave diffuser having a conical spike, if the angles of the conical steps are:

$$\omega_1 = 24°, \quad \omega_2 = 10°, \quad \omega_3 = 5°;$$

the terminal shock wave is normal and the velocity of the free stream flow $M_n = 3.5$.

The calculation will be carried out with the aid of the graphs.

We find the two dimensional angle, which produces the disturbance of the flow corresponding to the given cone angle $\omega'_{kon} = 24°$. According to the graph in Fig. 46, $\omega'_{kl} = 15°$. The incidence angle of the first shock wave and the parameters of the air behind the first shock wave when $M = 3.5$ and $\omega_1 = 15°$ are found by the graphs in Fig. 39, 40, 41, 42, and 43: $\alpha_1 = 29°$; $M_1 = 2.61$; $\dfrac{p_1}{p_n} = 3.24$; $\dfrac{\gamma_1}{\gamma_n} = 2.21$; $= 1.467$. The angle of the second shock wave relative to the direction of the flow

behind the first shock wave, and the parameters of the air behind the second shock wave are found by the same graphs for M_1 = 2.61 and ω_2 = 10°: α_2 = 29.7°; M_2 = 2.18; $\frac{P_2}{P_1}$ = 1.90; $\frac{\gamma_2}{\gamma_1}$ = 1.57 and $\frac{T_2}{T_1}$ = 1.212. One must observe the equality in both cases

$$\frac{p_1}{p_{\text{и}}} = \frac{\gamma_1}{\gamma_{\text{и}}}\frac{T_1}{T_{\text{и}}}; \quad \frac{p_2}{p_1} = \frac{\gamma_2}{\gamma_1}\frac{T_2}{T_1}.$$

The angle of the third shock wave relative to the direction of the flow behind the second shock wave α_3 and the parameters of the air behind the third shock wave are found by the same graphs for M_2 = 2.18 and ω_3 = 5°

$$\alpha_3 = 31.2°; \quad M_3 = 2.00; \quad \frac{p_3}{p_2} = 1.34;$$

$$\frac{\gamma_3}{\gamma_2} = 1.23; \quad \frac{T_3}{T_2} = 1.087; \quad \left(\frac{p_3}{p_2} = \frac{\gamma_3}{\gamma_2}\frac{T_3}{T_2}\right).$$

The stagnation parameters behind the terminal normal shock wave when M = 2 are found in accordance with the graph in Fig. 36:

$$\frac{p_{04}}{p_3} = 5.62; \quad \frac{\gamma_{04}}{\gamma_3} = 3.12; \quad \frac{T_{04}}{T_3} = 1.8.$$

The parameters behind the third shock wave, expressed as a ratio to the parameters of an undisturbed flow, are

$$\frac{p_3}{p_{\text{и}}} = \frac{p_1}{p_{\text{и}}}\frac{p_2}{p_1}\frac{p_3}{p_2} = 3.24\cdot1.90\cdot1.34 = 8.26;$$

$$\frac{\gamma_3}{\gamma_{\text{и}}} = \frac{\gamma_1}{\gamma_{\text{и}}}\frac{\gamma_2}{\gamma_1}\frac{\gamma_3}{\gamma_2} = 2.21\cdot1.57\cdot1.23 = 4.27;$$

$$\frac{T_3}{T_{\text{и}}} = \frac{T_1}{T_{\text{и}}}\frac{T_2}{T_1}\frac{T_3}{T_2} = 1.467\cdot1.212\cdot1.087 = 1.93.$$

The cross section ratio of the inlet slot is

$$\frac{S_{\text{щ}}}{S_{\text{вх}}} = \frac{M_{\text{и}}}{M_3}\frac{\gamma_{\text{и}}}{\gamma_3}\sqrt{\frac{T_{\text{и}}}{T_3}} = \frac{3.25}{2\cdot4.27}\sqrt{\frac{1}{1.93}} = 0.294.$$

The stagnation parameters behind the normal shock wave are

$$\frac{p_{04}}{p_{\text{и}}} = \frac{p_{04}}{p_3}\frac{p_3}{p_{\text{и}}} = 5.62\cdot8.26 = 46.3;$$

$$\frac{\gamma_{04}}{\gamma_{\text{и}}} = \frac{\gamma_{04}}{\gamma_3}\frac{\gamma_3}{\gamma_{\text{и}}} = 3.12\cdot4.27 = 13.3;$$

$$\frac{T_{04}}{T_{\text{и}}} = \frac{T_{04}}{T_3}\frac{T_3}{T_{\text{и}}} = 1.8\cdot1.93 = 3.47$$

or, otherwise,

$$\frac{T_{04}}{T_{\text{и}}} = 1 + \frac{k-1}{2}M_{\text{и}}^2 = 1 + 0.2\cdot3.5^2 = 3.45;$$

$$\frac{p_{04}}{p_{\text{и}}} = \frac{\gamma_{04}}{\gamma_{\text{и}}}\frac{T_{04}}{T_{\text{и}}} = 13.3\cdot3.47 = 46.3.$$

$$\frac{p_{04}}{p_n} = \left(\frac{T_{04}}{T_n}\right)^{\overline{k-1}} = 3.45^{3.5} = 77.$$

The pressure recovery factor is

$$\sigma = \frac{\dfrac{p_{04}}{p_n}}{\dfrac{p'_{04}}{p_n}} = \frac{46.3}{77} = 0.6.$$

If the flight occurs at an altitude of H = 25 km, where the pressure is equal

to 253 kg/cm^2, then the diffuser considered by us gives a pressure of p_{04} = 46.3 p_n =

11,700 kg/m^2 = 1.17 atm, totally sufficient to sustain combustion.

Section 8. The Operation of a Multi-Shock Wave-Diffuser at Off Design Point Condi-

tions. Additional Resistance.

The operation process of a multi-shock-wave diffuser is dependent upon two

factors: the Mach number of the free stream flow and the tube's exhaust opening

cross section. Let us examine the influence of these factors upon the operation of

a multi-shock-wave diffuser.

The operation of a multi-shock-wave diffuser at an off design point velocity

is: $M_n \neq M_{rasch}$. If the velocity of the free stream flow is greater than that of the

design value: $M_n > M_{rasch}$, then the incidence angles of the shock waves decrease

(see Fig. 43) and the surfaces of the shock waves fall not upon the forward edge,

but inside the throat (Fig. 71, a). During the approach of the free stream flow to

the exposed diffuser edge, a rarefaction wave appears, as during the supersonic flow

around an obtuse angle. The flow compressed in several oblique shock waves, and the

flow which has passed through the rarefication waves, will both penetrate into the

throat. The profiles of velocities and pressures at the inlet to the throat abruptly

becomes dissimilar. In the subsonic portion of the diffuser there will occur a gradual

straightening of the profiles, but the average stagnation pressure will prove to be less

than the possible maximum at a given velocity M. The pressure recovery factor σ_d will

be lowered. The dependence of σ_d on M_n is depicted in Fig 72. The diffuser mass flow

ratio at flight velocities higher than the design point remains equal to one, and the

wave drag equal to zero.

If the flight velocity is less than the design point: $M_n < M_{rasch}$, then the incidence angles of the shock waves increase (see Fig. 13). The shock waves cease to touch the inlet edge (Fig. 71,b) and increased pressure begins to act on the surface of the conical shell of the diffuser. The boundaries of the flow passing through the engine, which run parallel to the spike generatrix from the forward edge, are represented in Fig. 71,b, by a dotted line. The smaller the flow velocity M, the greater the incidence angles of the shock waves, the lesser the cross-section of the stream tube S_n, and the lesser the mass flow ratio $\varphi = \dfrac{S_n}{S_1}$.
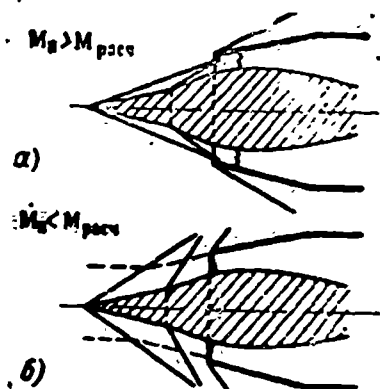
Fig. 71. Schematics of shock waves which appear at the inlet to a diffuser at off design point velocities.
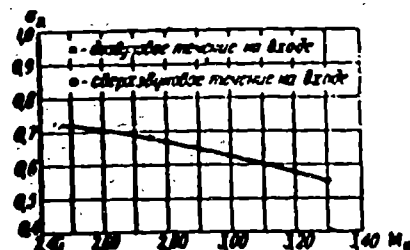
Fig. 72. The velocity characteristic of a diffuser $\omega = 22°$; $\dfrac{d_{кr}}{d_1} = 0.634$.

With a decrease of the mass flow ratio φ the additive wave drag X_d of the diffuser increases. After finding, as was shown above, the pressure ratios behind the first, second, third, and other shock waves are $\dfrac{p_1}{p_n}, \dfrac{p_2}{p_n}, \dfrac{p_3}{p_n} \ldots$, one may find the additive wave drag of the diffuser by assuming that the pressures which act on the surface of each step of the bullet are uniform.

The forces which act on the surface of each step are respectively equal to

$$X_1 = S_1(p_1 - p_n) = \frac{\pi}{4} d_1^2 p_n \left(\frac{p_1}{p_n} - 1 \right);$$

$$X_2 = (S_2 - S_1)(p_2 - p_n) = \frac{\pi}{4}(d_2^2 - d_1^2) p_n \left(\frac{p_2}{p_n} - 1 \right). \qquad (4.42)$$

The additive drag of the diffuser (see Chapter II, Section 8) is

$$X_d = X_1 + X_2 + \ldots + \left[(p_l - p_n) S_{ш} + \frac{G w_l}{g} \right] \cos \omega_{od} - \frac{G w_n}{g}. \qquad (4.43)$$

Additive diffuser drag in the case of conical spikes is more reliably determined experimentally by testing model diffusers in a supersonic wind tunnel (see Fig. 59, b).

Additive drag is determined by the mass flow ratio: when $\varphi = 1$, $X_d = 0$. With

a decrease of the mass flow ratio φ the additive drag increases (Fig. 73).

The additive wave drag coefficient referred to the maximum cross section, is equal to

$$c_{\text{A}} = \frac{X_{\text{A}}}{q S_{\text{M}}} .$$

(4.44)

The mass flow ratio is equal to the ratio of the actual flow rate through the engine to the maximum possible flow rate

$$\varphi = \frac{G}{w_{\text{H}} T_{\text{H}} S_1} = \frac{w_3 T_3 S_{\text{M}}}{w_{\text{H}} T_{\text{H}} S_1} = \frac{M_3 T_3}{M_{\text{H}} T_{\text{H}}} \sqrt{\frac{T_3}{T_{\text{H}}}} \frac{S_{\text{M}}}{S_1} .$$

(4.45)

The cross section area ratio of the inlet slot for a given diffuser is known: $f = \dfrac{S_{\text{shch}}}{S_1}$. We find the mass flow ratio φ after determining, as was shown above, M_3, γ_3, and T_3.

At sufficiently low M_n, the velocity of the flow before one of the steps becomes so small that the flow rake angle proves to be greater than critical: $\omega > \omega_{\text{cr}}$ (see Fig. 38). The oblique shock wave before this step is transformed into a normal one (see Fig. 71). The pressure behind the normal shock wave begins to act not only on the inlet section, but also on the steps of the spike which lie behind the normal shock wave, and the additive wave drag abruptly increases. With a subsequent decrease of M_n the normal shock wave is displaced to the point of the spike.

For example, in the case of the diffuser considered on page 126: $\omega_1 = 15°$; $\omega_2 = 10°$; $\omega_3 = 5°$, a normal shock wave appears in front of the third step, as seen in Fig. 38, when $M_2 = 1.24$, i.e., when $M_n \approx 2$ (see Fig. 39). A normal shock wave appears in front of the second step when $M_1 = 1.42$ or when $M_n = 1.94$. A normal shock wave appears in front of the first step at $M_n = 1.62$. If the diffuser is intended for operation through a wide range of velocities, beginning at $M_n < M_{\text{rasch}}$, then to decrease the inlet wave drag, diffusers are used with small inlet section area ratios $\dfrac{S_1}{S_{\text{M}}}$ and large mass flow ratios φ, i.e., large slot area ratios $f = \dfrac{S_{\text{shch}}}{S_1}$.

Example. Find the mass flow ratio of a 15°, 10°, 5° diffuser if $M_n = 2.5$ and $f = \dfrac{S_{\text{shch}}}{S_1} = 0.294$.

We find the parameters of the air behind the first shock wave on the basis of velocity $M_n = 2.5$ by the graphs in Fig. 39, 40, 41, and 42.

$$M_1 = 1,67; \quad \frac{p_1}{p_0} = 2,47; \quad \frac{\gamma_1}{\gamma_0} = 1,87; \quad \frac{T_1}{T_0} = 1,32$$

a)

b)
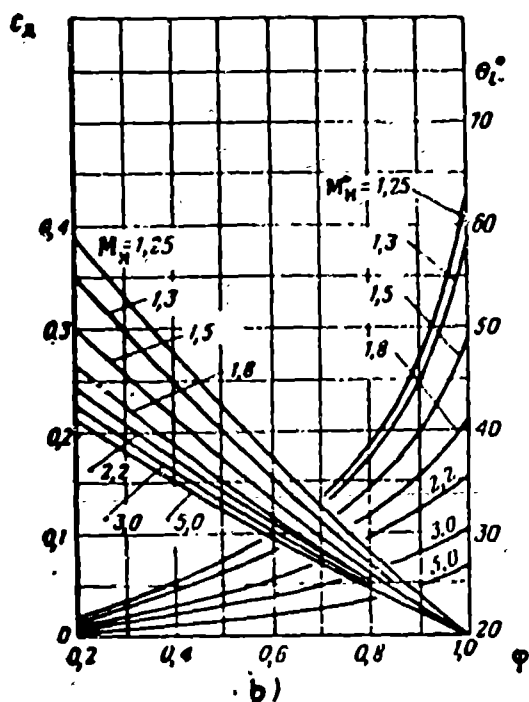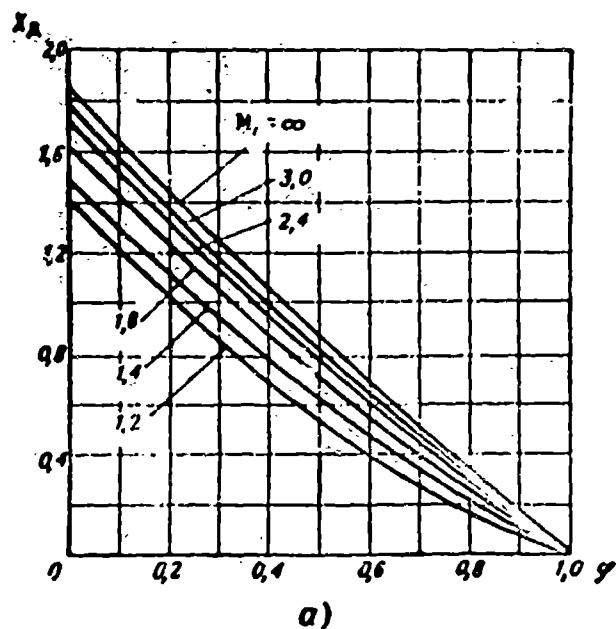
Fig. 73. Additive diffuser drag.
a -- the dependence of additive drag X_d upon the mass flow ratio φ; b -- the dependence of c_d upon the mass flow ratio, θ -- angle determining the position of the spike in relation to the inlet edge. (see Fig. 65, b)

On the basis of velocity $M_1 = 1.67$, we find the parameters of the air behind the second shock $M_2 = 1.33$, $\dfrac{p_2}{p_1} = 1.65$; $\dfrac{\gamma_2}{\gamma_1} = 1.42$; $\dfrac{T_2}{T_1} = 1.150$. On the basis of velocity M_2

$= 1.33$, we find the parameters of the air behind the third shock wave

$M_3 = 1.13$; $\dfrac{p_3}{p_2} = 1.31$; $\dfrac{\gamma_3}{\gamma_2} = 1.21$; $\dfrac{T_3}{T_2} = 1.08$. We determine the parameters which have

to do with the condition of the free stream flow:

$$\frac{\nu_3}{p_{\mu}}=2,47\cdot1,65\cdot1,31=5,35;$$

$$\frac{T_3}{T_{\mu}}=1,87\cdot1,42\cdot1,21=3,21;$$

$$\frac{T_3}{T_{\mu}}=1,32\cdot1,158\cdot1,08=1,65.$$

The mass flow ratio is

$$\varphi=\frac{M_3}{M_{\mu}}\frac{\gamma_3}{\gamma_{\mu}}\sqrt{\frac{T_3}{T_{\mu}}}f=\frac{1,13}{2,5}\ 3,21\ \sqrt{1,65\cdot0,294}=0,550.$$

The operation of a multi-shock wave diffuser with an off design point tube

exhaust section area. The location of the terminal normal shock wave de-

pends on the area of the exhaust section of the tube, which is connected to the dif-

diffused (see Fig. 59). At a certain "design point" cross section area of the ex-

haust opening $S_{\mu cr}$, a normal shock wave is located at the inlet slot (see Fig. 65).

If the exhaust section of the tube $S_{\mu cr}$ is greater than the design point one: $S_{\mu cr}$

$>S_{rasch}$ (Fig. 74), a normal shock wave does not form in the throat and the flow re-

mains supersonic. As a supersonic flow reaches the inlet edge, a rarefaction wave is

formed. The flow in the divergent portion of the diffuser will be accelerated and

will end with a powerful normal shock wave, accompanied by great losses. The air

flow will remain constant and equal to the maximum possible value:

$$G=w_3\gamma_3 S_{rop}=w_{\mu}\gamma_{\mu}S_1=const;\ \ \varphi=1.$$
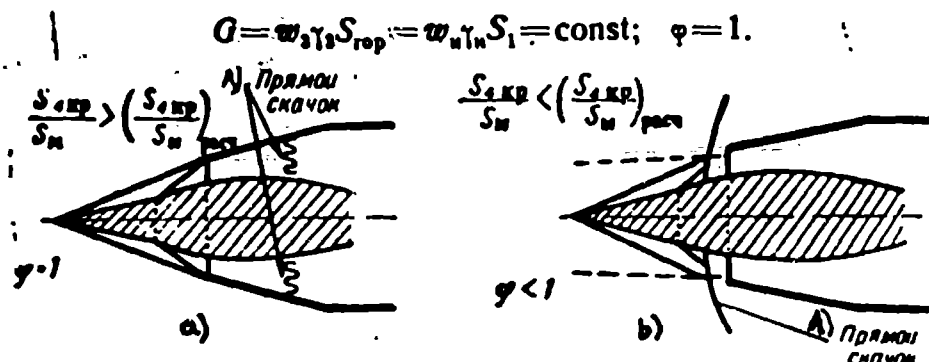
Fig. 74. Schematics of shock waves which appear at the diffuser inlet at off design
point hydraulic resistance.
a — φ = 1, b — φ < 1. A) normal shock wave.

The air pressure in front of the exit from the tube will be such as required in

order to discharge G = $w_n \gamma_n S_1$ kg of gas from the exhaust section every second (see

4.29).

With an increase of the area of the exhaust section S_{cr}, the pressure ahead of

the exit falls and the recovery factor decreases.

If the exhaust section becomes less than the design point value, then the stag-

nation pressure ahead of the exit will be almost constant: $S_{cr} < S_{rasch} \frac{p_{ocr}}{p_n} \approx const.$

The air flow through the diffuser, and, consequently, the mass flow ratio will be decreasing directly proportional to the exhaust cross section area. The incidence angles of the oblique shock waves on the individual diffuser steps will remain as before. A normal shock wave will move forward from the throat and be located at some distance in from of the inlet, decreasing the surface of the oblique shock waves. (Fig. 76, b). A portion of the compressed subsonic flow from the space behind the normal shock which, when $S_{vykh} \geqslant S_{rasch}$ was directed into the diffuser throat, will now flow past the throat around the diffuser along its sides. The mass flow ratio φ decreases; the surface exposed to the action of the pressure which has grown behind a normal shock wave, increases. The wave drag of the diffuser augments (Fig. 75). The location of the terminal shock wave becomes unstable and diffuser "buzzing" begins.
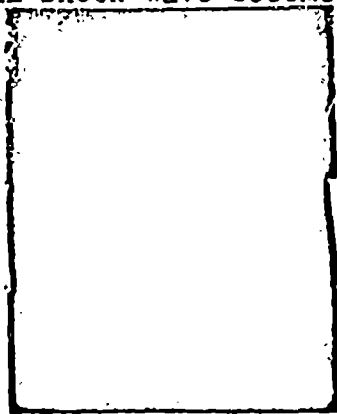
Fig. 75. A photograph of the shock waves which appear at a diffuser inlet when $\varphi < 1$.

The off design point characteristics of diffusers are usually tested experimentally, by flowing air at small diffuser models in wind tunnels. The directions of the oblique shock waves depend only upon the Mach number or upon the flow rake angle and not upon the absolute dimensions of the models; therefore the results of the tests performe on small-scale models may be carried over to full-scale diffusers with only a small correction for the relative value of the throat, since the relative thickness of the boundary layer on various scale models is not similar.

BIBLIOGRAPHY

1. Abramovich, G.N., "Drag of Diffusers," Prikladnaya gazovaya dinamika /Applied Gas Dynamics/, GITTL, Moscow-Leningrad, 1953, 290-303.

2. Limonad, Yu. G., Profilirovaniye vkhodnikh uchastkov tonneley i kapotov /Profiling the Inlet Portions of Tunnels and Housings/, TVF, 1942, No 2.

3. Sibulkin, M., "Theoretical and Experimental Research on Additive Drag," NACA Rep, 1954, No 1187.

4. Ferri, A. and Nucci, L., "Theoretical and Experimental Research on Circular Section Air Scoops with Low Drag at Mach Numbers of 3.3, 2.75, and 2.45," NACA Rep., 1954, No 1189.

5. Oswatisch, Kl., Der Druckruckgewinn bei Geschossen mit Ruckstossantrieb bei hohen Uberschallgeschwindigkeiten, 1944, (see NACA TM. 1140).

6. Hugonio, "Sur la propagation des mouvements dans les corps fluides et specialement dans les gas parfait," Journ. Ec. Phys., v. 58, 1889.

CHAPTER V

JET NOZZLES

The compressed gases, which are heated in a combustion chamber or in a heat exchanger, are exhausted through an exhaust nozzle. In the exhaust nozzle the gases' pressure falls and their velocity increases. The gases, which are exhausted from the nozzle, act on the engine with the force of their reaction; therefore, exhaust nozzles are often called jet nozzles. In a jet nozzle the enthalpy of the gases is changed to the kinetic energy of the flow.

If the relative pressure drop across the nozzle is less than critical, the velocity of the flow from the nozzle will be less than the local speed of sound.

If the relative pressure drop across the nozzle is greater than critical, the velocity of the gases which are exhausted from the nozzle may become greater than the local speed of sound.

In conformity with the discharge velocity, the nozzles are divided into subsonic and supersonic types. The contours of subsonic and supersonic nozzles are different.

In order to pass various inputs of gas at a given temperature and pressure or in order to pass a given gas input at a given pressure and various temperatures, the cross section of the nozzle must have a variable value. These nozzles, whose cross section may be changed, are called variable-area nozzles. Some makes of subsonic variable-area nozzles exist. A series of supersonic variable-area jet nozzles, suitable for exploitation, have been proposed.

SECTION 1. THE EQUATION OF A FLOW THROUGH A NOZZLE

A diagram of a nozzle is depicted on Fig. 76. If we disregard the comparatively weak heat exchange with the surrounding medium, then the stagnation temperature, and consequently, the critical velocity will remain constant: $T_{0i} = T_{03} = $ const;

$$a_i = \sqrt{\frac{2gkR}{k+1}T_{0i}} = a_r = \text{const.} \qquad (5.1)$$

The absolute and relative velocity of the gas, which moves through the nozzle, increases.

The flow velocity in the narrowest "critical" section of the nozzle S_{4cr}, as shown in Chapter II, section 7, may not become higher than the local speed of sound. When $w_i = w_{4cr} = w_g$ the gas flow through the nozzle reaches maximum value.
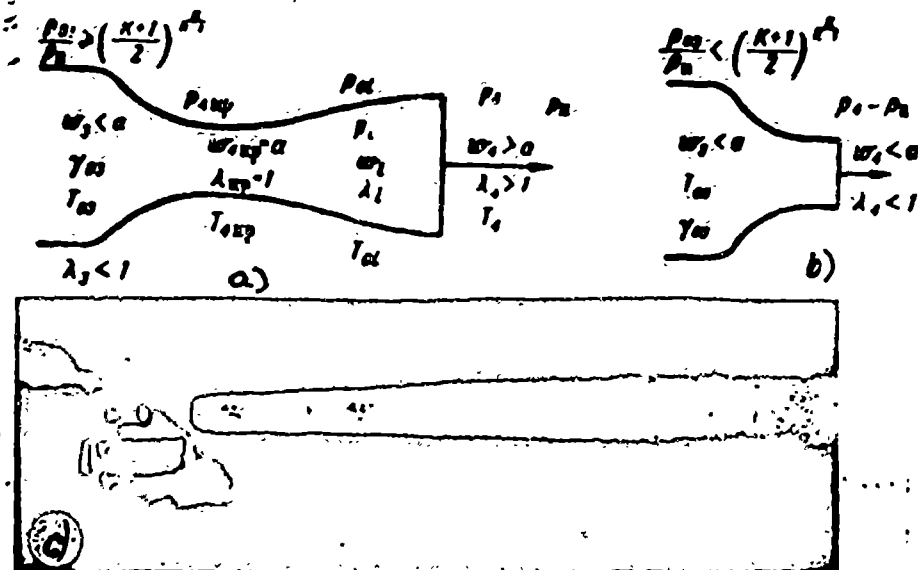
Fig. 76. Jet nozzles. a — supersonic, b — subsonic, c — a photograph of a supersonic stream, exhausting from a nozzle.

The relative velocity of the flow in any nozzle section is determined by the local ratio of total pressure to static pressure $\frac{p_{0i}}{p_i}$ (see 2.72).

$$\lambda_i = \sqrt{\frac{k+1}{k-1}\left[1-\left(\frac{p_i}{p_{0i}}\right)^{\frac{k-1}{k}}\right]} \quad (5.2)$$

The absolute velocity in a given section S_i according to (2.67) and (5.2):

$$w_i = a_i \lambda_i = \sqrt{\frac{2gkR}{k-1}T_{0i}\left[1-\left(\frac{p_i}{p_{0i}}\right)^{\frac{k-1}{k}}\right]} \quad (5.3)$$

The gas flow through a given section in conformance with (2.74):

$$G_i = \sqrt{\frac{2gk}{(k+1)R}}\frac{S_i p_{0i}}{\sqrt{T_{0i}}}q(\lambda_i). \quad (5.4)$$

After writing down the flow equations for any two sections S_i and S_j, we find a connection between the velocities and the sections:

$$\frac{S_i}{S_j}=\frac{p_{0j}\,q(\lambda_j)}{p_{0i}\,q(\lambda_i)}. \quad (5.5)$$

During a discharge without losses, the flow's total pressure does not vary:

$$p_{0i}=p_{0i}=p_{03}=\text{const.}$$

The section, in which the velocity reaches a sonic value: $\lambda_i = 1$, is called the "critical" /throat/ section S_{4cr}.

SECTION 2. SUBSONIC AND SUPERSONIC NOZZLES

If the pressure drop across the nozzle is greater than critical:

$$\frac{p_{03}}{p_n} > \left(\frac{k+1}{2}\right)^{\frac{k}{k-1}},$$ (5.6)

then the velocity in the narrowest section of the nozzle reaches sonic value: λ_{4cr} = 1. During this, the gas dynamic function is

$$q(\lambda_{4\kappa p}) = \left(\frac{2}{k+1}\right)^{\frac{1}{k-1}}.$$ (2.75)

We find the flow through the throat section by using (5.4)

$$G = \sqrt{\left(\frac{2}{k+1}\right)^{\frac{k+1}{k-1}} \frac{gk}{R} \frac{p_{0i} S_{4\kappa p}}{\sqrt{T_{0i}}}}$$ (5.7)

The stagnation pressure in the throat section decreases, but remains higher than that of the atmosphere:

$$p_{4\kappa p} = p_{03} \left(\frac{2}{k+1}\right)^{\frac{k}{k-1}} > p_{n}.$$ (5.8)

The surplus pressure may be used for accelerating the gas to supersonic velocity in the expanded portion of the nozzle (Fig. 76, a), called the supersonic portion. Supersonic nozzles were suggested at the end of the last century by the Swedish engineer Laval and carry his name.

The ratio of any section of a Laval nozzle to the critical section S_{4cr} may be found from (5.5), noting that when $S_j = S_{4cr}$, λ_j = 1:

$$\varepsilon_i = \frac{S_i}{S_{4\kappa p}} = \frac{\left(\frac{2}{k+1}\right)^{\frac{1}{k-1}}}{\lambda_i \left[1 - \frac{k-1}{k+1}\lambda_i^2\right]^{\frac{1}{k-1}}},$$ (5.9)

Substituting in place of λ_i its value from (5.2), we find the connection between the ratio of nozzle section $\varepsilon_i = \frac{S_i}{S_{4\kappa p}}$ and the relative pressure ratio $\frac{p_{0i}}{p_i}$:

$$\varepsilon_i = \frac{S_i}{S_{4\kappa p}} = \frac{\left(\frac{2}{k+1}\right)^{\frac{1}{k-1}} \left(\frac{p_{0i}}{p_i}\right)^{\frac{1}{k}}}{\sqrt{\frac{k+1}{k-1}\left[1 - \left(\frac{p_i}{p_{0i}}\right)^{\frac{k-1}{k}}\right]}}.$$ (5.10)

The exhaust area ratio of a Laval nozzle, necessary for the total utilization of the overall pressure drop, is determined from the last equation by replacing the ratio $\frac{p_{0i}}{p_i}$ by the ratio $\frac{p_{03}}{p_n}$.

With an increase of the overall pressure ratio $\frac{p_{03}}{p_n}$ the relative nozzle expansion,

necessary for the total effect of the pressure ratio, increases (Fig. 77). The
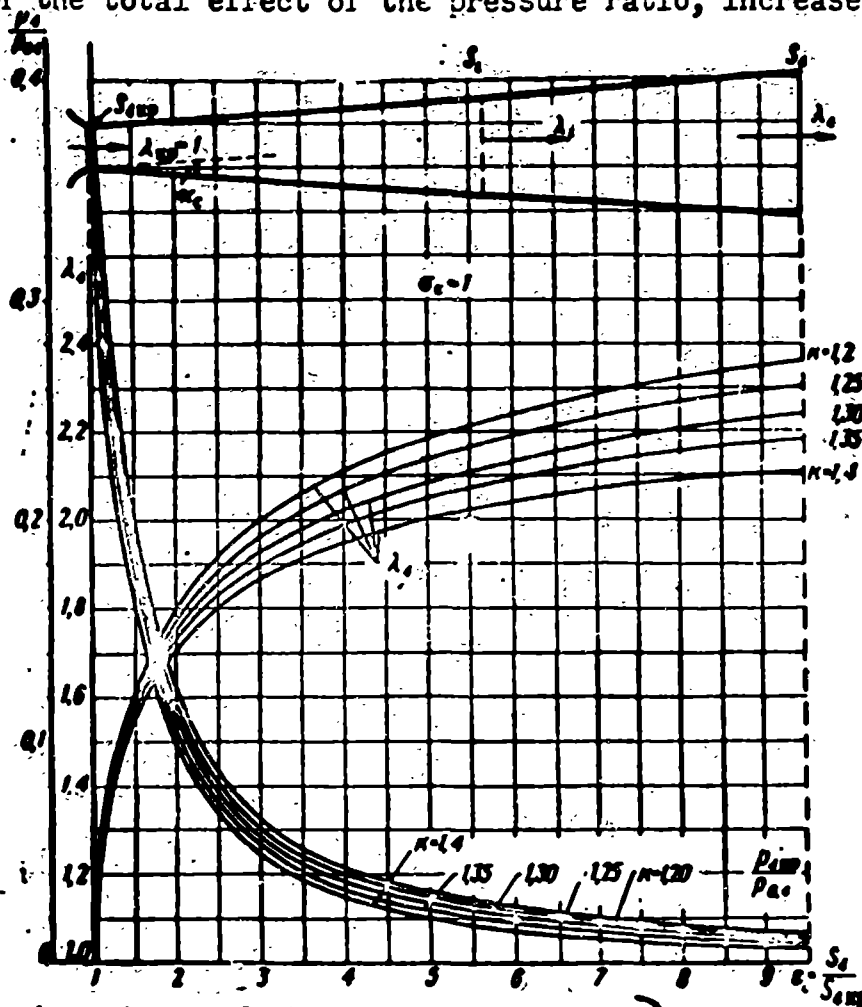
Fig. 77. The dependence of the relative velocity λ_4 and the relative pressure ratio $\pi (\lambda) = \dfrac{p_4}{p_{04}}$ on the degree of expansion of an ideal nozzle $\varepsilon_i = \dfrac{S_4}{S_{cr}}$ ..

necessary degree of nozzle expansion ε depends also on the parameter $k = \dfrac{c_p}{c_v}$. Thus, when $k = 1.4$ and when $\dfrac{p_{03}}{p_n} = 20$: $\varepsilon = \dfrac{S_4}{S_4} = 3$; $\lambda_4 = 1.87$; and with the same pressure ratio, but k being equal to 1.2: $\varepsilon = 3.6$ and $\lambda_4 = 2.07$. When the area ratio is computed to be $S_4 = \varepsilon S_{4cr}$, the pressure at the nozzle exhaust is equal to that of the atmosphere: $p_4 = p_n$.

If the overall pressure ratio is less than critical:

$$\frac{p_n}{p_0} < \left(\frac{k+1}{2}\right)^{\frac{k}{k-1}},$$
(5.11)

then the velocity in the narrowest nozzle section does not attain a sonic value $\lambda_4 < 1$. If one supplies a nozzle with an expanded portion, then not an increase but a decrease of the velocity will occur in it, and the reaction of the exhausting gases will diminish. Subsonic nozzles do not require an expanding portion (see Fig. 76, b). During a sub-critical discharge, the pressure at the nozzle exhaust is equal to the

pressure of the surrounding medium: $p_4 = p_n$.

A flow of gas through an actual nozzle is accompanied by losses from friction and shocks. Because of these, the energy is dissipated. The stagnation pressure during an irreversible discharge is decreased, and the discharge velocity will be less than during a flow without losses.

SECTION 3. ENERGY DISSIPATION AND LOSSES DURING DISCHARGE FROM A NOZZLE

The flow of heated gases through an actual nozzle is accompanied by the partial dissipation of kinetic energy and heat losses through the walls. The dissipation of energy is accompanied by a decrease of the flow's stagnation pressure and an increase of the gas entropy S.

We denote the overall relative stagnation pressure ratio accompanying the discharge from the nozzle by $\dfrac{p_{03}}{p_4}$.

The discharge velocity from an ideal nozzle $w_{4\mathrm{ID}}$ is expressed by the equation

$$w_{4\text{ид}} = \sqrt{\frac{2gkRT_{03}}{k-1}\left[1-\left(\frac{p_4}{p_{03}}\right)^{\frac{k-1}{k}}\right]}. \tag{5.12}$$

The discharge velocity from a real nozzle, owing to the dissipation of energy and thermal losses, will have a lesser value w_4:

$$w_4 = \sqrt{\frac{2gkR}{k-1}T_{03}\eta_c\left[1-\left(\frac{p_4}{p_{04}}\right)^{\frac{k-1}{k}}\right]}, \tag{5.13}$$

where p_{04} is the stagnation pressure at the nozzle exhaust:

$$p_{04} = \sigma_c p_{03}, \tag{5.14}$$

σ_s is the nozzle pressure coefficient;

η_s is the enthalpy conservation factor during a flow through a nozzle. If the thermal losses through the walls are absent, $\eta_s = 1$.

The dissipated kinetic energy during the absence of losses through the walls is equal to the difference of

$$\Delta E_{\text{дис}} = \frac{w_{4\text{ид}}^2 - w_4^2}{2g}. \tag{5.15}$$

The increase in entropy is equal to the dissipated energy divided by the temperature:

$$\Delta s = A \frac{\Delta E_{kc}}{T_4} \, . \tag{5.16}$$

Substituting (5.12) and (5.13) in (5.16), we obtain

$$\Delta s = \frac{c_p T_{03}}{T_4} \left(\frac{p_4}{p_{03}}\right)^{\frac{k-1}{k}} \left(1 - \frac{1}{\sigma_c^{\frac{k-1}{k}}}\right) = c_p \left(1 - \frac{1}{\sigma_c^{\frac{k-1}{k}}}\right) . \tag{5.17}$$

With a decrease of the nozzle pressure coefficient σ_s, the increase of entropy of the exhausting gases becomes greater.

The process of the dissipation of energy occurs in the subsonic and supersonic portions of the nozzle. To compute the gas flow G, the nozzle pressure coefficient must be properly divided into a pressure coefficient for the subsonic portion σ'_s, and that for the supersonic portion σ''_s:

$$\sigma'_c = \frac{p_{04kp}}{p_{03}}; \quad \sigma''_c = \frac{p_{04}}{p_{04kp}};$$

$$\sigma_c = \sigma'_c \sigma''_c. \tag{5.18}$$

The pressure coefficient of a well designed subsonic portion of a nozzle is usually high: $\sigma'_s = 0.97$ to 0.99. The pressure coefficient of the supersonic portion decreases with an increase in the relative discharge velocity because of the growth of the losses in the formation of shock waves and vortexes, and because of friction of the supersonic flow along the walls. The pressure coefficients of supersonic nozzles are determined by means of tests.

The losses in nozzles may also be expressed with the aid of the velocity coefficient φ_s:

$$\varphi_c = \frac{w_4}{w_{4u\lambda}} \frac{\lambda_4}{\lambda_{4u\lambda}} = \sqrt{\eta_c \frac{1 - \left(\frac{p_4}{\sigma_c p_{03}}\right)^{\frac{k-1}{k}}}{1 - \left(\frac{p_4}{p_{03}}\right)^{\frac{k-1}{k}}}} \, . \tag{5.19}$$

The dependence between the velocity coefficient and the pressure coefficient $\varphi_s = f(\sigma_s)$ in the absence of thermal losses ($\eta_s = 1$), is depicted in Fig. 78. For large overall pressure ratios $\frac{p_{03}}{p_4}$, i.e., for large relative discharge velocities: $\lambda_4 > 1.5$, the large changes in σ_s are accompanied by small changes in φ_s.

The flow through the nozzle /in conformance with (2.74)7, depends on the pressure
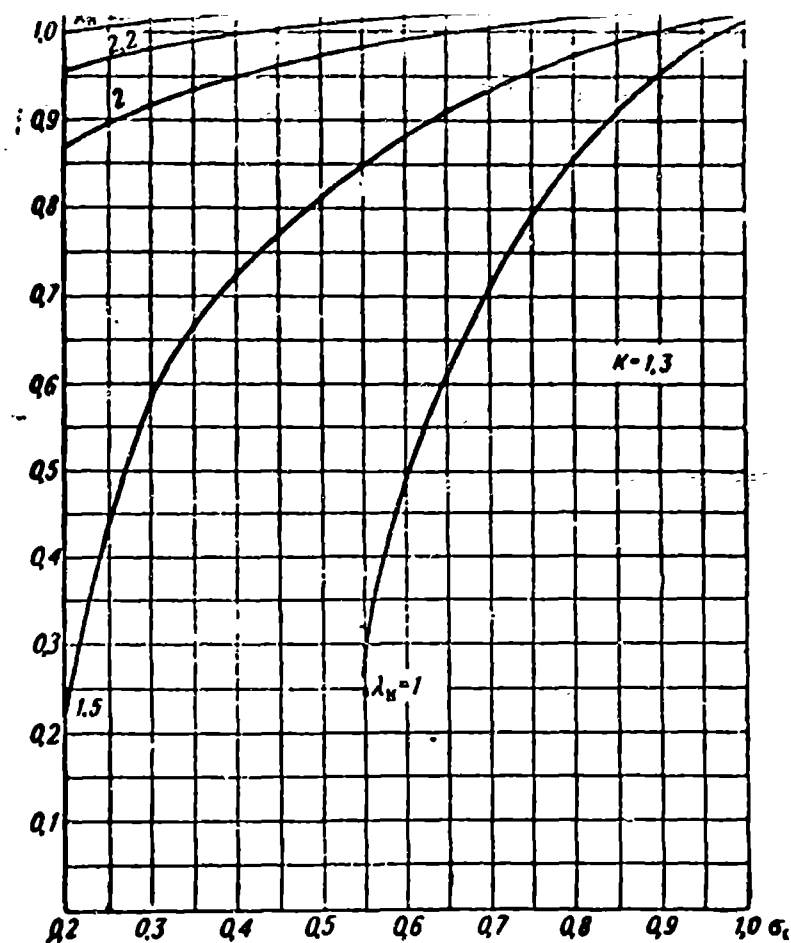
Fig. 78. The dependence of the velocity coefficient $\varphi_s = \dfrac{\lambda_4}{\lambda_{4\text{ID}}}$ on the nozzle pressure coefficient σ_s.

coefficient of the subsonic portion σ_s':

$$G = \sqrt{\left(\frac{2}{k+1}\right)^{\frac{k+1}{k-1}} \frac{gk}{R} \frac{p_{0\kappa p} S_{4\kappa p}}{\sqrt{T_{0s}}}} =$$

$$= \sqrt{\left(\frac{2}{k+1}\right)^{\frac{k+1}{k-1}} \frac{gk}{R} \frac{\sigma_c' p_{0s} S_{4\kappa p}}{\sqrt{T_{0s}}}}.$$

The calculated degree of nozzle expansion $\mathcal{E}_4 = \dfrac{S_4}{S_{4cr}}$, in conformance with (5.7), depends on the total pressure coefficient σ_s

$$\varepsilon_4 = \frac{S_4}{S_{4\kappa p}} = \frac{p_{0s}}{p_{04}} \frac{\left(\frac{2}{k+1}\right)^{\frac{1}{k-1}}}{q\,(\lambda_4)} = \frac{\left(\frac{2}{k+1}\right)^{\frac{1}{k-1}}}{\sigma_c q\,(\lambda_4)}. \qquad (5.20)$$

The discharge velocity for a given pressure ratio also depends on σ_s:

$$\lambda_4 = \sqrt{\frac{k+1}{k-1}\left[1-\left(\frac{p_4}{p_{04}}\right)^{\frac{k-1}{k}}\right]} =$$

$$= \sqrt{\frac{k+1}{k-1}\left[1-\left(\frac{p_{\scriptscriptstyle H}}{\sigma_c p_{0s}}\right)^{\frac{k-1}{k}}\right]}. \qquad (5.21)$$

Substituting (5.21) in (5.20), we find the connection of the degree of expan-

sion with the overall pressure ratio and coefficient σ_s of an actual supersonic nozzle

$$e_4=\frac{S_4}{S_{4\kappa p}}=\frac{\left(\frac{2}{k+1}\right)^{\frac{1}{k-1}}\left(\sigma_c\frac{p_{00}}{p_{00}}\right)^{\frac{1}{k}}}{\sigma_c\sqrt{\frac{k+1}{k-1}\left[1-\left(\frac{p_{00}}{p_c p_{00}}\right)^{\frac{k-1}{k}}\right]}}.$$

(5.22)

With a decrease in the pressure recovery coefficient σ_s, the calculated value of the exhaust cross section area ratio increases, since the discharge velocity diminishes. The pressure remains equal to the atmosphere, the static temperature increases insignificantly because of the decrease of velocity, and the static density decreases because of the increase of temperature.

The thrust of the exhausting gases varies with the degree of nozzle expansion and with the pressure coefficient.

SECTION 4. THE IMPULSE OF GASES EXHAUSTING FROM A NOZZLE. IMPULSE LOSS FACTOR

The impulse of the gases, which are exhausted from a nozzle, in conformance with (2.76) is equal to

$$F_4=\frac{G_4 w_4}{g}+p_4 S_4.$$

(5.23)

After making Kiselev's transformation, we express the impulse of the gases by the relative discharge velocity /see (2.81)7:

$$F_4=\frac{k_r+1}{2gk_r}a_r G_4\left(\lambda_4+\frac{1}{\lambda_4}\right).$$

(5.24)

Here and later the index "g" stands for the value belonging to the "hot" end of the engine.

The critical velocity of the discharge gases a_g is equal to

$$a_r=\sqrt{\frac{2gk_r R_r}{k_r+1}T_{0r}}.$$

(5.25)

The gas flow through the nozzle's critical section S_{4cr} in accordance with (2.74) will be

$$G_4=\sqrt{\left(\frac{2}{k_r+1}\right)^{\frac{k_r+1}{k_r-1}}\frac{gk_r}{R_r}\frac{p_{04\kappa p}S_{4\kappa p}}{\sqrt{T_{0r}}}}.$$

(5.26)

The critical discharge velocity is directly proportional to the square root of the stagnation temperature of gases and their flow is inversely proportional to this

quantity Therefore, the gas impulse does not depend on these temperatures:

$$F_4 = \left(\frac{2}{k_r+1}\right)^{\frac{1}{k_r-1}} p_{04kp} S_{4kp}\left(\lambda_4 + \frac{1}{\lambda_4}\right).$$ (5.27)

The impulse of the discharge gases is proportional to the product of the stagnation pressure in the critical section p_{04cr}, the area of the critical section S_{4cr}, and the gas dynamic function

$$z(\lambda_4) = \lambda_4 + \frac{1}{\lambda_4}.$$

With an increase in pressure ratio across the nozzle $\frac{p_{03}}{p_4}$, the computed degree of nozzle expansion $\mathcal{E} = \frac{S_4}{S_4} = f(\frac{p_{03}}{p_4})$ increases in accordance with equation (5.22); and the relative discharge velocity λ_4, together with the gas dynamic function $z(\lambda_4)$ and impulse of the gases, increases.

We find the critical impulse F_{4cr} by substituting $\lambda_4 = 1$ in (5.27):

$$F_{4kp} = 2\left(\frac{2}{k_r+1}\right)^{\frac{1}{k_r-1}} \sigma'_c p_{03} S_{4kp}.$$ (5.28)

The impulse coefficient c_λ for the expanding section of a Laval nozzle is equal to (see 2.86)

$$c_\lambda = \frac{F_4}{F_{4kp}} = \frac{z(\lambda_4)}{2} < \frac{k_c}{\sqrt{k_r^2 - 1}}.$$ (5.29)

The actual magnitude of the impulse during the use of an expanded nozzle is less than the calculated value. The impulse losses are attributed to the fact that the streams of gas which discharge from a conical nozzle are not parallel to one anothc . The gas streams which are adjacent to the axis are parallel to the axis; those streams which are close to the walls are parallel to the walls (Fig. 79). The reaction force is only caused by the normal impulse components $w_i G_i \cos a_i$, since the tangential components $w_i G_i \sin a_i$ counterbalance one another (see Fig. 79). The average value of the momentum of the discharge gases $(G_4 w_4)_{sr}$ is proportional to the average value of $\cos a_i$ for the entire nozzle exhaust section. In the first approximation one may accept

$$(G_4 w_4)_{cp} = G_4 w_4 \frac{1 + \cos \frac{a_c}{2}}{2}.$$ (5.30)

The impulse losses during the discharge from a nozzle are usually determined by means of experiments, by directly measuring the reaction force of the gases discharging from the nozzle.
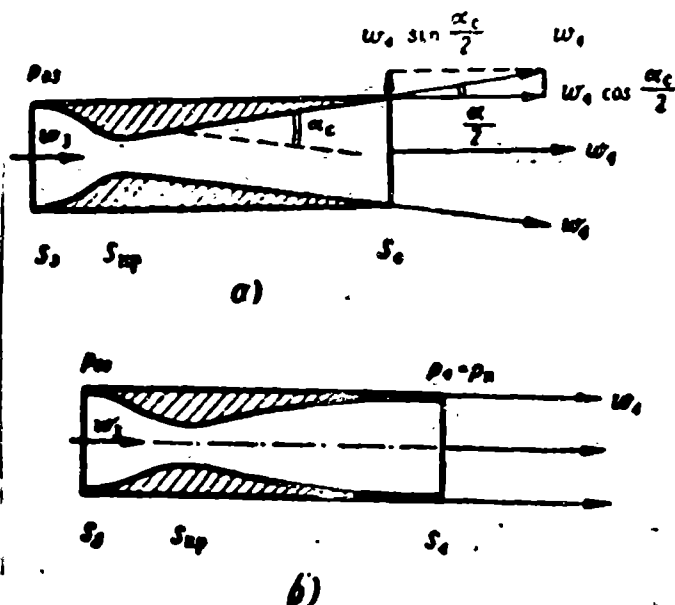
Fig. 79. The discharge from a nozzle.
a -- the stream lines at the exhaust of a conical Laval nozzle are not
parallel to one another, b -- the stream lines at the exhaust of a Frankl
nozzle are parallel to one another.

The reaction force of the gases acting on the nozzle during discharge into the

atmosphere, is equal to the impulse per second of the effluxing gases minus the force

of the atmospheric pressure on the shell $\int_S p_n dS = p_n S_4$, i.e., equal to the net im-

pulse F_{4izb}:

$$F_{4izb} = P_4 - p_n S_4 = \frac{G_4 w_4}{g} + S_4 (p_4 - p_n).$$

The calculated value of the net impulse during the total expansion of the gases

to the back pressure $p_4 = p_n$ depends on the overall pressure drop $\dfrac{p_{03}}{p_n}$

$$(F_{4izb})_{rasch} = \frac{G_4 w_4}{g}. \tag{5.31}$$

In practice, the measured reaction force of the gases is less than the calcu-

lated net impulse: $F_{4izb} < (F_{4izb})_{rasch}$.

The difference between the calculated net impulse $(F_{4izg})_{rasch}$ and the measured

reaction force is called the impulse loss ΔF:

$$\Delta F = (F_{4izb})_{rasch} - F_{4izb}. \tag{5.32}$$

The ratio of the impulse loss ΔF to the calculated net impulse $(F_{izb})_{rasch}$ is

called the impulse loss factor δ :

$$\delta = \frac{\Delta F}{(F_{4izb})_{rasch}} = 1 - \frac{F_{4izb}}{(F_{4izb})_{rasch}}. \tag{5.33}$$

The impulse loss factor is determined by the nozzle configuration, degree of

expansion ε, quality of the machining of the internal surface, nozzle expansion angle

α_s and thermal losses through the walls.

We will introduce the concept of the effective pressure coefficient $\sigma_{\text{эф}}$ for which the net impulse of the nozzle, operating with complete expansion $p_4 = p_n$, is equal to the measured impulse, $F_{4\text{izb}}$.

The effective pressure coefficient is uniquely connected to the impulse loss factor:

$$\delta = 1 - \frac{F_{4\text{изб}}}{(F_{4\text{изб}})_{\text{расч}}} = 1 - \frac{G_4 w_4}{G_4 w_{4\text{расч}}} = 1 - \frac{\lambda_4}{\lambda_{4\text{расч}}};$$

$$\delta = 1 - \sqrt{\frac{1 - \left(\frac{p_н}{\sigma_{\text{эф}} p_{03}}\right)^{\frac{k_r-1}{k_r}}}{1 - \left(\frac{p_4}{p_{03}}\right)^{\frac{k_r-1}{k_r}}}}.$$

(5.34)

The relationship between the effective pressure factor of the nozzle and the impulse loss factor is depicted on Figure 80. From this graph we see that, for example, when $\frac{p_{03}}{p_n} = 40$ an impulse loss of 1% corresponds approximately to a pressure loss of 12%.

The internal nozzle outlines should have such a contour that the impulse loss factor has the least value. The impulse loss factor of finely manufactured and contoured supersonic nozzles usually does not exceed 2%.
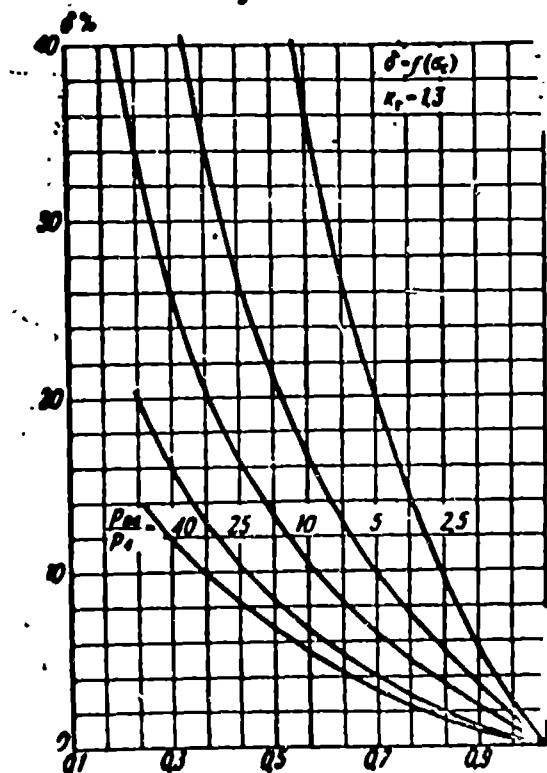
Fig. 80. The dependence of the impulse loss factor δ on the nozzle pressure coefficient σ_s.

SECTION 5. NOZZLE OPERATION DURING OFF-DESIGN POINT CONDITIONS

The relative pressure ratio of the gases in an expanding nozzle $\pi = \dfrac{p_{03}}{p_4}$ and the relative discharge velocity λ_4 depend on the degree of nozzle expansion $\varepsilon = \dfrac{s_4}{s_{4cr}}$ and on Poisson's index k_g (see 5.10). The relative velocity depends on the temperature of the gases T_4 only as much as the temperature depends on the value of k_g (see Figure 86, b).

The pressure ratio across a nozzle having a constant degree of expansion $\varepsilon = \dfrac{s_4}{s_4} = $ const when k = const is constant: $\pi = \dfrac{p_{04}}{p_4} = $ const and the relative discharge velocity is also constant: $\lambda_{4cr} = $ const.

The degree of expansion of an actual supersonic jet nozzle having fixed cross sections is set and cannot change during variations of flight conditions or of combustion chamber operating conditions. Therefore, the relative pressure ratio across a fixed geometry supersonic nozzle π and the relative velocity λ_4 are constant (if k = const).

The pressure ratio to free stream $\dfrac{p_{03}}{p_n}$ may not be equal to the pressure ratio to the exit $\pi = \dfrac{p_{03}}{p_4}$, since usually $p_4 \neq p_n$.

If the pressure ratio to free stream $\dfrac{p_{03}}{p_n}$ is greater than the pressure ratio to the exit

$$\frac{p_{03}}{p_n} > \pi = \frac{p_{03}}{p_4} = f(\varepsilon),$$

then the nozzle operates with underexpansion (Figure 81a). In this case the pressure at the nozzle exit p_4 is greater than the back pressure: $p_4 > p_n$, and the stream lines at the nozzle outlet suddenly widen.

If the pressure ratio to free stream is equal to the pressure ratio to the exit

$$\frac{p_{03}}{p_n} = \pi = \frac{p_{03}}{p_4} = f(\varepsilon),$$

then the nozzle operates at the design condition, the pressure at the exit is equal to the back pressure: $p_4 = p_n$, and the relative discharge velocity remains constant $\lambda_4 = f(\varepsilon) = $ const.

If the pressure ratio to free stream is less than the pressure ratio to the exit

$$\frac{p_\infty}{p_n} < \pi = \frac{p_{03}}{p_4} = f(\varepsilon),$$

then the nozzle operates with overexpansion and the pressure at the exit will be less than the back pressure: $p_4 < p_n$.
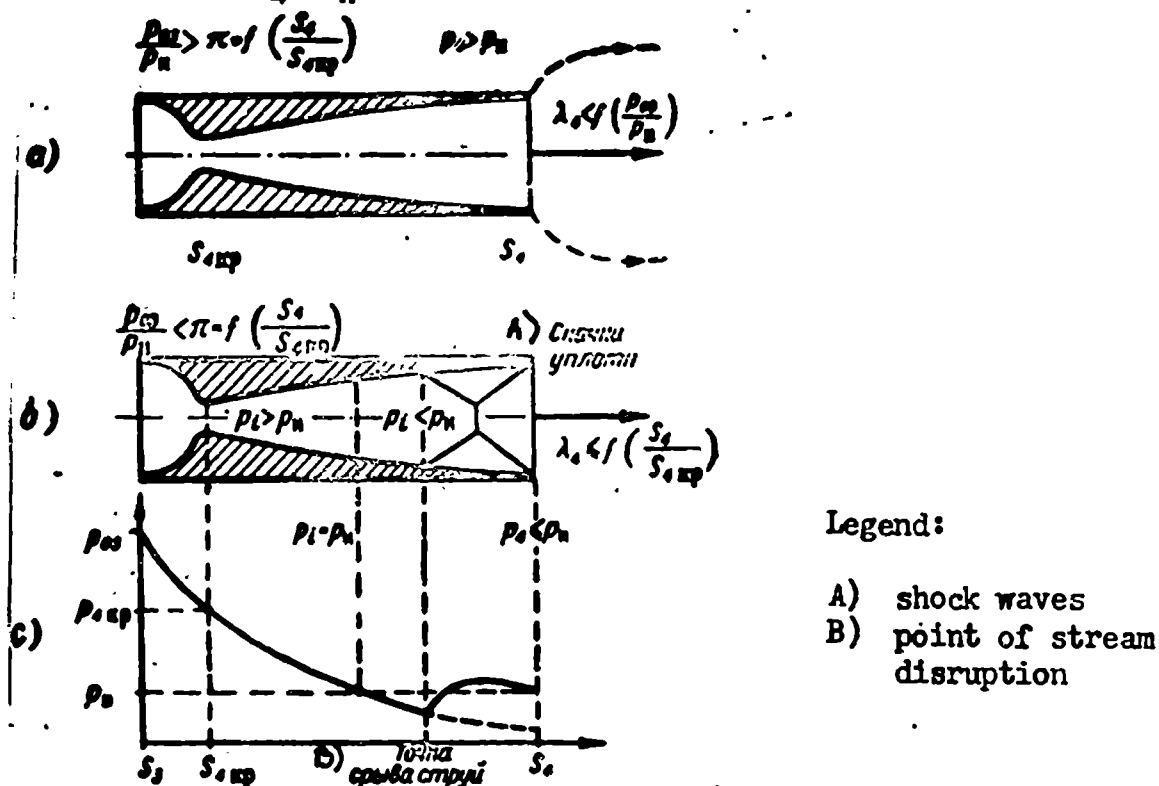
Fig. 81. Nozzle operation at off-design point pressure ratio.

$$a - \frac{p_{03}}{p_n} > f\left(\frac{S_4}{S_{4cr}}\right); \quad b - \frac{p_{03}}{p} < f\left(\frac{S_4}{S_{4cr}}\right); \quad c - \text{expansion diagram}$$

Legend:

A) shock waves
B) point of stream disruption

Separation of the supersonic flow from the nozzle walls may occur during large overexpansion (see Figure 81b and c). The supersonic flow, separating from the walls and interacting with the surrounding gases, suddenly loses velocity. A system of oblique shock waves appears in the nozzle, as a result of which the pressure grows and the velocity falls. The thrust of the gases during operation with overexpansion diminishes (Figure 82). Therefore, when designing supersonic nozzles a degree of expansion is chosen so that through the entire range of engine operation the nozzle works either at rated conditions or with underexpansion. If the pressure at the nozzle exit is greater than the pressure of the surrounding medium: $p_4 > p_n$, then the discharge velocity will be less than the maximum possible value: $\lambda_4 < \lambda'_{rasch}$. The thrust of the discharge gases F_4 will be less than calculated: $F_4 < F_{4rasch}$.

$$F_4 = \left(\frac{2}{k+1}\right)^{\overline{k-1}} p_{04} S_{\text{кр}} \left(\lambda_4 + \frac{1}{\lambda_4}\right) <$$

$$< \left(\frac{2}{k+1}\right)^{\frac{1}{k-1}} p_{04} S_{\text{кр}} \left(\lambda_{4\text{рас}} + \frac{1}{\lambda_{4\text{рас}}}\right).$$

(5.34)
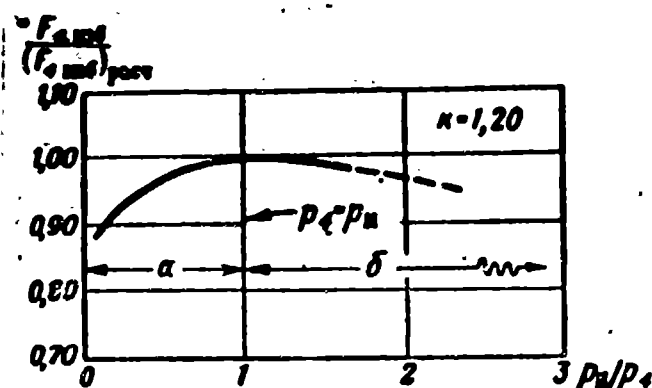
Fig. 82. The dependence of the relative variation of the gases' jet force upon the relative variation of the pressure ratio.

The relative decrease of the jet forces of the discharge gases owing to underexpansion is

$$\frac{F_4}{F_{\text{рас}}} = \frac{\lambda_4 + \dfrac{1}{\lambda_4}}{\lambda_{4\text{рас}} + \dfrac{1}{\lambda_{4\text{рас}}}}.$$

(5.35)

If, for example, $\lambda_{4\text{rasch}} = 2$, and $\lambda_4 = 1.5$, then $\quad \dfrac{F}{F_{\text{рас}}} = \dfrac{1.5 + \dfrac{1}{1.5}}{2 + \dfrac{1}{2}} = 0.87.$

With an increase in the nozzle exhaust cross section S_4 the drag due to atmospheric pressure acting on the engine shell $p_n(S_4 - S_n)$, increases because of the increase of the difference of the cross sections $S_4 - S_n$. Therefore, the jet thrust of the engine diminishes with an increase in overexpansion (see 2.76); (2.77) and (2.78).

$$R = F_4 - F_1 - p_n(S_4 - S_n).$$

(5.36)

At lean fuel/air ratios, the stagnation pressure ahead of a supersonic ramjet nozzle decreases (see Chapter IX). In the design of nozzles, the degree of expansion is chosen in conformance with the lowest operating pressure in the combustion chamber. Variable area nozzles may allow a substantial improvement of the parameters of a wide operating range supersonic ramjet engine intended for flight with variable velocities and, consequently, with variable pressures $\dfrac{p_{03}}{p_n}$.

SECTION 6. VARIABLE AREA NOZZLES

The most simple means of regulating the cross section of convergent nozzles consists of using a movable cone or "bullet". (Variable area nozzles with movable bullets are used in turbo-jet engines. Figure 83a). When the bullet shifts in the direction-of the diffuser, the nozzle cross section increases. One can, in principle, so profile the outside walls of a nozzle and the outlines of the bullet as to form an expanding duct between the walls and the tapering bullet. However, endeavors to construct supersonic nozzles with variable area bullets, which would operate without stream disruption or shock wave formation and would give the calculated thrusts have not been successful.

To simplify the control problems, sometimes axisymmetrical nozzles are abandoned, and two-dimensional nozzles are used (Figure 83, b and c).

A nozzle with movable sides (Figure 83b) consists of two flat sides, hinged to which are movable rigid contoured sides. As the contoured sides vary position, it is impossible to maintain parallel stream lines at the nozzle exit through the entire variable range. Due to this the thrust proves to be less than calculated.

Nozzles with flexible sides (Figure 83c) consist of two flat rigid sides and two flexible sides made from resilient steel sheets. Under the pressure of shaped cams, the flexible walls bend and change the area of the critical section, and consequently, the degree of nozzle expansion.

Nozzles with flexible sides are used in variable area supersonic wind tunnels. The difficulties in selecting materials, which are able to maintain their resilient qualities at the operating temperatures of ramjet engines, limit the usage of nozzles with flexible sides.

SECTION 7. NOZZLE CONTOURING AND DESIGNING

The internal contours of the nozzles are designed, in conformance with theoretical principles supported by numerous experiments, so as to make uniform the velocity profile at the nozzle exit, to form the flow stream lines into parallel paths, and to
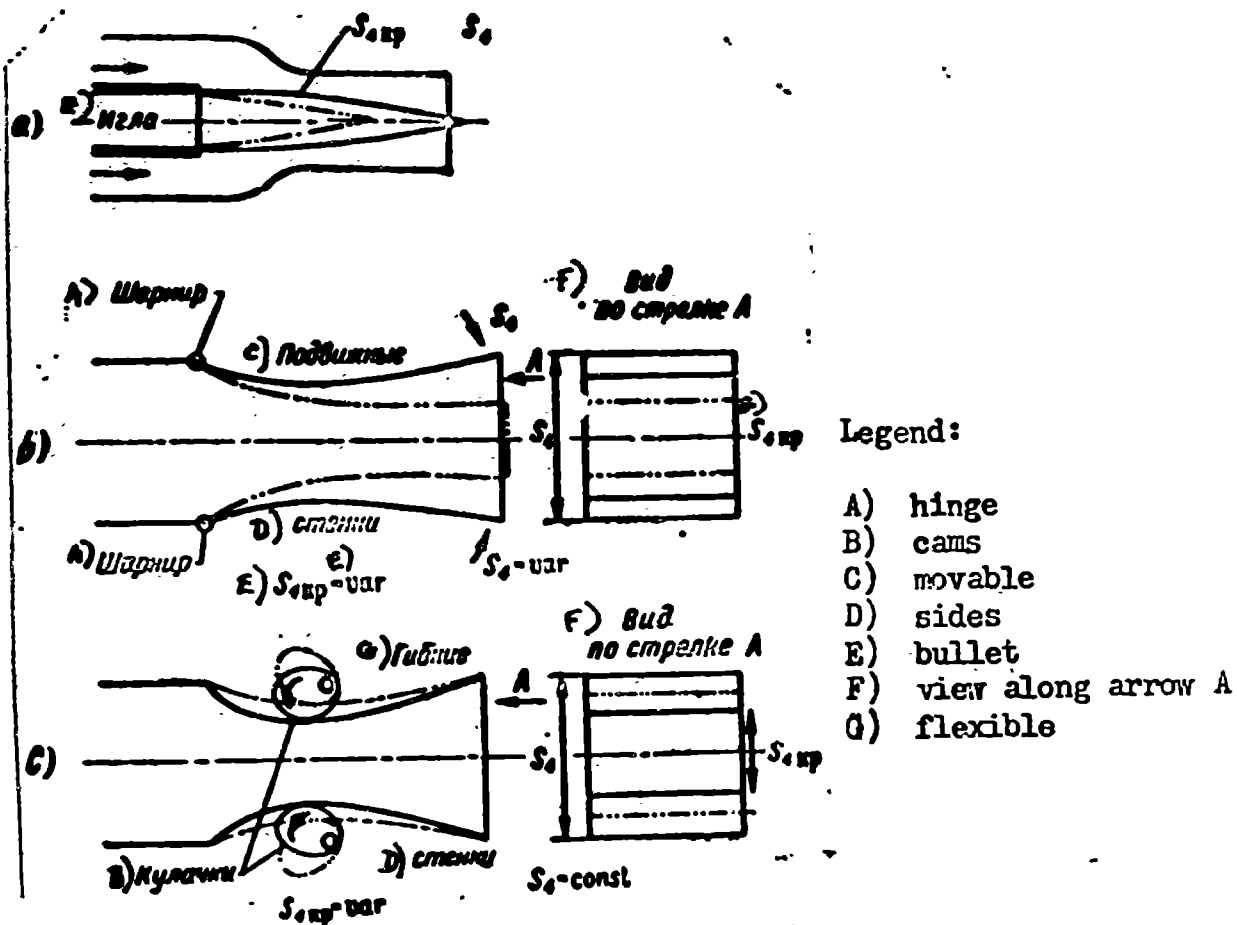
Fig. 83. Plans of variable area nozzles.
a -- nozzle with variable area bullet; b -- nozzle with movable sides;
c -- nozzle with flexible sides.

Legend:

A) hinge
B) cams
C) movable
D) sides
E) bullet
F) view along arrow A
G) flexible

prevent the flow from separating from the walls.

The subsonic portion of a nozzle is constructed according to Vitoshinskiy's

formula

$$\frac{d_{\text{кр}}}{d_x} = \sqrt{1 - \left[1 - \left(\frac{d_{\text{кр}}}{d_{\text{н}}}\right)^2\right]\frac{\left(1 - \frac{x^2}{l^2}\right)^2}{\left(1 + \frac{x^2}{3l^2}\right)^3}},$$

(5.37)

where d_{H} is the initial cross section;

d_x is the diameter at x distance from the initial cross section;

d_{cr} is the diameter of the critical section;

l is the nozzle length.

The profiling of a nozzle according to Vitoshinskiy's formula ensures the max
mum possible uniformity of the velocity profile at the exit of a convergent subsoni
nozzle and the maximum possible parallelism of the streamlines.

The supersonic portion of a nozzle is constructed according to a graphic-anal
ic method, worked out by the Soviet scientist F. I. Frankel. Frankel's supersoni

nozzles possess fine velocity profiles at the exit and have parallel supersonic flow. However, these nozzles are long and therefore primarily used in wind tunnels. Nozzles for jet engines are made much shorter and use flat surface elements to form the internal contour.

In a well-designed expanding portion of a nozzle, the supersonic velocity profile at the outlet appears to be uniform with stream lines parallel to the axis (see Fig. 79, b). In this case $c_\lambda \approx 1$.

To design a nozzle it is necessary to know the ambient pressure p_n, the stagnation pressure ahead of the nozzle p_{03}, the stagnation temperature T_{03}, and the gas weight flow rate through the nozzle G.

The throat section of the nozzle S_{4cr} is determined from the formula (5.26)

$$S_{кр} = \sqrt{\frac{R}{gk}\left(\frac{k+1}{2}\right)^{\frac{k+1}{k-1}}}\; \frac{G\sqrt{T_{03}}}{\sigma_c p_{03}},$$
(5.38)

where σ_s' is the pressure coefficient of the subsonic portion of the nozzle. In actual nozzles, when the internal walls are finely machined, the losses in the subsonic portion are small: $0.98 < \sigma_s' < 0.99$.

The temperature of the discharge gases T_4 is

$$T_4 = T_{04}\left(\frac{p_4}{p_{04}}\right)^{\frac{k-1}{k}}.$$
(5.39)

The relative velocity at the nozzle outlet λ_4, in accordance with the formula (5.21) is equal to

$$\lambda_4 = \sqrt{\frac{k+1}{k-1}\left[1 - \left(\frac{p_4}{\sigma_c p_{03}}\right)^{\frac{k-1}{k}}\right]}.$$
(5.40)

We express the degree of nozzle expansion ε in terms of the calculated pressure ratio π across the nozzle $\varepsilon = f(\pi)$ according to formula (5.22) or by the graph depicted in Figure 77.

After defining the diameters of the throat and exit cross sections S_{4cr} and S_4, we design the contour of the supersonic portion.

The inlet diameter of the subsonic portion of the nozzle d_3 is equal to the diameter of the combustion chamber: $d_3 = d_{к.sг}$.

We design the contour of the subsonic portion according to Vitoshinskiy's

formula (5.37).

Example of the Calculation. Design a nozzle with the following data:

$$T_{03} = 2100^\circ \text{ K}; \quad G_4 = 100 \text{ kg/sec}; \quad p_{03} = 3 \text{ kg/cm}^2$$

$$p_4 = 60 \text{ mm of mercury col.} \quad \sigma'_s = 0.96; \quad c_\alpha = 0.99$$

$$\sigma'_s = 0.95; \quad \delta_s = \sigma'_s \ \sigma''_s = 0.91$$

Poisson's index and the gas constant: $k = 1.25; \quad R_g = 30 \text{ kg m/kg deg.}$

The factor of B in the flow formula (2.53), according to table 2.1 is: B = 0.38. From this is derived the nozzle throat section:

$$S_{4\text{кр}} = \frac{G_4 \sqrt{T_{03}}}{0.38 \sigma_c \ p_{03}} = \frac{100 \sqrt{2100}}{0.38 \cdot 0.96 \cdot 3 \cdot 10^4} = 0.425 \text{ m}^2.$$

The diameter of the throat section $d_{4\text{cr}} = 738 \text{ mm.}$

The pressure ratio across the nozzle is

$$\pi = \frac{p_{03}}{p_4} = \frac{3 \cdot 735}{60} = 36.8.$$

The temperature ratio to the exit is

$$\frac{T_4}{T_{03}} = \left(\frac{p_4}{p_{03}}\right)^{\frac{k-1}{k}} = \frac{1}{(\sigma_c \pi)^{\frac{k-1}{k}}} = \frac{1}{(0.91 \cdot 36.8)^{\frac{0.25}{1.25}}} = 0.416.$$

The temperature of the discharge gases $T_4 = 872^\circ \text{ K.}$

The relative velocity at the exit, in accordance with (5.40) (see also Fig. 77) is

$$\lambda_4 = \sqrt{\frac{k+1}{k-1}\left[1 - \left(\frac{p_n}{p_{03}\sigma_c}\right)^{\frac{k-1}{k}}\right]} = \sqrt{\frac{2.25}{0.25}[1 - 0.416]} = 2.27.$$

The gas dynamic function (see also Fig. 207) is:

$$q(\lambda) = \lambda_4\left[1 - \frac{k-1}{k+1}\lambda_4^2\right]^{\frac{1}{k-1}} = 2.27\left(1 - \frac{2.27^2}{9}\right)^4 = 0.067.$$

The degree of nozzle expansion, in accordance with (5.20) is

$$\bar{s} = \frac{S_4}{S_{4\text{кр}}} = \frac{\left(\frac{2}{k+1}\right)^{\frac{1}{k-1}}}{\sigma_c q(\lambda)} = \frac{0.625}{0.91 \cdot 0.067} = 10.2$$

The diameter of the exit cross section is

$$d_{\text{вих}} = d_{\text{кр}} \sqrt{\bar{s}} = 738 \sqrt{10.2} = 2360 \text{ mm.}$$

The critical velocity, in accordance with (2.54) is

$$a_{\text{кр}} = \sqrt{\frac{2gkRT_{03}}{k+1}} = \sqrt{\frac{19.6 \cdot 1.25 \cdot 30 \cdot 2100}{2.25}} = 820 \text{ m/sec.}$$

The thrust of the exhaust gases (see 5.24) is

$$P_4 = \frac{k+1}{2gk} a_{\text{кр}} G_4\left(\lambda_4 + \frac{1}{\lambda_4}\right) = \frac{2.25 \cdot 820 \cdot 100}{2 \cdot 9.8 \cdot 1.25}\left(2.27 + \frac{1}{2.27}\right) = 7550 \cdot 2.71 = 20\,500 \text{ kg.}$$

BIBLIOGRAPHY

1. Astrov, V.; Levin, E.; Pavlov, L.; Khristianovich, S., "O raschyete sopel Lavalya," /The Calculation of a Laval Nozzle/, Prikladnaya matematika i mekhanika /Applied Mathematics and Mechanics/, 1943, Vol II, 1st Ed.

2. Bolgarskiy, A. V. and Shchukin, V. K., Rabochiye protsessi zhidkostno-reaktivnikh dvigatelyakh /Working Processes in Liquid-Fuel Jet Engines/ Oborongiz, 1953.

3. Vulis, L. A., Termodinamika gazovikh potokov /The Thermodynamics of Gas Flows/ Energoizdat, 1950.

4. Zauer, R., Vvedeniye v gazovuyu dinamiku /An Introduction to Gas Dynamics/, M.-L., 1947.

5. Ilyukhin, N. V., "Issledovaniye teploperedachi i poter' na treniye dlya ustanovivshegosya techeniya pri ochen' bol'shikh skorostyakh," /An Investigation of Heat Transfer and Losses due to Friction for a Constant Flow during Very High Velocities/. Izvestia of the Academy of Sciences, USSR, 5, 1946, 703-718.

6. Kochin, H. Ye.; Kibel', I. A.; and Roze, N. B., "Teoreticheskaya gidromekhanika," /Theoretical Fluid Mechanics/, GITTL, M.-L., 1948, parts I, II.

7. Kisenko, M.S., "Sravnitel'niye ispitaniya neskol'kikh variantov sopel," /Comparative Studies of Several Nozzle Variants/, Works of TSAGI, Edition 478, 1940.

8. Frankel, F. I.; Khristianovich, S.A. and Alekseyeva, R. N., "Osnovy gazovoy dinamika," /Principles of Gas Dynamics/, Works of TSAGI, No. 364, 1938.

9. Shapiro, Howthorne, "The Mechanics and Thermodynamics of Steady One-Dimensional Gas Flow," J. App. Mech, 14, 1947.

10. Stodola, A., Steam and Gas Turbines, New York and London, 1927.

11. Diehl, W.S., NACA TR, 218, 1940.

12. Warfield, C. N., NACA TN, 1200, 1947.

13. Sammerfield, M.; Foster C. R., and Swan, W.C., Flow Separation in Overexpacted Supersonic Exhaust Nozzles, Los Angeles, XI, 1948.

14. Beckwith, I. E., and Moore, I. A., "An Accurate and Rapid Method for the Design of Supersonic Nozzles," NACA TN, No 3322, Feb. 1955.

77)

BASIC PRINCIPLES OF MOLECULAR FUELS USED IN A RAMJET ENGINE, AND THEIR COMBUSTION

Ramjet engines may utilize the energy of atomic fuels or the energy of molecular (chemical) fuels which is released during combustion with air. Only several forms of fuel, which possess definite combinations of physical-chemical properties, are used in ramjet engines.

This chapter will show what qualities these fuels must have to be suitable for ramjet engines, and will cite basic data on the combustion of fuel-air mixtures.

SECTION 1. THE PHYSICO-CHEMICAL PARAMETERS OF RAMJET ENGINE FUELS

Ramjet engines create the thrust that is necessary to propel aircraft. Solid fuel and liquid fuel rockets with the same mid-section area and with the same weight are capable of developing greater thrust. In the ratio of frontal and weight thrust $R_M = \frac{R}{S_M}$ and $R_p = \frac{R}{P}$, ramjet engines are inferior to rocket engines. The advantage of a ramjet engine in comparison to a rocket is in the considerably less specific consumption of fuel, or, alternately, the significantly greater specific thrust $\underline{/sic\underline{7}}$[*] $I = \frac{R}{G}$.

The specific thrust and the thrust coefficient of a ramjet engine vary with change in the composition of the fuel mixture.

The maximum value of the thrust coefficient c_R or the specific thrust I depends on the nature of the fuel used.

In Chapter III the equation of the specific thrust of an ideal ramjet engine was found:

$$I = \frac{R}{G_r} = \frac{aL\mathbf{w}_1}{g}(\beta\sqrt{\theta} - 1). \tag{6.1}$$

The general efficiency coefficient is

$$\eta = \frac{AR\mathbf{w}_0}{G_r H_s}. \tag{6.2}$$

---

[*]Translator's Note: Should be "specific impulse".

Consequently,

$$I = \frac{H_s \eta}{A w_s}.$$
(6.3)

The temperature ratio during operation with a molecular fuel is

$$\theta = \frac{T_{0r}}{T_{0x}} = 1 + \frac{H_s}{[(1 + \alpha L) c_p T_{0x}]}.$$
(6.4)

At a given velocity and flight altitude the temperature ratio θ is determined by the excess air coefficient α. The correct mixture ratio for any fuel would produce a given temperature ratio so that the overall efficiency η would be a maximum (of course, if the required temperature ratio is not too great: $\theta < \theta_{max}$, $\alpha > 1$).

For a given temperature ratio θ, the overall efficiency of a ramjet engine does not depend on the nature of the fuel.

The specific thrust at constant efficiency is directly proportional to the lower heating value of the fuel. The greatest value of overall efficiency, as we will see further on (Chapter XI), depends only upon the losses in the engine and for practical purposes does not depend on the nature of the fuel. Therefore ramjet engines are capable of producing the highest specific thrust when operating on a fuel that has the highest H_u.

The thrust coefficient of an ideal ramjet engine is

$$c_R = 2 \left(1 - \frac{1}{\theta \sqrt{\theta}} \right).$$
(6.5)

A ramjet engine, operating on a fuel capable of insuring the greatest temperature ratio of the gases θ, will posses maximum thrust coefficient.

At a given velocity w_n and flight altitude H, the temperature ratio reaches a maximum, if the excess air coefficient is equal to one: $\alpha = 1$.

$$\theta = \theta_{max} = \frac{H_s}{c_p T_{0x}(1 + L)} + 1.$$
(6.6)

The amount of heat, which accompanies 1 kg of combustion products formed by a stoichiometric composition of the mixture, is called the calorific value of the fuel W:

$$W = \frac{H_s}{1 + L}$$
(6.7)

A ramjet engine, which uses the greatest heat-producing mixture, is capable of producing the highest thrust coefficient.

In those cases where the highest thrust coefficient c_R is required, a fuel with the highest calorific value W is used. When the greatest economy is desired, i.e., the highest specific thrust, a fuel having a high heating value H_u is used.

Along with the heating value and calorific value the suitability of a fuel is determined by its density and boiling point.

We will consider the influence of the fuel's density. We will assume that the weight of a winged missle, which uses various fuels, remains constant: P_{pol} = const. In this case the wing area and the wing's aerodynamic drag will be constants: S_{cr} = const

$$X_{кр} = \frac{P_{пол}}{k_{кр}} = \text{const}$$

(6.8)

where k_{cr} is the aerodynamic quality of the wing.
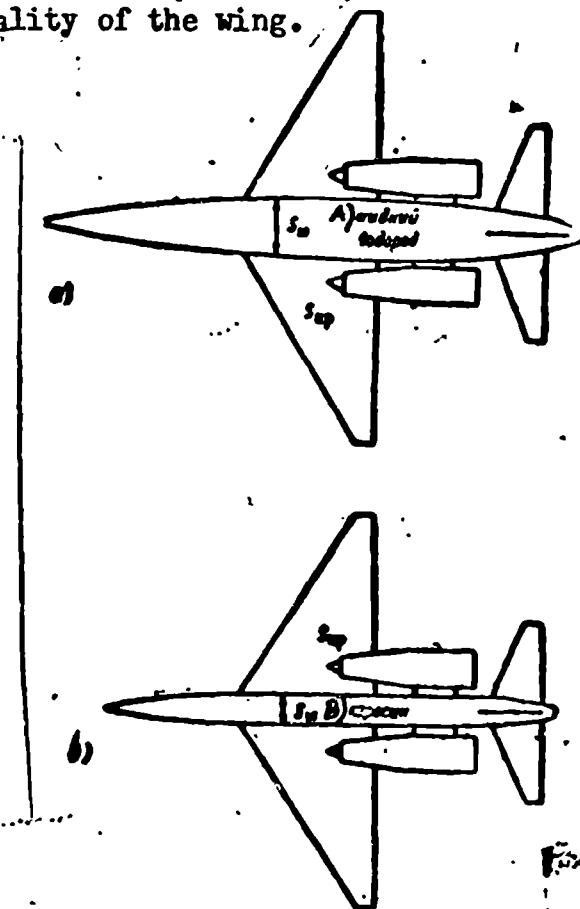
Fig. 84. Plans of winged missiles. With an increase of the density of the fuel γ_g, which is poured into the tanks, the calculated dimensions of winged long-range missiles decrease.
(P_{pol} = const).
a -- γ_g = 0.07 T/m³;
b -- γ_g = 0.8 T/m³

Legend:
A) liquid
hydrogen
B) kerosene

The weight of the fuel comprises a considerable portion of the take-off weight: P_g = νP_{pol}. With an increase of the fuel's density γ_g, the volume of the fuel tanks (which usually occupies the greater portion of the fuselage) and the necessary

area of the fuselage mid-section S_{mf} will be decreased. Together with this decrease, the weight of the tanks will be less (Figure 84).

The frontal drag and the required thrust R decrease

$$\mathbf{R} = X_{кр} + X_\phi =$$
$$= \frac{P_{пол}}{k_{кр}} + c_x S_{м.ф} q, \tag{6.9}$$

where X_{cr} and X_f are the aerodynamic drags of the wing and fuselage.

The aerodynamic quality of all aircraft, with an increase of fuel density, will grow until the fuel tanks become so small that they may be inserted into the thickness of the wing, then the aerodynamic quality of the entire aircraft approaches the maximum possible. Also the weight of the tanks' casing becomes smaller, but the relative amount of fuel stored will be greatest. Any further increase of fuel density ($\gamma > 2$) practically does not exert an influence on the possible flight range, since S_{mf} is minimum, P_{pol} = const and $k \approx k_{cr}$.

In Figure 84 schematics are shown of aircraft of equal weight, one uses kerosene as a fuel, the other -- liquid hydrogen. Owing to the low density of the hydrogen, the volume and frontal drag of the fuselage and the weight of the fuel tanks' casings prove to be so great, that the advantage presented by the high calorific value of the hydrogen is lost. Therefore, liquid hydrogen is not used as a fuel for missiles.

During a long flight at supersonic speed, an aircraft heats up to a temperature that is close to the stagnation temperature of the air, and the fuel in the tanks may boil. Therefore, for supersonic aircraft, intended for long flights, a fuel with a high boiling point is preferred.

The heating value, calorific value, density, boiling and melting points of various chemical elements and compounds are indicated in table 6.1.

SECTION 2. THE CALCULATION OF THE HEATING VALUE OF A FUEL FROM ITS COMPOSITION

The fractional weights of the individual elements from which the fuel is composed, is called the fuel's "elementary composition". The elementary composition is determined by a chemical analysis.

Table 6.1

THE PARAMETERS OF VARIOUS MOLECULAR FUELS[1]

Substance	Atomic number	Symbol	Density kg/m³	Temperature in °C — Boiling	Temperature in °C — Melting	L	Heating Value H_u kcal/kg	Calorific Value W kcal/kg
Elements								
Liquid hydrogen	1	H	70	—268	—270	34,5	28 550	807
Lithium	3	Li	534	1336	180	4,97	7 700	1290
Beryllium	4	Be	1840		1280	7,65	14 800	1700
Boron	5	B	1700	2500	2000	9,6	14 000	1460
Carbon[2]	6	C	1800	4000	3500	11,5	7 850	628
Compounds								
Liquid methane		CH₄	415	—161,5	—	17,25	12 000	656
Heptane		C₇H₁₆	684	98,4	—51,6	15,2	11 200	671
Benzol		C₆H₆	880	83,1	— 5,5	13,3	9 500	668
Gasoline		—	750	80	—70	14,9	10 500	663
Kerosene		—	810	140	—50	14,8	10 200	663
Diesel fuel		—	850	162	—40	14,8	10 200	663
Alcohol		C₂H₆O	790	78,0	—114	9,0	6 400	642
Pentabaron		B₅H₉	630	60	—46,9	13,0	16 200	1160

The energy, which is released during the formation of the fuel from the elements, is called heat of formation E'_{sv}. The heat of formation is determined by the data obtained from calorimetric experiments. For example, the heat of formation of one kilogram-molecule (kg mol) of methane CH_4 due to reaction of 4 kg of hydrogen and 12 kg of carbon is equal to 16,000 kcal:

$$C + 2H_2 \rightarrow CH_4 + 16,000 \text{ kcal.}$$
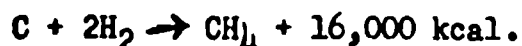
In order to break down a given combination into elements, it is necessary to subtract the energy which is equal to the heat of formation according to the law of conservation. For example, in order to decompose 1 kgmol of methane, it is necessary to subtract 16,000 kcal.

The energy, released by the combination of 1 kg mol of a combustion substance with the corresponding amount of oxygen is called the heat of reaction E (Table 6.2).

---

[1] D. Kay and T. Libby, "Spravochnik Fizika-Eksperimentator," /Handbook of a Physics Experimenter), Publishing House for Foreign Lit, 1950. NACA Report, No 1037, 1953.

[2] All the remaining chemical elements possess less heating value than carbon.

The heats of reactions of combustion elements are determined by means of calorimetric tests. For example, the heat of formation of water vapor from 1 kg mol of hydrogen and 0.5 kg mol of oxygen is equal to 57,100 kcal/kg mol

$$H_2 + \tfrac{1}{2}O_2 \longrightarrow H_2O + 57,100 \text{ kcal}$$
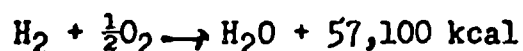
It follows from the law of the conservation of energy that the amount of heat, liberated during any chemical reaction, depends only upon the composition of the aggregate of the reaction products and upon the original substances and does not depend on the means of the reaction (G. I. Hess' law).

The reaction products of combustion are in the form of a gas at the moment of their generation. If the terminal temperature of the products is not great, then the oxides formed may change into a liquid, and then to a solid state, releasing heat because of condensation and hardening. Therefore, one distinguishes between the heats of reaction in a gaseous state (the original and final products are gaseous); heats of reaction in a liquid state (the original and final substances are liquids) and heats of reaction in a solid state (the original and final products are solid substances).

The heats of reaction in a solid state have the greatest value, and in a gaseous state -- the least.

The heat of condensation of 1 kg mol of water vapor is equal to 9700 kcal. Therefore, the heat of the combustion of hydrogen in a liquid state (if the water vapor condenses) is equal to 57,100 + 9700 = 66,800 kcal.

Dividing the heat of reaction E, expressed in kcal/kg mol, by the mass of fuel, entering the reaction, μ_g in kg, we find the amount of heat liberated during the combustion of 1 kg of a given substance, i.e., its heating value H:

$$H = \frac{E}{\mu} . \qquad\qquad (6.10)$$

The heating value of a multi-component fuel, composed of several chemical elements, may be computed, if the elementary composition, the heat reaction of the components, and the heat of formation of a fuel from these components are known.

The heating value of a fuel is equal to the sum of the products of the heating

Table 6.2

HEAT OF REACTION E AT ABSOLUTE ZERO IN KCAL/KG MOL*

Reaction	Chemical Formula	Heat of Reaction
The formation of carbon monoxide	$C + \frac{1}{2}O_2 \to CO$	27 400
The combustion of carbon monoxide	$CO + \frac{1}{2}O_2 \to CO_2$	66 760
The formation of methane	$C + 2H_2 \to CH_4$	16 000
The combustion of hydrogen	$H_2 + \frac{1}{2}O_2 \to H_2O$	57 100
The combination of hydrogen with hydroxyl	$\frac{1}{2}H_2 + OH \to H_2O$	63 000
The combustion of hydrogen with chlorine	$\frac{1}{2}H_2 + \frac{1}{2}Cl_2 \to HCl$	22 000
The decomposition of ozone	$O_3 \to 1.5O_2$	34 500
The oxidation of lithium	$2Li + \frac{1}{2}O_2 \to Li_2O$	107 000
" " " aluminum	$2Al + 1.5O_2 \to Al_2O_3$	327 000
" " " phosphorus	$2P + 2.5O_2 \to P_2O_5$	363 000
" " " boron	$2B + 1.5O_2 \to B_2O_3$	302 000
" " " magnesium	$Mg + \frac{1}{2}O_2 \to MgO$	144 000
" " " beryllium	$Be + \frac{1}{2}O_2 \to BeO$	133 000

Note: Metallic oxides, at the temperatures in the combustion chambers of ram-jet engines (near 2000°C), are transformed into a liquid or solid state, releasing heat of vaporization. Lithium oxide is an exception, boiling at 1230°C. Therefore, the heat of reaction of metals, with the exception of Li, includes the heat of vaporization.

values of its components multiplied by their fractional weights, less the heat of fuel formation from these components:

$$H = \sum \frac{E_i}{\mu_i} g_i - \frac{E_{av}}{\mu_g},$$ (6.11)

where g_i is the fractional weight of a given element in the fuel;

E_i is the heat of reaction of a given element;

μ_i is the mass of a given element in 1 kg mol of the combustion products;

E_{av} and μ_g are the heat of formation and the molecular weight of the fuel.

The elementary composition of an individual fuel may be found by its chemical formula. Let the composition of a fuel be expressed by the formula $C_nH_mO_k$. The molecular weights of the components are designated respectively by μ_C, μ_H, μ_O. The

*A Chemist's Handbook, vol I, Khimizdat, M.-L., 1952.
B. Lewis and G. von Elbe, Goreniye, plamya i vzryvy v gazakh /Combustion, Flame, and Explosions in Gases/, Pub. House for Foreign Lit., 1948.

molecular weight of the fuel is equal to the sum

$$\mu_r = n\mu_C + m\mu_H + k\mu_O.$$ (6.12)

The fractional weights of the components are

$$[C] = g_C = \frac{n\mu_C}{\mu_r} = 12\frac{n}{\mu_r},$$

$$[H] = g_H = \frac{m\mu_H}{\mu_r} = \frac{m}{\mu_r},$$

$$[O] = g_O = \frac{k\mu_O}{\mu_r} = 16\frac{k}{\mu_r}.$$ (6.13)

The heating value of the fuel is

$$H = \frac{E_C}{\mu_C}g_C + \frac{E_H}{\mu_H}g_H - \frac{E}{\mu_r},$$ (6.14)

The more atoms a hydrocarbon molecule is composed of, usually the less will be its density and the less will be the heat of formation. Methane possesses the highest heat of formation among the hydrocarbons of the paraffin series. The heat of formation of unsaturated hydrocarbons is usually less than that of saturated hydrocarbons. The heat of formation of acetylene C_2H_2 is negative.

The heat of formation of multi-component fuels is usually not known, and since it is not basic for large molecules, it is often disregarded. The computed heating values are confirmed more exactly by calorimetric experiments.

A distinction is made between the gross and net heating values of a fuel. During the determination of the gross heating value H, the temperature is lowered so much as to cause the combustion products (usually only steam) to condense. The determination of the net heating value H_u is carried out at such temperature that all the combustion products remain gaseous. For example, for hydrogen $n\mu_n = 2$ kg.

$$H_u = \frac{57,100}{2} = 28,550 \text{ kcal/kg}; \quad H = \frac{66,800}{2} = 33,400 \text{ kcal/kg}.$$

The combustion products of the majority of fuels used in ramjet engines remain gaseous. Therefore, usually the net heating value H_u has the greatest significance for operation in a ramjet engine.

Example. Find the heating value of methane CH_4.

The molecular weight of methane is

$$\mu_r = \mu_C + 4\mu_H = 12 + 4 = 16.$$

The elementary composition of methane is

$$\varepsilon_C = \frac{\mu_C}{\mu_r} = \frac{12}{16} = 0.75; \quad \varepsilon_H = \frac{4\mu_H}{\mu_r} = \frac{4}{16} = 0.25.$$

The heat of formation of methane is

$$E = 16,000 \text{ kcal/kg mol}$$

The heating value of methane is determined by the formula

$$H_u = \frac{!E_C}{\mu_C} \varepsilon_C + \frac{!E_H}{2\mu_H} \varepsilon_H - \frac{E}{\mu_r} =$$

$$= 28\,550 \cdot 0.25 + 7850 \cdot 0.75 - \frac{16\,000}{16} = 12\,000 \text{ kcal/kg.}$$

SECTION 3. CALCULATION OF THE AMOUNT OF AIR THEORETICALLY REQUIRED, THE COMPOSITION AND THERMODYNAMIC PARAMETERS OF THE COMBUSTION PRODUCTS

From the elementary composition, it is possible to find the amount of air theoretically necessary for the combustion of one kilogram of fuel and the composition and thermodynamic parameters of the combustion products.

According to the equilibrium equation, the amount of oxygen, necessary for the combustion of 1 kg of fuel is equal to

$$m_0 = \frac{2\mu_0}{\mu_C}[C] + \frac{\mu_0}{2\mu_H}[H] - [O] = \frac{8}{3}[C] + 8[H] - [O]. \tag{6.15}$$

Air is composed of 23.2% of oxygen by weight. The amount of air, necessary for the combustion of 1 kg of fuel is

$$L = \frac{m_0}{0.232} = 11.5[C] + 34.5[H] - 4.31[O]. \tag{6.16}$$

The amount of air, theoretically required for the combustion of G_g kg of fuel is equal to LG_g. The ratio of the amount of air, which enters the combustion chamber G_v, to the amount of air, which is required for the combustion of the fuel is called the <u>excess air coefficient</u> α:

$$\alpha = \frac{G_v}{LG_r}. \tag{6.17}$$

If the elementary composition of the fuel is known, it is possible to determine the composition of the combustion products for any excess air coefficient. The hot combustion products include CO_2, H_2O, N_2, O_2, and even products of incomplete oxidation: CO, NO, CH_4H_2, the products of dissociation: OH, O, H, N and others.

The total mass of the combustion products of 1 kg of fuel in the air is

$$m_{comb} = 1 + \alpha L.$$

We will determine the composition of the combustion products when $\alpha > 1$.

The mass of carbon dioxide gas in 1 kg of fuel is

$$m_{CO_2} = \frac{\mu_{CO_2}}{\mu_c} g_c.$$

The mass of the water vapor, formed during the combustion of 1 kg of fuel is

$$m_{H_2O} = \frac{\mu_{H_2O}}{2\mu_n} g_n.$$

The mass of the unreacted oxygen in the combustion products is

$$m_o = 0.232\alpha L - \frac{2\mu_o}{\mu_c} g_c - \frac{\mu_o}{2\mu_n} g_n.$$

The mass of nitrogen, including argon and other noble gases, in the combustion products is

$$m_N = 0.768\alpha L.$$

The fraction of the individual components by weight in the undissociated combustion products g_i^0 is found by dividing the mass of each component m_i by the total mass of the products $1 + \alpha L$ (Table 6.3);

$$g_i^0 = \frac{m_i}{1+\alpha L}; \quad \sum_1^i g_i^0 = 1. \tag{6.18}$$

The determination of the composition of dissociated combustion products is discussed in Section 5 of this chapter.

Table 6.3

THE COMPOSITION OF THE UNDISSOCIATED COMBUSTION PRODUCTS OF KEROSENE

		1,0	1,25	1,5	2,0	∞
Composition by weight	α_0					
	g_{CO_2}	0,1965	0,1592	0,1338	0,1014	0,0000
	$g_{H_2O}^0$	0,0838	0,0679	0,0571	0,0433	0,0000
	$g_{O_2}^0$	0,0000	0,0440	0,0740	0,1122	0,2320
	$g_{N_2}^0$*	0,7197	0,7289	0,7351	0,7431	0,7680
	$\sum g_i^0$	1,0000	1,0000	1,0000	1,0000	1,0000
Composition by volume	$r_{CO_2}^0$	0,1280	0,1040	0,0874	0,0663	0,0000
	$r_{H_2O}^0$	0,1340	0,1084	0,0911	0,0691	0,0000
	$r_{O_2}^0$	0,0000	0,0395	0,6555	0,1009	0,2090
	$r_{N_2}^0$*	0,7330	0,7481	0,7550	0,7636	0,7910
	$\sum r_i^0$	1,0000	1,0000	1,0000	1,0000	1,00000
R kgm/kg·gr		29,53	29,51	29,49	29,48	29,27
μ_0		28,72	28,75	28,77	28,78	29,93

*Inert gases are included with the nitrogen.

Knowing the fraction of all the components by weight g_i, it is possible to find the enthalpy, internal energy, entropy, gas constant, and the specific heat of the combustion products in accordance with the laws of the conservation of energy and matter.

The internal energy is

$$u = \sum_1^l u_i g_i \quad \kappa\kappa a \Lambda/\kappa z.$$ (6.19)

The gas constant is

$$R = \sum_1^l R_i g_i = \sum_1^l \frac{848}{\mu_i} g_i \quad \kappa z \Lambda/\kappa z. \; z p a \partial.$$ (6.20)

The enthalpy is

$$i = \sum_1^l i_i g_i = \sum_1^l (u_i + R_i T) g_i \quad \kappa\kappa a \Lambda/\kappa z.$$ (6.21)

The entropy is

$$s = \sum s_i g_i \quad \kappa\kappa a \Lambda/\kappa z. \; z p a \partial.$$ (6.22)

The average molecular weight of the combustion products is

$$\mu_0 = \frac{848}{R}.$$ (6.23)

The internal energy, enthalpy and entropy of each component depends on the temperature. The internal energy is determined by experimental means. The results of several determinations are indicated in Table 6.4.

Table 6.4

THE INTERNAL ENERGIES OF GASES IN kcal/mol*

Gas	μ T	600	1000	1400	1800	2200	2600	3000
O_2	32	3088	5511	8128	10852	13667	16570	19544
H_2	2	2936	4978	7151	9478	11954	14545	17231
N_2	28	3006	5216	7646	10207	12857	15500	18287
NO	30	3196	5534	8074	10724	13439	16197	18985
CO	28	3017	5247	7441	10334	13011	15725	18476
OH	17	3048	5118	7340	9740	12255	14890	17607
H_2O	18	3687	6577	9920	13655	17790	21945	26330
CO_2	44	4135	8247	12844	17698	22703	27819	33012

* B. Lewis and G. von Elbe, Goreniye, plamya i vzryvy v gazakh /Combustion, Flame, and Explosions in Gases7, Pub. House for Foreign Lit., 1948.

The enthalpy and entropy are found by calculation. The results of several calculations are shown in Tables 6.5 and 6.6.

GAS ENTHALPIES IN kcal/kg[*]

Gas \ T°K	600	1000	1400	1800	2200	2600	3000
O_2	133,8	234,2	340,8	450,8	5636	679,2	797,0
H_2	30620	32040	33520	35080	36720	38410	40150
N_2	150,0	257,2	372,4	492,2	615,2	740,0	866,0
NO	860	964	1075	1190	1307	1425	1545
CO	2535	2643	2760	2820	3005	3130	3257
OH	2275	2444	2621	2800	3004	3205	3412
H_2O	271	476	703	957	1226	1505	1794
CO_2	121,1	232,6	355,1	483,5	615,3	750,0	886
O	3854	3978	4102	4226	4350	4474	4598
H	82760	84760	86750	88730	90720	92700	94690
N	6256	6398	6540	6682	6824	6966	7108

GAS ENTROPIES IN $\frac{kcal}{kg\ deg}$ WHEN p = 1 kg/cm^2

Gas \ T°K	600	1000	1400	1800	2200	2600	3000
O_2	0,158	0,286	0,375	0,445	0,502	0,549	0,592
H_2	7,74	9,55	10,79	11,78	12,58	13,30	13,92
N_2	0,174	0,311	0,407	0,483	0,544	0,596	0,642
NO	0,264	0,397	0,491	0,563	0,622	0,672	0,714
CO	0,917	1,056	1,154	1,230	1,291	1,345	1,39
OH	0,823	1,038	1,188	1,306	1,404	1,488	1,562
H_2O	0,317	0,577	0,771	0,928	1,064	1,18	1,283
CO_2	0,160	0,301	0,403	0,484	0,549	0,606	0,655
O	1,085	1,246	1,351	1,432	1,495	1,547	1,593
H	20,56	23,11	24,78	26,03	27,02	27,85	28,57
N	1,238	1,405	1,516	1,606	1,672	1,736	1,786

The fraction by volume of each component r_i may be found by the well-known ratio

$$r_i = \frac{g_i}{\mu_i}\mu.$$ (6.24)

After calculating the composition of the combustion products, the internal energy and enthalpy at given temperatures are calculated and plotted on a graph (Figure 85).

After dividing the increase in internal energy or enthalpy by the corresponding temperature interval, we find the average specific heat for a given temperature

---

[*]Ya. B. Zel'dovich and A. I. Polyarnyy, Raschyoty teplovykh protsessov pri vysokikh temperaturakh /Calculations of Thermal Processes at High Temperatures/, BNT Printing House, 1947.
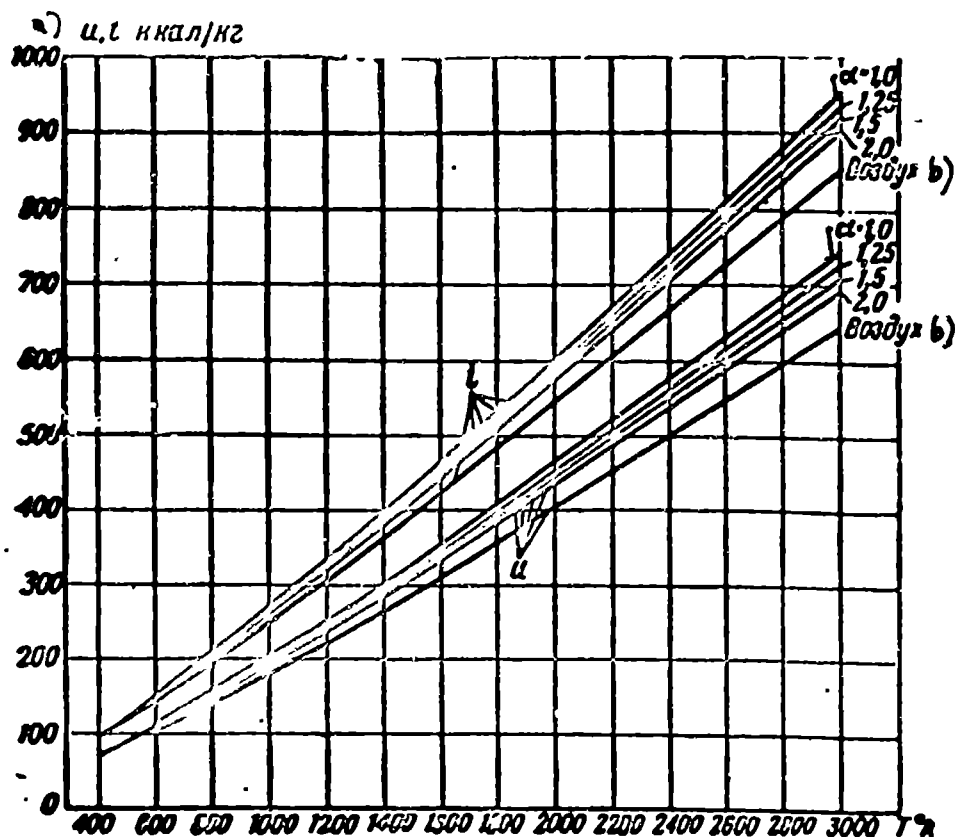
Fig. 85. The temperature dependence of the internal energy and enthalpy of the combustion products of kerosene (neglecting dissociation).
a) u, t kcal/kg; b) air.

interval

$$c_v = \frac{\Delta u}{\Delta T};$$ (6.25)

$$c_p = \frac{\Delta i}{\Delta T}$$ (6.26)

and the average value of Poisson's index

$$k = \frac{c_p}{c_v}.$$ (6.27)

As ΔT tends to zero, c_v, c_p and R approach their true values.

The average specific heats of hydrocarbon combustion products, such as those from kerosene, are depicted in the graphs in Figures 86, a and b, and are calculated by neglecting dissociation, i.e., when $p \to \infty$.

Example: Find the composition of the combustion products of octane C_8H_{18} when the excess air coefficient $\alpha = 2$.

The molecular weight of C_8H_{18} is: $\mu = 8 \cdot 12 + 18 = 114$.

The fractions by weight are

$$[C] = \frac{8 \cdot 12}{114} = 0.843; \quad [H] = \frac{18}{114} = 0.157.$$

The amount of air that is theoretically required is

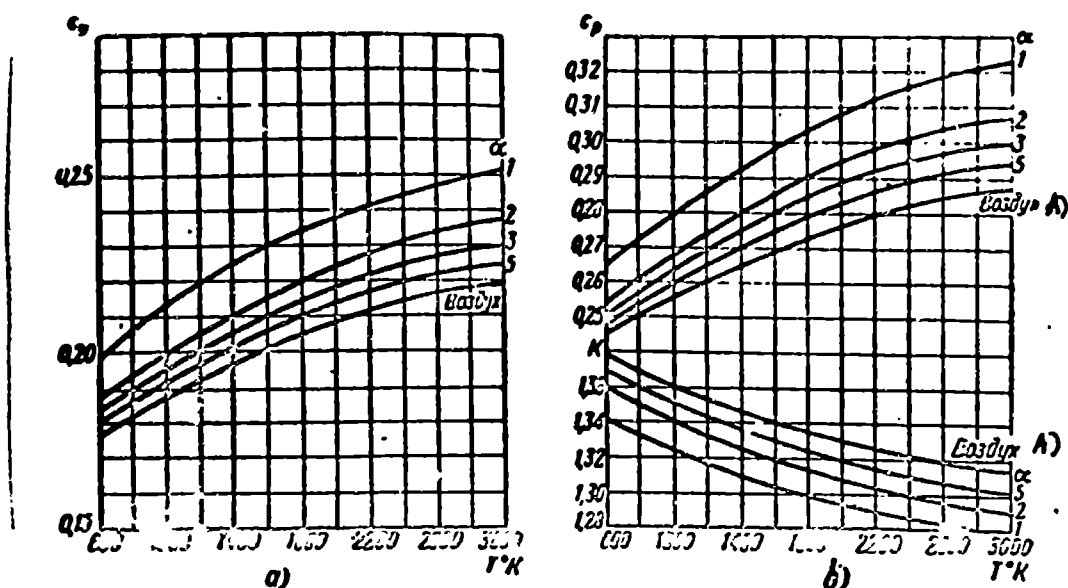$$L = 11.5 \cdot 0.843 + 34.5 \cdot 0.157 = 15.1.$$

Fig. 86. Temperature dependency of the average specific heat and Poisson Index neglecting dissociation.

a) $c_v = f(T)$; b) $c_p = f(T)$ and $k = f(T)$.

A) air.

The quantity of air when $\alpha = 2$ is

$$\alpha L = 30,2.$$

The weight of the carbon dioxide gas in the combustion products of 1 kg of octane is

$$\frac{\mu_{CO_2}}{\mu_C}[C] = \frac{44}{12}0,843 = 3,09.$$

The fraction of CO_2 by weight is

$$g^0_{CO_2} = \frac{3,09}{1+\alpha L} = \frac{3,09}{31,2} = 0,0992.$$

The weight of the water vapor in the combustion products of 1 kg of octane is

$$\frac{\mu_{H_2O}}{\mu_{H_2}}[H] = \frac{18}{2}0,157 = 1,41.$$

The fraction of the H_2O by weight is

$$g^0_{H_2O} = \frac{1,41}{1+\alpha L} = \frac{1,41}{31,2} = 0,0453.$$

The weight of the nitrogen in the air is

$$30,2 \cdot 0,768 = 23.$$

The fraction of nitrogen by weight is

$$g^0_{N_2} = \frac{23}{31,2} = 0,7435.$$

The fraction of the oxygen in the air by weight is

$$30,2 \cdot 0,232 = 7,00.$$

Half of this oxygen is spent in the formation of CO_2 and H_2O.

The fraction of the free oxygen by weight is

$$g_{O_2} = \frac{7,00}{2 \cdot 31,2} = 0,1120.$$

We will verify this:

$$g_{CO} + g_{H_2O} + g_{N_2} + g_{O_2} = 0,0992 + 0,0453 + 0,7435 + 0,1120 = 1,000.$$

The gas constant R and the average molecular weight μ of the combustion products are

$$R = 848 \left(\frac{g_{CO_2}}{\mu_{CO_2}} + \frac{g_{H_2O}}{\mu_{H_2O}} + \frac{g_{N_2}}{\mu_{N_2}} + \frac{g_{O_2}}{\mu_{O_2}} \right) =$$

$$= 848 \left(\frac{0,0992}{44} + \frac{0,0453}{18} + \frac{0,7435}{28} + \frac{0,112}{32} \right) = 29,5 \text{ kg m/kg deg;}$$

$$\mu = \frac{848}{R} = \frac{848}{29,5} = 28,75.$$

After multiplying the fractional values of the combustion products by the internal energies, the enthalpies, and the entropies of the components and after adding the products so obtained, we find the u, i and s of the combustion products at a given temperature. After this, the specific heats c_p and c_v and Poisson's index k may be calculated.

SECTION 4. THE CONCEPT OF CHEMICAL EQUILIBRIUM.
THE DISSOCIATION OF COMBUSTION PRODUCTS.

The substances forming the composition of a fuel mixture are capable of forming a chemical compond with one another: under certain conditions, the oxygen of the air unites with the hydrogen, carbon, and other fuel components.

Under normal conditions the oxidation of hydrocarbons does not occur.

In order for the reaction to begin, the fuel mixture must be heated to a certain temperature, called the ignition temperature T_{vsp}. If the heat of a reaction which is developed in an enclosed volume is greater than the heat lost by means of heat conductivity and radiation, then the mixture heats up. The speed of the reaction increases because of the increased velocity of the molecules and increased number of molecular collisions. The quiet reaction may be transformed into an explosive one.

The cooled combustion products consist of carbon dioxide CO_2, water vapor H_2O, carbon monoxide CO, and nitrogen N_2. Besides this, the nitrogen of the air, which

for all practical purposes, does not take part in the reaction, remains in the combustion products. Also remaining are those substances, which at the start of the reaction, were excess -- oxygen or unburned fuel components.

Spectrographic tests show that the hot combustion products contain, besides the enumerated final products, the original substances and a series of intermediate products of the reaction. Thus for example, the hot combustion products of hydrogen and oxygen contain not only the final product -- water vapor, but also the original substances O_2 and H_2, and even intermediate compounds and free atoms OH, H, and O. With an increase of the mixture's initial temperature T_{Ox}, the temperature of the combustion products increases and the percentage of the final products decreases.

We will consider the reaction of hydrogen with oxygen:

$$H_2 + \frac{1}{2}O_2 \rightleftarrows H_2O. \qquad (6.28)$$

The arrows, pointing in both directions, show that under the proper conditions the reaction may go either in one or the other direction. The hot products of the combustion of hydrogen in oxygen contain

$$H_2, \ O_2, \ H_2O, \ OH, \ H, \ and \ O$$
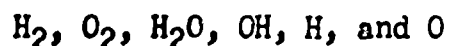
We indicate the partial pressures of the components, determined by the number of molecules of a given component in a unit of volume and temperature of a mixture, by p_{H2}, p_{O2}, p_{H_2O}, p_{OH}, p_H and p_O.

On the basis of the law of mass action, the principle of which is presented in courses in thermodynamics, one may describe the equation of chemical equilibrium:

$$k_{H_2O} = \frac{p_{H_2} p_{O_2}^{\frac{1}{2}}}{p_{H_2O}}. \qquad (6.29)$$

The constant k_{H_2O} is called the constant of chemical equilibrium for the reaction of the formation of water from hydrogen and oxygen. The degree to which each partial pressure enters the equation of chemical equilibrium, is equal to the number of molecules entering the reaction equation (6.28).

The equilibrium constants which are determined by experimental methods, are

functions only of temperature and depend neither upon the pressure to which the re-
acting mixture is exposed nor on the presence of different impurities (Table 6.7).

Table 6.7

EQUILIBRIUM CONSTANTS

(pressure is expressed in kg/cm^2)[*]

Reaction	Const.	$T=1800°$ K	$T=2200°$ K	$T=2600°$ K	$T=3000°$ K
$CO_2 \rightleftarrows CO + \frac{1}{2} O_2$	k_1	$2.04 \cdot 10^{-4}$	$6.41 \cdot 10^{-3}$	0.0622	0.339
$H_2O \rightleftarrows H_2 + \frac{1}{2} O_2$	k_2	$5.37 \cdot 10^{-5}$	$1.23 \cdot 10^{-3}$	0.010	0.049
$H_2O \rightleftarrows OH + \frac{1}{2} H_2$	k_3	$2.512 \cdot 10^{-5}$	$8.32 \cdot 10^{-4}$	$9.55 \cdot 10^{-3}$	0.0566
$H_2 \rightleftarrows H + H$	k_4	$1.574 \cdot 10^{-7}$	$3.767 \cdot 10^{-5}$	$1.702 \cdot 10^{-3}$	0.0283
$N_2 \rightleftarrows N + N$	k_5	$1.00 \cdot 10^{-14}$	$5.01 \cdot 10^{-11}$	$2.5 \cdot 10^{-8}$	$2.24 \cdot 10^{-6}$
$\frac{1}{2} N_2 + \frac{1}{2} O_2 \rightleftarrows NO$	k_6	0.011	0.0332	0.0708	0.124
$O_2 \rightleftarrows O + O$	k_7	$1.69 \cdot 10^{-8}$	$8.11 \cdot 10^{-6}$	$5.92 \cdot 10^{-4}$	0.01388

To determine the composition of the dissociated combustion products it is neces-
sary to solve simultaneously the equations of material balance of the (6.28) type, and
of chemical equilibrium of the (6.29) type for all substances that may be formed dur-
ing combustion (see Section 5 of this chapter).

The greater the temperature of the gas, the greater the portion of molecules
whose kinetic energy is sufficient for ionization by impact. With an increase of the
combustion products' temperature, the fraction of the molecules, which are split up
into elements, increases.

The kinetic energy of the molecules colliding together is transformed into the
potential energy of the dissociated products. Therefore, at a given enthalpy the
kinetic energy of the particles of a dissociated gas is less, and the potential
energy greater than that of a non-dissociated gas. The temperature of the gas is
proportional to the average kinetic energy of the particles, consequently, at a given
enthalpy the temperature of a dissociated gas is less than that of a non-dissociated
gas. At a temperature which is less than 1700°C, the amount of dissociated combustion

[*]B. Lewis and G. von Elbe, Goreniye, plamya i vzryvy v gazakh /Combustion, Flame,
and Explosions in Gases/, Pub. House for Foreign Lit., 1948.

F-TS-9740/V   170

products, H_2O, CO_2 and others, is small to the point of vanishing. At temperatures higher than 4000°C the combustion products are practically totally dissociated. If a fuel is introduced into air, the temperature of which is greater than 4000°C, combustion does not occur. On the other hand, the molecules of the fuel substance as well as the molecules of the air are broken down into atoms. Separation does not occur but energy is absorbed.

If the relative velocity is not too great during the collision of the dissociated products with one another, "moleculization" may occur: the particles reunite into whole molecules. The number of recombined molecules is increased by more frequent collisions which result in "moleculization". The number of the recombined molecules is the greater, the more molecules there are on the surface of the volume under consideration, and the more molecules there are or the periphery of the ambient medium. Thus, the degree of dissociation (i.e., the ratio of the number of disintegrated molecules to the number of those not disintegrated) at a given temperature is approximately inversely proportional to the square of the gas' density. During an increase of pressure the degree of dissociation decreases. As the pressure increases to infinity, the degree of dissociation approaches zero.

In calculations respecting the operation process in the combustion chambers of ramjets, it is necessary to consider dissociation if the temperature of the products exceeds 2000°K. Dissociation involves a decrease in temperature. The higher the pressure in the chamber, the lesser the degree of the products' dissociation. With an increase of flight altitude, the pressure in the chamber falls, the degree of dissociation increases and the decrease in temperature becomes more significant.

The determination of the composition of dissociated combustion products is produced by means of a combined solution of the equations of equilibrium and material balance and is accompanied by painstaking computations. These computations determine the volume and weight fraction of the components CO_2, CO, CH_4, H_2O, OH, H_2, H, NO, N_2,

O_2, O, and N. In the air there are traces of inert gases and possible traces of other elements which are not usually considered in relation to a fuel.

SECTION 5. THE CALCULATION OF THE COMPOSITION OF DISSOCIATED COMBUSTION PRODUCTS

During dissociation the number of particles and the volume of the combustion products increases, and their apparent molecular weight μ decreases.

The ratio of the molecular weight of a non-dissociated gas $\mu^{\bullet}$ to the molecular weight of a dissociated one μ is called the molecular change coefficient a:

$$a = \frac{\mu^o}{\mu} = \frac{R}{R_0} \geqslant 1. \qquad (6.30)$$

Carbon dioxide dissociates into carbon monoxide and oxygen

$$CO_2 \rightleftarrows CO + \frac{1}{2} O_2.$$
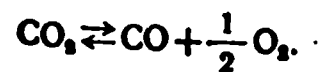
The partial pressures of the original and produced products p_i are related to each other by the equation of chemical equilibrium

$$k_1 = \frac{p_{CO} \sqrt{p_{O_2}}}{p_{CO_2}}.$$

The partial pressure of a given component p_i is equal to the product of the total pressure p and the volume fraction r_i

$$p_i = p r_i. \qquad (6.31)$$

Consequently,

$$k_1 = \frac{p r_{CO} \sqrt{p r_{O_2}}}{p r_{CO_2}} = \frac{r_{CO} \sqrt{p r_{O_2}}}{r_{CO_2}}, \qquad (6.32)$$

where k_1 is the equilibrium constant for the dissociation of carbon dioxide and is dependent only on the temperature of the gases.

During dissociation the mass of the substance must remain constant, but the volume of the mixture increases.

If one attributes the volumetric portions of the substances formed to a new volume of the mixture, then the equation of material balance of carbon presents this form:

$$\frac{1}{a} r_{CO_2}^0 = r_{CO_2} + r_{CO}. \qquad (6.33)$$

Water vapor dissociates into hydroxyl, molecular hydrogen and atomi, hydrogen. Therefore, for water just as for carbon dioxide, the following equations may be written:

$$H_2O \rightleftarrows H_2 + \frac{1}{2} O_2,$$
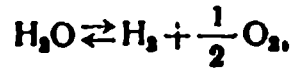
$$k_2 = \frac{r_{H_2} \sqrt{p r_{O_2}}}{r_{H_2O}}, \qquad (6.34)$$

$$H_2O \rightleftarrows OH + \frac{1}{2} H_2,$$

$$k_3 = \frac{r_{OH} \sqrt{p r_{H_2}}}{r_{H_2O}}. \qquad (6.35)$$

$$H_2 \rightleftarrows H + H,$$

$$k_4 = \frac{p r_H^2}{r_{H_2}}. \qquad (6.36)$$

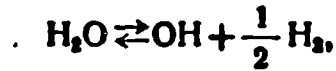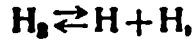The material balance equation of hydrogen for all of these reactions is

$$\frac{1}{a} r_{H_2O}^0 = r_{H_2O} + r_{H_2} + \frac{1}{2} r_{OH} + \frac{1}{2} r_H. \qquad (6.37)$$

Nitrogen dissociates into atomic components and oxidizes, forming nitrous oxide

$$N_2 \rightleftarrows N + N,$$

$$\frac{1}{2} N_2 + \frac{1}{2} O_2 \rightleftarrows NO.$$
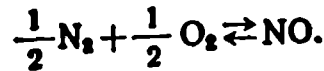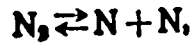
The equations of equilibrium and material balance have this form for all these reactions

$$k_5 = \frac{p r_N^2}{r_{N_2}}; \qquad (6.38)$$

$$k_6 = \frac{r_{NO}}{\sqrt{r_{N_2} r_{O_2}}}, \qquad (6.39)$$

$$\frac{1}{a} r_{N_2}^0 = r_{N_2} + \frac{1}{2} (r_N + r_{NO}). \qquad (6.40)$$

Molecular oxygen dissociates into its atomic components:

$$O_2 \rightleftarrows O + O,$$
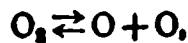
$$k_7 = \frac{p r_O^2}{r_{O_2}}. \qquad (6.41)$$

The equation of material balance of oxygen is

$$\frac{1}{a} \left(r_{O_2}^0 + r_{CO_2}^0 + \frac{1}{2} r_{H_2O}^0 \right) = r_{O_2} + r_{CO_2} +$$

$$+ \frac{1}{2} (r_{CO} + r_{OH} + r_{OH} + r_{H_2O} + r_O). \qquad (6.42)$$

The molecular change coefficient 'a' must have such a value which satisfies the condition

$$\sum r_i = 1. \qquad (6.43)$$

In this way, in order to determine the volumetric composition of the dissociated mixture of i components and the molecular change coefficient a, a total of i + 1 equations was produced. In principle, these equations permit one to determine all the component fractions of the mixture and the coefficient a. However, the simultaneous solution of this system of equations results in an equation higher than the third power, the solution of which is found by graphic means. The following method brings us quicker to our goal.

Let us consider a given excess of air, α, and a given elementary composition of a fuel mixture of C and H. We will find, as was shown in Section 3, the volumetric composition of a non-dissociated mixture $r^0_{CO_2}$, $r^0_{H_2O}$, $r^0_{N_2}$ and $r^0_{O_2}$. We will set up the temperature T, the pressure p, and the molecular change coefficient a (in the first approximation we will take care of the last value by guess work). We will set up a series of values of a volumetric concentration of oxygen r_{O_2}. We will find the parameter x:

$$x = \sqrt{p r_{O_2}}.$$ (6.44)

The volume fractions of carbon dioxide and carbon monoxide, which correspond to the tabulated fractions of oxygen, are found from the equations (6.32) and (6.33):

$$r_{CO_2} = \frac{r^0_{CO_2}}{a\left(1 + \frac{k_1}{x}\right)},$$ (6.45)

$$r_{CO} = \frac{k_1}{x} r_{CO_2}.$$ (6.46)

We will compute the auxiliary parameters

$$b = \frac{k_2}{x},$$ (6.47)

$$c = \frac{k_3}{4\sqrt{p}},$$ (6.48)

$$d = \frac{1}{4}\sqrt{\frac{k_4}{p}} b.$$ (6.49)

The volume fractions of water, hydroxyl, molecular and atomic hydrogen, which correspond to the tabulated fractions of oxygen, are found from the equations (6.34); (6.35); (6.36); (6.37); (6.47); (6.48) and (6.49)

$$r_{H_2O} = \sqrt{\left(\frac{c+d}{1+b}\right)^2 + \frac{r^0_{H_2O}}{a(1+b)}} - \frac{c+d}{1+b},$$ (6.50)

$$r_{H_2} = b r_{H_2O},$$ (6.51)

$$r_{OH} = \frac{c}{0.25} \sqrt{r_{H_2O}},$$

(6.52)

$$r_H = \sqrt{\frac{k_4 r_{H_2}}{p}}.$$

(6.53)

For any oxygen fraction r_{O_2}, the values determined for r_{CO_2} and r_{CO}, and also r_{H_2O}, r_{H_2}, r_{OH} and r_H must comply with the corresponding material balance equations (6.33) and (6.37).

The volume fractions of molecular nitrogen, atomic nitrogen and nitrous oxide are found from the equations (6.38); (6.39) and (6.40)

$$\sqrt{r_{N_2}} = \sqrt{\frac{r_{N_2}^0}{a} + \left(\frac{k_6}{4}\sqrt{r_{O_2}} + \frac{1}{4}\sqrt{\frac{k_5}{p}}\right)^2} - \left(\frac{k_6}{4}\sqrt{r_{O_2}} + \frac{1}{4}\sqrt{\frac{k_5}{p}}\right),$$

(6.54)

$$r_N = \sqrt{\frac{k_5}{p} r_{N_2}},$$

(6.55)

$$r_{NO} = k_6 \sqrt{r_{O_2} r_{N_2}}.$$

(6.56)

The volume fractions of atomic oxygen are found from the equation (6.41):

$$r_O = \sqrt{\frac{k_7}{p} r_{O_2}}.$$

(6.57)

After this, we select those values of the volumetric concentrations of r_i which comply with the material balance equation of oxygen (6.42). This is done by a graphic method. We put the assumed values of the volume concentration of oxygen r_{O_2} along the abscissa axis (Figure 87) and along the ordinate axis we plot the calculated volumetric fractions of the components and the summary amount of oxygen ω, which was determined from the material balance equation for oxygen:

$$\omega = r_{CO_2} + r_{O_2} + \frac{1}{2}(r_{H_2O} + r_{OH} + r_{NO} + r_{CO} + r_O).$$

(6.58)

Valid are those volumetric concentrations at which the material balance equation of oxygen is complied with, i.e. when

$$\omega = \frac{\omega_0}{a} = \frac{1}{a}\left(r_{CO_2}^0 + r_{O_2}^0 + \frac{1}{2} r_{H_2O}^0\right).$$

(6.59)

Dropping a perpendicular from the intersection point of the curve $w = f(r_{O_2})$ with a horizontal line $(r^0_{CO_2} + r^0_{O_2} + \frac{1}{2} r^0_{H_2O}) \frac{1}{a} = \frac{1}{a} \omega^0$, we find the volumetric fractions of the components of a dissociated mixture r_i.

Fig. 87. Diagram of calculation of the degree of dissociation.

If the molecular change coefficient a at the beginning of the calculation was assumed correctly, the sum of the volumetric fractions of all the components would be equal to one: when $a = a_{1st} = \dfrac{\mu_0}{\mu}$, $\sum r_i = 1$. Otherwise,

$$\sum r_i = a'. \tag{6.60}$$

Then

$$a_{H3} = a a'. \tag{6.61}$$

If $a' > 1,03$, one must repeat the calculation, using the corrected value of the molecular change coefficient a, as the initial value. An error in the value of a, which does not exceed 3%, does not have a noticeable influence on the composition and thermodynamic parameters of the combustion products.

The true values of the volumetric concentrations of the components are less than those found on the graph in Figure 87 by a' times

$$(r_i)_{HCT} = \frac{r_i}{a'}; \tag{6.62}$$
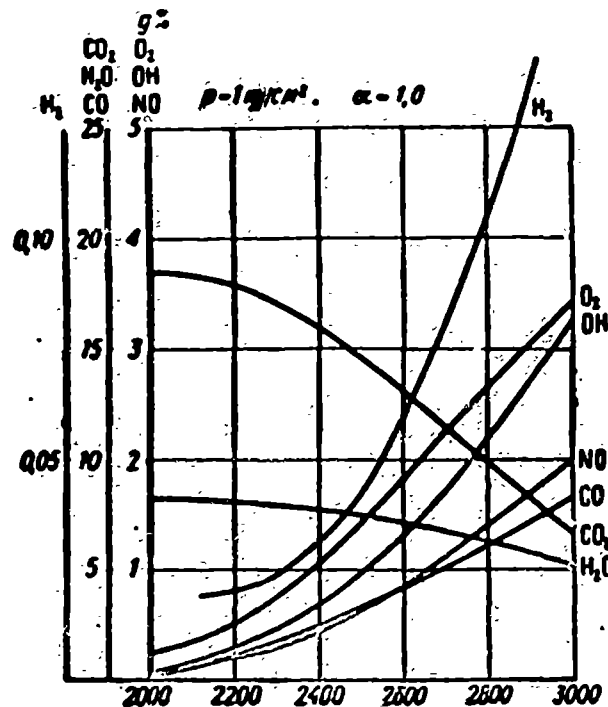
$$\sum (r_i)_{HCT} = 1. \tag{6.63}$$

Fig. 68. Temperature dependence of the composition of the dissociated combustion products of kerosene.

The apparent molecular weight of the dissociated mixture μ is

$$\mu = \sum \mu_i (r_i)_{act},$$ (6.64)

where μ_i is the molecular weight of a given component.

The gravimetric fractions of the components are found by the equation

$$g_i = \frac{\mu_i r_i}{\mu}.$$ (6.65)

With an increase of temperature, the volumetric and gravimetric fractions of the dissociation products grow, while the volumetric and gravimetric fractions of the original products decrease (Figure 88).

With an increase of pressure, the volumetric and gravimetric fractions of the dissociation products diminish (Figure 89).

The knowledge of the weight composition of a dissociated mixture is used to calculate the internal energy, enthalpy, gas constant, and entropy of combustion products at various temperatures and pressures and is also used to construct thermal /Mollier/ charts.

SECTION 6. THERMAL /MOLLIER/ CHARTS OF COMBUSTION PRODUCTS

It is possible to compute the internal energy u, the enthalpy i, and the entropy of 1 kg of combustion products u, i, R and s by the gravimetric composition of a dissociated mixture (see equations 6.19 - 6.22).
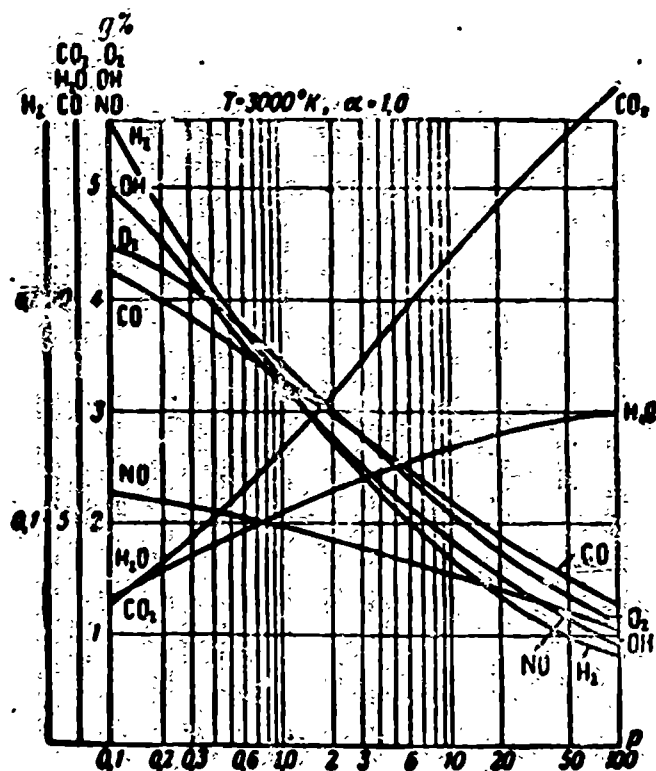
Fig. 89. The dependence on pressure of the composition of the dissociated combustion products of kerosene.

The internal energy u_i, the enthalpy i_i and the entropy s_i of a given component depend only on its temperature (see Tables 6.4, 6.5 and 6.6). The percentage of a given component depends on the composition of the mixture, i.e., on the excess air coefficient α, on the temperature T, and on the pressure p. In this way, special curves will correspond to each α and to each pressure p: $u = f(T)$ (Figure 90, a, b, c, d), $R = f(T)$ (Figure 91, a, b, c, d), $i = f(T)$ (Figure 92, a, b, c, d) and $s = f(T)$ The entropy diagrams, $i = f(s)$ (Figure 93, a, b, c, d) are constructed from the known i-T and s-T diagrams. The thermal /Mollier/ charts cited in the book for the hydrocarbon combustion products were computed and drawn by S. M. Il'yashenko, Ye. M. Germeier and V. N. Sokolovoy according to thermo-chemical data of 1947.

The computation of the stagnation temperatures and the temperatures of the combustion products is based upon the thermal /Mollier/ charts.

The computation of the stagnation temperature at very high velocities is based upon the i-T chart, which is plotted for unvitiated air (see Figure 92). The stagnation air enthalpy i_o is equal to

$$i_{\text{H}} = i_{\text{н}} + \frac{A w_{\text{н}}^2}{2 g} = i_{\text{н}} \left(1 - \frac{k-1}{2} M_{\text{н}}^2 \right),$$

where

$$i_{\text{н}} = c_p T_{\text{н}}.$$

Tentatively, we will find the stagnation pressure p_{02}, knowing the velocity of the free stream flow and the stagnation process. We locate the determined stagnation enthalpy i_{on} on the vertical axis and draw a perpendicular to the point where it intersects with the curve $i = f(T)$, which corresponds to the stagnation pressure p_{02} previously found. Dropping a perpendicular to the horizontal axis, we find the stagnation temperature accounting for the dissociation of the air.

The lowering of the stagnation temperature, caused by the change in specific heat and by the dissociation of the air, becomes perceptible only when $M > 5$.

The computation of the combustion products' temperatures is derived from the i-T chart, which corresponds to a given excess air coefficient α (Figure 92, a, b, c, d).

We find the stagnation enthalpy of the combustion products i_{cg} by:

$$i_{cg} = i_n + \frac{A w_n^2}{2g} + \frac{H_u \eta_{sg}}{1 + \alpha L} = i_{on} + \frac{H_u \eta_{sg}}{1 + \alpha L},$$

where η_{sg} is the total combustion efficiency.

We locate the enthalpy that was found on the vertical axis of the i-T diagram, draw a horizontal line to the point where it intersects with the curve $i = f(T)$, corresponding to the pressure in the combustion chamber p_{02}. Then, by dropping a perpendicular to the horizontal axis, we will find the temperature of the combustion products accounting for dissociation.

The closer the composition of the mixture is to stoichiometry ($\alpha = 1$) and the lower is the absolute pressure in the chamber, the more significant will be the lowering of the temperature, caused by the dissociation.

Thus, for example, when $\alpha = 1$, $M_0 = 4$, $T_n = 216.5°K$, $H_u = 10,500$ kcal/kg, the pressure in the chamber $p = 1$ kg/cm^2; $i_n = 52$ kcal/kg; $i_{on} = 218$ kcal/kg, and $\eta_{sg} = 1$; the temperature of the combustion products accounting for the dissociation is equal to 2500°K, but without accounting for dissociation ($p = \infty$) it is equal to 2810°K. Under these conditions, dissociation lowers the temperature by 310°.

Fig. 90. The u - T diagrams of the combustion products of kerosene accounting for dissociation.

a -- α = 1.0; b -- α = 1.5; c -- α = 2.0; d -- α = ∞.
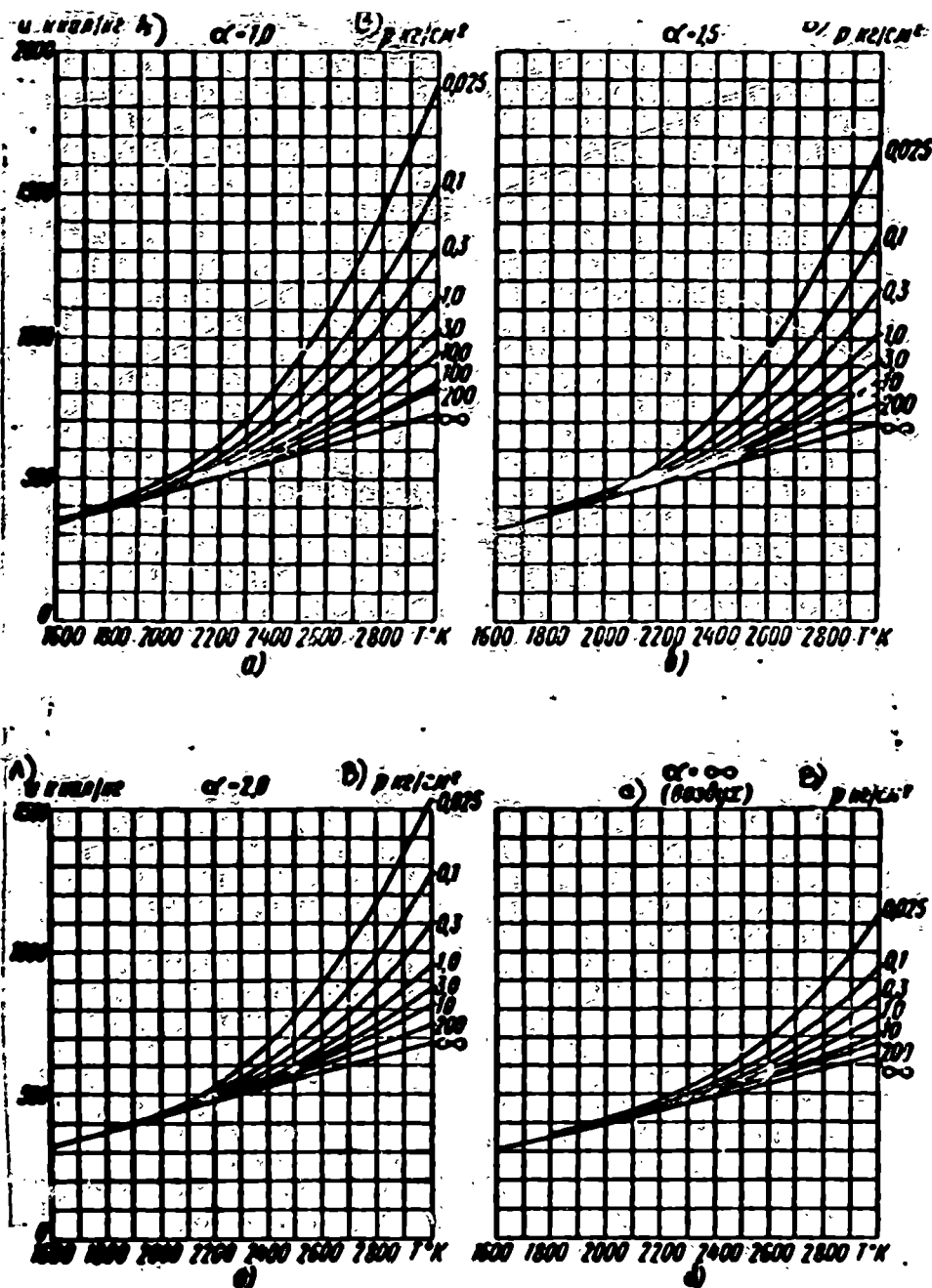
Legend:

A) u kcal/kg
B) p kg/cm^2
C) (air)

The determination of the adiabatic heat content drop h = i_1 - i_2 at a given pressure drop Δp = p_1 - p_2 is derived from the i - s diagram (see Figure 93 , the five inserts at the end of the book). We locate the enthalpy of the gases on the vertical axis and draw a horizontal line to the point where it intersects the curve i = f(s), corresponding to the initial pressure p_1. The decrease of gas enthalpy during an expansion without losses (s = const) from the pressure p_1 to the pressure p_2 is measured by the length of the vertical line AB, below the curve i = f(s) corresponding to the pressure p_2 (Figure 94);

$$h = i_1 - i_2$$
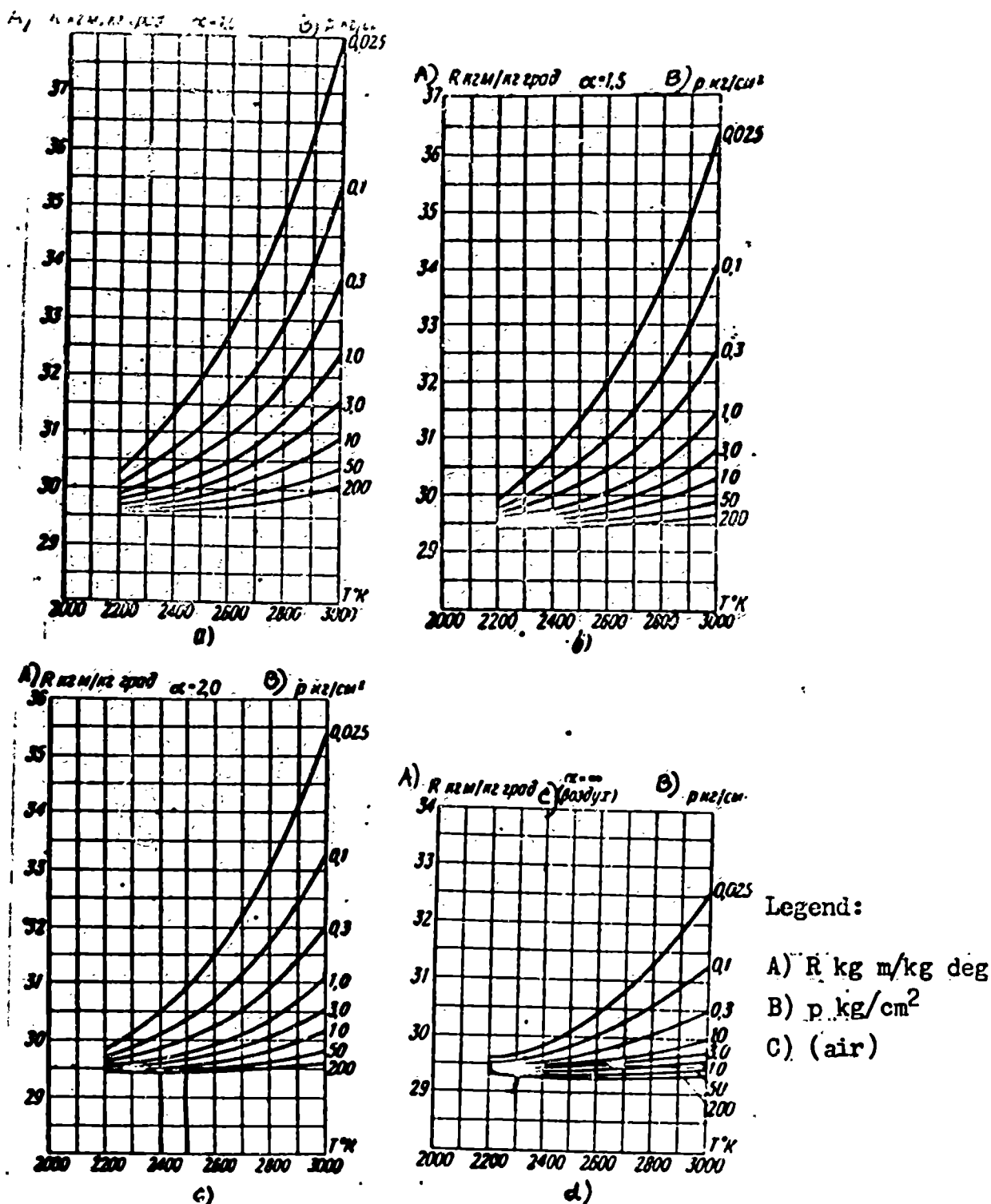
Fig. 91. The temperature dependence of the gas constants of the dissociated combustion products of kerosene.
a -- $\alpha = 1.0$; b -- $\alpha = 1.5$; c -- $\alpha = 2.0$; d -- $\alpha = \infty$.

An adiabatic drop during expansion with losses h' will be less by the value of

$BC = i_{pot} = h(1-\eta)$, where η is the efficiency of the expansion process. The gas

entropy during an expansion with losses increases (see page 139). An expansion with

losses is shown on the diagram by the inclined straight line AD. The greater the

losses, the more the straight line AD deviates from the vertical. In the extreme

case, during a flow with a constant velocity through porous bodies, the loss in

the heat capacity is equal to zero, h = 0; the straight line AD becomes horizontal.
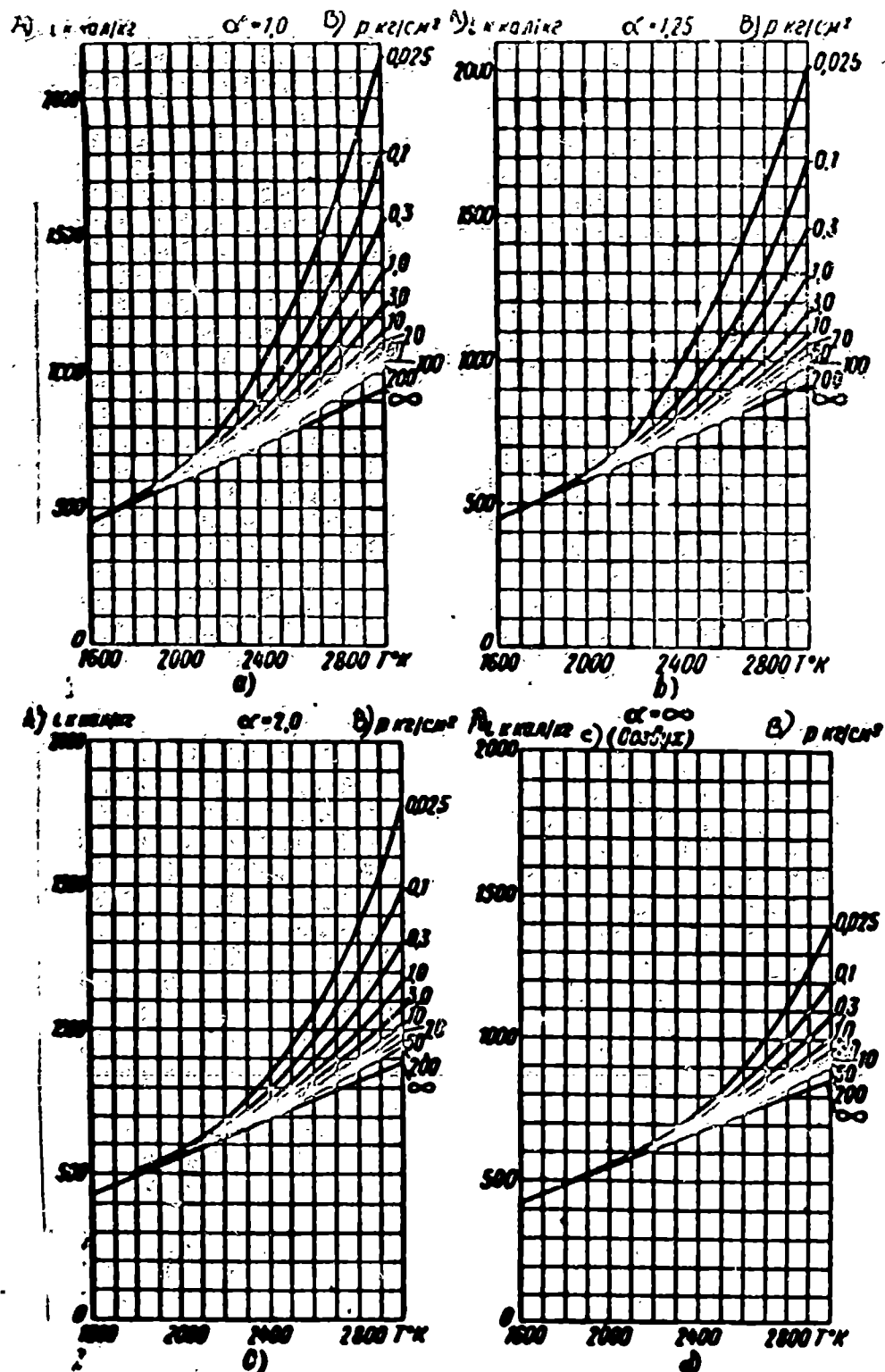
Fig. 92. The i - T diagrams of the combustion products of kerosene, accounting for
dissociation.

a -- α = 1.0; b -- α = 1.25; c -- α = 2.0; d -- α = ∞.

At high temperatures, when it is necessary to consider that the combustion

products are dissociated, the thermal drop during discharge from a nozzle is deter-

mined by the i - s diagram.

SECTION 7. THE COMBUSTION OF FUEL - AIR MIXTURES

The phenomena, which occur during the combustion of a fuel-air mixture, may be

divided into physical and chemical effects. The diffusion of the active nuclei from

Fig. 94. The determination of the heat content drop by the i - s diagram during an expansion with losses.
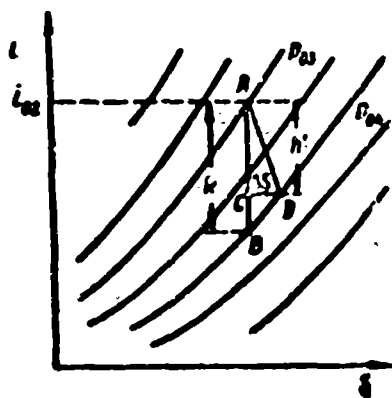
the combustion zone to the unburned gas; the thermal drop from the combustion area to the colder gas; the turbulent mixing of the burning gases with a fresh mixture; the radiant energy of the flames; and others belong to the physical phenomena. The disintegration of the fuel-complex molecules to more simple ones, occurring under the action of collisions with the fast moving molecules of the burning gases; the formation of intermediate products during the union of the dissociated fuel molecules with oxygen; the formation of the final combustion products; and others belong to the chemical phenomena.

During various combustion conditions with various fuel substances and with various fuel mixtures, the processes may be characterized by various physical and chemical phenomena. Therefore, attempts to cover all the problems of combustion by a single theory have not worked out well up to the present time.

Without going into a minute account of the theory of combustion, we will briefly describe those basic facts which will be encountered during a study of combustion chambers.

The combustion reaction of a fuel mixture with air occurs in a gaseous phase, since the ignition temperature of liquid fuels is far higher than the boiling temperature. Therefore, evaporation and mixing with the air precedes the ignition of a liquid fuel.

The ignition of a fuel-air mixture is accomplished by means of one or another ignition sources. The most prevalent are the following: an electric spark; a wire, heated to incandescence by a current; a pilot light; an incandescent body; adiabatic

compression; all of which increase the temperature to a point sufficient for ignition.
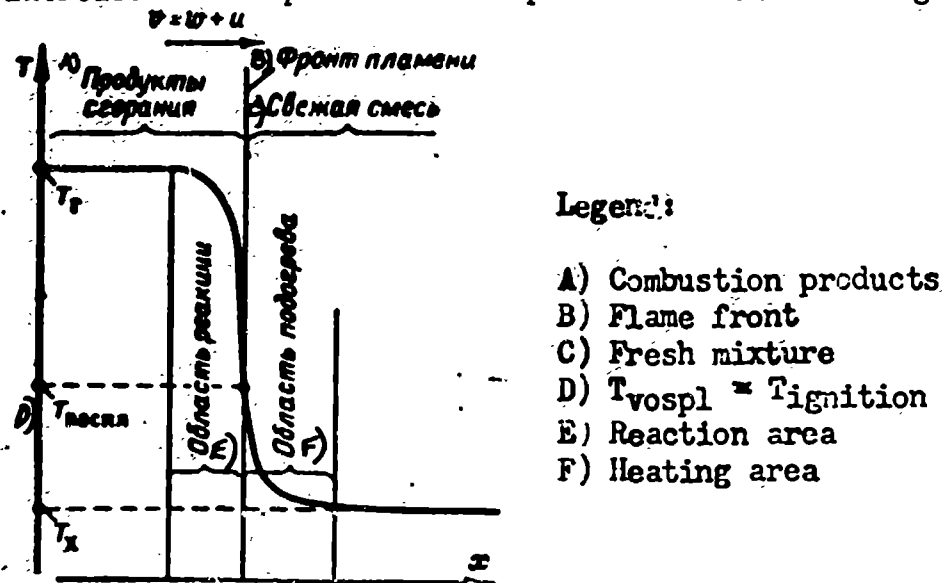
Fig. 95. A schematic of flame front formation during normal combustion.

The various possible forms of combustion: laminar, turbulent, and detonation, are dependent on the temperature, degree of turbulent mixing, and means of ignition.

These forms of flames correspond to their forms of combustion: laminar, turbulent, and detonation flames.

The surface, which separates the combustion area from the unburned gases is called the flame front (Figure 95).

The laminar diffusion of a flame is represented by the propagation of a flame front into the unburned gas, and is brought about by means of the molecular migration of heat and matter which is the determining factor in the matter of flame propagation: the migration of heat or diffusion, up until the present time, has not been definitely established. The velocity of the propagation of a laminar flame front into an unburned gas, measured along the normal to the flame front, is called the normal velocity of flame propagation or the fundamental velocity of flame spread u_n.

Burning gases become heated and expand. Therefore, the propagation of the flame front relative to a fresh gas is superimposed upon the movement of the gas as a whole, which (the movement) is brought about by thermal expansion, convection, and other factors. The velocity of the movement of the combustion zone is relative to the walls of the combustion chamber v. The velocity vector is normal to the flame front, and is equal to the geometric sum of the normal flame velocity u_n and the velocity of the

gas as a whole v:

$$\vec{v} = \vec{u_n} + \vec{w}.$$ (6.66)

The velocity of the gas motion w is determined by the conditions of test.

The normal velocity of the flame u_n depends upon the nature of the gas mixture, upon the temperature, and upon the pressure. With an increase of the temperature of the gases T, the velocity of the molecular movement increases, th chemical reaction develops faster, the heat conductivity and diffusion increase, and the normal velocity of the flame propagation augments. During a decrease of pressure p<1 abs. atm. the velocity of the flame spread increases somewhat. The influence of a pressure increase on the propagation velocity has been insufficiently investigated.

The normal flame velocity of stoichiometric hydrocarbon-air mixtures will be on the order of 0.4 m/sec at normal temperatures. During the leaning out or enrichment of a mixture, the normal flame velocity falls. The normal velocities of unsaturated hydrocarbon - air mixtures is usually somewhat higher than for saturated mixtures (Table 6.8).

Table 6.8

NORMAL FLAME PROPAGATION VELOCITIES OF HYDROCARBONS AT 20° C

Hydrocarbon	u_n cm/sec	Volume Concentration r %	Ratio of the Hydrocarbon Weight to the Air $\frac{1}{\alpha L}$
Ethane	40,1	6,28	0,153
Propane	39,0	4,54	0,0724
Butane	37,9	3,52	0,0732
Pentane	38,5	2,92	0,0748
Hexane	38,5	2,51	0,0764
Heptane	38,6	2,26	0,0798
Ethyne	68,2	7,40	0,0773
Propyne	43,8	5,04	0,0770
Butyne 1	43,2	3,87	0,0780
Pentyne 1	42,6	3,07	0,0766
Hexyne 1	42,1	2,67	0,0796

We will consider the formation of a laminar flame front (see Figure 95) which spreads in a fresh gas. We will designate the temperature of the unburned gas before the flame front by T_x, the temperature behind the front by T_g. This temperature is close to the possible maximum for a given composition of the mixture. At a normal

pressure, the thickness of the flame front, as shown by Schlieren photography,[1] will be on the order of 0.5 mm. During a decrease in the pressure, this thickness increases to several millimeters. The temperature of a fresh gas, which enters a flame front, increases, thanks to the heat supply from the reaction area, and finally, reaches ignition temperature T_{vsp} (see Figure 95), after which the chemical reaction of oxidation develops in the gas and is accompanied by the release of heat. The flame front may be divided into the heating zone and the reaction zone. The heat, which is released in the reaction zone, goes partially to heat the burning mixture and is partially passed on to the fresh gas before the flame front.

During the heating of a fresh mixture, the fuel molecules form radicals, several of which possess great chemical activity. The reaction of the fuel particles in combining with the oxygen of the air occurs with the assistance of the so-called active nuclei -- the radicals of H, OH, and O, which are formed in the reaction zone. The diffusion of the active kernels into a fresh mixture is one of the causes of flame propagation.

A flame front which is propagated into a gas, which is stationary in relation to the ignition source, is represented by a spherical surface (Figure 96a). The flame front which is propagated into a gas, which moves in relation to the ignition source at a velocity of w, is represented by a conical surface whose apex angle, as first shown by V. A. Michelson,[2] is such, that the normal component of the flow velocity $w_n = w \sin\alpha$ proves to be equal to the normal velocity of flame propagation u_n:

$$u_n = w \sin\alpha. \tag{6.67}$$

The velocity of the air flow w and the included angle of the combustion cone α are not difficult to measure by test. The normal velocity of flame propagation is computed according to Michelson's formula (6.67).

---

[1]Combustion Process, New York, 1956.

[2]V. A. Michelson, Normal'naya skorost' vosplameneniya v gremuchikh smesyakh /Normal Ignition Velocity in Detonating Mixtures/, 1890.

Legend:

A) Fuel mixture
B) Ignition source
C) Flame front
D) Matrix
E) Tube
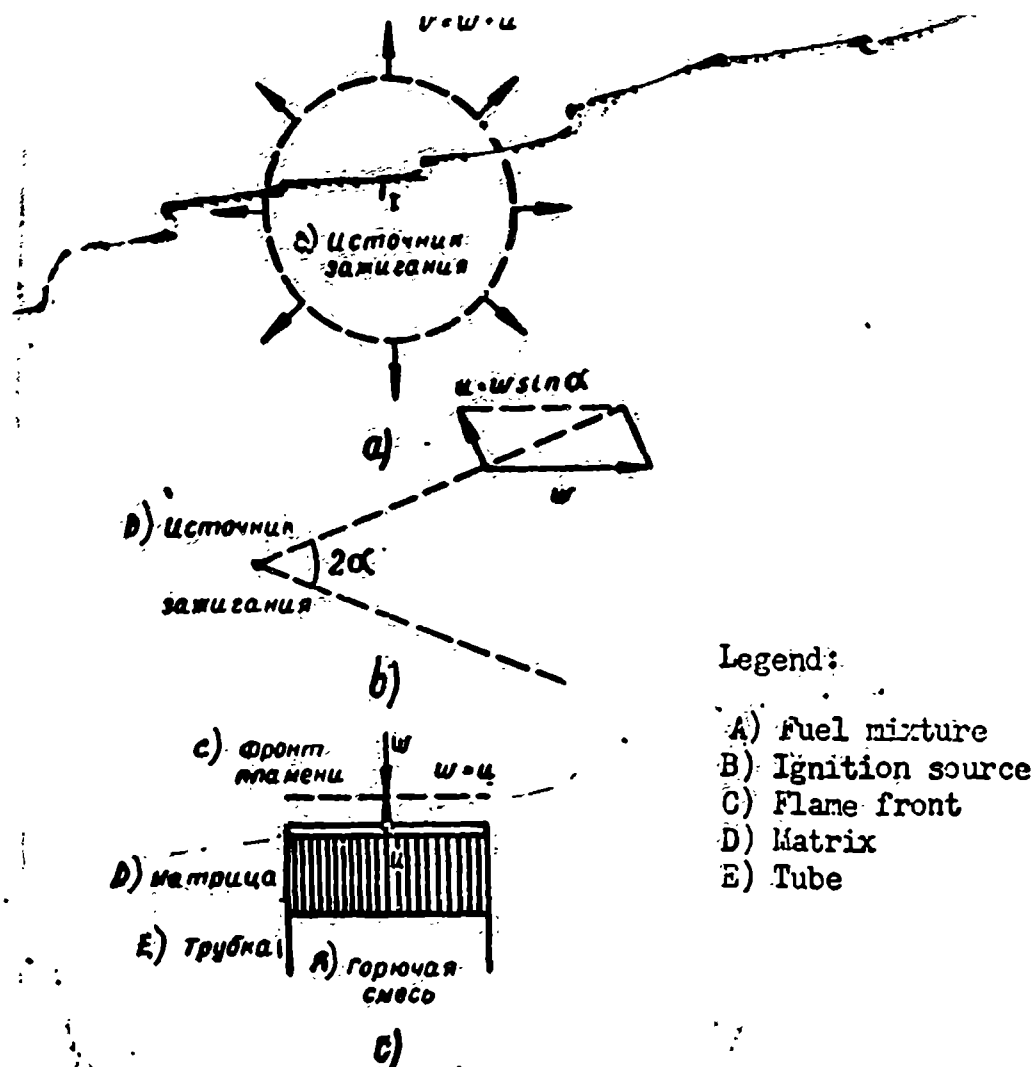
Fig. 96. Various cases of normal flame propagation.
a -- propagation in a stationary gas from a point source; b -- propagation in flow when $w > u_n$; c -- propagation in a flow when $w = u_n$.

During a decrease of flow velocity w, the included angle of the combustion cone increases to $180°$. During a subsequent decrease $w < u_n$, the front shifts to the flow.[1]

Laminar combustion occurs, for example, in a Bunsen burner or in the flame of a candle. Turbulent combustion takes place in the combustion chambers of jet engines.

Turbulent combustion is represented by the transfer of the combustion nuclei to the unburned gas by the turbulent masses or by the "kernels" of the gas (Figure 97). Turbulent kernels are those separate masses of gas, which preserve their individuality for some time and which may be detected by the eye (as during the movement of smoke) or may be observed in instantaneous photographs (see Fig. 101). The separate kernels of a gas in a turbulent flow create irregular vortex movements, reminiscent of the thermal movement of gas molecules. The value, which characterizes the size of the kernels, is

---

[1] V. A. Michelson, Normal'naya skorost' vosplameneniya v gremuchikh smesyakh /Normal Ignition Velocity in Detonating Mixtures/, 1590.

Fig. 97. Photography of a turbulent combustion flame during an exposure of two
microseconds.
a -- single-phase mixture; b -- two-phase mixture.

alled the scale of turbulence. The root mean square velocity of the kernels in re-
ation to the gas is called the pulsation velocity. This velocity always varies and
s vectorally added to the velocity of the flow. Therefore, the true velocity of a
urbulent flow in relation to the walls of a combustion chamber always varies (Figure
8). The variable velocity of a turbulent flow and, consequently, the value of the
ulsation velocity, may be measured with the aid of a hot wire anemometer, the sensi-
ive portion of which is a resistance thermometer, composed of a very thin wire heated
y an electric current. This wire is connected with one of the arms of a wheatstone
ridge (Fig. 99). The hot wire is inserted in the flow to be studied. The greater
he instantaneous velocity of the flow in relation to the heated wire, the greater
s the velocity of the heat conductivity, the more the temperature of the wire will
trop, and the less will be its resistance. The resistance measurement of the wire,
nserted in a turbulent flow, is recorded by a low-reluctance oscillograph (see
igure 99). The root mean square component of the pulsation velocity, determined by
n oscillogram, is directed along the axis of the flow $w_{syst} = \frac{1}{n}\sqrt{\sum_{n}^{a} \Delta w_x^2}$
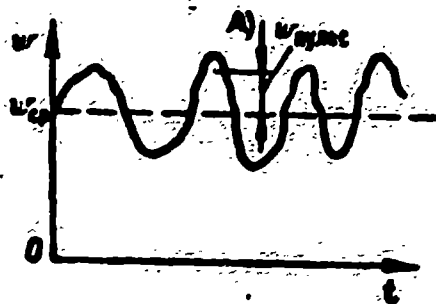
Fig. 98. The pulsation velocity of a turbulent flow, measured by a hot wire anemometer. A) $w_{pul's}$
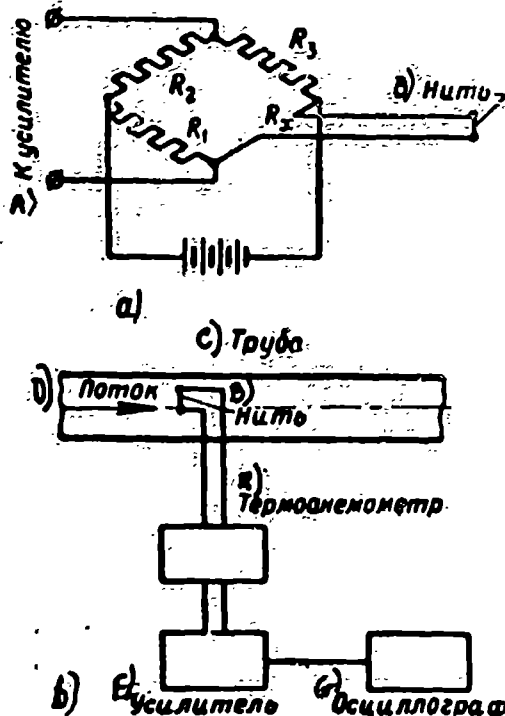
Legend:

A) To the amplifier
B) Filament.
C) Tube
D) Flow
E) Hot wire anemometer
F) Amplifier
G) Oscillograph

Fig. 99. The measurement of pulsation velocity by a hot wire anemometer.
a -- general schematic of a hot wire anemometer.
b -- instrumentation schematic.

The ratio of the root mean square pulsation velocity to the average velocity of the flow is called the turbulence intensity ε :

$$\varepsilon = \frac{w_{pul}}{w}.$$

(6.68)

Grilles made up of rods, plates or wires, and also poorly streamlined bodies, increase the degree of turbulence. The scale of the turbulence, i.e., the size of the turbulent kernels, is of the order of the size of the grille mesh. The intensity of the turbulence depends on the configuration of the rods, and on the relative blockage of the cross section.

Flame propagation in a turbulent flow is substantially different from that which is observed in a stationary medium or in a laminar flow.

The widely disseminated conception of turbulent combustion in use today was

1943. According to Shchelkin's theory, the turbulent pulsations of velocity distort a laminar flame front. The surface, which separates the burning and fresh gas in a
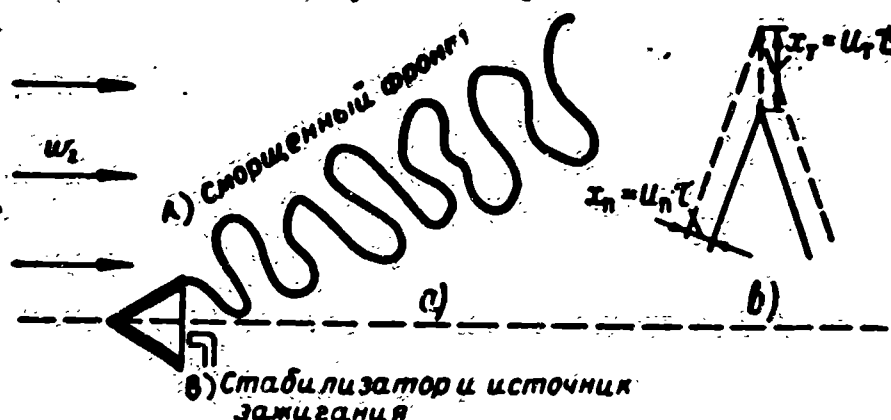
Fig. 100. Schematic of turbulent flame front formation (according to Shchelkin). Legend: A) Wrinkled front; B) Stabilizer and ignition source.

turbulent flow, proves to be wrinkled (Figures 97 and 100a). During the time in which the area of normal combustion spreads with a velocity of u_n and is displaced at a distance of $x_n = u_n \tau$, the apex of the turbulent "wrinkle" is displaced a greater distance $x_\tau = u_\tau \tau$ and transmits the combustion to the fresh mixture (Figure 100b). The velocity of the turbulent flame propagation u_τ is as many times greater than the normal velocity of flame propagation as the surface of the wrinkled front is greater than the smooth surface of a laminar front

$$\frac{u_\tau}{u_a} = \frac{S_\tau}{S_a} = \sqrt{1 + B\left(\frac{w_{nyak}}{u_a}\right)^2}, \tag{6.69}$$

where B is a certain coefficient, hardly distinguishable from 1 (one) and determined by an experimental method. Otherwise:

$$\frac{u_\tau}{u_a} = \sqrt{1 + B\left(\frac{\varepsilon w}{u_a}\right)^2}. \tag{6.70}$$

As long as the normal velocity of flame propagation u_n is measured in tens of centimeters per second (see Table 6.8), then during large pulsation velocities $w \gg u \gg u_n$.

$$u_\tau = w_{nyak} = \varepsilon w. \tag{6.71}$$

The velocity of turbulent combustion u_τ ceases to depend upon the nature of the fuel, and is determined by the pulsation velocity or the turbulence intensity that corresponds to it.

The incidence angle of the turbulent combustion zone to the direction of the

undisturbed flow, in accordance with Michelson's formula (6.67), is then determined only by the intensity of the turbulence $\mathcal{E}$.

$$\sin \alpha = \frac{u_t}{w} = \varepsilon. \tag{6.72}$$

Shchelkin's formulas are justified by experience only to the first approximation.

During the past years Ye. S. Shchetnikov and abroad, M. Summerfield, developed, independently from one another, the theories of volumetric turbulent combustion, in accordance with which combustion occurs not in a distorted flame front, but in the entire volume of the flame jet, whose temperature gradually increases as it recedes from the ignition source.

Schlieren photographs of the individual turbulent kernels of a burning gas are depicted in Figure 101.

The theoretical and experimental investigation of turbulent combustion is still far from being finished. The experimental data obtained at the present time seem to suggest that an increase of small-scale turbulence intensity contributes to an increase in the growth of combustion velocity.

Under certain conditions a quiet turbulent combustion may change into a pulsating or detonating combustion.

A detonating combustion is represented by the propagation of the reaction zone with an extremely high velocity: from 1000 to 3000 m/sec. A reaction zone, which is propagated with a high velocity, is called a detonation wave. The works of Ya. B. Zel'dovich brought an important contribution to the theory of detonation.
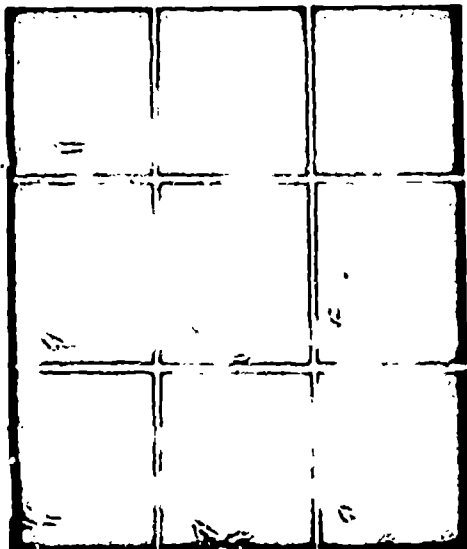

Fig. 101. Photographs of burning turbulent kernels.

Detonation waves possess certain important characteristics. The velocity of a detonation wave does not depend upon the dimensions of the combustion chamber if its diameter is greater than a certain limiting value. The propagation velocity of a detonation wave is little dependent upon the initial temperature and pressure. Thus, for example, the propagation velocity of a detonation in a stoichiometric mixture of hydrogen and oxygen during a pressure change from 200 to 1500 mm of mercury, i.e., 7 times more, changes from 2630 to 2870 m/sec, and during a temperature change from 10 to 100°C, -- from 2820 to 2790 m/sec.

The velocity of detonation waves depends, in a large degree, upon the nature of the fuel and oxidant and upon the composition of the mixture: during a leaning out of the mixture, the detonation velocity diminishes. With sufficient leaning out, detonating combustion changes to the usual slow flame spread. Detonation effects are connected with shock waves.

A combustion detonation appears when an increase of temperature in a shock wave is sufficient for the ignition of the mixture. The velocity of a detonation is equal to the propagation velocity of a shock wave in the combustion products at the temperature that is established at the end of combustion.

In piston engines a combustion detonation ("knock"), which leads to the chipping of the piston and combustion chamber walls, is extremely harmful. The possibility of using detonating combustion in jet engines has not yet been sufficiently studied.

SECTION 8. IGNITION LIMITS OF HYDROCARBONS. IGNITION LAG.

The flame from an ignition source may be propagated along the entire volume of the mixture only during certain conditions. If the heat liberated by an ignition source (sparks, for example) is insufficient, the mixture will not ignite. By changing the mixture composition certain limits may be reached beyond which no local ignition source can promote combustion.

The highest fuel-to-oxidant ratio in a mixture at which the ignition of the

The lowest fuel-to-oxidant ratio in a mixture at which the ignition of the mixture is still possible, is called the lower ignition limit (Table 6.9).

Table 6.9

IGNITION CONCENTRATION LIMITS OF HYDROCARBONS IN VOLUMETRIC PERCENTAGES WHEN p = 1 kg/cm² AND t = 15°C

Fuel	Formula	Molecular Weight	Ignition Limits	
			Lower	Upper
Methane	CH_4	16	5.00	15.00
Ethane	C_2H_6	29	3.22	12.45
Heptane	C_7H_{16}	100	1.00	6.00
Octane	C_8H_{18}	114	0.95	

Ignition limits depend upon the initial temperature and pressure of the mixture, upon the means of ignition, and upon the gas constant. With an increase of the temperature of the mixture, and with an increase in the energy of the ignition source, the ignition limits are expanded (Figure 102b). The ignition limits for a gas flow are usually different than those for a stationary gas.

A pressure variation also influences the ignition limits: if the pressure drops below that of the atmosphere, the ignition limits shrink and finally coincide: ignition becomes impossible. If the pressure becomes higher than that of the atmosphere, the ignition limits are altered insignificantly. For some mixtures an increase of pressure causes an expansion, for others -- a constriction of the ignition limits.

The ignition limits are connected with the flame propagation velocity u: if u = 0, the flame in the mixture is not propagated, combustion is impossible, and the upper and lower ignition limits coincide with one another. With an increase of propagation velocity, occurring for example during a temperature increase of the mixture, the ignition limits are expanded.

The fraction of fuel in a mixture at the upper and lower ignition limits is usually expressed in volumetric percentages r, from which it is not difficult to derive the gravimetric fraction or the excess air coefficient α, if the molecular weights of the fuel μ_g and of the air μ_v are known.
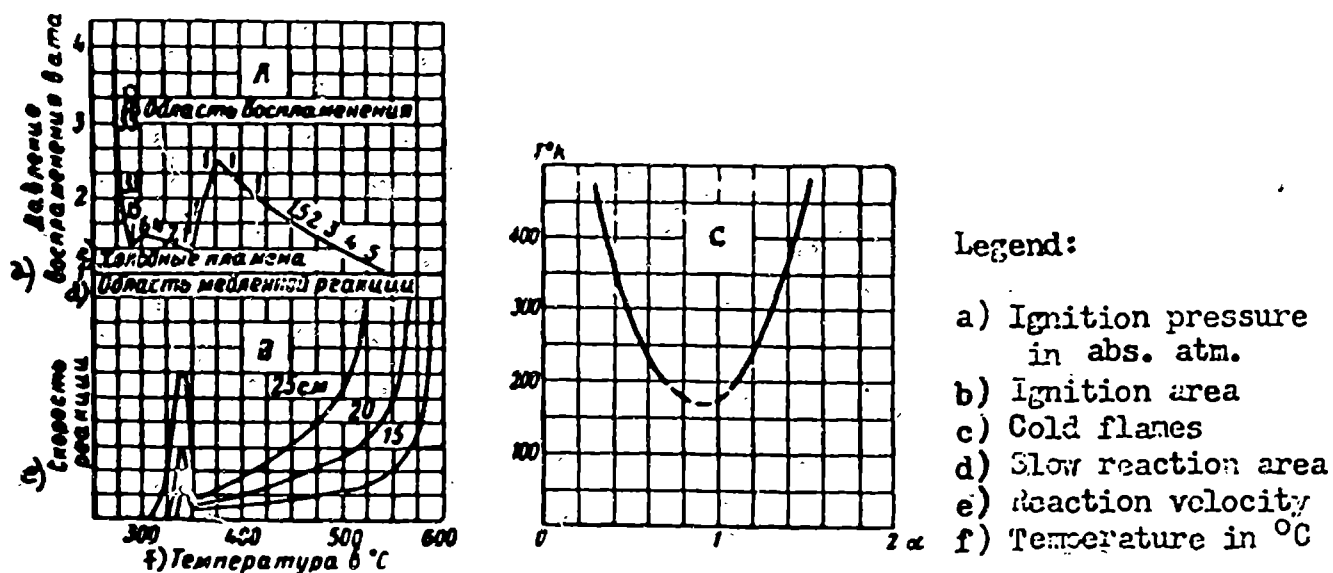
Fig. 102. Ignition limits.
A -- Dependence of the ignition pressure upon the temperature; B -- Dependence of the reaction velocity upon the temperature during various pressures (in mm of mercury); C -- Dependence of the composition of a mixture upon the temperature.

Legend:

a) Ignition pressure in abs. atm.
b) Ignition area
c) Cold flames
d) Slow reaction area
e) Reaction velocity
f) Temperature in °C

The partial pressure of the fuel and the air in a fuel mixture is

$$p_r = rp; \quad p_s = (1-r)p.$$ (6.73)

The gas constant of the fuel is

$$R_r = \frac{848}{\mu_r}.$$

The gravimetric fractions of the fuel and the air in 1 m³ of a mixture is

$$G_r = \frac{p_r}{R_r T} = \frac{rp}{R_r T}; \quad G_s = \frac{p_s}{R_s T} = \frac{(1-r)p}{R_s T}.$$ (6.74)

The excess air coefficient is

$$\alpha = \frac{G_r}{LG_s} = \frac{1-r}{rL}\frac{\mu_s}{\mu_r}.$$ (6.75)

The combustion of a mixture, which lies within the ignition limits for ignition by a spark, does not occur instantly, but after the passage of a measurable period of time. The time which elapses from the moment the fuel mixture is ignited to the moment the flame front appears, and may be registered is called the ignition lag. An ignition lag is usually observed during the ignition of a fuel mixture in a gas cylinder. The pressure increase in the cylinder is recorded by an oscillograph. During the ignition lag, the pressure does not increase greatly (Figure 103). At the expiration of the ignition lag, a pressure increase occurs at a great speed and ends when the entire mixture is burnt. An ignition lag is observed during the ignition of mixtures of hydrocarbons and air. The transformation from the ignition lag to the reaction,

which proceeds with a noticeable velocity, occurs gradually.

Legend:

A) Terminal pressure
B) Initial ressure
C) Time
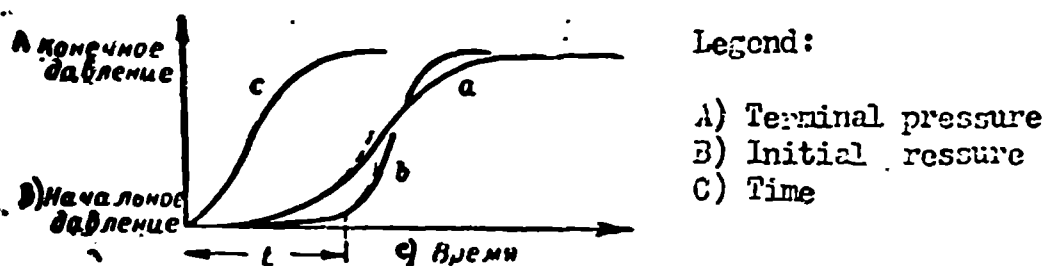
Fig. 103. Variation with time of the reaction rate of the oxidation of hydrocarbons. t -- ignition lag. The curves a and b refer to mixtures of hydrocarbons with oxygen, the curve c refers to the same mixture after an addition of aldehyde.

The existence of the ignition lag is explained by the fact that the hydrocarbon molecules do not unite immediately with the oxygen, and the reaction has a chain mechanism. In the course of the ignition lag, a sufficient quantity of active particles in the mixture accumulate, the presence of which is necessary for the development of chain reactions which result in the oxidation of the hydrocarbons. A small addition of aldehydes shortens the ignition lag (Figure 103, curve c).

Example. Find the greatest and least excess air, during which the combustion of heptane is possible when r_n = 1%; r_v = 6%.

The carbon content in heptane is 0.84, hydrogen -- 0.16, L = 0.84·11.5+0.16· 34.5 = 15.17.

Using formula (6.73), we determine: the greatest excess air (lower limit)

$$\alpha_{max} = \frac{99 \cdot 28,9}{1 \cdot 100 \cdot 15,17} = 1,89,$$

least excess air (upper limit)

$$\alpha_{min} = \frac{94 \cdot 28,9}{6 \cdot 100 \cdot 15,17} = 0,30$$

SECTION 9. FLAME STABILIZATION

If a flow of a fuel mixture, whose composition is within the ignition limits, passes an ignition source (an electric spark, for example), whose power is insufficiently great, at a high velocity (about 100 m/sec), then the heat balance proves to be unfavorable, the mixture temperature does not reach T_{vsp}, and the mixture does not ignite. To insure the uninterrupted ignition of the quickly moving flow of a fuel mixture, the ignition source (an electric spark, for example) is located behind a poorly streamlined body, for example, a cone, which faces towards the flow, or a

plate behind which a vortex zone is formed where the gas flow recirculates (Figures 104 and 105).

Legend:

A) Plane flame holder
B) Area of reversed flow

Fig. 104. Recirculation zone behind a poorly streamlined body.

The area of counter flow, in which the ignited masses of gas are recirculated, serves as an ignition source for a fresh mixture.

A poorly streamlined body, which holds back the flame in the recirculation zone is called a baffle flame holder.

Flat, conical, corrugated, cylindrical, and other forms of flame holders are used (see Figure 104). Flame stabilization is possible also in the boundary layer and in counter flow.
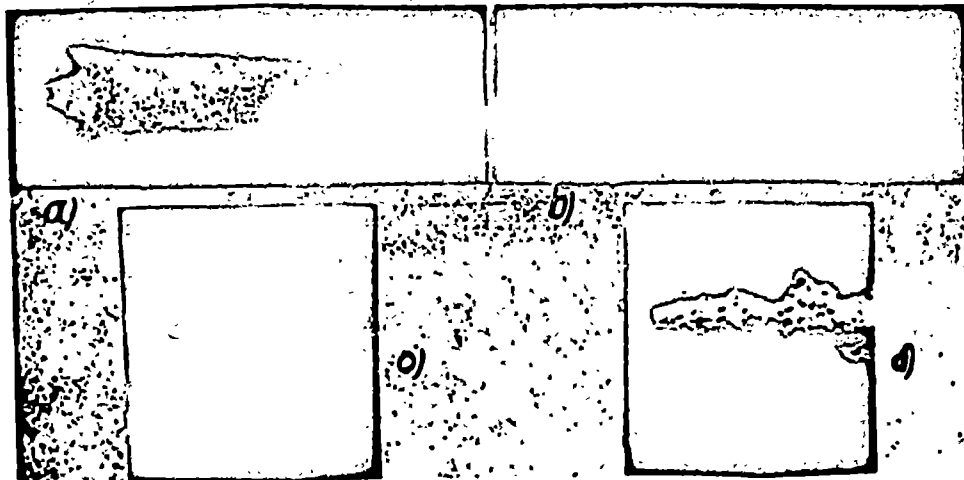
Fig. 105. Photographs of the combustion zone behind the flame holders.
a -- multiple flame holder (time exposure), b -- the same flame holder
(instantaneous Schlieren-photograph), c -- simple flame holder (time
exposure), d -- the same flame holder (instantaneous Schlieren-photograph).

At a certain flow velocity, w_{sr}, the flame of a homogeneous mixture, the composition of which is within ignition limits, blows away from the flame holder and combustion ceases.

According to the thermal theory, the action of a flame holder is as follows. Continuous combustion occurs in the vortex area behind the flame holder (see Figure 104). The cold, turbulent flow of gas, which flows around the flame holder, comes

into contact with the combustion area, and by means of a turbulent heat exchange, obtains the heat necessary for its ignition. If the velocity of its movement w is great or if the temperature of the gases in the combustion zone behind the flame holder is low, the quantity of heat that the fresh mixture receives will be insufficient for heating it to the ignition temperature T_{vsp}, and the mixture will not ignite: the flame will blow away from the flame holder.

During tests, a flame holder with a known relative cross section $S_{st} = \dfrac{S_{st}}{S_2}$ is installed in a combustion chamber and the velocity at the chamber inlet w_2 increased (by increasing, for example, the exhaust nozzle cross section) until combustion takes place. All the remaining parameters: the composition of the mixture α, the temperature T_2 and the air pressure p_{02}, the nature of the fuel, and the turbulence intensity of the flow ε -- must be constant if possible. That flame holder which, at a given relative cross section S_{st}, has the highest blow off velocity $w_{sr} = w_2$, is the best. Sometimes, in place of the relative cross section S_{st}, the drag coefficient of the flame holder ζ is given, and the velocity of the blow out determined at a given drag. However, to calculate the drag coefficient of a complicated flame-holder beforehand is usually impossible. Tests show that the blow out velocity at a given relative flame holder cross section $S_{st} = \dfrac{S_{st}}{S}$ depends upon the geometry of the flame holder and upon the parameters of the fuel mixture.

The geometry of a flame holder exerts complex influences upon the blow out velocity. Certain tests, the authenticity of which is in need of confirmation, show that the blow out velocity increases with an increase of the flame holder's perimeter so long as the transverse dimensions of its elements do not become less than a certain given value. Therefore complicated flame holders, constructed from radial or concentric gutters or of rods, retain the flame better than a conical holder if the loads applied to the cross-section S_{st} are equal. The blow out velocity increases with an increase of the rods' cross-section (Figure 116).

The composition of a mixture exerts a substantial influence upon the action of a flame holder. Usually the blow out velocity for a given flame holder has its

greatest value near the stoichiometric composition (Figure 1C7).

With a leaning out or an enrichment of the mixture, the blow out velocity decreases. If the composition of the mixture changes sufficiently, pulsating combustion begins and ends with the breaking away of the flame.

The temperature of the mixture. With an increase of the mixture temperature, the velocity of a turbulent combustion increases owing to the growth of the normal velocity of the flame propagation. The blow out limits, for a given velocity and composition of the mixture, expand. Therefore, in those supersonic combustion chambers, where the stagnation temperature is great, higher flow velocities are permissible, and the limits of stable combustion at a given composition of the mixture, prove to be wider than in subsonic combustion chambers.

The phase composition of the mixture exerts an influence upon the operation of the flame holder. A large portion of the drops, moving with the air, do not flow around the flame holder while moving along the air stream lines, but strike against its surface. Fuel vapors and the minutest drops penetrate into the space behind the flame holder. If the surface is not too hot, a liquid film forms on it and runs off the rear edges of the flame holder. Under the influence of heat transfer from the combustion zone through the material of the flame holder, and in co sequence of the diffusion of vapors into the oncoming air, the film evaporates intensively. The forming vapors are carried over to the turbulent area of the flame holder, enriching the mixture near its rear edges. The average excess air in the combustion chamber is seldom less than $\alpha_{sr} = 0.C$. Since the drops on flame holder evaporate, the mixture in the combustion zone is enriched without exceeding the combustion limits. If the average excess air in the chamber $\alpha_{sr} \gg 1.6$, combustion of the two-phase mixture is not curtailed, since the fuel evaporation of the flame holder enriches the mixture at its rear edges and the lean blow out occurs when $\alpha_{sr} > 1.6$. Consequently, in a two-phase mixture the blow out of the flames from the flame holder occurs at lower fuel-to-air ratios than during operation with a single-phase mixture. With an increase of the flow velocity, the portion of the drops which strike

the flame holder increases; therefore in a two-phase mixture poor blow out limits occur at large average air excesses α_{cr}, for high flow velocities. Two-phase mixtures are more suitable for combustion in a combustion chamber equipped with a flame holder than are single-phase mixtures.

Ignition source. An ignition source, such as an electric spark or a flame,

Legend:

A) Flow velocity at the chamber inlet in m/sec
B) Stoichimetry
C) Air/fuel ratio
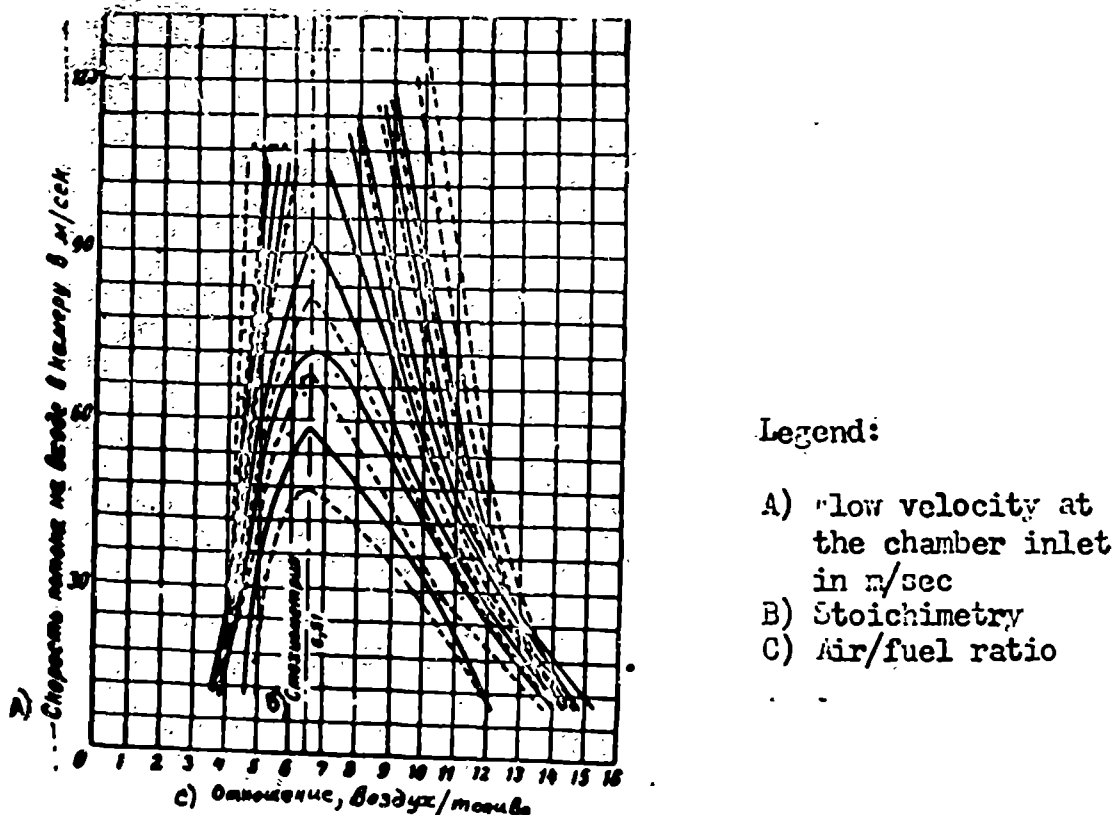
Fig. 106. The influence of the thickness of the flame-holding rods on the derangement velocity, with an increase of the thickness.

must be introduced into the space behind the flame holder for the initial ignition of the mixture. After ignition, the ignition source may remain connected and carry out the function of a "pilot light". With an increase of the heat energy of the ignition source, the blow out limits at a given velocity and given composition of the mixture are expanded. With an increase of the degree of turbulence, the blow out velocity changes. Turbulence-forming screens and grilles, used to make the flow turbulent, are installed at the chamber inlet. The installation of turbulence-forming screens during operation on rich mixtures decreases the blow out velocity. During operation on lean mixtures, the influence of the degree of turbulence is more complex.

The heating of the flame holder expands the stabilization limits at a given velocity and given composition of a mixture. Cooling of the flame holder shrinks the

stabilization limits.

В) Область измерений
w от 12 до 170 м/сек D)
p от 0,2 до 1,0 кг/см² E)
D от 0,6 до 2,5 см F)

C) Параметр стабилизации $Z = \dfrac{w}{p^{0,95}D^{0,85}}$

Legend:

A) Ratio $\dfrac{1}{\alpha L}$

B) Transition area

C) Stabilization parameter

D) w from 12 to 170 m/sec

E) p from 0.2 to 1.0 kg/cm²

F) D from 0.6 to 2.5 cm
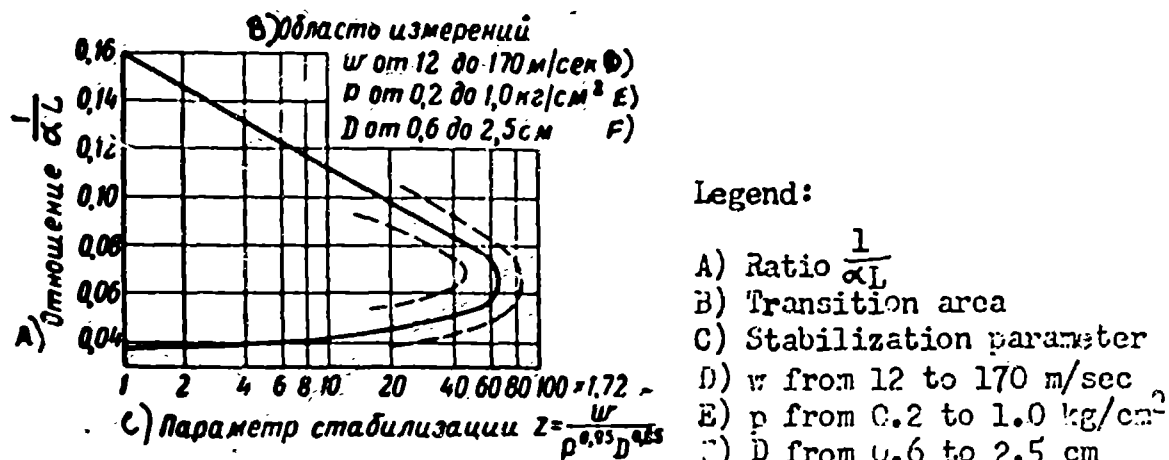
Fig. 107. Dependence of the stabilization parameter on the composition of the mixture

Calculation Formulae. Detailed research on flame stabilization was carried out by a series of scientists. Figure 107 depicts the experimental data of De Zubay who studied the stabilization of flames of previously prepared propane-air mixtures by bodies of various sizes and shapes and over a wide range of mixture compositions, pressures and flow velocities (from 0.2 to 1 atm and from 12 to 170 m/sec)[*].

De Zubay found that $\dfrac{G_r}{G_e} = \dfrac{1}{\alpha L}$, the blow out limit, is a function of the stabilization parameter $\dfrac{w}{p^{0,95}D^{0,85}}\left(\dfrac{T_0}{T}\right)^{1,5}$:

$$\frac{1}{\alpha L} = f\left[\frac{w}{p^{0,95}D^{0,85}}\left(\frac{T_0}{T}\right)^{1,5}\right],$$

(6.76)

where T_0 is the temperature at which all experiments were carried out; $T_0 = 390°K$;

T is the temperature of the flow in $°K$;

p is the pressure of the flow in kg/cm^2;

w is the velocity of the flow in m/sec;

f is the function, approximated by the curve in Figure 107;

D is the hydraulic diameter of the flame holder in cm.:

$$D = \frac{4S}{P};$$

(6.77)

S is the area of the flame holder in cm^2;

P is the wetted perimeter in cm.

Example: For a stoichiometric mixture of pentane with air: L = 15; when $\alpha = 1$, the fuel-air ratio $\dfrac{1}{\alpha L} = 0.0167$. The stabilization parameter according to the graph of Figure 107 is:

---

[*] De Zubay, Character of Disk Controlled Flames, Aero Digest, 61, 1950.

$$\frac{w}{p^{0.85} D^{0.15}} \cdot \frac{T_0}{T} = 67 \cdot 1.72 = 115. \tag{6.78}$$

From this it is possible to find the velocity, pressure, and temperature of the flow or the hydraulic diameter of the flame holder, for the blow out condition, if the remaining parameters are known.

If the velocity of a flow $v = 100 \text{ m/sec}$; $\frac{T}{T_0} = 1$; $p = 1 \text{ kg/cm}^2$, then the least hydraulic diameter of a flame holder capable of maintaining a flame is equal to

$$D = \sqrt[0.85]{\frac{100}{115}} = 0.94 \text{ cm} = 9.4 \text{ mm.}$$

SECTION 10. COMBUSTION IN CERAMIC TUBES

Flame holders are necessary for the combustion of hydrocarbon fuels in combustion chambers having metal walls, since the temperature of the metal walls usually remains lower than the ignition temperature of the fuel and metallic walls are not able to serve as igniters.
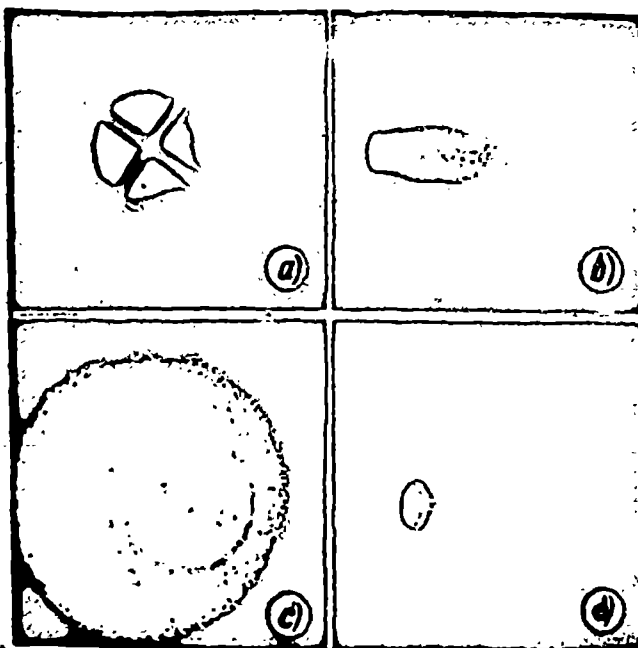
Fig. 108. Photographs of combustion in stabilized and in ceramic combustion chambers. a -- a stabilized combustion chamber, b -- flame at the outlet of a stabilized combustion chamber, c -- combustion in a ceramic combustion chamber, d -- flame at the outlet of a ceramic combustion chamber.

To decrease the drag of the combustion chamber ζ, experiments were carried out upon the ignition of a fuel mixture in an un-stabilized combustion chamber, whose sides may heat up to a temperature which was close to the flame temperature. In order that the walls should maintain a temperature which was much higher than the ignition temperature, ceramic tubes (Figure 108) were used as the combustion chamber.

The combustion efficiency of the hydrocarbons in a ceramic tube is close to 100%, and the drag ζ is less than that of a stabilized combustion chamber. However, the mechanical strength of ceramic chambers is significantly lower than that of metallic, and the surface unit weight is much higher. Therefore, up to the present time, ceramic combustion chambers have not found a use in jet technology. The heat-resistant and non-conductive converings of the internal surfaces of the plates of which combustion chambers are made are able to intensify the combustion process, decrease the length of the combustion zone, decrease heat losses through the walls, increase the combustion efficiency and decrease the burner drag.

BIBLIOGRAPHY

1. Vol', K., "Skorost' rasprostaneniya otkrytykh turbulentnykh plamen," /Propagation Velocity of Open Turbulent Flames/, "VRT" 1956, No. 4, 48-53.

2. Voprosy goreniya /Combustion Problems/, Collections 1 and 2, Publishing House for Foreign Literature, 1954.

3. Zel'dovich, Ya. B. and Polyarnyy, A. I., Raschety teplovykh protsessov pri vysokikh temperaturakh /Calculations of the Thermal Processes during High Temperatures/ Printing House "BHT", 1947.

4. Zel'dovich, Ya. B. "K teorii rasprostraneniya plameni," /The Theory of Flame Propagation/, "ZhFKh," 1948, col. 22.

5. Il'yashenko, S. M., Germeyer, Ye. M., and Sokolova, V. M., Teplovyye diagrammy dlya produktov sgoraniya kerosina v vozdukhye /Thermal (Mollier) Charts for the Combustion Products of Kerosene in Air/, 1950.

6. Cross, R. A., "Stabilizatsiya plameni v pogrannichnor sloye," /Flame Stabilization in the Boundary Layer/, Jet Propulsion, vol. 25, 1955, No. 6.

7. Kay, D. and Libby, T., Spravochnik fizika-eksperimentatora/Handbook of a Physics Experimenter/, Publishing House for Foreign Literature, 1950.

8. Lewis, B. and Elbe, G., Goreniya, plamya i vzryvy v gazakh /Combustion, Flame and Explosions in Gases/, Publishing House for Foreign Literature, 1948.

9. Mack, Clure and Berl, "Goreniye," /Combustion/ Ind. and Engineering Chemistry, vol. 45, 1953, No. 7.

10. Michelson, V. A., Normal'naya skorost' vosplameneniya v gremuchikh smesyakh /Normal Ignition Velocity in Detonating Mixtures/, 1890.

11. Prandtl, L., Gidromekhanika /Hydromechanics/, Publishing House for Foreign Literature, 1951.

12. Roberts, J., Teplota i termodinamika /Heat and Thermodynamics/, Publishing House

for Foreign Literature, 1950.

13. Semenov, N. N., Teoriya tsepnykh reaktziy /The Theory of Chain Reaction/ Gostechizdat /State Technical Printing House/, 1940.

14. Spravochnik khimika /A Chemist's Handbook/, vol. I, Khimizdat /Chemical Printing House/, M. - L., 1952.

15. Khritrin, L. N., Fizika goreniya i vzryva /The Physics of Combustion and Explosion/, Moscow University Press, 1957.

16. Shchelkin, K. I., "Turbulenthoye goreniye," /Turbulent Combustion/, ZhTF /Journal of Technical Physics/, 1943, vol. 13, No. 9.

17. NACA Report, 1953, No. 1037.

18. Summerfield, M. and others, "The Physical Structures of Turbulent Flames," Jet Propulsion, vol. 24, No. 4, 1954.

19. Bolz, R. E., and Burlage, H., "The Influence of Turbulence on Flame Propagation Rates," Jet Propulsion, vol. 25, 1955, No. 6.

20. Elbe, H., Fourth Simpos. on Combustion, 1953.

21. Combustion Processes, New York, 1956.

22. Dugger, G. and Simon D., "Prediction of Flame Velocities of Hydrocarbon Flames," NACA Rep., 1954, No. 1158.

23. Karman, Th., "Combustion in Turbulent Flames," Fourth Symposium on Combustion, 1953.

24. De Zubay, "Character of Disk Controlled Flames," Aero Digest, 61, 1950.

25. Schaffer, A. and Cambel, A. B., "The Effect of an Opposing Jet on Flame Stability," Jet Propulsion, vol. 25, 1955, No. 6.

26. Howland, A. H., and Simmonds, W. A., "Combustion inside Refractory Tubes," Fourth Symposium on Combustion, 1953.

27. Evans, M. W., "Current Status of Problems of Combustion Heat Trans. and Fl. Mech. Inst.," 1954.

28. Dugger, G. L., "Effect of Initial Mixture Temperature on Flame Speeds and Blow-off Limits of Propane -- Air Flames," NACA, TN, 2170, Aug. 1950.

29. Petrein, R. J., Longwell, J. P., and Weiss, M. A., "Flame Spreading from Baffles," Jet Propulsion, v. 26, 1956, No. 2.

30. Lewis, B., Pease, R. N., and Taylor, H. S.,"High Speed Aerodynamics and Jet Propulsion," vol. II, Combustion Processes, Princeton Univ. Press, 1956.

RAMJET ENGINES

BY: M. N. Bondaryuk and S. M. Il'yashenko

February 1960, 431 Pages

(Part 2 of 2 Parts)

CARBURETION

The fuel used in ramjet engines which operate on a molecular energy source is in a liquid state. The initial velocity of an air flow at the inlet to a combustion chamber amounts to tens of m/sec, and in some combustion chambers even exceeds 100 m/sec; the stay time of the fuel in a combustion chamber does not exceed several milliseconds. In order that the liquid fuel be able to burn completely in such a short interval of time, the ignition must be preceded by a careful preparation of the fuel-air mixture.

The preparation of the mixture by combining vapor and small drops of fuel with the air is called carburetion.

Carburetion consists of the following processes: the fuel injection; the breaking-down of the fuel stream into drops; the evaporation of the drops, and the mixing of the fuel vapor that is formed, with the air.

The speed and completeness of the combustion depends on the quality of the mixture preparation. Carburetion is one of the most important stages in the operation of the combustion chamber of a jet engine.

The fuel feed is accomplished by the aid of containers filled with a compressed gas or by the aid of a pump which is placed into operation by a special motor -- usually an air turbine.

The dispersion of the fuel is accomplished by the aid of fuel injectors: the fuel stream, which discharges from an injector, is broken down into separate minute drops, the diameters of which are usually measured in a tenth of a micron. The evaporation of the drops which are moving in the air, occurs because of the heat taken from the surrounding gases as well as from their own heat. The finer the drops, i.e. the greater their overall surface, and the greater the material and heat transfer coefficient, the quicker the transmission of heat and the evaporation of the drops will be. The injectors must be situated so that the local concentration of the fuel-air mixture that is formed in the combustion zone is within ignition limits. The evapora-

tion of the drops is usually accomplished in the same combustion zone.

The interspersion of the fuel vapor with the air occurs due to the turbulence of the flow and molecular diffusion. With an increase of turbulence intensity, the interspersion process is accelerated; the distance, at which the distribution across the entire cross section of the combustion chamber is made uniform, is shortened.

We will begin the study of carburetion with an account of the theory of fuel injectors.

SECTION 1. DIRECT-SPRAY INJECTORS

A direct-spray injector is represented by a small nozzle with a narrow opening, the diameter of which is usually in the region of a tenth of a millimeter (Figure 109).

The discharge velocity of the fuel w_g may be found from Bernoulli's equation. We will designate the excess pressure ahead of the injector inlet by Δp and the density of the fuel by γ_g. Then:

$$w_r = \sqrt{2g \frac{\Delta p - \Delta p_{not}}{\gamma_r}}.$$ (7.1)

A) Горючее   B) Сопло

e) p ≈ 100 атм   d_c < 1мм
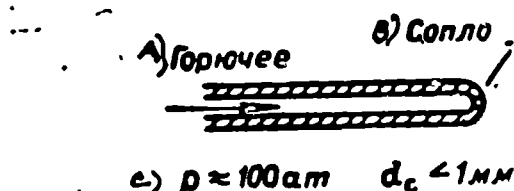
Legend:
A) Fuel
B) Nozzle
C) p ≈ 100 atm

Fig. 109. A schematic of a direct-spray injector.

The pressure losses Δp_{pot} are usually proportional to the square of the discharge velocity:

$$\Delta p_{not} = \zeta \frac{\gamma_r w_r^2}{2g}.$$ (7.2)

Here ζ is the loss factor or the drag coefficient, which is determined by an experimental method. Substituting the equation (7.2) in (7.1), we obtain

$$w_r = \sqrt{\frac{1}{1+\zeta} \frac{2g\Delta p}{\gamma_r}} = \varphi_w \sqrt{\frac{2g\Delta p}{\gamma_r}}.$$ (7.3)

The expression φ_w is called the velocity coefficient.

The velocity coefficient is related to the drag coefficient

$$\varphi_w = \frac{1}{\sqrt{1+\zeta}}.$$ (7.4)

The velocity coefficient usually lies between the limits of 0.92 to 0.98. For

$$\varphi_w = 0.95.$$

One may find the discharge of a liquid G from the velocity and size of the injector outlet section S:

$$G = \varphi w_r S_{\text{Tr}} = \varphi \varphi_w s \sqrt{2g\gamma_r \Delta p}. \tag{7.5}$$

The factor φ, which is equal to the ratio of the cross section area of a spray to the injector nozzle area, is called the <u>contraction coefficient</u>. When the discharge in direct-spray injectors is from an opening with sharp edges

$$\varphi \approx \frac{2}{3}.$$

The product of the velocity coefficient φ_w and the contraction coefficient φ is called the <u>discharge coefficient</u> μ

$$\mu = \varphi \varphi_w. \tag{7.6}$$

In practice, it is more convenient to measure the discharge coefficient by:

$$\mu = \frac{G}{S\sqrt{2g\gamma_r \Delta p}}. \tag{7.7}$$

The excess pressure of the fuel supply is measured by a manometer, the density of the liquid -- by a hydrometer; the flow per second is determined either by a direct weighing of the liquid, which flows out of an injector in t time, or with the aid of special fuel flow meters: calibrated orifices, flow meters, turbine meters and others.

For changes in the nature of the liquid (for example, when benzine is substituted for kerosene), for variations of the liquid's temperature or of the surplus pressure, the discharge coefficient of a direct-spray injector is insignificantly altered.

The stream of fuel, which discharges from an injector, breaks up into separate drops during interaction with the surrounding medium.

<u>Example</u>. Find the discharge velocity and the flow rate of benzine if the diameter of the injector nozzle $d_c = 1$ mm, the discharge coefficient $\mu = 0.6$, and the velocity coefficient $\varphi_w = 0.95$ if the density of the benzine $\gamma_E = 0.75$ kg/m^3 and the fuel-feed pressure $\Delta p = 10$ kg/cm^2.

$$w_r = \varphi_w \sqrt{2g \frac{\Delta p}{\gamma_r}}.$$

We express all values in the technical system of units: $\Delta p = 10$ atm. $= 10 \cdot 10^4$ kg/m^2; $\gamma = 0.75$ kg/ℓ $= 750$ kg/m^3;

$$w_2 = 0.95 \sqrt{19.6 \frac{10 \cdot 10^4}{750}} = 48.5 \text{ m/sec.}$$

The exhaust opening is

$$s = \frac{\pi}{4} d_c^2 = 0.78 \cdot 10^{-6} \ m^2 = 0.78 \text{ mm}^2.$$

The benzine flow rate (7.5) is

$$G = 0.6 \cdot 0.78 \cdot 10^{-6} \sqrt{19.6 \cdot 750 \cdot 10 \cdot 10^4} = 0.0179 \ \kappa z/c e \kappa = 17.9 \text{ gm/sec.}$$

SECTION 2. CENTRIFUGAL INJECTORS

Direct-spray injectors allow good dispersion for relative velocities of 100 m/sec and higher. To obtain good dispersion at smaller relative velocities, centrifugal injectors are used.

A vortex is created in a centrifugal injector, which directs the stream of liquid into a rapidly circulating motion, thanks to which the liquid, during discharge from the injector, moves not only along the nozzle axis but also in a tangential direction (Figure 110). The theory of "ideal" centrifugal injectors, neglecting the force of friction, was worked out by the Soviet scientist, Doctor of Technical Sciences, Professor G. N. Abramovich. L. A. Klyachko and other researchers refined this theory more precisely for the case of the flow of a viscous liquid.

Many forms of centrifugal injectors exist. The most widely used injectors are those with a tangential fuel supply (Figure 111). An injector with a tangential fuel feed consists of a vortex chamber and an exhaust opening -- with a nozzle and feeders which are located at a tangent to the vortex chamber. The fuel enters the vortex chamber at a tangential direction, moving in a spiral it goes into an intensive rotary movement and discharges through the exhaust nozzle. The annular velocity of a liquid during its movement from a vortex chamber to the exhaust opening of the nozzle increases in accordance with the law of the conservation of momentum. The particles of the liquid, which are exhausted from the nozzle, and are moving in an

axial as well as a tangential direction, expand into a conical shroud which, even during discharge into a vacuum, reaches maximum fineness at a certain distance from the injector, loses its stability and breaks down into minute drops (Figure 112).
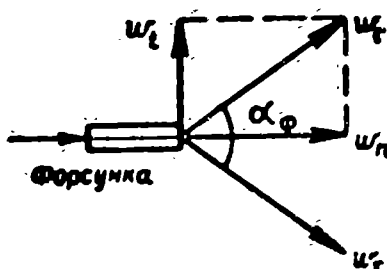
Fig. 110. Particles of a liquid, discharging from a centrifugal injector, move in axial and in radial directions. A) Injector.

Legend:
A) Fuel
B) Supply tube
C) Vortex chamber
D) Nozzle
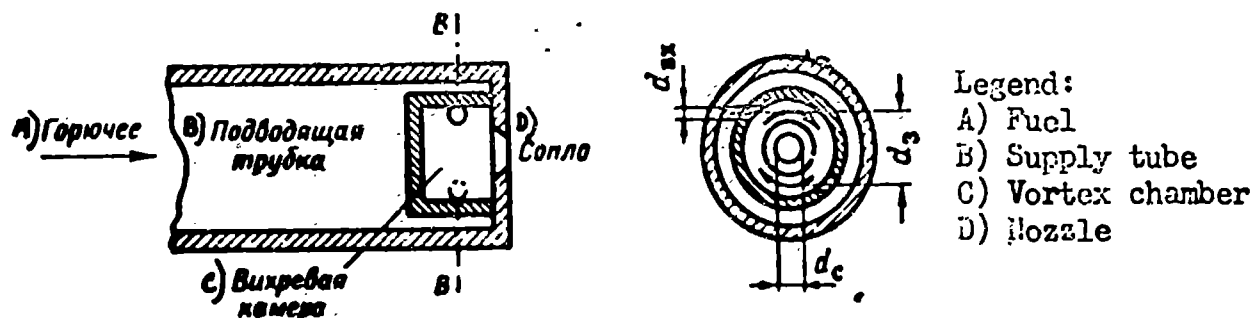
Fig. 111. A schematic of a centrifugal injector.

The velocity of the discharge from a centrifugal injector is determined by Bernoulli's equation:

$$w = \varphi_w \sqrt{2g \frac{\Delta p}{\gamma}},$$

(7.8)

where Δp is the surplus pressure, which represents the difference between the pressure at the injector inlet and the pressure of the surrounding medium;

γ is the density of the liquid;

φ_w is the speed ratio.

For an ideal injector $\varphi_w = 1$.

The velocity vector of the discharge is composed of the tangential w_t and axial w_n components:

$$w_t = w \sin \frac{\alpha}{2},$$

(7.9)

$$w_n = w \cos \frac{\alpha}{2},$$

(7.10)

$$w^2 = w_t^2 + w_n^2,$$

(7.11)

where α is the included spray angle of the dispersion jet.

The weight flow rate of the liquid is

$$G = \mu S \sqrt{2g\gamma \Delta p},$$
(7.12)

where S is the area of the nozzle exhaust opening;

μ is the discharge coefficient.

The theory of ideal centrifugal injectors is used to determine the discharge coefficient of an injector μ, the dispersion included spray angle α, the contraction coefficient ψ, and the thickness of the spray cone. The depth of the spray cone determines the fineness of the dispersion of a liquid by centrifugal injectors.
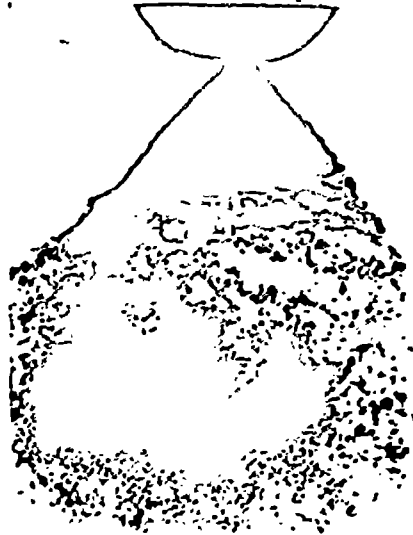
Fig. 112. Photograph of the breakdown of a liquid spray cone discharging from a centrifugal injector.

For non-viscous liquids, benzine or water for example, the theory of an ideal injector offers a sufficiently close agreement with practice; for more vis.. is liquids -- for example, kerosene or diesel fuel -- it is necessary to introduce corrections for the force of friction.

The momentum M of a liquid, which enters a centrifugal injector, is equal to the product of the velocity at the inlet tube w_3 and the radius of the twist r_3, which is equal to the distance from the axis of the injector to the axis of the inlet tube (see Figure 111):

$$M = w_3 r_3.$$

During the flow of a non-viscous liquid the momentum of any liquid particle under consideration remains constant:

$$w_3 r_3 = w_t r,$$

where w_t is the tangential component velocity at the nozzle outlet;

charge nozzle.

During the approach to the exhaust opening the radius of the circulation r decreases and the tangential velocity w_t grows.

Tending to move rectilinearly because of inertia, the particles of the twisted stream depart from the circulation axis and form a cylindrical spray cone with a depth of δ (see Figure 111) inside the nozzle. At the nozzle outlet the spray cone expands into a conical surface. The greater the tangential velocity of the stream, the smaller the relative depth of the spray cone $\frac{\delta}{d_c}$ and the smaller the contraction coefficient of the nozzle.

The ratio of the ring-shaped section of the discharging stream S_{str} to the nozzle exhaust section S_s is called the contraction coefficient:

$$\varphi = \frac{S_{cтp}}{S_c} = 1 - \frac{d_{вих}^2}{d_c^2},$$ (7.13)

where d_{vikh} is the diameter of the air vortex;

d_s is the nozzle diameter.

The thickness of the spray cone in the exhaust nozzle is:

$$\delta = \frac{1}{2}(d_c - d_{вих}).$$

The diameter of the air vortex in the exhaust nozzle is:

$$d_{вих} = d_c \sqrt{1 - \varphi},$$

consequently, the relative thickness of the spray cone is:

$$\frac{\delta}{d_c} = \frac{1}{2}(1 - \sqrt{1 - \varphi}).$$ (7.14)

In the theory of an ideal injector, which we will not set forth, it is indicated that the contraction coefficient φ, the discharge coefficient μ, and the included angle α are determined by the so-called geometric characteristic of the injector A:

$$A = \frac{d_s d_c}{n d_{вх}^2},$$ (7.15)

where d_3 is the diameter of the twist, which is equal to twice the distance from the injector axis to the axis of the inlet tube (tangential opening);

d_{vkh} is the diameter of the inlet opening;

n is the number of tangential openings at the vertex chamber inlet.

The contraction coefficient φ may be found from the equation:

$$A = \frac{1-\varphi}{\sqrt{\frac{\varphi^3}{2}}} .$$

(7.16)

The discharge coefficient from

$$\mu = \varphi \sqrt{\frac{\varphi}{2-\varphi}} .$$

(7.17)

The included spray angle of the injector α from

$$tg \frac{\alpha}{2} = \frac{(1-\varphi)\sqrt{8}}{(1+\sqrt{1-\varphi})\sqrt{\varphi}} .$$

(7.18)

All these formulae were obtained during a series of simplified assumptions. Therefore, even for a non-viscous liquid they are only approximately correct. The greater the viscosity of the liquid, the smaller the twist of the stream, the thicker the spray cone in the exhaust nozzle, the greater the contraction coefficient φ, and the greater the discharge coefficient μ. This paradoxical conclusion is confirmed by practice. The nozzle spray angle during an increase of the viscosity of the liquid decreases because of the decrease of tangential component velocity. The
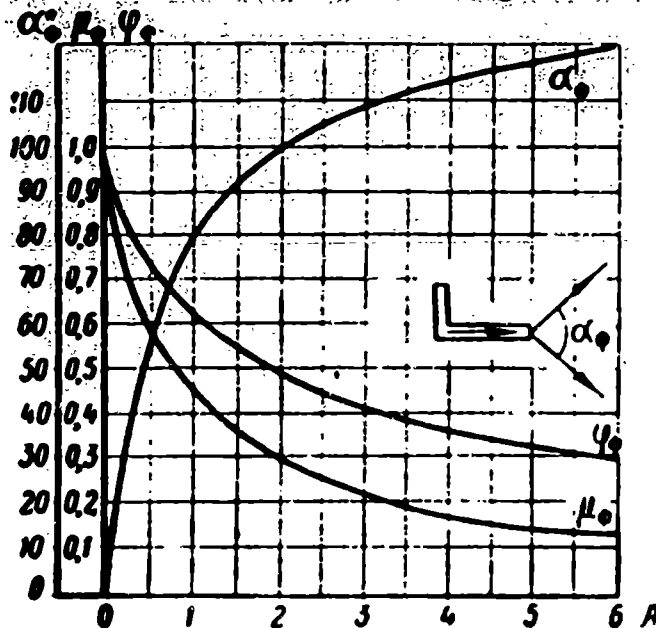
Fig. 113. The dependence of the contraction coefficient φ_f, the discharge coefficient μ_f, and the included spray angle α_f upon the geometric characteristic of the injector A.

dependence of φ, μ, and α upon the geometric characteristic of an ideal injector, calculated according to the formulae (7.16), (7.17), and (7.18) is depicted in Figure 113.

The discharge coefficients of a centrifugal injector during operation on kero-

sene and more viscous liquids, if the geometric characteristic $A > 2.5$, seems to be two and three times greater than the theory of an ideal injector, the basic conclusions of which were stated above, are suitable only for approximate preliminary calculations. The actual discharge coefficients and spray dispersion angles of centrifugal injectors are found by means of tests.

Example. Determine the geometric characteristic of an ideal centrifugal injector A, the coefficients φ and μ, the spray angle α, and the relative thickness of the spray cones δ, if $d_s = 0.5$ mm., $d_3 = 4$ mm., $d_{vikh} = 0.4$ mm., and the number of tangential openings $n = 3$.

The geometric characteristic (7.15) is:

$$A = \frac{d_c d_3}{n d_{bx}^2} = \frac{0.5 \cdot 4}{3 \cdot 0.4^2} = 4.16.$$

The coefficients φ and μ and the angle α are found by the graph in Figure 113:
$\varphi = 0.35; \ \mu = 0.18; \ \alpha = 120°$.

The relative thickness of the spray cone (7.14) is:

$$\frac{\delta}{\ell_c} = \frac{1}{2}(1 - \sqrt{1 - \varphi}) = \frac{1}{2}(1 - \sqrt{1 - 0.35}) = 0.0975.$$

The average diameter of the drops which are formed during the operation of a centrifugal injector depend upon the thickness of the liquid spray cone at the injector nozzle outlet.

SECTION 3. THE BREAK-DOWN OF LIQUID STREAMS AND DROPS

Liquid streams and drops, which are moving in a gaseous medium, break down.

A liquid, which discharges from the opening of a tube or from the nozzle of an injector into still air, comes under the action of surface tension and aerodynamic forces. Turbulent pulsations of velocity usually occur in a discharging stream: the stream as a whole moves in relation to the tube with a certain speed $w = \varphi \cdot \sqrt{2g \frac{\Delta p}{\gamma}}$.

Inside the stream the individual turbulent moles of the liquid move in a disorderly fashion, which is similar to the thermal movement of molecules. The character of the flow depends upon the discharge velocity, the density, viscosity, and surface tension of the liquid, and even upon the layout of the exhaust nozzle or injector.

During a very small surplus pressure, the discharge velocity is low; under the action of the force of gravity and the force of surface tension individual drops, the diameters of which usually lie between 1 to 5 mm (Figure 114a), will break off from the edges of the exhaust opening.

With an increase of the surplus pressure, the discharge velocity increases and the liquid discharges from the opening in the form of a laminar stream (Figure 114b).

With a further increase of the surplus pressure, the discharge velocity increases, and the stream becomes turbulent. Owing to the radial pulsations of the velocity, the surface of the stream is not uniform (Figure 114c). The aerodynamic forces, which act on the stream, tend to increase all the irregularities on its surface, while the surface tension forces tend to level them. The stream lines near a turbulent stream having a non-uniform surface is shown in Figure 115. In front of the irregularity, the air velocity decreases and the pressure increases; at the peak of the irregularity, the velocity of the flow increases and the pressure diminishes. The areas of increased pressure are indicated in Figure 115 by "+" signs; the rarefied areas by "-" signs.

It is obvious that under the action of aerodynamic forces, the disturbance on the surface of the stream will increase. For a sufficiently large relative velocity the individual disturbances will break away from the stream and form minute drops, the diameters of which are less than the diameter of the stream. At a great distance from the opening the entire stream will break down into drops whose diameters are commensurate with the initial diameter of the stream.

At very high stream velocities relative to the air (higher than 100 m/sec for kerosine), the break-down of the stream into drops begins right at the outlet opening (see Figure 114d).

The liquid drops become subject to the action of surface tension and aerodynamic forces as they move in the air.

Surface tension forces tend to impart a spherical shape to a drop. Aerodynamic forces tend to flatten out a drop (Figure 116. At a sufficient value of the dynamic

head (i.e., at a sufficient relative velocity) the drops of a given liquid disinte-
grate, forming a complete shower of more minute drops.
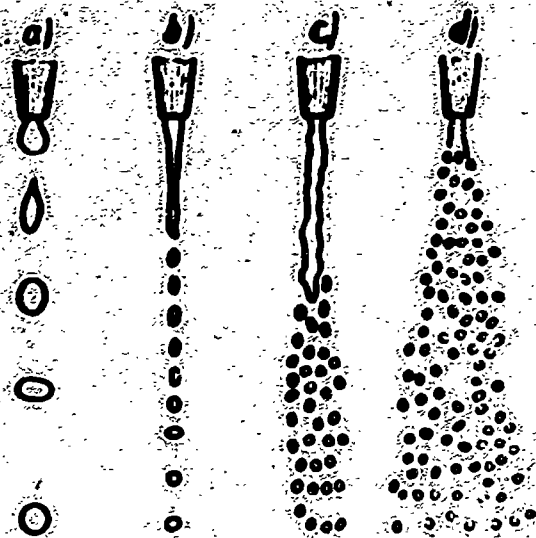
Fig. 114. The breakdown of a stream which discharges from an opening at various velocities.
a) v=0; b) v<10 m/sec; c) v>10 m/sec; d) v≥100 m/sec.

The breakdown of millimeter-sized drops is shown in Figure 117. When a velocity of approximately 23 m/sec is reached, a drop whose initial diameter is 2.5 mm, at first becomes flat, then forms a ring with a film in the center. Gradually this film blows out into a bubble, which finally bursts, breaking up into a series of almost imperceptible drops. The photographs in Figure 117 show the successive moments of deformation and breakdown of a spherical drop. In frame five we see that the bubble breaks near the apex. The broken edges of the film pull together towards the ring (Frames 6, 7, and 8) under the action of surface tension and collide with the ring, driving small droplets away from it (Frame 9). Finally, the same ring breaks into a series of minute drops and one or two large drops (Frame 10).
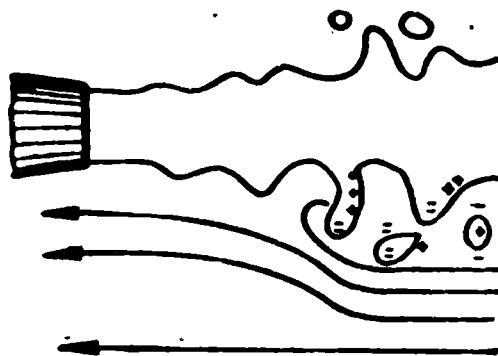
Fig. 115. The air flow around a turbulent stream.

The dynamic head, which appears during the movement of the drops relative to the air, is sufficient to cause the breakdown of the drop and may be found by substituting it for the internal pressure which appears in a drop because of surface ten-

sion. Although, as will be subsequently considered, a drop in flight does not have exactly a spherical shape, for the mathematical analysis of the problem it will be conditionally considered to be spherical.
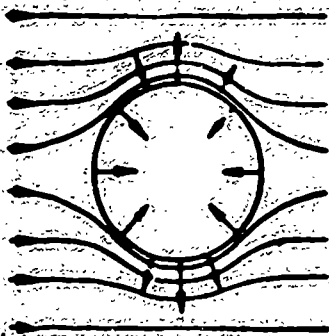
Fig. 116. Airflow around a drop.

If the surface tension of the drop is equal to σ, then the force f, with which one half of the drop attracts the other, will be equal to (Figure 116),

$$f = \pi d_\kappa \sigma.$$

(7.19)

This force creates a pressure which acts on the entire surface of the drop. The force f is equal to the sum of the products of elements of the area dS times the pressure projected to the normal to the element in question:

$$f = \int_{\left(\frac{S}{2}\right)} p\, dS \cos\varphi = p \int_{\left(\frac{\pi}{2}d_\kappa\right)} dS \cos\varphi = \frac{\pi}{4} d^2 p.$$

(7.20)
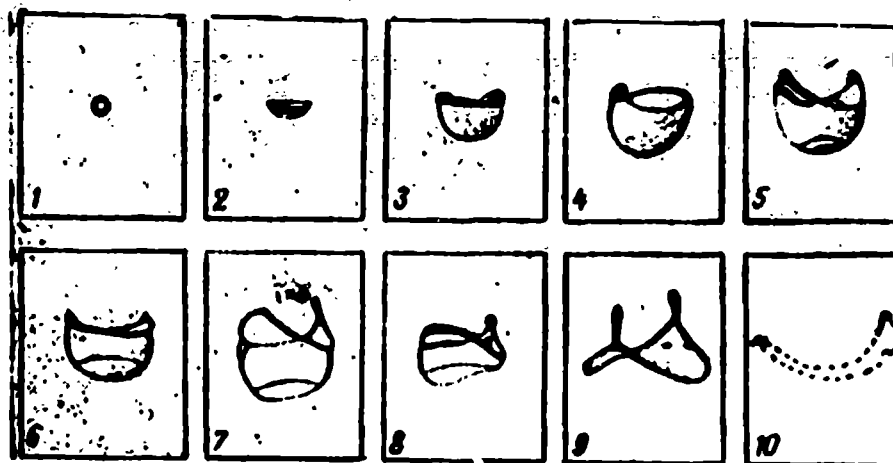
Fig. 117. A photograph of the breakdown of a millimeter-sized drop in an air flow.

By equating (7.19) and (7.20), we obtain the internal pressure which is created by the forces of surface tension:

$$p = \frac{4\sigma}{d_\kappa}.$$

(7.21)

If the dynamic head $\frac{\gamma_e w^2}{2g}$ has the same order of magnitude as the internal pressure caused by surface tension $\frac{4\sigma}{d_\kappa}$, the drop begins to disintegrate:

$$\frac{\gamma_b u^2}{2g} \approx \frac{4\sigma}{d_k}, \qquad (7.22)$$

From this

$$\frac{\gamma_b u^2 d_k}{g\sigma} = D, \qquad (7.23)$$

where D is the breakdown criterion.

The experiments of M. S. Volynskiy, made with various relative velocities of a drop of liquid having various surface tensions, showed the value of the breakdown criterion D for all the liquids investigated to be constant. When $D \geqslant 10.7$ splitting begins, and when $D > 14$ -- breakdown of the drop occurs.
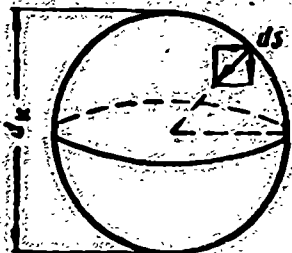
Fig. 118. Determining the internal pressure of a liquid in a drop.

The limiting velocity with which a drop is able to move in the air without disintegrating, in accordance with (7.23), is equal to

$$u_{max} = \sqrt{\frac{g\sigma D}{\gamma_b d_k}}. \qquad (7.24)$$

Here u is expressed in m/sec, σ in kg/m, γ_b in kg/m^3, d_k in m, and g = 9.81 m/sec^2.

If fuel discharges from a direct-spray injector into still air, then the breakdown of the stream begins when the pressure of the fuel feed is approximately 100 km/cm^2. After determining the discharge velocity from the equation (7.8), one may determine the value of the diameter of the larger drops which may be formed during the disintegration of the stream, from the equation (7.24):

$$d_{max} = \frac{g\sigma D}{\gamma_b u^2} = \frac{\sigma D}{2\Delta p_r}\frac{\gamma_r}{\gamma_b}. \qquad (7.25)$$

Besides the larger drops, a multitude of much smaller drops will be created in the dispersion jet (see section 4 of this chapter).

Centrifugal injectors disperse a fuel better at significantly lower fuel feed pressures than do direct-spray injectors.

Streams of a liquid, moving simultaneously in axial and tangential directions,

ever thinner, and finally, after losing its stability, breaks down into individual drops (see Figure 112). At low stream velocities relative to the air (u < 10-15 r/sec), the breakdown begins at a certain distance from the injector (as in Figure 112). At high relative velocities, the breakdown sets in right at the outlet edge of the injector nozzle. In photographs of shrouds, liquid braids, which encompass the spray cone along its circumference, are seen. The disintegrating spray cone breaks down into these braids which in turn disintegrate into separate drops.

The diameters of the larger drops formed during the disintegration of a liquid stream, shroud or other drops, may not be greater than d_{pred}, which is expressed by the formula (7.25).

The drops that are formed pulsate under the action of the force of surface tension, taking a form, now of an elongated, then of a flattened ellipsoid. Only in the first approximation may a drop be considered as spherical.

Example 1. Find the maximum diameter of a drop of kerosene that is formed during discharge into still air if the fuel feed pressure p_g = 10 kg/cm^2, γ_b = 1.22, and γ_g = 815 kg/m^3.

The limiting diameter in conformance with (7.25) is:

$$d_{npe\lambda} = \frac{D_2\gamma_r}{2p_r\gamma_a} = \frac{14 \cdot 0.002 \cdot 815}{2 \cdot 100\,000 \cdot 1.22} = 93 \cdot 10^{-6}\,\varkappa = 93\ \text{microns}$$

Example 2. Find the limiting velocity in relation to the air during which a 100-micron drop of kerosene disintegrates, if the temperature equals 15°C and the air pressure is 1 abs. atm.

According to Figure 126 the surface tension of the kerosene at 15°C is

$$\sigma = 26\ \text{dyne/cm} \approx 0.0026\ \text{kg/r}; \qquad \gamma_a = \frac{p_a}{RT_a} = \frac{10\,000}{29.3 \cdot 288} = 1.22\ \text{kg/r}^3$$

The limiting velocity is found according to the formula (7.24)

$$u_{npe\lambda} = \sqrt{\frac{g\sigma D}{\gamma_a d_\kappa}} = \sqrt{\frac{9.8 \cdot 0.0026 \cdot 14}{1.22 \cdot 100 \cdot 10^{-6}}} = 54\ \text{m/sec.}$$

SECTION 4. INJECTOR DISPERSION SPECTRA

The distribution of a fuel according to the sizes of the drops is called the

dispersion spectrum of an injector. Dispersion spectra are found by means of experiments. During the determination of the dispersion spectrum, the drops are conditionally divided into separate groups according to sizes (Table 7.1): for example, from 0 to 20 microns, from 20 to 40 microns, from 40 to 60 microns etc., to the limiting (maximum) diameter d_{pr}; the overall weight of a drop G and the **absolute and relative weights of each size-drops is found:**

$$G_{0-20}; \ G_{20-40}; \ G_{40-60} \ldots$$

$$x_{0-20} = \frac{G_{0-20}}{G}; \ x_{20-40} = \frac{G_{20-40}}{G}; \ldots ;$$

and

$$G_{0-20} + G_{20-40} + G_{40-60} + \ldots = G,$$

$$x_{0-20} + x_{20-40} + x_{40-60} + \ldots = 1.$$

(7.26)

A dispersion spectrum is expressed in the form of a graph, on the horizontal axis of which is plotted the size of the drops and on the vertical axis is plotted either the relative weight percentage of the drops whose diameters are less than the size which is plotted along the ordinate axis (Figure 119), or the relative weight of a given group of drops (see Figures 123, 124 and 125).

The numbers, cited in Table 7.1, indicate that the drops, the diameters of which lie within the limits of 60 to 80 microns, form every second 12 grams or 30% of the total weight of drops, and the drops with a diameter of less than 80 microns form 24.8 grams or 62% every second.

Table 7.1

INJECTOR DISPERSION SPECTRUM (DISTRIBUTION OF DROPS BY SIZES)

d microns	G_l gr/sec	$x_l = \frac{G_l}{G}$	G_{0-l} gr/sec	$\frac{G_{0-l}}{G}$ %	n (millions)	S m²
0	0,8	2	0	0	1900	0,96
20	4	10	0,8	2	354	1,0
40	8	20	4,8	12	153	1,2
60	12	30	12,8	32	84	1,285
80	7,2	18	24,8	62	23	0,6
100	4,8	12	32,0	80	8,6	0,33
120	3,2	8	40,0	92	3,5	0,185
d_{pr}				—		
Σ	40 gr	100%	—	100	2526,1	5,2 m²

The knowledge of dispersion spectra is necessary for the study of the evaporation and combustion of the drops.

If the weight of the drops, the diameters of which lie within **definite**

limits, is known, then it is possible to find the number of the drops and their total surface. If the weight of the group of drops is equal to G, and their average diameter equal to d_{sr}, then the weight of one drop is equal to:

$$\frac{\pi}{6}\gamma_r d_{cp}^3.$$ (7.27)

The surface of one drop is

$$s = \pi d_{cp}^2.$$ (7.28)

The number of drops is

$$n = \frac{6G}{\pi\gamma_r d_{cp}^3}.$$ (7.29)

The total surface of the drops is

$$S = ns = \frac{6G}{\gamma_r d_{cp}}.$$ (7.30)

If, for example, $d_{sr} = 100$ microns $= 10^{-4}$ m., $\gamma_g = 800$ kg/m^3, and G = 1 kg, then the number of drops is

$$n = \frac{6 \cdot 1}{3.14 \cdot 800 \cdot 10^{-12}} = 2.39 \text{ billions};$$

and their total surface is

$$S = \frac{6G}{\gamma_r d_{cp}} = \frac{6}{800 \cdot 10^{-4}} = 75 \text{ m}^2.$$
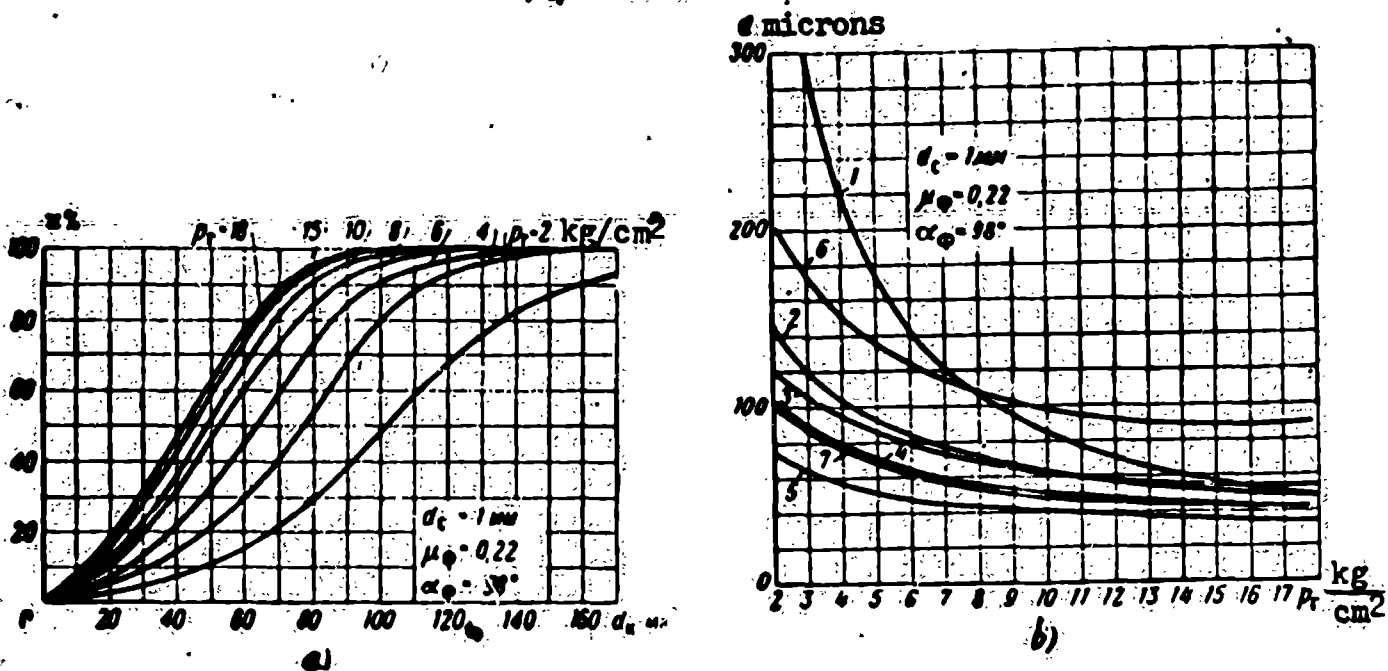
Fig. 119. Dispersion from centrifugal injectors.
a -- dispersion spectra at various pressure, b -- a comparison of measured drop diameters with calculated ones.
1 -- limiting drop diameter /formula (7.25)7, 2 -- median diameter (Longwell's formula), 3 -- the same (Nukiyama-Tanasawa formula), 4 -- measured median diameter, 5 -- median diameter (Bloch-Kichkin formula), 6 -- measured limiting diameter, 7 -- median diameter /formula (7.40)7.

Knowing the spectrum of dispersion, it is not difficult to estimate the

amount of drops which are contained in this or in another group (see Table 7.1).

It appears that groups of small drops, the general mass of which is small, are more numerous than groups of larger drops, which possess significantly greater weight. Thus, for example, the number of drops which are less than 20 microns, in the example in question, comprises 1,900,000,000, i.e. 70% of the total number of the drops, and at the same time their weight is equal to 2% of the total weight, and their surface is 11.5% of the total surface.

Often the fineness of a dispersion is characterized by a certain dimension. Various authors select different parameters for this characteristic dimension. That diameter, of which 50% of the overall mass of the drops is comprised, is called the median diameter. In Figure 119 the median diameter when $p = 18$ kg/cm^2 $d_M = 42\,\mu$.

In foreign literature the so-called Sutter or Zauter average diameter (abbreviated SDS) is accepted to characterize the fineness of a dispersion.[1]

Sutter's average diameter is equal to that diameter which drops of an identical size would have if their total surface $\sum \pi d_i^2$ and total weight $\sum \frac{\pi}{6} d_i^3$ would be the same as those in a stream composed of drops of various sizes. Consequently, SDS is

$$d_c = 6 \frac{V}{S} = \frac{\sum d_i^3}{\sum d_i^2}.$$ (7.31)

The non-uniformity of a dispersion k is characterized by the ratio of the true number of drops n to that number n_s which would be obtained if all the particles had the same diameter, equal to the SDS:

$$k = \frac{n}{n_c}.$$ (7.32)

In the example, analyzed before (see Table 7.1)

$$d_c = \frac{6G}{\gamma S} = \frac{6 \cdot 0.040}{800 \cdot 5.2} = 5.8 \cdot 10^{-5}\ \varkappa = 58\ \mu;$$

$$n_c = \frac{6G}{\pi \gamma d_c^3} = \frac{6 \cdot 0.040 \cdot 10^{18}}{3.14 \cdot 800 \cdot 58^3} = 0.486 \cdot 10^9 = 486\ \text{mm}.$$

---

[1] Griffin, E., "Atomisation of Fuel Sprays," Engineering, 4-VII, 1952, vol. 174, No. 4510.
Longwell, J., "Szhiganiye zhidkikh topliv" /Combustion of Liquid Fuels/. From the book Combustion Processes, New York, 1956.

The degree of non-uniformity is

$$k = \frac{n}{n_c} = \frac{25,26 \cdot 10^9}{4,86 \cdot 10^9} = 5,2.$$

SECTION 5. EXPERIMENTAL RESEARCH OF DISPERSION SPECTRA

The dispersion spectra of centrifugal and spray injectors may be investigated by means of experiments. The most widely used are the following methods: solidification method, absolute method, impression method, colorimetric method, and an optical method.

The solidification method that is used, for example in the work of Clair and Radcliffe, is based upon the fact that the density, viscosity, and surface tension of some substance in a molten state may be the same, at an increased temperature, as that of the test fuel during normal temperature. For example, the physical parameters of melted paraffin are close to the parameters of kerosene at room temperature. Such a molten substance, discharging from an injector, will be dispersed the same as the test fuel. Falling into the air, the drops of the melted paraffin are cooled and solidify, preserving an approximately spherical shape. The solidified drops collect

Fig. 120. A series of screens for sorting solidified drops.
A) Strainers; B) 100 and more μ.

and are sorted through a series of screens having various sized meshes. The sorted globules are weighed. Through the finest screen, having a size of 20 μ for example, come all the solidified drops with diameters of 0 to 20 μ; through the next screen come all the particles with diameters of, for example, 20 to 40 μ etc. To accelerate the process, all the screens are placed one atop the other (Figure 120). The widest-meshed screen is placed on top. The determination of the dispersion spectrum is accomplished by weighing the sifted particles remaining on each screen and those passing

through to the pan.

The draw-back of this solidification method is that it is difficult to select a substance, the physical parameters of which in a molten state would be sufficiently close to the fuel in question at the required conditions. The temperature of the fuel exerts a material influence upon the character of the dispersion and upon subsequent evaporation. To investigate the influence of temperature upon dispersion it is necessary to choose such substances, which in a molten state, would have the same physical parameters as would the fuel in question for a given succession of temperatures. This is usually only successful within a narrow temperature interval. Therefore, to expand the areas of research, along with the solidification method one must use other methods to investigate the dispersion.

The absolute method consists of entrapping the drops in a layer of a viscous liquid with which they do not mix and which fails to dissolve them--glycerine for example. The drops, stuck in the glycerine, preserve their spherical form. Their dimensions are measured under a microscope. The drawbacks of this absolute method are, first, its difficulty, and second -- the specimens obtained do not last a long time.

Legend:
A) Injector
B) Dispersion jet
C) Aperture
D) Slide plate
E) Plate with a layer
   of magnesium .
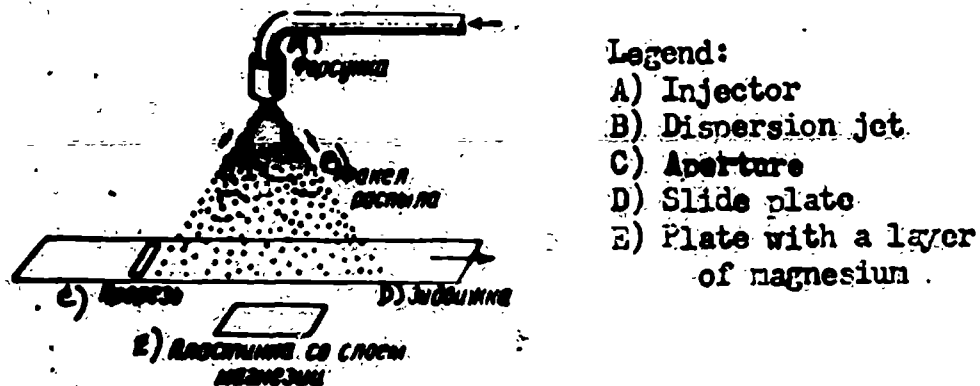
Fig. 121. The investigation of a dispersion spectrum by the impression method.

The impression method includes the capture of the liquid drops in a substance in which noticeable traces remain. To obtain the impressions, the drops are captured on a plate which is covered with a layer of magnesium or carbon black. Falling on these coverings, the drops imprint their traces which may be examined and computed under a microscope. The dimensions of the impressions are not equal to the dimensions of the drops. The relationship between the diameter of the impression and the diameter of the drop is determined by means of a special experiment by which

crops, the dimensions of which are determined by the absolute method, are entrapped on the layer.

In order that the impressions of the drops do not overlap one another during the investigation of the dispersion, the spray strikes the plate for a limited time. This time is set, for example, by the motion of a slide plate (Figure 121) with a slot or by a rotating disk with a slot.

The impression method, which requires the measurement and calculation of a large quantity of traces under a microscope, is extremely tedious and fatigueing.

Legend:
A) Priming funnel
B) Rotating disk
C) Filter
D) Injector
E) Collecting trays
F) Air
G) Fuel
H) Screen
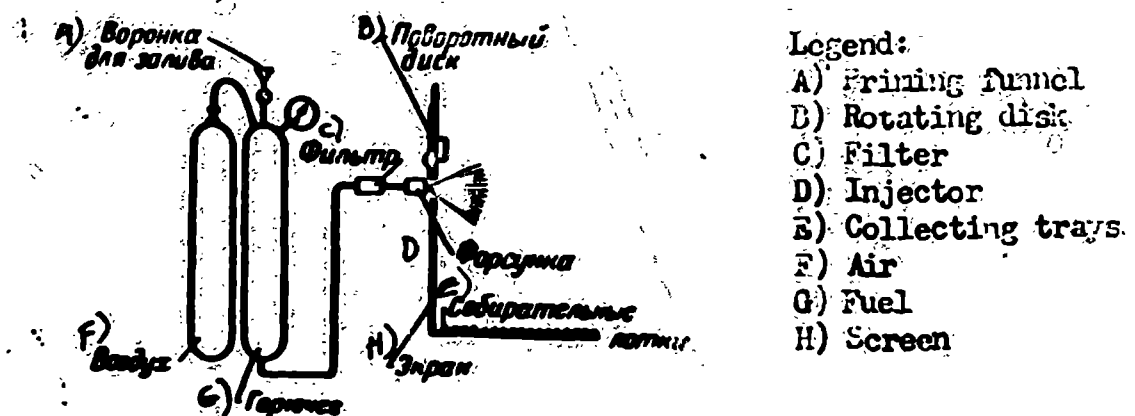
Fig. 122. The investigation of a dispersion spectrum by the colorimetric method.

The colorimetric method is based on the use of the fact that with a constant-pressure fuel feed and a very narrow dispersion angle, the larger drops from a horizontally-mounted injector fly further than do the small ones (Figure 122). The injector is located horizontally above a tray which is divided into grooves that are oriented at a right angle to the axis of the spray. A predetermined amount of the fuel in question is poured into a groove. A color is added to the fuel to be atomized. The greater the weight of the drops that fall in one or another groove, the more intensively the liquid will be colored in it. The intensity of the color is determined by a colorimetric method. The diameters of the drops of fuel which fall in one or another of the grooves is determined by covering the grooves with a plate coated with magnisium oxide and measuring the dimensions of the impressions. Similar experiments have shown that in each groove fall only those drops determined by the dimension of the group.

Not one of the above-described methods is used for the study of the dispersion

spectra of the lighter liquids such as benzine and kerosene that are preheated to a temperature that is close to their boiling temperature. Prior to all the drops being captured, a significant portion of them will be able to evaporate. In this case only an optical method is suitable.

The optical method used, for example, in the work of Blokh and Kichkin,[1] consists of photographing the flying drops with the aid of a camera having an objective lens with fine depth definition. The photographs of the drops that are obtained are examined and measured under a microscope. The distortion of the sizes of the drops at varying distances from the lens introduces a considerable error in an optical method.

SECTION 6. THE INFLUENCE OF THE PHYSICAL PARAMETERS OF THE LIQUID AND THE AIR ON THE DISPERSION AND THE FORM OF THE JET.

For a given injector, a given fuel feed pressure, and constant velocity, pressure and temperature of the air, the fineness of a dispersion depends upon the viscosity, density, and surface tension of the liquid.

Experiments have shown, that during an increase of the viscosity, the dispersion spectrum increases on the side of the larger drops (Figure 123). Not only does the average diameter of the drops increase during this, but the largest diameter increases sharply and the relative content of the larger drops become more significant.

Evaporation and combustion of the larger drops occurs so slowly that these processes may not successfully be completed in the combustion chamber of a ramjet engine. The presence of the larger drops may be one of the reasons for the incompleteness of the combustion and reduced efficiency of ramjet engines. Therefore, atomizing a liquid having a high viscosity is not recommended.

The influence of the viscosity upon the atomization of a fuel by centrifugal injectors, apparently, is dependent on its influence upon the thickness of the liquid spray cone that is formed in the injector nozzle (see Figure 111). With an increase

---

[1]Blokh, A. G. and Kichkina, Ye. S., "Sredniy diameter kapel' pri raspylivanii topliva tsentrobezhnymi forsunkami," /The Average Diameter of a Drop during Atomization of a Fuel by Centrifugal Injectors/. Teploenergetika, 1955, No. 9.

of viscosity, and due to the increase of friction, the twist of the fuel becores less, the tangential velocity decreases, and the thickness of the spray cone, and the sizes of the drops that are formed increase.

To increase the atomization of such viscous liquids as diesel fuel, solar oil /petroleum/, naptha or fuel oil, these are pre-heated since an increase of tempera-ture decreases the viscosity.

The influence of viscosity at room temperature (t = 20° C) upon atomization is seen from the comparison of Figures 123 and 124, in which the dispersion spectra arc plotted of a safe diesel fuel and of a light lubricating oil. These liquids have al-most identical surface tensions (23 and 32 dyne/cm) and materially different kinematic viscosities (1.8 and 32 centistokes). Experience shows that an increase of viscosity alters the form of the dispersion spectrum, increases the SDS, increases the size of the larger drops, and increases their content. Therefore the transition to a more viscous fuel for the same other parameters will be accompanied by a deterioration of the dispersion and the evaporation of the drops, which causes a decrease in the com-pleteness of the combustion. To increase combustion during operation on high-vis-cosity fuels, it is necessary to increase the temperature of the fuel or to decrease
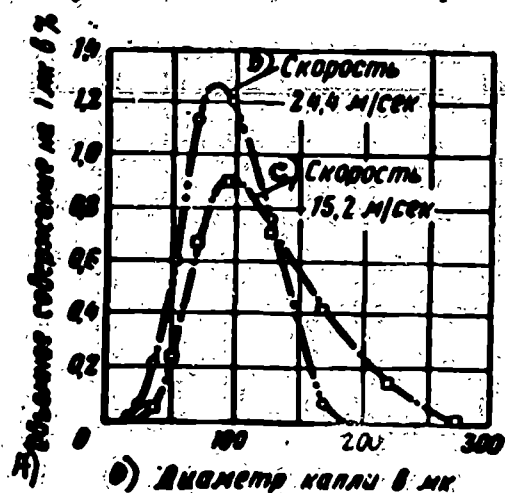
Legend:

A) Volumetric content per micron in %
B) Velocity 24.4 m/sec
C) Velocity 15.2 m/sec
D) Diameter of the drops in μ

Fig. 123. Atomization spectra of diesel fuel.

the discharge opening of the injector, simultaneously raising the fuel feed pressure, or to lengthen the combustion zone, or to augment the dispersion rate.

With an increase of surface tension, as seen from formula (7.25), the quality of the dispersion deteriorates. The effect of surface tension on dispersion is seen

Legend:

A) Volumetric content
per micron in %
B) Velocity 24.4 m/sec
C) Velocity 15.2 m/sec
D) Diameter of the drops
in μ
E) End

Fig. 124. Dispersion spectra of a light lubricating oil.

from a comparison of the dispersion spectra of a safe diesel fuel and water (Figures 123 and 125), which have similar viscosities (1.8 and 1.0 centistokes) and materially different surface tensions (23 and 73 dyne/cm).

An increase of the drop diameter occurs with an increase of surface tension in accordance with the formula (7.23). It is appropriate to mention that the surface tensions of hydrocarbon fuels have similar values (Table 7.2). Therefore, the change of the dispersion spectrum during the transition from one fuel to another is usually accompanied by a change of viscosity and not by a change of surface tension.
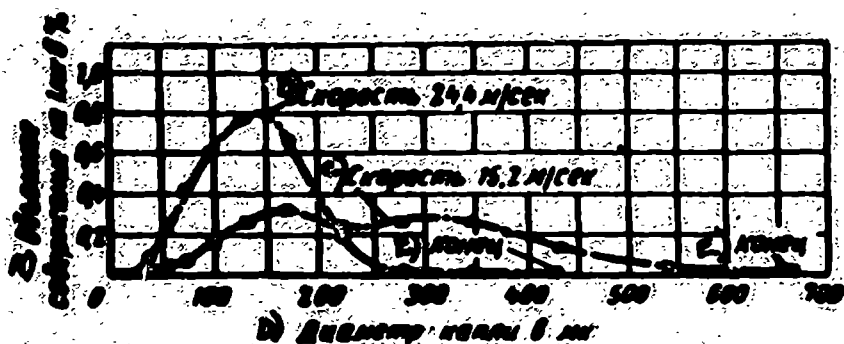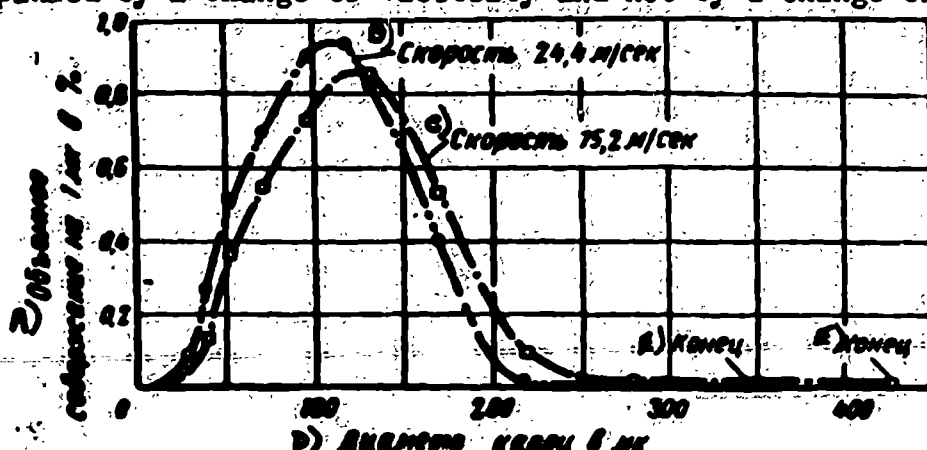
Legend:

A) Volumetric content per
micron in %
B) Velocity 24.4 m/sec
C) Velocity 15.2 m/sec
D) Diameter of the drops
in μ
E) End

Fig. 125. Dispersion spectra of water.

The compensation for the negative effect on dispersion of the surface tension may be effected in the same way as for that of increased viscosity, i.e. by heating the fuel (Figure 126).

The density of a fuel γ_6, as one may surmise, must also have an effect on the fineness of a dispersion. For other conditions being equal, if the density of the fuel increases, the inertness of the drops increases and the dispersion must deteriorate.

With an increase in the relative velocity w_{otn}, other conditions being equal, the aerodynamic forces which act upon the stream increase, and the fineness of the

ispersion grows. How the fineness of a dispersion increases during an increase of

Table 7.2

SURFACE TENSION AND VISCOSITY OF CERTAIN LIQUIDS

Fuel	Temperature, °C	Density γ_g kg/ℓ	Kinematic Viscosity ν_g in Centistokes	Surface Tension σ dynes/cm
Benzine	15	0,75	0,68	22,5
Kerosene	15	0,815	1,95	26,6
Water	20	1,00	1,01	73
Safe diesel fuel	20	0,87	1,60	23
Light lubricating oil	20	0,86	32	32
Heptane	20	0,684	0,692	20,9
Benzol	20	0,879	0,729	28,9
Ethyl alcohol	20	0,789	1,43	22,3

the relative velocity from 15.2 to 24.4 m/sec is seen in Figures 123, 124 and 125.

It is seen that the lower the relative velocity, the more noticeable will be the ef-

fect of the viscosity and surface tension upon dispersion.
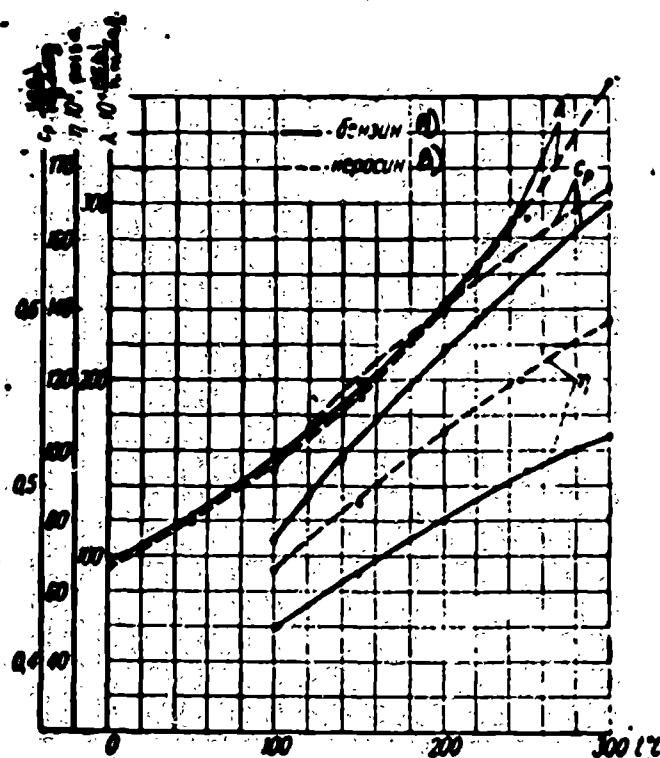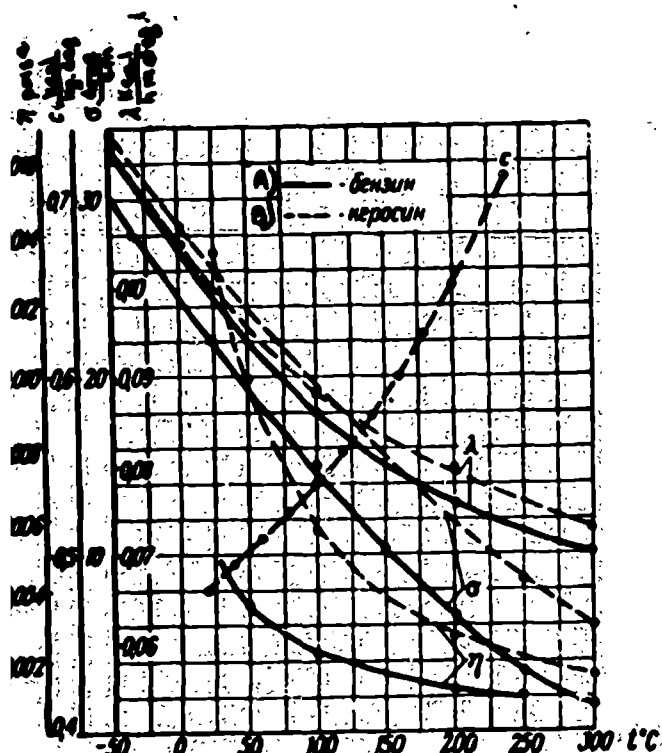
Fig. 126. The dependence of the parameters of kerosene and benzine upon temperature.
a -- liquid phase, b -- vapor phase.

$1 \dfrac{kg \cdot sec}{m^2} = 98$ poise

A) Benzine
B) Kerosene

The air pressure also has an effect upon the fineness of a dispersion. With

lowering of the pressure, the air density decreases, and the aerodynamic forces

diminish, other conditions being equal. According to certain data, dispersion de-

teriorates with a decrease of pressure, and the average drop diameter grows.[1] The effect of atmospheric pressure upon dispersion is shown in Figure 127.
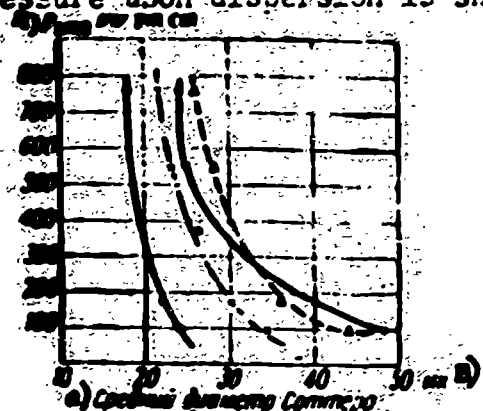
Legend:
A) P, ... in mm of mercury
B) microns
D) Sutter's average diameter
E) dynes/cm
F) γg/cm³
G) γcentistokes
H) p-heptane
I) kerosene
J) bnezene
K) toluene

Fig. 127. The effect of atmospheric pressure upon dispersion by a pneumatic injector.

The airtemperature also must have an effect upon the fineness of a dispersion (Figure 128). With a temperature increase, the density of the air decreases and the aerodynamic forces diminish, owing to which the dispersion must deteriorate. We do not know of any actual experiments that confirm the effect of air temperature on dispersion.
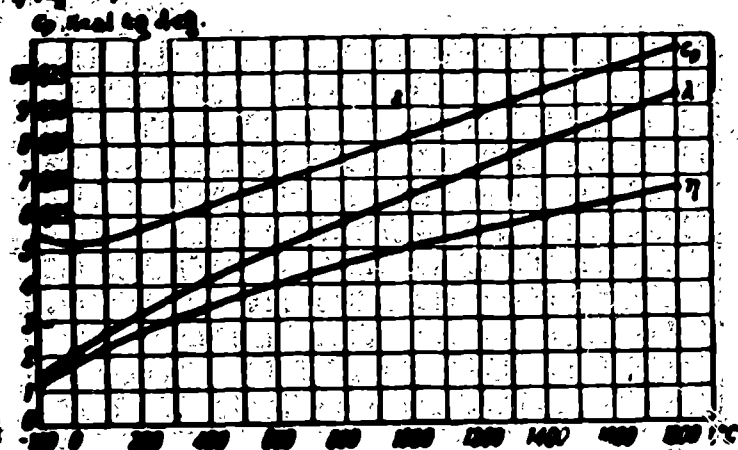
Fig. 128. The dependence of the parameters of dry air upon the temperature.

Aerodynamic forces influence not only the fineness of a dispersion, but also affect the configuration of the shape of the jet, i.e., the form of the drops' trajectory in relation to the stationary walls of the combustion chamber (Figure 129). The greater the density of the liquid, the diameter of the drops, and their initial velocity, the further the drops will deviate from the axis at a given injector spray cone

[1]Garner, F. H. and Henney, V. E., "Behavior of Sprays under High Altitude conditions," Fuel, vol. 32, 1953.

angle and the wider the dispersion jet will be. The greater the density and viscosity of the air, the faster the drops will lose their velocity, and the narrower the dispersion jet will be. The greater the velocity of the air, the faster the drops will be brought together in a flow, and the narrower will be the dispersion jet.

A division of drops according to size occurs during the operation of a centrifugal injector in an air stream. The larger drops, which have a certain tangential velocity at the breakdown of the shroud $w_t = w \sin \frac{\alpha}{2}$, deviate further from the injector axis than do the smaller drops which have the same tangential velocity (see Figure 129). Drops, the diameter of which is less than 10μ, lose their initial velocity at a distance of not further than several millimeters from the injector, and continue to move together with the air, taking part in the air's turbulent movement.

For an increase of flight altitude, if the Mach number is constant, the pressure and density of the air in a combustion chamber diminish, the dispersion deteriorates, and the dispersion jet broadens owing both to the increase of the drop diameters and to decrease in air density.

The number of kilograms of air, which pass through a combustion chamber every second, diminishes proportionally to the decrease of air density γ_n during an increase of flight altitude, if the Mach number is constant. In order that the composition of the mixture in the combustion chamber remains constant, the fuel feed G must diminish in direct proportion to the decrease in the density of the surrounding air

$$G = k \gamma_n.$$

If the fuel-feed-control variation with altitude is carried out only by changing the pressure p_g, then with an increase of flight altitude, the discharge velocity of the fuel will decrease, and the similar pressure decrease in the combustion chamber will be accompanied by a deterioration of the dispersion, an increase of the content of the large drops, and a decrease in the completeness of the combustion. If the altitude-control is accomplished by changing the number of injectors, or the cross-section of the injector, for a constant fuel feed pressure, then for an increase of flight altitude and a decrease of pressure in the combustion chamber, the dispersion will de-

teriorate because of the change in the air density. But the dispersion jet will widen at a constant discharge velocity so that the largest drops will be able to fall to the walls of the chamber.

The changes in the fineness of dispersion and the jet configuration, resulting from the altering flight altitude, must be taken into account in the designs of high-altitude chambers.
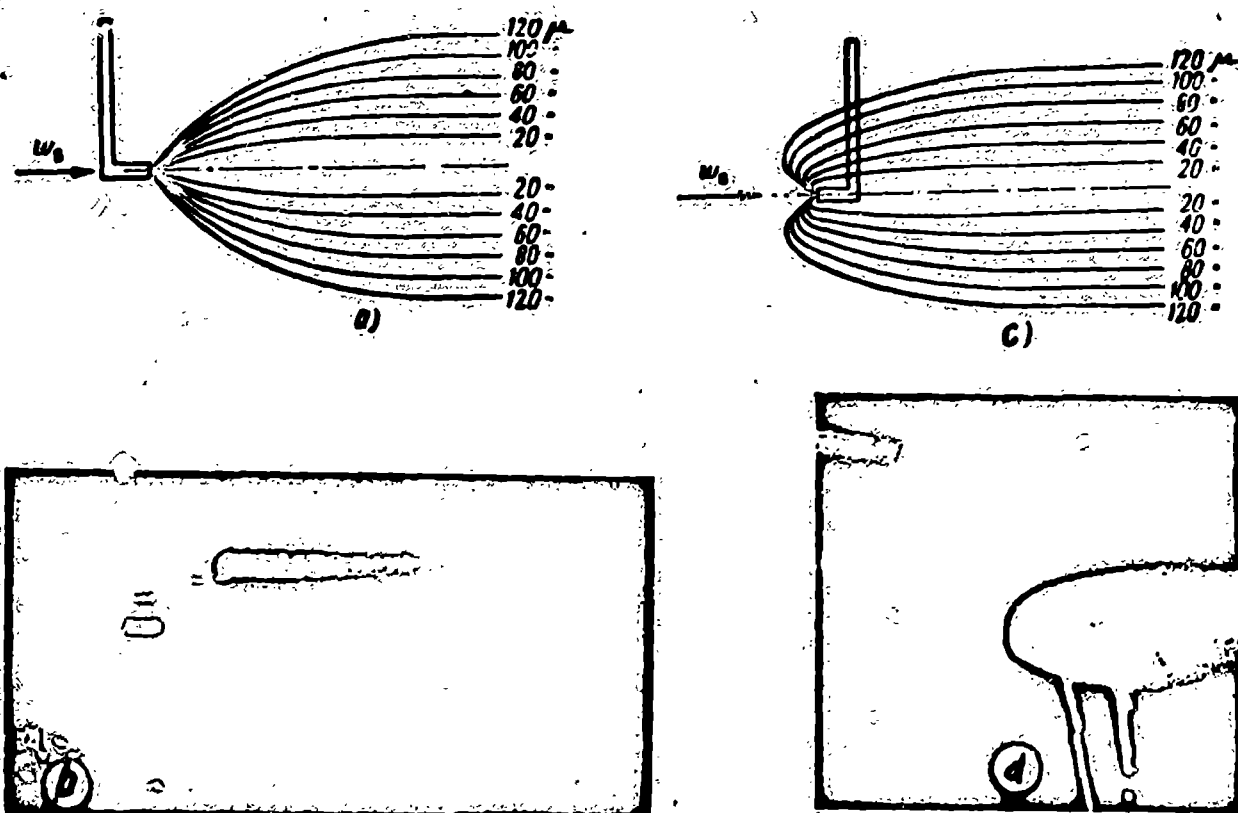
Fig. 129. A dispersion jet (trajectory of the drops' movement);
a and b -- injection with the flow; c and d -- injection against the flow.

SECTION 7. FORMULAE FOR COMPUTING DISPERSION SPECTRA

Not one of the investigations of atomization resulting from theoretical under-standings succeeded in obtaining calculated formulae which agreed with the data of an experiment. The numerous emperical formulae proposed at the present time are usually suitable only within narrow confines and coincide poorly with the experimental re-sults that were obtained by other authors.

A. G. Blokh and Ye. S. Kichkina, having investigated the dispersion spectra of centrifugal injectors by optical method, suggest the following emperical formula to compute the relationship between the median diameter of the drops and the nozzle diameter of the centrifugal injector:

$$\frac{d_m}{d_c} = \frac{47.8}{A^{0.4} \Pi^{0.1} Re^{0.7}} \cdot \tag{7.33}$$

e A is the geometric characteristic of the injector, which is determined by the formula (7.15).

Parameter II considers the quality of the fuel:

$$\Pi = \frac{g \nu_r^2}{\gamma_r \sigma d_c}; \tag{7.34}$$

γ_g is the density of the fuel in kg/m^3;

η_g is the dynamic viscosity of the fuel in $kg \ sec/m^2$;

σ is the surface tension of the liquid in $kg \ m$;

g is $9.81 \ m/sec^2$.

The Reynold's number is determined for the conditions which correspond to the discharge from the injector nozzle:

$$Re = \frac{\gamma_r w_r d_c}{g \eta_r}.$$

The number of drops whose diameter is greater than d is determined by the formula

$$x = \frac{G_{d-d_{max}}}{G} = e^{-\left(\frac{1}{n} + \frac{d}{d_m}\right)}. \tag{7.35}$$

The parameter n = 2.0 to 2.5 is dependent on the construction of the injector.

J. Longwell suggested the following formula to compute the median diameter of the drops that are formed during operation of centrifugal injectors:

$$\frac{d_m}{d_c} = \frac{0.32 e^{0.7 \nu_r}}{p_r^{0.3} \sin\frac{\alpha}{2}}. \tag{7.36}$$

The relative content of the drops whose diameter is greater than d is equal to

$$x = \frac{G_{d+d_{max}}}{G} = e^{-0.69 \left(\frac{d}{d_m}\right)^k}. \tag{7.37}$$

In these formulae:

γ_g is the kinematic viscosity of the fuel (from 0.08 to 0.8 cm^2/sec);

α is the dispersion angle of the injector;

p_g surplus pressure of the fuel feed (from 3 to 22 kg/cm^2);

k is the empirical factor of irregularity, which is dependent on the median diameter d_m (Figure 130).

When $d = d_{r}$, $\dfrac{3d \div d_{max}}{d} = 0.5$. With an increase of k, the dispersion becomes more even.

Longwell's formula does not consider the surface tension of a liquid and the parameters of the surrounding air. The geometric characteristic of the injector is taken into consideration only by introducing $\sin\dfrac{\alpha}{2}$.
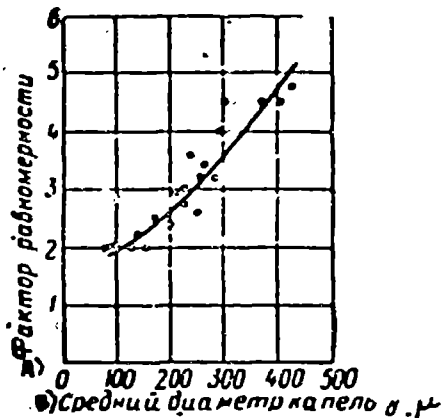
Fig. 130. The dependence of the uniformity factor upon the average diameter d_m. A) Uniformity factor; B) Average drop in diameter in μ.
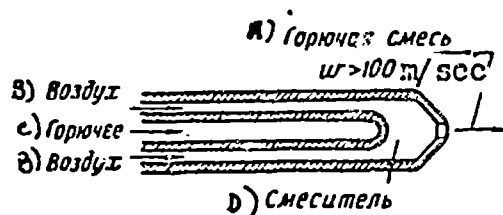
Fig. 131. Schematic of pneumatic injector. A) Fuel mixture; B) Air; C) Fuel; D) Mixer.

Apart from direct-spray and centrifugal injectors, there exist also pneumatic injectors in which the fuel atomization occurs during the interaction of the fuel and air streams. Air and fuel blend in the mixing chamber and discharge through the same nozzle where the velocity of the mixture increases to more than 100 m/sec. (Figure 131).

Pneumatic dispersion was investigated by Nukiyama and Tanasawa[1] who suggest the following formulae for the calculation of Sutter's diameter d_S and the dispersion spectrum:

$$d_c = \frac{586}{w}\sqrt{\frac{\sigma}{P_r}} + 597\left(\frac{\eta_r}{\sqrt{\sigma P_r}}\right)^{0.45}\left(\frac{1000 V_r}{V_s}\right)^{1.5};\qquad (7.38)$$

$$\frac{d\varkappa}{d\left(\frac{d}{d_m}\right)} = 286\left(\frac{d}{d_c}\right)^5 e^{-5.7\left(\frac{d}{d_m}\right)},\qquad (7.39)$$

d_m and d_0 are the median diameter and average Sutter diameter in microns;

w is the fuel velocity at the injector outlet in relation to the air in m/sec;

σ is the surface tension in dyne/cm (from 19 to 73);

η_g is the viscosity of the fuel (from 0.003 to 0.5 poise);

P_g is the density of the fuel (from 0.7 to 1.2 gm/cm^3);

[1]Tanasawa, Y. On the Combustion Rate of a Group of Fuel Particles Injected through a Swirled Nozzle, T. R. Tohk, Univ., v. 18, 1954.

V_V and V_g are the volumetric flow rates of air and fuel which pass through the injector.

According to the formula (7.39) one may determine the relative distribution of the drops in a given measured group provided that it is narrow. For example, the relative distribution of drops with a size from d_1 to d_2 is equal to

$$\frac{G_{d_1-d_2}}{G} = 286 \left(\frac{d_{cp}}{d_c}\right)^5 e^{-5.7\left(\frac{d_{cp}}{d_c}\right)} \frac{d_2 - d_1}{d_c},$$

where d_{sr} is the average diameter for a given group:

$$d_{cp} = \frac{d_1 + d_2}{2}.$$

If $\dfrac{V_V}{V_g} > 5,000$, then the second term in the formula (7.38) becomes negligibly small.

A detailed experimental investigation of atomization by the solidification method was introduced by N. N. Strulevich. The processing we did of his results showed that the formulae of a primary dispersion, suggested by Blokh and Kichkina, Longwell, and other authors, expressed the results of the experiments with an exactness inadequate for practical computations.

The experiments on atomization of Strulevich, Giffen and Murashev, Garner and Henney, and others may be best expressed by the empirical formulae shown below.

The ratio of the average drop diameter to the injector nozzle diameter is directly proportional to the product of the sum of certain functions of the surface tension and of the viscosity of the fuel and the flow rate of the injector, and are indirectly proportional to a certain function of the dynamic head during the motion of the drops in the air:

$$\frac{d_m}{d_c} = \frac{\left(\frac{\sigma}{\sigma_0}\right)^n + \left(\frac{\nu_f}{\nu_0}\right)^m}{A M^{0.817} \sqrt[3]{\frac{p_a}{760}}} \mu_\phi, \tag{7.40}$$

where $\sigma_0 = 24$ dyne/cm and $\nu_0 = 2.0$ centistokes is the surface tension and kinematic viscosity of kerosene at 20° C;

σ and ν_g are the surface tension and viscosity of an atomized fuel;

M is the Mach number of the movement of the drops in relation to the air;

p_v is the air pressure in mm of mercury;

n, m, and A are the dimensionless values which are determined experimentally.

From the data of Strulevich and Giffen one may find:

$$n=0.77; \quad m=0.44; \quad A=41.5.$$

The number of drops, the diameter of which is less than d, is expressed approximately by the distribution formula

$$z = 1 - e^{-0.695\left(\frac{d}{d_m}\right)^{2.5}}.$$

The results of the calculations are compared with the experimental data of Strulevich in Figure 119, a and b. The results of the calculations are compared with the data of Giffen in Table 7.3.

Table 7.3

DEPENDENCE OF THE MEDIAN DROP DIAMETER ON THE PHYSICAL PARAMETERS OF A FUEL.   CENTRIFUGAL INJECTOR WITH $d_c = 1$ mm

AND $\mu_c = 0.22^*$

	Kerosene		Lubricating Oil		Water	
σ dyne/cm	23.4		32		73	
ν centistokes	1.8		32		1.01	
ρ gr/cm^3	0.77		0.86		1.0	
w m/sec	15.2	24.4	15.2	24.4	15.2	24.4
$(d_m)_{rasch}$ microns	123	80.5	296	192	192	126
$(d_m)_{rasch}$ microns	121	90	301	193	193	126

*The discharge coefficient of the injector, used in Giffen's experiments, is not known. We assumed that for a usual centrifugal injector $\mu_f = 0.22$.

SECTION 8.   THE EVAPORATION OF AN ATOMIZED FUEL

Drops of a fuel, moving in the air, evaporate. The investigation of the problem of the evaporation of moving drops represents a highly complicated task, since during this process the diameter of the drops, their temperature, relative velocity of motion, the saturated vapor tension (pressure), heat transfer coefficient, and even the temperature difference between the surface of the drops and the surrounding air change simultaneously. Attempts to express the drop evaporation rate as a function of its initial temperature, of its discharge velocity, and of the parameters of the surrounding flow in the form of a closed system of equations have not been successful up to the present time. The solving of this task is usually accomplished by a method

of numerical integration.

The evaporation speed of a drop is determined by the speed of the diffusion of the vapors that form on its surface into the surrounding air, and by the speed of the heat transfer from the surrounding air to the drop (Figure 132).

The flow of a diffused substance, considering the convection transfer, is expressed by Fik's equation:

$$q_m = -D_p \, \text{grad} \, p + w \frac{p_n}{RT_a}. \tag{7.41}$$

Here q_m is the flow rate of a substance diffused through a unit of surface for a unit of time, in kg/sec. m^2;

D_p is the diffusion coefficient relative to the pressure gradient in m/sec;

w is the velocity of the vapors which leave the surface of the drop in m/sec;

p_p is the pressure of the saturated vapor at the surface temperature of the drop in kg/m^2 (Figure 133);

T_p is the temperature of the vapor on the drop's surface;

grad p is the pressure gradient in the boundary layer of the drop in kg/m^3.

A) Граница температурного градиента
B) Граница проникновения паров
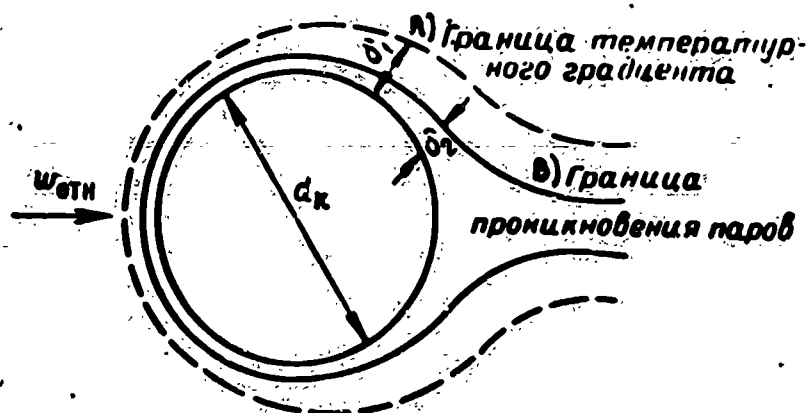
Legend:

A) Limit of the temperature gradient
B) Penetration limit of the vapors

Fig. 132. Schematic of the evaporation and cooling of a drop.

The "minus" sign shows that the flow direction of a substance is in the direction of decreased pressure.

During the evaporation of a drop, the transport of the vapors that are formed is accomplished by two different processes: by their own diffusion, i.e., by the movement of the molecules of the evaporating substance between the molecules of the surrounding air; and by the convection transport of the vapors which depart from the drop with a speed of w.

For a low diffusion velocity $D_p \to 0$:

$$q_m = w \gamma_m = \frac{A}{RT_a} w.$$

For a low convection velocity $w \to 0$:

$$q_m = -D_p \operatorname{grad} p.$$

The diffusion coefficients may be calculated on the basis of molecular-kinetic considerations or may be determined by an experimental method.

The diffusion coefficient of a given substance in the air, D_p, depends upon the temperature and upon the pressure:

$$D_p = D_{po} \frac{760}{p} \left(\frac{T}{273} \right)^a. \qquad (7.42)$$

where D_{po} is the diffusion coefficient when $p = 760$ mm. of mercury and $T = 273°$. For benzine $D_{po} = 2.42 \cdot 10^{-9}$ m/sec; for kerosene $D_{po} = 3.11 \cdot 10^{-9}$ m/sec.

With an increase of pressure the diffusion coefficient diminishes, and with an increase of temperature it increases.

The indicator a lies within the following limits

$$0.75 \leqslant a < 1.$$

Generally speaking, the surface temperature of a drop is not equal to the temperature of the surrounding air. Therefore, evaporation is accompanied by a heat exchange: the temperature of the evaporating drop changes. The speed of the heat exchange, or thermal flow q_t, in the absence of radiation, is determined by Fourier equation:

$$q_t = -\lambda \operatorname{grad} T + q_m c_n \Delta T_p. \qquad (7.43)$$

where λ is the heat conductivity of the gases that surround the drop, in kcal/m sec degree;

gradient T is the temperature gradient in the boundary layer of the drop in degrees/m;

c_p is the specific heat of the vapor at constant pressure in kcal/kg, degrees;

ΔT_p is the temperature increase of the vapor in the boundary layer of the drop.

The "minus" sign indicates that the heat flow is in the direction of the lower temperature.

Heat transmission is carried out by means of various processes: by means of a heat transfer due to flow of a substance, and by means of heat transmission owing to
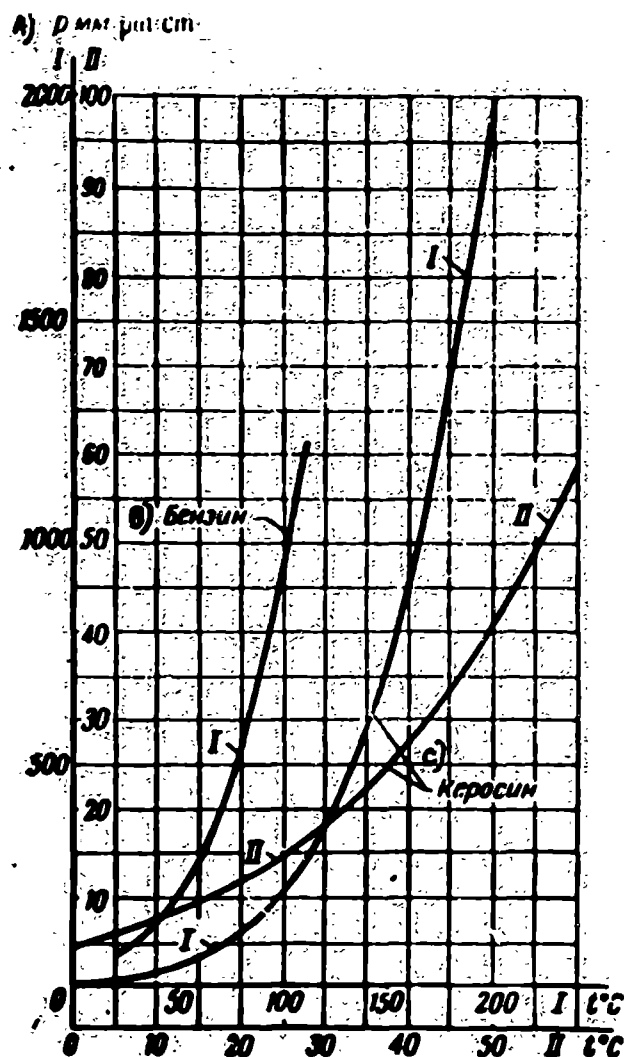
Fig. 133. The saturated vapor pressure of benzine and kerosene at various temperatures molecular collisions.

If the heat conductivity is low ($\lambda \to 0$), then the heat transmission will be carried out only by convection:

$$q_r = q_m c_m \Delta T_r$$

If the temperature increase of the vapor is insignificant $\Delta T_p \to 0$, then

$$q_r = -\lambda \operatorname{grad} T.$$

The temperature gradients and concentrations at various points of the boundary layer of a drop are not alike. The determination of the true value of the gradients T and p, at various distances from the surface of a drop which is evaporating in an air stream, represents a very difficult task which has not been successfully solved in a basic form up to the present time.

To obtain the numerical results the true value of the concentration and temperature gradients are changed to average values:

$$\operatorname{grad} p = \frac{p_n - p_o}{\delta_D}; \quad \operatorname{grad} T = \frac{T_c - T_t}{\delta_t}. \tag{7.44}$$

Here p_p is the pressure of the vapor on the drop's surface, equal to saturation

pressure at a temperature of T_k;

p_∞ is the partial pressure of the fuel vapor in the air at a great distance from

the drop;

δ_D is the characteristic depth of the layer in which a noticeable change of the

partial pressure of the vapor occurs;

T_k is the temperature of the drop's surface;

T_v is the air temperature;

δ_T is the depth of the layer, in which the temperature change occurs.

According to a proposal of D. A. Frank-Kamenetskiy, the area of gas around a

drop, in which a change in the concentrations of the vapors and temperatures occurs,

is called the _associated film_.

The thickness of the associated film is determined experimentally from the value

of the heat or mass transfer.

In the theory of heat transfer and diffusion the transfer of heat and substance

is characterized by the generalized coefficients called _Nusselt's numbers_ and indi-

cated by the symbols Nu_T and Nu_D.

An attempt to find Nusselt's number theoretically for an evaporating drop,

by analysis of the processes that occur in the boundary layer of a drop, was made

in 1947 by the Academician L. S. Leybenzon.

The dependence of Nusselt's number upon the physical parameters and relative

velocity of the flow is usually determined by means of a generalized large quantity

of experimental data.[1] For this Nusselt's number is expressed by Reynold's number.

[1] J. Longwell, Szhiganiye Zhidkikh Topliv _/Combustion of Liquid Fuels/_ from the book "Combustion Processes," New York, 1956.

N. P. Tverskaya, Ispareniye Padayushchey Kapli _/The Evaporation of a Falling Drop/_, Transactions of LGU _/Leningrad State University/_, physics series, 1949, issue 7.

V. A. Fedoseyev and D. I. Polishchuk, Ispareniye Kapel' Vody _/The Evaporation of Water Drops/_ ZhTF _/Journal of Technical Physics -- a periodical/_, vol XXIII, issue 2, 1953.

The thermal criterion of Nu_T is expressed by Vyrubov's formula when $Re > 200$:

$$Nu_T = 2 + 0.16 \sqrt[3]{Re^2}.$$

(7.45)

When $Re < 200$ the criterion Nu_T is expressed by Sokol'skiy's formula:

$$Nu_T = 0.54 \sqrt{Re}.$$

(7.46)

When $Re = 200$, the criteria Nu_T, determined by Vyrubov's and Sokol'skiy's formulae, coincide: $Nu_T = 0.54 \sqrt{200} = 2 + 0.16 \cdot 200^{2/3} = 7.6$.

The Reynold's number for a drop, which is moving in the air at a relative velocity of w, will be

$$Re = \frac{w d_k}{v} = \frac{w d_k \gamma}{g \eta} = \frac{w d_k p}{g R T \eta},$$

(7.47)

where η is the viscosity of the air in kg sec/m^2.

If the thermal criterion Nu_T is known, it is possible to determine the heat transfer coefficient

$$\alpha_T = \frac{Nu_T \lambda}{d_k}.$$

(7.48)

where d_k is the drop diameter;

λ is the average heat conductivity factor of a mixture of the vapors of fuel with air.

The flow of heat, i.e., the amount of heat, which is transferred in a unit of time per unit of surface is:

$$q_T = \alpha_T (T_k - T_0) = \lambda \frac{T_k - T_0}{b_T} = \frac{Nu_T \lambda}{d_k}(T_k - T_0).$$

(7.49)

From this

$$b_T = \frac{d_k}{Nu_T}.$$

(7.50)

In this way, the thickness of the associated film is less, the greater the criterion Nu_T, i.e. the quicker the thermal transfer takes place.

The last equation may be considered for the determination of the thickness of the associated film.

During evaporation in still air $w = 0$; $Re = 0$; according to Sokol'skiy's formula $Nu_T = 2$ and $\frac{b_T}{d_k} = \frac{1}{Nu} = \frac{1}{2}$ -- the thickness of the associated film is equal to the radius of the drop. At limiting velocity (before the breakup of the drop) $w_{pred} = \sqrt{\frac{D g \sigma}{\gamma_v d}}$ in accordance with (7.24).

$$Re_{cpea} = \frac{w_{cpea} d_{To}}{g \tau_o} = \sqrt{\frac{D_3 d_x T_o}{g \tau_o}}. \qquad (7.51)$$

Nusselt's number Nu and the transfer factor for drops flying in the air also may not exceed the limiting values:

$$Nu_{cpea} = 0,54 \sqrt{Re_{cpea}} = 0,54 \sqrt[4]{\frac{D_3 d_x T_o}{g \tau_o^2}} < 10,$$

$$a_{cpea} = \frac{Nu_{cpea} \lambda}{d_x}, \qquad \delta_{cpea} = \frac{d_{x, cpea}}{Nu_{cpea}}.$$

With an increase of drop diameter, the relative thickness of the associated film decreases. When $T_y = 288^\circ$ K and d = 200 μ, $\frac{\delta}{d} = 0.1$. In this way, the relative thickness of the associated film for various sized drops which are moving at various velocities, lies within the limits: $0.1 < \frac{\delta}{d} < 0.5$.

If the effect of the convection of the flow is not taken into account during diffusion and heat transfer, then the processes of mass and heat transfer will be similar to one another. During an increase of the relative velocity, w, Reynold's number -- Re and Nusselt's numbers for heat transfer and diffusion, Nu_T and Nu_D, will grow.

If Nu_D is known, it is possible to find the flow rate of the substance by:

$$q_m = \beta (p_a - p_w). \qquad (7.52)$$

The coefficient of mass transfer β is:

$$\beta = \frac{Nu_D D_p}{d_x}, \qquad (7.53)$$

D_p is the diffusion coefficient, which is relative to the pressure gradient;
d_k is the drop diameter.

The drop obtains a portion of the heat that is required for evaporation from the surrounding gases and a portion from the substance from which it is composed. The thermal balance of the drop is composed of the following quantities.

The heat, which is required for the evaporation of a mass dm = $q_m$sdt, during a small increase of temperature between the surrounding air and the drops T_v -- T_k is:

$$\Delta Q_m = l dm = l q_m s dt.$$

Here l is the heat of evaporation during a temperature of T_k in kcal/kg;
s is the surface of the drop in m^2: s = πd_k^2.

d_k is the diameter of the drop in m;

dt is the time interval in sec.

The heat, which is released by the mass of the drop, is $\Delta Q_k = c_g \, m dT_k$.
Here m is the mass of the drop in kg;

c_g is the specific heat of the fuel in a liquid phase in kcal/kg deg

dT_k is the temperature change per dt time in degrees.

The amount of heat, that is obtained by the drop from the surrounding gases in
the absence of radiation, is
$$\Delta Q_\tau = \alpha_\tau S (T_s - T_k) dt = q_\tau S dt.$$

according to the law of the conservation of energy
$$\Delta Q_m = \Delta Q_\tau - \Delta Q_k \tag{7.54}$$

or
$$c_r m \, dT_k = q_\tau S dt - l q_m S dt. \tag{7.55}$$

The speed of the temperature change of a drop is
$$\frac{dT_k}{dt} = \frac{S}{c_r m} (q_\tau - l q_m) = \frac{6}{c_r \gamma_k d_k} (q_\tau - l q_m), \tag{7.56}$$

If the temperature of the gases is higher than the temperature of the drop
$T_v > T_k$ and $q_g > l g_m$, the drop will be heated.

During evaporation the diameter of a drop decreases; simultaneously the rela-
tive velocity and the temperature of the drop, the vapor pressure at its surface,
the Re number, the Nu_T and Nu_D numbers, and the mass transfer coefficient β change.

A combined analytical solution of the equations for the diffusion, heat transfer
and movement of the drops, moving in relation to the air is difficult to effect. The
problem of the movement, evaporation, and cooling of the drops which are formed during
the atomization of a stream of fuel is usually solved by means of numerical integration.

Similar calculations show that the higher the initial temperature of the drops
T_k and the corresponding vapor pressure p_p, and also the greater the initial velocity
of the fuel and the lesser the drop diameter — the quicker evaporation occurs and
the quicker the temperature of the drops changes (Figure 134).

The greater the flow velocity, the faster is the drop transported by the ambi-
ent air, and the faster it traverses a given distance. Consequently, with changing
flow velocity, the quantity of vapor, forming at a given distance from the injector,
changes but insignificantly for drops of a given size.

Within a certain time interval, the surface of the drop acquires a temperature r_{av} at which the amount of heat, obtained by the drop from the surrounding gases, becomes equal to the amount of heat that is necessary for evaporation. The drop temperature ceases to change:

$$q_s = lq_m, \quad T_x = \text{const.}$$

The equilibrium temperature at which the quantity of heat which is required for vaporation is equal to the amount of heat that is obtained from the surrounding gas, is called the equilibrium isothermal evaporation temperature.
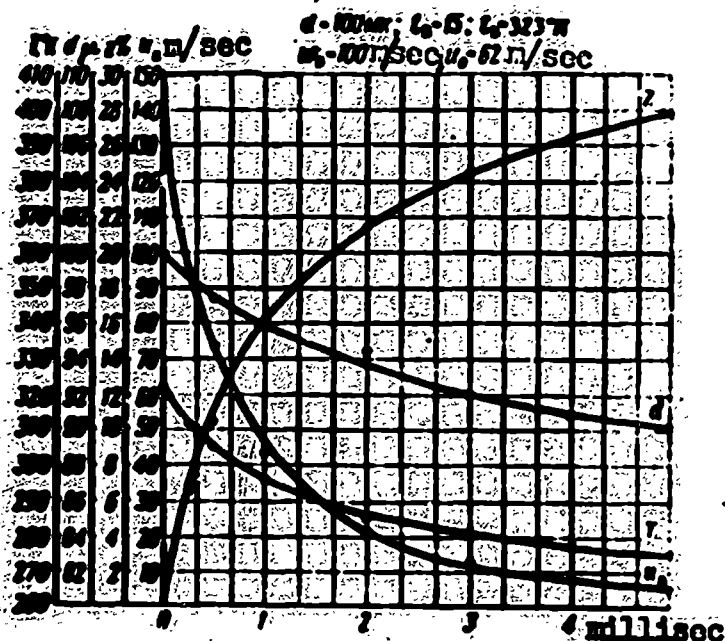
-g. 134. The dependence of the parameters of an evaporating drop upon time.

The lesser the initial diameter of a drop and the greater the saturated fuel vapor pressure, then the quicker evaporation equilibrium sets in.

The temperature equilibrium of a drop T_{rav} was determined by Fuchs in 134. From the thermal balance equation (7.55) when $dT_k = 0$, we obtain

$$q_s = lq_m,$$

$$\frac{Nu \lambda}{d_k}(T_s - T_{pas}) = \frac{Nu_p D_p}{d_k} l(p_{si} - p_\infty).$$

From this, when $p_\infty = 0$ and small differences of $T_v - T_k$:

$$T_s - T_{pas} = \frac{lD_p}{\lambda} \cdot \frac{Nu_p}{Nu_r} \cdot p_{si}. \tag{7.57}$$

The equilibrium temperature is always less than the air temperature. The differnce of $T_v - T_{rav}$ is directly proportional to the product of the heat of evaporation l times the diffusion factor D_p and the saturated vapor pressure, and inversely proportional to the heat conductivity of the mixture of fuel vapors with the air λ.

For the development of the formula for the temperature of equilibrium evaporation, the effect of the convective flow upon the transfer of mass and heat was not taken into consideration. At high air temperatures, a convection flow noticeably increases the transfer of mass and decreases the flow of heat. Therefore, the true temperature of equilibrium evaporation (Figure 135) appears to be substantially less than that which the approximation equation (7.57) gives. To determine the temperature of equilibrium evaporation of kerosene when $T_v < 300^\circ$ C, it is possible to use the equation (7.57) with a sufficient degree of accuracy.

During evaporation in the combustion zone ($T_v \not= 1000^\circ$ C), the temperature of equilibrium evaporation of the drops approaches the boiling point of the liquid without ever reaching it: $T_{rav} < T_{kip}$.
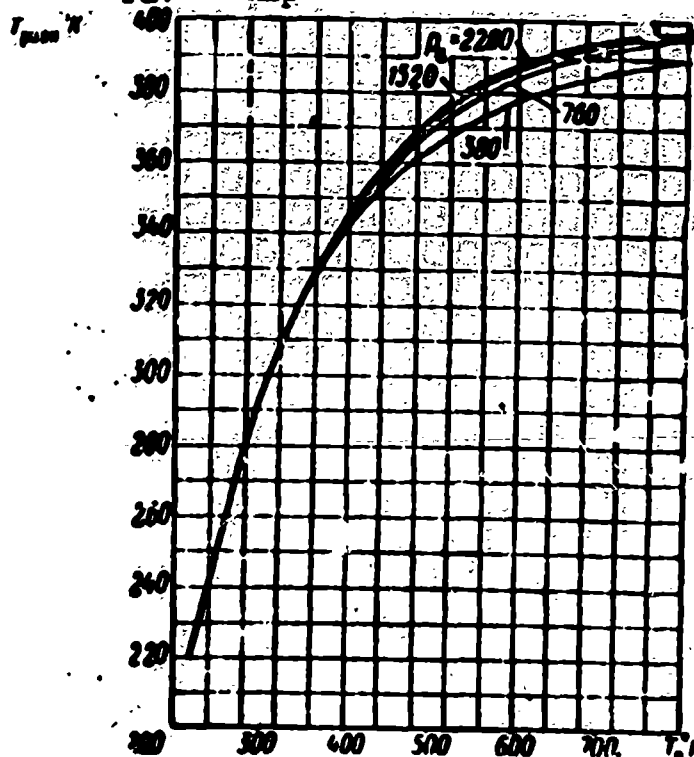
Fig. 135. The computed equilibrium evaporation temperature of a drop of kerosene for various air temperatures and pressures.

Calculations show that the evaporation process of the drops occurs at high relative velocities on the curvilinear portions of the drops' trajectory (see Figure 129) and ends in the combustion zone. The evaporation of the drops at low relative velocities, on those portions of the trajectory which are close to rectilinear, proceeds less intensively.

Example. Find the air temperature at which an evaporating drop of benzine will

maintain the temperature which the fuel had in the tanks: $T_{rav} = 15°$ C, if $r_h = 735$ pm of mercury $= 10,000$ kg/m^2; $\lambda = 0.02$ kcal/hr m degree $= 5.6 \cdot 10^{-6}$ kcal/sec m degree, $D_p = 2.4 \cdot 10^{-9}$ m/sec; $l = 80$ kcal/kg; $\frac{Nu_D}{Nu_T} = 1$.

According to the formula (7.57):

$$T_0 = T_{sm} + \frac{l D_p Nu_D \rho_n}{\lambda Nu_T} = 15 + \frac{80 \cdot 2.4 \cdot 10^{-9} \cdot 1970}{5.6 \cdot 10^{-6}} = 82° C.$$

SECTION 9. THE EFFECT OF THE PARAMETERS OF THE FUEL AND AIR UPON EVAPORATION

An entire series of physical parameters influences the evaporation of atomized fuel. We will consider the effect of each of them separately, considering the remaining values as constants.

The Geometry of the Injector. Centrifugal injectors disperse fuel better than do direct-spray injectors. By a decrease of the outlet injector nozzle diameter and by an increase of the twist, the spray cone thickness diminishes, the fineness of the dispersion is increased and, together with these factors, the evaporation of the drops is improved. The dispersion jet contracts with a decrease of the drops' maximum diameter.

The Fuel Feed Pressure. By an increase of the fuel feed pressure, the relative velocity of the discharging stream increases, the fineness of the dispersion increases, and evaporation is improved. The jet broadens at first and then narrows, since the increase of the speed of the drops is offset by the decrease of the diameter of the largest drops.

Viscosity and Surface Tension of the Fuel. An increase of the fuel's viscosity impairs the twist of the spray, and increases the spray cone thickness. The force which is required for the disintegration of a drop increases. This, along with the increase of surface tension detrimentally affects dispersion. The diameter of the drops increases, the jet widens, and the evaporation rate decreases because of the increase of the average drop diameter. Therefore, the atomization and evaporability of kerosene are inferior to those of benzine.

Fuel Vapor Pressure. With an increase of the volatility of the fuel, i.e.,

with an increase of the vapor pressure, the pressure gradient in the boundary layer of the drop increases; the mass transfer increases and evaporability is improved. Atomized benzine evaporates quicker than kerosene due to its greater vapor pressure.

Heat of Evaporation of the Fuel. With an increase of heat of evaporation, evaporability decreases.

The Temperature of the Fuel has a decided effect upon atomization and evaporability. With an increase of its own temperature, the fuel's viscosity and surface tension diminish; therefore the fineness of the dispersion is increased, the diameter of the larger drops decreases, and the dispersion jet narrows. The vapor pressure and the enthalpy of the fuel grow, while evaporability augments owing both to improved dispersion and to increasing mass flow caused by the growth of pressure gradient.

During the heating of the fuel under pressure in a fuel system to a temperature which exceeds the boiling point in the combustion chamber, the drops, during flight from the injector, boil and evaporate because of their internal energy; evaporability rises sharply. When $T_k - T_{rav} > \frac{1}{c}$, the drops evaporate completely.

The Specific Heat of the Fuel. If the fuel temperature is higher than the equilibrium evaporation temperature, then by an increase of the specific heat, evapor ability is improved because of the increase of the enthalpy of the drops. The growth of the drops' specific heat lowers the evaporability.

The Velocity and Pressure of the Air. With an increase of air velocity, the relative velocity of the drops increases, dispersion is improved, and the dispersion jet contracts. The drift of the drops with the oncoming flow increases. The evaporability of the fuel at a given distance from the injector increases.

The Temperature of the Air. With an increase of air temperature, its viscosity heat conductivity and density are changed. The speed of the heat transfer to the drop grows because of the growth of the temperature gradient and the evaporability increases. An increase of air temperature exerts a substantially lesser influence on evaporability than does the same increase of the fuel temperature.
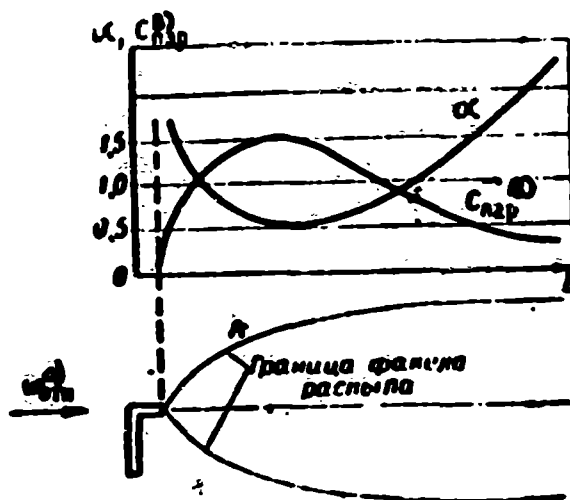
Fig. 136. The variation of the vapor concentration and the excess air coefficient along the axis of the jet. A) Limit of the dispersion jet; B) vapor; C) relative.

The vapor, which is formed during the evaporation of the drops, intermixes with the surrounding air. Therefore, with an increase of the axial distance from the edge of a single injector, the local concentration of the fuel vapor at first grows because of the growth of the evaporability of the drops, and later begins to diminish because of the turbulent intermixing of the fuel with the air.

Experience shows that the total vapor concentration and the drop-liquid fuel concentration diminishes in inverse proportion to the distance from the injector (Figure 136), and that consequently, the excess air coefficient grows in direct proportion to the distance from the injector.

That portion of the jet where the concentration of vapor has a value that is most favorable for combustion, is the most suitable for the location of ignition units and stabilizers.

The concentrations become similar along the entire combustion chamber at a sufficient distance from the injector due to turbulent intermixing. The concentration profiles may be calculated theoretically and investigated by an experimental method.

SECTION 10. THE EXPERIMENTAL DETERMINATION OF LOCAL FUEL CONCENTRATIONS

To measure the total concentration of the liquid and vapor phases of a fuel, a sample is taken by means of a tube, the plane of the inlet opening of which is situated perpendicular to the stream lines (Figure 137). The speed of sampling must be

equal to the velocity of an undisturbed flow or else the ratio between the quantity of the air drawn in and the general mass of the drops entrained will be upset. If the velocity of the sample drawn-off is less than the velocity of the flow, the air stream lines at the inlet of the intake tube will diverge. A portion of the air will flow into the tube along the walls, but the drops of the fuel, which are driven almost rectilinearly by their inertia, will fall into the tube. In this way, if the speed of the sampling operation is less than the velocity of the flow, almost all the drops from the stream tube will enter the sampling probe, (the cross-section of the former being equal to the intake tube inlet) and only a fraction of the air will penetrate from the stream tube. The fuel-air ratio in the drawn-off sample will be greater than in an undisturbed mixture.
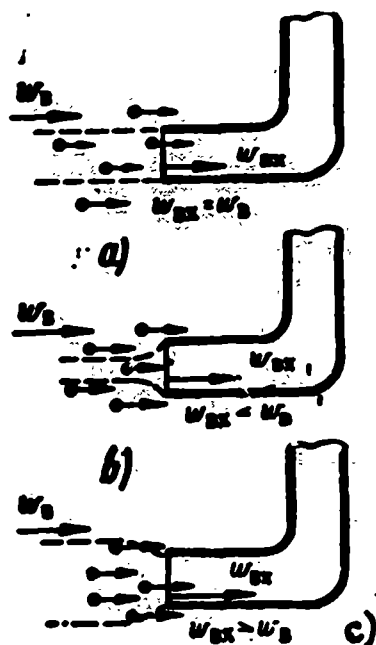
Fig. 137. The selection of a sample of the liquid and vapor phases of a fuel-air mixture.
a) $w_{vkh} = w_v$; b) $w_{vkh} < w_v$; c) $w_{vkh} > w_v$

If the speed of the sample abstraction is greater than the velocity of an undisturbed flow, the relative amount of liquid fuel in the selected sample will be less than in an undisturbed flow since a portion of the drops which are contained in the abstracted portion of air flow around the sample probe (Figure 137c).

The equality of the velocities of sampling and of an undisturbed flow is obtained by throttling the inlet opening of the sampling tube in such a way that the static pressure at the inlet to the sampling tube p_{ots} is equal to the static

pressure of an undisturbed flow:

$$P_{ots} = P_n$$

To sample a mixture of fuel vapor with air which does not contain drops of liquid, the plane of the inlet opening of the sampling tube must be situated parallel to the stream lines (Figure 138, tube b), to protect it from penetration of both the individual drops carried along by the flow and the liquid film which forms on the surface of the tube itself.
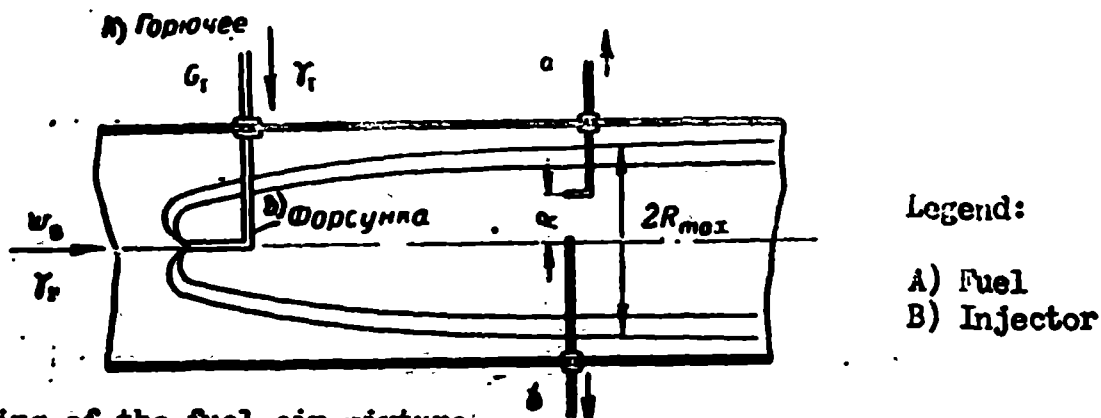
Fig. 138. Sampling of the fuel-air mixture.

Legend:

A) Fuel
B) Injector

To entrap only the liquid (free from vapors) the sampling tube is placed with its inlet opening perpendicular to the flow. The drops, because of their inertia, will penetrate the tube and settle on its walls (Figure 138, tube a). The finest (micron-sized) drops will pass around the tube, moving approximately along the air stream lines. However, the portion of the substance carried along by these drops is not large (see Table 7.1).

It is necessary to take special precautions in order that the liquid settled on the walls of the sampling tube does not spill outside. The volume of liquid which has penetrated the sampling tube is measured by a burette.

The contents of the vapor and liquid phases of the fuel in the sampled portions of the mixture after complete evaporation are determined by a method of gas analysis (by means of an absorption or electric gas analyzer) after having been diluted with a known quantity of air and burned in a catalytic furnace.

Without the investigation of these concentration fields it would be impossible to study the processes which take place in the combustion chambers of jet engines.

On the basis of the foregoing deliberations about the configuration of a jet and about the evaporation of the drops, moving along their ballistic trajectories, one may first of all consider the local concentrations of fuel mixtures which will take place in the separate zones of combustion chambers. Calculations, corroborated by test, show that the concentration zones of fuel in the areas of the stabilizers are not similar. This circumstance presents the possibility of a combustion chamber operating in those cases when the average composition of the mixture lies far below the limits of lean blow out, since the mixture on the sides of the flame-holder is re-enriched by the fuel.

To determine the local concentrations, one is required to carry out the difficult computations of the trajectories of the evaporating drops and their evaporability, and to take into account the mixing of the vapor formed with the surrounding air, and also the mutual overlapping of overlapping jets from neighboring injectors.

As the first approximation for the solution of the problem covering the dispersion of a fuel which is sprayed into an air flow by a single injector, Longwell and Weiss[1] consider the injector as a point source of matter that is diffused into a turbulent flow.

The diffusion equation may be described in the form of

$$q_m = -D_c \frac{\gamma_p \partial \left(\frac{f}{a}\right)}{\partial R},$$ (7.58)

where $\frac{f}{a}$ is the local concentration, or fuel-air ratio, i.e., the ratio of the weight of the fuel to the weight of the air:

$$\frac{f}{a} = \frac{1}{aL}.$$

γ_p is the density of the fuel vapor in kg/m^3;

q_m is the flow rate of the diffused matter in $kg/sec\ m^2$;

D_c is the turbulent diffusion factor, relative to the concentration gradient in m^2/sec.

---

[1] J. Longwell and M. A. Weiss, Ind. Eng. Chem., vol. 45, 1953, 667-676.

The work of Longwell and Weiss presents a solution to the differential equation, recorded above, for a point source of fuel at zero relative velocity:

$$\frac{f}{a} = \frac{1}{al} \cdot \frac{G_r}{\pi w_a \gamma_a} \cdot \frac{w_a}{4D_C x} e^{-\frac{w_a}{4D_C x} \cdot R}$$

(7.59)

x is the distance from the edge of the injector to the section of the combustion chamber in question (Figure 139);

R is the distance from the injector axis to the point A in question in meters;

w_v and γ_v are the velocity and density of the air in m/sec and kg/m^3;

G_g is the fuel consumption in kg/sec.

Legend:

A) Fuel
B) actual concentration
C) concentration according to Longwell's calculation
D) without consideration of mixing
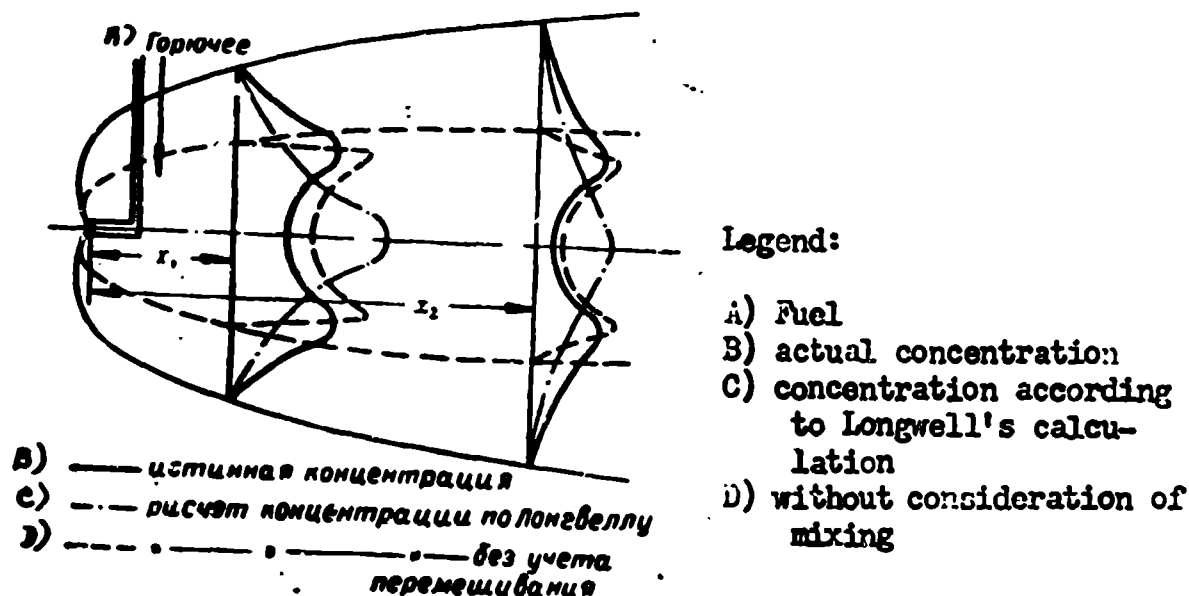
Fig. 139. The effect of turbulent mixing on local concentrations.

The equation (7.59) shows that the axial concentration of the fuel immediately downstream of the injector changes in inverse proportion to the distance from its edge. This conclusion is supported by experiment.

The decrease of the concentration in a radial direction is

$$\frac{f}{a} = \left(\frac{f}{a}\right)_{ax} e^{-\frac{w_a}{4D_C x} \cdot R}$$

[on axis] (7.60)

In passing on from the fuel-air ratio $\frac{f}{a}$ to the excess air coefficent, α, we obtain

$$\alpha = \frac{4\pi \gamma_a D_C x}{L G_r} e^{\frac{w_a R}{4D_C x}}$$

(7.61)

If the distance from the injector nozzle x is greater than the maximum width of the jet, and is calculated without considering turbulent mixing R_{max} (see Figure 138),

and the fuel is dispersed and evaporates well, then the formula (7.60) offers re-

sults which are close to the true concentrations. For small distances or during poor

dispersion, Longwell's formula offers overrated axial concentrations.

Fig. 140. The calculation of local concentrations.
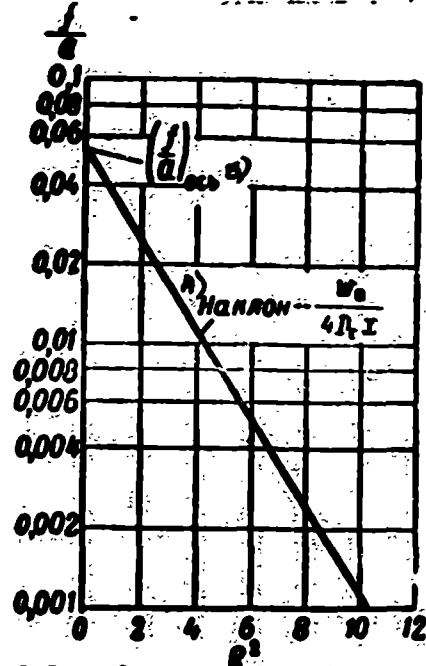
Legend:

A) Inclination
B) axis

The dependence of a calculated concentration upon the radial distance R is de-

picted in Figure 140. The concentrations computed from Longwell's formula are com-

pared in Figure 139 with the experimental values. The "bumps" on the experimental

concentration curves (Figure 139) stipulate that the drops of fuel depart from the

axis of a centrifugal injector and enrich the peripherial areas of the jet. Only the

micron-sized drops and vapors that are formed are pulled into the axial area.

During operation with a pre-heated fuel that is dispersed into hot air, evapora-

tion is completed close to the edge of the injector nozzle. In this case, the con-

centration profile of the fuel at a distance from the injector approaches that which

Longwell's formula gives.

The drawback of Longwell's theory is the circumstance that the value of the

turbulent diffusion factor, which depends on the degree of turbulence, the nature of

the fuel, and the temperature of the flow (and is usually not known beforehand,) is

used as the basis of the calculations.

The concentration zones of a single injector may also be found by using the

theory of a turbulent spray, which was developed by a series of authors and was

generalized by G. N. Abramovich.

The outer boundary of a turbulent spray of vapor or gas, on the average with respect to time, is represented by the surface of a cone, the cone angle of which α_f increases, with increasing intensity of the flow turbulence ε (Figure 141):

$$\sin \frac{\alpha_\varphi}{2} = \frac{w_{turb}}{w_0} = \varepsilon. \tag{7.62}$$

The distance from the axis of the jet to the stream boundary R_{gr} is directly proportional to the distance x from the injector nozzle edge and the intensity of the turbulence ε

$$R_{гр} = x \sin \frac{\alpha_\varphi}{2} = \varepsilon x. \tag{7.63}$$

The concentration along the axis of the jet, which is measured by the fuel-air ratio $\frac{f}{a}$, changes in inverse proportion to the distance x:

$$\left(\frac{f}{a}\right)_{ao} = \frac{1}{\varepsilon \omega L} = \frac{CO_r}{w_0 \varepsilon x}. \tag{7.64}$$

Here C is a constant, determined from experimental data.

g. 141. The change of concentration with distance.
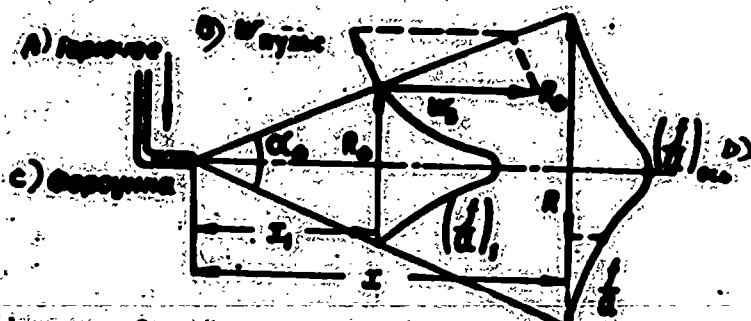
Legend:
A) Fuel
B) Wpulse
C) Injector
D) axis

The drop of the concentrations as a function of the distance from the axis of the jet may be expressed by the "three-halfs" law.

$$\frac{f}{a} = \left(\frac{f}{a}\right)_{ao}\left[1 - \left(\frac{R}{R_{гр}}\right)^{\frac{3}{2}}\right]^2 = \frac{CO_r}{w_0 \varepsilon x}\left[1 - \left(\frac{R}{\varepsilon x}\right)^{\frac{3}{2}}\right]^2.$$

when $R = 0;\ \frac{f}{a} = \left(\frac{f}{a}\right)_{ao};$ when $R = R_{гр}: \frac{f}{a} = 0.$ $$\tag{7.65}$$

After determining the axial concentration $\left(\frac{f}{a}\right)_1$ at a certain distance x_1 from the edge of the injector nozzle, it is possible to compute the concentration at any point of the jet A by

$$\frac{\left(\frac{f}{a}\right)_A}{\frac{f}{a}} = \frac{a}{a_1} = \frac{x}{x_1}\left[\frac{1 - \left(\frac{R_1}{\varepsilon x_1}\right)^{\frac{3}{2}}}{1 - \left(\frac{R}{\varepsilon x}\right)^{\frac{3}{2}}}\right]^2. \tag{7.66}$$

The theory of turbulent sprays offers the possibility to express the local concentrations or air excesses as a function of the distances x and R, the degree of turbulence ε, and only one constant C, which is determined experimentally.

Example: The fuel consumption through a centrifugal injector C = 10 gm/sec. Find the constant C, if during a flow velocity of w_v = 100 m/sec and an air density of γ_v = 1.22 kg/m³, the excess air coefficient α_{oo} = 1 per distance of x_1 = 100 mm from the injector nozzle. Find also the excess air coefficient at a distance of R = 20 mm from the axis in a cross-section located at a distance x - 200 mm from the injector, if the degree of turbulence ε = 15%.

We find the constant C from the formula (7.64):

$$C = \frac{w_v \gamma_v x}{\alpha_{oo} \varepsilon G_r} = \frac{100 \cdot 1.22 \cdot 0.1}{15 \cdot 0.01} = 81 \frac{1}{m}.$$

The excess air coefficient from the formula (7.66):

$$a = \frac{\alpha_1 \frac{x}{x_1}}{\left[1-\left(\frac{R}{\varepsilon x}\right)^{\frac{3}{2}}\right]^2} = \frac{\frac{200}{100}}{\left[1-\left(\frac{20}{30}\right)^{\frac{3}{2}}\right]^2} = \frac{2}{(1-0.545)^2} = 9.7.$$

BIBLIOGRAPHY

1. Abramovich, G. N., Gazovaya dinamika vozdushno-reaktivnikh dvigateley, /The Gas Dynamics of Air Breathing Engines/, "BNT", 1947, 122-134.

2. Abramovich, G. N., Turbulentniye svobodniye strui zhidkostey i gazov, /Turbulent Free Streams of Liquids and Gases/, "Energoizdat", M. -- L., 1948.

3. Blokh, A. G. and Kichkina, Y. S., Sredniy diametr kapel' pri raspylivanii topliva tsentrobezhnymi forsunkami, /The Average Diameter of Drops During the Atomization of a Fuel by a Centrifugal Injector/, "Teploenergetika", 1955, No. 9.

4. Volynskiy, M. S., O droblenii kapel' v potoke vozdukha, /The Dispersion of Drops in an Air Stream/, DAN /Reports of the Academy of Sciences/ of the USSR, 1948, vol LXII, No. 3. Izucheniye drobleniya kapel' v gazovom potoke, /The Study of the Dispersion of Drops in a Gas Flow/, DAN USSR, 1949, No. 2., vol XLVIII.

5. Kigi, V. R. and Ellis, H. H., Primereniye shliren-metoda dlya kolichestvennogo issledovaniya smesheniya gazov v struye /The Use of the Schlieren Method for the Qualitive Investigation of the Mixing of Gases in a Stream/, Voprosy goreniya /Combustion Problems/, collection 2, printed in Foreign Literature Pub. House, 1953.

6. Clair H. and Radcliffe, A., Pnevmaticheskaya forsunka dlya raspylivaniya vyazkikh topliv /A Pneumatic Injector for the Dispersion of Viscous Fuels/, "VRT", 1956, No. 2.

7. Leybenzon, L. S., Ob isparenii kapel' v gazovom potoke /The Evaporation of Drops

in a Gas Flow_7, Publishing House of the Academy of Sciences, USSR, series of geography and geodesy, 1940, vol. 4, issue 3.

8. Levich, V. G., Fiziko-khimicheskaya gidromekhanika /Physico-Chemical Hydromechanics_7, Publishing House of the Academy of Sciences, USSR, 1952.

9. Hanson, N., Banerzhe, S., and Eddy, P., Mikrofotograficheskoye issledovaniye raspylivaniya zhidkikh topliv /Microphotographic Research of the Dispersion of Liquid Fuels_7, "VRT", 1956, No. 4.

10. Kissye, K., Obrabotka eksperimental'nogo issledovaniya raspada struy zhidkosti s pomoshch'yu bezrazmernykh kriteriyev /Processing Experimental Data on the Disintegration of Streams of Liquids with the Aid of Non-dimensional Criteria_7, "VRT", 1956, No. 5.

11. Prandtl, L. Gidromekhanika /Hydromechanics_7, printed in Foreign Literature Pub. House, 1951, 427-433.

12. Sreznevskiy, B., Ob isparenii zhidkostey /The Evaporation of Liquids_7 Journal of the RF-KhO /Russian Society of Physics and Chemistry_7, Physics portion, vol. XIV, 1882, 420-469 and 483-500.

13. Sokol'skiy, A. P., Issledovaniye protsessa goreniya natural'nogo topliva /Research on the Combustion Process of a Natural Fuel_7, "Gosenergoizdat", 1948, 175-184.

14. Tverskaya, N. P., Isparentye padayushchey kapli /The Evaporation of a Falling Drop_7 Transactions of LGU, physics series, 1949, issue 7.

15. Fedoseyev, V. A. and Polishchuk, D. I., Isparentye kapel'vody /The Evaporation of a Water Drop_7, ZhTF, vol XXIII, issue 2, 1953.

16. Frank-Kamenetskiy, D. A., Teploprovodonost' i diffuziya v khimicheskoy kinetike /Heat Conductivity and Diffusion in Chemical Kinetics_7, Printing House of the Academy of Sciences, USSR, 1947.

17. Fuchs, N. O., O skorostyakh isparentya kapelek v atmosfere gaza /The Evaporation Velocities of Drops in a Gaseous Atmosphere_7, ZhTF /Journal of Experimental and Theoretical Physics_7, vol. 4, issue 7, 1934, 747-759.

18. Giffen, E.,"Atomization of Fuel Sprays," Eng., 4 -- VII, vol. 174, 1952, No. 4510.

19. Stefan, Wien -- Ber., 1873, 68, 385, 1881, 83, 913.

20. Longwell, J. and Weiss, M. A., Ind. Eng. Chem., 1953, vol. 45, 667-676.

21. Longwell, J., Szhiganiye zhidkikh topliv /Combustion of Liquid Fuels_7 from the book "Combustion Processes," New York, 1956.

22. Tanasawa, Y., On the Combustion Rate of a Group of Fuel Particles, Injected through a Swirled Nozzle TR. Tohk. Univ., v. 18, 1954.

23. Garner, F. H. and Henney, V. E., "Behavior of Sprays under High Altitude Conditions," Fuel, vol. 32, 1953.

24. Penner, S. S., "On Maximum Evaporation Rates for Liquid Droplets in a Rocket Motor," J. Am. Rocket Soc., vol. 23, III-IV, 1953.

25. Maxwell, C., Scient. Papers, 1890, 11, 63

COMBUSTION CHAMBERS OF RAMJET ENGINES

Contemporary data about fuels, about the processes of carburation, and about combustion in a high-speed flow present not only the possibility to understand, but also to evaluate numerically the phenomena that occur in the combustion chambers of ramjet engines, by carrying out gas dynamic and thermo-physical calculations.
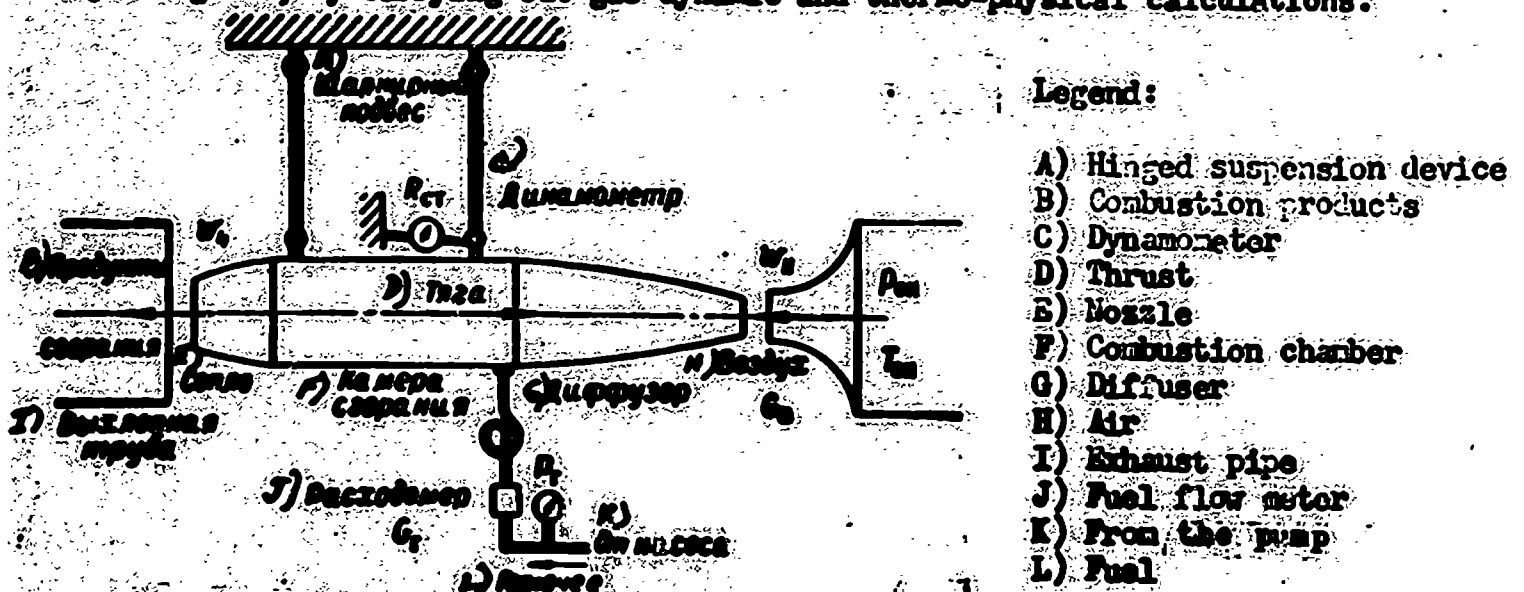
Fig. 142. A ramjet engine on a test stand.

Legend:

A) Hinged suspension device
B) Combustion products
C) Dynamometer
D) Thrust
E) Nozzle
F) Combustion chamber
G) Diffuser
H) Air
I) Exhaust pipe
J) Fuel flow meter
K) From the pump
L) Fuel

The chambers, which are designed and constructed on the basis of theoretical ideas and calculations, are tested and refined on special test stands (Figure 142).

To test large-scale combustion chambers, which require hundreds of kilograms of air and tens of kilograms of fuel per second, powerful and expensive test stands are required (Figure 143). The power of the compressors, which supply the air that is required for the operation of the combustion chamber, reaches hundreds of thousands of kilowatts.
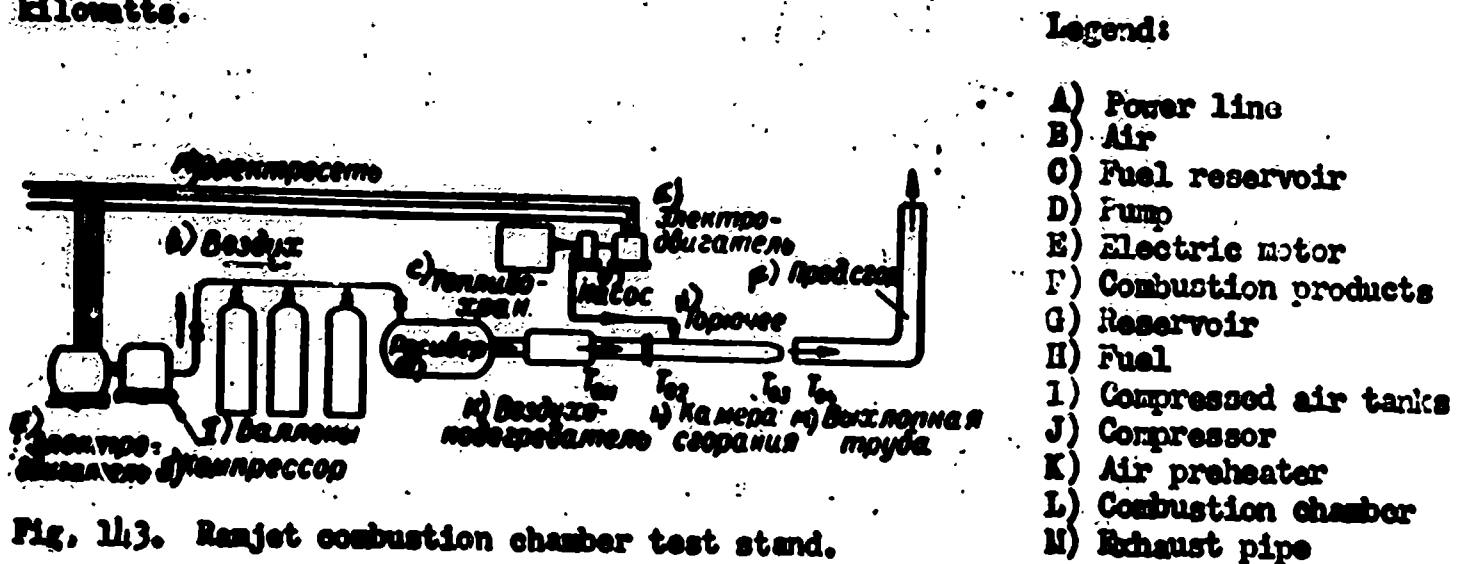
Fig. 143. Ramjet combustion chamber test stand.

Legend:

A) Power line
B) Air
C) Fuel reservoir
D) Pump
E) Electric motor
F) Combustion products
G) Reservoir
H) Fuel
I) Compressed air tanks
J) Compressor
K) Air preheater
L) Combustion chamber
M) Exhaust pipe

SECTION 1. THE CLASSIFICATION OF COMBUSTION CHAMBERS

A standard classification of combustion chambers does not exist.

Depending upon the velocity of the flow which enters the engine, ramjet combustion chambers may be divided into subsonic ramjet engine combustion chambers and supersonic ramjet engine combustion chambers. From the standpoint of gas dynamics, supersonic combustion chambers differ from subsonic ones in that the air flow rate through the combustion chamber of a supersonic ramjet engine is limited by the condition of $\varphi = 1$, which, within a wide range of fuel mixtures, remains constant. A temperature variation of the combustion products does not effect the air consumption in a supersonic combustion chamber. The air flow rate in a subsonic combustion chamber depends on the temperature. The stagnation temperature of the flow at the inlet to a supersonic ramjet engine combustion chamber is higher than that of a subsonic chamber. This circumstance makes unnecessary special installations for pre-heating the fuel.

The combustion chambers of subsonic and supersonic ramjet engines may be divided into single-regime, which are intended for operation within a narrow range of fuel mixtures, velocities, air pressures, and fuel flow rates; and into multiple-regime, which are intended for operation over a wide range of velocities and flight altitudes, and consequently, over a wide range of velocities and flow pressures in the combustion chamber, fuel mixtures, and fuel flow rates.

Combustion chambers may be divided into single-stage (Figure 144) and two-stage (Figure 145) according to the organization of their combustion processes. The fuel in single-stage combustion chambers is fed into the entire air flow. These combustion chambers are more suitable for operation on rich mixtures: $\alpha \gg 1$. In two-stage combustion chambers, the air is divided into primary and secondary flows, as in the combustion chambers of gas turbine engines. Fuel is introduced into the primary flow, combustion occurs at the most suitable composition of the mixture, close to stoichiometric. Later the combustion products are mixed with fresh air, with the idea of lowering their temperature to the required value. Two-stage combustion

chambers are intended for operation on lean mixtures: $\alpha > 2$. Single-stage and two-stage combustion chambers may be of the vortex type (as gas turbine engines have) or

Legend:

A) Fuel
B) Air
C) Precombustion chamber
D) Combustion zone
E) Flame-holder
F) Injectors
G) Carburation zone
H) Additional burner
I) Afterburner
J) Injector
K) Flame-holder
L) Thermocouples
M) Supply pipe
N) Collector
O) Hinged bracing
P) Stabilizing cone
Q) Bullet
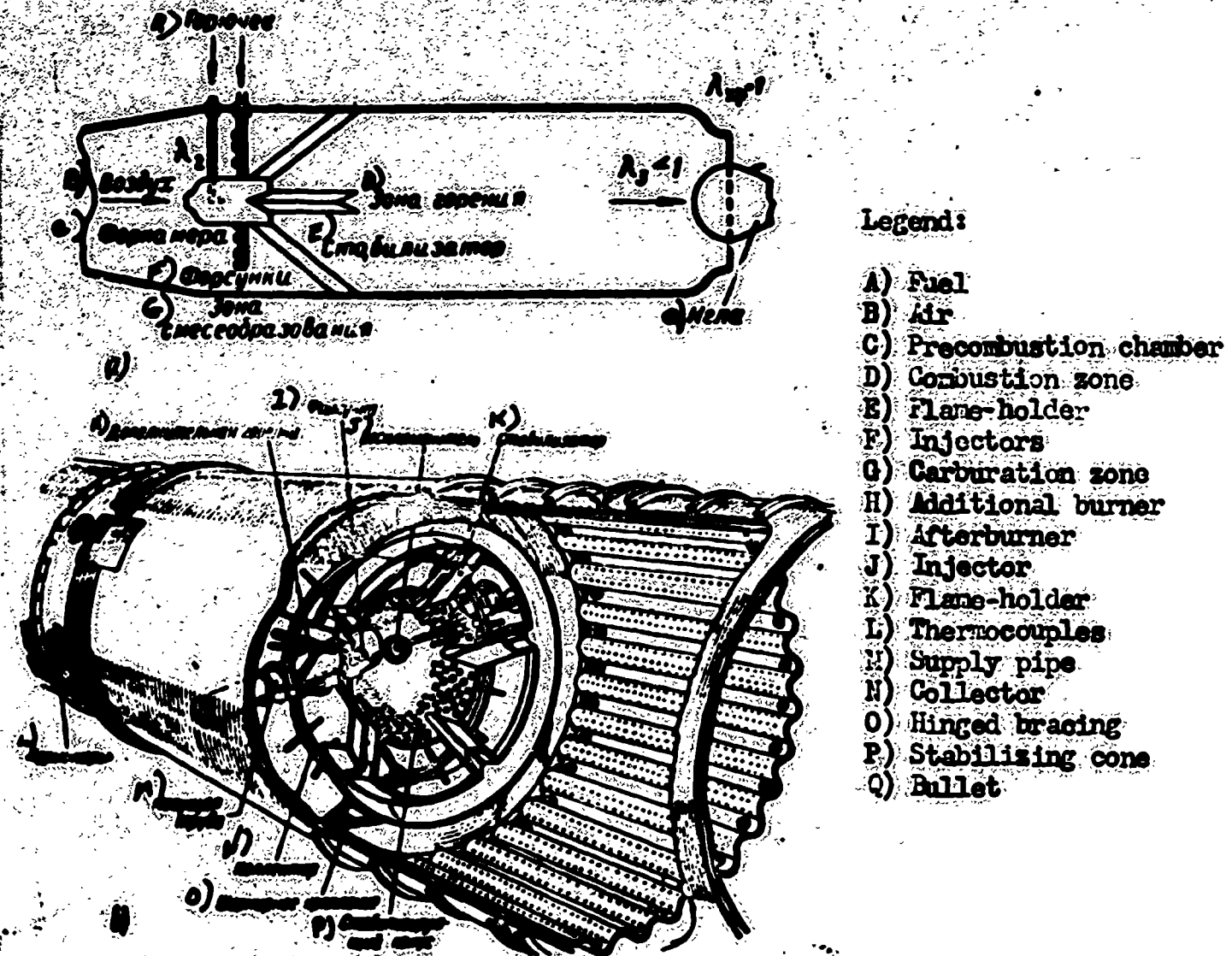
Fig. 144. A single-stage combustion chamber.
a — schematic, b — perspective cut-away view.

a stabilizing type. Vortex combustion chambers may be used only in those cases where their diameter is not too great (not more than 300-400 mm). The utilization, as flame-holders, of impinging jets, ceramic wedges, and radioactive combustion activators is also possible.

Legend:

A) Primary stage
B) Fuel
C) Secondary stage
D) Combustion and mixing zone
E) Injectors
F) Flame-holders
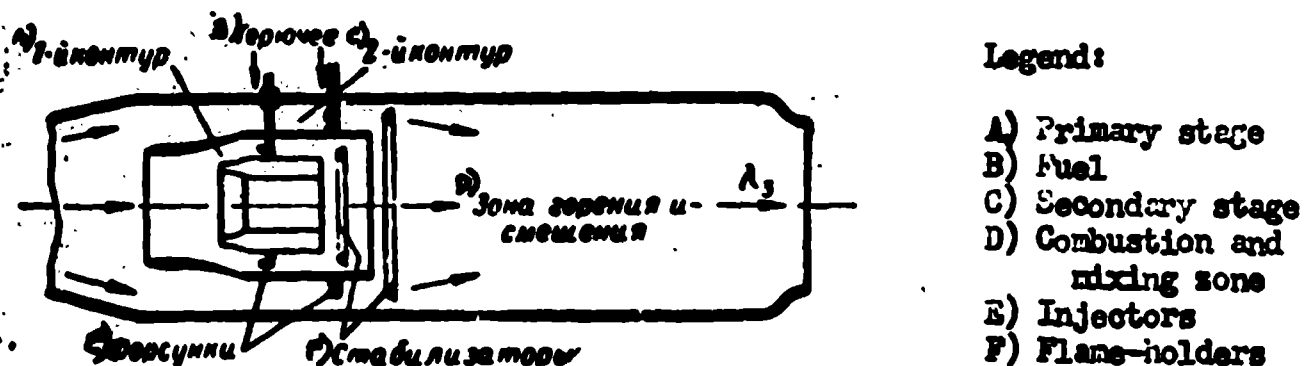
Fig. 145. A diagram of a supersonic two-stage combustion chamber.

Spark ignition, ignition by an incandescent wire, and pyrotechnic ignition are possible means of igniting the fuel mixture. At very high supersonic velocities, when the stagnation temperature of the flow is greater than the ignition temperature: $T_{Ox} > T_{vsp}$, ignition is possible by compression (Figure 146).[1]
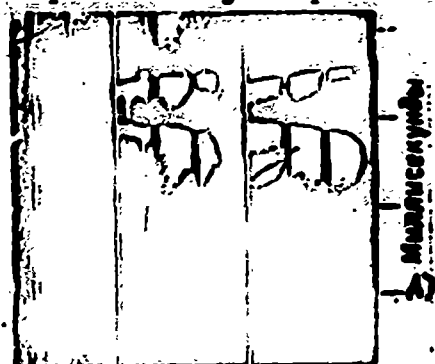
Legend:

A) Milliseconds

Fig. 146. The combustion of a mixture prepared beforehand in a shock wave.

Spray, swirl, and pneumatic injectors are used to feed the fuel into the combustion chamber. Evaporative fuel feed, in which the fuel before being introduced into the combustion chamber is evaporated in a special vaporizer and the forming vapors are mixed with the air, is another possibility.

Combustion chambers are designated either as combustion chambers with gradual mixing or as combustion chambers with instantaneous mixing in accordance with the particular method of mixing the fuel and the combustion products with the air. Theoretical calculations show that in the case of instantaneous mixing when combustion terminates at a distance which is equal to the thickness of the turbulent flame front, a considerable decrease in engine weight may be obtained.[2]

SECTION 2. STABILIZING ELEMENTS OF A COMBUSTION CHAMBER

A stabilized combustion chamber (see Figures 144 and 145) includes the following elements: 1) an installation for the introduction and atomization of the fuel; 2) ignition units; 3) turbulence rings (turbulizers); 4) flame-holders; 5) mixers.

_____

[1] Sheferd, U. F., Vosplameneniye gazovykh smesey impul'sami davleniya /The Ignition of Gas Mixtures by Pressure Impulses/, Collection Voprosy goreniya /Combustion Problems/, Part 2, printed in Foreign Literature Pub. House, 1953.

[2] Avery, W. H. and Hard, R. W., "Combustor Performance with Instantaneous Mixing," Ind. and Eng. Chem., vol. 45, VIII, 1955, 1634-1637.

The design of the individual elements depends upon the purpose and upon the dimensions of the combustion chamber.

The apparatus for the injection and atomization of the fuel consists of centrifugal or direct-spray injectors. Small-diameter combustion chambers are supplied with one injector; large combustion chambers -- many injectors. Injectors are selected so that, over the entire operating range of the combustion chamber, the local concentration of the mixture remains within the limits of combustion in the areas of the flame-holders. The local concentration of the mixture is usually greater than the average concentration.

The injectors must be so situated in relation to the air flow as to insure the best dispersion, evaporation, and mixing of the fuel with the air. In order to increase the stay time of the drops in the space in front of the flame-holder, it is advantageous to install them facing the stream. At very high flow velocities, the differences in atomization as produced by centrifugal and direct-spray injectors will cease to be noticeable. To increase the vaporization and mixing of the fuel with the air, it is advantageous to locate the injectors in the high-velocity areas.

Legend:

A) Precombustion chamber
B) Flame-holder

A) Форкамера Б) Стабилизатор
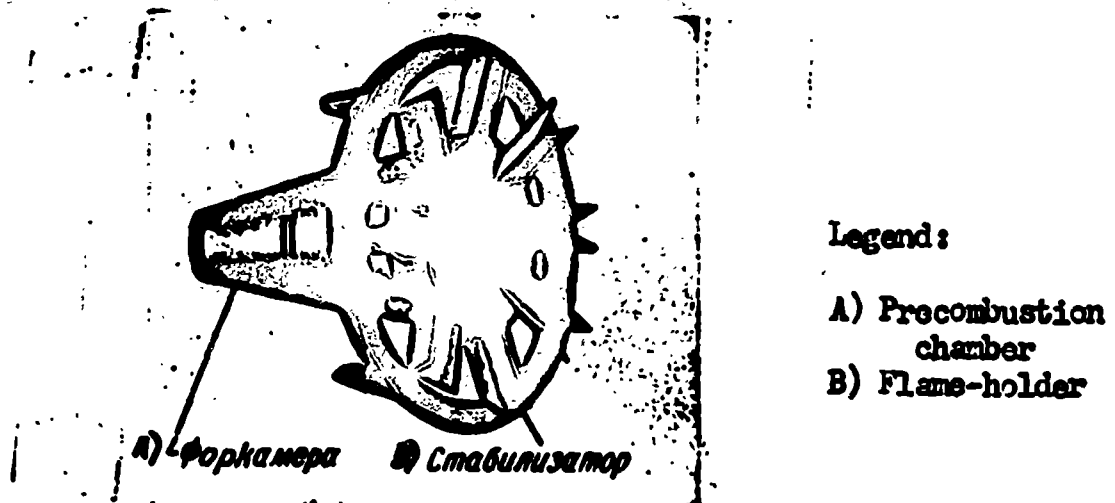
Fig. 147. An external view of a pre-combustion chamber with a ring-shaped flame-holder.

The space between the injectors and the combustion zone behind the flame-holders is called the carburation zone.

Vaporization and mixing in the carburation zone usually do not end; therefore, a mixture, non-homogeneous in composition and containing a significant percentage of fuel in drop-liquid form, penetrates into the combustion zone behind the flame-holders. A

heterogeneous combustion of a two-phase mixture, i.e., the combustion of a mixture which contains both the vapors and drops of a fuel, takes place in the combustion chambers of ramjet engines.

The ignition units of a combustion chamber are usually electric spark plug igniters. To facilitate the ignition system, and to increase the reliability of starting the combustion chambers of ramjet engines, the chambers may be supplied with a pyrotechnic cartridge with an electric squib, similar to those in the combustion chambers of liquid fuel rocket engines of the V-2 type.

To facilitate the starting and stabilization of the combustion process, the combustion chambers are usually equipped with a pilot light or preliminary combustion chambers -- precombustion chambers and flame-holders (Figure 147).

The preliminary combustion chamber maintains a powerful, constantly operative jet of flame, which ignites the basic mixture. The precombustion chamber is located at the beginning of the main combustion chamber (see Figure 144b). The inlet cross section of the precombustion chamber has a small relative value so that the velocity of the flow through the precombustion chamber is sufficiently low so that the ignition and combustion of the mixture is reliable. One centrifugal injector, which gives fine atomization during low relative flow velocities, is usually located in the preliminary combustion chamber. The ignition spark plug is located in the same area of the precombustion chamber, where there is a sufficient concentration of fuel vapor. The tongue of flame, which extends from the precombustion chamber, must reach the turbulent zone that is formed behind the flame-holders.

The flame-holders are usually manufactured from steel channels and are placed in the form of rays, concentric rings, or transverse grates (see Figure 144b and 147). The use of ceramic, quartz, and catalytic flame-holders is possible.

The outside walls and the nozzles of supersonic combustion chambers are usually cooled by air.

During the manufacture of the elements of combustion chambers care should be taken to assure that the chamber cross-section should not be overloaded, i.e., that

the drag coefficient ζ should not be excessively high. An increase in ζ increases the combustion efficiency η_{sg} but lowers the pressure ahead of the exhaust nozzle and decreases the impulse of the exhaust gases.

SECTION 3. A STUDY OF COMBUSTION IN A CYLINDRICAL COMBUSTION CHAMBER

The basic problems of combustion and flame holding may be investigated with the aid of an experimental device, depicted in Figure 148.

Air from the compressors enters a <u>plenum</u> or reservoir, the diameter of which is several times greater than the diameter of the combustion chamber. The static pressure p in the plenum is close to the stagnation pressure p_0. To reproduce the stagnation temperatures which take place in flight during high Mach numbers, the reservoir

Legend:
A) Pitot tube; B) Spark igniter;
C) Fuel spray; D) Air;
E) Flame-holder with pilot light;
F) Oxyhydrogen;
G) Air preheater; H) Thermometer;
I) Combustion zone.
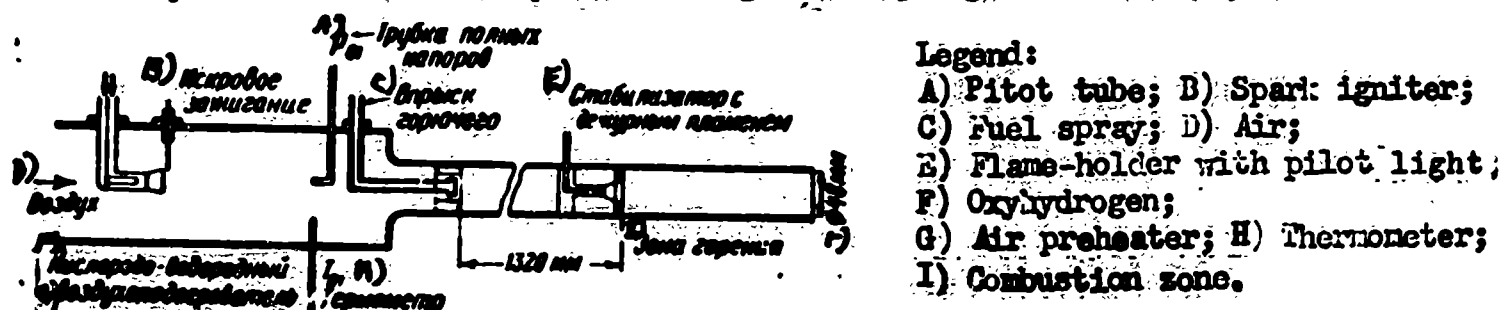
Fig. 148. A diagram of an experimental constant cross-section combustion chamber.

is supplied with a preheater, which is usually represented by a small combustion chamber, operating, for example, on acetylene and oxygen, on benzine and air, or on hydrogen and oxygen. The preheater contaminates the air with combustion products. One must tolerate this occurence. To preheat 1 kg/sec of air at 100° requires a thermal power of $N_Q = c_p \, G\Delta T = 0.24 \cdot 100 = 24$ kcal/sec = 100 kilowatts. (The corresponding benzine consumption G_g is equal to $G_g = \dfrac{N_Q}{H_u} = \dfrac{24}{10,500} = 2.3$ gm/sec.) The compressed and preheated air enters the combustion chamber through a throttling orifice or nozzle (which, at the same time, serves to measure the air output). The combustion chamber, represented by a cylindrical tube, is equipped with an injector, a mixer, a flame-holder with an ignition unit, and an exhaust nozzle. It is possible to reproduce exactly those conditions which take place in a combustion chamber at various altitudes by varying the temperature and pressure in the chamber T_0 and p_0 and by matching the diameter of the exhaust nozzle.

It is necessary to know the following values to judge the combustion process

(see Figure 150).

Legend:

A) to the booster
B) Vaned turbine
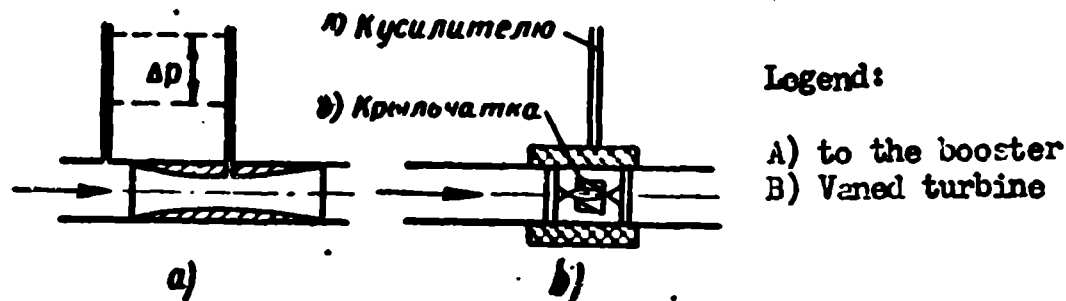
Fig. 149. Schematics of fuel flow meters.
a -- venturi meter, b -- vaned flow meter.

The _air_ _output_ is G_v. The air output is measured according to the pressure drop $\dfrac{p_{01}}{p_1}$ in a measured nozzle (or an output disk), the through section of which S_1 is known. From (2.49) and (2.74)

$$G_e = \sigma'_c S_1 p_{01} \sqrt{\frac{2gk}{(k-1)RT_{01}}\left[\left(\frac{p_1}{\sigma_c p_{01}}\right)^{\frac{2}{k}} - \left(\frac{p_1}{\sigma_c p_{01}}\right)^{\frac{k+1}{k}}\right]} =$$

$$= \sigma'_c \sqrt{\frac{2gk}{k+1}}\, \frac{p_{01} S_1) \cdot (\lambda)}{\sqrt{RT_{01}}}, \tag{8.1}$$

where p_{01} and T_{01} are the stagnation pressure and temperature before the delivery

nozzle;

p_1 is the static pressure behind the delivery nozzle;

σ'_s is the pressure factor, measured by experimental method.

Good nozzles have $0.99 < \sigma'_s < 1.00$. The rules for measuring consumptions are given in special wor..s.[1]

The _fuel_ _consumption_ is G_g . The fuel consumption is measured with the aid of a flow meter (Figure 149a) or by a vaned flow meter (Figure 149b). If the absolute pressure drop in the flow meter is equal to Δp mm of mercury or $13.6\,\Delta p$ mm of water and the cross section of the flow meter is equal to

$$G_r = \mu S \sqrt{2g\gamma_r 13.6\Delta p}, \tag{8.2}$$

where μ is the flow coefficient of the flow meter, determined by means of experiments;

γ_g is the fuel density in kg/m^3.

---

[1]Makarov, A. N. and Sherman, N. Ya., Raschet drossel'nkh ustroystv /The Computation of Orifice Plates/ Metallurgizdat /Metallurgical Printing House/, 1953.

Consumption is determined by the rotation speed of the vanes when an electric flow meter is used.

The static and total pressures in the beginning of the combustion chamber are p_2 and p_{02}; in front of the discharge -- p_3 and p_{03}; at the exhaust nozzle edge -- p_4 and p_{04}. The pressure is measured by means of static and dynamic tubes.

The stagnation temperatures at the combustion chamber inlet $T_{01} = T_{0x}$ (i.e., temperature before combustion); after combustion they are $T_{03} = T_{0g}$ (i.e., before discharge), are equal to the stagnation temperature of the effluxing gases T_{04}. However, to carry out an exact measurement of the combustion products temperatures when the compositions of the mixtures are close to stoichiometric is ($\alpha \approx 1$) difficult, since the measured temperatures, which exceed 2,000° C, lie beyond the heat resistance limits of existing thermocouples. The measurement of very high temperatures is carried out spectrographically, by a method of rotating the D lines of sodium. This labor-consuming method requires intricate equipment and qualified personnel. Therefore, only those temperatures before combustion T_{0x} are usually measured. The stagnation temperature after combustion is calculated by the flow equation (2.49), after measuring the pressure p_{03} and p_3 in the exhaust section of the combustion chamber S_3, the area of which is known:

$$T_{04} = \frac{2g k_c}{(k_r - 1) R_r} \left(\frac{p_{03} S_3}{G_3}\right)^2 \left[\left(\frac{p_3}{p_{03}}\right)^{\frac{2}{k_r}} - \left(\frac{p_3}{p_{03}}\right)^{\frac{k_r+1}{k_r}}\right]. \tag{8.3}$$

The smaller the flow of gases through a unit of the nozzle through section $\frac{G_4}{S_4}$ (i.e., mass flow is $\gamma_4 w_4$ kg/sec m²) at a given stagnation pressure in the outlet p_{04}, the greater is the temperature of the effluxing flow.

Example. We will find the temperature of the exhaust gases, if the stagic pressure at the outlet edge of the combustion chamber $p_4 = 1.02$ kg/cm²; the total pressure $p_{04} = 1.06$ kg/cm²; the combustion chamber exhaust section $S_4 = 100$ cm², and the output of the gases $G_4 = 1.29$ kg/sec; the gas constant R = 29.5 kg m/kg degree.

We will assume that for the heated gases $k_g = 1.3$.

We find the stagnation temperature by the formula (8.3), by substituting the

values with the index "3" for the values with the index "4".

$$T_{44} = \frac{2g}{R_e} \cdot \frac{k_r}{l_r - 1} \left(\frac{p_{04}S_4}{G_4}\right)^2 \left[\left(\frac{p_4}{p_{04}}\right)^{\frac{2}{k_r}} - \left(\frac{p_4}{p_{04}}\right)^{\frac{k_r+1}{k_r}}\right] =$$

$$= \frac{19.6 \cdot 1.3}{29.3 \cdot 0.3} \left(\frac{1.6 \cdot 100}{1.29}\right)^2 \left[\left(\frac{1.02}{1.6}\right)^{\frac{2}{1.3}} - \left(\frac{1.02}{1.6}\right)^{\frac{2.3}{1.3}}\right] = 2175^\circ \text{ K.}$$

SECTION 4. COMBUSTION CHAMBER PARAMETERS

Combustion chambers serve for the combustion of a fuel, i.e., for the conversion of its chemical energy into the enthalpy of the combustion products. The more complex the units for carburation, ignition, and flame stabilization, the more complete the combustion, but the greater the energy losses in overcoming local resistances, the pressure ahead of the exhaust is smaller, and the exit velocity and jet thrust of the exhaust gases are smaller.

In this way, the quality of the combustion chamber is characterized by two parameters: by the drag coefficient ζ and by the combustion efficiency ψ_{sg}.

The Determination of the Drag Coefficient of a Combustion Chamber

In order to determine the drag coefficient of a combustion chamber ζ, one measures the stagnation pressure p_{02} and the static pressure p_2 at the combustion chamber inlet, and also the stagnation pressure p'_{02} directly behind the flame-holder. In order to exclude pressure losses which are produced by the initial heating, a more reliable measurement is carried out in the absence of combustion, but at the same flow rate as in an operating combustion chamber. During cold flow tests the air output is regulated by means of a bullet or valve, which is installed in the exhaust nozzle (Figure 150).
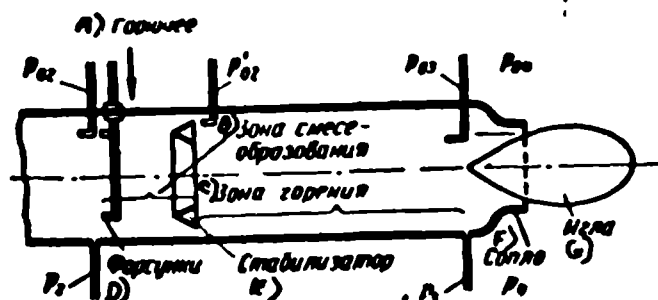
Legend:
A) Fuel
B) Carbueration zone
C) Combustion zone
D) Injectors
E) Flame-holder
F) Nozzle
G) Bullet

Fig. 150. A diagram of the measurements in a combustion chamber.

The local drag coefficient of the combustion chamber is found from the equation (4.19) with the consideration of (2.67):

$$\zeta = \frac{k+1}{M_3^2}\frac{\Delta p}{p_{04}z(\lambda_3)} = \frac{k-1}{k}\frac{\frac{\Delta p}{p_{03}}}{1-\left(\frac{p_3}{p_{03}}\right)^{\frac{k-1}{k}}}.$$ (8.4)

Here: $\Delta p = p_{04}-p'_{03}$; $z(\lambda_3) \approx 1$.

Only those pressures which may be measured directly are included in the formula (8.4).

The Determination of the Combustion Efficiency

The ratio of the enthalpy increase of the combustion products $G\Delta i$ to the chemical energy of the fuel $G_g H_u$ introduced into the combustion chamber is called the combustion efficiency φ_{sg}:

$$\varphi_{cr} = \frac{G\Delta i}{G_r H_u} = (1+\alpha L)\frac{\Delta i}{H_u} = (1+\alpha L)\frac{c_{p\,r}T_{04}-c_{p\,x}T_{02}}{H_u},$$ (8.5)

where C_{pg} is the average heat capacity of the combustion products in a temperature range from 0 to T_{04};

C_{px} is the average heat capacity of the air in a temperature range from 0 to T_{02}.

The excess air coefficient α, is determined by the fuel flow rate into the combustion chamber and is set experimentally.

To calculate the combustion efficiency, it is necessary to know the air flow G_v, which is determined by a measuring orifice at the combustion chamber inlet, the fuel consumption G_g, the cross section of the combustion chamber S_3 or the cross section of the exhaust nozzle S_4; and the static and total pressure in one of these sections p_4 and p_{04}, or p_3 and p_{03}.

We find the combustion efficiency φ_{sg} from the equation (8.5), after substituting the stagnation temperature of the combustion products ($T_{04} \approx T_{03}$) from the equation (8.3) in it:

$$\varphi_{cr} = \frac{G_0+G_r}{G_r H_u}\left\{2gA\left(\frac{k_r}{k_r-1}\frac{p_{03}S_3}{G_0+G_r}\right)^2\left[\left(\frac{p_3}{p_{03}}\right)^{\frac{2}{k_r}}-\left(\frac{p_3}{p_{03}}\right)^{\frac{k_r+1}{k_r}}\right]-i_{0x}\right\}.$$ (8.6)

The drag coefficient ζ and the combustion efficiency φ_{sg} characterize the suitability of a combustion chamber to operate on a given fuel at a given air surplus, but not the quality of the fuel, since under corresponding combustion conditions any fuel may burn out almost completely. If the combustion chamber is inadequately constructed, even a fuel like benzine burns poorly. There are cases known, when combustion chambers, which were intended for the combustion of kerosene, operated poorly on benzine. This is explained by the fact that during operating on the more volatile benzine mixture, the mixture ahead of the flame-holders appeared to be over-enriched ($\alpha \leqslant 1$), but downstream of the flame-holder the mixture ration failed to decrease enough for combustion with the amount of unused air.

The best combustion chamber would be one for which $\zeta = 0$ and $\varphi_{sg} = 1$. Such combustion chambers do not exist. To increase the combustion efficiency, the combustion chambers are equipped with mixers, flame-holders and other units. These devices, which serve to increase the combustion efficiency φ_{sg}, usually increase the drag coefficient of the combustion chamber ζ. In designing combustion chambers one should compromise by striving for a ration between φ_{sg} and ζ, at which the specific air impulse of the gases, which exit from the combustion chamber at a given mixture composition, appear to be the greatest.

One cannot find analytically the optimum ratio between φ_{sg} and ζ because of the impossibility of establishing a single-valued analytical connection between these values. Therefore, the problem of the optimum arrangement of a combustion chamber must be solved by an experimental method.

The Determination of the Air Specific Impulse

The ratio of the thrust of a flow, which acts in the exhaust section S_4 to the air output is called the air specific impulse:

$$I_a = \frac{R_4}{G_a} .$$

$$(8.7)$$

A force, which acts in any section of the flow, as is known, is expressed by the formula (2.76). For the section S_4

Consequently,

$$\mathbf{I} = \frac{G_a w_a}{g} + p_a S_a = p_a S_a (1 + kM_a^2).$$

$$I_a = \frac{p_a S_a}{G_a}(1 + kM_a^2) = \frac{p_a}{w_a \gamma_a}(1 + kM_a^2). \tag{8.8}$$

During discharge with a critical velocity

$$w_{cr} = \sqrt{\frac{2gkR}{k+1} T_{04}}.$$

$M_4 = 1$, the critical specific air impulse $I_{a\ cr}$ will be equal to

$$I_{a\,cr} = \beta \frac{RT_4}{w_{cr}}(1 + k) = \beta \sqrt{\frac{RT_4}{kg}}(1 + k).$$

Considering that $T_{cr} = \frac{2}{k+1} T_{04}$ we obtain

$$I_{a\,cr} = \beta \sqrt{2 \frac{k+1}{kg} RT_{04}}. \tag{8.9}$$

The ratio of the true specific impulse I_a to the possible maximum with a given fuel I_{max} (when $\zeta = 0$ and $\varphi_{sg} = 1$), is called the impulse efficiency η_i:

$$\eta_i = \frac{R_4}{I_{max}}. \tag{8.10}$$

The impulse efficiency, which is dependent on losses from incomplete combustion and from local drags, characterizes the perfection of a combustion chamber. ζ and φ_{sg} must be such so that η_i will be maximum.

Example 1. Find the drag coefficient of a combustion chamber ζ if the pressure at the inlet $p_{02} = 1.80$ kg/cm^2, and $p_2 = 1.72$ kg/cm^2, but the pressure drop $\Delta p = 0.29$ kg/cm^2. According to the formula (8.4),

$$\zeta = \frac{k-1}{k} \frac{\Delta p}{p_{02}} \frac{1}{1 - \left(\frac{p_2}{p_{02}}\right)^{\frac{k-1}{k}}} = \frac{0.4}{1.4} \frac{0.29}{1.80} \frac{1}{1 - \left(\frac{1.72}{1.80}\right)^{\frac{0.4}{1.4}}} \approx 3.8.$$

Example 2. Find the combustion efficiency φ_{sg}, if $G_v = 2.34$ kg/sec, $S_4 = 130$ cm^2; $p_4 = 1.006$ kg/cm^2, $p_{04} = 1.67$ kg/cm^2, $G_g = 71$ g/sec, $T_{0x} = 435°$ K, $H_u = 10,300$ kcal/kg, and $L = 14.9$.

We will assume, that for the heated gases $k_g = 1.3$. The enthalpy of the air at the combustion chamber inlet i_{0x} is found by the i-T diagram (see Figure 93); $i_{0x} = 118$ kcal/kg.

According to formula (8.6) the completeness of combustion is

$$\tau_r = \frac{G_0 + G_r}{G_r H_a} \left\{ 2 g A \left(\frac{h_r}{h_r - 1} \right)^2 \left(\frac{p_{04} S_4}{G_0 + G_r} \right)^2 \left[\left(\frac{p_4}{p_{04}} \right)^{\frac{2}{k_r}} - \left(\frac{p_4}{p_{04}} \right)^{\frac{k_r + 1}{k_r}} \right] - h_a \right\} =$$

$$= \frac{2.24 + 0.07}{0.071 \cdot 10300} \left\{ \frac{19.6}{427} \left(\frac{1.3 \cdot 1}{0.3} \frac{1.67 \cdot 130}{2.34 + 0.7} \right)^2 \left[\left(\frac{1.006}{1.67} \right)^{\frac{2}{1.3}} - \left(\frac{1.006}{1.67} \right)^{\frac{2.3}{1.3}} \right] - 118 \right\} \approx 0.81.$$

SECTION 5. THE EFFECT OF THE MIXTURE PARAMETERS ON THE COMBUSTION EFFICIENCY

The combustion efficiency depends on the parameters of the mixture which approaches the flame-holders. In order to eliminate the effect of carburation, we will investigate the variation of the combustion efficiency with the surplus air factor α, the initial temperature, the degree of turbulence, and the nature of the premixed fuel mixture, i.e., the fuel was vaporized and mixed with the air so that the composition of the flow would be the same across its entire cross-section.

The effect of the composition of the mixture. Experience shows that the combustion chambers may operate on similar premixed mixtures only within narrow limits of the excess air coefficient. Thus, in Mullen's tests, a combustion chamber operated on a homogeneous mixture prepared beforehand only over the range of $0.7 < \alpha < 1.6$.

Legend:

A) Combustion efficiency
B) Impulse efficiency
C) Air specific impulse
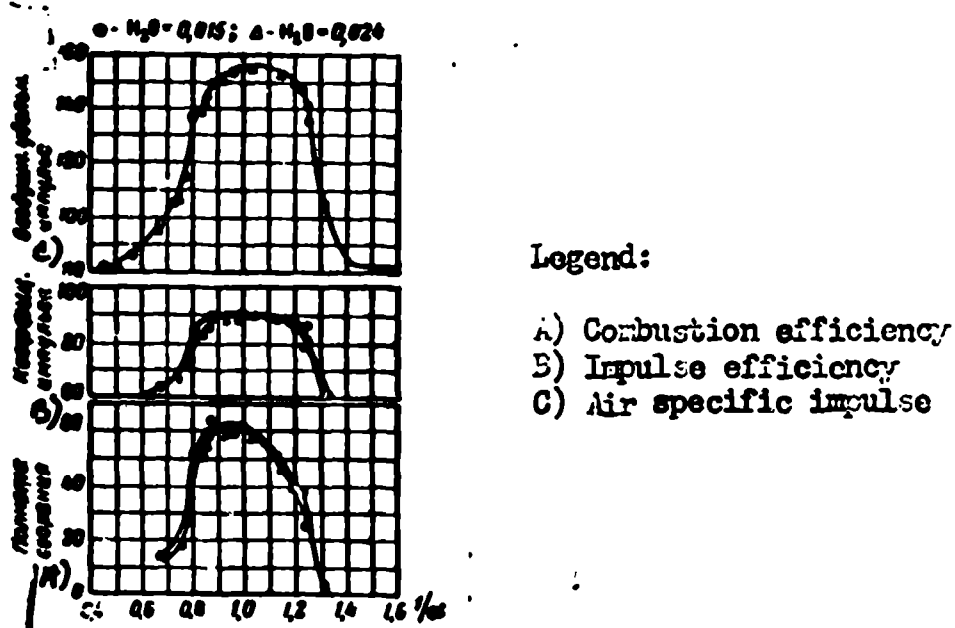
Fig. 151. Effect of the composition of a premixed mixture on φ, I_a, and η_i.

The combustion efficiency has a maximum value which lies approximately at $1.0 < \alpha$ to 1.2 (Figure 151). Within the range of the composition of a mixture from $\alpha = 1$ to $\alpha = 1.2$, the combustion efficiency varies insignificantly, but with a further leaning out of the mixture, it falls rapidly. When $\alpha \approx 1.6$, combustion ceases. In

mixtures enriched to $\alpha < 1$, η_{sg} gradually decreases, since there is not sufficient oxygen for total combustion. When $\alpha \sim 0.7$ the combustion of a homogeneous premixed mixture ceases.

The _temperature_ T_2 effects the combustion efficiency of a homogeneous premixed mixture. With an increase of air temperature, the combustion efficiency increases and the operating limits are broadened (Figure 152). The initial temperature also affects the ignition limits and the combustion of a stationary gas in an enclosed area. The combustion chambers of supersonic ramjet engines, into which the air comes preheated to several hundreds of degrees due to the stagnation of the oncoming flow, operate under more favorable conditions than the combustion chambers of subsonic ramjet engines.

The effect of the initial temperature of the combustion efficiency of a homogeneous mixture is attributable to the fact that with increasing temperature, the normal velocity of flame propagation increases. The turbulent moles of a gas burn out quicker and at a given degree of turbulence, combustion is completed at a lesser distance, and the combustion efficiency for a given length of the combustion chamber increases.

The _nature_ _of_ _the_ _fuel_ used in the turbulent combustion of homogeneous premixed mixtures affects the reaction velocity and the normal flame propagation velocity. The normal combustion velocities of hydrocarbons as heptane, octane, benzine, kerosene, diesel fuel, etc., have about the same values if their initial temperatures are equal.

The normal flame propagation velocities of such fuel substances as hydrogen, acetylene, or ether, are greater than those of the hydrocarbons; therefore, other conditions being equal, the combustion efficiency of the mixtures of these substances with air will be greater.

Flow _Velocity_ _of_ _the_ _Mixture._ With an increase of the mixture's flow velocity w, the velocity of the turbulent pulsations grows $w_{pul's} = \varepsilon w$ and the turbulent flame propagation velocity u_T increases. The increase of the flame propagation velocity usually lags behind the increase of the flow velocity w_n. Therefore, the

cone angle of the jet α_f, is determined from the equation

$$\sin\frac{\alpha_\phi}{2} = \frac{u_t}{w},$$

and, with an increase of flow velocity, it decreases.
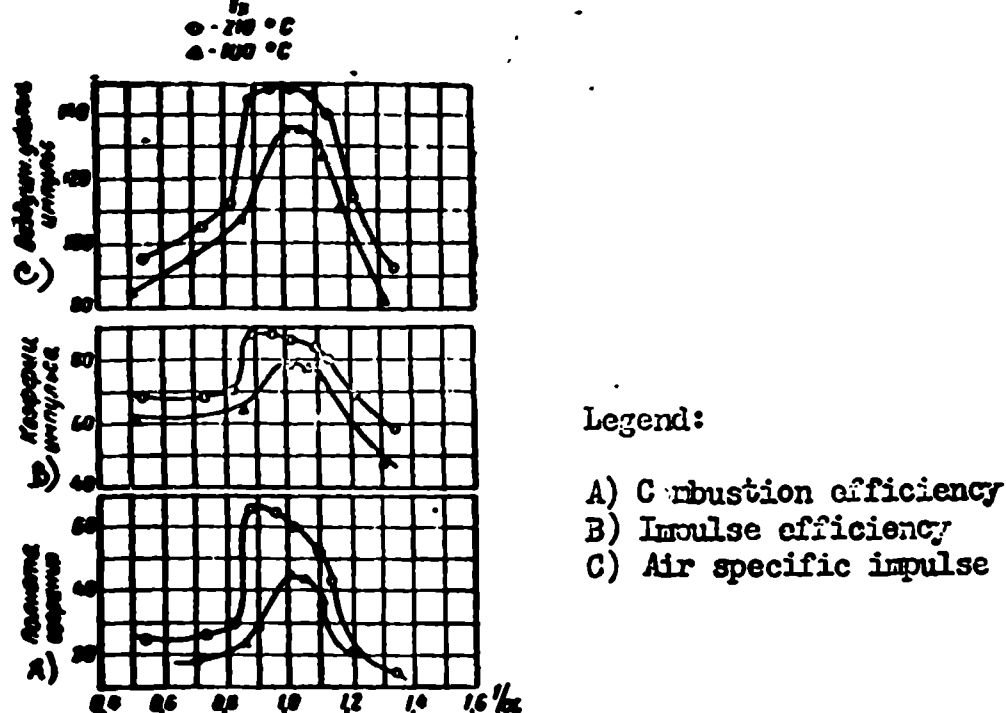
Fig. 152. Effect of the initial temperature upon the combustion efficiency φ_{sg}, air specific impulse I_a and impulse efficiency η_i.

Legend:

A) Combustion efficiency
B) Impulse efficiency
C) Air specific impulse

The length of the jet increases with an increase of flow velocity, but the combustion efficiency for a given combustion chamber length decreases (Figure 153).

At a sufficiently large flow velocity w, the flame breaks away from the flame-holder and combustion ceases. The value of the velocity, at which this break-away occurs, depends on the design and dimensions of the flame-holder, on the strength of the pilot light, and upon the parameters of the fuel mixture (see Section 9, Chapter VI).

Because of the break-away of the flame it is not possible to investigate the effect of the flow velocity on the combustion efficiency through the entire range of compositions of a mixture.

The humidity of the air has a certain effect on the combustion efficiency (Figure 154). With an increase of humidity the combustion efficiency decreases insignificantly. Thus, during an increase of water vapor content from 1.4 to 2.7 per cent by weight, the combustion efficiency decreases by 5-10%. The decrease in com-

bustion efficiency is more noticeable as the composition of the mixture departs from a stoichiometric ratio, and as the length of the combustion chamber becomes smaller (Figure 154). The effect of humidity is connected, it seems, with the fact that the normal flame velocity for humid mixtures is less than for dry mixtures. With
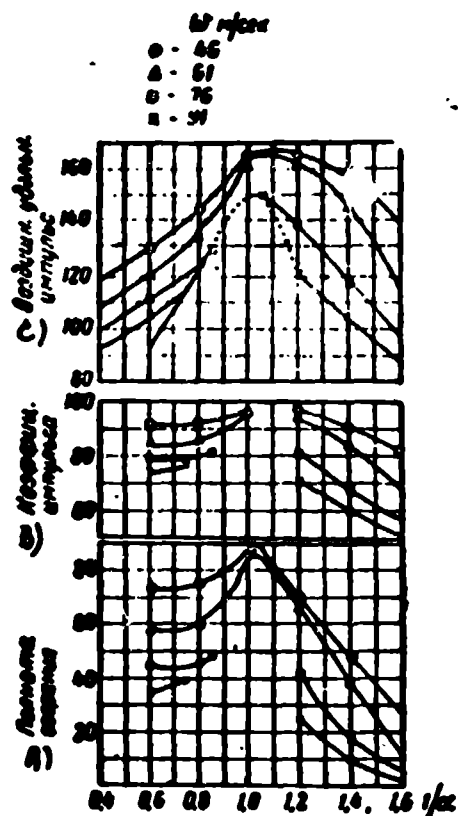
Fig. 153. The effect of the flow velocity on φ_{sg}, I_a, and η_i.
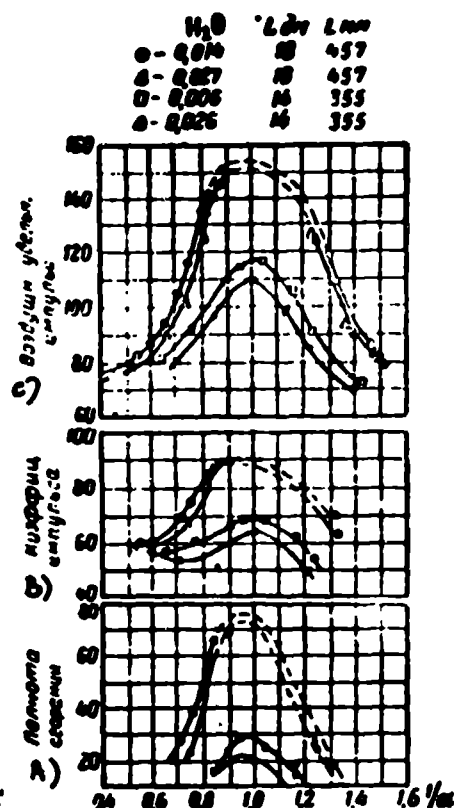
Fig. 154. The effect of the humidity of the air on φ_{sg}, I_a, and η_i.

Legend: A) Combustion effeciency; B) Impulse efficiency; C) Air specific impulse.

increase of humidity, the combustion becomes smoother. We will mention that the addition of water into the cylinders of piston engines eliminates detonating combustion, i.e., also decreases the flame propagation velocity. The effect of the humidity of the air must be considered for flights under trying weather conditions.

The degree of the **flow** turbulence has a substantial effect on the operation of a combustion chamber. Large-scale turbulence, in which the dimensions of the turbulent moles compare with the diameter of the combustion chamber and exceed the dimensions of the flame-holders, makes the operation of the combustion chamber difficult and lowers the value of the flow velocity at which blow out occurs. A small-scale turbulence, for which the dimensions of the turbulent moles are less than the diameter of the flame-holder, increases the velocity of turbulent flame propagation u_T and, other conditions being equal, increases the combustion efficiency.[1]

---

[1] Mullen, J., Fenn, J. B., and Garmon, R. C., Burners for Supersonic Ramjets,
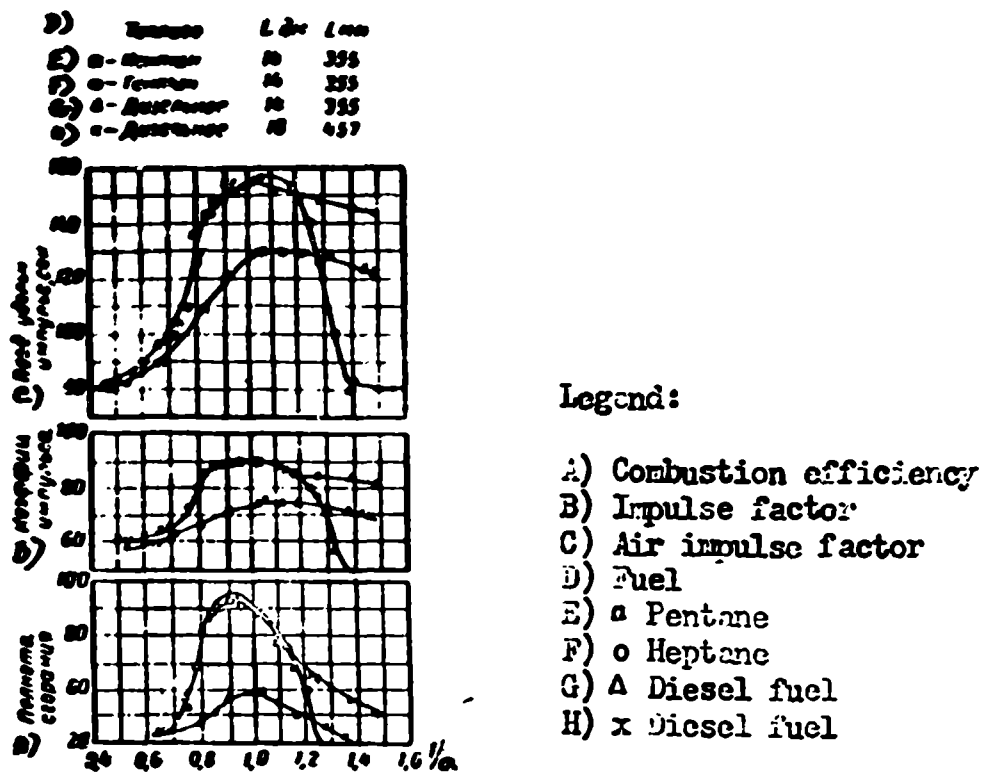
Fig. 155. The effect of the contents of a non-vaporized fuel on φ_{sg}, I_a, and η_i.

The effect of the phase composition of a mixture. During operation on fuel substances with low vapor pressure, for example, kerosene or diesel fuel, the larger drops of the atomized liquid do not successfully vaporize completely. Therefore, a mixture, which approaches the flame-holders, contains, in addition to the vapor phase of the fuel, a drop-liquid phase also. The presence of the liquid phase has an effect upon the character and upon the combustion efficiency (figure 155). Only that portion of the fuel which was vaporized enters the combustion reaction in the area behind the flame-holder. The fuel, which enters the combustion zone in a liquid state, must be vaporized before it enters into the reaction. The vaporization of the fuel drops occurs at the flame ignition source, the precombustion chamber for example (Figure 144). With a sufficiently powerful source, a two-phase mixture of hydrocarbons and air will ignite and burn with a greater velocity for finer degrees of atomization. During a great leaning out ($\alpha > 1.5$), two-phase mixtures burn better than do single-phase. The more non-vaporized fuel the mixture, that approaches the flame-holder, contains (and the larger the drops), the more powerful must be the ignition source (see Section 7).

The parameters of the mixture have a noticeable effect only on the operation of

Indust. and Eng. Chemistry, vol. 43, I, 1951, 195-211.

a short combustion chamber, in which combustion does not succeed to totally cease. During a correct organization of the process, if the length of the combustion chamber is sufficiently great and the sides of the chamber are isolated from thermal losses, any mixture, the composition of which lies within the ignition limits and $\alpha > 1$, will be practically totally burned.

If the parameters of the mixture are given, then the drag coefficient and the combustion efficiency will depend on the construction and on the dimensions of the flame-holders and igniters, on the power of the pilot light, on the fuel feed system, and on the length of the combustion chamber.

SECTION 6. THE EFFECT OF THE COMBUSTION CHAMBER ARRANGEMENT ON THE DRAG COEFFICIENT AND COMBUSTION EFFICIENCY.

The most important parameters of a combustion chamber which effect the combustion efficiency and local drags are the apparatus for fuel atomization and carburation, the geometry of the flame-holder, the length of the combustion chamber, and the diameter of the exhaust nozzle. The inlet cross section and exhaust nozzle have an effect on the flow velocity in the combustion chamber. To eliminate the effect of velocity, we will consider that the combustion chamber is, each time, equipped with such a nozzle at which the flow velocity has a given value.

We will consider the effect of each of the parameters of a combustion chamber on the combustion efficiency φ_{sg} and on the drag factor ζ.

The Geometry of the Flame-Holder. The form of the flame-holder effects the operation of the combustion chamber (see Chapter VI, Section 9).

During the flow around the sharp edges of the flame-holder, a break-away of the stream occurs, which is accompanied by an intensive vortex formation.

With an increase of the relative cross section of the flame-holder $s_{cr} = \dfrac{S_{cr}}{S_{g}}$ the relative velocity of the flow, which flows around the flame-holder $\dfrac{w_{cr}}{w}$, increases until the velocity of the flow between the edges of the flame-holder and the walls of the combustion chamber becomes equal to the local speed of sound. Besides, flame-holders with such large relative cross-sections are not used.

The average velocity of the turbulent pulsations $w_{pul's}$ is the greater, the greater the velocity of the streams which break away from the edges of the flame-holder. A growth of the intensity of the turbulence increases the velocity of turbulent flame propagation u_T, and the expansion angle of the combustion zone behind the flame-holder a_f widens. Therefore, with an increase of S_{st}, other conditions being equal, the length of the combustion zone decreases and the combustion efficiency at a given distance from the flame-holder increases (see Chapter VI, Section 9). However, very large flow velocities along the edges of the flame-holder may cause the flame to break away. It is possible to show that the optimum relative section of a conical flame-holder $S_{st} = \frac{1}{3}$ and that of a ring-shaped one $S_{st} = \frac{1}{2}$.

The arrangement of radial grooves (gutters) (Figure 156) aids the transfer of the hot gases from the ignition source to the fresh mixture and, other conditions being equal, shortens the length of the combustion area and increases the combustion efficiency. Ring-shaped grooves (gutters), located concentrically around the ignition source, may serve as flame-holders in very wide combustion chambers (see Figure 144b).

From the sides which are turned towards the diffuser, a flame holder is washed by air, the temperature of which is close to the stagnation temperature of the oncoming flow, and from the side of the exhaust nozzle, the flame-holder is washed by the products of incomplete combustion, since combustion near the flame-holder is not totally ended. Photographs of the combustion zone after a flame-holder show that the maximum luminescence intensity of the gases is reached at a distance of several centimeters from the flame-holder (see Figure 105). In this way, a flame-holder has the forward side cooled by air, the temperature of which is close to the stagnation temperature of the oncoming flow, while its rear-side is heated by gases, the temperature of which is on the order of 1,000° C. Considering that the heat emission coefficient from the rear side of the flame-holder is less than from the forward side, a flame-holder, which is constructed of heat-resistant steel, cannot overheat as a result of the combustion which takes place in its aerodynamic trail. A flame-holder does not

$$S_{cr} = \frac{\pi}{4} D_{cr}^2 \qquad S_{cr} = \frac{\pi}{4} D_{cr}^2 \qquad S_{cr} = \frac{\pi}{4}\left(D_1^2 - D_2^2\right)$$

$$P = \pi\left(D_1 + D_2\right)$$

$$D_{cr} = \frac{4S_{cr}}{P} = 2h$$

a)   b)   c)

d)
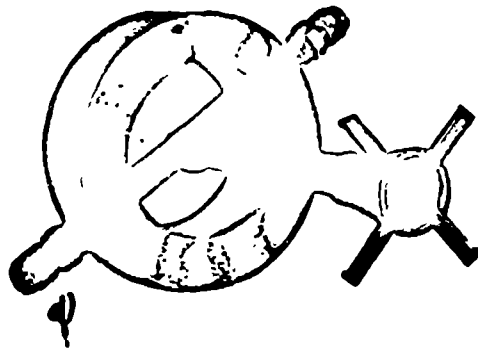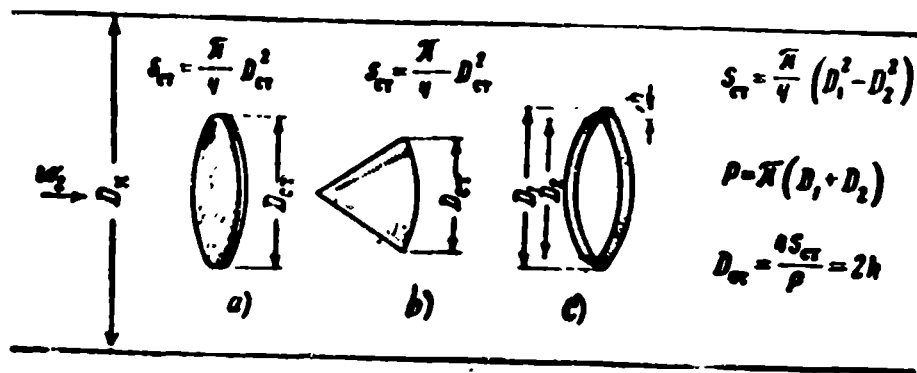
ig. 156. Forms of flame-holders.

a — disk; b — conical; c — ring-shaped; d — V-shaped.

urn from its own flame.

The combustion efficiencies, obtained by a simple conical flame-holder (Figure 56b) or by a complex flame-holder, composed of a cone with grooves (Figure 156d), are ompared in Figure 157. The combustion efficiency with a complex flame-holder is reater than with a simple conical one. The drag factor of the combustion chamber ncreases with an increase of the relative section of the flame-holder.

The length of the combustion chamber has a substantial effect on the combustion fficiency, since the stay time of the gases in the combustion zone depends on it. ith an increase of the length of the combustion chamber the combustion efficiency increases and at a certain length l_0, approaches 100%. Increasing the length of a comustion chamber above this value does not make sense, since with an increase of length he contact surface of the hot gases with the walls of the combustion chamber and the eat losses through the walls grow. In addition to this, the friction losses of the ot gases on the sides of the combustion chamber and the drag factor ζ of the comustion chamber increases. The most suitable is that length at which the specific

impulse of the gases is maximum. The effect of the length of the combustion chamber
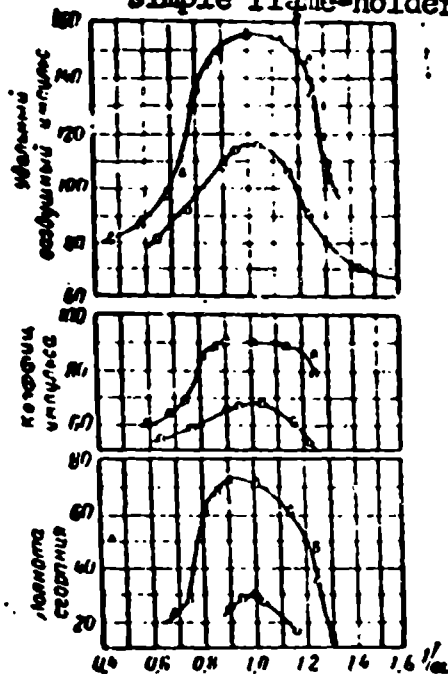
Fig. 157. The effect of the form of the flame-holder on φ_{sg}, $\dfrac{I_a}{I_{max}}$ and η.
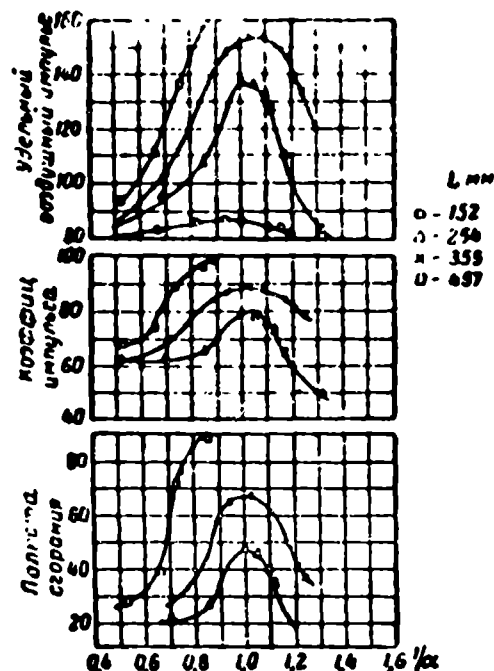
Fig. 158. The effect of the length of the combustion chamber on φ_{sg}, $\dfrac{I_a}{I_{max}}$, and η.

on the combustion efficiency is depicted in Figure 158. The combustion efficiency is low at a length of 150 mm of the area behind the flame-holder and when $\alpha \approx 1$. With an increase of length the combustion efficiency of a homogeneous mixture increases and when $l = 450$ mm, it reaches 100%. Increasing the length of the combustion zone higher than 450 mm may only lower the impulse of the effluxing gases, since the efficiency cannot increase further, the heat-and-friction losses in the area behind the flame-holder will grow with an increase of length.

The *relative cross-section of the exhaust nozzle* $S_4 = \dfrac{S_4}{S_3}$ has a substantial effect on the operation of a combustion chamber, since it determines the character of the flow of the gases. Depending upon the conditions which exist in the inlet section of a combustion chamber S_1, the change of the exhaust section may be accompanied by either a variation of the gas discharge, or by a variation in pressure (see Chapter X, Section 2).

SECTION 7. THE COMBUSTION OF LIQUID DROPS

Streams of a liquid, which are thrown out by direct-spray or centrifugal injec-

tors, disintegrate into separate drops. Moving in the air, the drops gradually vaporize. The higher the vapor pressure of the saturated fuel vapors, the quicker evaporation occurs. But even during operation on such volatile liquids such as benzine, the drops do not successfully completely vaporize into the space between the precombustion chambers and the combustion zone behind the flame-holder, so that the mixture, approaching the flame-holder, contains a significant percent of fuel in a drop and liquid state. Therefore, not only vapors, but also individual drops, burn in a combustion chamber.

We will consider certain combustion problems about liquid drops.

To stimulate the combustion reaction, it is necessary to elevate the temperature of the reacting substances to the ignition temperature T_{vsp}.

The ignition temperature is always higher than the boiling point of liquid fuels $T_{vsp} > T_{kip}$. Therefore, the liquid surface of the fuel fundamentally cannot burn. Vaporization always precedes combustion. The vapor pressure of such liquid ~~liquid fuels~~ as benzine is sufficiently great so that at temperatures below minus 50° C there are enough vapors over the surface of the liquid for ignition. The fractional pressure of the fuel vapors p_{nas} with the molecular weight μ_g, that is required for the formation of the mixture with the surplus air α, is equal to

$$p_{nas} = p_{ir} \frac{\mu_{ca}}{\mu_r} \frac{1}{1+\alpha L}.$$

When

$$L = 15; \quad \mu_{ca} = 29; \quad \mu_r = 110 \ \& \ \alpha = 1.5; \quad p_{nas} = 0.0123 p_{ir}.$$

If p_{atm} = 760 mm of mercury, then p_{nas} = 8.5 mm. The vapors of benzine have such a pressure at a temperature of -53° C, of kerosene at +13° C, and of diesel fuel at +50° C. Combustible substances, the vapors of which possess a pressure, which at normal temperature is insufficient to form a mixture capable of ignition, are called safe.

The vapors, which form on the surface of a drop, diffuse into the surrounding air; the greater the distance from the drop the lesser is the contents of

vapors in the air. At a certain distance from the drop, the fuel mixture

reaches a stoichiometric ratio. If one ignites a large separate drop, a "covering"

flame will appear around it (Figures 159 and 160).

In order to ignite a drop of fuel with a low vapor pressure, for example like a

drop of kerosene, it must first be heated to a point so that the vapor pressure

should reach a value that is sufficient for the formation of a fuel mixture.

This preheating may be accomplished either in the tanks before the efflux from the

injectors, or by atomization into hot air, as in the combustion chambers of super-

sonic ramjet engines, where the stagnation temperature is very great.

In the presence of a sufficiently powerful ignition unit the preheating of the

drops occurs in the ignition flame. Falling in the area of the heated gases, the

drops are heated; the content of the vapors reaches the required value and the mix-

ture burns.

Legend:

A) Combustion zone
B) Oxygen
C) Vapors
D) Combustion zone limit
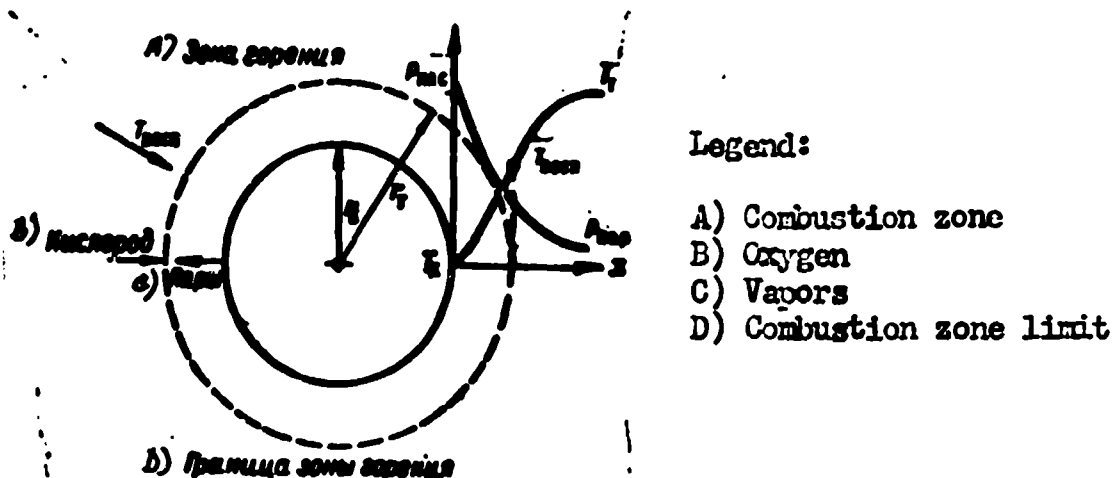
Fig. 159. Diagram of the vaporization and combustion of a drop.

It is not difficult to show that during a fine atomization the average distances

between the individual drops X are less than the thickness of the combustion zone of

the drops (Figure 161).

The number of drops, which are contained in a cube with a side a : $n = \left(\dfrac{a}{x}\right)^3$.

The mass of these drops is $G_f = \dfrac{\pi}{6} d_{s}^3 \gamma_f n = \dfrac{\pi}{6} \gamma_f \left(\dfrac{a d_s}{x}\right)^3$. The mass of the air in a selected

volume is $G_v = \gamma_v a^3$ (disregarding the volume of the drops). The composition of the

mixture is:

$$\frac{G_s}{G_f} = aL = \frac{6}{\pi} \frac{\gamma_0}{\gamma_f} \frac{x^3}{d^3}.$$

From this

$$\frac{x}{d} = \sqrt[3]{\frac{\pi}{6} \cdot \frac{\gamma_g}{\gamma_v} \alpha L}.$$

(8.11)

When $\gamma_g = 800$ kg/m^3; $\gamma_v = 1.225$ kg/m^3; $L = 15$; $\alpha = 1.5$ the average distance between the drops will be

$$x = d_k \sqrt[3]{\frac{3.14 \cdot 800 \cdot 1.5 \cdot 15}{6 \cdot 1.225}} \approx 20 d_k.$$

If $d_k = 100 \mu$, then $x = 2$ mm.

The theoretical investigation of the vaporization and combustion of drops, which are stationary in relation to the surrounding air, was carried out in 1945 by G. A. Varshavskiy. He considered that the vapors that were formed on the surface of a drop were diffused into the surrounding air, meeting diffused oxygen (see Figure 159). At a certain distance from the drop a spherical flame front appears, where the chemical reaction of fuel oxidation takes place and the heat of combustion is released. Partially it spreads in the direction of the diffusing fuel vapors and is used in the process of vaporization, and partially it diffuses into the ambient gases. The calculated radius of the combustion zone is several times greater than the radius of the drop. The combustion products are dispersed into the surrounding air after diffusing with the oxygen encountered. In this way, a "covering" flame appears around a heated drop. In accordance with Varshavskiy's ideas isolated drops are capable of burning in an atmosphere of pure oxygen, since an area which is sufficiently enriched with oxygen and fuel exists at a certain distance from the surface of each drop.
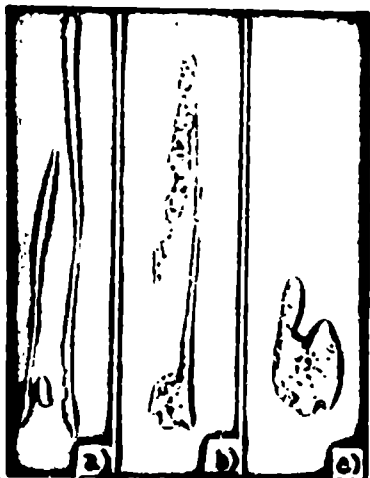
Fig. 160. A photograph of the combustion of a single drop.
a -- still air; b -- w<10 m/sec;
c -- w→w$_{sryv}$
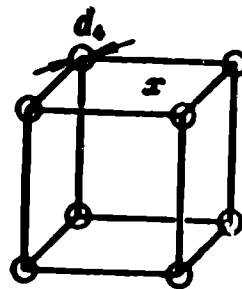
Fig. 161. Towards the determination of the average distance between drops in the jet of an injector.

An experimental investigation of the combustion of single drops, falling

in the atmosphere of a hot gas or suspended on a special device, was carried out by many researchers.[1] These investigations showed that covering flames (Figure 160a) actually appear around the drops at low relative velocities. During an increase of the relative velocity, the combustion zone is displaced towards the rear of the drop, and after this, combustion occurs only within its trail (Figure 160b). Investigations at relative velocities measured in tens of meters per second were not carried out. The speed of vaporization and combustion of the drops quickly grows with an increase of their relative velocity. The vaporization speed of drops immobile in relation to the air is not great.

The assumption that the drops are still in relation to the surrounding air, is only the first approximation to that which occurs in a ramjet engine. First of all, the drops are blown out by the turbulent movement of the air, secondly, after temperature of a burning gas increases, its specific volume grows, the flow velocity grows, the pressure decreases: $p_{03} < p_{02}$, and the velocity of the drops in relation to the gas varies. The velocity of the drops at the moment of penetration into the combustion zone is approximately equal to the velocity of the flow: $w_2 \approx w_k$. The burning gases begin to move faster than the drops of fuel. The gases flow around the drops with a relative velocity of: $u = v = w_k$, an aerodynamic force f arises thereby:

$$f = c_x S_k \frac{\gamma_0 u^2}{2g},$$ (8.12)

where C_x is the aerodynamic drag coefficient of the drop

S_k is the cross section area of the drop.

During a sufficient relative velocity u_{pr}, the aerodynamic force becomes so great that it imparts a boost to the drops, which then approach the velocity of the flow j; the vaporization speed grows.

SECTION 8. THE GAS DYNAMICS OF A COMBUSTION CHAMBER

The temperature of the burning gas mixture flowing through a combustion chamber

[1]Burgoyne, J. and Richardson, J., Fuel, vol. 28, 1949, 2.
Spalding, D. B., Eksperimenty po goreniyu i gasheniyu zhidkogo topliva na sharovykh poverkhnostyakh /Experiments on the Combustion and Quenching of a Liquid Fuel on Spherical Surfaces/, Fuel, vol. 32, 1953, No. 2, 169.

increases. During this its velocity increases, but the pressure falls. The gas dynamics of a combustion chamber establish a connection between the temperatures of the gases in the various sections of the combustion chamber on the one side, and with the velocities, pressures, and densities of the gases on the other side.

During the research of the gas dynamics of a combustion chamber an assumption is made that the temperatures, velocities, and pressures in the investigated sections are the same. These allowances are sufficiently correct for the inlet section of a combustion chamber S_2 and only approximately correct for the exhaust section S_3. The zones of temperature and velocity in the in-between sections of the combustion chamber, where combustion occurs, may not be considered as uniform even in the first approximation.

We will designate the temperature and other thermodynamic parameters of the air at the inlet to the combustion chamber by T_2, γ_2, p_2, and w_2. The stagnation parameters at the inlet to the combustion chamber we will designate by T_{02}, p_{02}, and γ_{02}.

The critical velocity of the incoming flow is

$$a_2 = \sqrt{\frac{2gkRT_{02}}{k+1}}.$$ (8.13)

The relative velocity at the combustion chamber inlet is

$$\lambda_2 = \frac{w_2}{a_2} = w_2 \sqrt{\frac{k+1}{2gkRT_{02}}}.$$ (8.14)

The ratio between the stagnation parameters and the static parameters at the combustion chamber inlet may be found by using the gas dynamic function:

$$T_2 = T_{02}\tau(\lambda_2); \quad p_2 = p_{02}\pi(\lambda_2); \quad \gamma_2 = \gamma_{02}\varepsilon(\lambda_2).$$ (8.15)

The stagnation temperature at the inlet to the combustion chamber T_{02} may be measured by screened resistance thermometers or by thermocouples. The stagnation pressures are measured by Pitot tubes, the static pressures -- by tubes, the openings of which are parallel to the stream lines (see Figure 150). Relative to the pressure ratio $\frac{p_{02}}{p_2}$ it is possible to find the relative velocity at the inlet to the combustion chamber λ_2 (see 2.68):

$$\lambda_2 = \sqrt{\frac{k+1}{k-1}\left[1 - \left(\frac{p_2}{p_{02}}\right)^{\frac{k-1}{k}}\right]}.$$ (8.16)

The density of the incoming air is determined by the equation of state:

$$\gamma_2 = \frac{p_2}{RT_2} = \frac{p_{02}}{RT_{02}}\, \varepsilon(\lambda_2).$$ (8.17)

The air flow through the combustion chamber may be calculated by knowing the inlet section S_2 and the parameters p_2, p_{02}, and T_{02} (see 2.74):

$$G_a = w_2 S_2 \gamma_2 = \sqrt{\frac{2gk}{(k+1)R}}\, \frac{S_2 p_{02}}{\sqrt{T_{02}}}\, q(\lambda_2).$$ (8.18)

A portion of the total pressure situated at the inlet to the combustion chamber p_{02} is dissipated in friction and shocks during the flow around the turbulence rings (turbulizers), fuel collectors, flame-holders, and other units which are located at the combustion chamber inlet.

The pressure preservation factor during the flow around the local resistances, as was shown in Chapter IV, Section 2, is equal to

$$\sigma_m = \frac{p_{02}'}{p_{02}} = 1 - \frac{\Delta p}{p_{02}} = 1 - \zeta\frac{\gamma_2 w_2^2}{2g p_{02}} = 1 - \frac{k\zeta}{k+1}\lambda_2^2 \varepsilon(\lambda_2).$$ (8.19)

At low velocities $(\lambda_2 < 0.2 \div 0.3)$

$$\sigma_m \approx 1 - \frac{k\zeta}{k+1}\lambda_2^2.$$ (8.20)

To determine the local drag coefficient factor ζ in addition to the pressures p_2 and p_{02}, one measures the pressure drop Δp, which takes place during the flow around the obstacles: $\Delta p = p_{02} - p_{02}'$.

From (8.19) we obtain

$$\zeta = \frac{k+1}{k\lambda_2^2 \varepsilon(\lambda_2)}\, \frac{\Delta p}{p_{02}} \approx \frac{k+1}{k\lambda_2^2}\, \frac{\Delta p}{p_{02}}.$$ (8.21)

The local drag coefficient may first be calculated if the ratio of the blockage area S_{cr} to that of cross-section S_2 is known:

$$\zeta \approx \left[\frac{S_2}{a(S_2 - S_{cr})} - 1\right]^2;\quad a = 0.63 + 0.37\left(\frac{S_2 - S_{cr}}{S_2}\right)^3.$$ (8.22)

We determine the relative velocity behind the flame-holder λ_2' from the flow equation $q(\lambda_2) = \sigma_m q(\lambda_2')$, $\lambda_2' < 1$, after solving it graphically.

The enthalpy of the flow at the combustion chamber inlet i_{02}, disregarding the enthalpy of the fuel, is found by the i-T diagram (see Figure 92), or by calculation, if the heat capacity c_{p2} is known:

$$i_{02} = c_{p2} T_{02}.$$ (8.23)

During the combustion of the fuel the enthalpy of the gases grows:

$$i_{03} = \left(i_{02} + \frac{H_u}{1 + \alpha L}\right) \eta_{tep},$$ (8.24)

where η_{tep} is the heat utilization coefficient, which accounts for the losses due to incomplete combustion and heat conduction through the walls.

The stagnation temperature of the combustion products of rich mixtures $\alpha \leqslant 1.5$, considering dissociation, is more reliably determined by the i-T diagram (see Figure 92). During the combustion of lean mixtures one may use the data for the average heat capacities, without considering dissociation, as given in Figure 85. Then,

$$T_{03} = \frac{i_{03}}{c_{p3}}.$$ (8.25)

Along with the burning out of the mixture, which occurs along the entire length of the combustion chamber, the temperature of the products increases, their velocity increases and the pressure falls. According to the continuity equation

$$w_2 \gamma_2 S_2 = w_3' \gamma_3' S_3'.$$ (8.26)

The velocity w_3 may not be determined from this, since the pressures p_{03}, p_3, and consequently, the density of the combustion products γ_3 are not known.

The relationship between the stagnation pressures up to and after combustion p_{02}' and p_{03} in the section S_2' directly behind the front sections and in the section S_3 in front of the nozzle may be found from the flow equation (2.74)

$$\beta G_2 = G_3.$$

$$\beta \sqrt{\frac{2 g k_2}{(k_2 + 1) R_2}} \frac{S_2 p_{02}' q(\lambda_2')}{\sqrt{T_{02}}} = \sqrt{\frac{2 g k_3}{(k_3 + 1) R_3}} \frac{S_3 p_{03} q(\lambda_3)}{\sqrt{T_{03}}}.$$ (8.27)

Hence, the pressure recovery during combustion σ_{sg} is equal to

$$\sigma_{sg} = \frac{p_{03}}{p_{02}'} = \beta \xi \sqrt{\theta} \frac{q(\lambda_2')}{q(\lambda_3)} \frac{S_2}{S_3}.$$ (8.28)

Here

$$\theta = \sqrt{\frac{T_{02}}{T_{03}}},$$

$$\xi = \sqrt{\frac{k_3}{k_2} \frac{k_2 + 1}{k_3 + 1} \frac{R_3}{R_2}} > 1.$$ (8.29)

The relationship between the relative velocities up to and after combustion λ_2 and λ_3 may be found from Kiselev's equation for the thrust of a flow (see 2.84):

$$I=\sqrt{\frac{k_3+1}{2k_3}R_3T_{03}}G_3\left(\lambda_3+\frac{1}{\lambda_3}\right)-\sqrt{\frac{k_2+1}{2k_2}R_2T_{02}}G_2\left(\lambda_2'+\frac{1}{\lambda_2'}\right). \tag{8.30}$$

In the case of a cylindrical combustion chamber $S_3 = S_2$; $R = 0$ and the equation (8.30) is simplified:

$$\frac{z(\lambda_2')}{z(\lambda_3)}=\frac{\lambda_2'+\frac{1}{\lambda_2'}}{\lambda_3+\frac{1}{\lambda_3}}=\beta\sqrt{\theta}. \tag{8.31}$$

After solving the last quadratic equation in relation to λ_2, we obtain

$$\lambda_2'=\Pi-\sqrt{\Pi^2-1}. \tag{8.32}$$

Here

$$\Pi=\frac{\beta\epsilon}{2}\sqrt{\theta}\left(\lambda_3+\frac{1}{\lambda_3}\right). \tag{8.33}$$

The pressure recovery during combustion in a cylindrical combustion chamber is from (8.28) and (8.31)

$$\sigma_{cr}=\beta\sqrt{\theta}\frac{q(\lambda_2')}{q(\lambda_3)}=\frac{z(\lambda_2')q(\lambda_2')}{z(\lambda_3)q(\lambda_3)}. \tag{8.34}$$

The overall pressure ratio across the combustion chamber is equal to the product of

$$\sigma_x=\frac{p_{03}}{p_{02}}=\frac{p_{03}}{p_{02}'}\frac{p_{02}'}{p_{02}}=\sigma_{cr}\sigma_u, \tag{8.35}$$

$$\sigma_x=\left[1-\frac{k}{k+1}\lambda_2^2\varepsilon(\lambda_2)\right]^2\frac{z(\lambda_2')q(\lambda_2')}{z(\lambda_3)q(\lambda_3)}. \tag{8.36}$$

Here

$$\lambda_3=\sqrt{\frac{k_3+1}{k_3-1}\left[1-\left(\frac{p_3}{p_{03}}\right)^{\frac{k_3-1}{k_3}}\right]}. \tag{8.37}$$

The flow of the gases through the combustion chamber is determined by the throat section of the diffuser S_{1cr} or the critical section of the exhaust nozzle S_{4cr}. In not one of these sections is the flow velocity able to become greater than the local speed of sound. The problem of flow through subsonic and supersonic engines is discussed in Chapters IX and X.

The stagnation temperature of the combustion products of lean mixtures $\alpha > 1.5$, may be measured with the aid of a shielded thermocouple; the stagnation temperature of the combustion products of rich mixtures $\alpha < 1.5$ may be found by calculating the flow of gases G_3 and the static and total pressures ahead of the nozzle p_3 and p_{03}:

$$VT_{03} = \sqrt{\frac{2k\cdot k_1}{(k_1+1)R_3}}\frac{S_3 p_{03} q(\lambda_3)}{G_3}.$$ (8.38)

The heat release coefficient is determined from the equation (8.24).

If there is no convergent nozzle at the combustion chamber outlet, then the velocity after combustion in a cylindrical tube may reach a sonic value. If $S_3 = S_{4cr}$, then $\lambda_3 = 1$. This is the most possible value of the relative velocity of a flow in a constant cross-section combustion chamber. The velocity at the inlet to a combustion chamber without constriction at the outlet, i.e., when $\frac{S_4}{S_3} = 1$, may not be greater than the limiting value, which corresponds to $\lambda_3 = 1$:

$$\lambda_{2max} = \beta\xi\sqrt{\theta} - \sqrt{\beta^2\xi^2\theta - 1}.$$ (8.39)

In the absence of heating $\theta = 1$; $\beta\xi = 1$; $\lambda_{2max} = 1$. With an increase of relative heating $\theta = \frac{T_{02}}{T_{0x}}$ λ_{2max} decreases.

When $\beta\xi = 1.15$ and $\theta = 4$; $\beta\xi\sqrt{\theta} = 2.3$; $\lambda_{2max} = 2.3 - \sqrt{2.3^2 - 1} = 0.23$.

Substituting the value λ_{2max} in the formula (8.34) we find the loss of total pressure during combustion.

The loss of pressure in a constant cross-section combustion chamber is the highest then, when the velocity at the end of combustion reaches a sonic value. This may take place only in those combustion chambers that do not have a convergent exhaust nozzle ($S_4 = S_3$; $\lambda_3 = Y_4 = 1$).

Substituting $\lambda_3 = 1$ and $\lambda_2 = \lambda_{2max}$ in the formula (8.34) we find the maximum possible decrease of total pressure in the combustion chamber, i.e., the least pressure ratio during combustion $\sigma_{ag\ min}$.

$$\sigma_{cr\ min} = \left(\frac{p_{03}}{p_{02}}\right)_{min} = \frac{\left[k - (k-1)\left(1 - \sqrt{1 - \frac{T_{02}}{T_{03}}}\right)\frac{T_{03}}{T_{02}}\right]^{\frac{k}{k-1}}}{1 + k\sqrt{1 - \frac{T_{02}}{T_{03}}}}.$$ (8.40)

The dependence of the relative variation of the total pressure in a constant cross-section combustion chamber without constriction at the outlet $\frac{S_4}{S_3} = 1$, $\lambda_3 = 1$, on the relative increase of the temperature, is depicted in the following table:

$$\theta = \frac{T_{00}}{T_{02}} \qquad 1 \quad 1,5 \quad 2 \quad 4 \quad 6 \quad 8 \quad \infty$$

$$\sigma_{\text{г min}} = \frac{p_{00}}{p_{02}} \qquad 1 \quad 0,89 \quad 0,86 \quad 0,82 \quad 0,81 \quad 0,80 \quad 0,79$$

__Example.__ Find the pressure ratio for a combustion chamber σ_k, if the velocity of the gases before the discharge $\lambda_3 = 0.5$, the temperature ratio during combustion $\theta = 3$, the local drag factor $\zeta = 1.2$, $k_3 = 1.3$, $\frac{R_3}{R_2} = 1.02$, and $\beta = 1.05$.

We will determine the functions of ξ and Π :

$$\xi = \sqrt{\frac{k_2}{k_3} \frac{k_3+1}{k_2+1} \frac{R_3}{R_2}} = \sqrt{\frac{1,4}{1,3} \frac{2,3}{2,4} 1,02} = 1,03,$$

$$\Pi = \frac{\beta \xi}{2} \sqrt{\theta} \left(\lambda_3 + \frac{1}{\lambda_3}\right) = \frac{1,05 \cdot 1,03}{2} \sqrt{3}\left(0,5 + \frac{1}{0,5}\right) = 2,343.$$

The relative velocity after the flame-holder is

$$\lambda_2' = \Pi - \sqrt{\Pi^2 - 1} = 2,343 - \sqrt{2,343^2 - 1} = 2,343 - 2,120 = 0,223.$$

The determined λ_2' value must be checked by substitution in the initial equation (8.31).

The pressure recovery for combustion is

$$\sigma_{\text{гr}} = \frac{z(\lambda_2') q(\lambda_2')}{z(\lambda_3) q(\lambda_3)} = \frac{4,7}{2,5} \frac{0,223}{0,5} \frac{\left(1 - \frac{0,223^2}{6}\right)^{2,5}}{\left(1 - \frac{0,5^2}{7,67}\right)^{3,33}} = 0,923.$$

The relative velocity at the combustion chamber inlet is found by solving the discharge equation graphically:

$$\frac{q(\lambda_2)}{1 - \frac{k\zeta}{k+1}\lambda_3^2} = q(\lambda_2') = 0,22.$$

From this:

$$\lambda_2 = 0,216; \quad \sigma_{\text{м}} = 0,965.$$

The overall pressure ratio across the combustion chamber is:

$$\sigma_k = \sigma_{\text{м}}\sigma_{\text{гr}} = 0,965 \cdot 0,923 = 0,890.$$

SECTION 9. THE OPERATING PROCESS IN A STABILIZED COMBUSTION CHAMBER

The processes of atomization, vaporization, and combustion of a fuel, which end by the turbulent intermixing of the combustion products with fresh air, occur in a stabilized combustion chamber (Figure 162).

The fuel consumption G_g in kg/sec is determined by the number of injectors n, the cross section of the injector nozzle S_f in m^2, the fuel feed pressure Δp in kg/m^2 and the density of the fuel γ_g in kg/m^3:

$$O_r = \mu_\phi \mu S_\phi \sqrt{2g\gamma_r \Delta p}. \qquad (8.41)$$

The flow coefficient of an injector μ_f depends on its geometric characteristic and on the viscosity of the fuel η_g. With an increase of viscosity the twist of the fuel in a centrifugal injector deteriorates, the thickness of the shroud increases, and the flow coefficient μ_f grows, remaining less than one. The flow coefficient of direct-spray injectors diminishes with an increase of viscosity due to increased friction losses. Other conditions being equal, the flow coefficient of a centrifugal injector is less than that of a direct-spray injector.

The temperature of the fuel influences the viscosity and density; with an increase of the fuel temperature when Δp = const. the flow coefficient μ_f diminishes until the viscosity of the liquid becomes negligibly small; then the injector approaches ideal.

The atomization of the fuel is determined by the relative velocity, the density, and the viscosity of the air, by the density, surface tension, and viscosity of the fuel. With an increase of fuel temperature, the atomization is improved. The air temperature has a small effect on the atomization.

The form of the dispersion jet depends on the flow velocity, the fineness of the dispersion, the density and viscosity of the air, and also on the location of the injector in relation to the oncoming flow. With an increase of flow velocity, with an increase of the dimensions of the drops, and also with a decrease of air density, the dispersion jet widens. When the injector is located with the flow the jet is somewhat wider than when the injector is located against the flow, although the widening of the jet occurs at a considerable distance from it. During the widening of the jet the local fuel concentration in the trail of the injector diminishes, other conditions being equal.

With increase of flight altitude the absolute pressure and density of the flow in the combustion chamber fall and the jet widens so that the drops are able to fall on the sides of the chamber. The variation of the form of the jet must be considered during the calculation of a combustion chamber which must operate at various altitudes.
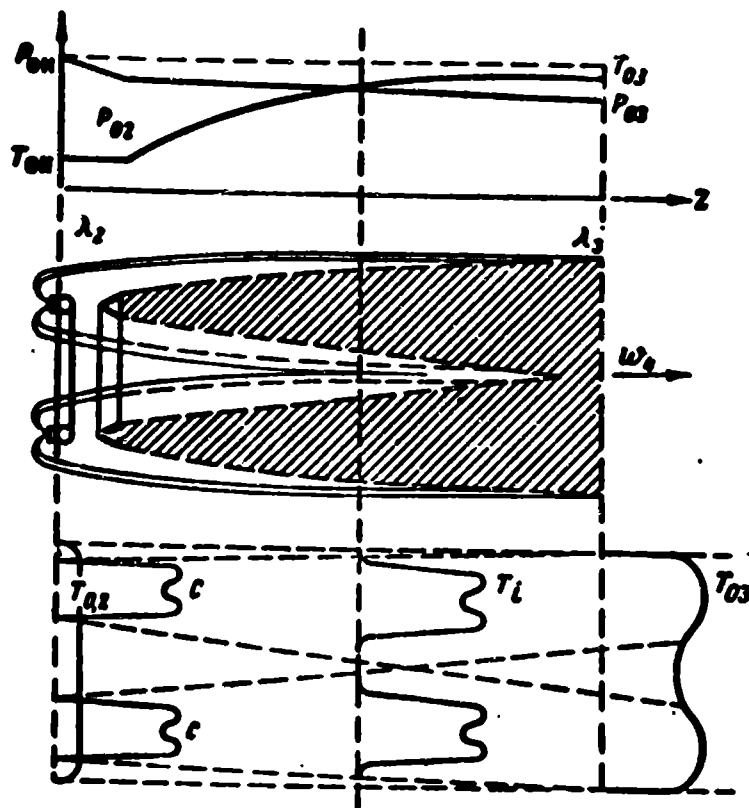
Fig. 162. A diagram of the operating process in a stabilized combustion chamber.

The evaporability of the fuel depends on its volatility and temperature, on the fineness of the dispersion, on the relative velocity of the drops, and on the temperature of the air. The evaporability increases with an improvement of the dispersion, with an increase of the volatility of the fuel, with an increase of the relative velocity of the drops, the temperature of the air, and especially the temperature of the fuel. The vapors that are formed during the motion of the drops are carried away along the stream lines of the air. Therefore, with an increase of fuel evaporability the vapor concentration in the injector trail increases. The basic evaporation of the fuel occurs during high relative flow velocities, i.e., during the movement of the drops along curvilinear portions of the trajectory directly after leaving the injector and while flowing around the flame-holders. Therefore, the content of the fuel vapors noticeably increases only at a small distance from the injector. With a subsequent increase of distance, the evaporability increases slower than the turbulent interspersion of the air occurs, which is accompanied by a widening of the jet and the concentration of fuel vapors in the injector trail begins to diminish.

The relative position of the flame-holders and the injectors has an effect on

the operation of a combustion chamber only when the distance between them is not greater that that at which the local concentration of fuel ceases to vary, i.e., until the concentration zones become even. When the flame-holders and the injectors are located too close together, a narrow jet, which contains less drops and more liquid fuel, will fall on the flame-holders; conditions will be unsuitable for ignition and combustion. When the flame-holder is located further from the injectors the width of the jet will grow, the evaporability of the fuel and the concentration of the vapor phase will increase, but the concentration of the liquid phase will decrease; conditions for combustion will improve, and will finally become perfect. During a further increase of the distance between the flame-holder and the injectors, the width of the jet will slowly increase due to turbulent intermixing; the evaporability of the fuel will grow until it finally reaches 100%. The contents of the liquid phase of the fuel will decrease, and the concentration of vapors will slowly diminish, until the concentration zones become even.

At a given relative position of the injectors and flame-holder of definite design and dimensions, the composition of a mixture in the area of the flame-holder edges will be determined by the fuel feed pressure, the temperature and nature of the fuel, and the velocity, pressure, and temperature of the air. With an increase of the fuel feed pressure, the fuel consumption increases, dispersion is improved, the local concentration at first begins to grow as a result of rising proportions of small drops, and the improvement of vaporization. With an increase of fuel temperature, consumption decreases insignificantly owing to diminishing fuel density and reduction in the thickness of the film. Dispersion improves because of diminishing surface tension and the local concentrations grow because of the improvement of vaporization, the increase of proportion of small drops, and the narrowing of the jet. It is for the same reasons that a growth of axial concentration is registered as a result of kerosene replacement by benzine.

With rising temperature of the air, but constant fuel temperature T_g = const., dispersion deteriorates insignificantly due to a reduction in air density, and the

evaporability of the fuel increases because a greater quantity of heat is imparted to the drops. The fuel concentration in the injector trail grows due to the growth of the content of the vapor phase; the conditions for combustion improve.

With an increase of the flow velocity the dispersion improves, the jet constricts, the evaporability of the drops increases and the fuel content in the trail of the injector increases.

Depending on which has the predominant value — the growth of the air flow or the growth of the fuel flow — the mixture concentration either diminishes or increases. A stabilized combustion chamber is able to operate within a wide range of velocities of the oncoming flow.

Legend:

A) Undisturbed flow
B) Turbulent trace
C) Counter current zone
D) air stream lines
E) drop trajectories
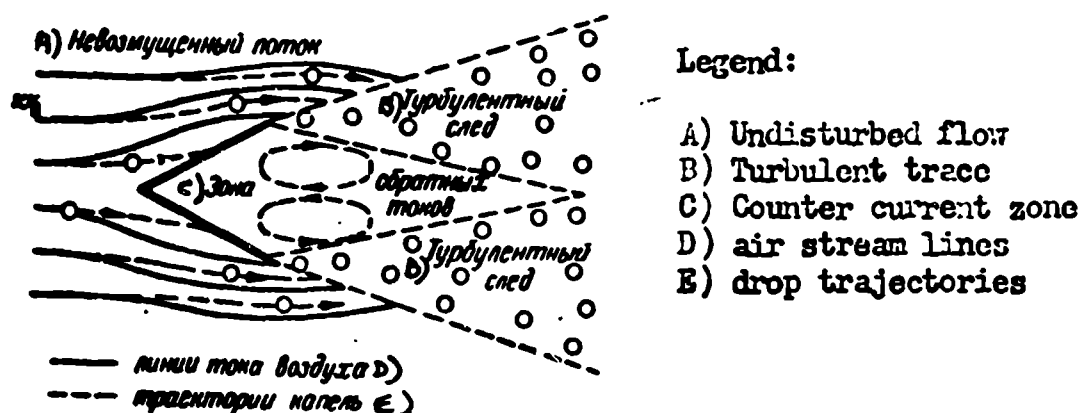
Fig. 163. Diagram of a flame-holder facing a two-phase flow.

With an increase of air pressure the dispersion is improved, the jet quickly constricts, evaporization increases because of the improvement of the dispersion, and the flow of the fuel in the injector trace increases. The flow of air grows slower than the flow of fuel and the fuel concentration along the injector axis grows during an increase of air pressure.

During an increase of any parameter which leads towards enriching the mixture in the trace of the injectors, i.e., during an increase of the fuel feed pressure, the temperature or volatility of the fuel, and a decrease of the flight altitude, it is possible to raise the concentration of the mixture to the upper ignition limit; a rich blow-out occurs, which may be preceded by concentration pulsations (see Chapter VIII, Section 12).

During a decrease in the fuel feed pressure, the temperature and volatility of

the fuel, and also during an increase in flight altitude, it is possible to raise the concentration of the mixture up to a lean blow-out, which sometimes may be preceded by lean concentration pulsations.

Carburation has a substantial effect on the operation of a combustion chamber.

During the flow around the flame holders, the stream lines of the air warp. The drops, which have a much higher density than the air, continue to move almost rectilinearily (Figure 163). The greater the diameter of the drops, the smaller is the curvature of their trajectories in comparison with the curvature of the air stream lines. Therefore, only the finest — the micron-sized drops — flow around the flame-holder which is located in the trace of the injector, but the larger drops strike against it, forming a liquid film on the flame-holder surface. A flame-holder enriches a two-phase mixture.

Owing to the irregularity of the concentrations in the dispersion jet to the transport of vapors and the evaporization of the liquid film formed on the flame-holder, the mixture on the edges of the flame-holder contains a significantly higher percent of fuel than does the flow which moves past the flame-holders:

$$\alpha_{st} < \alpha_{ar}.$$

If an electric sparkplug, located behind the flame-holder so that no drops of the liquid fall on it, serves as an ignition source, then a quantity of vapor sufficient for burning must arise in the carburation zone, since only vapors and micron-sized drops actually penetrate into the space behind the flame-holder. If a precombustion chamber or pilot light serve as the ignition source, then the evaporation of the drops may reach the required value in the ignition jet, wherefrom the evaporation and combustion gradually diffuse to the entire flow. Sometimes the growth process of the combustion area takes several seconds.

Evaporation in the combustion zone is determined by the speed of the heat transmission, the evaporation heat of the fuel, and the fineness of the dispersion. Evaporation in the combustion zone practically does not depend on the fuel vapors pressure.

the fuel, and also during an increase in flight altitude, it is possible to raise the concentration of the mixture up to a lean blow-out, which sometimes may be preceded by lean concentration pulsations.

Carburation has a substantial effect on the operation of a combustion chamber.

During the flow around the flame holders, the stream lines of the air warp. The drops, which have a much higher density than the air, continue to move almost rectilinearily (Figure 163). The greater the diameter of the drops, the smaller is the curvature of their trajectories in comparison with the curvature of the air stream lines. Therefore, only the finest -- the micron-sized drops -- flow around the flame-holder which is located in the trace of the injector, but the larger drops strike against it, forming a liquid film on the flame-holder surface. A flame-holder enriches a two-phase mixture.

Owing to the irregularity of the concentrations in the dispersion jet to the transport of vapors and the evaporization of the liquid film formed on the flame-holder, the mixture on the edges of the flame-holder contains a significantly higher percent of fuel than does the flow which moves past the flame-holders:

$$\alpha_{st} < \alpha_{sr}.$$

If an electric sparkplug, located behind the flame-holder so that no drops of the liquid fall on it, serves as an ignition source, then a quantity of vapor sufficient for burning must arise in the carburation zone, since only vapors and micron-sized drops actually penetrate into the space behind the flame-holder. If a precombustion chamber or pilot light serve as the ignition source, then the evaporation of the drops may reach the required value in the ignition jet, wherefrom the evaporation and combustion gradually diffuse to the entire flow. Sometimes the growth process of the combustion area takes several seconds.

Evaporation in the combustion zone is determined by the speed of the heat transmission, the evaporation heat of the fuel, and the fineness of the dispersion. Evaporation in the combustion zone practically does not depend on the fuel vapors pressure.

In the beginning of the combustion area the zones of velocities, concentrations, and temperatures are sharply irregular. The equalization of the zones takes place only at a sufficiently great distance from the flame-holders (see Figure 162): the greater the degree of turbulence, the quicker the zones equalize. The temperatures, pressures, and velocities which enter into the gas dynamic equations, derived in Section 8 of this chapter, represent but cross-section averages. Thus, one may speak about average velocities, average pressures, and average accelerations of the flow in a combustion chamber.

The disintegration, evaporation and combustion of the drops, ending by the mixing of the combustion products with the air and the equalization of the temperature and velocity profiles, must proceed in but a few milliseconds. In combustion chambers of insufficient length these processes are not successfully completed. The incompleteness of combustion and the irregularity of the zones before the nozzle inlet reduce the thrust characteristics of a combustion chamber. If $w_2 \simeq 100$ m/sec and the degree of turbulence of the flow in the combustion chamber is $\varepsilon = 0.1$, then $w_{\text{пульс}} = \varepsilon w_2 \sim 0.1 \cdot 100 = 10$ m/sec, i.e., the pulsation velocity, which determines the velocity of the turbulent flame propagation, will be ten times greater than the normal velocity, which computed for hydrocarbons is near 0.4 m/sec. In this way, the combustion of a fuel-air mixture and the uniformity of the concentration, temperature, and velocity zones, are determined by the intensity of the flow turbulence in the combustion chamber, the fineness of the dispersion, and the relative positioning of the injectors and flame-holders. By increasing the degree of turbulence, it is possible to substantially shorten the combustion area.

Pressure drops along the combustion chamber as the mixture burns out and the average flow velocity increases. According to the pressure drop along the combustion chamber, it is possible to approximately judge the combustion of the mixture. Combustion terminates at that point where the pressure practically ceases to decrease (see Figure 152).

Subsonic ramjet engines are sometimes used to rotate helicopter rotors. The helicopter ramjet engines are located at the ends of the rotor blades, the circumferential velocity of which lies within the limits from 200 to 300 m/sec (Figure 164).

An engine, which is located at the end of a rotating blade, undergoes a very large centripetal acceleration:

$$j = \frac{u^2}{R} \cdot \qquad (8.42)$$

Here u is the circumferential velocity;

R is the radius of rotation, i.e., the distance from the axis of the rotor to the axis of the engine.
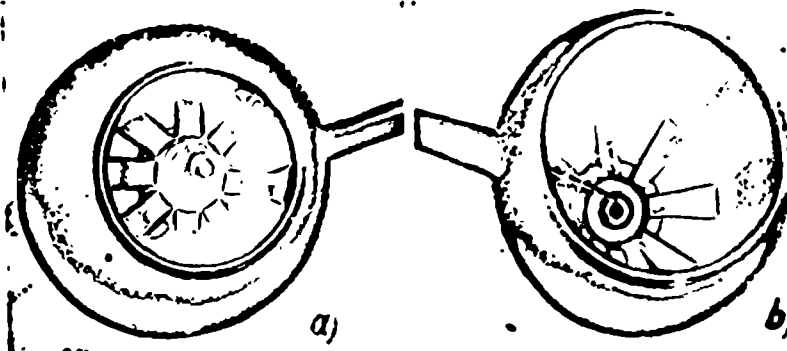
Fig. 164. The combustion chamber of a helicopter engine.
a -- front view, b -- back view.

When R = 5 m and u = 250 m/sec, $j = \frac{250^2}{5} = 12,500$ m/sec^2 = 1,250 gm.

Tremendous centripetal accelerations, more than a thousand times greater than the accelerating forces of gravity, have a substantial effect on the operation of a combustion chamber of a helicopter ramjet engine.

It is convenient to consider the combustion chambers of a helicopter ramjet engine in a system of coordinates, which are connected with the revolving rotor (Figure 165).

From the viewpoint of an observer who moves together with engines, a centrifugal force df acts on each element of mass dm:

$$df = j \frac{dm}{g} = \frac{\gamma u^2}{gR} dV. \qquad (8.43)$$

Here γ is the density in kg/m^3;

dV is the element of volume.

The centrifugal forces act on the structural elements of the engine, creating elastic stresses in them, on the gases which flow through the engine, and on the drops that are carried along by the flow. The centrifugal forces, tending to tear the engine away from the rotor, act on each gram of structural mass, exceed one kg of force. The engine support, which weighs 5 kg, must endure a force of nearly 6 m.

The centrifugal forces tend to draw the flow away from the axis of the engine: gradients of pressures and densities appear in the flow (Figure 166):

$$\operatorname{grad} p = \frac{dp}{dx} = \frac{df}{sdx} = \frac{df}{dV} = \frac{\gamma u^2}{gR} = \gamma \frac{j}{g}. \qquad (8.44)$$

When j = 1,250 gm; grad p = 0.125·1,250 = 150 kg/m^2·m = 0.015 atm/m.

The pressure gradient may be considered as constant along the entire section of the combustion chamber, since the radius of rotation R is large in comparison with the diameter of the combustion chamber.
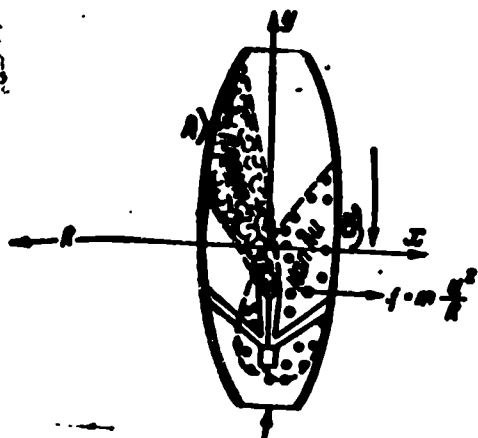
Fig. 165. The system of coordinates for computation of rotating helicopter engines.
A) Flame; B) Drops.
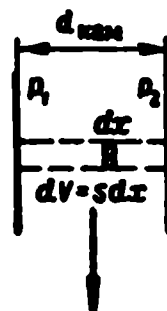
Fig. 166. The calculation of the pressure gradient in centrifugal force fields.

The difference of the gas pressures on the outside and inside of the engine is

$$\Delta p = d_{kam} \operatorname{grad} p = \frac{\gamma u^2}{g} \frac{d_{kam}}{R}, \qquad (8.45)$$

where d_{kam} is the diameter of the combustion chamber.

When

$$d_{kam} = 0.2\,\text{m and}\,\operatorname{grad} p = 0.015\,\text{atm/m}$$
$$\Delta p = d_{kam} \operatorname{grad} p = 0.2 \cdot 0.015 = 0.03\,\text{atm} = 3\ \text{kg/m}^2.$$

In this way it is possible to disregard the pressure difference at the walls of the helicopter engine and the corresponding difference of densities.

From the viewpoint of an observer, who moves with the engine, centrifugal forces, while acting on the drops which move within the chamber, impart a centrifugal acceleration to them. Under the action of the centrifugal forces, the drops depart from the axis of rotation (see Figure 166).

For dt time the drops break away from the rotation axis at a distance of dx:

$$dx = \frac{1}{2} j (dt)^2. \tag{8.46}$$

The radial velocity of the drops for this time grows with an increase of dw_R:

$$dw_R = j dt. \tag{8.47}$$

With the increase of the radial velocity w_R the aerodynamic drag of the drops grows and their acceleration decreases.

If the time of the drops' movement from the injectors to the flame-holder is equal to three microseconds and the acceleration $j = 12{,}500$ m/sec^2, then the displacement of the drops from the axis of rotation would reach 56 mm. Besides, during such great time intervals, the radial velocity may grow by $\Delta w = j \Delta t = 12{,}500 \cdot 0.003 = 37.5$ m/sec, and the acceleration of the drops may not be considered as constant; the true displacement of the drops is less than 56 mm.

The differential equations of the drops' movement in a field of centrifugal forces may be successfully integrated only in the event if one assumes that the aerodynamic forces are proportional to the first degree of velocity. This is correct when Re <1, i.e., for micron-sized drops. Their contribution of fuel to the dispersion spectrum is very small.

Within a certain time, the radial velocity of the drops reaches such a value, at which the aerodynamic force f_a becomes equal to the centrifugal force f:

$$c_x \frac{\pi d_k^2}{4} \frac{\gamma_b w_{oтн}^2}{2g} = m \frac{j}{g} = \frac{\pi d_k^3 \gamma_k}{6g} \frac{u^2}{R}. \tag{8.48}$$

From this

$$\frac{w_{oтн}}{u} = \sqrt{\frac{4}{3 c_x} \frac{\gamma_k}{\gamma_b} \frac{d_k}{R}}. \tag{8.49}$$

If $\gamma_k = 800$ kg/m^3; $\gamma_v = 1.225$ kg/m^3; $c_x = 1.2$, then

$$\frac{w_{oтн}}{u} = \sqrt{\frac{4}{3 \cdot 1.2} \frac{800}{1{,}225} \frac{d_k}{R}} = 26{,}9 \sqrt{\frac{d_k}{R}}.$$

When $d_k = 100 \, \mu = 10^{-4}$ m, $R = 5$ m and $u = 250$ m/sec

$$\frac{w_{otn}}{u} = 26.9 \sqrt{\frac{10^{-4}}{5}} = 0.12; \quad w_{otn} = 30 \text{ m/sec.}$$

The maximum possible displacement is equal to the product of the relative velocity w_{otn} and the time interval Δt:

$$\Delta x_{max} = w_{otn} \Delta t = u \sqrt{\frac{4}{3c_x} \frac{\gamma_k}{\gamma_o} \frac{d_k}{R}} \Delta t, \tag{8.50}$$

The time of the drops' movement through the combustion chamber has the following magnitude:

$$\Delta t \approx \frac{l}{w_2} \approx \frac{nl}{u}. \tag{8.51}$$

Here l is the length of the combustion chamber;

n is the relative expansion of the engine

$$n = \frac{S_2}{S_u} \approx \frac{u}{w_2}. \tag{8.52}$$

In this way

$$\frac{\Delta x_{max}}{l} = \frac{w_{otn} \Delta t}{l} = \frac{w_{otn}}{u} \cdot n = n \sqrt{\frac{4}{3c_x} \frac{\gamma_k}{\gamma_o} \frac{d_k}{R}}. \tag{8.53}$$

The maximum possible relative displacement of the drops, if $\dfrac{\gamma_k}{\gamma_v}$ and n are given, depends only on their diameters and on the radius of rotation.

The last formula is for a tentative calculation of the centrifugal displacement of the drops in the combustion chambers of helicopter engines.

The centrifugal forces which act upon the cold air and upon the combustion products are not similar, since their densities are different. According to the general law of relativity, the movement of hot and cold gases in the field of centrifugal forces, may be likened to motion in the field of gravity. The hot gases "float up" in the direction opposite to that of the actuating forces, while the suspended drops and the cold gases "sink", i.e., move away from the center of rotation (see Figure 166). The denser air masses and the suspended drops move away from the axis of rotation, while the combustion products with a lesser density approach this axis.

The force which compels one volume element of hot gas dV — which has a density γ_g and is surrounded by cold air with density γ_v — to move towards the axis of rotation, just like the lifting force of gas (in the field of gravity), is equal to:

$$df = \frac{u - u_r}{\ell} \frac{u}{R} dV.$$ (8.54)

Acceleration j, with which the examined gas mass $dm = \gamma_{gaz} dV$ will approach the axis of rotation, is equal to (8.55)

$$J = \frac{g \, df}{dm} = \left(\frac{T_x}{T_{ras}} - 1\right) \frac{u^2}{R}.$$

If the initial velocity of the gases in a combustion chamber $w_2 = \frac{u}{n}$ and the temperature ratio $\theta = \frac{T_g}{T_x}$, then the velocity towards the combustion end will be equal to

$$w_r = w_x \frac{T_r}{T_x} = \frac{u}{n} \frac{T_r}{T_x}.$$

The average velocity of the movement of gases through the combustion chamber is

$$w_{cp} = \frac{w_x + w_r}{2} = \frac{u}{2n}\left(1 + \frac{T_r}{T_x}\right).$$

The stay of gases in the combustion zone Δt is approximately equal to

$$\Delta t = \frac{l_r}{w_{cp}} = \frac{2l_r n}{u} \frac{T_x}{T_r + T_x},$$ (8.56)

where l_g is the length of the combustion zone.

The density variation of the hot gases is

$$\frac{T_x}{T_{ras}} = \frac{T_r}{T_x}; \quad \frac{T_x}{T_{ras}} - 1 = \frac{T_r - T_x}{T_x}.$$

On the basis of (8.55) and (8.56) the displacement of the hot gases towards the axis of rotation during combustion is approximately equal to

$$\Delta x = \frac{1}{2} J (\Delta t)^2 = \frac{u^2}{2R} \frac{T_r - T_x}{T_x} \frac{4 l_r^2 n^2 T_x^2}{u^2 (T_r + T_x)^2}.$$

The relative displacement of the gases is

$$\frac{\Delta x}{l_r} = \frac{2n^2 T_x l_r}{R} \frac{T_r - T_x}{(T_r + T_x)^2} = n^2 \frac{l_r}{D} \frac{T_x \Delta T}{T_{cp}^2}.$$ (8.57)

Here D is the rotor diameter

$$T_{cp} = \frac{T_r + T_x}{2}.$$

The last formula is suitable for the approximate calculation of the displacement of the hot jet in the combustion chamber of a helicopter engine.

To decrease the relative displacement of the burning stream one must equalize the temperature gradient so the temperature difference ΔT between the combustion products and the gas surrounding them would be the least. When $\Delta T = 0$, $\Delta y = 0$.

After equating Δx to the radius of the combustion chamber r_{kam}, it is possible to find the length l_{pred} at which the combustion products would be displaced from the center of the combustion chamber to the side. If $\Delta x = r_{kam}$, then from (8.57) we obtain

$$\frac{l_{\text{зон}}}{r_{\text{кам}}} = \frac{T_{cp}}{n}\sqrt{\frac{D}{r_{\text{кам}}T_x\Delta T}}.\tag{8.58}$$

It is necessary to consider the displacement of the hot combustion products during the design of helicopter engine combustion chambers.

__Example.__ Find the relative length of the combustion zone which is sufficient for the hot streams to be displaced from the center out to the side of a helicopter combustion chamber, if r_{kam} = 100 mm, D = 10 m, n = 5; T_x = 300° K, and T_g = 2,300° K

$$\Delta T = T_r - T_x = 2300 - 300 = 2000°; \quad T_{cp} = \frac{T_r + T_x}{2} = 1300° \text{ K};$$

$$\frac{l_r}{r_{\text{кам}}} = \frac{T_{cp}}{n}\sqrt{\frac{D}{r_{\text{кам}}T_x\Delta T}} = \frac{1300}{5}\sqrt{\frac{10}{0,1\cdot 300\cdot 2000}} = 3,4$$

SECTION 11. CHARACTERISTICS OF COMBUSTION CHAMBERS

The characteristics which describe the dependence of the heat release coefficient or combustion efficiency φ_{sg} and the drag coefficient of the combustion chamber ζ upon the air surplus α for a given stagnation pressure of the freed stream flow and for a given nozzle area ratio, have the highest importance.

Such a combustion chamber, in which through the entire operating range of mixture compositions the combustion efficiency φ_{sg} is close to one, φ = 1, and drag coefficient is close to zero ζ = 0, is ideal.

In practice an ideal combustion chamber could not be built.

With an increase of the fuel feed to $\alpha < 1$ the combustion efficiency decreases due to insufficient oxygen. The pressure factor of the combustion chamber σ_k, which is dependent on the velocity of the flow, increases with a decrease of the surplus air α because of velocity losses in the beginning of the combustion chamber w_2 and the decrease of the relative velocity λ_2.

An increase of the inlet area ratio $S_{hcr} = \frac{S_{hcr}}{S_k}$, which determines the gas flow through the chamber, is accompanied by an increase of velocity in the beginning of the chamber w_2 and an increase of the relative velocity λ_2. The local pressure losses increase thereby and the combustion efficiency φ_{sg} diminishes.

With an increase in flight altitude H the pressure in a combustion chamber decreases and may become lower than 760 mm of mercury. During an excessive pressure drop the conditions for carburation and combustion deteriorate and the combustion efficiency decreases. Especially noticeable is the drop of φ_{sg} with altitude in subsonic combustion chambers in which the stagnation pressure may exceed the atmospheric pressure by no more than 1.8 times. Supersonic combustion chambers, in which the stagnation pressure is tens of times greater than that of the atmosphere, maintain good combustion efficiency to significantly greater altitudes than do subsonic chambers.

With increasing flight velocity the stagnation pressure and temperature of the free stream flow are increased. With an increase of flight velocity M_n, the velocity in the beginning of the combustion chamber w_2 increases until the relative critical section of the exhaust nozzle remains constant. When $M_n > 3$ the compressibility of air becomes so significant, that the necessity to decrease the critical section of the engine appears, as was shown in Chapter III for ideal ramjet engines (see Figure 54). After passing $M_n \approx 3$ the through sections of the engine must be reduced, the velocity in the beginning of the combustion chamber diminishes, but the stagnation pressure and temperature continue to grow. The greater the velocity of the oncoming flow M_n, the better the combustion conditions in supersonic engines; the greater the altitude, the more complete the combustion, and the lesser the drag of the chamber. It is more simple to organize combustion in supersonic combustion chambers than in subsonic ones.

The temperature of the boundary layer of a body, which is swept over by a supersonic flow, is 10-15% less than the stagnation temperature. At supersonic velocities the temperature of the outside walls of the compression and carburation sections of an engine is hundreds of degrees above zero, while during a flight in the stratosphere at subsonic velocities, it falls to several tens of degrees below zero.

The walls of the combustion chamber in the combustion zone are swept over from the outside by the air flow, the temperature of which is close to the stagnation tempera-

ture T_{Cn}, and from the inside, by the hot gases, whose temperature is close to T_{Og}.

The cooling of the combustion chamber by the surrounding air is possible, if $O_n < 700°$ K, i.e., when $M_n < 3.5$. During higher flow velocities it is impossible to permit direct contact between the combustion products and the walls of the combustion chamber: it is necessary to arrange this by blowing air along the walls from the inside.

If the unburned gases contact the walls of the chamber the temperature of the gases falls below the ignition temperature T_{VOSD} and combustion ceases -- the presence of the cold walls lowers the combustion efficiency. Therefore, for a high-efficiency combustion chamber the intensive cooling of the walls is undesirable. The most advantageous temperature for the inner walls is $T_{VOSD} > 800°K$.

SECTION 12. PULSATIONS IN COMBUSTION CHAMBERS

The column of air, which is enclosed in a combustion chamber at each moment, may oscillate with its natural frequency. The portions of the oscillating air column move parallel to the axis of the combustion chamber (Figure 167a). The movement of the individual masses of the oscillating gas column is similar to the movement of connected pendulums, the suspension line of which moves along the axis of the chamber with a velocity of w, equal to the average flow velocity (Figure 167b).

The velocity at which the pressure impulses pass from one mass of air to another, is equal to the local speed of sound $c = \sqrt{gkRT}$. During the combustion of the flow, the temperature of the gases T, and together with it, the average velocity of the impulse propagation varies. The average speed of sound in the combustion products is always higher than the average speed of the gases' movement through the combustion chamber; therefore the masses of gas, which flow through the combustion chamber, moving from the inlet section to the outlet, successfully accomplish several complete oscillations. If the frequency of the impulses which cause the oscillations coincides with the natural oscillation frequency of a gas column in a combustion

chamber; then the amplitude of the oscillations may become very large.

The gases, which flow through the chamber, perform a complex movement: they move along the combustion chamber at variable velocity and oscillate. The oscillation propagation velocity in the chamber is not constant; therefore, the oscillatory phenomena which accompany combustion are very complex. It is possible to draw the following simple picture in the first approximation.
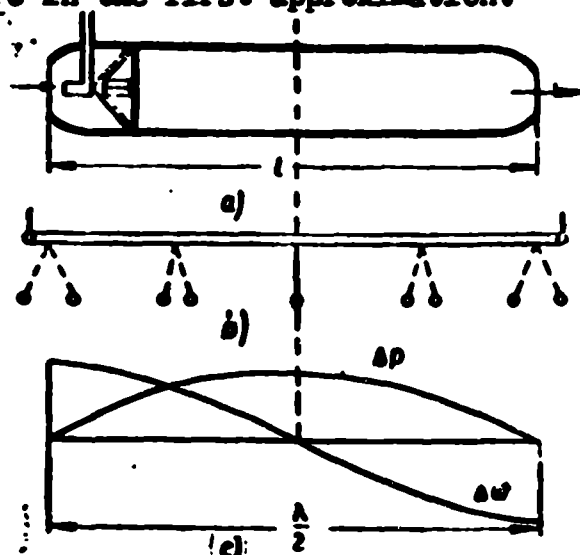
Fig. 167. The oscillation of the air column in a combustion chamber.
a -- a diagram of the chamber, b -- a mechanical analogy, c -- pressure and velocity waves.

Standing waves appear in the flow which passes through a combustion chamber. The average velocity of the flow and the average pressure of the gases in a standing wave vary. The greatest variations of the average velocity -- velocity antinodes -- take place at the chamber inlet and at the outlet after it. The variation
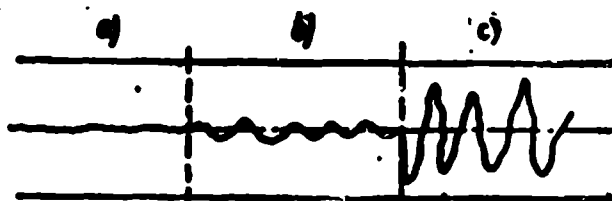
Fig. 168. An oscillogram of the pressures in a combustion chamber.
a -- quiet combustion, b -- rough combustion, c -- pulsating combustion.

of the flow velocity in the center of the chamber is insignificant: a velocity node is formed in the center of the combustion chamber (Figure 167c). The pressure variations at the combustion chamber inlet and outlet are insignificant: pressure nodes appear on the edges of the chamber. The greatest average pressure variations -- the pressure antinodes -- take place in the center of the chamber.

One half of a standing wave fits the air column, the length of which is equal

of the total length of the combustion chamber $l \div r$.

$$l = \frac{\lambda}{2}.$$

It is possible to find the natural acoustical frequency of the oscillations of an air column f_{sob} from the known ratio

$$f_{sob} = \frac{c_{sr}}{\lambda} = \frac{\sqrt{gkRT_{sr}}}{2l},$$

where C_{sr} is the average velocity of sound for the entire chamber.

When $k = 1.4$ and $R = 29.3$ kg m/kg degree:

$$f = \frac{10}{l}\sqrt{T_{sr}} \; 1/cek.$$

If $l = 2$ m and $T_{sr} = 400^\circ$ K, $f = \frac{10}{2}\sqrt{400} = 100 \; 1/sec$

With an increase of the average temperature of the gases T_{sr}, their natural frequency increases, but with an increase of chamber length it decreases.

The oscillations of the air in a combustion chamber at a frequency of f_{sob} may be measured with the aid of an oscillograph (Figure 168). In the absence of combustion the amplitudes of the velocities and pressures Δv and Δp are insignificant in comparison with the average velocity w_{sr} and the average pressure in the chamber p_{sr} (Figure 168a).

The combustion process usually increases the amplitude of oscillations of gases in a combustion chamber. If the amplitudes of pressure during combustion and during the absence of combustion are approximately the same, the combustion is called quiet (Figure 168a). If the amplitudes of the oscillations increase several times during combustion, but remain substantially less than the average pressure in the chamber, the combustion is called "rough" (Figure 168b). Rough combustion is accompanied by a loud noise. If the amplitudes of the pressure become commensurate with the average excess pressure in the combustion chamber, the combustion is called pulsating (Figure 168c). The pulsations of the pressure cause a heavy jolting and may lead to engine break-up. Rough and pulsating combustions are inadmissable in ramjet engines.

In order to predict in each concrete instance, what changes in heating will be caused by the velocity variations of the flow, it is necessary to have an exhaustive understanding about the processes in the combustion zone.

Contemporary information about turbulent combustion is insufficient for this. The formation of turbulent combustion is usually sudden in each definite case. The pulsations are stopped by shortening the length of the combustion chamber, by changing the composition and temperature of the mixture, and by changing the shape of the flame-holders and the relative location of the flame-holders and the injectors.

One of the basic reasons for the formation of rough and pulsating combustion is carburation during the combustion of a two-phase homogeneous mixture. Actually, during operation on very rich mixtures, the mixture in the flame-holder area may go out of the ignition limits during a chance increase of the fuel concentrations (for example, during a pressure increase of the fuel feed or during a decrease in the air output). Combustion deteriorates or ceases. The combustion efficiency decreases, the flow velocity grows, the dispersion and evaporability of the fuel improves, and the dispersion jet constricts.

If the increase of the fuel flow seems greater than the increase of the air flow, the mixture is enriched still further and a rich blow-out occurs: combustion ceases. If the effect of the increase of the air consumption will be stronger than the effect of the increase of the fuel concentrations, the mixture becomes lean, enters the ignition limits, and combustion is restored. The thermal resistance increases, the air flow decreases, and the mixture again leaves the ignition limits; combustion deteriorates etc. Rough combustion appears, which, if it envelopes the entire flame-holder, is transformed into pulsating combustion.

If during operation on very lean mixtures, a deterioration of the combustion or a lean blow-out occurs, then the flow velocity increases, the dispersion (which was poor on lean mixtures) is improved, the evaporability increases, and the jet constricts. If the effect of the increase of the fuel concentrations will be stronger than the effect of the increase of the air flow, the mixture enters the ignition limits and combustion is renewed. The velocity decreases, the dispersion deteriorates, the fuel content is lowered, and combustion again ceases, etc. Rough combustion begins, which may be transformed into pulsating combustion.

1. Voprosy raketnoy tkhniki /Problems of Rocket Technology/ 1956, No. 4, 173.

2. Berkley, J., Metodika rascheta kamer sgoraniya PVRD i forsazhnykh kamer na osnove kharakteristik ustoychivosti goreniya i raspredeleniya topliva /A Method for Calculating the Combustion Chambers of Ramjet Engines and Precombustion Chambers on the Basis of the Characteristics of the Stability of the Combustion and the Atomization of the Fuel/, "VRT", 1956, No. 2.

3. Inozemtsev, N. V., Aviatsionnyye gazoturbinnyye dvigateli /Aircraft Gas Turbine Engines/, Oborongiz, 1955.

4. Idel'chik, I. Ye., Spravochnik po gidravlicheskomu soprotivleniyu fasonnykh i pryamykh chastey truboprovodov /A Handbook on the Resistance of Shaped and Straight Sections of Piping/ TSAGI /Central Aero-Hydrodynamic Institute/, 1950.

5. Makarov, A. N. and Sherman, N. Ya., Raschet drossel'nykh ustroystv /The Calculation of Throttle Units/, Metallurgizdat /Metallurgical Printing House/, 1953.

6. Spalding, D. B., Eksperimenty po goreniyu i gasheniyu zhidkogo topliva na sharovikh poverkhnostyakh /Experiments in the Combustion and Quenching of a Liquid Fuel on Spherical Surfaces/, Fuel, vol. 32, 1953, No. 2, 169.

7. Khudyakov, G. N., O gorenii kapli zhidkogo topliva, nakhodyashcheysya v polete /About the Combustion of the Drops of a Liquid Fuel which are in Flight/ Academy of Sciences, USSR, OTN /Department of Technical Sciences/, 1949, 4.

8. Sheferd, U. F., Vosplameneniye gazovykh smesey impul'sami davleniya /The Ignition of Gas Mixtures by Pressure Impulses/ Collection Voprosy goreniya /Combustion Problems/, Part 2, printed in foreign literature, 1953.

9. Burgoyne, J. and Richardson, J., Fuel, v. 28, 1949, 2.

10. Longwell, J., "Combustion Problems in Ramjet Desing.," Journ. of the Aer. Sciens. v. 16, XII, 1949.

11. Godsave, G., Fourth Symposium on Combustion, 1953, 818.

12. Mullen, J., Fenn, J. B. and Garmon, R. C., "Burners for Supersonic Ramjets," Indust. and Eng., Chemistry, v. 43, I, 1951, 195-211.

13. McClure, F. T. and Berl, W. G., "Combustion," Ind. and Engin. Chemistry, v. 45, 1953, No. 7.

14. Coward, H. F., Hartwell, F. J., and Georgson, E. H., Journ. Chem. Soc., 1937, 1482

15. Rex, J. F., Fuhs, A. E. and Penner S. S., "Interference Effects During Burning in Air for Stationary n-Heptane, Ethyl Alcohol and Methyl Alcohol Droplets," Jet Propulsion, v. 26, 1956, No. 3.

16. Goldsmith, M., "Experiments on the Burning of Single Drops of Fuel," Jet Propulsion, v. 26, 1956, No. 3.

17. DeZubay, A., "Comparative Investigation of a Homogenous Combustion Chamber with a Two-Stage Combustion Chamber," Jet Propulsion, v. 26, 1956, No. 2.

19. Avery, W. H., and Hard, R. W., "Combustor Performance with Instantaneous Mixing," Ind. and Eng. Chem., v. 45, VIII, 1955, 1634-1637.

20. Issledovaniye fizicheskikh osnov rabochego protsessa topok i pechey /An Investigation of the Physical Foundations of the Operating Process of Furnaces and Ovens/ Edited by Vulis, L. A., Printing House of the Academy of Sciences of the Kasakh SSR, Alma Ata, 1957.

CHAPTER IX

SUBSONIC RAMJET ENGINES

Subsonic ramjet engines are intended for flights with velocities that are less than the speed of sound: $w_n < c$; $M_n < 1$; $\lambda_n < 1$.

The stagnation pressure of the oncoming flow exceeds the pressure of the atmoshere not more than 1.89 times during subsonic flight velocities:

$$\frac{p_{0n}}{p_n} = \left(1 + \frac{k-1}{2} M_n^2\right)^{\frac{k}{k-1}} < \left(\frac{k+1}{2}\right)^{\frac{k}{k-1}} = 1.89.$$

Therefore, the thermal efficiency of a subsonic engine is not great:

$$\eta_t = 1 - \left(\frac{p_4}{p_{04}}\right)^{\frac{k-1}{k}} = \frac{k-1}{k+1} \lambda_n^2 < \frac{k-1}{k+1} = 0.167.$$

The total efficiency of a subsonic ramjet engine η does not exceed 7%.

The specific thrust of a subsonic ramjet engine is low even during the most suitable operating conditions:

$$I < \frac{H_u \eta}{A w_n} = \frac{10\,300 \cdot 0.07 \cdot 427}{340} < 1000.$$

With a decrease of flight velocity the efficiency and specific thrust of a subsonic ramjet engine quickly diminish. Therefore, at those velocities, which are less than half the speed of sound, ramjet engines are not used.

The jet thrust of a subsonic ramjet engine changes approximately in proportion to the square of the flight speed; when $w_n = 0$, the static thrust equals zero: a ramjet engine is incapable of self-starting. Rocket and turbo-jet boosters are used for starting aircraft equipped with ramjet engines.

SECTION 1. THE PRINCIPLE DIAGRAM OF A SUBSONIC RAMJET ENGINE

A subsonic ramjet engine consists of a divergent subsonic diffuser, a combustion chamber, and a convergent exhaust nozzle (Figure 169). The stagnation pressure of the oncoming flow is less than critical. A portion of the disposable velocity goes to overcome local resistances and to boost the preheated gases. Therefore, the stagnation pressure ahead of the exit from a subsonic ramjet engine p_{03}, is less than the stagnation pressure of the oncoming flow p_{0n}, and always substantially less than

critical; the velocity of the exhaust gases is less than the speed of sound:

$$M_{l_4} = K \ M_n < 1.$$
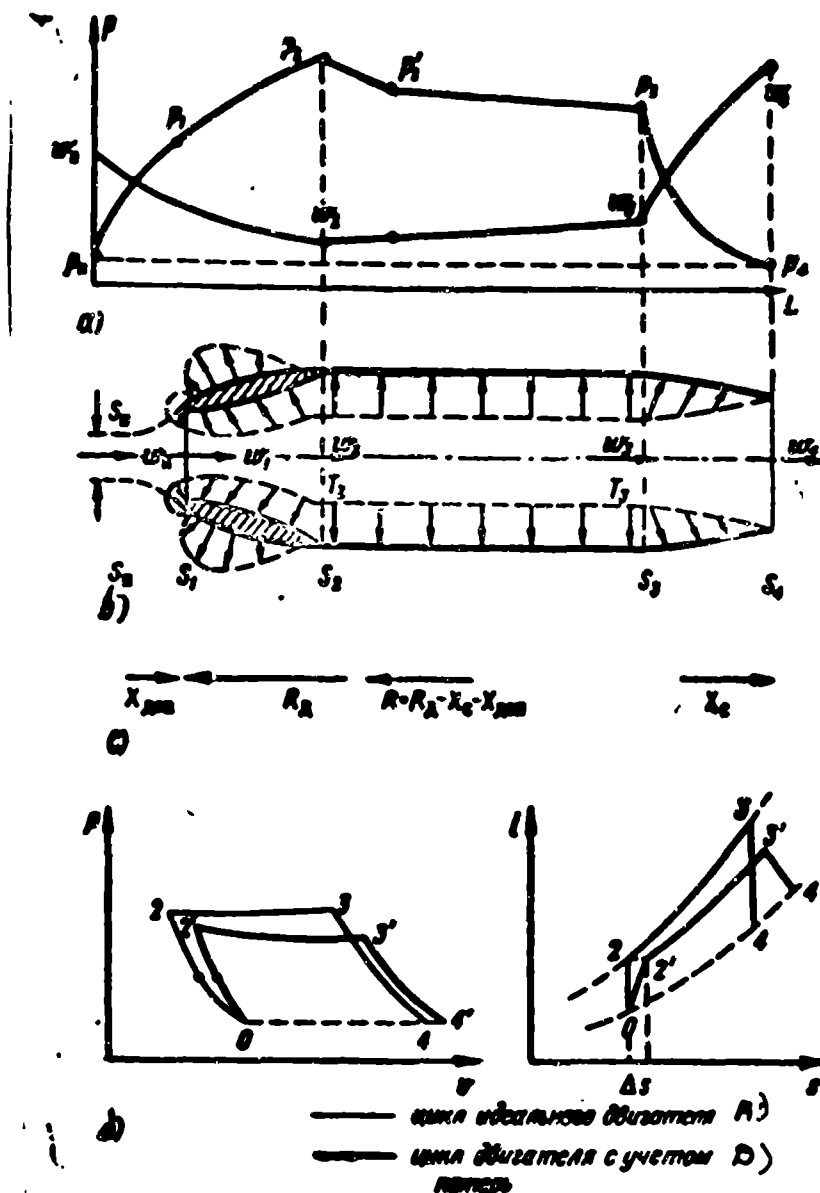
Fig. 169. An actual subsonic ramjet engine.
    a -- a diagram of the velocities, temperatures, and pressure along the engine duct,
    b -- diagram of the pressures on the walls, c -- direction of the actuating forces, d -- p-v and i-s diagrams of the operating cyclo of an engine.
Legend: A) cycle of an ideal engine; B) cycle of an engine with losses calculated.

The velocity at the inlet section is not equal to the flight velocity:

$w_1 \gtrless w_n$. With a small relative exhaust section $\dfrac{S_{l_4}}{S_1}$ or for a large relative preheating of the gases $\theta = \dfrac{T_{0l_4}}{T_{0n}}$, the air flow G through the engine is low and the velocity at the inlet w_1 is less than the velocity of the oncoming flow: $w_1 < w_n$; the diffuser operates with external ramming. With an increase of the exhaust section of the engine S_{l_4} or with a decrease of the relative preheating θ, the air flow G through the engine increases, the velocity at the diffuser inlet increases and may become greater than the velocity of the oncoming flow w_n, but may not exceed the

speed of sound $M_1 \lesssim M_n < 1$.

The flow through the diffuser is accompanied by losses which have their greatest value the greater the velocity is at the inlet to the engine w_1. The stagnation pressure of the oncoming flow at the diffuser exhaust is less than the stagnation pressure of the oncoming flow:

$$\sigma_2 = \frac{p_{02}}{p_{0n}} < 1.$$

Turbulence rings, fuel injectors, ignition units, and flame-holders are installed at the inlet to the combustion chamber. The static air pressure grows during the flow through the diffuser: $p_2 > p_n$, but during the flow around the local burner resistances somewhat decreases. During preheating in the combustion chamber, the flow velocity of the gases increases and the stagnation pressure and static pressure decrease.

$$T_{04} > T_{02}; \quad w_{04} > w_2; \quad \frac{p_{04}}{p_{02}} = \sigma_{cr} < 1,$$

The pressure of the gases in the exhaust nozzle lowers to approximately that of the back pressure: $p_4 \approx p_n$, the flow velocity increases, remaining less than the local speed of sound:

$$w_4 = \varkappa K w_2 \sqrt{\theta} < c_4.$$

With a sufficiently large preheating θ, the flow velocity w_4 becomes greater than the velocity of the oncoming flow:

$$\frac{w_4}{w_2} = \frac{c_4 \lambda_4}{c_2 \lambda_2} = \varkappa K \sqrt{\theta} > 1.$$

Because of the increased amount of the air's movement, jet thrust R appears:

$$R = \frac{G_4 w_4}{g} - \frac{G_2 c_2}{g} + S_4 (p_4 - p_n).$$

The flow rate of the gases through a subsonic ramjet engine is determined by the relative stagnation pressure after exhaust $\dfrac{p_{04}}{p_4}$, the temperature of the gases T_{04}, and the cross-section of the exhaust nozzle S_4:

$$G_4 = w_4 \gamma_4 S_4 = p_{04} S_4 \sqrt{\frac{2g k_r}{(k_r - 1) R_r T_{04}} \left[\left(\frac{p_4}{p_{04}} \right)^{\frac{2}{k_r}} - \left(\frac{p_4}{p_{04}} \right)^{\frac{k_r + 1}{k_r}} \right]}.$$

The velocity of the flow, which flows around the forward edge of the diffuser shell increases and its pressure decreases (see Figure 169b). A vacuum may appear on the profiled outline of the shell close to the inlet opening. The pressure inside

the diffuser increases and becomes greater than that of the atmosphere. The force of the excess pressure, which acts on the inner surface of the diffuser, is oriented in the direction of motion. The surplus pressure forces, which act on the side walls from within, mutually equalize themselves. The surplus pressure forces, which act on the inner walls of the nozzle, are oriented in the direction opposite to that of the flight (Figure 169c).

The jet thrust of a ramjet engine, which is equal to the difference between the forces of the surplus pressure, applied to the inner walls of the diffuser and nozzle and the additive drag of the diffuser X_{dop}, is applied to the diffuser. This circumstance should be studied in designing.

SECTION 2. THE GAS DYNAMICS OF A SUBSONIC RAMJET ENGINE

It is necessary to have the following data for the gas dynamic calculation of a subsonic ramjet engine: inlet, midship, and exhaust cross sections of the engine S_1, S_M, and S_4; the parameters of the oncoming flow M_n (or λ_n), p_n and T_n; the drag coefficient of the combustion chamber ζ, the pressure recovery in the diffuser σ_d, and the pressure ratio of the nozzle σ_s.

In the gas dynamic calculations a series of the possible values of the temperature ratio θ are set up:

$$\theta = \frac{T_{cr}}{T_{ox}}.$$

(9.1)

The stagnation enthalpy of the engine is constant on all portions up to the heat supply:

$$i_{o_1} = \overline{i_{o_1} = i_{o_2}} = i_{ox}.$$

(9.2)

The specific heat of the air is practically constant, consequently, the stagnation temperature before combustion is constant:

$$T_{o_1} = T_{o_1} = T_{o_2} = T_{ox}.$$

(9.3)

Heat losses through the engine walls are usually comparatively low, therefore, it is possible to assume that the enthalpy of the combustion products also remains constant:

$$i_{o_2} = i_{o_1} = i_{or}$$

(9.4)

$$c_{p3}T_{03} = c_{p4}T_{04} = c_{pr}T_{0r}.$$

If the change of heat capacity is disregarded during the efflux, then

$$T_{03} = T_{04} = T_{0r}.$$

The stagnation temperature after combustion may be considered as constant only insofar as exhaust gases may be disregarded. In reality, the thermodynamic temperature, and consequently, the heat capacity, decrease.

The stagnation parameters of the oncoming flow T_{On}, P_{On}, and γ_{On} are determined from graphs of the gas dynamic functions or by the known formulae:

$$\frac{T_n}{T_{0n}} = \tau(\lambda_n) = 1 - \frac{k-1}{k+1}\lambda_n^2, \tag{9.5}$$

$$\frac{p_n}{p_{0n}} = \pi(\lambda_n) = [\tau(\lambda_n)]^{\frac{k}{k-1}} = \left[1 - \frac{k-1}{k+1}\lambda_n^2\right]^{\frac{k}{k-1}}, \tag{9.6}$$

$$\frac{\gamma_n}{\gamma_{0n}} = \varepsilon(\lambda_n) = [\tau(\lambda_n)]^{\frac{1}{k-1}} = \left[1 - \frac{k-1}{k+1}\lambda_n^2\right]^{\frac{1}{k-1}}. \tag{9.7}$$

The stagnation pressure at the diffuser outlet is

$$\frac{p_{02}}{p_n} = \sigma_d \frac{p_{0n}}{p_n} = \frac{\sigma_d}{\pi(\lambda_n)}. \tag{9.8}$$

The stagnation pressure before combustion p_{02}', p_{02}, depends on the relative velocity λ_2 and on the local drag factor ζ (see 7.17).

$$\frac{p_{02}'}{p_{02}} = 1 - \frac{\zeta k}{k+1}\lambda_2^2 = \sigma_{drag}. \tag{9.9}$$

The relative velocity behind the flame-holder λ_2' is:

$$q(\lambda_2') = \frac{q(\lambda_2)}{\sigma_{drag}}.$$

The lowering of the stagnation pressure during combustion is determined by the equation (8.44)

$$\sigma_{cr} = \frac{p_{03}}{p_{02}} = \beta\sqrt{\theta} \frac{\lambda_{pr}(\lambda_2')}{\lambda_{pr}(\lambda_3)} = \frac{z(\lambda_2')q(\lambda_2')}{z(\lambda_3)q(\lambda_3)}. \tag{9.10}$$

Here

$$\beta = 1 + \frac{1}{\alpha L} = 1 + \frac{G_r}{G_a}; \quad \xi = \sqrt{\frac{k_r + 1}{k + 1}\frac{k}{k_r}\frac{R_r}{R}}. \tag{9.11}$$

The relative velocity after combustion λ_3 is also as yet unknown.

The relative stagnation pressure after exit is

$$\frac{p_{04}}{p_{03}} = \sigma_c. \tag{9.12}$$

$$\frac{p_{04}}{p_{04}} = \sigma_{\Lambda}\sigma_{\text{вест}}\sigma_{0}\sigma_{c}, \quad \frac{p_{04}}{\bar{p}_{4}} = \frac{\sigma_{06}}{\pi(\lambda_{4})}.$$ (9.13)

The relative velocity at the nozzle exhaust λ_4 is:

$$\lambda_4 = \sqrt{\frac{k_r+1}{k_r-1}\left[1-\left(\frac{p_4}{p_{04}}\right)^{\frac{k_r-1}{k_r}}\right]} =$$

$$= \sqrt{\frac{k_r+1}{k_r-1}\left[1-\left(\frac{p_4}{\sigma_{06}p_{04}}\right)^{\frac{k_r-1}{k_r}}\right]} = K\lambda_*.$$ (9.14)

The gas dynamic coefficient of a ramjet engine is

$$K = \frac{1}{\lambda_*}\sqrt{\frac{k_1+1}{k_r-1}\left\{1-\left[\frac{\pi(\lambda_4)}{\sigma_{06}}\right]^{\frac{k_r-1}{k_r}}\right\}}.$$ (9.15)

The flow rate of the gases through the exhaust nozzle (see 2.49 and 2.74) is

$$G_3 = S_4 p_{04}\sqrt{\frac{2gk_r}{(k_r-1)R_rT_{0r}}\left[\left(\frac{p_4}{p_{04}}\right)^{\frac{2}{k_r}}-\left(\frac{p_4}{p_{04}}\right)^{\frac{k_r+1}{k_r}}\right]} =$$

$$= \sqrt{\frac{2gk_r}{(k_r+1)R_r}}\frac{p_{04}S_4 q(\lambda_4)}{\sqrt{T_{0r}}}.$$ (9.16)

We find the relative velocity ahead of the exit by the continuity equation:

$$G_4 = G_3 = G_{mb},$$

$$\sqrt{\frac{2gk_r}{(k_r+1)R_r}}\frac{p_{04}S_4 q(\lambda_4)}{\sqrt{T_{0r}}} = \sqrt{\frac{2gk_r}{(k_r+1)R_r}}\frac{p_{03}S_3 q(\lambda_3)}{\sqrt{T_{0r}}}.$$

From this

$$m = \frac{S_3}{S_4} = \sigma_c\frac{\lambda_4}{\lambda_3}\frac{\varepsilon(\lambda_4)}{\varepsilon(\lambda_3)} = \sigma_c\frac{\lambda_4}{\lambda_3}\left[\frac{1-\frac{k_r-1}{k_r+1}\lambda_4^2}{1-\frac{k_r-1}{k_r+1}\lambda_3^2}\right]^{\frac{1}{k_r-1}}.$$ (9.17)

If the engine is totally open: $S_4 = S_3$, then $\lambda_3 = \lambda_4$. The greater the degree of constriction of the engine $m = \dfrac{S_3}{S_4}$, the lesser the ratio $\dfrac{\lambda_3}{\lambda_4}$ (Figure 170).

If $\lambda_4 = 1$, the equation (9.17) gives (2.53).

We find the relative velocity before combustion by the equation (8.50):

$$\lambda_2 = \frac{\theta}{2}\sqrt{\theta}\left(\lambda_3+\frac{1}{\lambda_3}\right)-\sqrt{\frac{\theta^2}{4}\theta\left(\lambda_3+\frac{1}{\lambda_3}\right)^2-1}.$$ (9.18)

When $\lambda_2 \ll 1$ and $\lambda_3 \ll 1$: $\dfrac{\lambda_3}{\lambda_2} = \beta\dfrac{}{}\sqrt{\theta}$.

On solving this system of six equations (9.9); (9.10); (9.12); (9.14); (9.17); and (9.18) it is possible to find all the parameters of a subsonic ramjet engine λ_2, λ_3, λ_4, $T_{\text{газ}}$, σ_{sg}, and σ_{ob}.
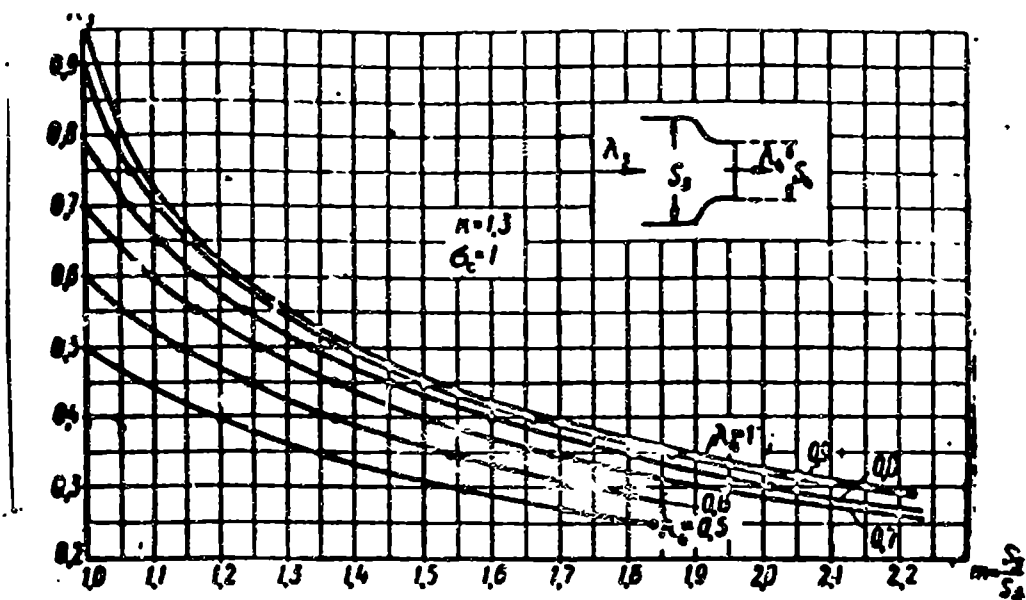
Fig. 170. The dependence of the relative velocity ahead of the nozzle upon the relative velocity at the end of the nozzle.

However, this system boils down to an equation with fractional exponents, the a braic solution of which is not possible. Therefore, a gas dynamic computation of a subsonic ramjet engine is usually carried out by method of successive approximatio:

SECTION 3. A METHOD OF SUCCESSIVE APPROXIMATIONS

The parameters of the free stream flow λ_n, p_n, and T_n, the factors σ_o, ζ, and σ_s, and the engine cross sections S_1, S_k, and S_4 must be known. We will set up the temperature ratio of the gases in the chamber:

$$\theta = \frac{T_{Og}}{T_{Ok}}$$

Let $\lambda_n = 0.9$, $p_n = 140$ mm of mercury, and $T_n = 216.5°$ K, $\sigma_d = 0.95$; $\zeta = 3$, $\sigma_s = 0.97$; $S_1 = 0.3$ m^2; $S_k = 1$ m^2, $S_4 = 0.7$ m^2; $\theta = 7$.

We will calculate the stagnation parameters of the free stream flow

$$\frac{T_{0n}}{T_n} = \frac{1}{\tau(\lambda)} = \frac{1}{1-\frac{k-1}{k+1}\lambda_n^2} = \frac{1}{1-\frac{\lambda_n^2}{6}} = \frac{1}{1-\frac{0.9^2}{6}} = \frac{1}{0.865} = 1.159,$$

$$\frac{p_{0n}}{p_n} = \frac{1}{\tau(\lambda)} = \frac{1}{\left[\tau(\lambda)\right]^{\frac{k}{k-1}}} = \frac{1}{0.865^{3.5}} = 1.159^{3.5} = 1.665,$$

$$\frac{\rho_{0n}}{\rho_n} = \frac{1}{\tau(\lambda)} = \left[\frac{1}{\tau(\lambda)}\right]^{\frac{1}{k-1}} = 1.159^{2.5} = 1.447.$$

The stagnation enthalpy of the oncoming flow is

$$i_{0n} = \frac{i_n}{\tau(\lambda_n)} = \frac{c_p T_n}{\tau(\lambda_n)} = \frac{0.24 \cdot 216.5}{0.865} = 60 \text{ kcal/kg.}$$

The stagnation temperature after combustion is

$$T_{cr} = \theta T_{0a} = 7 \cdot 216,5 \cdot 1,159 = 1760° \, K.$$

While at this temperature according to Figure 86b, $k_g \approx 1.32$; $R_g \approx 29.5$; $\beta \approx 1.04$.

$$\xi = \sqrt{\frac{k}{k_r} \frac{k_1+1}{k+1} \frac{R_r}{R}} = \sqrt{\frac{1,4}{1,32} \frac{2,32}{2,4} \frac{29,5}{29,3}} = 1,017.$$

Noting that the relative velocity at the exhaust differs slightly from the relative velocity of the oncoming flow: $\lambda_4 = K \lambda_n \approx 0.9 \lambda_n$ and after using the graph, which is depicted on Figure 170, or the equation (9.17), we find the first approximation of the reduced velocity ahead of the exit λ_3:

$$\lambda_3 = f\left(\frac{S_4}{S_k} \lambda_4\right) = 0,48.$$

The gas dynamic function is

$$\epsilon(\lambda_3) = \left(1 - \frac{k-1}{k+1}\lambda_3^2\right)^{\frac{1}{k-1}} = \left(1 - \frac{0,35}{2,35}0,48^2\right)^{\frac{1}{0,35}} = 0,902.$$

$$\Pi = \frac{\theta \sqrt{\theta}}{2}\left(\lambda_3 + \frac{1}{\lambda_3}\right) = \frac{1,01 \cdot 1,04 \sqrt{7}}{2}\left(0,48 + \frac{1}{0,48}\right) = 3,455.$$

The relative velocity before combustion, in accordance with (9.18), is

$$\lambda_2' = \Pi - \sqrt{\Pi^2 - 1} = 3,455 - \sqrt{3,455^2 - 1} = 0,148.$$

The pressure coefficient during the flow around the internal units of the combustion chamber and the relative velocity before the flame-holder are found by solution of the graphic equation

$$\frac{q(\lambda_2')}{\sigma_{\text{внеш}}} = q(\lambda_2').$$

From this

$$\lambda_2 = 0,145; \quad \sigma_{\text{внеш}} = 0,962.$$

The pressure preservation factor during combustion (see 8.44) is

$$\sigma_{cr} = \xi \beta \sqrt{\theta} \frac{\lambda_{2a}(\lambda_2)}{\lambda_{2f}(\lambda_3)} = \frac{1,017 \cdot 1,04 \sqrt{7} \cdot 0,148 \cdot 0,991}{0,48 \cdot 0,902} = 0,95.$$

The total pressure recovery factor in the engine is

$$\sigma_{ad} = \sigma_d^2 \sigma_{\text{внеш}}^2 \sigma_{cr} \sigma_c = 0,95 \cdot 0,962 \cdot 0,95 \cdot 0,97 = 0,84.$$

The relative stagnation pressure ahead of the nozzle is

$$\frac{p_{0d}}{p_a} = \sigma_{ad} \frac{p_{0n}}{p_a} = 0,84 \cdot 1,665 = 1,405.$$

Pressure

$$p_{0d} = p_a \frac{p_{0d}}{p_a} = 140 \cdot 1,405 \cdot 13,6 = 2670 \; \kappa z/\mu^2.$$

$$\lambda_4 = \sqrt{\frac{k_r+1}{k_r-1}\left[1-\left(\frac{p_4}{p_{04}}\right)^{\frac{k_r-1}{k_r}}\right]} =$$

$$= \sqrt{\frac{2,35}{0,35}\left[1-\left(\frac{1}{1,405}\right)^{\frac{0,35}{1,35}}\right]} = 0,78.$$

The gas dynamic function is

$$\varepsilon(\lambda_4) = \left(1-\frac{k_r-1}{k_r+1}\lambda_4^2\right)^{\frac{1}{k_r-1}} = \left(1-\frac{0,35}{2,35}0,78^2\right)^{\frac{1}{0,35}} = 0,750.$$

After determining the relative velocity of the exhaust gases λ_4 in the first approximation, we will find a more exact value of the relative velocity ahead of the nozzle by the equation (9.17) or by the graph in Figure 170: λ_3 = 0.46. We will repeat the calculations, using the value of λ_3 that is found.

By a certain practice in the selection of the initial values of the relative velocity ahead of the nozzle λ_3, one succeeds in obtaining a satisfactory coincidence already in the second approximation.

The gas dynamic factor of a ramjet engine is

$$K = \frac{\lambda_4}{\lambda_4} = \frac{0,78}{0,90} = 0,87.$$

The flow rate through the engine is determined by the formula (9.16)

$$G_{rm} = \sqrt{\frac{2gk_r}{(k_r+1)R_r}} \frac{p_{04}S_4}{\sqrt{T_{0r}}} \lambda_4 \varepsilon(\lambda_4) =$$

$$= \sqrt{\frac{2,98\cdot1,35}{2,35\cdot29,5}} \cdot \frac{2670\cdot0,7\cdot0,78\cdot0,75}{\sqrt{1760}} = 16,6 \text{ kg/sec.}$$

Knowing the relative velocity at the exit λ_4 and the flow rate of the gases G_{gas}, it is possible to find the fuel flow and thrust parameters of the engine.

SECTION 4. THE CALCULATION OF THE THRUST PARAMETERS OF AN ACTUAL RAMJET ENGINE

After the relative velocity at the exit λ_1 and the flow rate of the gases G_{gas} have been determined, it is possible to find the fuel flow G_g that is necessary to obtain a given temperature ratio θ, the composition of the mixture, and the thrust parameters of the engine R, c_R, I, and η.

The heating value of the fuel that is used in the engine is denoted by H_u.

According to the law of the conservation of energy

$$i_{0r} = i_{0x} + \frac{H_u \varphi_{cr}}{1 + \alpha L},$$
(9.19)

where φ_{sg} is the combustion efficiency determined by the combustion chamber arra';' ment.

The enthalpy of the combustion products when $T_{0g} = \theta T_{0kh} = 1760^\circ$ K is found by the i-T diagram without allowance for dissociation (see Figure 85) while setting up the possible value of the surplus air $\alpha \approx 2$,

$$i_{0r} = f(T_{0r}, a).$$

$i_{0g} = 490$ kcal/kg
(9.20)

From (9.19) we find

$$\alpha = \frac{H_u \varphi_{cr}}{(i_{0r} - i_{0x}) L} - \frac{1}{L}.$$
(9.21)

When $\varphi_{sg} = 0.95$, $H_u = 10,300$ kcal/kg; $L = 14.9$ and $i_{0kh} = 52$; $\alpha = 1.78$.

The coefficient is

$$\beta = 1 + \frac{1}{\alpha L} = 1.037.$$

The fuel flow is

$$G_r = \frac{G_{ras}}{1 + \alpha L}.$$
(9.22)

The air flow G_v is

$$G_v = G_{ras} - G_r = G_{ras}\left(1 - \frac{G_r}{G_{ras}}\right) = \frac{G_{ras}}{1 + \frac{1}{\alpha L}} = \frac{G_{ras}}{\beta}.$$
(9.23)

The velocity of the free stream flow is

$$w_u = \lambda_u \sqrt{\frac{2g k R T_{0u}}{k + 1}} = \lambda_u \sqrt{\frac{2g k R T_u}{(k + 1)\tau(\lambda_u)}} = 18.3 \lambda_u \sqrt{\frac{T_u}{\tau(\lambda_u)}}.$$

When $\lambda_u = 0.9$ and $T_u = 216.5^\circ$ K; $T_{0u} = \frac{T_u}{\tau(\lambda_u)} = \frac{216.5}{0.865} = 251^\circ$ K,

$a = 18.3\sqrt{251} = 290$ m/sec; $w_u = \lambda_u a = 0.9 \cdot 290 = 261$ m/sec.

The relative velocity increase during discharge is

$$\frac{w_4}{w_u} = \frac{\lambda_4}{\lambda_u} \sqrt{\frac{k_r}{k} \frac{k + 1}{k_r + 1} \frac{R_r}{R}} \sqrt{\frac{T_{0r}}{T_{0u}}} = K_x \sqrt{\theta}.$$
(9.24)

$$\frac{w_4}{w_u} = 0.87 \sqrt{\frac{1.35}{1.4} \frac{2.4}{2.35} \frac{29.5}{29.3}} \sqrt{7} = 2.29.$$

Jet thrust R is determined by the equation (2.91)

$$R = \frac{G_{ras}w_4}{g} - \frac{G_a w_a}{g} + S_4(p_4 - p_a).$$

The static pressure at the exhaust edge of a subsonic engine may only be found experimentally. It usually exceeds the pressure of the surrounding medium insignificantly. For calculations it is assumed that

$$p_4 = p_n$$

Then

$$R = \frac{G_a w_a}{g}\left(\beta\frac{w_4}{w_a} - 1\right) = \frac{G_{ras}w_a}{g\beta}(\beta_x K\sqrt{\theta} - 1). \qquad (9.25)$$

For our example

$$R = \frac{16,6\cdot261}{1,037\cdot9,81}(1,037\cdot2,29 - 1) \approx 600 \quad \text{kg.}$$

or else

$$R = \frac{G_{ras}w_4}{g}\left(1 - \frac{w_a}{\beta w_4}\right);$$

$$R = \frac{K_x\sqrt{\theta}\,G_{ras}w_a}{g}\left(1 - \frac{1}{K\beta_x\sqrt{\theta}}\right) \qquad (9.26)$$

We will use the formula (9.16) for the flow rate of the gases, an express the velocity w_n by the relative and critical velocities:

$$G_{ras} = \sqrt{\frac{2gk_r}{k_r+1}}\frac{p_{ea}S_4q^2(\lambda_4)}{\sqrt{R_r T_{er}}};$$

$$w_a = \lambda_a\sqrt{\frac{2gk}{k+1}RT_{ea}};$$

$$p_{0a} = \frac{p_4}{\pi(\lambda_4)}; \quad \lambda_4 = K\lambda_a.$$

After simple conversions, we obtain a formula in which jet thrust is expressed only by the initial values:

$$R = \frac{2k_r}{k_r+1}\frac{p_{ea}S_4 K^2 q_a^2}{1 - \frac{k_r-1}{k_r+1}K^2 q_s^2}\left[1 - \frac{1}{\beta_x K\sqrt{\theta}}\right]. \qquad (9.27)$$

The frontal, or maximum, thrust R_M is:

$$R_M = \frac{R}{S_M} = \frac{2k_r}{k_r+1}\frac{p_a K^2 q_a^2}{\pi\tau(K\lambda_a)}\left[1 - \frac{1}{\beta_x K\sqrt{\theta}}\right]; \qquad (9.28)$$

Here

$$n = \frac{S_4}{S_M}$$

When the difference decreases $1 - \dfrac{1}{\beta_x K\sqrt{\theta}}$ the thrust diminishes. The relative temperature ratio, at which thrust reverts to zero, is

$$\theta_{\text{пред}} = \frac{1}{\beta_{\text{м}}^2 K^2}.$$ (9.29)

At low temperature ratios $x \to 1$, $\beta \to 1$, and $K = 0.8$. In this case $\theta_R = 0 \to 1.57$.

After expressing the dynamic head as a function of relative velocity λ_n and the atmospheric pressure p_n, we will find the thrust coefficient of a subsonic ram-jet engine c_R by (see 2.70):

$$q = \frac{\gamma_n \omega_n^2}{2g} = \frac{k}{k+1} \frac{p_n \lambda_n^2}{\tau(\lambda_n)};$$ (9.30)

$$c_R = \frac{R_x}{q} = \frac{2k_r}{k_r+1} \frac{k+1}{k} \frac{K^2}{m} \frac{\tau(\lambda_n)}{\tau(K\lambda_n)} \left[1 - \frac{1}{x\beta K \sqrt{\theta}} \right];$$

$$c_R = \frac{2}{m} \frac{R}{R_r} x^2 K^2 \frac{\tau(\lambda_n)}{\tau(K\lambda_n)} \left[1 - \frac{1}{x\beta K \sqrt{\theta}} \right].$$ (9.31)

Here R and R_g are the gas constants of the fresh air and the combustion products.

For an ideal ramjet engine $x = 1$; $K = 1$; $\lambda_u = \lambda_n$; and $R = R_g$, consequently,

$$c_{R\text{ид}} = \frac{2}{m} \left(1 - \frac{1}{\beta \sqrt{\theta}} \right).$$

We obtained this last formula in Chapter III by another method.

During an unlimited temperature ratio $\theta \to \infty$, the thrust coefficient asymptotically approaches the limiting value

$$c_{R\text{пред}} = \frac{2x^2 K^2 R \tau(\lambda_n)}{m R_r \tau(K\lambda_n)}.$$ (9.32)

When $n = 1$, $K = 0.9$, $R_g = R$, and $x = 0.9$ -- $c_{R\text{pred}} < 1.3$.

The economy of the engine is characterized by the specific thrust I:

$$I = \frac{R}{G} = \frac{R \cdot \alpha L}{G_u} = \frac{R(1 + \alpha L)}{G_{r\text{аз}}}.$$ (9.33)

After utilizing the thrust formula (9.25), we obtain

$$I = \frac{\alpha L \omega_n}{g} \left(\beta \frac{\omega_4}{\omega_n} - 1 \right) = \frac{\alpha L c M_n}{g} (x \beta K \sqrt{\theta} - 1) =$$

$$= \frac{\alpha L c M_n}{g} \left(x \beta K \sqrt{1 + \frac{H_a \eta_{cr}}{(1 + \alpha L) c_{p,r} T_{0x}}} - 1 \right).$$ (9.34)

During a leaning out of the mixture, i.e., during an increase of the excess air α, the first factor in the specific thrust equation grows, and the second factor

diminishes. The surplus of air, at which the specific thrust reaches its maximum value, is called the state of maximum economy (see Section 5).

The specific thrust of the fuel C_s, i.e., the fuel consumption per hour per kilogram of thrust, is:

$$C_s = \frac{3600}{I}.\qquad(9.35)$$

The specific fuel consumption becomes least during a condition of maximum economy.

With diminishing temperature ratio, i.e., by increasing α, the gas dynamic factor of a ramjet engine decreases due to the increased losses in the diffuser and in the flow around local resistances (flame-holder). It is not advisable, therefore, to lean out the mixture to $\alpha > 4$.

The total efficiency of an actual ramjet engine is measured by the ratio of the thrust power, which is developed by the engine, to the energy, introduced into the engine per second together with the fuel:

$$\eta = \frac{\overline{N_{ye}}}{N_Q} = \frac{A N_{ye}}{H_u G_r} = \frac{A R w_n r_{cr}}{c_p G_4 (I_{cr} - I_{cx})} = \frac{R w_n r_{cr}}{\frac{kR}{k-1} G_4 T_{cx}\left(\frac{T_{cr}}{T_{cx}} - 1\right)}.\qquad(9.36)$$

After noting that

$$\frac{T_{cr}}{T_{cx}} = \theta,$$

$$R = \frac{G_r w_4}{g} - \frac{G_n w_n}{g} = \frac{G_n w_n}{g}\left(\beta \frac{w_4}{w_n} - 1\right)$$

and

$$\frac{w_4}{w_n} = \varkappa K \sqrt{\theta},$$

we obtain

$$\eta = \frac{w_n^2 r_{cr}}{\frac{g kR}{k-1} T_{cx}} \cdot \frac{\beta \varkappa K \sqrt{\theta} - 1}{\beta(\theta - 1)}.$$

But

$$\frac{w_n^2}{\frac{g kR}{k-1} T_{cx}} = 2\frac{k-1}{k+1}\lambda_n^2 = 2\eta_{y\,ai}.\qquad(9.37)$$

Consequently,

$$\eta = \frac{k-1}{k+1}\lambda_{ny}^2 r_{cr}\frac{\beta \varkappa K \sqrt{\theta} - 1}{\beta(\theta - 1)} = \eta_t \eta_{tr.\,a}.\qquad(9.38)$$

The first fraction represents the thermal efficiency of an ideal ramjet engine the second fraction may be called the active thrust efficiency:

$$\eta_{mr.A} = 2\frac{\beta x K \sqrt{\theta}-1}{\beta(\theta-1)}\varphi_{cr}. \tag{9.39}$$

For an ideal ramjet engine: $\varphi_{sg} = 1$, $x = 1$, and $K = 1$. When $\beta = 1$, we obtain

$$\eta_{mr.ua} = 2\frac{\sqrt{\theta}-1}{\theta-1} = \frac{2}{\sqrt{\theta}+1} = \frac{2}{\frac{w_1}{w_g}+1}. \tag{9.40}$$

The thrust efficiency of an actual ramjet engine goes to zero when $\beta x K\sqrt{\theta} = 1$, i.e., when

$$\theta_{pred} = \frac{1}{(\beta x K)^2}. \tag{9.41}$$

For an ideal ramjet engine $\theta_{pred} = 1$.

The specific thrust of a ramjet engine is connected with the overall efficiency:

$$\eta = \frac{A R w_u}{G_r H_u} = \frac{A l w_u}{H_u},$$

$$l = \frac{H_u \eta}{A w_u} = \frac{H_u \eta}{A a_x \lambda_u}, \tag{9.42}$$

$$l = 2\frac{k-1}{k+1}\frac{H_u}{A}\frac{\lambda_u}{a_x}\frac{\beta x K \sqrt{\theta}-1}{\beta(\theta-1)}\varphi_{cr}. \tag{9.43}$$

The specific thrust is directly proportional to the heating value of the fuel H_u and depends on the relative flight velocity λ_n, the gas dynamic factor K, and on the temperature ratio θ. At a certain optimum temperature ratio θ_{opt} the specific thrust and the thrust efficiency reach maximum (see Section 5). The thermal efficiency η_{tid} of an ideal ramjet engine does not depend on the temperature ratio.

Example. Find the efficiency of a subsonic ramjet engine if $\lambda_n = 0.9$; $\theta = 7$; $x = 0.97$; $K = 0.87$; $\beta = 1.037$; and $\varphi_{sg} = 1$.

The ideal thermal efficiency is

$$\eta_{ui} = \frac{k-1}{k+1}\lambda_u^2 = \frac{0.9^2}{6} = 0.135.$$

The active thrust efficiency is

$$\eta_{mr.A} = 2\varphi_{cr}\frac{\beta x K \sqrt{\theta}-1}{\theta-1} = 2\frac{1.037\cdot0.97\cdot0.87\sqrt{7}-1}{7-1} = 0.437.$$

The total efficiency is

$$\eta_i = \eta_{ui}\eta_{mr.A} = 0.135\cdot0.437 = 0.059.$$

SECTION 5. THE STATE OF MAXIMUM ECONOMY

To compute the surplus air factor at which the specific thrust of an engine reaches its maximum value, we will express the specific thrust by the surplus air factor α [see (9.34)].

$$I = \frac{\alpha L w_n}{g}\left[\frac{1+\alpha L}{\alpha L}\varkappa K\sqrt{1+\frac{H_u v_{cr}^2}{(1+\alpha L)c_{p\,r}T_{ox}}}-1\right] \qquad (9.44)$$

or else

$$I = \frac{w_n}{g}\left[(1-\alpha L)\varkappa K\sqrt{1+\frac{H_u v_{cr}^2}{(1+\alpha L)c_{p\,r}T_{ox}}}-(1-\alpha L)+1\right]. \qquad (9.45)$$

We will introduce the designation

$$1+\alpha L=a; \quad \frac{H_u v_{cr}^2}{c_{p\,r}T_{ox}}=t. \qquad (9.46)$$

Then

$$I = \frac{w_n}{g}\left[\varkappa K\sqrt{a^2+at}-a+1\right]. \qquad (9.47)$$

To determine the state of maximum economy we will find the derivative from I with respect to a and equate it to zero:

$$\frac{dI}{da} = \frac{w_n}{g}\left[\frac{\varkappa K(2a+t)}{2\sqrt{a^2+at}}-1\right]=0. \qquad (9.48)$$

From this

$$\varkappa Ka+\frac{t}{2}\varkappa K=\sqrt{a^2+at}$$

or else

$$a^2+at-\frac{\varkappa^2 K^2 t^2}{4(1-\varkappa^2 K^2)}=0.$$

After solving this quadratic equation, we find

$$a=1+\alpha_{opt}L=\frac{H_u v_{cr}^2}{2c_{p\,r}T_{ox}}\left[\frac{1}{\sqrt{1-\varkappa^2 K^2}}-1\right]=\frac{H_u v_{cr}^2}{2c_{p\,r}T_{ox}}\frac{1-\sqrt{1-\varkappa^2 K^2}}{\sqrt{1-\varkappa^2 K^2}}. \qquad (9.49)$$

The surplus of air, which corresponds to the state of maximum economy, is

$$\alpha_{opt}=\frac{H_u v_{cr}^2}{2Lc_{p\,r}T_{ox}}\left[\frac{1}{\sqrt{1-\varkappa^2 K^2}}-1\right]-\frac{1}{L}. \qquad (9.50)$$

The optimum temperature ratio is:

$$\theta_{opt}=\frac{H_u v_{cr}^2}{(1+\alpha_{opt}L)c_{p\,r}T_{ox}}+1=\frac{2\sqrt{1-\varkappa^2 K^2}}{1-\sqrt{1-\varkappa^2 K^2}}+1,$$

$$\theta_{opt}=\frac{1+\sqrt{1-\varkappa^2 K^2}}{1-\sqrt{1-\varkappa^2 K^2}}. \qquad (9.51)$$

When $\varkappa K = 1$; $\theta_{opt} = 1$; and $\alpha_{opt} = \infty$; when $K \rightarrow 0$; $\theta_{opt} \rightarrow \infty$.

We will note here that the temperature ratio depends only on the gas dynamic factor of a ramjet engine and depends neither on the parameters of the fuel nor on the flight velocity, or the parameter of the surrounding atmosphere.

In a state of maximum economy it may be accepted that

$$\beta_{opt} = 1.$$

The specific thrust in a state of maximum economy is determined from the equations (9.44 and 9.49):

$$I_{cor} = \frac{w_n}{g}\left[(1 + \epsilon_{cor}L) - 1\right]\left[\varkappa K\sqrt{\theta_{cor}} - 1\right],$$

$$I_{cor} = \frac{w_n}{g}\left[\frac{H_u\varphi_{cr}}{2c_{pr}T_{0c}}\frac{1 - \sqrt{1 - \varkappa^2 K^2}}{\sqrt{1 - \varkappa^2 K^2}} - 1\right]\left[\varkappa K\sqrt{\frac{1 + \sqrt{1 - \varkappa^2 K^2}}{1 - \sqrt{1 - \varkappa^2 K^2}}} - 1\right]. \tag{9.52}$$

The thrust efficiency in a state of maximum economy is found by substituting (9.51) in (9.39) and after making simple conversions:

$$(\eta_{tar})_{max} = 2\frac{\varkappa K\sqrt{\theta_{cor}} - 1}{\beta(\theta_{cor} - 1)} \qquad \varphi_{ac} = \left(\frac{1}{\beta} - \frac{1 - \beta\varkappa^2 K^2}{\beta\sqrt{1 - \varkappa^2 K^2}}\right)\varphi_{cr}. \tag{9.53}$$

When $\beta = 1$ and $\varphi_{sg} = 1$, $(\eta_{tyag})_{max} = 1 - \sqrt{1 - x^2 K^2}$.

Thrust efficiency as a function of the gas dynamic factor of a ramjet engine K is depicted in Table 9.1.

Table 9.1

THE DEPENDENCE OF THE OPTIMUM PARAMETERS OF A RAMJET ENGINE ON THE GAS DYNAMIC FACTOR $K = \frac{\lambda_4}{\lambda_n}$ when $x = 1$, $\lambda_n = 0.9$; $T_n = 216.5^\circ$ K; $\beta \approx 1$; $\eta_{tid} = 0.135$.

K	0,95	0,90	0,85	0,80	0,75
$\sqrt{1 - K^2}$	0,317	0,434	0,524	0,60	0,663
$(\eta_{tar})_{cor}$	0,683	0,566	0,476	0,400	0,337
θ_{cor}	1,94	2,53	3,2	4,0	4,92
$\left(\frac{w_4}{w_n}\right)_{cor} = \varkappa K\sqrt{\theta}$	1,32	1,43	1,52	1,60	1,66
$1 + \epsilon_{cor}L$	178	107	75	55	41,5
ϵ_{cor}	12	7,15	4,96	3,62	3,35
I_{max}	1530	1230	1040	875	730
C kg/kg hr	2,35	2,93	3,46	4,11	4,93

At any given flight velocity λ_n or M_n, after determining the gas dynamic factor K, it is possible to choose a temperature ratio so that the specific thrust and the thrust and total efficiencies would be the greatest.

With an increase of flight velocity the thermal and overall efficiencies increase in direct proportion to the square of the relative flight velocity λ_n. When $\lambda_n^2 = \frac{k + 1}{k - 1}$, $\eta_{tid} = 1$.

With a decrease of K the specific thrust of an engine quickly diminishes. During a decrease of K from 0.9 to 0.8 the specific thrust diminishes by 40%.

The relative discharge velocity in a state of maximum economy is:

$$\left(\frac{w_4}{w_3}\right)_{opt} = \varkappa K \sqrt{\bar{\vartheta}_{opt}} = \varkappa K \sqrt{\frac{1+\sqrt{1-\varkappa^2 K^2}}{1-\sqrt{1-\varkappa^2 K^2}}} \ . \tag{9.54}$$

The relative growth of velocity in a state of maximum economy depends only on the gas dynamic factor K. If $\varkappa K = 1$, then $\left(\frac{w_4}{w_3}\right)_{opt} = 1$.

It is seen from Table 9.1 that to increase the economy of the engine at high gas dynamic factors, it is advisable to strongly lean out the mixture. It is necessary to consider that a significant leaning out causes the thrust and the thrust coefficient to drop. If the thrust factor C_R becomes less than the external resistance factor of the engine shell c_x : $C_R < C_x$, then the ramjet engine will not only be unsuitable to serve as an aircraft engine, but may even not be able to move itself. Therefore it is practically impossible to operate during large α's.

The greater the degree of constriction in the engine $m = \frac{S_M}{S_4}$, the lesser the relative velocities λ_2 and λ_3, the lesser the losses in the engine, the greater the total pressure recovery σ_{ob} and the gas dynamic factor K, but the lesser the engine thrust factor C_R and the transverse thrust R_M.

In this way, the geometric parameter of an engine $m = \frac{S_M}{S_4}$, shows a substantial effect on the thrust parameters and optimum air surplus.

Foreign subsonic ramjet engines, for example, the American Hiller helicopter engine or Marquardt's engine, which are installed in target drones of the Gorgon IV type (see Figure 17a), have a low degree of constriction: $m \approx 1.4$.

SECTION 6. CONTROL CHARACTERISTICS OF SUBSONIC RAMJET ENGINES

The control of subsonic ramjet engines may be accomplished by varying the fuel supply. During the enrichment of the mixture to $\alpha = 1$, the temperature of the combustion products and the temperature ratio increase. The mass flow rate of the gases changes in accordance with (9.16) approximately in inverse proportion to $\sqrt{T_{0g}}$.

$$G_4 = \sqrt{\frac{2gk_r}{(k_r+1)R_r}} \frac{\sigma_{ob}p_{ow}S_4}{\sqrt{T_{0r}}} q(\lambda_4). \tag{9.55}$$

The relative velocity of the exhaust gases λ_4 varies insignificantly, since the losses in heat dispersion increase and the losses in the diffuser and local losses decrease; the overall pressure recovery remains almost constant

$$\sigma_{ob} = \sigma_d \, \sigma_m \, \sigma_{sg} \, \sigma_\varepsilon \approx const.$$

The discharge velocity w_4 grows approximately in direct proportion to T_{og}:

$$w_4 = a_* \lambda_* = \sqrt{\frac{2gk_r}{k_r-1} R_r T_{o*} \left[1 - \left(\frac{\pi(\lambda_u)}{\sigma_{ob}}\right)^{\frac{k_r-1}{k_r}}\right]};$$ (9.56)

The stagnation impulse of the free stream flow decreases because of the decrease of the air flow rate. Additional drag of the diffuser grows.

The impulse of the exhaust gases, as it follows from (9.55) and (9.56) does not depend on the temperature of the gases (or on fuel feed), since an increase of the exit velocity is compensated by an equally large air flow rate:

$$(F_*)_{ax6} = \frac{G_4 w_4}{g} = \frac{2gk_r}{k_r+1} \frac{\sigma_{ob} p_{0n} S_4}{\pi(\lambda_u)} \lambda_4^2 z(\lambda_4) = k_r S_4 p_4 M_4^2.$$ (9.57)

Jet thrust slowly increases with the growth of heating because of the decrease of the braking impulse of the oncoming flow (9.27).

In certain cases thrust may be conveniently expressed by the Mach number:

$$R = \frac{G_4 w_4}{g} - \frac{G_n w_n}{g} = k_r S_4 p_4 M_4^2 - k S_n p_n M_n^2.$$ (9.58)

The cross section of the stream tube flow is expressed by the flow rate factor φ:

$$S_n = \varphi \, S_1$$

According to Kiselev's formula

$$R = S_4 [\sigma_{ob} p_{0n} (\lambda_4^2 - 1) z(\lambda_4) - p_n] - S_1 [p_{0n} (\lambda_1^2 - 1) z(\lambda_1) - p_n].$$ (9.59)

Here p_n is the static pressure of the undisturbed flow, which acts upon the shell;

p_{0n} is the stagnation pressure of the oncoming flow;

λ_1 is the relative velocity at the engine inlet;

S_1 and S_4 are the engine terminal sections;

$\sigma_{ob} = \sigma_d \, \sigma_M \sigma_{sg} \, \sigma_g$ is the total pressure recovery of a ramjet engine.

During an increase of the fuel feed, the thrust force grows because of the decrease of air consumption, i.e., because of the decrease of relative velocity at the inlet λ_1 and because of the increase of stagnation pressure after the exit p_{04}; an increase of p_{04} is accompanied by a decrease of λ_4.

The thrust factor of a ramjet engine C_R varies during a change in the fuel flow rate just as the thrust R, because we consider the flight velocity and altitude

The curves that depict the dependence of the thrust parameters of a ramjet engine upon the fuel flow rate G_g (or on the surplus air factor α) are called the control characteristics (Figure 171). Owing to the fact that the supply of a liquid fuel is usually regulated by means of throttling the fuel line, the control characteristics of a ramjet engine are called the throttle characteristics.

The form of the control characteristics depends upon the flight altitude and velocity M_n and H, upon the fuel parameters, and upon the factors σ_d, ζ, σ_s, and $m = \dfrac{S_k}{S_4}$.
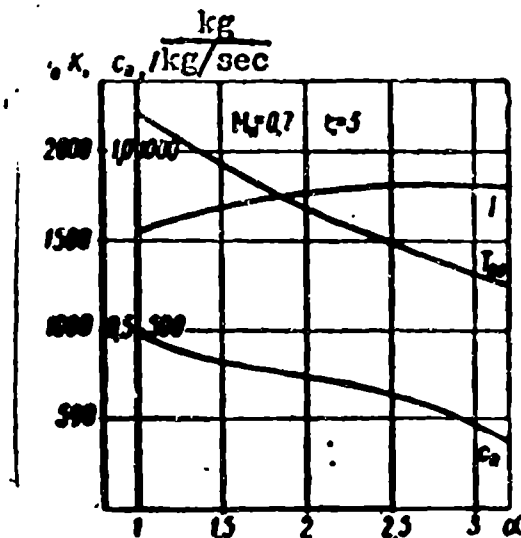
Fig. 171. The control characteristics of a subsonic ramjet engine.

During a leaning out of the mixture the thrust force R and the thrust factor C_R slowly diminish at first. When α are large the velocities λ_1 and λ_2, and the losses along the engine duct quickly grow, the pressure ahead of the nozzle decreases and the thrust parameters diminish rapidly.

The specific thrust of a ramjet engine I is equal to

$$I = \frac{aL w_4}{g}\left(\beta \frac{w_4}{w_n} - 1\right) = \frac{aL w_n}{g}\left[\beta \varkappa K \sqrt{1 + \frac{H_u \eta_{cr}}{(1 + aL)c_p T_{cr}}} - 1\right]. \tag{9.60}$$

During an increase of the surplus air α the first of the factors grows, but the second $- \beta \dfrac{w_4}{w_n} - 1 -$ decreases because of the decrease of the relative growth of the velocity $\dfrac{w_4}{w_n}$ (see Section 5). During a leaning out of the mixture the thrust forces diminish slowly at first; therefore the specific thrust increases, passes the maximum and then, as the thrust begins to diminish rapidly (faster than the fuel flow rate),

also begins to decrease. The total pressure recovery σ_{ob}, during a strong leaning out of the mixture, decreases because of the increase of λ_2 and the increase of the losses in the diffuser and on the local burner resistances. The combustion efficiency is maximum when the surplus air is somewhat greater than one.

It is immaterial for the aircraft designer at what cost were any of the parameters achieved -- important for him are only the thrust coefficient C_R and the specific thrust I. Therefore, the control characteristic is often represented in the form of curve $C_R = f(I)$ (Figure 172).

The calculati n of the control characteristics is accomplished by method of successive approximations, stated in Section 3, according to the flow parameters w_n, p_n, and T_n, coefficients σ_d, ζ, σ_s, and φ_{sg}, the fuel parameters H_u and L, and the degree of engine constriction $m = \dfrac{S_k}{S_4}$.
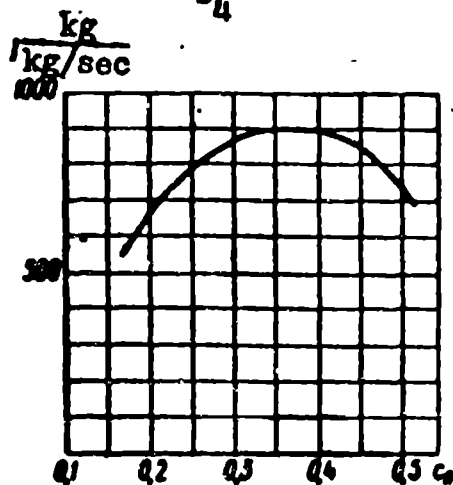
Fig. 172. The depenaence of the specific thrust upon the thrust coefficient.

SECTION 7. THE VELOCITY CHARACTERISTICS OF SUBSONIC RAMJET ENGINES

During a variation of the flight velocity the stagnation temperature and pressure of the flow, which enters the diffuser, change and together with them, all the thrust parameters of the engine change. The dependence of the parameters of a ramjet engine on the flight velocity, on the Mach number of the flight or on the relative velocity λ_n are called the velocity characteristics of a ramjet engine (Figure 173).

With an increase of the flight velocity w_n the relative velocity λ_n increases and the flow rate of the gases increases. After using (9.6 and 9.16), we obtain

$$G = \sqrt{\frac{2gk_r}{(k_r+1)R_r}} \frac{p_{04}S_4}{\sqrt{T_{04}}} \frac{\lambda_4}{\tau(\lambda_4)} = \sqrt{\frac{gk_r}{R_r}} \frac{p_{04}S_4}{\sqrt{T_4}} M_4. \qquad (9.61)$$

In order that the composition of the mixture remains constant during a variation in flight velocity, the engine must be equipped with a regulator which varies the fuel supply in proportion to the air input, i.e., approximately in proportion to M_4.

The relative velocities along the duct of the engine λ_1 and λ_2 increase with an increase of λ_n. The pressure factors decrease (9.9) during the flow around local resistances σ_M and the diffuser σ_d. The stagnation temperature and pressure T_{0n} and p_{0n} grow and the temperature ratio decreases:

$$\theta = \frac{T_{0r}}{T_{0a}} \approx 1 + \frac{H_{u}\alpha_{cr}\tau(\lambda_a)}{c_p T_a(1+\alpha L)}. \qquad (9.62)$$

The pressure recovery during combustion σ_{sg} (IX, 2, 10) increases because of the decrease of the temperature ratio and the decrease of the velocity of the combustion products. The total pressure recovery σ_{ob} and the gas dynamic factor K of a subsonic ramjet engine changes insignificantly with an increase of velocity. The ratios $\frac{M_4}{M_n}$ and $\frac{4}{n}$ remain constant in the first approximation.
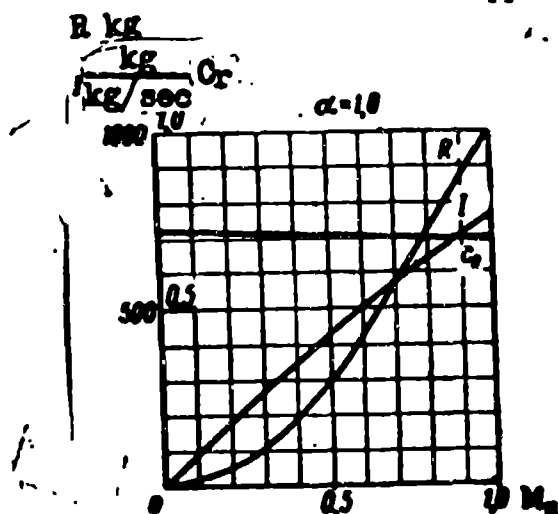
Fig. 173. The velocity characteristics of a subsonic ramjet engine.

At first, while the temperature ratio remains practically constant, the thrust of a subsonic ramjet engine changes proportionally to M_n^2:

$$R = \frac{G_r w_4}{g} - \frac{G_n w_n}{g} = k p_n S_4 M_n^2 \left(\frac{k_r}{k} \frac{M_4^2}{M_n^2} - \frac{S_n}{S_4} \right). \qquad (9.63)$$

During a further increase of velocity, $\theta = \frac{T_{0g}}{T_{0kh}}$ decreases, the relative section of the stream tube flow $\frac{S_n}{S_4} = \frac{1}{x\theta K\sqrt{\theta}}$ increases and the thrust increase slows down.

The thrust coefficient slowly decreases with an increase of velocity because of

the decrease of K and the temperature ratio θ (see Figure 173):

$$c_R = \frac{2u^2K^2}{m} \frac{\tau(\lambda_n)R}{\tau(K\lambda_n)R_f} \times \left[1 - \frac{1}{\beta K\sqrt{\theta}}\right].$$ (9.64)

The specific thrust of a subsonic ramjet engine increases with an increase of velocity due to the increase of the stagnation pressure after the exit p_{04} and the increase of the thermal efficiency η_r, although θ decreases insignificantly:

$$\eta_r = 1 - \left(\frac{p_4}{p_{04}}\right)^{\frac{k-1}{k}} = 1 - \left[\frac{\tau(\lambda_n)}{\varepsilon_{06}}\right]^{\frac{k_r-1}{k_r}},$$ (9.65)

$$I = \frac{aL_cM_s}{g}(\beta K\sqrt{\theta} - 1).$$ (9.66)

The optimum heating θ_{opt} increases during an increase of flight velocity M_n due to the decrease of K (see 9.51).
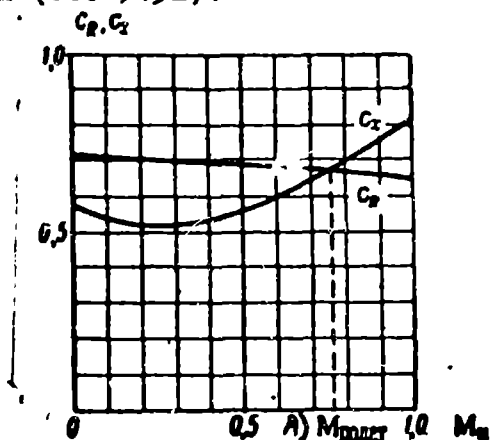
Fig. 174. A flight occurring with such a velocity that the thrust coefficient and the drag coefficient are equal to one another. A) M_{flight}.

The optimum surplus air factor α_{opt} decreases with an increase of velocity (see 9.50).

Owing to the fact that the thrust coefficient of a ramjet engine diminishes with an increase of M_n when α = const, the flight of an aircraft with a subsonic ramjet engine is stable for a chance variation of velocity. Actually, the thrust coefficient of an engine C_R diminishes insignificantly with an increase of velocity, and the drag coefficient C_x increases (Figure 174). A flight may occur with such a velocity u_n at which C_R = C_x. If, because of some reason, the flight velocity decreases, the thrust proves to be greater than the drag force and the velocity again returns to its former value. During a chance increase of velocity, the thrust proves to be less than the drag and the flight slows down.

If during the flight, the fuel supply is constant G_g = const, then the mix-

ire will lean out with an increase of velocity and the change of the thrust co-
fißient C_R will be sharper than when α = const. The flight will be still more
able in relation to accidental velocity variations.

CTION 8. ALTITUDE CHARACTERISTICS OF SUBSONIC RAMJET ENGINES

During a change of flight altitude H, if the flight velocity and fuel supply
-e constant: M_n = const and α = const, the parameters of a ramjet engine change be-
iuse of the change of the pressure p_n and temperature T_n of the surrounding air.

The curves, which depict the dependence of the parameters of a ramjet engine
i the flight velocity H are called the altitude characteristics of a ramjet engine
Figure 175).

ig. 175. The altitude characteristics of subsonic ramjet engine.
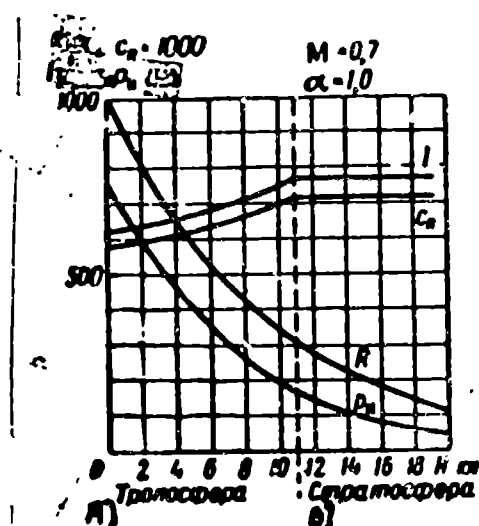
Legend:

A) Troposphere
B) Stratosphere

The pressure p_n diminishes with increasing flight altitude (see Table 11.1).
hen this happens, the flow rate of the gases and the thrust force decrease approxi-
ately in direct proportion to p_n (9.61 and 9.63).

In order that the mixture composition does not change during an increase of
ltitude, the fuel supply should be decreased. The air temperature diminishes with
ltitude until the boundary of the troposphere is reached (according to the inter-
ational standard, the atmosphere H_{st} = 11 km).

With a diminishing temperature T_n the enthalpy of the air i_{0x} decreases, but
he temperature ratio increases up to H = 11 km.

The thrust coefficient C_R and the specific thrust I, in accordance with (9.31)
nd (9.34) increase (see Figure 175) for an increase of the temperature ratio θ.

The optimum temperature ratio, at which the specific thrust reaches the maximum value, does not depend on the flight altitude (see 9.51). The optimum surplus air λ_{opt} increases with an increase of altitude H because of the decrease of T_n (see 9.50), right up to an altitude of 11 km.

After the passage into the stratosphere, where $T_n \approx$ const, all the parameters of a ramjet engine, with the exception of thrust, would remain constant if the combustion efficiency $\mathcal{q}_{sg}$ would be constant. In actuality, the density of the gases in the combustion chamber diminishes with an increase of altitude. If the altitude control of the fuel composition is accomplished by a change of the fuel feed pressure, then the coarseness of the fuel dispersion will increase with an increase of altitude. Because of the decrease of density, the speed of the heat transmission from the surrounding flow to the drops will diminish and evaporation of the fuel in the carburation zone and in the combustion zone will deteriorate. The dispersion jet will be broadened and, other conditions being equal, the mixture in the area of the flame-holders may be leaned out. The combustion efficiency decreases with an increase of altitude because of the deterioration of carburation. The decrease of the combustion efficiency, which is topped off by the total cessation of combustion, establishes the altitude limit for subsonic ramjet engines.

SECTION 9. THE USE OF SUBSONIC RAMJET ENGINES

The first tests of the practical use of subsonic ramjet engines took place in the USSR in 1932-1935 under the leadership of Professor Yu. A. Pobedonostsev. In 1939 the Soviet designer I. A. Merkulov installed two ramjet engines of his own design (figure 176) under the wings of the I-15 fighter, designed by N. N. Polikarpov. These ramjet engines were to serve as boosters, i.e., to impart a further increase of velocity to the aircraft, after the basic power plant would have reached its peak output.

Merkulov's ramjet engine had a diameter of 400 mm, a length of 1,500 mm, and a weight of 12 kg. The engine used the same brand of fuel as the aircraft's main power

thrust or at a velocity of 600 km/hr -- nearly 2 kg/hr per one horse power, i.e., it was eight times greater than that of the main power plant of the aircraft.
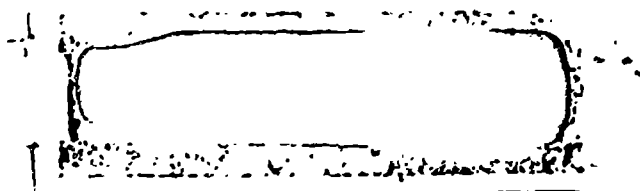
Fig. 176. I. A. Merkulov's ramjet engine, which was installed on the Polikarpov I-15 fighter.

By including a ramjet engine, the speed of an aircraft was increased by 40-50 km/hr. However, with the inoperative boosters, which had great aerodynamic drag, the speed of the aircraft proved to be substantially less than without boosters.

An attempt to use a ramjet engine as a booster for a propeller-driven aircraft was also made by the German designer Senger in 1943..

Even during the Second World War, projects of fighter aircraft with ramjet engines as the main power plants were carried out in Germany. One such project belonged to Senger (Figure 177). The aircraft was carried aloft by a mother-aircraft, was released and proceeded to independent flight. The Mach number of the flight was to be equal to 0.7, and the flight range was to be 800 km. Benzine was to serve as the fuel for the ramjet engine.

Another similar project was developed in 1944 by Lippisch and Pabst at the Fokke-Wulf plant in Vienna. The aircraft was also to be carried aloft by a mother-aircraft. After the ramjet engine started, the aircraft gained the design velocity by diving. Carbon, which filled the combustion chamber, was to serve as the fuel for Lippisch's aircraft. The low heating value of carbon (7850 kcal/kg) is compensated by its high density (higher than 1500 kg/m^3), owing to which, the volume and frontal drag of the combustion chamber prove to be less than a tank with benzine would have. The calculated flight duration with a velocity of more than 1,000 km/hr was to be 30 minutes.

The projects were not completed because of Germany's defeat in the war and the cessation of all projects on the design of military aircraft.
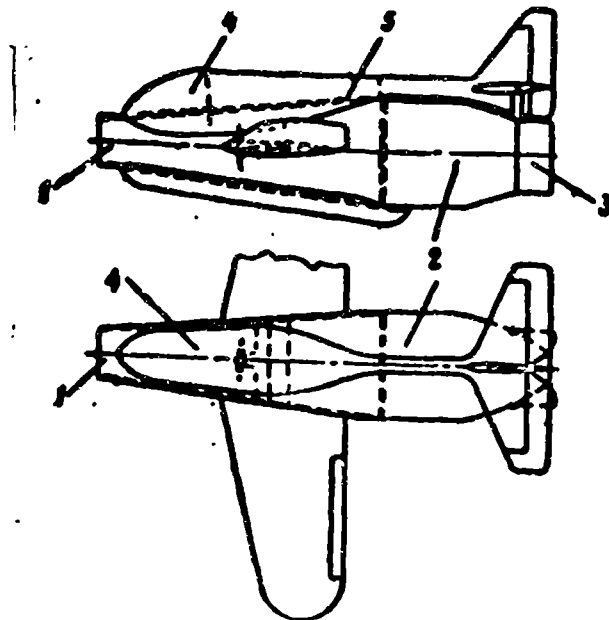
Fig. 177. Senger's project of a fighter with a ramjet engine, 1944.
1 -- diffuser, 2 -- combustion chamber, 3 -- nozzle, 4 -- pilot's cabin,
5 -- fuel tank.

Back in 1938 the French designer R. Leduc began to work on the project of a
fighter aircraft with a ramjet engine. At the present time Leduc's aircraft is
undergoing flight testing. Although this aircraft has not yet developed supersonic
speeds, it is intended for a flight at M ≈ 3. Therefore, it will be discussed in
greater detail in the following chapter.

The American designer R. Marquardt developed (1947) a subsonic ramjet engine
system, tested it in flight in the aircraft "Shooting Star" (see Figure 3), and form-
ed a firm to produce ramjet engines.[1]

At the present time subsonic ramjet engines are used in target drones, guided
missiles, and on helicopters.

The American firm Martin developed a target drone -- the Gorgon IV -- equipped
with a Marquardt ramjet engine and guided by radio (see Figure 17a). A target drone,
the speed of which is close to that of jet bombers, is used for training personnel
and for testing various means of antiaircraft defense.[1]

Guided missiles, which are directed by radio and supplied with self-guidance
instruments, are used to defeat enemy ships at distances where artillery is impracti-
cable. Ramjet engines, which consume several times less fuel than a liquid-fuel

[1]R. Marquardt, American Aviation, vol. 17, No. 18, I-II, 1954, 24-28.

suitable for launching pilotless single-flight guided missiles.

Subsonic ramjet engines, which are installed at the ends of rotor blades, are used as primary helicopter engines.[1] As an example we will cite the American helicopter, the H-32, produced by Hiller (see Figure 18), which has ramjet engines installed at the ends of the seven-meter-long two-bladed rotor. At the design rotor speed, the engines develop a power of more than 40 hp each. The diameter of the engine is 200 mm, the length is 600 mm; the weight is 2.5 kg; the thrust -- nearly 14 kg; and the fuel -- kerosene. The total weight of the helicopter is 250 kg; the useful load is nearly 140 kg; the cruising speed is 100 km/hr; the flight range is 50 km; the flight duration is 30 minutes; and the rate of climb is 0.3 km/min. The starting of the engine is accomplished with the aid of a hand-operated inertia starter. Due to their extreme simplicity, helicopters with ramjet engines may find wide usage as a means of transportation, in agricultural aviation, and even in war during landing operations and ferrying.

Subsonic ramjet engines are not widely used. Supersonic ramjet engines possess greater possibilities.

BIBLIOGRAPHY

1. Varshavskiy, G.A., and Makarov, B.V., Tekhnika vozdushnogo flota /Air Fleet Engineering/, 1940, No. 6.

2. Inozemtsev, N. V., Aviatsionnyye gazoturbinnyye dvigateli /Aircraft Gas Turbine Engines/ Oborongiz, M.-L., 1955.

3. Merkulov, I. A., Reaktivnaya aviatsiya /Jet Aviation/, Printing House Znaniye /Knowledge/, 1954.

4. Stechkin, B. S., Teoriya vozdyshnogo reaktivnogo dvigatelya /The Theory of a Ramjet Engine/, TVF, 1929, No. 2.

5. Avery, W. H., Dvadtsat' pyat' let razvitiya pryamotochnykh dvigatelyey /Twenty-Five Years of Ramjet Engine Development/, Jet Propulsion. IX, 1955, 601-611.

---

[1] P. R. Payne, "Subsonic Ramjet of Helicopter," Flight, vol. 66, No., 1954.
R. T. De Vault, "Augmenting Helicopters Take-off Power by Ramjet," Aircraft Eng., v. 27, No. 312, Feb. 1955.

6. Shapiro, A. H., The Dynamics and Thermodynamics of Compressible Fluid Flow. New York, 1953.

7. Bailey, N. P., "The Thermodynamics of Air at High Velocities," Journ. of Aeron. Sciences, v. 11, July, 1944, 227-238.

8. Chambre, P. and Lin, C., "On the Steady Flow of a Gas through a Tube with Heat Exchange or Chemical Reaction," J. of Aer. Scienc., v. 13, Oct. 1946, 537-542.

9. Hicks, B. L. and Montgomery, D. I., "The One -- Dimensional Theory of Steady Compressible Flow in Ducts with Friction and Heat Addition," NACA TN, 1336, 1946.

10. Rudnic, P., "Momentum Relations in Propulsive Ducts," J. of Aer. Scienc., v. 14, Sept., 1947.

11. Sanders, N. D., "Performance Parameters of Jet Propulsion Engines," NACA TN, 1106 1946.

12. Marquardt, R., American Aviation, v. 17, No. 18, I-II, 1954, 24-28.

13. Payne, P. R., "Subsonic Ramjet of Helicopters," Flight, v. 66, Nov. 1954.

14. De Vault, R. T., "Augmenting Helicopters Take-off Power by Ramjet Aircraft," Eng., v. 27, No. 312, Feb. 1955.

CHAPTER X

SUPERSONIC RAMJET ENGINES

Supersonic ramjet engines (SPVRD) are intended for flights at speeds that are higher than the speed of sound, i.e., at $M > 1$. The upper limit of the velocity to which ramjet engines may be used, is determined by the temperature of the gases before exit T_{03}. The greater the difference $T_{03}-T_{02}$, the greater the terminal flight velocity. During operation on high-calorific fuels or on atomic energy, the velocity of a prolonged flight is limited by the heat resistance quality of the materials, since the stagnation temperature at $M > 6$ becomes greater than the melting point of steel.

The geometry of a supersonic ramjet engine is determined by the design flight velocity and the purpose of the engine.

The specific fuel consumption of a supersonic ramjet engine at $M \approx 4$ is less than and the total efficiency is greater than that for any other type of engine ($\eta_{obshch} > 40\%$).

Supersonic ramjet engines, like subsonic ramjet engines, are incapable of self-starting. Supersonic ramjet engines must be accelerated to their initial velocity with the aid of a special booster. A rocket booster is the most effective means of accelerating a supersonic ramjet engine. The air-to-air and air-to-ground missiles that are launched by high-speed aircraft do not need boosters.

The theory of supersonic ramjet engines was formulated by Stechkin, Zuyev, Abramovich, Crocco, Senger, Willey, Trommsdorf, and many other Soviet and foreign authors. The present status of supersonic ramjet engine theory is stated below.

SECTION 1. THE PRINCIPLE SCHEMATIC OF A SUPERSONIC RAMJET ENGINE

Supersonic ramjet engines (Figure 178) have the same basic parts as subsonic ramjet engines: a diffuser, a combustion chamber, and an exhaust nozzle.

The shape of a supersonic diffuser is determined by the design flight velocity and the purpose of the engine. At design velocities of $M_n = 1$ to $M_n = 2$ the engine

is supplied with a diffuser having a normal shock wave at its inlet (Figure 178a). The pressure recovery factor after a normal shock wave diminishes from $\sigma_{pr} = 1.0$ to $\sigma_{pr} = 0.70$ for a velocity increase of $M_n = 1$ to $M_n = 2$. An assembly of oblique shock waves at the inlet when $M \leqslant 2$ may increase the pressure by not more than 10-20%. If the pressure in the combustion chamber p_{03} is higher than critical, a supersonic nozzle may be installed at the engine outlet. The nozzle divergence $\varepsilon = \frac{S_4}{S_{4cr}}$ must be the greater the larger is the pressure ratio in the combustion chamber ahead of the exit $\frac{p_{03}}{p_n} \gg \frac{p_{04}}{p_4}$ (see Figure 77).

Legend:

1) Normal shock wave
2) Oblique shock waves
3) Acceleration diffuser
4) Bullet
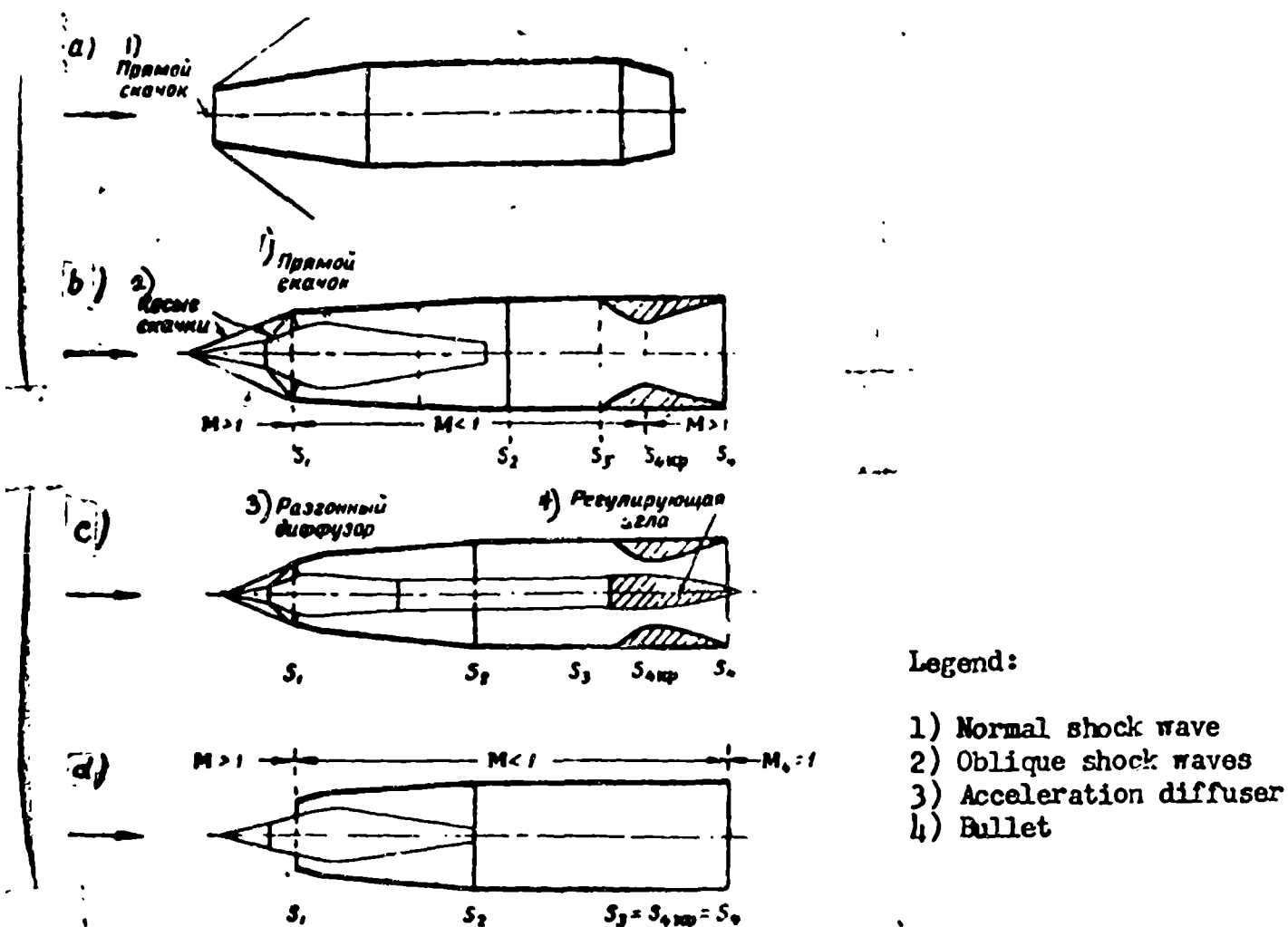
Fig. 178. Schematics of supersonic ramjet engines.
a -- a supersonic ramjet engine with a normal shock wave at the inlet,
b -- a ramjet engine with a multi-shock wave diffuser and a fixed-geometry nozzle,
c -- a supersonic ramjet engine with a multi-shock wave diffuser and a variable-geometry nozzle,
d -- a supersonic ramjet engine with no exit nozzle.

At high design flight velocities ($M \geqslant 2$) a multi-shock wave diffuser (for which the pressure increase is significantly more effective than during a single normal

shock wave) is installed at the inlet to the engine. Thus, when $M_n = 3$; $\frac{G_{0n}}{P_n} = 37$.

The pressure increases approximately 12 times in a diffuser with a normal shock wave, so that $\sigma_d = 0.3$. In a multi-shock wave diffuser the pressure increases more than 20 times, so that $\sigma_d \approx 0.65$. Thus, an arrangement of obliqud shock waves at the inlet when $M > 3$ increases the stagnation pressure at the diffuser outlet more than 2 times. With a further increase of the design flight velocity, multi-shock wave diffusers, in comparison with normal shock wave diffusers, give still greater benefits.

The most suitable configuration of a deflecting spike and the value of the diffuser throat cross section $\frac{S_{cr}}{S_M}$ depend upon the design velocity. As M_n increases the most suitable number of shock waves increases, the optimum turning angles of the flow ω_1, ω_2, and ω_3 decrease, the compression of the air increases, and the critical section of the throat S_{1cr} diminishes. The design critical cross section of the exhaust nozzle $\frac{S_{4cr}}{S_M}$ also decreases with an increase of M_n. An engine with a fixed-geometry may operate under the design conditions only at one flight speed. A single regime engine with a fixed-geometry, which is designed for flight at a predetermined velocity, is shown in Figure 178b. A multi-regime engine, which is intended for flight at various velocities for various temperature ratios, must be equipped with a variable-geometry diffuser and nozzle (see Figure 178c). A maximum thrust engine, which is designed for high combustion temperatures, is sometimes constructed without a constriction at the outlet: $S_3 = S_{4cr} = S_4$ (see Figure 178d).

The diffuser portion of a supersonic ramjet engine may be divided into supersonic and subsonic portions (Figure 179b). The flow in front of the oblique diffuser shock wave is supersonic. The flow through the divergent portion of the diffuser, through the combustion chamber, and through the nozzle up to its critical section is subsonic; the flow from the nozzle throat section to the exhaust plane and after it is supersonic.

The greater the design free stream flow velocity M_n for a given inlet area ratio $\frac{S_1}{S_2}$, the smaller the critical inlet section ratio $\frac{S_{1cr}}{S_2}$, the larger the widening of the subsonic portion of the diffuser, and the smaller the relative velocity at the combus-

tion chamber inlet λ_2. The absolute value of the velocity in the exhaust section

S_2 of a diffuser of a supersonic ramjet engine, i.e., at the combustion chamber in-

let, is nearly 100 m/sec. The velocity at a combustion chamber outlet which has no

exit nozzle constriction ($S_3 = S_{\mu cr} = S_4$) may reach the local speed of sound (see

Figure 178d).

The flow through the subsonic portion of a diffuser depends, to a significant

degree, upon the divergent angle of a right circular cone α. If this angle α_d ex-

ceeds 10°, the pressure recovery in the subsonic portion $\sigma_d"$ diminishes (see Figure

61c). This is caused by a separation from the walls and the appearance of turbulence

in the flow, and is accompanied by a dissipation of energy. At angles which are less

than 5°, pressure recovery decreases, due to surface friction losses which increase

with an increase in the diffuser length $\ell = \dfrac{d_2 - d_1}{2 \sin \dfrac{\alpha_d}{2}}$. The optimum divergence angle

of a right circular cone lies within the area of $5^\circ < \alpha_d < 10^\circ$.

Legend:

1) Diffuser
2) Combustion chamber
3) Fuel pump
4) Injectors
5) Flame-holder
6) Nozzle
7) Supersonic flow
8) Subsonic flow
9) Fuel injection and
   Flame stabilization
10) Incoming air
11) Compression
12) Combustion
13) Expansion
14) Hot Gases
15) Shock wave
16) Inlet diffuser
17) Exhaust nozzle
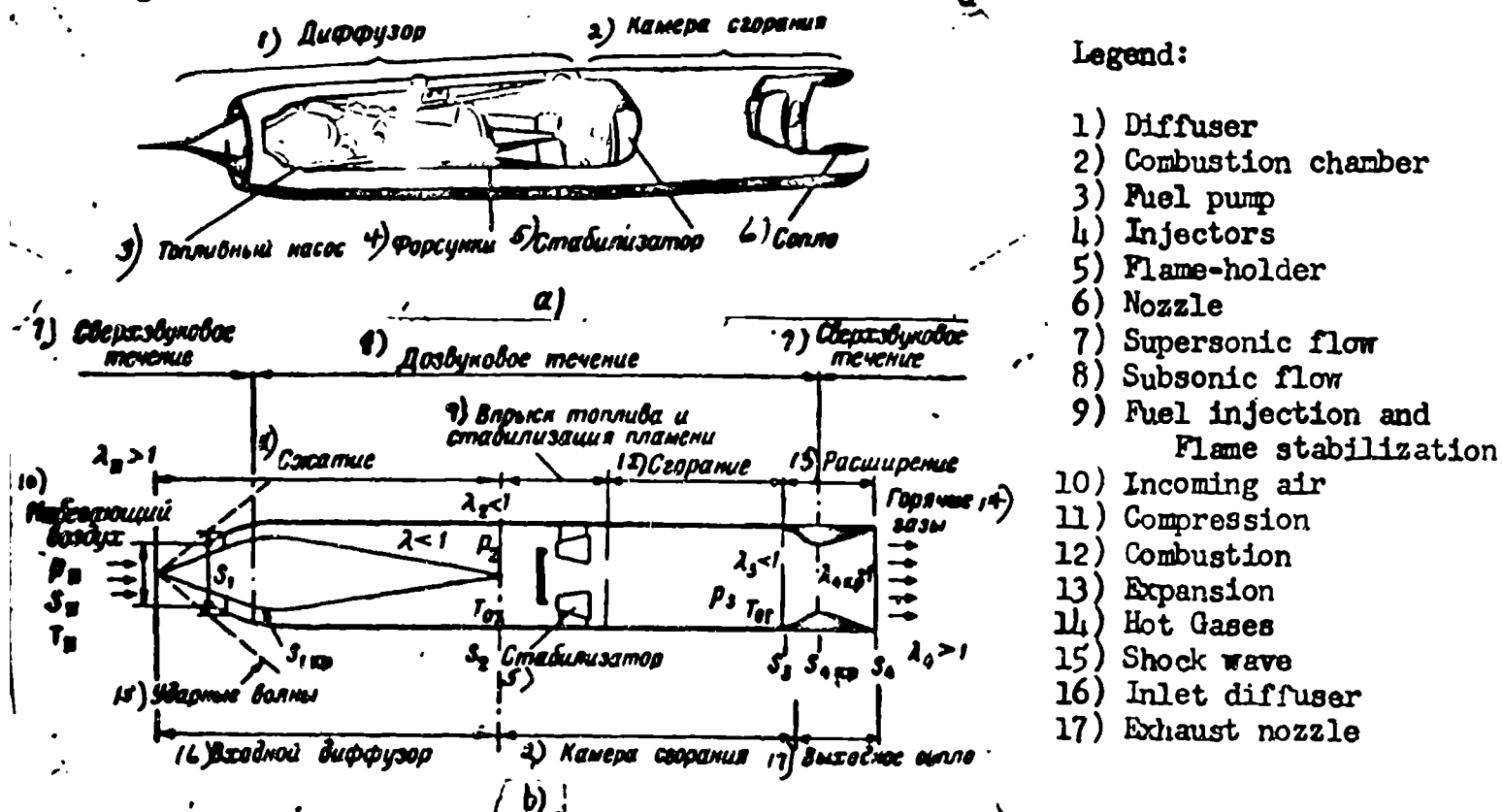
Fig. 179. The internal arrangement of a supersonic ramjet engine.
a -- perspective cross section, b -- diagram

In principle, the combustion chamber of a supersonic ramjet engine (Figure 179)

is constructed like the combustion chamber of a subsonic ramjet engine. We note that

with an increase of flight velocity M_n, the stagnation temperature and pressure in the

combustion chamber inlet increase, the relative velocity diminishes, and the opera-
tion of the combustion chamber is improved.

SECTION 2. THE GAS DYNAMICS OF A SUPERSONIC RAMJET ENGINE

A diagram of the gas flow through a supersonic ramjet engine having a multi-
shock wave diffuser is depicted in Figure 180. Oblique shock waves appear on the
multi-step spike of a diff ser as the supersonic flow approaches (see Chapter II,
Section 11). The air temperature, pressure, and density variations in the oblique
shock waves, which are expressed by (2.118, 2.119, 2.122, and 2.123), are depicted
in Figures 39, 40, 41, and 42.

The velocity of the flow during its passage through the oblique shock waves
diminishes, while the pressure and density increase. The direction of the flow
through the oblique shock waves changes. The air stream lines along the surface of
the spike are parallel to its surface.

Legend:

1) Last oblique shock wave
2) Rarefaction wave
3) Terminal shock wave
4) Normal shock wave
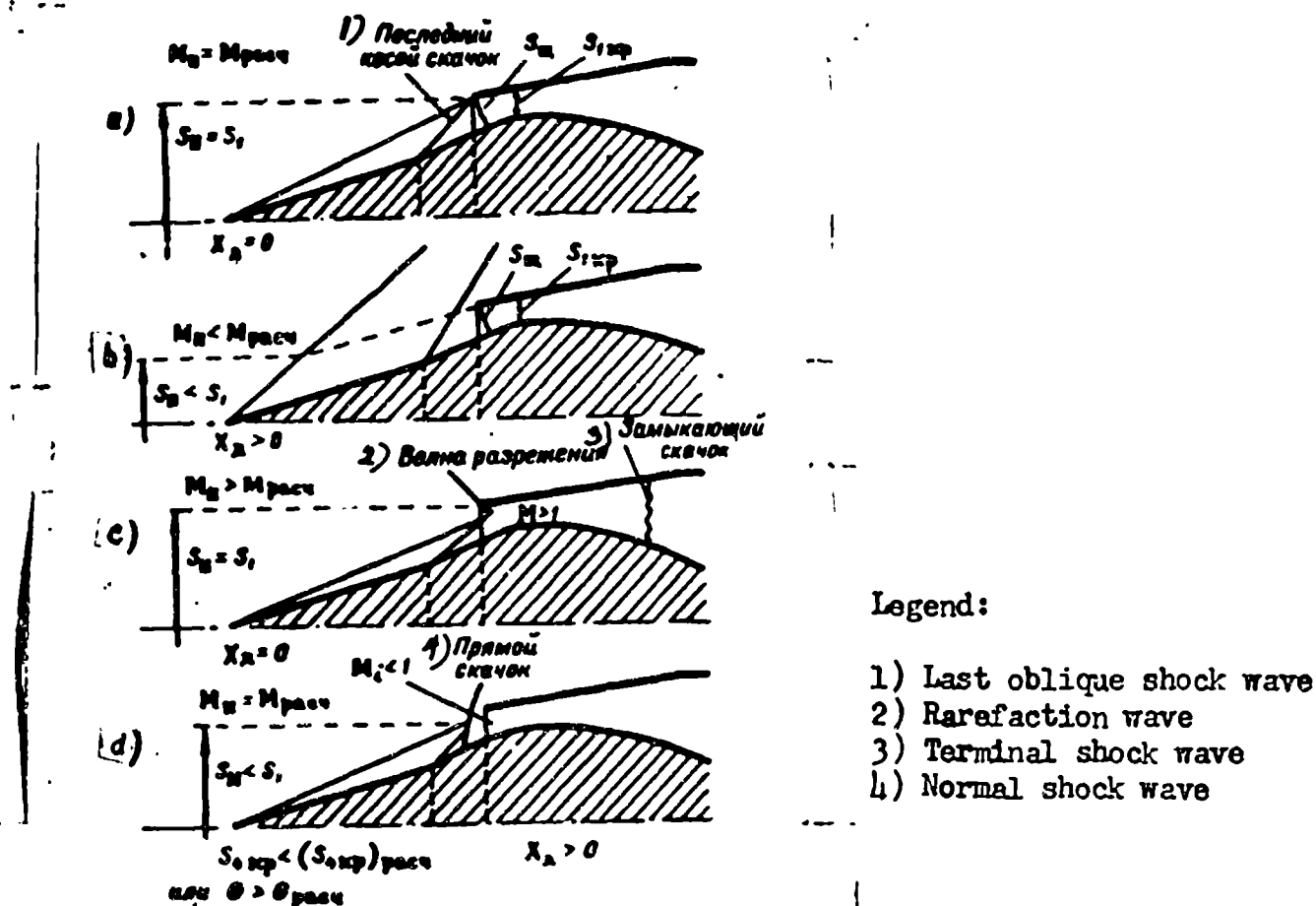
Fig. 180. A schematic of the shock waves in a diffuser inlet.
a -- design case; b -- $M_n < M_{rasch}$; c -- $M_n > M_{rasch}$; d -- $M_n = M_{rasch}$,
$S_{4cr}(S_{4cr})_{rasch}$

The final shock wave is usually formed inside the diffuser duct.

The air flow through a supersonic engine G_v is determined by the cross section of the diffuser inlet slot S_{shch}, which is measured normal to the stream lines in the diffuser inlet; and by the velocity and the density of the flow after the last oblique shock wave w_i-1 and γ_i-1 (i is the number of shock waves in the diffuser):

$$G_v = k S_m w_{i-1} \gamma_{i-1},$$ (10.1)

where k is the factor that is determined by the depth of the boundary layer at the diffuser inlet. The greater the depth of the boundary layer thirtation to the, height of the inlet slot, the less becomes K.

The air flow may be expressed by the parameters of the free stream flow and the inlet cross section S_1 (see Figure 180):

$$G_v = \varphi S_1 w_n \gamma_n,$$ (10.2)

where φ is the mass flow ratio of the diffuser.

If the shock waves are focused on the inlet edge of the diffuser (Figure 180a), then $\varphi = 1$; additive drag is absent: $X_d = 0$. In order to bring the diffuser mass flow ratio φ up to one when the inlet throat is "choked" by a boundary layer, the cross section of the inlet slot S_{shch} is made greater than design:

$$S_m = \frac{(S_m)_{des}}{k}.$$ (10.3)

If the flight velocity M_n is less than design point, then the shock wave incidence angles α_1, α_2, α_3, and others, will be greater than design point values and the air flow through the diffuser will become less than the maximum possible value $S_1 w_n \gamma_n$, since a portion of the flow is directed around the diffuser inlet slot (Figure 180b). The mass flow ratio φ decreases and additive wave drag X_d appears.

If the flight velocity is M_n greater than the design value, the shock wave incidence angles become less than design values and the oblique shock waves will enter the diffuser (Figure 180b). The pressure recovery σ_d will be less than design for a given velocity. The air flow will remain the maximum possible: $\varphi = 1$, and additive drag will be absent: $X_d = 0$.

The flow of the gases through any section of the engine S_i, is determined by the relative flow velocity λ_i, and the stagnation temperature and pressure in this

section p_{Oi} and T_{Oi} (see 2.74):

$$O_i = \left[\sqrt{\frac{2gk}{(k+1)RT_0}} p_0 S q(\lambda) \right]. \tag{10.4}$$

This index belongs to all the variations that enter into the flow equation.

The flow equation is used to find the relationship between the cross sections of the engine on one hand and the flows stagnation pressures and temperatures of the gases on the other.

Any two sections S_i and S_n may be described as:

$$\frac{O_i}{O_n} = \sqrt{\frac{k_i}{k_n} \frac{k_n+1}{k_i+1} \frac{R_n}{R_i} \frac{S_i}{S_n} \frac{p_{Oi}}{p_{On}} \frac{q(\lambda_i)}{q(\lambda_n)}}. \tag{10.5}$$

For any "cold" section, for example, for the free stream flow section S_n and for the diffuser exhaust section S_2

$$k_n = k_2 = k; \quad T_{On} = T_{O2} = T_{Ox}; \quad G_n = G_2 \text{ and } \frac{p_{O2}}{p_{On}} = \sigma_d$$

Consequently,

$$\frac{S_2}{S_n} = \frac{1}{\sigma_d} \frac{q(\lambda_n)}{q(\lambda_2)} = \frac{\lambda_n \epsilon(\lambda_n)}{\lambda_2 \epsilon(\lambda_2) \sigma_d}. \tag{10.6}$$

For low λ_n and λ_2 the compressibility of the air is insignificant:

$$\frac{T_2}{T_{O2}} = \epsilon(\lambda_2) \approx 1; \quad \frac{T_n}{T_{On}} = \epsilon(\lambda_n) \approx 1$$

and the relative velocities are inversely proportional to the sections:

$$\frac{\lambda_n}{\lambda_2} \approx \frac{S_2}{S_n}.$$

,For the critical and exhaust section of the diffuser S_{1cr} and S_2, considering that

$$\lambda_{1cr} = 1 \text{ and } \epsilon(\lambda_{1cr}) = \left(\frac{2}{k+1}\right)^{\frac{1}{k-1}},$$

from (10.6) we obtain

$$S_{1cr} = S_2 \left(\frac{k+1}{2}\right)^{\frac{1}{k-1}} \sigma_d'' q(\lambda_2) = S_n \left(\frac{k+1}{2}\right)^{\frac{1}{k-1}} \frac{1}{\sigma_d'} q(\lambda_n). \tag{10.7}$$

Here

σ_d'' is the pressure recovery of the subsonic portion of the diffuser

$$\sigma_d'' = \frac{p_{O2}}{p_{O1cr}};$$

σ_d' is the pressure recovery of the supersonic portion of the diffuser

$$\sigma_{A}' = \frac{p_{01\kappa p}}{p_{00}}.$$

With an increase of the relative velocity λ_n, the gas dynamic function $q(\lambda_n)$ decreases, the density of the air in the critical section of the diffuser grows and the calculated cross section of the throat $\frac{S_{1cr}}{S_n}$ decreases. With a decrease of pressure recovery in the supersonic portion of the diffuser σ_d'', the density of the air in the throat γ_{1cr} decreases and the critical section S_{1cr} increases.

Relationships analogous to (10.6) and (10.7) may be described also for the "hot" sections S_3, S_{4cr}, and S_4, by considering that $k_3 = k_4 = k_g$; $T_{03} = T_{04} = T_{0g}$; and $G_3 = G_4$ as:

$$S_{4\kappa p} = \left(\frac{k_r+1}{2}\right)^{\frac{1}{k_r-1}} S_4 \sigma_c' q(\lambda_4) = \left(\frac{k_r+1}{2}\right)^{\frac{1}{k_r-1}} S_3 \frac{q(\lambda_3)}{\sigma_c'}. \tag{10.8}$$

Here

σ_s' is the pressure recovery of the subsonic portion of the nozzle

$$\sigma_c' = \frac{p_{04\kappa p}}{p_{03}} \approx 0.97;$$

σ_s'' is the pressure recovery of the supersonic portion of the nozzle:

$$\frac{p_{04}}{p_{04\kappa p}} = \sigma_c'' = f\left(\frac{S_4}{S_{4\kappa p}}\right).$$

The relative velocity of the exhaust gases λ_4 depends on the ratio of the stagnation pressure to the static pressure at a given section: $\frac{p_{04}}{p_4}$

$$\lambda_4 = \sqrt{\frac{k_r+1}{k_r-1}\left[1-\left(\frac{p_4}{p_{04}}\right)^{\frac{k_r-1}{k_r}}\right]}. \tag{10.9}$$

Consequently, $\varepsilon(\lambda_4) = \left(\frac{p_4}{p_{04}}\right)$ and the design degree of divergence of the nozzle is

$$\sigma = \frac{S_4}{S_{\kappa p}} = \frac{\left(\frac{2}{k_r+1}\right)^{\frac{1}{k_r-1}}}{\sigma_c'' \sqrt{\frac{k_r+1}{k_r-1}\left[\left(\frac{p_4}{p_{04}}\right)^{\frac{2}{k_r}}-\left(\frac{p_4}{p_{04}}\right)^{\frac{k_r+1}{k_r}}\right]}}. \tag{10.10}$$

The stagnation pressure ratio of the exhaust gases $\frac{p_{04}}{p_4}$ is smaller than the stagnation pressure of the free stream flow $\frac{p_{0n}}{p_n}$:

$$\frac{p_{04}}{p_4} = \frac{p_{04}}{p_{03}} \frac{p_{03}}{p_{02}} \frac{p_{02}}{p_{02}} \frac{p_{02}}{p_{0n}} \frac{p_{0n}}{p_n} \frac{p_n}{p_4} = \sigma_c \sigma_{cr} \sigma_n \sigma_A \frac{p_4}{\pi(\lambda_n)} = \frac{\sigma_{o6}}{\pi(\lambda_n)} \frac{p_n}{p_4}. \tag{10.11}$$

Basically, the design ratio of the hot and cold throat sections is determined by the temperature ratio $\theta = \frac{T_{0g}}{T_{0x}}$.

$$\frac{S_{np}}{S_{np}} = \frac{p_1 \sqrt{\theta}}{\sigma_\Lambda \sigma_\pi \lambda_{cr} \lambda_t}. \tag{10.12}$$

re

$$\beta = \frac{G_4}{G_1} = 1 + \frac{1}{\alpha L}; \quad \chi = \sqrt{\frac{k_t R_t}{k_r R} \frac{\left(\frac{2}{k+1}\right)^{\frac{k+1}{k-1}}}{\left(\frac{2}{k_r+1}\right)^{\frac{k_r+1}{k_r-1}}}}, \tag{10.13}$$

The design ratio of the engine terminal cross sections is

$$\frac{S_4}{S_1} = \frac{\beta\sqrt{\theta}}{K\sigma_{o6}} \frac{\varepsilon(\lambda_n)}{\varepsilon(\lambda_4)} = \frac{\beta\sqrt{\theta}}{K} \frac{\tau(\lambda_4)}{\tau(\lambda_n)} \frac{p_n}{p_4}. \tag{10.14}$$

e,

$$K = \frac{\lambda_4}{\lambda_n}; \quad \xi = \sqrt{\frac{k}{k_r} \frac{k_r+1}{k+1} \frac{R_r}{R}}. \tag{10.15}$$

If the composition of the mixture is given, then with an increase of flight locity the temperature ratio θ diminishes:

$$\theta = \frac{T_{\theta r}}{T_{\theta s}} = 1 + \frac{H_u \eta_{cr} \tau(\lambda_n)}{c_p(1+\alpha L)T_n}. \tag{10.16}$$

The nozzle exhaust section may not be greater than the midships section of the $gine: S_4 \leqslant S_M$. The design cross section of the inlet $\frac{S_1}{S_M}$ and the ratio of the 'oat sections of the diffuser and nozzle $\frac{S_{1cr}}{S_{4cr}}$ increase with growing velocity due the decrease of the temperature ratio.

The relative velocity ahead of the exit λ_3, in accordance with (10.8), is de-mined by the ratio of the sections $\frac{S_3}{S_{4cr}}$. The relative velocity before combustion is determined by Kiselev's ratio (8.32). The pressure recovery for combustion is .ermined by the ratio of (8.34). The pressure recovery for the flow around local ner resistances is determined by the ratio of (8.19).

The pressure recoveries of the diffuser σ_d and the nozzle σ_s are determined flow tests.

We will assume that the geometry of an engine is given. To operate within the 'ign conditions, the engine will be at only one temperature ratio θ_{rasch} and at ' design flight velocity $(\lambda_n)_{rasch}$. For an increase of the ratio $\theta > \theta_{rasch}$, ' velocity ahead of the exit λ_3 does not vary, but the mass flow rate of the gases 'ies because of the increase of temperature and the decrease of the density of the

exhaust gases (see 10.4). The flow velocity in the cold sections S_1, S_{1cr}, and S_2 decreases while the pressure recovery σ_H grows during the flow around the local burner resistances. The pressure recovery during preheating σ_{sg} decreases because of the increase of the temperature ratio. The pressure recovery of the combustion chamber $\sigma_k = \sigma_H = \sigma_{sg}$ remains practically constant. The final shock wave is expelled from the diffuser inlet slot with an increase of the temperature ratio above the calculated value and the mass flow factor φ diminishes and a "buzz" condition begins. The pressure recovery σ_d remains practically constant (see Figure 180d).

With a decrease of the temperature ratio to a value that is less than the design, the air flow rate is limited by a choke point in the diffuser throat and remains constant $\varphi = 1$. The relative velocities λ_2, λ_3, and λ_4, are determined only by the geometry of the engine and do not change. The stagnation pressure ahead of the exit p_{03} and the static pressure at the nozzle exhaust edge p_4 decrease; and the overall pressure recovery σ_{ob} decreases:

$$p_{04} = \sqrt{\frac{R_r}{gk_r}\left(\frac{k_r+1}{2}\right)^{\frac{k_r+1}{k_r-1}}\frac{\beta G_s\sqrt{T_{0r}}}{\varepsilon_c S_{4cp}}},\tag{10.17}$$

$$\sigma_{ob} = \frac{p_{04}}{p_{0n}} = \frac{\varepsilon_c p_{03}}{p_{0n}}.\tag{10.18}$$

With a decrease of flight relative velocity λ_n, the stagnation temperature of the free stream flow $T_{0n} = \dfrac{T_n}{\tau(\lambda_n)}$ decreases. If the stagnation temperature of the exhaust gases T_{04} or the mixture ratio, α, are constants, then the temperature ratio θ will increase and the calculated cross section of the inlet S_{1cr} and S_1 will decrease. But when S_{1cr} is constant, one must increase the throat section of the nozzle S_{4cr}. The pressure recovery of the supersonic portion of the diffuser increases with a decrease in flight velocity.

If the engine must operate in design conditions at any flight speed $S_4 = S_M$, $p_4 = p_n$, then with a reduction of flight speed, the degree of divergence of the exhaust nozzle $\varepsilon = \dfrac{S_4}{S_{4cr}}$ decreases and together with it, the relative velocity and the stagnation pressure of the exhaust gases λ_4 and $\dfrac{p_{04}}{p_4}$.

In order for the same ramjet engine to operate at any speed and at any temperatu

-atio at the design condition, i.e., at the greatest possible pressure before the nozzle and with the least additive diffuser drag X_d, its terminal and throat sections must be controllable.

SECTION 3. THRUST PARAMETERS OF A SUPERSONIC RAMJET ENGINE

To determine the thrust parameters of a supersonic ramjet engine, it is necessary, at first, to find its jet thrust R (see 2.90):

$$R = F_4 - F_n - p_n(S_4 - S_n).$$

(10.19)

The impulse of the exhaust gases F_4 is determined by the equation (2.86):

$$F_4 = \frac{G_4 w_4}{g} + p_4 S_4.$$

(10.20)

After utilizing (5.27), we obtain

$$F_4 = \left(\frac{2}{k_r - 1}\right)^{\frac{1}{k_r - 1}} p_{04\sigma} S_{kp} \left(\lambda_4 + \frac{1}{\lambda_4}\right) = F_{kp} \frac{z(\lambda_4)}{2}.$$

(10.21)

The maximum relative discharge velocity $(\lambda_4)_{max}$ is determined by the intended pressure ratio $\frac{p_{04}}{p_n}$:

$$\lambda_{4max} = \sqrt{\frac{k_r + 1}{k_r - 1}\left[1 - \left(\frac{p_n}{\sigma_c p_{03}}\right)^{\frac{k_r - 1}{k_r}}\right]}.$$

(10.22)

The design degree of nozzle divergence ε_{rasch} is expressed by the equation 10.10)

$$\varepsilon_{rasch} = \frac{S_{vych}}{S_{kp}} = f\left(\frac{p_{03}}{p_n}, \sigma_c\right).$$

(10.23)

With a decrease of the nozzle pressure coefficient, σ_s, the relative velocity f the exhaust gases λ_4 diminishes, the static temperature of the gases T_4 increases, he density of the gases γ_4 decreases, and the calculated degree of nozzle diverence ε_{rasch} increases.

With an increase of the degree of divergence ε the nozzle pressure coefficient σ_s decreases, the dissipation of energy in the nozzle grows and the pressure losses ncrease.

$$\frac{p_{04}}{p_4} = \sigma_c \frac{p_{03}}{p_4} \frac{p_4}{p_n} = \sigma_{c4} \frac{p_{03}}{p_n} = \frac{\sigma_{c4}}{\pi(\lambda_n)}.$$

(10.24)

The pressure coefficient or impulse loss in nozzles of various configurations nd with various degrees of divergence are determined by experimental tests.

With an increase of the design flight velocity λ_n, the losses in the diffuser and nozzle increase and the gas dynamic coefficient of the engine $K = \dfrac{\lambda_4}{\lambda_n}$ decreases.

The stagnation impulse of the oncoming flow, which acts on the inlet section of the engine S_1, is equal to the sum of the momentum and the unbalanced pressure forces which act on the inlet slot and the deflecting spike. Considering the forces which act on both sides of the control surface, formed by the surface of the spike and the section of the inlet slot S_{shch} (Figure 183), we obtain

$$F_1 = \left[\frac{G_l w_l}{g} + p_l S_{uu}\right] \cos \omega_{o6} + \int p \, dS = F_{\text{m}} + X_{\text{доп}} =$$
$$= \frac{G_{\text{н}} w_{\text{н}}}{g} + p_{\text{н}} S_{\text{н}} + X_{\text{доп}}, \tag{10.25}$$

where ω_{ob} is the summary rake angle of the flow: $\omega_{ob} = \omega_1 + \omega_2 + \omega_3 + \ldots$

The integral $\int p dS$ represents the geometric sum of the pressure forces on the surface of the spike which protrudes from the diffuser (see Figure 179).

If the oblique shock waves are focused on the forward edge of the diffuser, additive drag resistance is absent: $X_d = 0$. In all cases, when the shock waves move away from the forward edge of the diffuser, additive drag, which is determined experimentally, appears.

The effective thrust R_{ef} is

$$R_{\text{эф}} = R - X_{\text{доп}} = \frac{G_4 w_4}{g} - \frac{G_{\text{г}} w_{\text{г}}}{g} - (p_4 - p_{\text{н}}) S_4 - X_{\text{доп}}. \tag{10.26}$$

The stagnation impulse of the stream tube flow F_n depends on the relative flight velocity λ_n, on the atmospheric pressure p_n, and on the cross section of the stream tube at infinity S_n.

After utilizing (2.71); (2.74); and (2.81), we obtain

$$F_{\text{н}} = \frac{G_{\text{н}} w_{\text{н}}}{g} + p_{\text{н}} S_{\text{н}} = \frac{k+1}{2gk} a_{\text{ж}} G_{\text{н}} z(\lambda_{\text{н}}) =$$
$$= p_{\text{н}} S_{\text{н}} \frac{\lambda_{\text{н}} r(\lambda_{\text{н}})}{\tau(\lambda_{\text{н}})} = p_{\text{0н}} S_{\text{н}} q(\lambda_{\text{н}}) z(\lambda_{\text{н}}), \tag{10.27}$$

where a_x is the critical velocity before heating.

The cross section of the stream tube flow S_n is determined from the continuity equation

$$S_{\text{н}} = \frac{G_{\text{н}}}{w_{\text{н}} \gamma_{\text{н}}} = \varphi S_1. \tag{10.28}$$

The mass flow ratio φ during heatings, which are less than calculated $\theta < \theta_{rasch}$, is determined by the flight velocity λ_n, the configuration, and the location of the center body diffuser. At temperature ratios which are more than calculated $\theta > \theta_{rasch}$, the mass flow ratio φ is determined by the cross section of the exhaust nozzle S_{4cr} and the parameters of the gases ahead of the exit p_{03} and T_{03}, and also by the pressure coefficient of the subsonic portion of the nozzle σ_s'.

At design point conditions, when the shock waves are focussed on the inlet edge, $p_1 = p_n$ and $X_{dop} = 0$. Then $S_n = S_1$, $= 1$.

After substituting (10.20) and 10.27) in (10.19), we obtain

$$R = p_{04} S_4 q(\lambda_4) z(\lambda_4) - p_{0n} S_n q(\lambda_n) z(\lambda_n) - p_n(S_4 - S_n);$$

$$R_n = \frac{R}{S_m} = p_n \left\{ \left[\frac{p_4}{p_n} \frac{\lambda_z(\lambda)}{\tau(\lambda)} \frac{S}{S_m} \right]_4 - \left[\frac{\lambda_z(\lambda)}{\tau(\lambda)} \frac{S}{S_m} \right]_n - \frac{S_4}{S_m} + \frac{S_n}{S_m} \right\}.$$

$$(10.29)$$

Jet thrust R is determined by the relative flight velocities and the exhaust λ_n and λ_4, by the atmospheric pressure p_n, by the mass flow ratio φ, and by the inlet and exit sections of the engine, S_1 and S_4. The temperature of the gases does not enter into the final thrust formula in an obvious form.

Heating of the gases is the only means of maintaining the high stagnation pressure of the exhaust gases, i.e. a high λ_4 when $S_{4cr} > S_{1cr}$. A thrust effect such as is obtained by heating, may be obtained by introducing an imaginery gas into the combustion chamber of the engine, so that the specific volume increases the required number of times.

The thrust coefficient C_R is

$$c_R = \frac{R}{S_m}. \qquad (10.30)$$

The effective thrust coefficient is

$$c_{R\,ef} = c_R - c_{x\,dop} \qquad (10.31)$$

where C_{xdop} is the additive wave drag coefficient, which is relative to the midships section and is determined experimentally.

The net thrust coefficient C_R chist is

$$c_{R\,chist} = c_R - c_{x\,dop} - c_{x\,ob}, \qquad (10.32)$$

where c_{xob} is the drag coefficient of the engine envelope (friction drag).

The net thrust of a supersonic ramjet engine R_{chist} must be greater than the

aerodynamic drag of the wings, fuselage, tail assembly, and the other portions of the aircraft. Figure 181 shows the drag of a V-2 rocket at supersonic flight speeds. The drag of the envelope of an air-breathing jet engine is caused primarily by
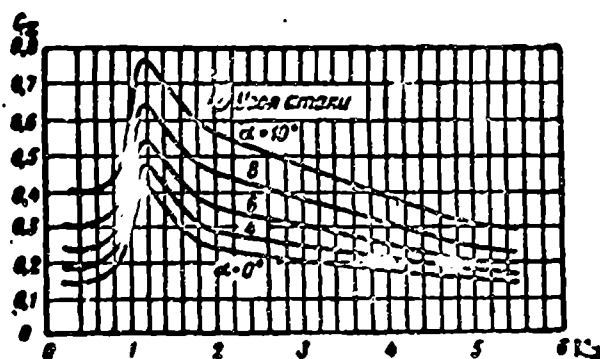
Legend:

-- A) Angle of attack

Fig. 181. The variation of the drag coefficient of a V-2 rocket with Mach number and angle of attack.

surface friction and by the pressure on the diffuser shell, since the drag of the center body diffuser is considered during the determination of the thrust and boat tail drag is absent when $S_4 = S_M$. Therefore, the drag of the shell comprises 50-70% of the drag of the ogive body that is depicted in Figure 181.

At high supersonic flight velocities the degree of nozzle divergence ε must be great. Therefore the area of the exhaust and midships sections are comparable: $S_4 = S_M$ (see Figure 183).

If the shock waves focus on the forward edge, then $S_n \cdot S_1$ and the additive drag $X_{dop} = 0$. If, during this, the exhaust section has the value computed from equation (10.14), then the pressure at the exhaust edge is equal to the back pressure $p_4 = p_n$, and the jet thrust formula may be simplified; using (2.55) and (2.74), we obtain

$$ \mathbf{R} = \frac{w_4 G_4}{g} - \frac{w_n G_n}{g} = \frac{2k_r}{k_r+1} S_4 p_{04} \lambda_4^2 \varepsilon(\lambda_4) - \frac{2k}{k+1} S_1 p_{04} \lambda_n^2 \varepsilon(\lambda_n). \tag{10.33} $$

Substituting the computed ratio of the inlet and exit sections $\dfrac{S_1}{S_4}$ in (10.14), we obtain a formula which is similar to the one which was introduced before for subsonic ramjet engines (see 9.27):

$$ \mathbf{R} = \frac{2k_r}{k_r+1} S_4 p_{04} \lambda_4^2 \varepsilon(\lambda_4) \left[1 - \frac{1}{x \beta K \sqrt{\theta}}\right]. \tag{10.34} $$

The thrust factor $C_R = \dfrac{R}{q S_M}$.

After using (2.70) and (10.34), we obtain

$$c_R = 2\pi^2 K^2 \frac{\bar{r}(\lambda_n)}{k_\tau \tau(\lambda_n)}\left[1 - \frac{1}{2K\beta\sqrt{\theta}}\right].$$ (10.35)

For a given temperature ratio θ = const, the thrust coefficient varies insignificantly with an increase of flight speed λ_n. At a given maximum temperature T_{0g} = const or for a given mixture composition α = const, the thrust coefficient diminishes with an increase of velocity.

Generally the specific thrust is equal to

$$I = \frac{R}{G_r} = \frac{H_s \eta}{A w_n}.$$ (10.36)

The magnitude of the thrust is determined by the equation (10.26) or (10.29).

When $p_4 = p_n$ and $S_n = S_1$, the specific thrust of a supersonic ramjet engine is expressed by the formula (9.34) or (9.43)

$$I = \alpha L a_x \lambda_n \frac{\beta_n K \sqrt{\theta} - 1}{\beta_s} = 2\frac{k-1}{k+1} \frac{H_s}{A} \frac{\lambda_n}{a_x} \frac{\beta_n K \sqrt{\theta} - 1}{\beta(\theta-1)} \varphi_{cr}.$$ (10.37)

The overall efficiency is

$$\eta = \frac{A R w_n}{N_Q} = \frac{A R w_n \varphi_{cr}}{\beta G_s c_p T_{0x}(\theta - 1)} = \frac{A L a_x \lambda_n \tau(\lambda_n)\varphi_{cr}}{\beta G_s c_p T_n(\theta - 1)}.$$ (10.38)

When $S_n = S_1$ and $p_4 = p_n$

$$\eta = 2\frac{k-1}{k+1}\lambda_n^2 \varphi_{cr} \frac{\beta K x \sqrt{\theta} - 1}{\beta(\theta-1)}.$$ (10.39)

The thermal power that is required by the engine N_Q, is

$$N_Q = c_p G_s \beta T_{0x} \frac{\theta-1}{\varphi_{cr}} = H_s G_r \quad \text{kcal/sec,}$$

$$N_Q = \frac{k\beta}{k-1}\sqrt{\frac{2gkR}{k+1}T_{0x}} \frac{p_n S_n \lambda_n(\theta-1)}{\varphi_{cr}\tau(\lambda_n)} \quad \text{kg m/sec.}$$ (10.40)

For a given temperature ratio, θ, the required thermal power N_Q increases quickly with an increase of λ_n owing to the increase of the air flow G_v and the final temperature of the gases $T_{0g} = \theta \dfrac{T_n}{\tau(\lambda_n)}$.

At a given temperature T_{0g} = const, the thermal power at first increases with an increase of velocity, reaches a maximum, and falls to zero when $T_{0g} = \dfrac{T_n}{\tau(\lambda_n)}$.

The flight range of a winged flying vehicle with an air-breathing jet engine is expressed by a formula of Tsiolkovskiy's (1.15):

$$l = w_n/k_a \ln \frac{1}{1-v} = DK.$$ (10.41)

From (10.36), it follows that the range factor $D = w_n I$ is equal to the product of the heating value of the fuel H_u (in mechanical units) and the overall efficiency of the air-breathing engine:

$$D = w_n I = \frac{H_u \eta}{A} \cdot m. \qquad (10.42)$$

The overall efficiency of an air-breathing jet engine η together with the aerodynamic quality k_a and the relative fuel weight ratio $\nu = 1 - \Psi$ determine the flight range. Here Ψ is the relative structural weight, which is equal to the ratio of the terminal flight weight to the initial weight.

$$\tau = \frac{P_{\text{кон}}}{P_{\text{нач}}} .$$

The ideal thermal efficiency η_t increases with an increase of flight speed, approaching one:

$$\eta_t = \frac{k-1}{k+1} \lambda_n^2 \rightarrow 1.$$

The effective thrust efficiency $(\eta_{tyag})_{ef}$ is determined by the temperature ratio θ and the gas dynamic factor of the engine K (ratio of specific heats). The variations of thrust efficiency with velocity are stated in Section 5 of this chapter.

Here is an example of designing a supersonic ramjet engine: We will assume that the flight speed is equal to the design point value: $M_n = M_{rasch} = 4$, $\varphi \leq 1$; $\lambda_n = 2.14$. We will assume that at this velocity, the pressure recovery of the diffuser (which must be determined by an experimental method) $\sigma_d = 0.3$. The flight altitude $H = 25$ km. According to the ICAD standard atmosphere:

$P_n = 18.6$ mm of mercury $= 253$ kg/m^2; $T_n = 216.5°$ K, $\gamma_n = 0.04$ kg/m^3; $c = 295$ m/sec.

We will find the thrust parameters of an engine which operates on kerosene, if $\alpha = 2.0$; $H_u = 10,200$ kcal/kg; $L = 14.8$ $\rho_{sg} = 1$. The midships cross section $S_M = 1$ m^2; the inlet cross section $S_1 = 0.9$ m^2, the mass flow ratio factor $\varphi = 1$, the exit cross section of the nozzle is equal to the midships $S_4 = S_M$. The nozzle pressure coefficient $\sigma_s = 0.9$. The drag coefficient of the combustion chamber $\zeta = 3$.

The stagnation parameters of the free stream flow (Figures 204 and 205) are

$$\frac{T_a}{T_{0a}} = \tau(\lambda_a) = 1 - \frac{k-1}{k+1}\lambda_a^2 = 1 - \frac{2.14^2}{6} = 0.238;$$

$$T_{0a} = \frac{T_a}{0.238} = \frac{216.5}{0.238} = 909^\circ K;$$

$$\frac{p_a}{p_{0a}} = \pi(\lambda_a) = [\tau(\lambda_a)]^{\frac{k}{k-1}} = 0.238^{\frac{1.4}{0.4}} = 0.00667;$$

$$p_{0a} = \frac{253}{0.00667} = 38\,000\,kg/m^2 = 3.8\ abs.\ atm.$$

The maximum possible pressure at the combustion chamber inlet is

$$p_{02} = \sigma_d p_{0n} = 0.3 \cdot 38,000 = 11,400\ kg/m^2 = 1.14\ abs.\ atm.$$

The stagnation enthalpy of the free stream flow is

$$i_{0x} = \frac{c_p T_a}{\tau(\lambda_a)} = \frac{0.24 \cdot 216.5}{0.238} = 218\ kcal/kg.$$

The stagnation enthalpy of the combustion products is

$$i_{0r} = i_{0x} + \frac{H_u \eta_{cr}}{1 + \alpha L} = 218 + \frac{10\,200}{1 + 2 \cdot 14.8} = 218 + 333 = 551\ kcal/kg.$$

After noting that the pressure ahead of the exit $p_{03} \approx 1\ kg/cm^2$ we will find

the stagnation temperature after combustion according to the i - T diagram (see

Figure 88):

$$T_{0g} = 1,920^\circ\ K$$

The temperature ratio is

$$\theta = \frac{T_{0r}}{T_{0x}} = \frac{1920}{909} = 2.11.$$

The adiabatic indicator (ratio of specific heats) when $\alpha = 2$ and the temperature is

$1,920^\circ$ K is: k = 1.312. The velocity of the free stream air is

$$w_a = c M_1 = 295 \cdot 4 = 1180\ m/sec.$$

The air flow through the engine is

$$G_v = \varphi w_n \gamma_n S_1 = 1,180 \cdot 0.040 \cdot 0.9 = 42.5\ kg/sec$$

The fuel flow is

$$G_g = \frac{G_v}{\alpha L} = \frac{42.5}{2 \cdot 14.8} = 1.435\ kg/sec$$

The flow of the gases through the exhaust nozzle is

$$G_g = G_v + G_g = 42.5 + 1.435 \approx 4\ kg/sec$$

The critical velocity of the oncoming air is

$$a_x = \sqrt{\frac{2gkRT_{0x}}{k+1}} = \sqrt{\frac{19.6 \cdot 1.4 \cdot 29.3}{2.4}}\ 909 = 18.3\ \sqrt{909} = 550\ m/sec.$$

The critical temperature is

$$T_{cr\ x} = \frac{2}{k+1} T_{0x} = \frac{T_{0x}}{1.2} = \frac{909}{1.2} = 756^\circ\ K$$

The critical pressure is

$$P_{\text{кр}} = \left(\frac{2}{k+1}\right)^{\frac{k}{k-1}} p_{01} = \frac{p_{01}}{1,89} = \frac{11\,400}{1,89} = 6030 \ \text{кг}/\text{м}^2 = 0,603 \ \text{abs. atm.}$$

The critical density is

$$\gamma_{\text{1кр}} = \frac{P_{\text{1кр}}}{RT_{\text{1кр}}} = \frac{6030}{29,3 \cdot 756} = 0,272 \ \text{kg}/\text{m}^3.$$

The cross section of the diffuser throat is

$$S_{\text{1кр}} = \frac{G_{\text{в}}}{\gamma_{\text{1кр}} w_{\text{1кр}}} = \frac{42,5}{0,272 \cdot 550} = 0,284 \ \text{m}^2.$$

We will find the calculated throat cross section of the exhaust nozzle after substituting

$$\sigma'_{\text{A}} \sigma_{\text{м}} \sigma_{\text{cr}} \sigma'_{\text{c}} \approx 0,9:$$

$$S_{\text{4кр}} = \frac{\xi \beta \sqrt{\theta}}{\sigma_{\text{A}} \sigma_{\text{м}} \sigma_{\text{cr}} \sigma_{\text{c}}} S_{\text{1кр}} = \frac{1,01 \cdot 1,03 \sqrt{2,11}}{0,9} \, 0,284 = 0,476 \ \text{m}^2.$$

In order to rule out the possibility of expelling the final (normal) shock wave from the diffuser throat in the event of a change decrease of flight velocity or an increase of temperature ratio θ, we will make the critical exhaust cross section somewhat greater than calculated:

$$S_{\text{4cr}} = 0.500 \ \text{m}^2$$

The degree of nozzle divergence is

$$s = \frac{S_4}{S_{\text{4кр}}} = \frac{1}{0,5} = 2.$$

We will find the relative velocity in the exhaust, and the pressure ratio across the nozzle by the graph which is depicted in Figure 77: $\lambda_4 = 1,75; \ \varepsilon = \frac{p_{04}}{p_4} = 10,3;$

$$\lambda_4 + \frac{1}{\lambda_4} = 1,75 + \frac{1}{1,75} = 2,32.$$

Jet thrust (see 2.90) is: $R = F_4 - F_{\text{в}} - p_{\text{н}}(S_4 - S_{\text{в}}).$

The reaction force of the exit gases is

$$F_4 = \sqrt{\frac{k_{\text{г}}+1}{2gk_{\text{г}}} R_{\text{г}} T_{04} G_{\text{г}} \left(\lambda_4 + \frac{1}{\lambda_4}\right)} =$$

$$= \sqrt{\frac{2,312 \cdot 29,5 \cdot 1920}{19,6 \cdot 1,312} \, 44 \cdot 2,32} = 1,635 \sqrt{1920 \cdot 44 \cdot 2,32} = 7300 \ \text{kg.}$$

The stagnation impulse of the stream tube flow, when $\varphi = 1, \ S_{\text{в}} = S_1$ is

$$F_{\text{в}} = \sqrt{\frac{k+1}{2gk} RT_{01} G_{\text{в}} \left(\lambda_{\text{в}} + \frac{1}{\lambda_{\text{в}}}\right)} = \sqrt{\frac{2,4 \cdot 29,3}{19,6 \cdot 1,4} \, 909 \cdot 42,5 \left(2,141 + \frac{1}{2,141}\right)} =$$

$$= 5360 \ \text{kg.}$$

Jet thrust is

$$R = F_4 - F_{\text{в}} - p_{\text{н}}(S_4 - S_{\text{в}}) = 7300 - 5360 - 253 (1 - 0,9) = 1915 \ \text{kg.}$$

The specific thrust is

$$I = \frac{R}{G_r} = \frac{1915}{1,435} = 1330 \text{ sec.}$$

The specific fuel flow is

$$Ce = \frac{3600}{I} = \frac{3600}{1300} = 2,7 \text{ 1/hr.}$$

The dynamic head is

$$q = \frac{k}{2} p_n M_n^2 = 0,7 \cdot 253 \cdot 4^2 = 2830 \text{ kg/m}^2.$$

The thrust coefficient is

$$c_R = \frac{R}{S_M q} = \frac{1915}{2830} = 0,677.$$

We will carry out a gas dynamic computation of the combustion chamber.

The stagnation pressure ahead of the exit nozzle is

$$p_{03} = \sqrt{\left(\frac{k_r+1}{2}\right)^{\frac{k_r+1}{k_r-1}} \frac{R}{g k_r} \frac{G_r \sqrt{T_{0r}}}{S_{\text{kp}}}} =$$

$$= \sqrt{\left(\frac{2,312}{2}\right)^{\frac{2,312}{0,312}} \frac{29,5}{9,8 \cdot 1,312} \frac{44 \sqrt{192}}{0,5}} = 10\,000 \text{ kg/m}^2.$$

The velocity ahead of the exit nozzle λ_3, according to Figure 170, is

$$\lambda_3 = 0,31; \quad z(\lambda_3) = 3,54.$$

The relative velocity before combustion is

$$z(\lambda_2') = \sigma \sqrt{\bar{\theta}} z(\lambda_3') = 1,01 \cdot 1,03 \sqrt{2,11} \cdot 3,54 = 5,37.$$

From this

$$\lambda_2' = \frac{z(\lambda_2')}{2} - \sqrt{\left[\frac{z(\lambda_2')}{2}\right]^2 - 1} = 2,685 - \sqrt{2,685^2 - 1} = 0,195.$$

The pressure coefficient for combustion is

$$\sigma_{gr} = \frac{z(\lambda_2')}{z(\lambda_3)} \frac{q(\lambda_2')}{q(\lambda_3)} = \frac{5,37}{3,54} \frac{0,195}{0,31} \frac{0,984}{0,96} = 0,985.$$

The pressure recovery for the flow around local resistances (flame-holders) is

$$\sigma_m \approx 1 - \frac{k}{k+1} \lambda_3^2 = 1 - \frac{1,4 \cdot 3}{2,4} 1,9^2 \approx 0,93.$$

The stagnation pressure at the diffuser outlet is

$$p_{0a} = \frac{p_{03}}{\sigma_m \sigma_{gr}} = \frac{10\,000}{0,93 \cdot 0,985} = 10\,900.$$

The pressure recovery in the diffuser is

$$\sigma_a = \frac{p_{0a}}{p_{0n}} = \frac{10\,900}{38\,000} = 0,287$$

somewhat less than the maximum possible value. In this way a chosen nozzle matches up

with a given diffuser.

The over-all pressure recovery in the engine is

$$\sigma_{o6} = \sigma_{A} \cdot \sigma_{M} \cdot \sigma_{cr} \cdot \sigma_{c} = 0,287 \cdot 0,93 \cdot 0,985 \cdot 0,9 = 0,238.$$

The overall efficiency of the engine is

$$\eta = \frac{A?w}{H_{u}G_{r}} = \frac{AIcM}{H_{u}} = \frac{1330 \cdot 295 \cdot 4}{427 \cdot 10200} = 0,36.$$

The flight range with a relative fuel weight ratio γ_{g} = 0.68 and an aerodynamic

quality (lift/drag ratio) k = 4 is:

$$l = cMlk \ln\frac{1}{1-0,68} = 295 \cdot 4 \cdot 1330 \cdot 4 \ln\frac{1}{0,32} = 7160 \text{ km},$$

Not a single other type of engine, only a supersonic ramjet engine, may achieve

a similar range of guided active flight at M_{n} = 4.

SECTION 4. COMPUTATION OF THRUST PARAMETERS OF A SUPERSONIC RAMJET ENGINE AS A FUNCTION OF MACH NUMBERS

The thrust parameters of a supersonic ramjet engine may be computed not by using

the relative velocities, as we did in the foregoing paragraph, but by the Mach numbers.

This last method of computation persists in American literature.[1]

The jet thrust of an engine, as is known, is determined from the difference

between the unbalanced pressure forces and the momentum at the exit of the engine in

an undisturbed flow:

$$R = \frac{G_{4}w_{4}}{g} + p_{4}S_{4} - S_{a}p_{a} - \frac{G_{a}w_{a}}{g_{i}} - p_{a}S_{a} + p_{a}S_{4} =$$

$$= \frac{G_{4}w_{4}}{g} + p_{4}S_{4} - \left(\frac{G_{a}w_{a}}{g} + p_{a}S_{a}\right) - p_{a}(S_{4} - S_{a}).$$ (10.43)

The flow impulse (mass flow parameter) in any section is

$$F = \frac{Gw}{g} + pS = pS(1 + kM^{2}),$$ (10.44)

since

$$\frac{Gw}{gpS} = \frac{\gamma w^{2}}{gp} = \frac{kw^{2}}{gkRT} = kM^{2}.$$ (10.45)

From (10.45), we obtain

$$pS = \frac{G}{M}\sqrt{\frac{RT}{gk}}.$$

[1] Marsh, B. W. and Sears, G. A., Introduction to the Analysis of Supersonic Ramjet Powerplants. Jet Propulsion, vol. 24, 1954, No. 3.
    Avery, W. H., Twenty-five Years of Ramjet Development. Jet Propulsion, vol. 25, Nov. 1955, No. 11.

Substituting for static temperature, the stagnation temperature, we obtain

$$F = G \sqrt{2 \frac{k+1}{gk} RT_0} \frac{1 + kM^2}{\sqrt{2(k+1)M^2 \left(1 + \frac{k-1}{2}M^2\right)}}.$$ (10.46)

The flow impulse (mass flow parameter) depends on the gas dynamic function of the Mach number

$$f(M) = \frac{1 + kM^2}{\sqrt{2(k+1)M^2 \left(1 + \frac{k-1}{2}M^2\right)}}.$$ (10.47)

The critical impulse of the gases, which discharge at sonic velocity from a convergent nozzle, is found after substituting M = 1 in (10.46). During this ·(M) = 1.

$$F_{sp} = G \sqrt{2 \frac{k+1}{gk} RT_{04}}.$$ (10.48)

After using (10.47) and (10.48), we obtain

$$F_4 = F_{sp} f(M).$$ (10.49)

After comparing (10.49) and (10.21), we find:

$$f(M) = \frac{1}{2} z(\lambda).$$ (10.50)

The function f(M) represents the relative increase of the impulse of the exhaust gases during the use of a divergent nozzle, in which the flow velocity grows from 4 = 1 to M_4.

The critical impulse, which is related to the air flow is called the air specific impulse I_a (see Chapter VIII, Section 4):

$$I_a = \sqrt{2 \frac{k_r + 1}{gk_r} R_r T_{04}}.$$ (10.51)

The critical impulse, which is related to the fuel consumption, is called the fuel specific impulse I_f:

$$I_f = \alpha L \sqrt{2 \frac{k_r + 1}{gk_r} R_r T_{04}}.$$ (10.52)

$$G_a I_a = G_f I_f = F_{sp}.$$ (10.53)

The impulse of the exhaust gases is

$$F_4 = p_4 S_4 (1 + k_r M_4^2) = G_a I_a f(M).$$ (10.54)

The impulse of the free stream flow is

$$X_n = p_n S_n (1 + kM_n^2) = G \sqrt{2 \frac{k+1}{gk} RT_{0n}} f(M_n).$$ (10.55)

The ratio of the exhaust cross section S_4 to the cross-section of the enclosed flow S_n, is found from the continuity equation

$$w_4 T_4 S_4 = \beta w_{\text{H}} T_{\text{H}} S_{\text{H}};$$
$$M_4 \sqrt{g k_r R T_4}\, S_4 \frac{p_4}{R T_4} = \beta M_{\text{H}} \sqrt{g k R T_{\text{H}}}\, S_{\text{H}} \frac{p_{\text{H}}}{R T_{\text{H}}}. \quad \Bigg\}$$

(10.56)

The calculated ratio of the inlet and exit sections when $p_1 = p_n$ and $S_n = S_1$ is:

$$\frac{S_4}{S_{\text{H}}} = \left(\frac{S_4}{S_1}\right)_{\text{pacu}} = \beta \sqrt{\frac{k}{k_r} \frac{R_r}{R} \frac{T_4}{T_{\text{H}}} \frac{M_{\text{H}}}{M_4} \frac{p_{\text{H}}}{p_4}}. \quad (10.57)$$

Converting from the static temperatures to the stagnation temperatures, we

obtain

$$\left(\frac{S_4}{S_1}\right)_{\text{pacu}} = \beta \frac{M_{\text{H}}}{M_4} \frac{p_{\text{H}}}{p_4} \sqrt{\frac{k R_r T_{04}}{k_r R T_{C_1}} \frac{1 + \frac{k-1}{2} M_{\text{H}}^2}{1 + \frac{k_r-1}{2} M_4^2}}. \quad (10.58)$$

For complete expansion of the exhaust gases $p_4 = p_n$, jet thrust is expressed by
a simplified formula

$$\mathbf{R} = \frac{G_4 w_4}{g} - \frac{G_{\text{H}} w_{\text{H}}}{g}.$$

After substituting $w = M\sqrt{g k R T}$, $G = w\gamma S$ and $\gamma = \frac{p}{RT}$, we obtain

$$\mathbf{R} = k_r p_4 S_4 M_4^2 - k p_{\text{H}} S_{\text{H}} M_{\text{H}}^2. \quad (10.59)$$

The thrust per unit area from (10.59) and (10.58) is

$$\mathbf{R}_{\text{H}} = \frac{\mathbf{R}}{S_4} = k_r p_4 M_4^2 \left(1 - \frac{k}{k_r} \frac{M_{\text{H}}^2}{M_4^2} \frac{S_{\text{H}}}{S_4}\right) =$$
$$= k_r p_4 M_4^2 \left[1 - \frac{M_{\text{H}}}{\beta M_4} \sqrt{\frac{k R T_{0\text{H}}}{k_r R_r T_{04}} \frac{1 + \frac{k_r-1}{2} M_4^2}{1 + \frac{k-1}{2} M_{\text{H}}^2}}\right]. \quad (10.60)$$

We find the thrust coefficient C_R from (10.59) and (10.58)

$$c_R = \frac{\mathbf{R}}{\frac{k}{2} p_{\text{H}} M_{\text{H}}^2 S_{\text{H}}} = 2\left(\frac{k_r}{k} \frac{M_4^2}{M_{\text{H}}^2} - \frac{S_{\text{H}}}{S_4}\right) =$$
$$= 2 \frac{k_r}{k} \frac{M_4^2}{M_{\text{H}}^2}\left[1 - \frac{M_{\text{H}}}{\beta M_4} \sqrt{\frac{k R T_{0\text{H}}}{k_r R_r T_{04}} \frac{1 + \frac{k_r-1}{2} M_4^2}{1 + \frac{k-1}{2} M_{\text{H}}^2}}\right]. \quad (10.61)$$

The Mach number of the discharge gases is less than that of the free stream:

$$\frac{M_4}{M_{\text{H}}} = \frac{1}{M_{\text{H}}} \sqrt{\frac{2}{k_r - 1}\left[\left(\frac{p_{04}}{p_4}\right)^{\frac{k_r-1}{k_r}} - 1\right]} =$$

$$-\frac{1}{M_n}\sqrt{\frac{2}{k_r-1}\left[\sigma_{ob}^{\frac{k_r-1}{k_r}}\left(1+\frac{k-1}{2}M_n^2\right)^{\frac{k}{k-1}\cdot\frac{k_r-1}{k_r}}-1\right]}<1. \qquad (10.62)$$

SECTION 5. AN ANALYSIS OF A SUPERSONIC RAMJET ENGINE

The thrust parameters of a supersonic ramjet engine R, C_R, I, and the overall efficiency are determined by the relative flight velocity λ_n, the flight altitude H, the temperature ratio θ, the ratio of the inlet to exit sections of the engine $\frac{S_1}{S_4}$, and the pressure losses through the engine duct. We will analyze the effect of each of these parameters.

Flight Speed. First we will consider the effect of the flight speed at constant temperature ratio θ = const and when H = const.

Legend:

A) normal shock wave
B) oblique shock wave + normal shock wave
C) two oblique shock waves and a normal shock wave
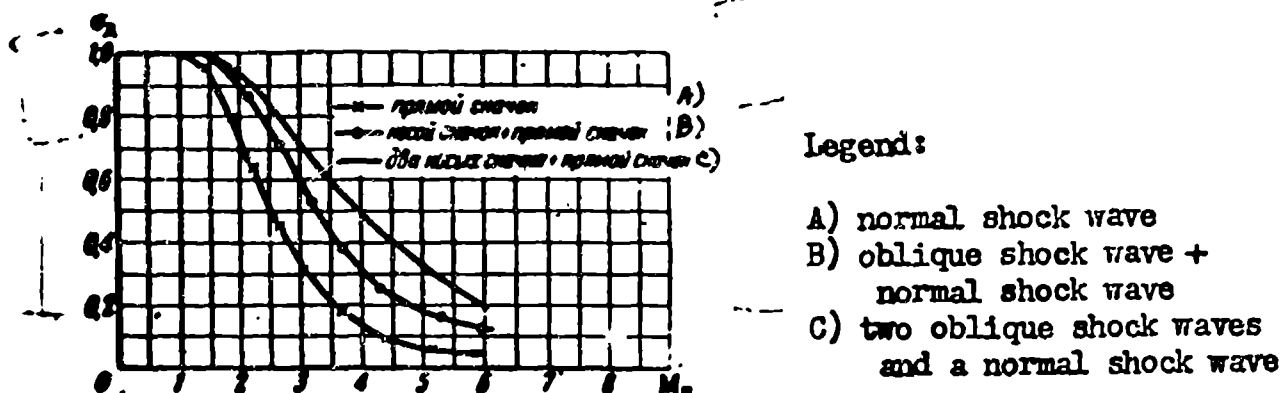
Fig. 182. The calculated variation of pressure recovery in a diffuser with Mach number.

The stagnation temperature of the heated gases increases with an increase of flight speed:

$$T_{0r}=\frac{T_{0r}}{T_{0x}}T_{0x}=\theta\frac{T_{a}}{\tau(\lambda_n)}. \qquad (10.63)$$

Poisson's index k_g decreases due to the increase of T_{0g}, and the function x diminishes while the function ξ grows.

The overall pressure recovery σ_{ob} decreases with an increase of velocity because of the pressure losses in the diffuser (Figure 182) and in the nozzle.

The gas dynamic coefficient $K = \frac{\lambda_4}{\lambda_n}$ slowly diminishes with an increase of velocity due to the decrease of σ_{ob}.

The thrust coefficient C_R, at constant temperature ratio θ, increases with an increase of velocity, asymptotically approaching the limiting value.

Jet thrust, at constant temperature ratio, increases approximately in direct

proportion to the square of the Mach number for an increase of velocity.

The ideal thermal efficiency approaches unity for an unlimited increase of velocity. When $\lambda_n^2 \to \frac{k+1}{k-1}$

$$\eta = \frac{k-1}{k+1}\lambda_a^2 \to 1.\tag{10.64}$$

The effective thrust efficiency at first diminishes with a decrease of K at constant temperature ratio θ; (see Table 10.2).

The specific thrust of a supersonic ramjet engine as follows from (9.43) is directly proportional to the ratio λ_n/a_x for constant temperature ratio θ and constant heating value of the fuel H_u, when θ = const, η_{tyag} = const.

$$I = \frac{k-1}{k+1}\frac{H_u}{A}\eta_{tar}\frac{\lambda_a}{a_x} = \frac{k-1}{\sqrt{2(k+1)}}\frac{H_u\gamma_{tar}}{Ac_a}\lambda_a\sqrt{1-\frac{k-1}{k+1}\lambda_a^2},\tag{10.65}$$

since

$$\frac{\lambda_a}{a_x} = \frac{\lambda_a}{\sqrt{\frac{2gkRT_a}{(k+1)\tau(\lambda_a)}}} =$$

$$I = \sqrt{\frac{k+1}{2gkRT_a}}\lambda_a\sqrt{1-\frac{k-1}{k+1}\lambda_a^2} = \sqrt{\frac{k+1}{2}}\frac{\lambda_a}{c_a}\sqrt{1-\frac{k-1}{k+1}\lambda_a^2}.$$

After equating the first derivative of the gas dynamic function $\lambda_n^2 - \frac{k-1}{k+1}\lambda_n^4$, with respect to λ_n, to zero, we find the optimum relative flight velocity at which the specific thrust will become the greatest for constant temperature ratio θ:

$$\frac{d}{d\lambda_a}\left(\lambda_a^2 - \frac{k-1}{k+1}\lambda_a^4\right) = 2\lambda_a - 4\frac{k-1}{k+1}\lambda_a^3 = 0.$$

From this, when k = 1.4

$$\lambda_{a.\,opt} = \sqrt{\frac{1}{2}\frac{k+1}{k-1}} = \frac{\lambda_{max}}{\sqrt{2}} = \sqrt{3} = 1.73.\tag{10.66}$$

The optimum flight Mach number is

$$M_{a.\,opt} = \sqrt{\frac{2}{k+1}\frac{\lambda_{a.\,opt}}{\tau(\lambda_{a.\,opt})}} = \sqrt{\frac{2}{k-1}} = \sqrt{5} = 2.24.\tag{10.67}$$

The optimum flight speed is greater than the speed of sound: $\lambda_{n\,opt} > 1$. In the subsonic area the specific thrust of a ramjet engine increases with an increase of flight speed.

The maximum value of the specific thrust from (10.65) and (10.66) at constant temperature ratio is:

$$I_{max} = \sqrt{\frac{k-1}{2g k R T_{a}}} \frac{\varphi_{cr} H_{a}}{A} \frac{\beta_{n} K \sqrt{\theta}-1}{\beta(\theta-1)} = \sqrt{\frac{k-1}{g}} \frac{H_{a}}{A c_{a}} \eta_{r.\,a}. \tag{10.68}$$

When $\lambda_n = \lambda_{n\ opt} = 1.73$; $H_u = 10{,}200$ kcal/kg and $c_n = 295$ m/sec: $I_{max} = 3{,}340 \hat{n}_{t.d.}$. When $xK = 0.92$, $\beta \approx 1$, $\varphi_{sg} = 1$, and $\theta = 3$.

$$\eta_{r.\,a} = 2\varphi_{cr} \frac{\beta_{n} K \sqrt{\theta}-1}{\beta(\theta-1)} = 2 \frac{0.92\sqrt{3}-1}{3-1} \approx 0.6; I_{max} = 3340 \cdot 0.6 \approx 2000 \text{ sec.}$$

The heat resistant quality of the material limits the maximum possible heating temperature T_{Og}.

We will consider the effect of the flight speed upon the parameters of a supersonic ramjet engine at a constant temperature $T_{Og} = $ const.

The temperature ratio θ, when $T_{Og} =$ const, diminishes with an increase of velocity λ_n because of the increased stagnation temperature of the free stream flow:

$$\theta = \frac{T_{Og}}{T_a} \tau(\lambda_n).$$

The thrust coefficient C_R decreases to zero for an increase of λ_n due to the decreased temperature ratio. When $x\beta K\sqrt{\theta} = 1$, $C_R = 0$. Hence, the limiting flight velocity λ_{pr} is:

$$[\tau(\lambda_n)]_{np} = \frac{T_a}{T_{Og}} \frac{1}{\beta_n^2 K^2}, \tag{10.69}$$

$$\lambda_{np} = \sqrt{\frac{k+1}{k-1}\left(1 - \frac{T_a}{T_{Og}} \frac{1}{\beta_n^2 K^2}\right)}. \tag{10.70}$$

With an increase of the permissable temperature T_{Og}, the limiting velocity grows. When $\beta xK = 1$ and $\frac{T_{Og}}{T_n} = 15$, then $\lambda_{pr} \approx 2.4$ and $M_{pr} \approx 10$. Such, apparently, is the limiting velocity of a supersonic ramjet engine.

The specific thrust at constant temperature, $T_{Og} =$ const, is found from (10.37) with consideration (10.63).

$$I = \frac{k-1}{k+1} \frac{H_a \varphi_{cr} \lambda_n}{A\sqrt{\frac{2g k R T_a}{(k+1)\tau(\lambda_n)}}} \frac{\beta K \sqrt{\frac{T_{Og}}{T_a}\tau(\lambda_n)}-1}{\beta\left[\frac{T_{Og}}{T_a}\tau(\lambda_n)-1\right]}.$$

After substituting $\lambda_n = \sqrt{\frac{k+1}{k-1}[1-\tau(\lambda_n)]}$ и $c = \sqrt{g k R T_a}$, and after a conversion we obtain

sion we obtain

$$I = \sqrt{2(k-1)} \frac{H_u \varphi_{cr}}{A\ell} \frac{\sqrt{\tau(\lambda_n) - [\tau(\lambda_n)]^2} \left\{ \varkappa K \sqrt{\frac{T_{0r}}{T_n} \tau(\lambda_n)} - \frac{1}{\beta} \right\}}{\frac{T_{0r}}{T_n} \tau(\lambda_n) - 1} .$$

(10.71)

At a certain value of the gas dynamic function $\tau(\lambda_n)$, i.e., at a certain flight speed λ_n, the specific thrust of a supersonic ramjet engine for a temperature T_{0g} = const reaches a maximum (Table 10.1). When $\frac{T_{0g}}{T_n}$ = 8, $\varkappa K$ = 0.92 and $\lambda_{opt} \approx 1.9$.

Jet thrust, when T_{0g} = const, passes the maximum and falls to zero with an increase of velocity in accordance with the condition expressed by the equation (10.70). The higher the velocity values, the greater is the temperature T_{0g}.

The thrust efficiency, when T_{0g} = const, passes a maximum and falls to zero together, with the thrust force, with a variation in velocity.

Table 10.1

THE DEPENDENCE OF THE SPECIFIC THRUST OF A SUPERSONIC RAMJET ENGINE UPON THE VELOCITY λ_n WHEN H_u = 10,500 kcal/kg, $\varkappa K$ = 0.92 = const and β = 1; φ_{sg} = 1 and H > 11 km.

λ_n	1,4	1,6	1,8	2,0	2,1	2,2
$\tau(\lambda_n)$	0,673	0,557	0,460	0,333	0,265	0,194
$\lambda_n \sqrt{\tau(\lambda_n)}$	1,150	1,195	1,222	1,153	1,081	0,968
$\theta = 1,5 \quad \eta_{r,л} = 0,50$						
I	1470	1520	1560	1470	1360	1235
$\theta = \theta_{opt} = 2,28 \quad \eta_{r,л} = (\eta_n)_{opt} = 0,61$						
I	1790	1860	1900	1800	1680	1510
$\theta = 3 \quad \eta_{r,л} = 0,593$						
I	1740	1810	1850	1750	1640	1470
$\theta = 4 \quad \eta_{r,л} = 0,56$						
I	1650	1710	1750	1650	1550	1380
$\frac{T_{0r}}{T_n} = 8$						
θ	5,38	4,45	3,68	2,66	2,12	1,553
$\eta_{r,л}$	0,518	0,546	0,570	0,606	0,600	0,535
I	1525	1670	1780	1790	1670	1330

Temperature Ratio. The effect of the temperature ratio $\theta = \frac{T_{0g}}{T_{0x}}$ at constant flight velocity was investigated before in Chapter IX. The conclusions that are made remain correct even when $\lambda_n > 1$.

The thrust and thrust coefficient grow with an increase of temperature ratio and the calculated inlet section ratio $\frac{S_1}{S_M}$ = f decreases. The specific thrust I and the thrust efficiency reach their maximum value at the optimum temperature ratio θ_{opt}

$$\theta_{cr} = \frac{1 + \sqrt{1 - x^2 K^2}}{1 - \sqrt{1 - x^2 K^2}} . \tag{10.72}$$

When

$$\theta \gtrsim \theta_{cr}, \quad I < I_{max} \text{ and } \eta_{rel} < \eta_{rel. max}$$

If the relative velocity has an optimum value, which is expressed by the equation (10.66), and the temperature ratio also has an optimum value, which is e..pressed by the equation (10.72), then the specific thrust I reaches the highest possible value of all $I_{max\ max}$:

$$I_{max\ max} = \sqrt{\frac{k-1}{8} \frac{H_u \varphi_{cr}}{Ac} \left(\frac{1}{\beta} - \frac{1 - \beta x^2 K^2}{\beta \sqrt{1 - x^2 K^2}} \right)} . \tag{10.73}$$

When $\beta \approx 1$

$$I_{max\ max} = \sqrt{\frac{k-1}{8} \frac{H_u \varphi_{cr}}{Ac} (1 - \sqrt{1 - x^2 K^2})} .$$

For an ideal ramjet engine $xK = 1$ and $\varphi_{sg} = 1$. Consequently,

$$(I_{max\ max})_{ad} = \sqrt{\frac{k-1}{8} \frac{H_u}{Ac}} . \tag{10.74}$$

This is the limit, to which the specific thrust of a ramjet engine approaches when the losses tend toward zero and the temperature ratio θ approaches one.

When $k = 1.4$; $A = 1/427$; $c = 295$ m/sec, and $H_u = 10.500$ Kcal/kg

$$(I_{max\ max})_{ad} = \sqrt{\frac{0.4}{8} \frac{10500 \cdot 427}{295}} = 3400 \text{ sec.}$$

The Location of the Center Body Diffuser and the Inlet area Ratio $f = \frac{S_1}{S_M}$. The inlet area ratio and the location of the center body diffuser influence the air flow and in this way determine the thrust parameters of a ramjet engine.

The highest value of the inlet ratio $\frac{(S_1)}{(S_M)_{max}} = 1$. The lowest value may be zero $\frac{(S_1)}{(S_M)_{min}} = 0$. In this case the flow is equal to zero: $G_v = 0$ and thrust is absent: $R = 0$ (Figure 183).

The maximum possible air flow $G_{v\ max}$ is equal to

$$G_{s\ max} = w_s \gamma_s S_s \tag{10.75}$$

The calculated cross sections of the inlet slot S_{shch} and the diffuser throat

S_{lcr} are determined from the equation of continuity for the maximum possible flow coefficient $\varphi = 1$:

$$w_n \gamma_n S_1 = w_{shch} \gamma_{shch}(S_{shch})_{rasch} = w_{lcr} \gamma_{lcr}(S_{lcr})_{rasch}$$

The actual cross sections of S_{shch} and S_{lcr} must be always greater than calculated in order to compensate for the partial closing of the slot by the boundary layer. An increase of the throat section of the diffuser, when the location of the center body diffuser is fixed and at a given velocity λ_n = const and given inlet cross section, does not influence the value of the maximum possible flow through the engine. The cross section of the stream tube of flow and the configuration of the shock waves does not change during this increase.

For a decrease of flight velocity or a forward movement of the center body diffuser, the leading shock wave breaks away from the forward edge of the diffuser (see Figure 184b) and the cross section of the stream tube of flow and the flow coefficient φ diminish. If the flight speed is given: λ_n = const, then the flow coefficient, and together with it, the pressure recovery depends upon the location of the center body diffuser. The location is determined by the angle θ_1 between the lines which connect the apex of the spike with the diffuser lip and with the longitudinal axis of the engine (see Figures 65b and 184). The stream lines behind the leading shock wave are approximately parallel with the spike generatrix. With a forward movement of the center body diffuser, this angle θ_1 decreases and, as seen from Figure 184, the stream tube constricts and φ diminishes. The system of shock waves which appear at
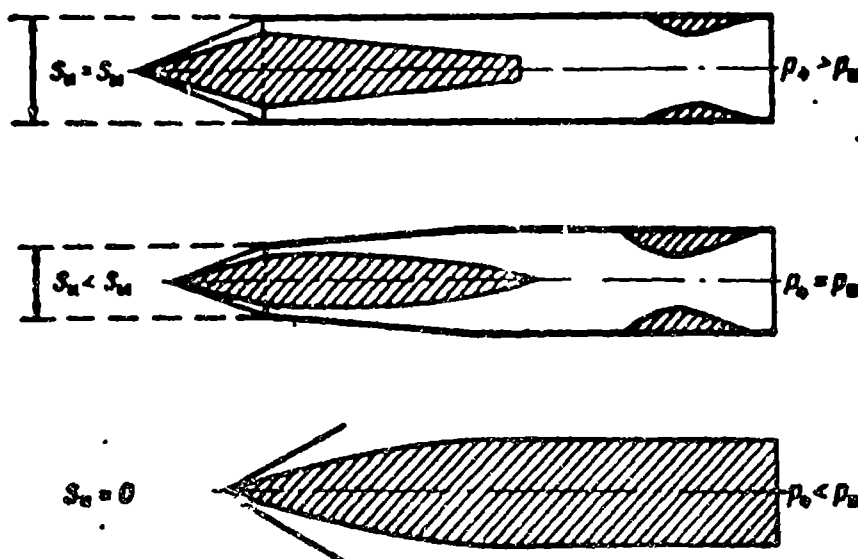

Fig. 183. The dependence of the air flow through a supersonic ramjet engine upon the inlet area ratio.

the inlet slot varies, and the pressure recovery becomes less than the maximum possible value (Figure 185). For a backward movement of the center body diffuser, θ_l increases, a supersonic flow enters the throat, and σ_d decreases (Figure 185). The flow coefficient remains constant: $\varphi = 1$.

The location of the center body diffuser at which the pressure recovery factor becomes the greatest is determined experimentally. It usually occurs when the leading shock wave falls on the diffuser lip (see Figures 184a and 185b).

For a calculated location of the center body diffuser, the air flow through a supersonic ram jet engine is determined by the inlet area ratio $\dfrac{S_1}{S_M}$. With an increase of the inlet area ratio, the calculated throat cross section of the nozzle $\dfrac{S_{4cr}}{S_M}$ increases. From the flow equation (2.74) and with consideration of (2.53) we obtain

$$\frac{S_{cp}}{S_M} = \frac{S_1}{S_M}\frac{p\lambda_1 q(\lambda_1)}{p_c^2\lambda\, q_{cr}}\sqrt{\frac{2}{k+1}\left(\frac{k_r+1}{2}\right)^{\frac{k_r+1}{k_r-1}}\frac{k}{k_r}\frac{R}{R_r}}\,\theta. \tag{10.76}$$

Fig. 184. The dependence of the flow factor upon the location of the center body diffuser.

a -- $\theta_l = \alpha_1$; $\varphi = 1$; b -- $\theta_l < \alpha_1$; $\varphi < 1$; c -- $\theta_l > \alpha_1$; $\varphi = 1$

When $k = 1.4$; $k_g = 1.3$; and $\dfrac{R_g}{R} = 1.01$

$$\sqrt{\frac{2}{k+1}\frac{k}{k_r}\frac{R}{R_r}\left(\frac{k_r+1}{2}\right)^{\frac{k_r+1}{k_r-1}}} \approx 1.6.$$

value (Figure 185). For a backward movement of the center body diffuser, θ_{ℓ} increases, a supersonic flow enters the throat, and σ_d decreases (Figure 185). The flow coefficient remains constant: $\varphi = 1$.

The location of the center body diffuser at which the pressure recovery factor becomes the greatest is determined experimentally. It usually occurs when the leading shock wave falls on the diffuser lip (see Figures 184a and 185b).

For a calculated location of the center body diffuser, the air flow through a supersonic r jet engine is determined by the inlet area ratio $\dfrac{S_1}{S_M}$. With an increase of the inlet area ratio, the calculated throat cross section of the nozzle $\dfrac{S_{4cr}}{S_M}$ increases. From the flow equation (2.74) and with consideration of (2.53) we obtain

$$\frac{S_{4cr}}{S_M} = \frac{S_1}{S_M} \frac{\varphi \lambda_{1} f(\lambda_1)}{\sigma_c^2 \lambda^* \sigma^* _{cr}} \sqrt{\frac{2}{k+1}\left(\frac{k_r+1}{2}\right)^{\frac{k_r+1}{k_r-1}} \frac{k}{k_r}\frac{R}{R_r}\theta} \quad (10.76)$$
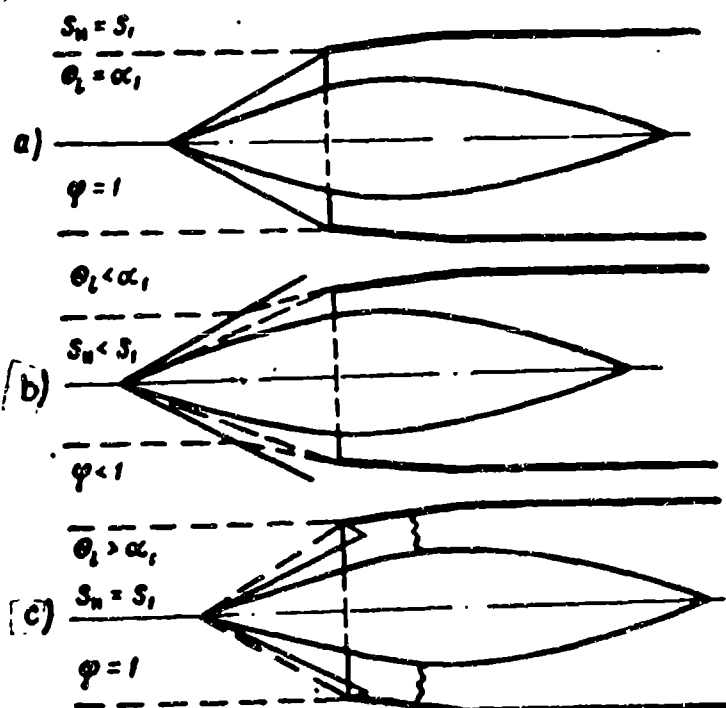

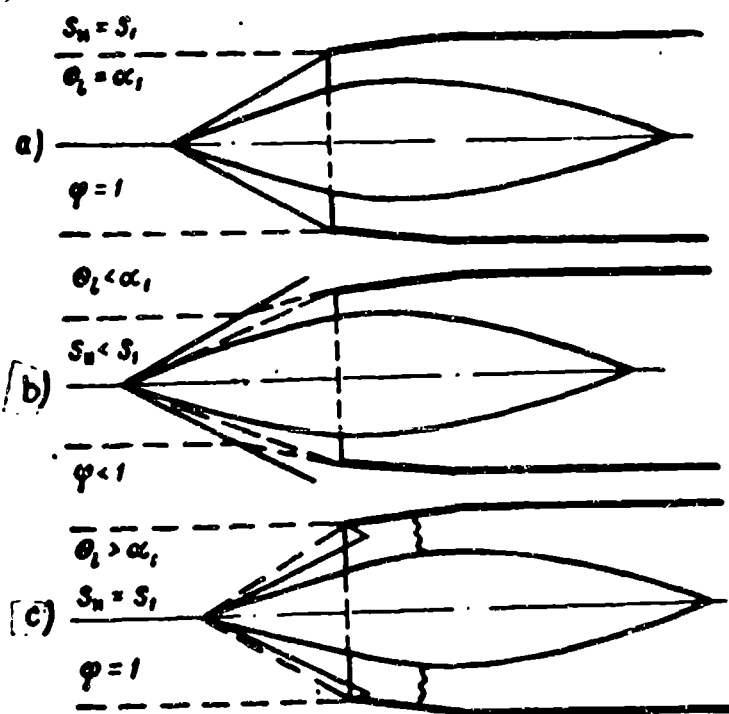Fig. 184. The dependence of the flow factor upon the location of the center body diffuser.
a -- $\theta_{\ell} = \alpha_1$; $\varphi = 1$; b -- $\theta_{\ell} < \alpha_1$; $\varphi < 1$; c -- $\theta_{\ell} > \alpha_1$; $\varphi = 1$

When $k = 1.4$; $k_g = 1.3$; and $\dfrac{R_g}{R} = 1.01$

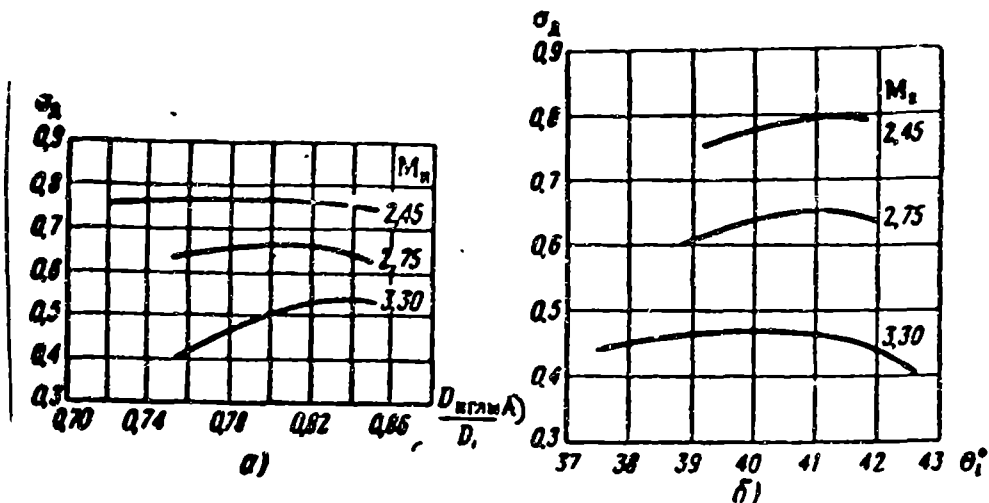$$\sqrt{\frac{2}{k+1}\frac{k}{k_r}\frac{R}{R_r}\left(\frac{k_r+1}{2}\right)^{\frac{k_r+1}{k_r-1}}} \approx 1.6.$$

Fig. 185. The characteristics of a supersonic diffuser.
a -- the dependence of the pressure recovery upon the relative diameter of the center body diffuser.
b -- the dependence of the pressure recovery of the diffuser upon the location of the center body diffuser.
A) of center body diffuser.

If the velocity λ_n and the temperature ratio θ are given, then at a certain value of the inlet $f_{1\ max} = \dfrac{S_1}{S_M}$ the calculated throat cross section of the nozzle becomes equal to the midships cross section: $\dfrac{S_{4cr}}{S_M} = 1$. A further increase of the inlet area ratio may be accompanied by forcing out the normal shock wave from the throat and a transition into a "buzzing" condition. The limiting value of the inlet area ratio $f_{1\ max}$ for a given λ_n and θ is determined by the equation (10.76), if $\dfrac{S_{4cr}}{S_M} = 1$.

The degree of expansion of the exhaust nozzle ε may not become greater than the ratio of the middle of an uncowled engine to the throat cross section of the nozzle:

$$\varepsilon < \frac{S_M}{S_{4cp}} .$$

With an increase of the inlet area ratio f_1 the degree of nozzle expansion decreases and together with it, the relative velocity of the exhaust gases λ_4 and the pressure ratio in the nozzle $\dfrac{P04}{P4} = \sigma_s \dfrac{P03}{P4}$. The static pressure at the nozzle inlet edge p_4 increases $/$see Graph 77 and formula $(10.10)/$.

The jet thrust at first increases with an increase of the inlet area ratio due to the increased air flow G_v, reaches a maximum value and begins to diminish because of the decrease of the gas dynamic function $\lambda_4 + \dfrac{1}{\lambda_4}$. The net thrust reaches a maximum at a somewhat larger inlet ratio, since with an increase of $\dfrac{S_1}{S_M}$, the external drag of the diffuser envelope X_{ob} decreases. The value of the inlet area ratio, at

the temperature ratio θ, and upon the losses in the engine.

The specific thrust of the engine at a constant composition of the mixture α = const, (as follows from (9.34), depends on the relative velocity of the exhaust gases $\frac{w_4}{w_n}$. The velocity increases with an increase of the degree of expansion of the exhaust nozzle, and reaches a maximum at

$$ \epsilon = \left(\frac{S_4}{S_{\text{мир}}}\right)_{\text{раст}} = f\left(\frac{r_{04}}{p_4}\right). $$

The ratio of the inlet to exit sections $\frac{S_1}{S_4}$ also has a calculated value which is expressed by the equation (10.14). Consequently, the specific thrust is maximum for the design point ratio of the inlet to exit sections.

The minimum cross section of the inlet is determined by equation (10.14). At this value the specifi. thrust is maximum. The maximum permissible inlet cross section, at which a "buzzing" condition may occur, is determined by the equation (10.76) under the condition that the throat cross section of the nozzle merges with the midships section: $\frac{S_{4\text{cr}}}{S_M} = 1_o$ If the heating is not too intensive, the "buzz" may occur at $\frac{S_1}{S_M} = 1$. The relative inlet cross-section, at which the net thrust reaches maximum, lies between $\frac{S_1}{S_M} = \frac{(S_1)}{(S_4)_{\text{rasch}}}$ and $\frac{S_1}{S_M} = 1$.

With an increase of λ_n when θ = const, $\frac{(S_1)}{(S_4)_{\text{rasch}}}$ decreases. With an increase of flight speed when θ = const, $\frac{(S_1)}{(S_4)_{\text{rasch}}}$ decreases insignificantly due to the decrease of the gas dynamic factor $K = \frac{\lambda_4}{\lambda_n}$. When T_{0g} = const (or when α = const) with an increase of λ_n,

$$ \epsilon = \frac{T_g}{T_a} \tau(\lambda_n) $$

diminishes and the inlet area ratio grows, gradually approaching ono.

The discussions covered in this paragraph refer to a series of engines whose cross-sections and inlet and exit sections have design point values for any flight conditions and at any temperature ratio, while the pressure recovery is at the maximum.

An engine, the cross-sections of which may be controlled, is called a _variable geometry engine_. A variable geometry engine differs from an optimum engine, since

maximum, depends upon the flight speed. It is, apparently, impossible to change the rake angle (cone angle) in accordance with the change of flight speed.

Usually the position of the spike (or cone) and the throat section of the nozzle is controlled.

The regulating, velocity, and altitude characteristics of a supersonic ramjet engine differ.

The characteristics may be plotted for a variable position of the bullet and adjustable throat section of the nozzle; for a constant position of the bullet and adjustable throat section; and, finally, for a fixed geometry of the engine. In this way, the characteristics of a variable-geometry engine, the characteristics of a partially variable-geometry engine, and the characteristics of a fixed-geometry supersonic ramjet engine differ.

SECTION 6. THE REGULATING CHARACTERISTICS OF A SUPERSONIC RA JET ENGINE WITH A VARIABLE-GEOMETRY NOZZLE

The regulating characteristics describe the dependence of the parameters of a supersonic ramjet engine upon the temperature of the gases, which is determined by the heat liberation in the combustion chamber (Figure 186). If the engine operates on a molecular fuel, then the heat liberation is determined by the composition of the fuel-air mixture and the combustion efficiency φ_{sg}.
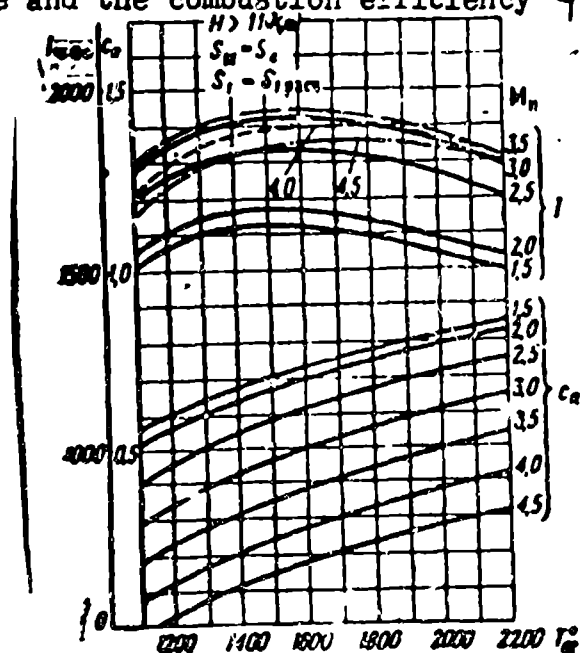

Fig. 186. The regulating characteristic of a supersonic ramjet engine with a variable-geometry nozzle.

During operation on a molecular fuel, the control of heat liberation is accomplished by varying the fuel feed G_T, changing the fuel feed pressure, or by changing the number of operating injectors.

The throat section of the nozzle is controlled so that the air flow remains constant and equal to the maximum possible value

$$G_s = w_s T_s S_1 = \sqrt{\frac{g^k}{RT_s}}\, p_s S_1 M_s,$$

and the flow coefficient would be equal to one, $\varphi = 1$.

If the cross section of the nozzle has a calculated value, which is determined the equation (10.76), then the pressure recovery will have the maximum possible value for a given diffuser at a given velocity (see Figure 182).

With an increase of the temperature ratio θ and with a decrease of the pressure coefficients σ''_d, σ_M, σ_{sg}, and σ'_s the calculated throat cross section of the nozzle S_{4cr} increases. If $M_n = 3\text{-}4$ then during a variation of the temperature ratio from the optimum value $\theta_{opt} = 2.3$ to the maximum possible on a hydrocarbon fuel when $\alpha = 1$ and $\theta_{max} = 4$, the calculated throat cross section of the nozzle creases approximately $\sqrt{\dfrac{\theta_{max}}{\theta_{opt}}} = \sqrt{\dfrac{4}{2.3}} \approx 1.3$ times.

The control of a supersonic ramjet engine within a wide range of temperatures requires a variation of the nozzle's throat cross section by less than one third.

The computation of the regulating characteristics of a supersonic ramjet engine with a variable-geometry nozzle is carried out in the following order: the velocity, flight altitude, and nature of the fuel are given. A diffuser, which will insure the ghest pressure recovery σ_d at a given flight speed, is chosen. The enthalpy of the stagnation flow $i_{0n} = \dfrac{i_n}{\tau(\lambda)_n}$ is computed and the stagnation temperature T_{0n} is found according to the i-T diagram.

A series of air excess ratios α is given and the enthalpy of the combustion products is determined.

$$i_{gt} = i_{0n} + \frac{H_n \eta_{cr}}{1 + \alpha L}.$$

The stagnation temperature of the combustion products is found by the i-T

diagram for the corresponding composition of the mixture and the pressure p_{03}. The combustion efficiency is obtained by the experimental characteristics of the combustion chamber.

Poisson's index k_g, found with the aid of the u-T and i-T diagrams, (see Figures 90 and 92) is:

$$k_r = \frac{\Delta i}{\Delta u}; \quad k_r = \frac{c_p}{c_v}.$$

Without considering disassociation, k_g may be found by graph 86. After determining k_g, the functions x, χ, and ξ are calculated.

The relative velocity at the chamber inlet λ_2 is determined by the degree of diffuser expansion $\frac{S_2}{S_{1cr}}$ (Figure 187).

The velocity at the inlet to the combustion chamber $w = a_x \lambda_2$. The Reynolds number of the flow, in the forward portion of the engine is: $Re = \frac{w_2 d_2}{\gamma_2}$.

The coefficient of local resistance ζ is determined by the Re-number and the chamber design.

The air flow through an engine with a variable geometry nozzle is constant and does not depend on the fuel feed: $G =$ const and $w_2 =$ const. The local pressure losses, which are expressed by the formula (8.19), also remain constant $\sigma_M =$ const.
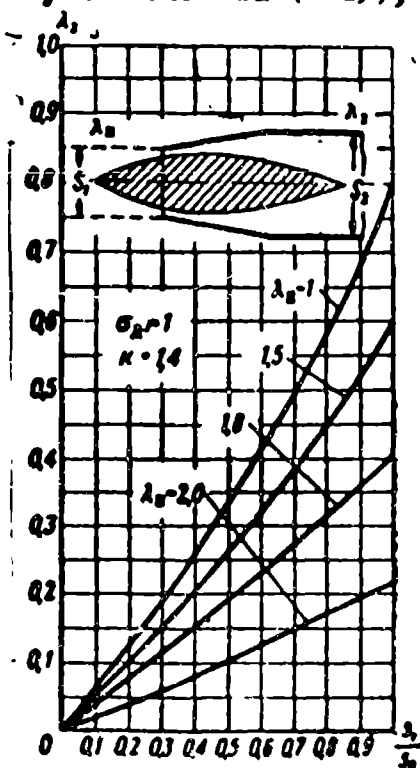

Fig. 187. The dependence of the relative velocity at the diffuser outlet λ_2 upon the inlet area ratio $f_1 = \frac{S_1}{S_2}$.

The temperature ratio increases with the enrichment of the mixture: $\theta = \frac{T_{0g}}{T_{0x}}$.

The relative velocity before exhaust λ_3, in accordance with (8.31), increases

with an increase of heating. The pressure coefficient decreases during combustion (8.34).

The stagnation pressure ahead of the discharge from the nozzle, diminishes with an increase of heating:

$$p_{0g} = \sigma_\kappa \sigma_H \sigma_{cr} \frac{p_s}{\pi(\lambda_s)}.$$

The throat cross section of the nozzle S_{4cr} increases in conformance with (10.76) during an increase of heating θ. If the exhaust cross section of the nozzle S_4 is constant, then the degree of nozzle expansion $\mathcal{E} = \dfrac{S_4}{S_{4cr}}$ and the relative velocity of the discharge gases λ_4 decrease with an increase of heating while the pressure at the exhaust section $p_4 = \dfrac{p04}{\pi} = \dfrac{p04}{f(\mathcal{E})}$ increases.

The velocity of the exhaust gases w_4 increases with an increase of heating θ owing to the increased temperature $T_{0g} = \theta \, T_{0x}$:

$$w_4 = \lambda_4 a_r = \lambda_4 \sqrt{\frac{2g k_r R}{k_r + 1} \theta T_{0x}}. \tag{10.77}$$

Jet thrust R and the thrust coefficient C_R grow with an increase of heating:

$$R = F_4 - F_x - p_4(S_4 - S_x) \tag{10.78}$$

The stagnation impulse of the free stream flow does not depend upon the temperature ratio when using a variable-geometry nozzle.

The impulse of the exhaust gases, at low temperature ratio, becomes equal to the stagnation impulse of the free stream flow while the thrust force falls to zero, if $\theta_{min} = \dfrac{1}{\beta^2 z_x^2 K^2}$.

The specific thrust of a supersonic ramjet engine at first increases during a decrease of the fuel flow and then reaches maximum at optimum heating

$$\theta_{opt} = \frac{1 + \sqrt{1 - z^2 \lambda^2}}{1 - \sqrt{1 - z^2 K^2}}.$$

During a subsequent decrease of heating from $\theta = \theta_{min}$ the specific thrust falls to zero.

If the flight speed is less than calculated, additive wave drag X_{dop} appears. The effective thrust R_{ef} is equal to

$$R_{ef} = R - X_{dop}.$$

The effective thrust, relative to a unit of fuel consumption, is called

the _effective_ _specific_ _thrust_ (specific impulse) I_{ef}:

$$I_{ef} = \frac{R_{ef}}{G_t}.$$

The effective specific thrust (specific impulse) reaches maximum at a somewhat greater temperature ratio, i.e., at lower air excesses, than does the specific thrust I, since the difference of $F_4 - F_n - p_n(S_4 - S_n) - X_{dop}$ diminishes quicker with a decrease of θ than does the difference of $F_4 - F_n - p_n(S_4 - S_n)$.

SECTION 7. THE REGULATING CHARACTERISTICS OF A SUPERSONIC RAMJET ENGINE WITH A FIXED-GEOMETRY NOZZLE

If the engine is equipped with a fixed-geometry nozzle S_{4cr} = const and S_4 = const, then when $T_{04} < T_{0x} \theta_{rasch}$ the pressure ahead of the exit nozzle p_{03} will be determined by the stagnation temperature of the combustion products T_{0g} (see 10.17).

The nozzle throat cross section S_{4cr} must be chosen sc that during the highest temperature for which the combustion chamber is calculated $T_{0g\ max}$, the pressure p_{03} remains less than the maximum possible value:

$$p_{03} < \sigma_A \sigma_m \sigma_{cr} \frac{p_3}{\pi(\lambda_4)}.$$

The relative velocity of the gases, which discharge from the fixed-geometry nozzle, λ_4 is constant: $\lambda_4 = f \frac{(S_4)}{(S_{4cr})}$ = const; $z(\lambda_4)$ = const. The discharge velocity w_4 increases in proportion to $\sqrt{T_{0g}}$

$$w_4 = \lambda_4 a_r = \lambda_4 \sqrt{\frac{2gkR}{k+1} T_{0r}} = \sqrt{2g \frac{kR}{k-1} T_{0r}\left[1 - \left(\frac{p_4}{\sigma_c p_{03}}\right)^{\frac{k-1}{k}}\right]}.$$

The pressure at the nozzle exhaust edge p_4 increases with the growth of T_{0g} due to the decrease of pressure p_{03}:

$$p_4 = \frac{p_{04}}{\pi} = \frac{p_{03}\sigma_c}{\pi} = \frac{p_{0m}\sigma_A^2\sigma_m^2\sigma_{cr}^2\sigma_c}{\pi},$$

since the normal shock wave moves from the diffuser exhaust section S_1 /sic S_2/ to its throat S_{1cr} with an increase of the temperature T_{0g} and σ_d increases because of the decreased losses from the normal shock wave.

For a temperature ratio at which the pressure p_{03} has a maximum possible value i.e., $\theta = \theta_{rasch}$, the parameters of engines with variable and fixed-geometry nozzles match. At the other temperature ratios the parameters of a fixed-geometry engine are

lower than those of a variable geometry engine. For a temperature ratio that is higher than calculated, the pressure ahead of the nozzle reaches its maximum possible value $p_{03} = \sigma_d \sigma_M \sigma_{sg} p_{0n}$ and the discharge of the gases decreases in inverse proportion to $\sqrt{T_{0g}}$ until the "buzzing" actually appears. G_v is constant in a controllable engine. When $\theta > \theta_{rasch}$ the thrust of a fixed-geometry engine is less than that of a variable-geometry one, due to the decreased air flow rate.

If $\theta < \theta_{rasch}$, then the pressure in a fixed-geometry engine decreases and the degree of nozzle expansion $\varepsilon = \frac{S_4}{S_{4cr}}$ and the relative exhaust velocity λ_4 remain constant. At the same time, as the pressure before the exhaust in a variable-geometry engine remains constant, the nozzle throat section decreases, the degree of expansion $\varepsilon = \frac{S_4}{S_{4cr}}$ increases and together with it, the relative velocity of the exhaust gases λ_4 grows. Therefore, the thrust of a variable-geometry engine is greater than of a fixed-geometry one when the heatings are less than calculated $\theta < \theta_{rasch}$ because the velocity of the exhaust gases is greater in the former than in the latter. The thrust of an engine with a constant-area nozzle falls to zero when the heating decreases, and during larger heatings (during lesser α) than those of an engine with a variable-geometry nozzle.

The specific thrust of an engine with a fixed-geometry nozzle is equal to that of an engine with a variable-geometry nozzle when $\theta = \theta_{rasch}$. During all the remaining heatings, the specific thrust of an engine with a fixed-geometry nozzle is less than that of an engine with a variable-geometry nozzle. The specific thrust of an engine with a fixed-geometry nozzle goes past the maximum value and falls to zero at much richer mixtures (at lesser α) than does an engine with a variable-geometry nozzle.

The increase of the specific thrust I and the thrust coefficient C_R, determinable by the nozzle geometry, depend on the ratio of the actual heating to the design heating $\frac{\theta}{\theta_{rasch}}$ and on the flight speed.

During a variation of flight speed M_n the relative pressures, temperatures, and densities in the shock waves (see Figure 39, 40, 41, and 42) change as do the incidence angles α of the shock waves (see Figure 43). The critical velocity in the diffuser throat and the stagnation parameters in the combustion chamber of a supersonic ramjet engine change, and together with them, the thrust parameters of the engine.

It is possible to select for each flight speed a diffuser which offers the highest pressure recovery σ_d; the optimum heating θ_{opt}, at which the specific thrust of the supersonic ramjet engine reaches its highest value, and finally, the location of the center body diffuser and the throat section of the exhaust nozzle at which the shock waves focus on the inlet edge, while the pressure in the combustion chamber ahead of the exit p_{03} attains the maximum.

Legend:

a—completely variable
b—variable-geometry nozzle
c—fixed-geometry ramjet
    engine
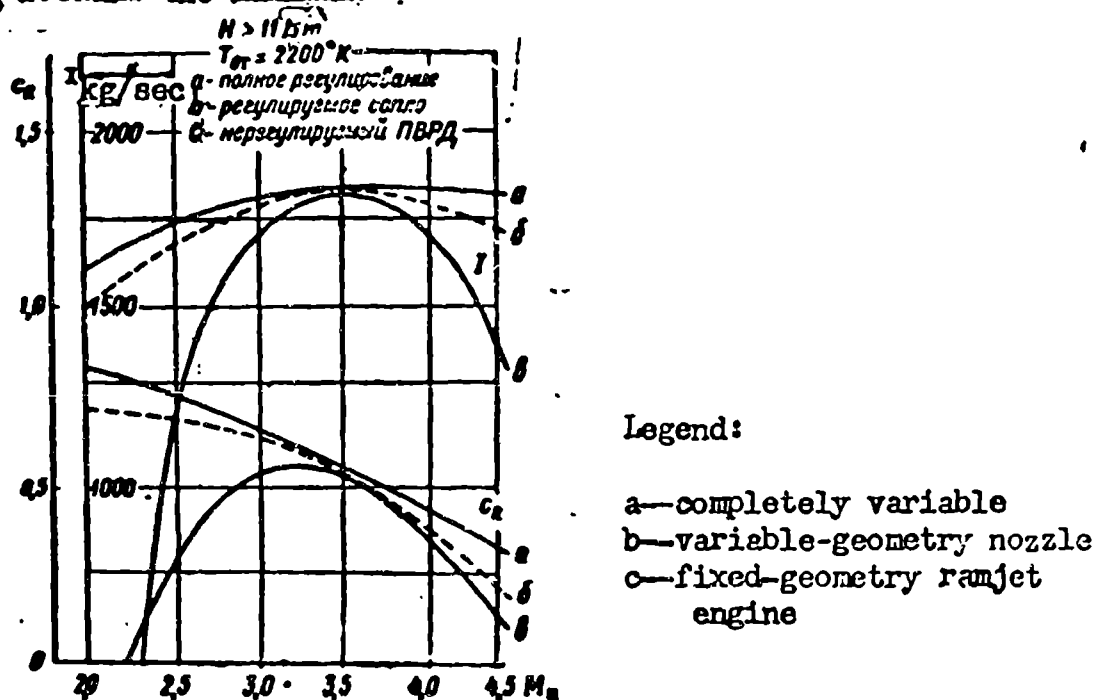
Fig. 188. The velocity characteristics of a supersonic ramjet engine.

The dependence on the flight speed of the parameters of a series of optimum engines, for which the pressure recovery σ_d, the cross sections S_1 and S_{ucr}, temperature ratio θ, and the other parameters have an optimum value, are called the velocity characteristics of optimum engines. If it were possible to manufacture an engine with a variable-geometry diffuser and nozzle, then its velocity characteristics at the same temperature ratio, would be comparable with the characteristics of a series of optimum engines.

The velocity characteristics of a supersonic ramjet engine with a fixed geometry for a certain calculated flight speed have a common point, while at all other speeds they lie below it. Therefore, the velocity characteristics of a variable-geometry engine present an interest as those representing the upper limit for fixed-geometry or partially variable geometry engines.

The Velocity Characteristics of Optimum Engines (Figure 188a). For the calculation of the velocity characteristics of a series of optimum engines, a series of flight speeds, for example, Mach numbers 2, 3, 4, and 5 are selected, and for each Mach number the most suitable diffuser which offers the maximum pressure recovery σ_d is selected. When $M \leqslant 1.5$ a diffuser with a normal shock wave at the inlet is usually chosen. When $M \geqslant 2$ a diffuser with a system of oblique shock waves is selected. The selection of a diffuser represents the most painstaking portion of the calculation, since it is necessary to test a series of diffusers which have various numbers of shock waves and various flow rake angles for each of the velocities given. The design of a multi-shock-wave diffuser may be accomplished as was stated in Chapter IV. Experimental data about diffusers are stated, for example, in the work of Ferri and Nucci.[1] The design velocity characteristic of diffusers, which offer the maximum possible pressure recovery at any speed, is depicted in the graph in Figure 182. The σ_d and $\dfrac{S_{1cr}}{S_1}$ for any velocity are determined by a similar experimental graph. For a flight with a design point velocity for a given diffuser, the shock waves are focused on its forward edge. Then the cross section of the stream tube flow is equal to the cross section of the inlet: $S_n = S_1$. With an increase of velocity the air flow increases in direct proportion to M_n.

With an increase of λ_n the gas dynamic function $q(\lambda_n)$ quickly diminishes and the calculated throat section $\dfrac{S_{1cr}}{S_1}$ decreases in accordance with (10.7) and the inlet area ratio $\dfrac{S_1}{S_4}$ increases (10.14) when $\alpha = $ const or $T_{0g} = $ const.

_____

[1] Ferri and Nucci, NACA Rep., No. 1189, 1954.

During a decrease of the pressure recovery in the diffuser σ_d the air in the throat seems to be less compressed and the calculated section S_{1cr} increases.

The relative velocity in the outlet section of the diffuser λ_2 may be found by Figure 187 (10.6). With an increase of flight velocity λ_2 diminishes due to the increase of the ratio $\dfrac{S_2}{S_{1cr}}$.

The pressure coefficient increases during the flow around the local resistances (flame holders) σ_M, with an increased initial velocity λ_n, because of the decrease of λ_2.

The temperature of the combustion products T_{0g}, is determined from the i-T diagram and is dependent upon the stagnation enthalpy i_{0g}. T_{0g} increases with an increase of velocity due to the increased stagnation enthalpy of the free stream flow $i_{0n} = \dfrac{i_n}{\tau(\lambda_n)}$.

The temperature ratio for a constant composition of the mixture α = const or for a constant temperature of the combustion products T_{0g} = const, decrease: with an increase of flight speed: $\theta = \dfrac{T_{0g}}{T_n}\tau(\lambda_n)$.

The relative velocity after combustion λ_3, which is expressed by the equation (8.42), decreases with an increase of flight speed λ_n due to diminishing temperature ratio θ and the relative velocity λ_2. The pressure recovery for combustion σ_{gg} increases.

The total pressure recovery of the engine σ_{ob} diminishes with an increase of speed due to the rapid increase of losses in the diffuser and nozzle, although the local losses and losses during combustion decrease.

The design throat section of the nozzle S_{4cr} diminishes with an increase of λ_n (10.76). The degree of nozzle expansion $\varepsilon = \dfrac{S_4}{S_{4cr}}$ and the relative velocity of the exhaust gases λ_4 increase with the growth of λ_n. The ratio $\dfrac{\lambda_4}{\lambda_n}$ does not depend on the velocity in an ideal ramjet engine: $\dfrac{\lambda_4}{\lambda_n} = 1$. In an actual supersonic ramjet engine the ratio $\dfrac{\lambda_4}{\lambda_n}$ at first diminishes with an increase of velocity due to the rapid decrease of σ_d and σ_g, then passes the minimum and increases insignificantly due to

the decrease of Poisson's index k_g of the combustion products (Table 10.2).

Table 10.2

THE DEPENDENCE OF THE PARAMETERS OF OPTIMUM SUPERSONIC RAMJET ENGINES ON THE FLIGHT SPEED

$$k = 1.4, \quad \beta = 1$$

λ_a	1.5	2.0	2.1	2.2	2.3
M_a	1.72	3.16	3.72	4.56	6.2
$\dfrac{p_{0a}}{p_a}$	5.2	46.8	105	316	1950
k_r	1.33	1.35	1.33	1.32	1.31
$T_0 \degree K$	600	1400	1900	2300	3200
s_{o6}	0.87	0.41	0.24	0.13	0.05
K	0.97	0.935	0.93	0.94	0.97
θ_{opt}	1.7	2.2	2.3	2.2	1.84
η	0.375	0.667	0.735	0.807	0.871
$(r_n)_{max}$	0.56	0.63	0.615	0.63	0.71
η_{max}	0.228	0.42	0.45	0.51	0.62

The thrust quickly increases with an increase of the flight speed, passes the maximum and then falls to zero when $\lambda_n = \lambda_{n \, pred}$ due to the losses of temperature ratio and the pressure recovery decrease in the diffuser and nozzle σ_d and σ_s.

The specific thrust I grows with an increase of velocity λ_n, passes the maximum when $\lambda_n = \lambda_{n \, opt}$ and falls to zero together with the thrust.

The overall efficiency of a supersonic ramjet engine increases at first with the increase of the velocity, then passes a maximum and begins to diminish.

The Velocity Characteristics of an Engine with a Given Diffuser and a Variable-Geometry Nozzle. The diffusers of engines are usually fixed geometry ones. The inlet section of a fixed-geometry diffuser is constant: S_1 = const. Pressure recovery depends on the flight speed. It is possible to select a diffuser which will produce the highest pressure recovery when the design flight speed $M_n = M_{rasch}$. At all speeds that are lower than calculated ($M_n < M_{rasch}$) the diffuser will produce a lesser pressure recovery than a diffuser which is designed for a given velocity: $\sigma_d < \sigma_{rasch}$. At off-design velocities the flow factor decreases: $\varphi < 1$ and additive wave resistance X_{dop} appears. Therefore, at velocities, which are less than calculated

$(M_n < M_{rasch})$, a supersonic ramjet engine with a fixed-geometry diffuser will have a lower thrust coefficient, specific thrust, and total efficiency than those engines which have diffusers designed for a given velocity (compare curves 'a' and 'b' in Figure 188).

We will examine in greater detail how a supersonic ramjet engine with a given diffuser operates in off-design velocities. If the velocity is less than design: $M_n < M_{rasch}$, then the incidence angle of the shock waves increases (see Figure 180b) and a portion of the air, which was compressed in the last oblique shock wave, is directed past the inlet slot of the diffuser: the flow coefficient φ diminishes.

The flow rake angle ω proves to be less than required to obtain the maximum pressure increase during stagnation. The coefficient σ'_d will be less than for an optimum selection of flow rake angles, and the pressure in the combustion chamber turns out to be less than the possible maximum. In order to eject all the gas in the combustion chamber which can pass through the diffuser throat for a given pressure drop, it is necessary to either decrease the temperature of the combustion products or to increase the nozzle's throat section S_{4cr}.

During acceleration an engine usually operates at a state of maximum thrust at a possibly large temperature T_{0g} = max, i.e., when α = 1. In order to avoid "buzzing" at a given diffuser inlet area ratio $f_1 = \dfrac{S_1}{S_M}$ an engine may be started at such a Mach number M_{min} at which S_{4cr} has a maximum possible value (for example S_{4cr} = S_3 = S_M) at θ_{max} (α = 1). During further acceleration, the throat section of the nozzle must be decreased, but remain greater than the minimum value $\dfrac{(S_{4cr})}{(S_3)_{min}}$ at which the normal shock wave still remains in the diffuser. The pressure ahead of the nozzle has a maximum possible value with a given diffuser and a given M_n. If during acceleration $\dfrac{S_{4cr}}{S_3}$ will be insufficient for the passage of the hot gas, then the terminal normal shock wave is expelled from the diffuser duct and will be located in front of the inlet slot, "buzzing" occurs, and the operation of the combustion chamber may fluctuate.

The Velocity Characteristics of a Fixed-Geometry Engine. At off-design conditio

engines with fixed-geometry nozzles have poorer parameters than do engines whose throat sections may be varied (see Figure 18"c). In order to decrease the velocity at which the operation of the engine becomes unstable, the exit throat area ratio of the engine $\frac{S_{4cr}}{S_M}$ is made larger (up to one) and the inlet area ratio $\frac{S_1}{S_M}$ is made less than one. Then at the beginning of independent operation when $\alpha \approx 1$, the pressure ahead of the exit p_{03} is close to the maximum possible value: $p_{03} \leq \sigma_d \sigma_M \sigma_{sg} p_{0n}$.

With an increase of flight speed, the pressure recovery of the diffuser σ_d will be decreased and become lower than in an engine which is designed for maximum pressure recovery. However, the engine thrust will be sufficient to overcome the frontal drag of the device, and the specific thrust will prove to be several times greater than that of a ZhRD /Liquid-fuel rocket engine/ For this reason the use of variable-geometry supersonic ramjets, in certain cases, is more advisable than that of liquid-fuel rocket engines. The use of a variable-geometry nozzle may increase the thrust and economy of an engine by more than 25%. However, for various types of flight vehicles with short flight ranges, such an increase of economy does not justify the construction complications and weight increase that are inevitable with the addition of a variable-geometry nozzle. Therefore, in self-accelerating missiles, which are intended for short and medium flights, the use of fixed-geometry supersonic ramjet engines with convergent diffusers and fixed-geometry nozzles having large openings may prove to be more advisable (see Figure 178d).

Single-regime engines, which are intended for flight at a constant velocity at a single altitude, should be equipped with an optimum diffuser and a fixed-geometry nozzle, which are designed for a cruising flight speed. At this speed their parameters are comparable to the parameters of a totally variable geometry engine.

SECTION 9. ALTITUDE CHARACTERISTICS OF A SUPERSONIC RAMJET ENGINE

The altitude characteristics are defined as the dependence of the parameters of a supersonic ramjet engine during constant speed (M_n = const) and a constant mixture composition (α = const) upon flight altitudes (Figure 189).

With an increase of flight altitude, the air flow through the engine varies in

direct proportion to the atmospheric pressure p_n at a given altitude H, and in inverse proportion to the square root of the ambient temperature T_n:

$$G_a = \varphi S_1 M_a p_a \sqrt{\frac{gk}{RT_a}}.$$

For a flight in the stratosphere $T_n \approx const$, and the flow depends only on p_n.

The fuel flow rate $G_g = \frac{G_v}{aL}$ when M_n = const and α = const is directly proportional to the atmospheric pressure p_n

$$G_r = \frac{G_a}{aL} = p_a \frac{\varphi M_a S_1}{aL} \sqrt{\frac{gk}{RT_a}}.$$

The fuel flow rate diminishes with an increase of flight altitude H.

The thrust coefficient C_R and the specific thrust of the engine I increase insignificantly during an increase of the flight altitude up to the stratosphere due to the increased temperature ratio since θ diminishes.

$$\theta = \frac{T_{0r}}{T_{0a}} = 1 + \frac{H_a \varphi_{cr} \tau(\lambda_n)}{(1 + aL) c_p T_a}.$$
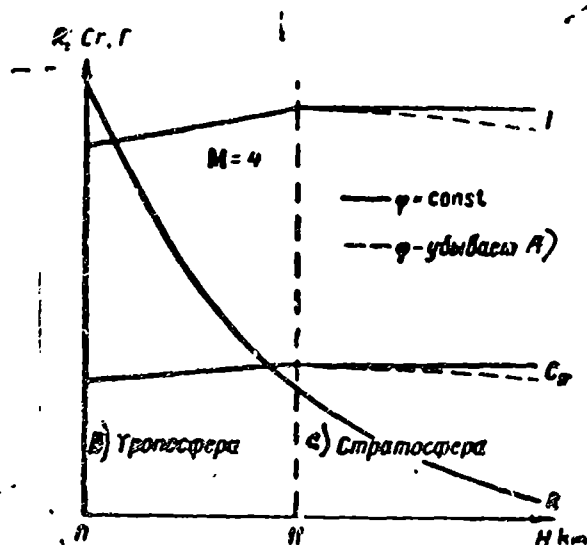
During a flight in the stratosphere C_R and I remain constant. The frontal thrust of the engine varies in direct proportion to p_n:

$$R_a = c_R q = \frac{k}{2} c_R p_a M_a^2.$$

The pressure in the combustion chamber diminishes in direct proportion to p_n:

$$p_{c1} = \sigma_A \sigma_a p_{0a} = p_a \frac{\sigma_A \sigma_a}{\pi(\lambda_a)}.$$

The pressure recovery factor in the diffuser σ_d does not depend on the flight altitude H.

Fig. 189. The altitude characteristics of a supersonic ramjet engine when M_n = const and α = const.

During a pressure drop in the combustion chamber the dispersion of the fuel deteriorates, the drops become larger, and the jet widens. The heat exchange between the drops and the air deteriorates because of the decrease in density. Therefore, the evaporation and combustion of the drops in the combustion chamber is slowed during an increase of flight altitude and the combustion efficiency q_{sg} drops. The combustion chambers of engines that are intended for high-altitude operation must be equipped with special devices that improve carburation and intensify combustion.

At very high altitudes the pressure in the combustion chamber falls so low that the evaporation and combustion of a common hydrocarbon fuel becomes impossible.

The greater the flight speed M_n, the greater the pressure ratio increase in the combustion chamber $\frac{P03}{Pn}$, and the greater the altitude to which the absolute pressure in the combustion chamber retains a value that is sufficient for rapid and complete combustion (Figure 190). At a flight speed $M_n = 6$ and $\sigma_d = 0.25$ the pressure in the combustion chamber does not fall below 0.5 kg/cm^2 even at an altitude that exceeds 40 km.

SECTION 10.   THE USE OF SUPERSONIC RAMJET ENGINES

At high supersonic flight speeds ($M_n > 3.0$), ramjet engines develop a higher specific thrust than do all other types of engines. Their frontal thrust is sufficiently great to overcome the aerodynamic drag of the flying vehicle. Information about several important flying vehicles with supersonic ramjet engines, as printed in the foreign press, is stated below.

Winged Long-Range Missiles   The American firm -- North American -- developed a project of an intercontinental supersonic winged missile, the "Navaho", which is propelled by supersonic ramjet engines (see Figure 21). The flight speed $M_n \approx$ 2.5-3.0 at an altitude of more than 15,000 m. The design flight range is 8,000 km. The guidance of the missile is accomplished by astronavigation method. The payload is sufficient to carry heavy atomic and hydrogen bombs from one continent to another[1].

[1]Gardner, G. W. H, Guided Missiles, Engineering, Nov. 26, 1954.
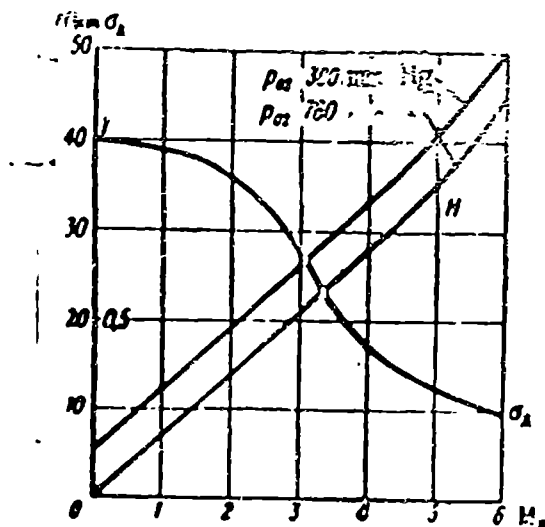Voprosy raketnoy tekhniki /Problems of Rocket Technology/, 1956, No. 1.

Fig. 190. The dependence of the limiting flight altitude of an actual supersonic ramjet engine upon the Mach number M_n when the given pressure in the combustion chamber p_{02} = const.

Supersonic Fighters   The French designer Rene Leduc is engaged for several years now in developing a supersonic fighter-interceptor. The take-off weight of the aircraft is almost six tons; the diameter of the engine is 2.28 m. The aircraft starts with the help of small turbo-jet engines installed on the wing tips or is carried to a high altitude by a mother-aircraft. The supersonic interceptor, which is intended for flights at varying altitudes and at varying speeds should be equipped with a multiple regime engine having an accelerating diffuser, a two-stage combustion chamber (pilot and main burners), and a variable-geometry nozzle. The difficulties which appeared during the creation of such an engine were so great that the development of Leduc's aircraft, the flight tests of which began in 1952, is still not finished. The experimental models still fly with subsonic speeds, although the shape of the center body diffuser in the diffuser inlet shows that the design velocity lies between M_n = 2.5 and M_n = 3.

Fighter aircraft with supersonic ramjet engines, carried on mother-aircraft and launched into the air at the far approaches to defended targets, may serve to intercept supersonic piloted and pilotless bombers and missiles of the "Navaho" type.[1]

_____

According to the data of the American press published in the year 1957, the work on the "Navaho" project was interrupted in order to increase the design speed.

[1]Sutton, G. P., History, Problems, and Status of Guided Missiles, Jet Propulsion, vol. 25, 1955, No. 11.

Projects of piloted interceptor aircraft, propelled t. ramjet engines with divergent supersonic diffusers, were developed in 1943-1944 by Senger (see Figure 177) and Lippisch in Germany. Their projects, as was mentioned in Chapter IX, were not translated into reality.

Fig. 191. An experimental aircraft -- the Leduc 010 with a multiple regime supersonic ramjet engine.

Antiaircraft Missiles   Supersonic ramjet engines may also be used to propel the second stage of guided and unguided antiaircraft missiles (Figure 192).

The missile starts under the action of a PRD /Solid Fuel Rocket_7 or a ZhRD, which is installed in the first stage. At the moment when the fuel contained in the first stage burns out the missile has successfully gained the altitude and develops the speed that is necessary for the operation of the supersonic ramjet engine. Figure 192a shows a photograph of the English antiaircraft missile "Thor", taken at the moment the booster rockets are released. The second stage continues to gain altitude and speed under the action of the supersonic ramjet engine.

Owing to the fact that supersonic ramjet engines have a significantly higher specific thrust than do rocket engines, the duration of the powered flight of the second stage, propelled by a supersonic ramjet engine, is several times greater than for a missile of the same weight propelled by a liquid fuel rocket engine.

Several English firms manufacture antiaircraft missiles, the second stages of which are propelled by supersonic ramjet engines.

In England, apart from the "Thor" missile mentioned, the Napier firm, in order to study free supersonic flight, built the NR-J1 rocket /sic, missile_7 with a supersonic ramjet engine. This vehicle was equipped with a simple divergent diffuser, and started with the aid of four pairs of solid-fuel rockets which surrounded the engine body (Figure 192b). The length of the rocket is 6.1 m ard its diameter is 0.45 m.
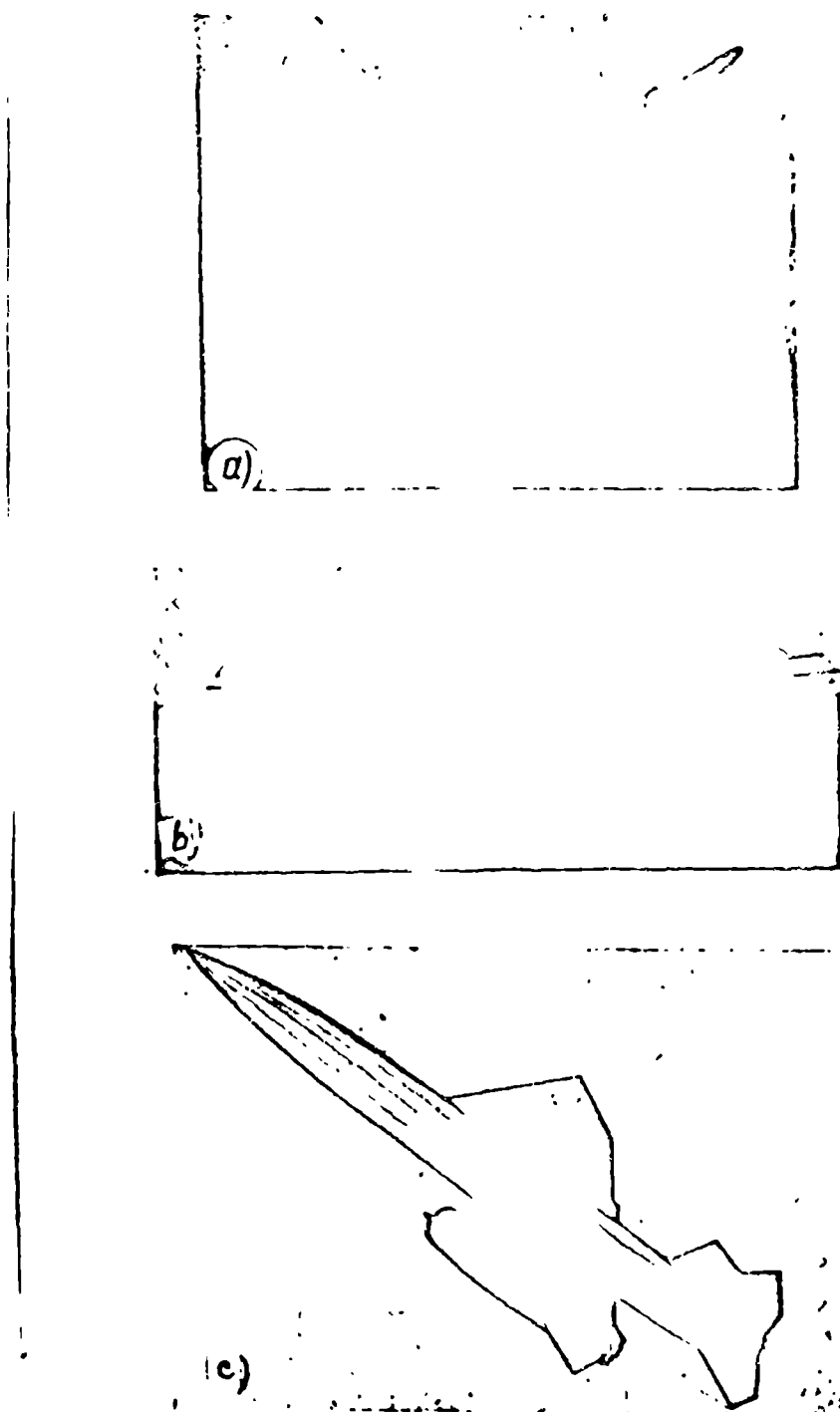
Fig. 192. Guided missiles with supersonic ramjet engines.
a -- the English guided missile "Thor" with a supersonic ramjet engine
at the moment the starting rockets release, b -- an English guided
missile of the Napier firm, c -- the American winged antiaircraft
missile, the "Bomarc".

Another English rocket with two supersonic ramjet engines from the Bristol firm was
first demonstrated at the Farnborough Air Show in 1954. The design velocity of the
rocket /sic -- missile/ was equal to twice the speed of sound.

Rockets /sic/ of a similar type are also developed in the USA, for example the
XSAM N-6 "Talos", "Cobra" (M ⁼ 2), and others.

A second stage equipped with wings is able to fly a greater distance than a wing-

ss rocket of the same weight. The American guided antiaircraft missile manufactured the Boeing and Marquardt firms, the IM-99 "Bomarc" (Figure 192c), belongs to the ruly of two-stage winged rockets /sic/. The length of the missile is 20 m, the igspan 11 m, the weight 3,860 kg, the speed M = 2.5, the ceiling is 18,300 m, and o range is 80 km. The "Bomarc" missile, which is intended for the interception of my aircraft, is guided by radio command. Its armament consists of the GAR-98 air- air missiles. The missile takes off under the action of an Aerojet liquid-fuel ket engine. Two Marquardt supersonic ramjet engines located under the fuselage, installed in the second stage.

Winged antiaircraft rockets of the "Bomarc" type, located on a launch pad in vicinity of the defended target, are capable of overtaking enemy aircraft from tever side they approach the target. Wingless antiaircraft rockets with liquid- rockets of the "Niko" type, the range of which is almost 20 km, must be arranged ι ring around the defended target, since their range is too short to intercept e aircraft which approach the target from the opposite side (see Figure 14).

Air-to-Air Type Missiles. Supersonic ramjet engines have been successfully used he primary engines in air-to-air type missiles. The "Orion" missile of the Martin is an example. The take-off weight of the missile is 680 kg, the flight speed = 3, and the range is 32 km. The missile, which is launched from an aircraft, quipped with radio guidance and a homing system control. It is intended to des- enemy bombers.

BIBLIOGRAPHY

oprosy raketnoy tekhniki /Problems of Rocket Technology7, 1956, No. 1.

techkin, B. S., Teoriya vozdushnogo reaktivnogo dvigatelya /The Theory of an Air- Breathing Jet Engine/ TVF, 1929, No. 2.

occo, G. A., Sui corpi aerodinamici a resistienza negativa. Atti della Reale Accademia dei Lincei. Classe di scienci fisiche, matematiche et naturali, Roma, Rendiconti, Ser. 6, v. 13, 1931.

hubauer, G. B., "Jet Propulsion with Special Reference to Thrust Augmenters," NACA TN, No. 422, 1933.

5. Willey. I., L'aviation a de tres grandes vitesse par les tuyeres de la Science Aerienne, IX 1936.

6. Sänger, E., Wirkungsgrade und Gossenverhältnisse von Lorintriebwerken. Deut. Luftfahrtforschung, FB, 996, Berlin, 1938.

7. Keenan, I. H., Kaye I., Rieke C. A. and Morrisson, R., The Calculated Performance of Certain Jet Propulsion Devices. NACA ACT, 3029, April, 1943.

8. Lippisch A., Die flugmechanischen Beziehungen des Flugzeuges mit Strahlantrieb. Deutsche Luftfahrforschung, ZWB Berichte, No. 7, FB 1791, 1943.

9. Hill, P. R., Parameters Determining Performance of Supersonic Pilotless Airplanes Powered by Ramjet Compression Power Plants. NACA ACT, L. 6, a17, WR. No. L-755, June, 1946.

10. Krebs, R. and Palasics, I., Analitical Comparison of Standard Turbojet Engine with a Tail-Pipe Burner and a Ramjet Engine. NACA Research Memo. No E6Lii, Feb. 1947.

11. Hill, P. R. and Gammal, A. A., An Analysis of Ducted -- Airfoil Ramjets for Supersonic Aircraft, NACA RM L. 7124, July 1948.

12. N. N., Supersonic Ramjet Performance Calculations. Marquardt Aircraft Co., Rep. A-23, Van-Nuys, Calif., 1948.

13. Harned, M. S., A Fundamental Consideration of the Supersonic Ramjet Aero Dig., v. 58, N. 4, April 1949.

14. Connors, J. F., Effect of Ramjet Pressure Pulsations on Supersonic Diffuser Performance, NACA RM NE-50, H-22, Nov., 1950.

15. Roid, J., The Gas Dynamic Theory of the Ramjet. British Aerop. Res. Counc. R. and M., 2370, 1950.

16. Henry, J. B. and Bennet, J. B., Method for Calculation of Ramjet Performance, NACA TN N 2357, June, 1951.

17. Oswatisch, R., Gasdynamik. Verlag Springer, Wien, 1952.

18. Harned, M., Ramjet Application to Aircraft Propulsion, Aviat. Age, vol. 2, Nov. 1953.

19. Kilrain, W. A., Mach 2--4: Ramjet Stamping Ground. Am. Aviat., vol. 16, Feb. 2, 1953.

20. Lukaschewicz, I., Supersonic Ramjet Performance. Aircr. Eng., vol. 25, Oct., 1953.

21. Marquardt, R. E., Tomorrow's Aircraft Today. Av. Age, vol. 20, July, 1953.

22. Marsh, B. W., and Sears, G. A., Introduction to the Analysis of Supersonic Ramjet Powerplants. Jet Propulsion, vol. 24, N 3, 1954.

23. Reiniger, S. H., Ramjet or Rocket for Missiles? Av. W ek., vol. 58, Jan. 12, 1953.

24. Gardner, G. W. H., Guided Missiles. Engineering, Nov. 26, 1954.

25. Tromsdorf, W., Staustrahltriebwerke bei hohen Mach--Zahlen. Z. Flugvissenschaften vol. 2, N 9, Sept. 1954.

26. Avery, W. H., Twenty-five Years of Ramjet Development. Jet Propulsion, vol. 25, N 11, Nov. 1955.

27. Anderson, D. A., Leduc-021 Puts Ramjet Spotlight. Av. Week, vol. 63, July 11, 1955.

28. Maire V. A. and others, Définition of the Thrust of a Jet Engine and of the Internal Drag of a Ducted Body. Brit. A.E.C. CP, 190, 1955.

29. Sänger, E., Die Wege des Strahlflugs. Mitteilung, N 3, 1955.

30. Sutton, G. P., History, Problems and Status of Guided Missiles. Jet Propulsion, v. 25, 1955, N 11.

CHAPTER XI

ATOMIC RAMJET ENGINES

Those ramjet engines, in which the heating of the air is accomplished by a controlled fission reaction of atomic nuclei in an atomic reactor, are called atomic ramjet engines. An atomic reactor is substituted for the combustion chamber of an ordinary ramjet engine, which operates on a molecular fuel (Figure 193).

As was mentioned in Chapter I, two methods of heat exchange between the atomic reactor and the air are fundamentally possible: direct heating, in which the air flows through the reactor (see Figure 7a), and heating with the aid of an intermediate heat-transfer agent (see Figure 7b). In the latter case, a liquid <u>heat-transfer agent</u> flows through the reactor and in a special heat exchanger transfers the heat obtained to the air. Helium under very high pressure, or molten metals: sodium, potassium, and others, may serve as the heat-transfer agent for jet engines.

The exact computation and design of reactors represents a special section of atomic power engineering which requires special training. From the viewpoint of an aircraft engineer, an atomic reactor is a heat liberating and heat exchanging unit, which, in order to be suitable as an energy source for aircraft, must have a weight and dimensions which do not exceed certain permissible limits. From this viewpoint we will consider the present problem, limited by the scanty information about these reactors.

SECTION 1. A SUMMARY OF INFORMATION ABOUT ATOMIC REACTORS

A fission reaction of the atoms of U^{233}, U^{235}, or Pu^{239}, which takes place under the action of neutrons, is used to obtain atomic energy.

During fission the nucleus of a radioactive substance, after having captured a neutron, splits into two smaller nuclei of approximately equal mass and into a number of neutrons; for example,

$$U^{235} + n \rightarrow A_1 + A_2 + \nu n. \tag{11.1}$$

Here the symbols A_1 and A_2 indicate the atomic weights of the fission products,
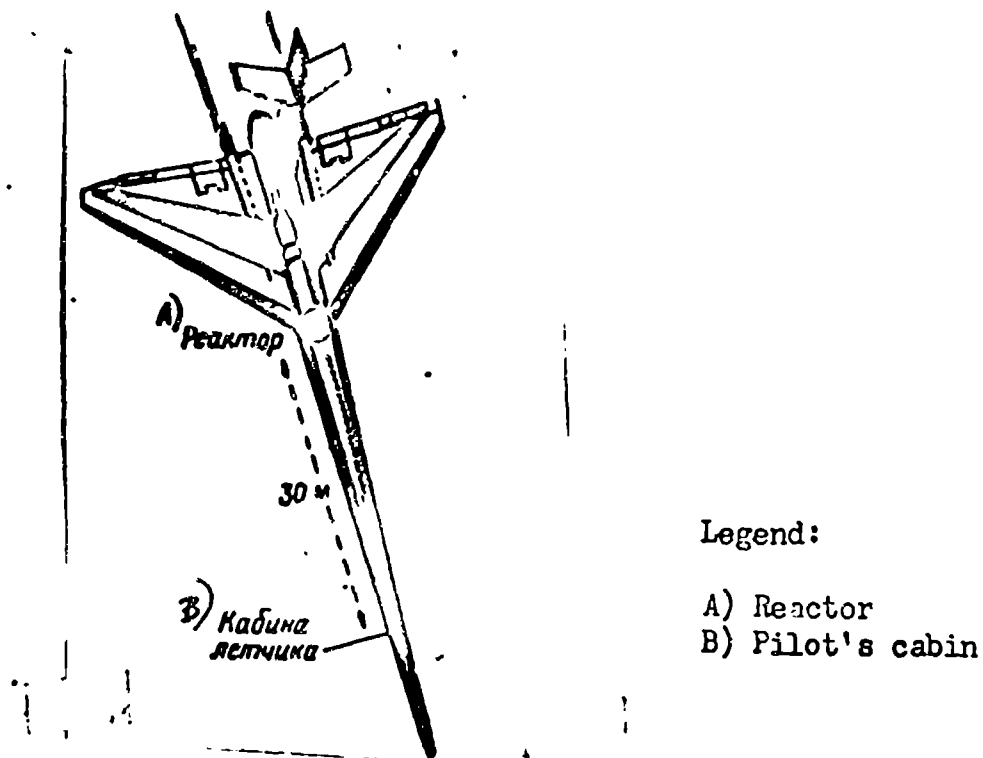
Fig. 193. A schematic of an atomic aircraft.

which vary within the limits of 72 to 162. The symbol ν indicates the average number of neutrons formed during fission. For uranium-235: $\nu = 2.5$.

The total mass of the fission products is less than the mass of the fissioned atom with a captured neutron:

$$A_1 + A_2 + \nu n < U^{235} + n. \tag{11.2}$$

The loss or "defect" of the mass is apparently equal to

$$\Delta m = U^{235} + n - A_1 - A_2 - \nu n.$$

Experience shows that for the fission of U^{235}, the average mass defect is $\Delta m \approx 0.21$ amu. One amu is an atomic mass unit.

The mass "loss" is transformed into energy which is released during fission. The fission energy is found from the mass defect by using Einstein's equation, considering that an atomic mass unit is equal to $1.66 \cdot 10^{-24}$ g $= 1.66 \cdot 10^{-24} \cdot 3.13 \cdot 10^{-3}$ ergs.

$$E = c^2 \Delta m = (3 \cdot 10^{10})^2 \cdot 0.21 \cdot 1.66 \cdot 10^{-24} = 3.13 \cdot 10^{-4} \, \text{ergs}.$$

In atomic power engineering, the energy of the particles is usually expressed in electron volts and mega-electron-volts (ev and mev). The charge of an electron is equal to $1.6 \cdot 10^{-19}$ coulombs. Consequently,

1 ev $= 1.6 \cdot 10^{-19}$ coulombs. 1 v $= 1.6 \cdot 10^{-19}$ joules $= 1.6 \cdot 10^{-4}$ ergs.

Legend:

A) Reactor
B) Pilot's cabin

1 mev = 10^6 ev = 1.6 · 10^{-6} ergs = 1.6 · 10^{-13} joules = 1.6 · 10^{-16} kilowatt seconds

$$= 0.24 \cdot 1.6 \cdot 10^{-16} = 0.384 \cdot 10^{-16} \text{ Kcal.}$$

$$1 \text{ amu} = 1.49 \cdot 10^{-3} \text{ ergs} = 931 \text{ mev.}$$

The fission energy is

$$E = 0.21 \text{ amu} = 0.3 \cdot 10^{-3} \text{ ergs} = 200 \text{ mev} = \frac{1}{3 \cdot 10^{13}} \text{ kilowatt seconds}$$

$$1 \text{ kilowatt} = \frac{1}{1.6} \cdot 10^{16} \frac{\text{mev}}{\text{sec}} = \frac{0.625}{200} \cdot 10^{16} \approx 3 \cdot 10^{13} \text{ fissions per second.}$$

The fission energy is distributed between the fission products approximately as follows:

The energy of the fission fragments. . . . . nearly 166 m. '

The energy of the fission neutrons. . . . . "   5   "

The energy of γ radiation . . . .   "   10   "

The energy of the electrons and their accompanying
neutrinos . . . .   "   18   "

The number of atoms which are contained in one kg of uranium-235 is equal to

$N = \frac{1000}{235 \cdot 1.66 \cdot 10^{-24}} = 2.56 \cdot 10^{24}$ atoms. Consequently, the energy of 1 kg of uranium-235 that is released during complete fission is: $H_{U235} = 2.56 \cdot 10^{24} \cdot 200 \text{ mev} = 512 \cdot 10^{24} \cdot 0.384 \cdot 10^{-16} = 1.96 \cdot 10^{10} \text{ Kcal}$, i.e., $\frac{19.6 \cdot 10^9}{10,500} = 1.87 \cdot 10^6$ times greater than the combustion of benzine. In other words, the complete fission of 1 g of uranium 235 releases almost as much energy as does the combustion of 2 tons of petroleum products.

The neutrons which are released during fission promote the fission of new atoms of the active substance and support a continuous or even a growing atomic chain reaction.

The fission neutrons move with very high velocities. By assuming that the average energy of each fission neutron is equal to $E_n = 2 \text{ mev} = 2 \cdot 1.6 \cdot 10^{-6}$ ergs, and that the mass of the neutron $m_n = 1.66 \cdot 10^{-24}$ g, we find

$$w = \sqrt{\frac{2E_n}{m_n}} = \sqrt{\frac{2 \cdot 2 \cdot 1.6 \cdot 10^{-6}}{1.66 \cdot 10^{-24}}} \approx 2 \cdot 10^9 \text{ cm/sec} =$$
$$= 20000 \text{ km/sec.} \tag{11.4}$$

The probability of capturing these fast neutrons by the atoms of uranium-235

is small. Therefore, a larger portion of the fission neutrons penetrate the small bar of uranium-235 and fly out, without producing new fission. In order to be sure that the neutrons are absorbed by the fissionable substance, its mass must not be less than the, so-called, "critical" value: on the order of 1 kg. In a quantity that is less than critical, uranium-235 is safe. Following the rapid approach of two bars of uranium-235, the mass of each of which is somewhat greater than half of critical, an atomic explosion occurs. The uncontrolled explosive fission reaction is used in the atomic bomb.

An atomic reactor is a system in which a controlled atomic reaction by moderated neutrons takes place. The deceleration of the neutrons is accomplished for the following reasons: the probability of catching a slow neutron by the active substance is greater than for the fast ones; the reaction of slow neutrons does not develop as uncontrollably as for fast neutrons and the reactor is easier to control, i.e., a reactor operating with slow neutrons is easier to control and is not so explosively dangerous.

The neutrons released in fission, or in other nuclear reactions, move and collide with the atomic nuclei.

Three forms of nuclear interaction with neutrons are known: scattering, capture, and capture leading to fission.

During the collisions which lead to scattering, the magnitude and directions of the velocities of the neutron and nucleus change, in accordance with the laws of collision of elastic balls. Thus, during a direct collision of a neutron with the nucleus of a hydrogen atom (a proton H^1_1), the mass of which is approximately equal to the mass of the neutron, the neutron completely loses its velocity. The proton that was stationary before, now begins to move with a velocity that is equal to the initial velocity of the neutron. Therefore the momentum remains constant. During a collision with a nucleus, the mass of which is many times greater than the mass of the neutron, the velocity of the neutron changes only in direction and the magnitude of the velocity remains practically constant. Almost no deceleration of the neutron occurs.

On the basis of the laws of the conservation of energy and of momentum, it is

possible to prove that the relative energy loss of the neutron during a collision with a nucleus with a mass M is equal to

$$\frac{\Delta E}{E} = \frac{4Mm}{(M+m)^2},$$

(11.5)

where m is the mass of the neutron, equal to one atomic mass unit.

The lower the atomic weight of a substance $A = \frac{M}{m}$, the better it will slow down neutrons.

During the collisions which lead to capture, the neutron penetrates the nucleus, forming a new isotope of the given element which is usually unstable — radioactive. For example, during the exposure of hydrogen H^1_1 to neutrons, deuterium H_1^2 is produced:

$$H^1_1 + n = H^2_1.$$
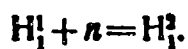
During a collision resulting in fission, the nucleus which captures the neutron splits into two fragments with the release of two or three new neutrons.

The interaction of the neutrons with the nuclei is quantitatively characterized by the so-called cross section of the nucleus.

The cross sections, which characterize the probability of a neutron collision with an atomic nucleus, are not equal to the geometric cross section of the nucleus.

Barn serves as a unit of measurement for the cross sections of atomic nuclei:

$$1 \text{ barn} = 10^{-24} \text{ cm}^2.$$

(We will recall that the diameter of an atomic nucleus is on the order of 10^{-12} cm.)

The cross sections of scattering σ_s, capture σ_a, and fission σ_f are not equal to one another. All these values are determined experimentally (Table 11.1).

The cross sections are complex velocity functions of the neutron velocities or their kinetic energies, which are usually expressed in electron volts.

Elements used as neutron moderators in atomic reactors have low capture cross sections σ_a, (since they absorb less neutrons); and low atomic weight A, since for each collision of a neutron with a nucleus, the more significant are its energy losses, the less the mass of the target-nucleus differs from the mass of the neutron (see

equation 11.5). After a series of collisions with the nuclei of the moderator, the velocity of the fission neutrons decreases to a "thermal" value, which corresponds to the average kinetic energy of the thermal movement of the surrounding molecules. From the viewpoint of the amount of the energy losses, hydrogen is an ideal moderator.

Table 11.1

CROSS SECTIONS FOR THERMAL NEUTRONS

Element		A	Z	Cross section in barns		
				σ_s	σ_a	σ_f
Hydrogen	H	1	1	38	0,33	0
Deuterium	D	2	1	—	0,00046	0
Beryllium	Be	9,01	4	7	0,010	0
Boron	B	10,8	5	4	750	0
Carbon	C	12	6	4,8	0,0045	0
Oxygen	O	16	8	4,2	0,0002	0
Iron	Fe	55,85	26	11	2,43	0
Cadmium	Cd	112,4	48	7	2400	0
Uranium 235	U	235	92	8,2	650	549
Uranium 238	U	238	92	8,2	2,8	0*
Plutonium	Pu	239	94	—	1025	664

*For fast neutrons $\sigma_f > 0$, since uranium-238 fissions under the action of fast neutrons.

However, it absorbs neutrons with the formation of heavy hydrogen -- deuterium D. The capture cross section of hydrogen is not large. Therefore, hydrogen, in conjunction with oxygen, is used as a moderator in nuclear reactors. Heavy water D_2O, beryllium Be, and carbon C in the form of graphite are also used as moderators. Oxygen, owing to its comparatively heavy atomic weight, slows neutrons poorly. However the absorbtion of neutrons by oxygen is insignificant. Therefore the presence of oxygen in connection with such moderators as hydrogen, deuterium, or beryllium does not disrupt the operation of a reactor. Stationary reactors, the weight and dimensions of which are not important, usually have graphite as a moderator.

An atomic reactor is represented by an assembly of fissionable substance and a moderator, surrounded by a neutron reflector and a shielding layer, and which is equipped with control rods and ducts for the coolant (Figure 194).

There are heterogenous and homogeneous reactors. In heterogeneous reactors the fissionable substance is prepared in the form of individual blocks — the heat liber - ating (fuel) elements (Figure 195) are located inside the moderator blocks (graphite, beryllium) or submerged in ordinary or heavy water (Figure 196). Tubes, through which the air, water, or liquid metal coolant flows, are laid out through the boiler. Reactors, the active rods of which are submerged in water, are called "submerged" or "swimming pool" reactors. Cooling is accomplished by the circulation of the water. In this way, the water serves simultaneously as a moderator and as a coolant.

In homogeneous reactors, the atoms of the active substance are uniformly distrib- uted between the atoms of the moderator, (graphite for example) (Figure 194). One homogeneous reactor is the, so-called, boiling reactor or boiler (Figure 197) in which a uranium salt (uranyl nitrate, for example) serves as the active substance. The salt is dissolved in water and serves as the moderator.

Legend:

A) U^{238} shell
B) A mixture of U^{238} with graphite
C) Helium ducts
D) From the pump
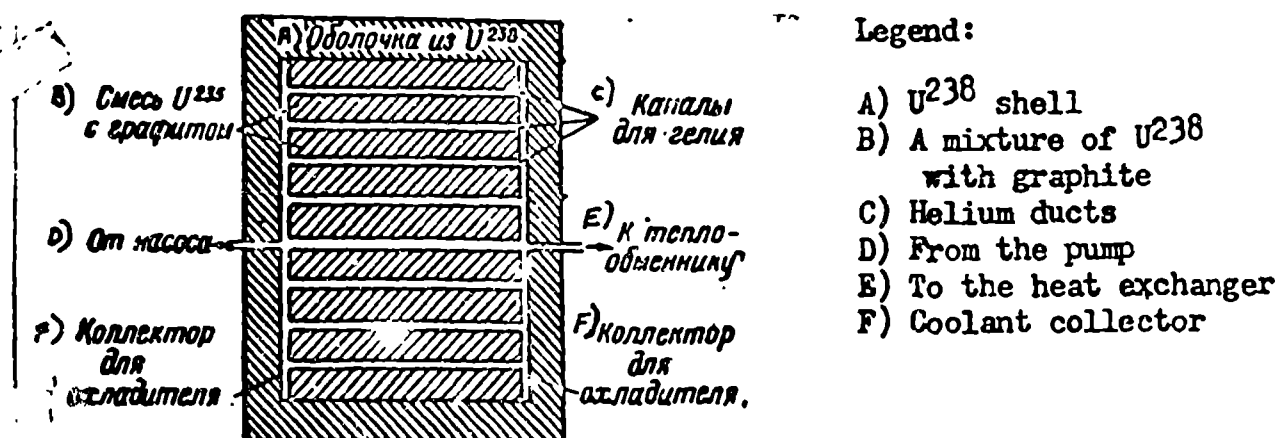E) To the heat exchanger
F) Coolant collector

Fig. 194. A schematic of a homogeneous reactor.

So that a continuous atomic reaction may be developed in the reactor, the average number of neutrons which ply in the reactor, must remain constant.

Each fission releases ν neutrons. A certain portion of them is absorbed by the uranium-235 without provoking fission. The so-called radiative capture occurs, ac- companied only by γ-radiation. The average number of neutrons which are released after the capture of a single neutron is equal to

$$\eta = \frac{\nu}{1+\alpha},$$
(11.6)

where α is the ratio of the radiative capture and fission cross sections. For uranium-235: $\alpha = 0.19$; $\eta = 2.1$.

There are heterogenous and homogeneous reactors. In heterogeneous reactors the fissionable substance is prepared in the form of individual blocks — the heat liber - ating (fuel) elements (Figure 195) are located inside the moderator blocks (graphite, beryllium) or submerged in ordinary or heavy water (Figure 196). Tubes, through which the air, water, or liquid metal coolant flows, are laid out through the boiler. Reactors, the active rods of which are submerged in water, are called "submerged" or "swimming pool" reactors. Cooling is accomplished by the circulation of the water. In this way, the water serves simultaneously as a moderator and as a coolant.

In homogeneous reactors, the atoms of the active substance are uniformly distrib uted between the atoms of the moderator, (graphite for example) (Figure 194). One homogeneous reactor is the, so-called, boiling reactor or boiler (Figure 197) in which a uranium salt (uranyl nitrate, for example) serves as the active substance. The salt is dissolved in water and serves as the moderator,

Legend:

A) U^{238} shell
B) A mixture of U^{238} with graphite
C) Helium ducts
D) From the pump
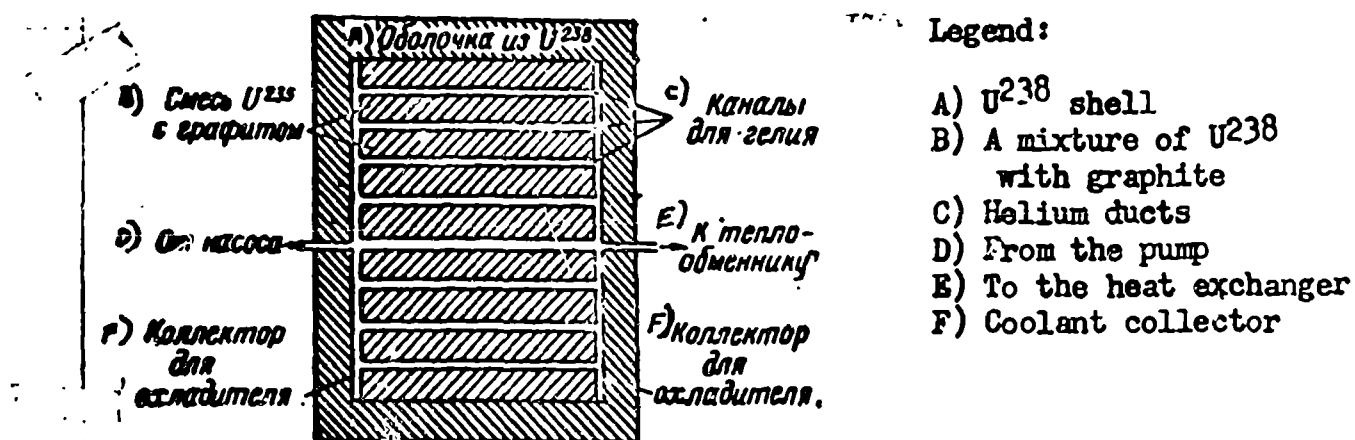E) To the heat exchanger
F) Coolant collector

Fig. 194. A schematic of a homogeneous reactor.

So that a continuous atomic reaction may be developed in the reactor, the average number of neutrons which ply in the reactor, must remain constant.

Each fission releases ν neutrons. A certain portion of them is absorbed by the uranium-235 without provoking fission. The so-called radiative capture occurs, accompanied only by γ-radiation. The average number of neutrons which are released after the capture of a single neutron is equal to

$$\eta = \frac{\nu}{1 + \alpha},$$ (11.6)

where α is the ratio of the radiative capture and fission cross sections. For uranium-235: $\alpha = 0.19$; $\eta = 2.1$.
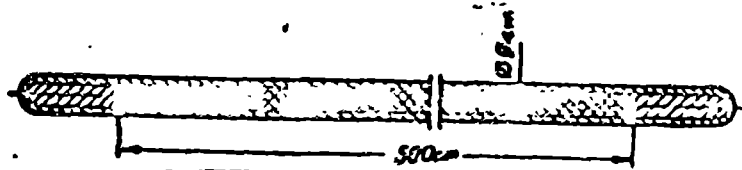
Fig. 195. A uranium block, the heat liberating (fuel) element.

A portion of the fast fission neutrons are captured by the nuclei of uranium-238, which is alway contained in a mixture of uranium isotopes and causes their fission. The relative increase of the number of neutrons resulting from the fission of the uranium-238 nuclei is called the fast fission (multiplication) constant ε. For natural uranium, this value somewhat exceeds one.

A proportion of fission neutrons is being captured by the uranium-238 nuclei without causing fission. The probability of avoiding resonant capture is designated by p. For natural uranium p = 0.9.

A portion of the fission neutrons is absorbed by the nuclei of the moderator in the slowing down process. The probability of avoiding absorbtion in the process of slowing down to "thermal" velocity is called the thermal utilization factor f.

The probability L of avoiding leaks through the surface of the reactor increases with an increase of the volume per unit of surface, i.e., with an increase of the linear dimensions of the reactor.
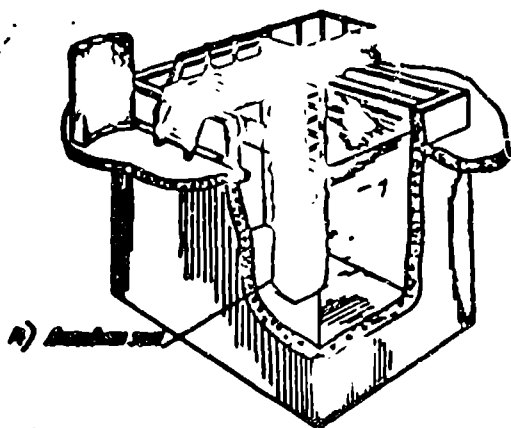

Fig. 196. A schematic of a heterogeneous "submerged" or "swimming pool" reactor.
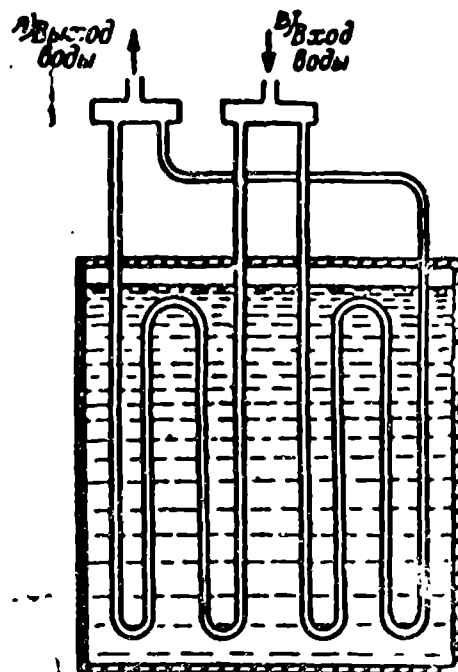Legend: A) Active zone.

Fig. 197. A schematic of a boiling water reactor -- a "boiler".
Legend: A) Water output
B) Water input

The ratio of neutrons which remain in a reactor after leakage and other losses to each original fast neutron is called the effective multiplication factor k_{ef}.

(11.7)

$$k_{ef} = \eta p f L$$

In order that the reactor develops a continuous fission reaction, the effective multiplication factor must be equal to, or greater than, one:

$$k_{ef} \geqslant 1.$$

The difference k_{ef} - 1 is called the reactivity of the reactor. A reactor, whose reactivity is somewhat greater than zero, is called critical. If one gradually accumulates blocks of nuclear fuel and moderators in a pile, then the dimensions of this pile will become critical. This name pile -- "kucha" (incorrectly translated by the word "kotel"*)is used in reactor terminology in American literature. The achievement of criticality is made known by the sharp increase of reactor radiation.

SECTION 2. THE NEUTRON FLUX AND THERMAL POWER OF A REACTOR

The quantity of heat which is released in a reactor every second is called the thermal power. The thermal power of a reactor N_Q is usually expressed in kilowatts:

1 kw = 0.24 Kcal/sec = 0.625 · 10^{16} mev/sec.

The thermal power per unit of the reactor's weight is called the specific power N_{ud}:

$$N_{ya} = \frac{N_Q}{P} \text{ kw/kg},$$

(11.8)

where P is the mass of the reactor, equal to the sum of the mass of the active zone [core] P_{akt}, the protective shield P_{zashch}, and the equipment P_{ob}:

$$P = P_{akt} + P_{zash} + P_{ob}.$$

The number of fissions which occur in a unit of mass of the active zone per second is called the activity, A fissions/sec g.

The thermal power is proportional to the product of the activity A, the mass of the active zone P_{akt}, and the fission energy E:

$$N_Q = \frac{AP_{akt}E}{0.625 \cdot 10^{16}} = \frac{AE}{0.625 \cdot 10^{16}} V\rho V \approx \frac{AV\rho V}{3 \cdot 10^{12}} \text{ kw},$$

(11.9)

where V is the volume of the active zone in cm^3;

ρ is the average density of the active substance, i.e., of the mixture of nuclei

*boiler

fuel with the moderator in g/cm^3;

∇ is the relative density, which is measured by the ratio of the volume of the active substance to the volume of the active zone;

P_{akt} is the mass of the active zone in grams:

$$P_{akt} = V\rho\nabla.$$ (11.10)

The activity of the reactor A is determined by the number of atoms of fissioning substance in each unit of mass of the active zone, by the fission cross section, and by the, so-called, neutron flux φ.

The number of neutrons which pass through a unit area (1 cm^2) per second is called the neutron flux. The thermal neutrons in a reactor move randomly. Therefore the neutron flux does not depend on the orientation of the area.

In various portions of the active zone the neutron flux is dissimilar. In the center of the active zone it is greater than at the periphery.

We will consider a unit volume of the active zone (Figure 198). The number of atoms of the fissioning substance with atomic weight A_{del} per unit volume, i.e., the atomic concentration, is denoted by N. The mass of a unit volume is equal to the density of the active substance ρ g/cm^3. The number of atoms in a gram-atom -- Avogadro's number -- is denoted by N_A, and is equal to $6 \cdot 10^{23}$ atom/mol. The ratio of the mass of the fissioning substance to the mass of the active zone is denoted by $\frac{P_{del}}{P_{akt}}$. The atomic concentration, apparently, is equal to

$$N = \frac{N_A \rho}{A_{del}} \frac{P_{del}}{P_{akt}}.$$ (11.11)

The probability of a collision, resulting from fission, of one neutron with any of N atoms of the fissioning substance per unit volume, or macroscopic cross section, is equal to

$$\sum_f = N\sigma_f = \frac{N_A \rho \sigma_f}{A_{del}} \frac{P_{del}}{P_{akt}}.$$ (11.12)

Consequently, the activity A is equal to

$$A = \varphi\frac{\sum_f}{\rho} = \varphi \frac{N_A \sigma_f}{A_{del}} \frac{P_{del}}{P_{akt}} \quad \text{fissions/sec gram,}$$ (11.13)

After substituting the value of the activity that is found (11.13) into the thermal power equation (11.9), and using (11.10), we obtain

$$N_Q = \frac{\beta N_A \sigma_f \varphi}{0.625 \cdot 10^{16} A_{_{gel}}} \frac{P_{_{gel}}}{P_{_{aKT}}} V \rho \nabla = \frac{N_A \sigma_f}{3 \cdot 10^{13} A_{_{gel}}} \varphi P_{_{gel}} \text{ kw.}$$ (11.14)

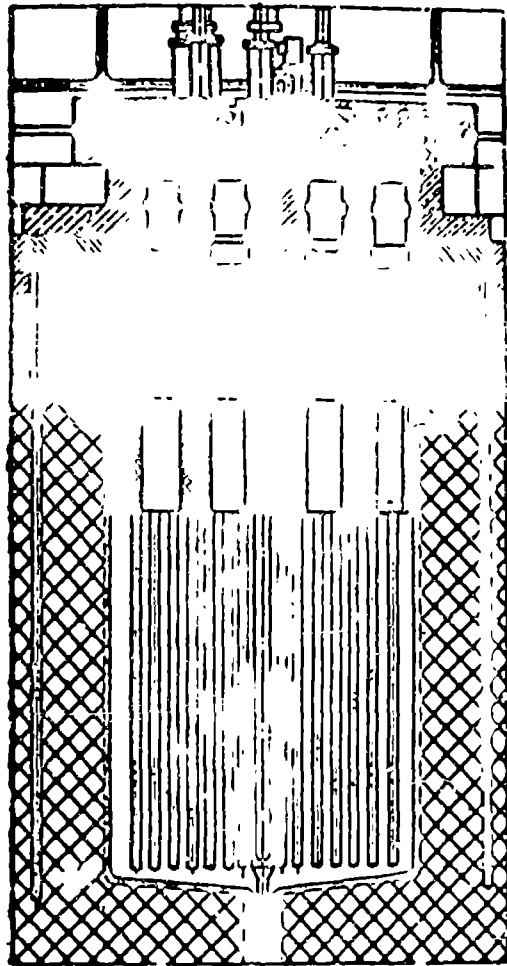The fission cross section of an atom of uranium-235 $\sigma_f = 549 \cdot 10^{-24}$ cm^2; A_{del}

Fig. 198. A schematic of the active zone of a heterogeneous reactor.

~~25 g/mole;~~ N_A $6 \cdot 10^{23}$ atom/mole. The thermal power of a reactor is determined by the product of the neutron flux and the mass of the fissioning substance

$$N_Q = \frac{6 \cdot 10^{23} \cdot 549 \cdot 10^{-24}}{3 \cdot 10^{13} \cdot 235} \varphi P_{_{gel}} \approx 4.6 \cdot 10^{-14} \varphi P_{_{gel}} \text{ kw.}$$ (11.15)

Subsequently we will see, that the neutron flux, and consequently, the thermal power of the reactor may be changed from zero to maximum by varying the location of the control rods.

The heat which is released in a reactor must be taken out by a coolant. The higher the thermal power, the greater the heat removal, the higher the temperature of the active zone, and the higher the required coolant flow. The limiting temperature which a reactor is capable of maintaining is determined by the thermal properties of the fissionable substance, the moderator, the coolant, and the materials

from which it is constructed.

In heterogeneous reactors, the heat is released only in blocks of nuclear fuel. In homogeneous reactors the liberation of the heat occurs in the entire mass of the active zone /core/.

The neutron flux in existing power reactors, as described in open literature, does not exceed 10^{15} neutrons per second per cm^2.

Example 1. Find the power that is released in 1 kg of pure uranium-235, if the neutron flux is $\varphi = 10^{14}$ neutrons per second per cm^2.

After substituting $P_{del} = 1,000$ grams in the formula (11.15), we obtain

$$N_Q = 4.6 \cdot 10^{-14} \varphi P_{del} = 4.6 \cdot 10^{-14} \cdot 10^{14} \cdot 1000 = 4600 \text{ kw/kg.}$$

In order to remove such a high specific power, the active block must be cooled with an intensive flow of coolant.

Example 2. Find the average neutron flux at which the specific power, i.e., the power per unit of mass a homogeneous reactor, reaches 100 kw/kg, if the weight content of the nuclear fuel is $\dfrac{P_{del}}{P_{akt}} = 0.01$.

From (11.14) we obtain

$$\varphi = \frac{0.625 \cdot 10^{16} A_{del} N_{yd}}{\sigma_f E N_A} \frac{P_{akt}}{P_{del}} = \frac{0.625 \cdot 10^{16} \cdot 235 \cdot 100 \cdot 10^{-4}}{549 \cdot 10^{-24} \cdot 200 \cdot 6 \cdot 10^{23} \cdot 0.01} =$$
$$= 2.24 \cdot 10^{14} \text{ neutrons/sec.cm}^2.$$

The neutron flux that was calculated does not exceed the limits already attained in existing power installations.

SECTION 3. REACTOR RADIATION AND SHIELDING

The operation of a reactor is accompanied by powerful radiation. During the disintegration of a fissionable substance, fission fragments, neutrons, electrons, and gamma-quanta are formed. The larger part of the fission fragments is represented by radioactive isotopes, which continue to decay spontaneously, releasing all forms of radioactive radiation: alpha particles, beta particles, and gamma quanta. The leakage neutrons which have abandoned the reactor are captured by the nuclei of atoms of the surrounding substances forming new radioactive isotopes. Gamma rays and neutrons are destructive to a human organism, since under their action the molecules of albumin

and living biological cells decompose.

The roentgen is the unit of gamma-exposure. One roentgen is the quantity of radiant energy such that it forms in one cubic centimeter of air so many ions of the same sign that their total charge constitutes one electrostatic unit of a quantity of electricity.

Gamma-exposure has a cumulative effect. The damages which accompany the exposure are accumulated. Experience shows that any irradiation dose is harmful. The amount of radiation which a person may receive in his life-time, without endangering his health and the health of his descendants, may not exceed 35 roentgens. A dose of 450 roentgens is usually fatal.

Shielding from Gamma Radiation. Gamma-rays are absorbed by the medium. Therefore, with an increase in the path length of the gamma-quanta, the intensity of the radiation decreases. The number of particles passing through a unit surface per second (the surface located normally to the direction of the ray) is called the flux. We will denote the gamma-quanta flux at the entrance to a given medium by I_0; the flux after passing a distance x we will denote by I_x. It is possible to show, that for a parallel flux

$$I_x = I_0 B e^{-\mu x},$$ (11.16)

where x is the distance in cm;

B is the accumulation factor, measured experimentally; $B \approx 1$;

μ is the attenuation factor (Table 11.2).

Table 11.2

THE TOTAL ATTENUATION FACTOR μ FOR GAMMA RAYS WITH ENERGIES OF 2 mev per cm^{-1}

Material	μ cm^{-1}	ρ g/cm^3	Material	μ cm^{-1}	ρ g/cm^3
Air	$0.065 \cdot 10^{-3}$	0.00122	Iron	0.35	7.8
Water	0.047	1.00	Lead	0.53	11.3
Concrete	0.09	~2	Uranium	0.95	19
Aluminum	0.12	2.7			

The flow at x distance from a point source which radiates N quanta per second in all directions is, apparently, equal to

$$I_0 = \frac{N}{4\pi x^2} \;\gamma\text{-quanta/sec cm}^2.$$

<div align="right">(11.17)</div>

Considering absorption in the atmos, here, we obtain

$$I_s = \frac{BN}{4\pi x^2} e^{-\gamma x}.$$

<div align="right">(11.18)</div>

The local radiation intensity can be measured by means of an ionization chamber. The chamber contains two plates to which a potential difference is applied, insufficient to cause a discharge. Under the effect of gamma-radiation, the gas between the plates is ionized and ionization current arises in the circuit. The current strength will be greater the larger the flow of ionizing particles. The irradiation dose is proportional to the quantity of electricity flowing in the circuit. The current is measured by means of a meter included in the circuit. A serial dosimeter, which is manufactured by our industry, is shown in Figure 199. The scale of the meter is often calibrated in roentgens.

We will calculate how great will be the radiation of a reactor whose thermal power is equal to the power of a modern jet bomber.

Fig. 199. A general view of a dosimeter.

Each nuclear fission is accompanied by radiation of nearly 5 gamma-quanta with energies on the average of 2 mev. The permissable radiation intensity in radiometric laboratories consists of 800 gamma-quanta per cm^2 per second. We will recall that the power in one kilowatt is equivalent to $3 \cdot 10^{13}$ fissions per second. The thermal power of an eight engine heavy jet bomber with a total thrust of R = 36,000 kg and a specific fuel consumption C_e = 0.9 kg per hour per kg is equal to

$$N_Q = H_s^{'} O_r = H_s \frac{R C_e}{3600} = \frac{10\,500 \cdot 36\,000 \cdot 0.9}{3600} =$$

$$= 94\,500 \text{ kcal/sec} \approx 400\,000 \text{ kw}.$$

In a reactor with a similar thermal power $3 \cdot 10^{13} \cdot 0.4 \cdot 10^6 = 1.2 \cdot 10^{19}$ fissions per second will occur, during which $N = 5 \cdot 1.2 \cdot 10^{19} = 6 \cdot 10^{19}$ gamma-quanta will be generated. Noting that the reactor is represented by a sphere with a radius of 50 cm, we find that the flow of gamma-quanta at the edge of the reactor is

$$\varphi = \frac{N}{4\pi r^2} = \frac{6 \cdot 10^{19}}{4 \cdot 3.14 \cdot 50^2} \approx 2 \cdot 10^{15} \text{ gamma-quanta/sec cm}^2.$$

After substituting the attenuation factor from Table 11.2 in the equation (11.18) and noting that $B = 1$, it is possible to find the distance at which the flow of gamma radiation will be reduced to a permissible value $I_x = 800$ gamma-quanta per second per cm^2. For air $\mu = 0.065 \cdot 10^{-3}$; $x = 1.6$ km. For lead $\mu = 0.53$ and $x = 54$ cm.

The foregoing calculation shows how great the radiation of a reactor is, and how great the weight and the thickness of the shielding layer must be.

It is seen from equation (11.16) that if the attenuation ratio of the flow $\frac{I_0}{I_x}$ is known, then the product of μx also must be known:

$$\mu x = \ln \frac{I_0}{I_x}.$$

It follows that the thickness of the face of the shielding layer is inversely proportional to the total attenuation factor:

$$x = \frac{\ln \frac{I_0}{I_x}}{\mu}. \tag{11.19}$$

The weight of the shielding layer is

$$P_s = Sx\rho = \frac{\rho}{\mu} S \ln \frac{I_0}{I_x}. \tag{11.20}$$

where S is the surface of the face of the shielding layer.

The ratio of the density to the attenuation factor is approximately one and the same for the majority of substances:

$$\frac{\rho}{\mu} \approx 20.$$

Therefore, the faces of the shielding screens, which are made from various materials, weigh approximately the same but have different thicknesses.

If the reactor is air-cooled, then the cooling air which is irradiated by neutrons, becomes radioactive because of the transformation of the nitrogen N^7_{14} into

a radioactive isotope of carbon C_6^{13} with a half-life period of 5,700 years. The contamination of the atmosphere by radioactive carbon makes the use of air-cooled reactors with an open air-cooling cycle objectionable.

To insure the safety of the service personnel, operating reactors are equipped with monitoring instruments. The reactors are always operated automatically by remote-control instruments. During the assembly of a reactor, manipulators and other remote-control mechanisms are used. Supervision during assembly is conducted with the aid of periscopic instruments or television units.

SECTION 4. THE ASSEMBLY, STARTING, AND CONTROL OF A REACTOR

The assembly of heterogeneous reactors may be accomplished by the following method: the unit is assembled with the use of corresponding construction materials, cooling systems, moderators, and protective shields in the absence of a fissionable material for which special ducts are left. Later, in the finished reactor, a certain amount of active rods is inserted so that the mass of the fissionable substance becomes critical and a continuous fission chain reaction develops in the reactor. The approach to criticality is made known by rapidly increasing radiation. Observations of the radiation are carried out with the aid of instruments which are built into the reactor core. This is how the assembly of the Soviet first atomic power station in the world was accomplished.[1]

The assembly of a heterogeneous reactor may also be carried out in the presence of the active substance consisting, for example, of blocks of uranium and moderators This is how the first Chicago reactor was constructed.

To prevent an explosion which may occur during a chance increase of the critic. dimensions, safety rods, which are constructed of materials which absorb neutrons, are used. These rods are automatically inserted into the active zone $\underline{/}$core$\underline{7}$ when th neutron flux passes the permissible limit. Safety and control rods are constructed

---

[1] Reactor Construction and Reactor Theory. Reports of the Soviet Delegation at the Conference for the Peaceful Use of Atomic Energy, Geneva, 1955, Printing House o the Academy of Sciences, USSR, 1955.

of materials with large capture cross sections: from cadium, boron, or from their compounds (see Table 11.1).

The value of the neutron flux, and consequently, even the power of the reactor depend on the immersion depth of the rods. With an increase of immersion, the absorption of the neutrons increases, the reactivity decreases and together with it, the neutron flux diminishes. At a sufficient immersion, the multiplication factor becomes less than one and the reaction dies out.

A foreign neutron source, for example, an ampule which contains a mixture of metallic beryllium with some sort of natural radioactive alpha emitter -- radium or polonium -- is sometimes inserted to set a reactor into operation. The collisions of the alpha particles with the nuclei of beryllium is accompanied by neutron radiation:

$$Be_4^9 + \alpha_2^4 \to C_6^{12} + n_0^1.$$
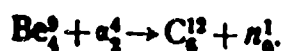
The neutrons from the beryllium-polonium source or stray neutrons bring about the fission of the nuclei of uranium-235. So that the reaction might increase, the safety rods are pulled out and the control rods inserted, and the multiplication factor does not become greater than one. The neutron flux in the reactor increases, the liberation of heat increases, and the temperature of the active zone grows. The length of the diffusion of the neutrons and the distance in which the fast neutrons are slowed down to a "thermal" velocity increases, the density of the active substance diminishes, the leakage of the neutrons grows, and the reactivity decreases. In this way, the process of the increasing power is, to a certain degree, self-regulating. The control rods move in more for greater neutron flux and consequently, greater thermal power. The reactivity of the reactor falls to zero.

The thermal power of a reactor is determined by the location of the control rods.

The level to which it is possible to raise the thermal power is determined by the cooling system and the heat-resistant quality of the reactor.

The movements of the control and safety rods is accomplished by motors, which are connected with probes that are sensitive to the neutron flux in the reactor.

The dependence of the neutron flux and the thermal power upon the immersion depth of the control rods is shown in Figure 200. The S-shaped form of the curve shows that the neutron flux at the reactor's periphery is low, so that the insertion of the rods only decreases insignificantly the overall number of neutrons in the reactor. The insertion of the rods into the central area of the active zone, where the neutron flux is great, has a much greater effect on the overall neutron balance and produces a greater change of the thermal power.

The operation of a reactor is completely controllable.

As the fissionable substance "burns out" and the fission fragments accumulate the reactivity of the reactor diminishes and the control rods must be pulled out.

The consumption of the nuclear fuel is not difficult to calculate in relation to the thermal power of the reactor N_Q kw:

$$G = 0.24 \frac{N_Q}{H} \text{ kg per sec} = 864 \frac{N_Q}{H} \text{ kg per hour,}$$

where H is the amount of energy that is liberated during the fission of 1 kg of uranium-235, in kcal/kg: $H = 1.9 \cdot 10^{10}$ kcal/kg.

Legend:

A) Power
B) Power in kw
C) Temperature
D) Temperature of the Solution in $^{\circ}C$
E) Extracted
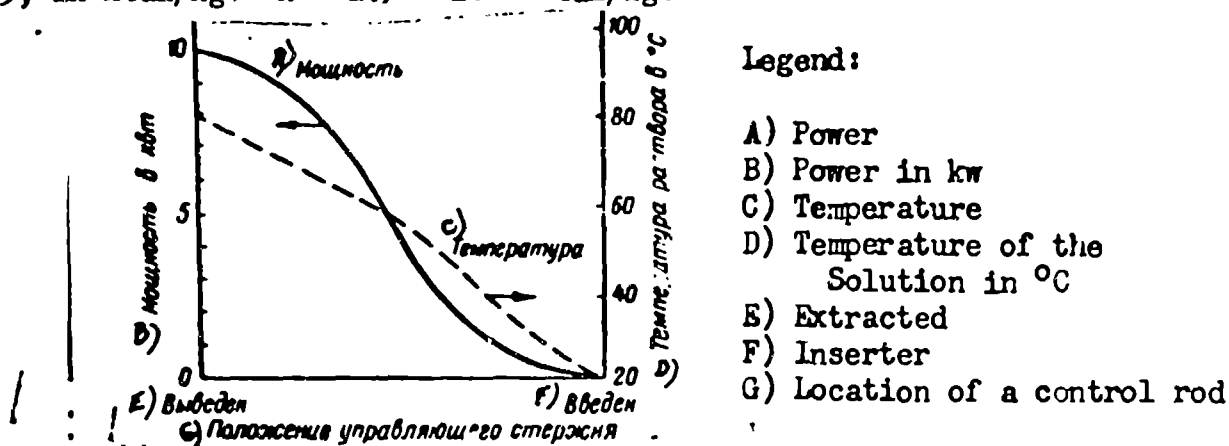F) Inserter
G) Location of a control rod

Fig. 200. The dependence of the neutron flux in a reactor and the thermal power of a reactor on the immersion depth of the control rods.

The consumption of the nuclear fuel in a heavy atomic aircraft with eight turbojet engines with thermal power of $N_Q = 400,000$ kw.

$$G = 864 \frac{400,000}{1.9 \cdot 10^{10}} = 0.018 \text{ kg per hour} = 18 \text{ g per hr} = 5 \text{ mg per sec.}$$

For a 40-hour around-the-world flight with a speed of 1,000 km/hr altogether 72 grams of a nuclear fuel will be required.

SECTION 5. THE COOLING OF A REACTOR AND THE PREHEATING OF THE AIR

The air which flows through a heat exchanger of a reactor for a ramjet engine must be preheated to an optimum temperature T_{03}. After determining this temperature and giving the required thrust, we will find the air flow G_v through the heat exchanger of a reactor.

After setting the permissible value of the relative velocity of the heated air at the heat exchanger outlet λ_3, we will determine the required cross section of the heat exchanger from (2.74):

$$S_3 = \frac{G}{\gamma_3 w_3} = \sqrt{\frac{(k_r + 1) R_r T_{03}}{2 g k_r}} \frac{G}{p_{03} q(\lambda_3)}.$$

(11.21)

The cross section that is found comprises a certain portion of the middle section of the engine S_M:

$$\frac{S_M}{S_3} = n > 1.$$

(11.22)

The geometry of the heat exchanger must be calculated so that the air flowing through it will be heated to the required temperature T_{03}.

The calculation of the heat exchanger for the heating of the air is carried out by a common method.

The air temperatures at the heat exchanger inlet and at its outlet are denoted by T_{02} and T_{03}. The temperature of the heat-transfer agent at the heat exchanger inlet and at its outlet we denote by T_2' and T_3' (Figure 201).
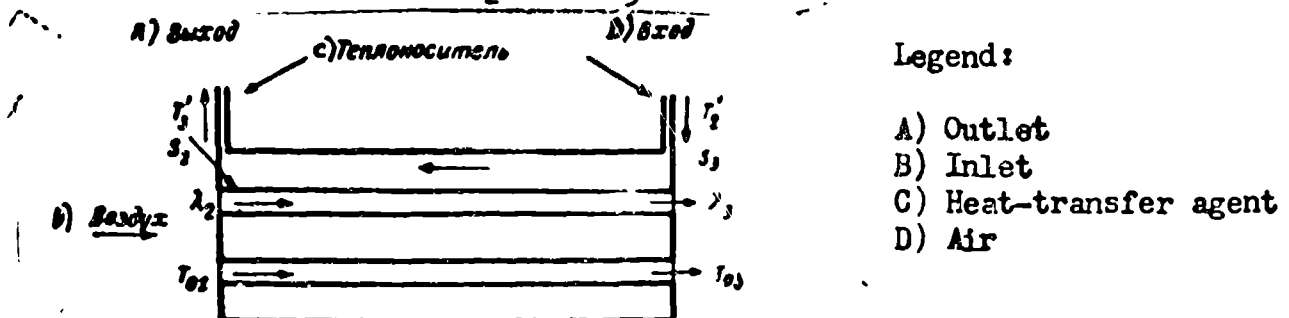

Fig. 201. A diagram of a heat exchanger.

Legend:

A) Outlet
B) Inlet
C) Heat-transfer agent
D) Air

The quantity of heat, which is received by the air in the heat exchanger, is equal to the thermal power N_Q:

$$N_Q = \alpha_v S_{repl} \Delta T.$$

(11.23)

where α_v is the heat transfer coefficient;

S_{repl} is the transfer surface between the air and the heat exchanger;

ΔT is the average temperature difference.

It is known from the theory of heat exchanger installations that the average temperature difference, in the case of a constant heat transfer coefficient through the heat exchanger α_v = const, is equal to

$$\Delta T = \frac{(T_2' - T_{02}) - (T_3' - T_{03})}{\ln \frac{T_2' - T_{02}}{T_3' - T_{03}}}.$$

(11.24)

The temperature of a reactor with direct air heating will be calculated in the first approximation by assuming the entire active zone at constant temperature: $T_2 = T_3 = T_p$. In this case

$$\Delta T = \frac{T_{03} - T_{02}}{\ln \frac{T_p - T_{02}}{T_p - T_{03}}}.$$

(11.25)

The heat transfer coefficient a_{tepl} is dependent upon Nusselt's number which is determined by the Reynolds' and Prandtl's numbers, and also by the heat conductivity λ :

$$\alpha_{tepl} = \frac{Nu \lambda}{d},$$

(11.26)

$$Nu = f(Re, Pr),$$

(11.27)

$$Re = \frac{wd}{\nu} = \frac{wd\gamma}{g\eta}, \quad Pr = \frac{c_p \eta}{\lambda}.$$

(11.28)

For gases Pr = 0.72.

d is the size of the heat exchanger that was determined;

c_p and λ are the specific heat and the heat conductivity of the air, ν is its

  kinematic viscosity;

η is the dynamic viscosity;

w is the velocity of the gas flow.

The temperature of the air which flows through a heat exchanger increases, the velocity of the flow increases and together with them the parameters of the air λ, ν, γ, and also the Re and Nu numbers and the heat transfer coefficient vary. We express the heat transfer coefficient as a function of the temperature in a clear form.

When $S_2 = S_3$

$$\gamma_2 w_2 = \gamma_3 w_3.$$

The product of γw is a constant value for a tube having a constant cross section. Consequently, the Reynolds' number during the flow through the heat exchanger varies in inverse proportion to the dynamic viscosity η :

$$Re = \frac{wd}{\nu} = \frac{w\eta}{g} \frac{d}{\eta}. \qquad (11.29)$$

The Nu number is determined by the Re and Pr numbers, and also by the shape of the heat exchanger. For cylindrical tubes

$$Nu = 0.023\, Re^{0.8}\, Pr^{0.4}. \qquad (11.30)$$

The heat transfer coefficient from the walls to the air α_v is

$$a_v = \frac{Nu\,\lambda}{d} = 0.023\, \frac{w^{0.8}\gamma^{0.8}d^{0.8}\lambda c^{0.4}\gamma_i^{0.4}}{g^{0.8}\eta_i^{0.8}d^{0.4}\lambda^{0.4}} = 0.023\, \frac{(w\gamma)^{0.8}\lambda^{0.6}c^{0.4}}{g^{0.8}\eta_i^{0.4}d^{0.2}}. \qquad (11.31)$$

The viscosity η, the heat capacity c, and the heat conductivity λ increase with an increase of temperature. The expression $\dfrac{c^{0.4}\,\lambda^{0.6}}{\eta^{0.4}}$ slowly increases with the increase of temperature. In the first approximation, the heat transfer coefficient may be considered as constant throughout the entire heat exchanger. The heat transfer coefficient decreases insignificantly with an increase of the diameter of the tubes

The thermal power, which is taken from the heat exchanger for a constant heat transfer coefficient α_v = const, is directly proportional to its surface. If the thermal power is given, then depending upon the diameter of the tubes, it is possible to find the surface of the heat exchanger S_{tepl}.

The overall cross section of a tube of a heat exchanger S_2 is determined by the air flow required G_v and the permissible flow velocity in the tubes w_2. The pressure of the heated air p_{02} is determined by the velocity and flight altitude, and by the pressure recovery of the diffuser σ_d. The number of tubes n is inversely proportional to the square of their diameter d:

$$n = \left(\frac{D}{d}\right)^2.$$

After equating the thermal power which is taken up by the air that is heated in a heat exchanger

$$N_Q = c_p w_3 \gamma_3 S_3 (T_{03} - T_{02}), \qquad (11.32)$$

to the thermal power which is transmitted through the walls of the heat exchanger

$$N_Q = a_s S_{\tau e_{\mu}} \Delta T,$$

and considering that

$$\frac{S_{\tau e_{n3}}}{S_2} = \frac{4\pi d l n}{\pi d^2 n} = 4\frac{l}{d},$$

we obtain

$$\frac{l}{d} = \frac{c_p \gamma_2 w_2}{4 a_s} \frac{T_{03} - T_{02}}{\Delta T}.$$

(11.34)

After using (11.28, 11.29, and 11.26) and after simple conversions, we obtain an equation which connects the relative length of the heat exchanger ducts with the temperature difference $T_{03} - T_{02}$ and the temperature drop ΔT by the Re, Pr, and Nu numbers:

$$\frac{l}{d} = \frac{\text{Re Pr}}{4 \, \text{Nu}} \frac{T_{03} - T_{02}}{\Delta T}.$$

(11.35)

SECTION 6. REACTORS COOLED BY MOLTEN METAL

To decrease the dimensions of a reactor and to avoid the contamination of t e air coolant by radioactive isotopes, reactors are constructed with liquid coolants. The heat liberated in the reactor is absorbed by the liquid heat-transfer agent, and carried to a heat exchanger where it is transferred to the heated air. It is clear that the temperature of the heat-transfer agent at the reactor outlet must be greater than the air temperature ahead of the nozzle exit. Therefore, water, the critical temperature of which is $650°$ K, is not suitable as a heat-transfer agent. More suitable heat-transfer agents for atomic ramjet engines are molten metals, the melting points of which are less than the temperature at the heat exchanger outlet T_3'. The vapor pressure at the temperature of T_2', which the heat-transfer agent has at the reactor outlet, cannot be too great, i.e., cannot exceed the stagnation pressure in the combustion chamber p_{02} by far.

As possible heat-transfer agents for reactors, the Institutes of the Academy of Sciences of the USSR investigated molten tin, lead, bismuth, sodium, and also alloys: sodium and potassium, lead and bismuth.

By the works of the academician M. A. Mikheyev with his associates, and also by

series of foreign scientists, it was proven that the heat transfer coefficient for metal which flowed along a cylindrical tube, is determined by Nusselt's (Nu) and clet's (Pe) numbers:

$$Pe = Re\,Pr = \frac{d w \eta c}{g \lambda}.$$

(11.36)

To determine the Nu number, Lyon, Dwyer and others suggested the following rmula:

$$Nu = 3{,}2 + 0{,}021\,Pe^{0{,}8}.$$

(11.37)

In the investigated heat exchangers Pe = 100--10,000, Nu = 10--30;

= 0.01--0.10 k cal per meter per second per degree. Because of the high heat conctivity of metal, the heat transfer coefficient was much higher than that for gas oling: $a_{\mu} = \frac{Nu\lambda}{d} = $ 1--300 kcal per square meter per second per degree, hundreds of mes greater than for heat transference to the air.

For the computation of a heat exchanger between the active zone /core/ of a retor and the heat-transfer agent, one considers the heat conductivity of the material om which the heat transfer agent tubes are prepared and the heat conductivity of the tive material.

We will introduce the concept of thermal resistance R_t after determing it from the following equation:

$$q_t = \frac{\Delta T}{R_t} = \alpha_{tepl} S_{tepl} \Delta T,$$

(11.38)

ere q_t is the heat flow;

ΔT is the average temperature drop.

om here

$$R_t = \frac{1}{\alpha_{tepl} S_{tepl}},$$

(11.39)

·re α_{tepl} is the heat transfer coefficient,

S_{tepl} is the heat exchanger surface.

The heat transfer from the active zone /core/ of the reactor to the molten metal be written as (Figure 202):

$$R_t = R_t + R_{\omega} + R_{\mu} = \frac{1}{a_t S_t} + \frac{\delta}{\lambda_{\omega} S_{\omega}} + \frac{1}{a_{\mu} S_{\mu}},$$

(11.40)

where δ is the thickness of the tube wall;

λ_w is its heat conductivity;

a_1 and a_M are the heat transfer coefficients from the active zone /core/ to the tube
wall and from the tube wall to the molten metal.

For air cooling, the temperature resistance is many times greater during heat
transfer from the tube wall to the air than during heat transfer from the active
material to the tube wall, or during heat transfer through the substance of the tube
or of the active zone /core/. Therefore it is possible to disregard these last re-
sistances, after considering only the first.

During the elimination of the heat from a reactor with a heavy active zone, the
primary heat resistance is concentrated on the mutual surface with the tube inside
the active zone. The heat resistance for the transfer from the tube walls to the
molten metal is insignificant. The overall heat resistance during cooling by a molten
metal, and the surface of the heat exchanger is ? as of times less than for air
cooling of a reactor.

A heat exchanger for heating the flowing air is computed as stated in the fore-
going paragraph.

A) кипящая вода

B) Жидкий
материй

Legend:

A) Boiling water
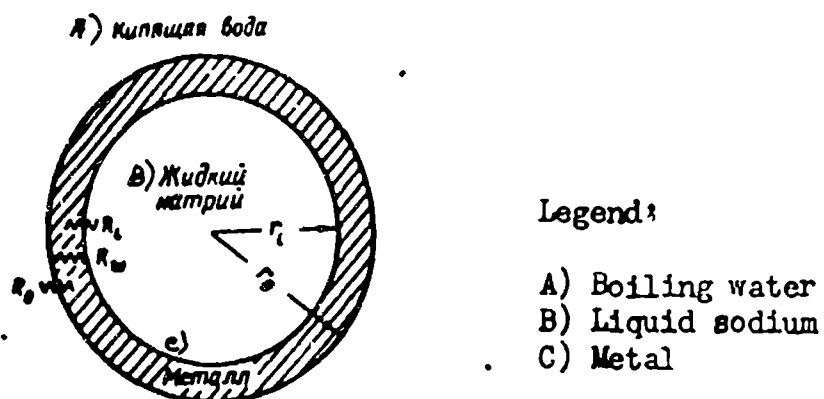B) Liquid sodium
C) Metal

Fig. 2υ2. The calculation of the heat transfer through the wall of a heat-exchanger.

Example. A reactor with a thermal power of $N_Q = 400,000$ kw is cooled by special
alloy. The temperature of the active zone is $T_p = 2,000°$ K. The temperature of the
heat-transfer agent at the reactor inlet is $T_2 = 600°$, at its outlet $T'_3 = 1,800°K$.
The parameters of the alloy are $\gamma = 700$ kg/m^3, $\lambda = 0.00\zeta$ kcal/м. sec degree, $c = 0.25$ kcal/kg degree. The coolant speed is $w = 10$ m/sec. The diameter of the tubes

is d = 25 mm.

The heat-transfer agent consumption is

$$G_T = \frac{N_Q}{c\,(T'_3 - T'_2)} = \frac{0.24 \cdot 400\,000}{0.25\,(1600 - 800)} = 384 \text{ kg/sec.}$$

The cross section of the heat-transfer agent tubes is

$$s = \frac{G}{w_T} = \frac{384}{10 \cdot 700} = 0.055\ м^2 = 550\ \text{cm}^2.$$

The number of tubes is

$$n = \frac{4s}{\pi d^2} = \frac{4 \cdot 550}{3.14 \cdot 2.5^2} = 112.$$

Peclet's number is

$$Pe = \frac{dw_T c}{g\lambda} = \frac{0.025 \cdot 10 \cdot 700 \cdot 0.25}{9.8 \cdot 0.006} = 740.$$

Nusselt's number is

$$Nu = 3.2 + 0.021 Pe^{0.8} = 3.2 + 0.021 \cdot 740^{0.8} = 7.3.$$

The heat transfer coefficient from the wall to the liquid metal is

$$a_u = \frac{Nu\lambda}{d} = \frac{7.3 \cdot 0.006}{0.025} = 1.75 \text{ kcal/sec } m^2 \text{ degree.}$$

The mean logarithmic temperature drop is

$$\Delta T = \frac{T'_3 - T'_2}{\ln \dfrac{T_p - T'_2}{T_p - T'_3}} = \frac{1600 - 800}{\ln \dfrac{2000 - 800}{2000 - 1600}} = 640°.$$

We will assume that the tubes are made of heat-resistant steel for which

λ_T = 0.01 kcal/m sec degree, the thickness of the walls is δ = 2.5 mm. We may disregard the heat resistance of the active zone.

We find the surface of the heat exchanger from the equation

$$N_Q = a_{Tcu} S \Delta T;$$

$$\frac{1}{a_{Tcu} S_{Tcu}} \approx \frac{\Delta T}{N_Q} = \frac{1}{a_u S_u} + \frac{\delta}{\lambda_T S_T} = \frac{\lambda_T S_T + a_u S_u \delta}{a_u \lambda_T S_T S_u},$$

$$S_{Tcu} = \frac{N_Q}{\Delta T}\left(\frac{1}{a_u} + \frac{\delta}{\lambda_T}\right) = \frac{96\,000}{640}\left(\frac{1}{1.75} + \frac{0.0025}{0.01}\right) = 123\ m^2.$$

where

$$S_u \approx S_T \approx S_{Tcu}.$$

The overall perimeter of the tubes is

$$P = \pi dn = 3.14 \cdot 0.025 \cdot 112 = 8.8\ m,$$

the total length of the tubes is

$$l = \frac{S}{P} = \frac{123}{8.8} = 14\ m.$$

The volume of the heat-transfer agent in the reactor is

$$V = ls = 14 \cdot 0.055 = 0.77 \text{ m}^3,$$

its weight is

$$P_{\text{теп}} = V\gamma = 0.77 \cdot 700 = 540 \text{ kg}.$$

To transfer the heat to the air requires a special heat exchanger, which is computed as was stated above in Section 5. If the reactor is equipped with a shield, then a system with an intervening heat-transfer agent permits a considerable decrease of the reactor's dimensions and a lower weight of the shielding.

Shielded reactors may be installed only in very heavy aircraft.

SECTION 7. ELECTROMAGNETIC PUMPS FOR MOLTEN METALS

Electromagnetic Faraday pumps, which are based on the power interaction of an electric current with a magnetic field, are often used to transfer molten metals. A diagram of an electromagnetic pump is shown in Figure 203. A portion of the tube, through which the molten metal flows, is flattened and placed between the fields of a strong electromagnet. A strong electric current from a step-down transformer is carried to the molten metal with the aid of two thick copper bars. From the side of the magnetic field to the bars with the current a force acts, which is directed , left-hand rule, the way the thumb points when the palm of the hand is turned to meet the magnetic lines of force and the four extended fingers show the direction of the current in the conductor. In Figure 203 this force is direct.d towards us.

The magnitude of the force F in dynes is equal to one tenth of the product of the force of the current I in amperes and the induction B of the magnetic field in gausses and the length l of the bar between the poles of the magnet in centimeters:

$$F = 0.1 \, IBl \text{ dynes.} \qquad\qquad (11.41)$$

After dividing this force by the cross section S of the tube, we find the pressure that is created by the pump:

$$p = \frac{F}{S} = 0.1 \frac{IBl}{S} \text{ dynes/cm}^2 = \frac{IB}{9.8 \cdot 10^9 \, b} \text{ kg/cm}^2. \qquad (11.42)$$

Here the quotient $b = \dfrac{S}{l}$ represents the inter-polar interval. After expressing

the current in kiloamperes and the induction in kilogauss, we obtain

$$p = \frac{IB}{9.8b}\ \kappa z/c\mu^3 \approx \frac{IB}{b_{(\mu\mu)}}\ \text{atm.}$$ (11.43)

The magnetic induction B during the use of good magnetic alloys may reach 10 kilo-gauss and higher. Let the inter-polar interval b = 1 mm. Then in order to create a pressure on the order of 10 atm, it is necessary to have a current with a force of $I = \dfrac{9.8bp}{B}\ \ \dfrac{1 \cdot 10}{10} = 1$ kiloampere $\stackrel{\Delta}{=} 1{,}000$ amps.
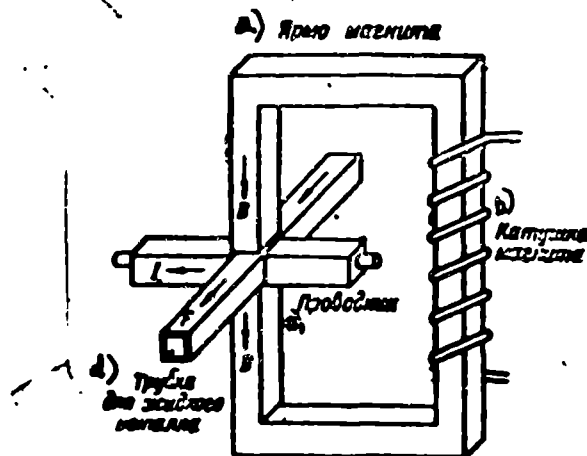
Legend:

a) Magnet yoke
b) Magnet coil
c) Conductor
d) Tube for molten metal

Fig. 203. The diagram of an electromagnetic pump to transfer liquid metals.

During the movement of the molten metal between the magnet poles, an electro-motive force with the induction E appears in it as it does in any conductor:

$$E = 10^{-8}Blw/\text{volt}$$ (11.44)

where w is the speed of the metal in cm/sec;

B is the induction of the magnetic poles in gauss;

l is the length in cm.

If B = 10 kilogauss; l = 10 cm; w = 10 m/sec, then E = $10^{-8} \cdot 10^4 \times 10 \cdot 10^3$ = 1 volt.

The voltage on the busbars must be greater than the electromotive force of induction, which appears in the moving wire:

$$U = E + IR,$$ (11.45)

R is the ohmic resistance of the molten metal between the bars:

$$R = \rho\frac{l}{s},$$

ρ is the specific resistance in ohms/centimeters;

s is the cross section in the direction of the normal to the electric current. If

the width of the interpolar interval is equal to a, then

$$s = ba$$

The power, which is spent on transferring the metal and in overcoming its ohmic resistance, will be equal to

$$N = UI. \tag{11.46}$$

__Example.__ The specific resistance of a heat-transfer agent is $\rho = 13 \cdot 10^{-6}$ ohms (molten sodium); a = 10 cm; b = 0.1 cm; and 1 = 10 cm.

$$R = 13 \cdot 10^{-6} \frac{10}{10 \cdot 0.1} = 1.3 \cdot 10^{-4} \text{ ohm},$$

$$U = E + IR = 1 + 1000 \cdot 1.3 \cdot 10^{-4} = 1.13 \text{ v};$$

$$N = UI = 1.13 \cdot 1000 = 1130 \text{ watts} = 1.13 \text{ kw.}$$

SECTION 8. THE GAS DYNAMIC CALCULATION OF A NUCLEAR SUPERSONIC RAMJET ENGINE

The gas dynamic calculation of a nuclear supersonic ramjet engine is identical with the calculation of an engine that operates on a molecular fuel. In the first case, the cross section of a heat exchanger is not equal to the mid-cross-section of the engine, and the mass of the exhaust gases is equal to the mass air flow:

$$S_2 < S_u; \quad \beta = 1 + \frac{1}{aL} = 1.$$

The required heating of the air in a heat exchanger $\theta = \frac{T_{03}}{T_{02}}$ is determined either by the given thrust coefficient, or by the conditions of maximum economy: $\theta = \theta_{opt}$ (see Chapter X, Section 5).

The minimum allowable thrust coefficient is determined by the aerodynamic computation for the entire aircraft as a whole.

For an established horizontal flight, the thrust coefficient is equal to the drag coefficient, which is computed relative to the area of the engine's mid-section

$$c_{R \text{ потр}} = c_x. \tag{11.47}$$

By knowing the required thrust coefficient, and after setting up the probable value of the gas dynamic coefficient of the engine K, from the formula of the thrust coefficient for a flight at the design condition, the required temperature ratio of the air in a heat exchanger θ is found (see formula 10.35)

$$c_{R \, omp} = 2 \varkappa^3 K^2 \frac{\tau(\lambda_4)}{\tau(\lambda_4)} \left(1 - \frac{1}{\varkappa K \sqrt{\theta}}\right).$$ (11.48)

In the last formula it is assumed that $R_r \approx R$.

The optimum temperature ratio, at which the total efficiency of an engine reaches its highest value, is equal to (see Chapter IX, Section 5)

$$\theta_{opt} = \frac{1 + \sqrt{1 - \varkappa^3 K^2}}{1 - \sqrt{1 - \varkappa^3 K^2}}.$$ (11.49)

The required thrust R is determined by the flight weight and the aerodynamic quality (lift-drag ratio) of the aircraft k_a

$$R = \frac{P_{nol}}{k_a}.$$ (11.50)

The total efficiency of a ramjet engine η is:

$$\eta = 2 \frac{k-1}{k+1} \lambda_\pi^2 \frac{\varkappa K \sqrt{\theta} - 1}{\theta - 1}.$$ (11.51)

The required thermal power N_Q is:

$$N_Q = A \frac{R w_n}{\eta} \text{ kcal/sec.}$$ (11.52)

The air flow G_v, that is required for the transfer of the required thermal power N_Q is,

$$G_v = \frac{N_Q}{c_p(T_{03} - T_{02})} = \frac{N_Q}{l_{0n}(\theta - 1)} \text{ kg/sec.}$$ (11.53)

We will set up an acceptable value for the relative velocity at the heat exchanger outlet, noting that it may not exceed one: $\lambda_3 < 1$. We will find the cross section of the heat exchanger S_3.

We will determine the required cross-section area ratio of the exhaust nozzle from (5.20):

$$\frac{S_3}{S_{mp}} = \frac{\sigma_c' \left(\frac{2}{k_r + 1}\right)^{\frac{1}{k_r - 1}}}{q(\lambda_3)}.$$ (11.54)

(See graph in Figure 170).

The velocity at the heat exchanger inlet is determined from the flow equation:

$$q(\lambda_2) = \frac{\varkappa}{\sqrt{\theta}} \frac{p_{03}}{p_{02}} q(\lambda_3).$$ (11.55)

The stagnation pressure of the free stream air $p_{0n} = \frac{p_n}{\pi(\lambda_n)}$. The stagnation pressure ahead of the heat exchanger inlet p_{02} depends upon the pressure coefficient of the diffuser σ_d:

$$\bar{p}_{01} = \frac{\epsilon_1 p_1}{\pi(\lambda_1)}.$$
(11.56)

The required cross section for the passage of the air through the heat exchanger S_2, is found from (2.74)

$$S_2 = \frac{G_0}{w_2 \tau_2} = \sqrt{\frac{k+1}{2gk} RT_{01}} \cdot \frac{G_0}{p_{01} q(\lambda_2)}.$$
(11.57)

SECTION 9. AN APPROXIMATE DETERMINATION OF THE CRITICAL DIMENSIONS OF A REACTOR

A reactor with cross sections and a thermal power of the required value must have a positive reactivity; its dimensions must be greater than critical. Below is found a simplified calculation of a reactor which operates on thermal neutrons without a reflector.

The critical dimensions of the reactor depend on the nature of the nuclear fuel and on the moderator, on the concentration of uranium-238, on the ratio of the masses of the fissionable substance and the moderator, on the volume (void) fraction of the active zone, on the nature of the heat-transfer agent, and on the construction of the reactor.

An approximate calculation for a homogeneous reactor which operates on thermal neutrons, is to be found below.

The ratio of the volume of the fissioning material and the moderator to the total volume of the active zone or the volume (void) fraction ∇ is equal to

$$\nabla = \frac{V_{akt}}{V_{akt} + V_{okl}},$$
(11.58)

where V_{akt} is the volume of the active material;

V_{okhl} is the volume of the cooling ducts and the construction materials.

The greater the volume that is occupied by the cooling ducts, the lesser the volume (void) fraction.

The shape of the reactor is determined by its usage. Cylindrical or spherical reactors are more suitable to be installed on aircraft. In order that the reactor may develop a continuous nuclear reaction, the effective multiplication factor of the reactor, which was discussed in Section 1 of this chapter, must be not less than one:

$$k_{ef} = \epsilon p f \eta L \geqslant 1.$$
(11.59)

The multiplication factor for fast neutrons ε and the probability of avoiding absorption into uranium-238 p depends on the presence of uranium-238. For natural uranium $\varepsilon \approx 1.03$; p = 0.9; for a pure fission substance ε = 1 and p = 1.

The thermal use factor f is equal to the ratio of the number of neutrons which are absorbed in the fissioning substance to the overall number of the neutrons which are absorbed by the fissioning substance and also by the moderator.

The atomic concentration of the fissioning substance, the number of atoms in 1 cm³, is denoted by N_{del}:

$$N_{яеэ} = \frac{\rho}{A_{яеэ}} N_A \frac{P_{яеэ}}{P_{экт}},$$ (11.60)

and the atomic concentration of the moderator is designated by N_3:

$$N_э = \frac{\rho}{A_э} N_A \frac{P_э}{P_{экт}},$$ (11.61)

where ρ is the density of the active substance, which is composed of a mixture of a moderator and the nuclear fuel.

The overall weight of the active zone /core/ of the reactor is

$$P_{акт} = P_{яеэ} + P_э,$$

where P_{del} and P_3 are the weights of the uranium and the moderator.

The macroscopic capture cross sections of the neutrons in the fissioning substance and in the moderator will be equal to

$$\Sigma_{яеэ} = N_{яеэ} \sigma_{яеэ}; \qquad \Sigma_э = N_э \sigma_э.$$ (11.62)

The coefficient of thermal use is, consequently, equal to

$$f = \frac{\Sigma_{яеэ}}{\Sigma_{яеэ} + \Sigma_э} = \frac{1}{1 + \frac{\Sigma_э}{\Sigma_{яеэ}}} = \frac{1}{1 + \frac{N_э \sigma_э}{N_{яеэ} \sigma_{яеэ}}},$$ (11.63)

The number of fission neutrons per one captured neutron for uranium-235 η = 2.1.

In reactor theory it is proven that the probability of avoiding leakage for fast neutrons in the slowing down process L_f is equal to

$$L_f = e^{-K^2 \tau}.$$ (11.64)

The probability for avoiding leakage for slow neutrons, before they will be absorbed by the fissioning substance L_t is equal to

$$L_f = \frac{1}{1 + K^2 L^2}. \tag{11.65}$$

Here L is the diffusion length, which depends on the nature of the moderator, on the coefficient of thermal use f, and on the volume (void) fraction V^2 (see Table 11.3)

$$L^2 = L_0^2 \frac{1-f}{V^2}. \tag{11.66}$$

τ is the square of the moderator length, which is dependent on the nature of the moderator and on the relative density ρ otn:

$$\tau = \frac{\tau_0}{V^2}, \tag{11.67}$$

where τ_0 is the square of the slowing-down length when $V = 1$ (Table 11.3)

K is the geometric parameter of the shape factor, which is dependent on the shape of the reactor.

For a sphere with a radius of R cm

$$K = \frac{\pi}{R}.$$

For a cylinder with a radius of R and a length of H

$$K^2 = \left(\frac{2.405}{R}\right)^2 + \left(\frac{\pi}{H}\right)^2. \tag{11.68}$$

The probability of avoiding leakage in the slowing down process and in diffusion is

$$L = L_t L_f = \frac{1}{(1 + K^2 L^2) e^{K^2 \tau}}. \tag{11.69}$$

The parameters L_0 and τ_0 are determined experimentally (Table 11.3).

Table 11.3

THE LENGTH OF DIFFUSION AND THE SQUARE OF THE MODERATOR LENGTH
OF CERTAIN MODERATORS

Substance	Formula	A	L_0 cm	τ_0 cm^2
Ordinary water	H_2O	18	2,88	33
Heavy water	D_2O	20	171	120
Graphite	C	12	50	300
Beryllium	Be	9,013	24	98

The weight of the reactor's active zone /core/ is a function of its volume, density, and volume (void) fraction:

$$P_{akt} = V \rho V_{akt}. \tag{11.70}$$

SECTION 10. A DESIGN EXAMPLE FOR AN AIR-COOLED REACTOR

We will determine the critical dimensions of a reactor which operates on pure uranium-235, with metallic beryllium as a moderator, and with air cooling.

We will assume the relative quantity of fissioning substance: $\frac{P_U}{P_{Be}} = 0.01;$ the volume (void) fraction $\triangledown = 0.5$ (a half of the volume of the active zone is occupied by air ducts), and we will assume that the reactor has the shape of a cylinder, the height of which is equal to the diameter: $H = 2R = D.$

We will determine at what diameter the reactor becomes critical, and we will find its weight and what thermal power it is possible to take from it.

The ratio of the number of the atoms of the moderator to the number of atoms of the active substance is, from (11.60) and (11.61):

$$\frac{N_{Be}}{N_U} = \frac{P_{Be}}{P_U} \frac{A_U}{A_{Be}} = \frac{235}{0.01 \cdot 9,013} = 2610.$$

The coefficient of the thermal use of the neutrons /see Table 11.1 and the formula (11.63)/ is

$$f = \frac{1}{1 + \frac{N_{Be}}{N_U} \frac{\sigma_{Be}}{\sigma_U}} = \frac{1}{1 + 2610 \frac{0.01}{650}} = 0.96.$$

The diffusion length and the square of the slowing-down length in beryllium when the volume fraction is $\triangledown = 0.5$ from (11.66) and (11.67)

$$L^2 = L_0^2 \frac{1-f}{\gamma^2} = 24^2 \frac{1-0,96}{0,5^2} = 92 \text{ cm}^2,$$

$$\tau = \frac{\tau_0}{\gamma^2} = \frac{98}{0,5^2} = 392 \text{ cm}^2.$$

The effective multiplication factor k_{ef} is determined from the equations (11.59) and (11.69) when $\varepsilon = 1$ and $p = 1$

$$k_{ef} = \frac{\eta f}{(1 + K^2 L^2) e^{K^2 \tau}}.$$

By considering that the number of neutrons which are liberated during the capture of a single neutron by uranium-235, $\eta = 2.1$ and that for a critical reactor $k_{ef} > 1$, we obtain an equation from which it is possible to find the reactor shape factor K:

$$(1 + 92 K^2) e^{392 K^2} = 2.1 \cdot 0.96.$$

After solving it by means of matching of, by a graphic method, we find

$$K^2 = 0.0015$$

The radius of the cylinder is found from the equation

$$K^2 = \left(\frac{2.405}{R}\right)^2 + \left(\frac{\pi}{2R}\right)^2 = \frac{8.25}{R^2};$$

$$R = \sqrt{\frac{8.25}{K^2}} = \sqrt{\frac{8.25}{0.0015}} = 74 \; cm = 0.74 \; m.$$

In order to obtain the positive reactivity, we express

$$D = H = 2R = 160 cm > 2 \cdot 74 \; cm.$$

The total cross section of the active zone $S_{akt} = \pi R^2 = 2 \; m^2$.

The flow cross section is $S_2 = (1 - \nabla) S_{akt} = 1 \; m^2$.

The weight of the active zone of the reactor is $P_{akt} = \gamma S_{akt} H_t = 0.5 \cdot 2 \cdot 1.6 \cdot 1.82 = 2.91 \; r.$

The amount of fissioning substance is $P_{del} = 0.01 P_{akt} = 29.1 \; kg = 29,100 \; grams.$

The thermal power of the reactor N_Q is determined by the average neutron flux in the active zone /core/ φ, determined by the position of the control rods.

The average neutron flux which is necessary to obtain the thermal power $N_Q = 400,000$ kw, is found from (11.15)

$$\varphi = \frac{10^{14} N_Q}{4.6 \cdot P_{del}} = \frac{10^{14} \cdot 400\,000}{4.6 \cdot 29\,100} \approx 3.1 \cdot 10^{14} \; \text{neutrons/sec.cm}^2.$$

An aircraft reactor, which is described by Hawthorne, possess very similar parameters.

BIBLIOGRAPHY

1. Glasstone, E. and Edlund, Teoriya i raschet yadernykh reaktorov /The Theory and Design of Nuclear Reactors/, Printed in Foreign Literature, 1955.

2. Murray, R., Vvedeniye v yadernuyu energetiku /An Introduction to Nuclear Power Engineering/, Printed in Foreign Literature, 1955.

3. Namias, M., Yadernaya energiya /Nuclear Energy/, Printed in Foreign Literature, 1955.

4. Reaktorostroeniye i teoriya reaktorov /Reactor Construction and Reactor Theory/. Reports of the Soviet Delegation at the Conference for the Peaceful Use of Atomic Energy, Geneva, 1955, Printing House of the Academy of Sciences, USSR, 1955.

5. Fizicheskiye issledovaniya /Physics Investigations/, Reports of the Soviet Delegation at the Conference for the Peaceful Use of Atomic Energy, Geneva, 1955, Printing House of the Academy of Sciences, USSR, 1955.

6. Avion Atomique. Atomes, No. 115, X, 1955.

7. Eksperimen!'haya yadernaya fizika /Experimental Nuclear Physics/ edited by E. Segre, vols. 1 and II, Printed in Foreign Literature, 1955 and 1956.

8. Lyon, R. N., Liquid Metals Handbook, 2 ed., Washington, 1952.

9. Kaeppeler, H. I., "Aspects of Nuclear Power Application for Jet Propulsion," Astronautics, vol. 2, No. 2 and 3, 1955.

10. Hawthorne, The Aeroplane, Nov. 9, 1956.

CHAPTER XII

THE DEVELOPMENT PERSPECTIVES OF RAMJET ENGINES

SECTION 1. SPEEDS AND ALTITUDES

The subsequent development of ramjet engines will, apparently, proceed along the lines of perfecting the individual elements of the engines, i.e., diffusers, combustion chambers, and nozzles, just as along the lines of mastering higher flight speeds, greater altitudes, and new forms of energy.

At flight speeds from $M_n = 0.8$ to $M_n = 2.5$ ramjet engines are suitable only for one-time flying vehicles, i.e., on target drones and winged missiles, and also on some types of helicopters since within this velocity range ramjet engines yield to turbo-jet engines both in thrust and in economy.

In the interval from $M_n = 2.5$ to $M_n = 3.0$ the competition between turbo-compressor and ramjet engines occurs with varying success. Up to the present time there is no data in open literature about three-Mach turbo-jet engines. In order for turbo-jet engines to compete with ramjet engine at $M_n - 3$ it is first necessary to solve the problem of lubricating the turbo-jet engine at such high stagnation temperatures. Calculations show that when $M_n \approx 4.0$ the optimum degree of compression in a turbo-jet compressor approaches one. This means, that with a sufficient increase of flight speed, a turbo-jet engine is transformed into a ramjet. The region of speeds like $M > 3$ and altitudes of more than 25 km belong to ramjet engines and rockets.

SECTION 2. DEVELOPMENT PERSPECTIVES OF DIFFUSERS

The pressure recovery coefficients of fixed-geometry multi-shock wave diffusers c increases with an increase of the design flight velocity: if when $M_n = 2.75$ $\sigma_d = 0.7$, then when $M_n = 3.3$ $\sigma_d = 0.55$ (see Figure 70). Calculations, which were confirmed by experiments, show that variable-geometry diffusers or diffusers which are manufactured in the shape of an inverted Laval nozzle, may possess significantly greater pressure recovery coefficients.[1]

---

[1] Time, 30/I, 1956, 37-40.
Aviation Age, Vol. 23, No. 6, 1955, 68-73, Vol. 25, II, 1956, No. 2, 29-31.

Other conditions being equal, the thrust of a ramjet engine grows and the economy and altitude increase with an increase of the pressure recovery coefficient.

SECTION 3. DEVELOPMENT PERSPECTIVES OF RAMJET ENGINE COMBUSTION CHAMBERS

Ramjet combustion chambers of the stabilizer type, in which the turbulent combustion of a two-phase mixture occurs, have been described in open literature.

The subsequent development of combustion chambers could consists of the following for example:

1. Perfection of the methods of preparing the fuel mixture.

2. The decrease of the hydraulic resistance of the combustion chamber with a simultaneous increase in combustion efficiency by means of the transition from the stabilization of poorly streamlined bodies to other types of stabilization.

3. The utilization of hypergolic fuels.

4. The development of combustion chamber operation at low internal air pressures.

5. A simplification of combustion chamber construction by transition from spark ignition to compression ignition.

The final aim of all these improvements is the reduction of the weight and the length of the combustion chamber, a lowering of the hydraulic losses, and an increase of the combustion efficiency, and, as a result, to increase the impulse of the gases in the exhaust section of the chamber. The decrease of the weight of the combustion chamber permits the fuel supply to be increased so that a certain increase of the duration and range of the flight will occur.

A substantial decrease of the specific fuel consumption and a corresponding increase of the flight range may be obtained by switching to a fuel with a higher calorific value than a hydrocarbon.

It is known from thermochemistry that only three elements: hydrogen, beryllium, and boron possess a higher calorific value than carbon. Hydrogen is unsuitable as a fuel for aircraft, since even in a liquid state it has a very low specific weight: nearly 0.07 kg/m^3. Flight range can be increased by switching from hydrocarbon fuels

to borohydrides. According to the latest information, long-range bombers using borohydride fuels have been developed in the USA.[1]

Borohydrides of the diborane and pentaborane types are hypergolic in air. The combustion chambers for these fuels do not require an ignition system.

Other conditions being equal, the increase in flight range when changing from hydrocarbons to borohydrides is proportional to the increase of the calorific value:

$$\frac{\Delta L}{L} = \frac{\Delta H_s}{H_s} = \frac{16\,000 - 10\,500}{10\,500} \approx 52\%.$$

SECTION 4. DEVELOPMENT PERSPECTIVES OF JET NOZZLES

The pressure coefficient of the subsonic portion of a jet nozzle usually has a large value: $\sigma'_s = 0.98$--0.99. The pressure coefficient of the supersonic portion of a well-profiled nozzle when $M = 3$ is on the order of 0.9. It is impossible to increase the pressure coefficient of the nozzle substantially after it approaches one since it is impossible to completely exclude the losses on friction and shocks. Therefore, there is no basis to expect that the thrust characteristics of an engine with a fixed-geometry may be noticeably improved because of the increase of the total pressure coefficient of the nozzle.

Usually in designing an engine with a fixed geometry the throat section of the nozzle is chosen with a higher value than is necessary for operation in the design conditions to prevent a "buzzing" condition during an increase of the temperature ratio. An over-sized nozzle lowers the pressure in front of the exhaust, and consequently, lowers the thrust and economy of the engine. This "shortage" of thrust may be avoided by employing supersonic nozzles with variable throat sections.

Multi-purpose engines, which must have a high degree of efficiency during various flight speeds and at various mixture compositions, must have variable-geometry nozzles. Such nozzles offer the possibility of operating with an optimum degree of expansion of the exhaust gases during varying flight speeds and during varying temperatures in the combustion chamber.

---

[1]Anderton, D. A., Aviation Week, vol. 65, 12/XI, 1956, No. 20, 51-57.
    Flight, 1957, No. 2531, p. 134.

The development of supersonic jet nozzles must proceed along the way of per-
fecting variable-geometry systems.

SECTION 5. THE UTILIZATION OF THE POTENTIAL ENERGY OF THE IONOSPHERE

In addition to the energy of a molecular fuel, it is possible to use the poten-
tial energy of the ionosphere for supersonic ramjet engines.

Under the action of solar and cosmic radiation oxygen and other gases in the
upper layers of the earth's atmosphere dissociate into ions. According to the opin-
ion of Ya. B. Zel'dovich and certain other scientists, the ion concentration in the
ionosphere must have a large value. These ideas have still not received experimental
confirmation.[1]

An ionized gas possesses a high reserve of potential energy which is accumulated
by absorbing the energy of the ionized particles and quanta. Thus, for example, 1
mole of oxygen, which is totally dissociated into atoms, contains 117 kcal of energy
or 3,650 kcal per kg, i.e., almost six times more than 1 kg of a fuel mixture of
benzine vapors with air of a stoichiometric composition contains.

If a catalyst or another factor would be found which is capable of producing
an association of the dissociated gas in the combustion chamber of a ramjet engine
flying in the ionosphere, then the flight may take place at the expense of the ion-
ized gases which enter the diffuser. Such an "ion" engine will not need a special
heat-transfer agent.

However, the density of the gases in the atmosphere is so small[2] that the thrust
of ion engine will be insignificant.

SECTION 6. RAMJET ENGINES WHICH OPERATE ON NUCLEAR FUEL.

The next task of ramjet technology is the creation of a supersonic ramjet en-
gine which operates on nuclear fuel. Chapter XI is devoted to this question. The
basic problem requiring a solution, is the development of a reactor, capable of main-

---

[1]Ya. B. Zel'dovich, UFN /Progress of Physical Sciences (a periodical)/ vol. LX,
1 September 1956, 161-162.
[2]Mitra, S. K., Verkhnyaya atmosfera /The Upper Atmosphere/, GTTI, 1955.

taining a temperature necessary to obtain the thrust required for flight.[1]

SECTION 7. RAMJET ENGINES WHICH OPERATE ON RADIOACTIVE ISOTOPES

In addition to the atomic reactors radioactive isotopes, which have a short half life and are obtained in atomic reactors,[2] may be used as an energy source for atomic ramjet engines.

Elementary calculations show that in a nuclear reactor having a thermal power in tens of millions of kilowatts, it is possible to obtain such a quantity of a radio active isotopes, which, when disintegrating will release a power on the order of 100,000 kw. This is sufficient for an intercontinental missile to fly at a supersonic speed.

It is impossible to control the heat emission of a radioactive isotope. When the flow of the incoming air is stopped a high energy radioactive isotope will quickly melt, due to the energy it releases. The thrust control of a ramjet engine which operates on radioactive isotopes may be accomplished, for example, by the variation of the throat section of the exhaust nozzle.

Handling high-activity isotopes is an extremely difficult matter.

SECTION 8. RAMJET ENGINES WHICH OPERATE ON BETA BATTERIES

Artificial radioactive isotopes may be used to create the so-called beta-batteries which develop electrical energy directly because of the energy of the radioactive dis-integration. The electric current from a beta-battery may be used to produce a pow-erful electrical arc or a spark discharge, which will heat the air that enters from the diffuser into a discharge chamber to any given temperature. The side of the cham-ber may be air cooled, as the combustion chamber of engines using a molecular fuel.[3]

---

[1] Atomnaya energiya /Atomic Energy/, 1956, No. 5, 1957.

[2] Namias, M., Yadernaya energiya /Nuclear Energy/, Foreign Literature Printing House, 1955, 202-206.

[3] Aeronautics, vol. 35, 1956, No. 1, 156, No. 2, 51.

The liberation of energy in a beta-battery is, apparently, uncontrollable. On the hardstand, the excess power may be bled off into the public power net. The thrust of an engine may be controlled in flight by varying the thrust section of the nozzle.

A ramjet engine which operates on beta-batteries is suitable for flight with very high velocities, since the air temperature in the discharge chamber may be raised to very high values.

Ramjet engines may operate on molecular as well as on atomic energy. Ramjet engines are unrivaled for powered and controlled flights at velocities from $M_n = 3.5$ to 4.0 and higher.

BIBLIOGRAPHY

1. Zel'dovich, Ya. B., UFN /Progress of Physical Sciences7, vol. LX, 1 September 1956 issue, 151-162.

2. Namias, M., Yadernaya energiya /Nuclear Energy7, Foreign Literature Printing House, 1955, 202-206.

3. Time, 30/I, 1956, 37-40.

4. Aviation Age, Vol. 25, II, 1956, No. 2, 29-31.

5. Aviation Age, Vol. 23, No. 6, 1955, 68-73.

6. Anderton, D. A., Aviation Week, v. 65, 12/XII, 1956, No. 20, 51-57.

7. Aeroplane, XI, No. 2359, 1956, 710.

8. Aeronautics, Vol. 35, 1956, No. 1, 156.

9. Aeronautics, Vol. 35, 1956, No. 2, 51.

10. Porter, W. H. L., Nuclear Power for Aircraft. Atomics and Nuclear Energy, v. 8, 1957, No. 1, Jan., 7-14.

11. Anderton, D. A., Aviation Week, v. 64, 1956, No. 23, 50-55.

12. Air Pictorial, 1956, No. 3, 85-86, 5 fig.

13. Flight, 1956, No. 2464, 415.

14. J. Crecknell, High-Energel Fuels, Flight, No. 2512, 1957, 332-334.

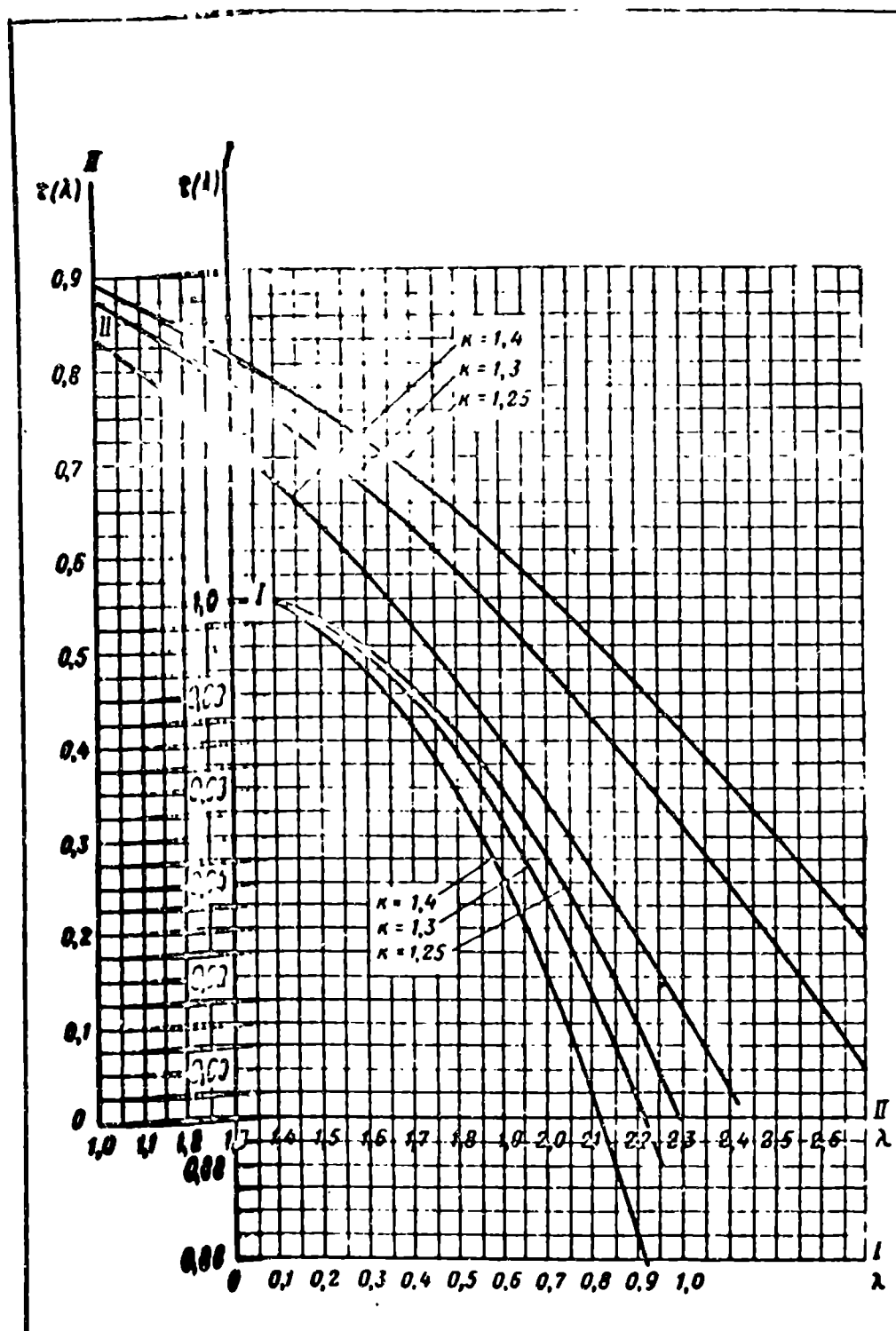15. Mitra, S. K., Verkhnyaya atmosfera /The Upper Atmosphere7, GTTI, 1955.

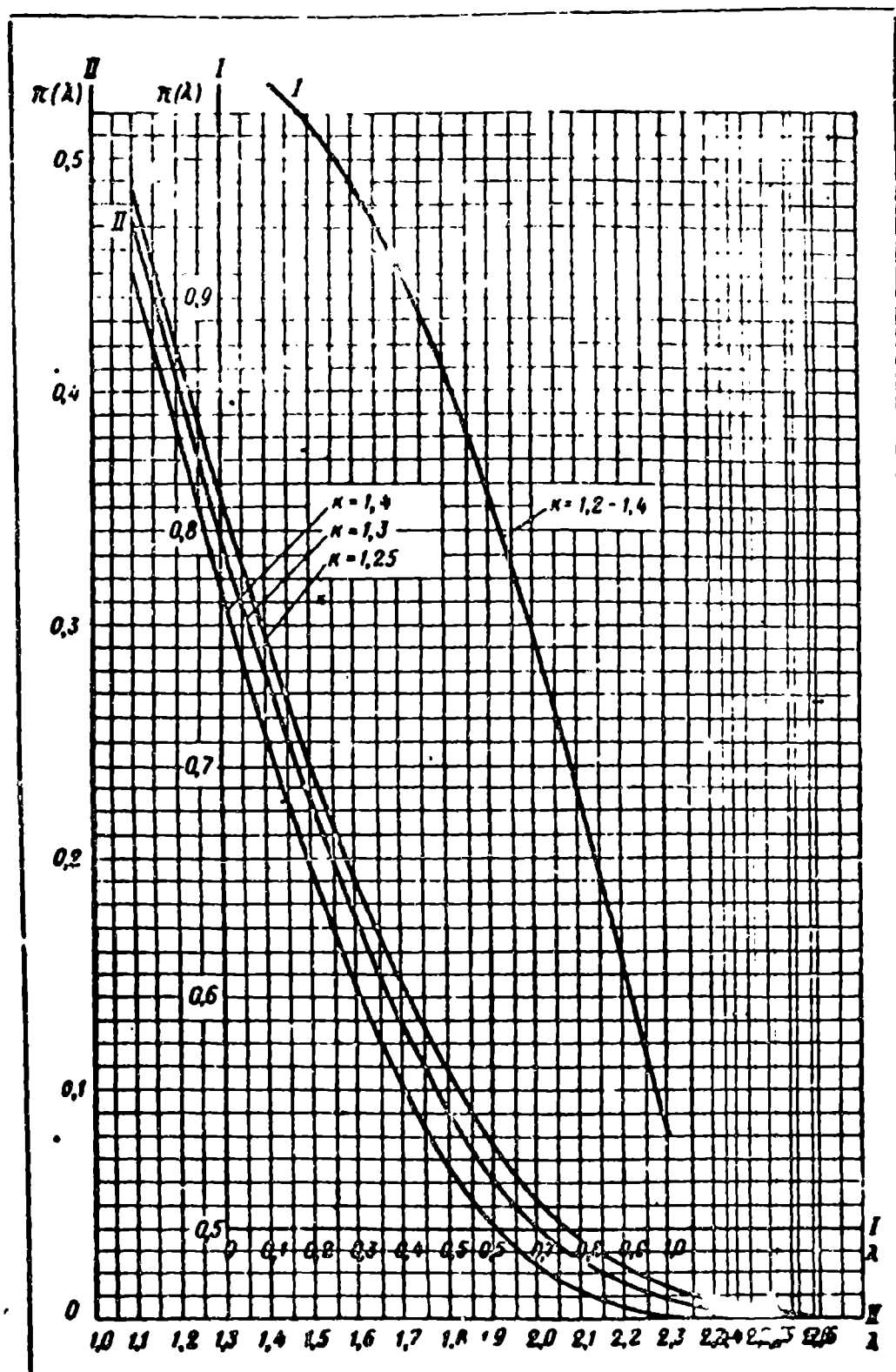Fig. 204. A graph of the gas dynamic function $\tau(\lambda) = 1 - \frac{k-1}{k+1}\lambda^2$.

Fig. 205. A graph of the gas dynamic function $\pi(\lambda) = \left[\tau(\lambda)\right]^{\frac{k}{k-1}}$.
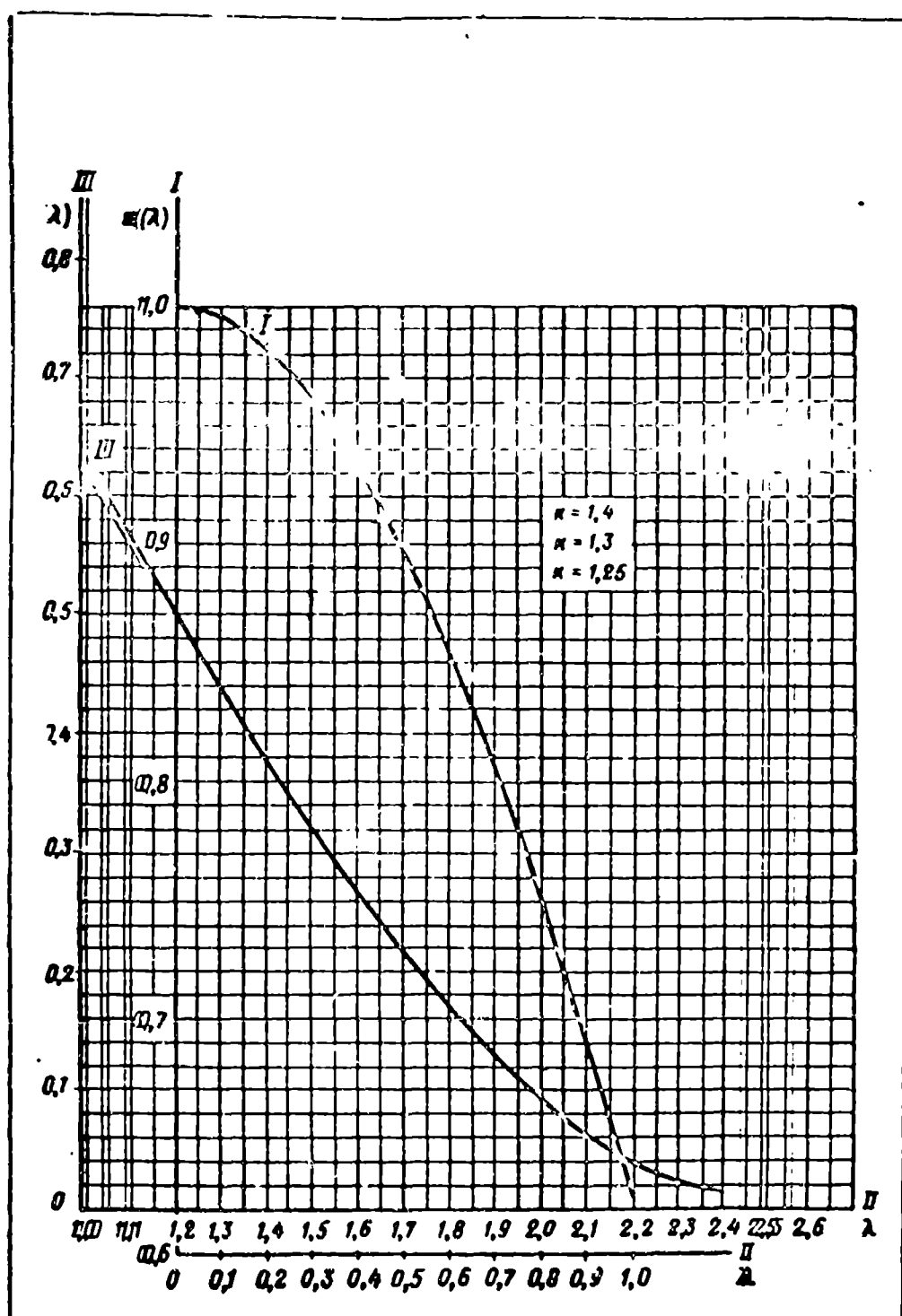
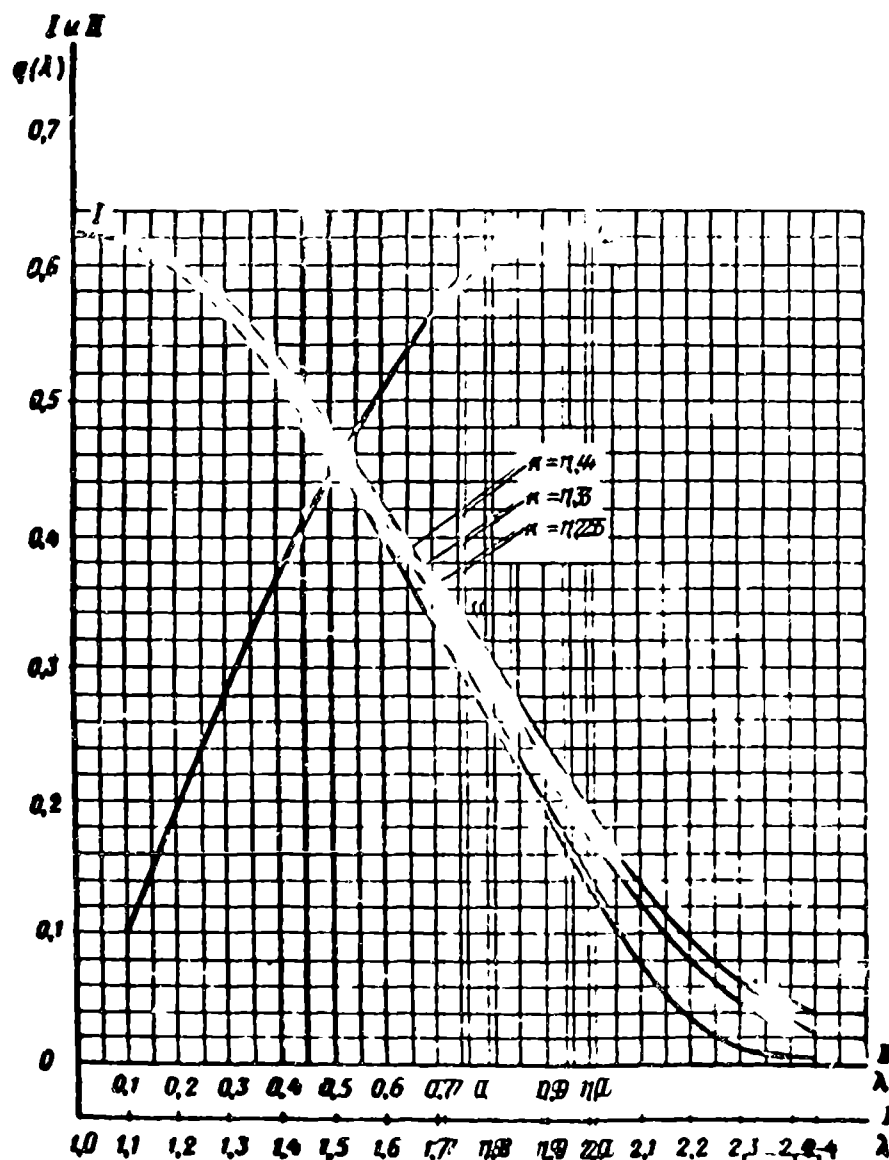Fig. 206. graph of the gas dynamic function $\varepsilon(\lambda) = [\tau(\lambda)]^{\frac{1}{k-1}}$.

Fig. 207. A graph of the gas dynamic function $\tau(\lambda) = \lambda \epsilon(\lambda\lambda) =$

$$= \lambda \left(1 - \frac{k-1}{k+1}\lambda^2\right)^{\frac{1}{k-1}}$$
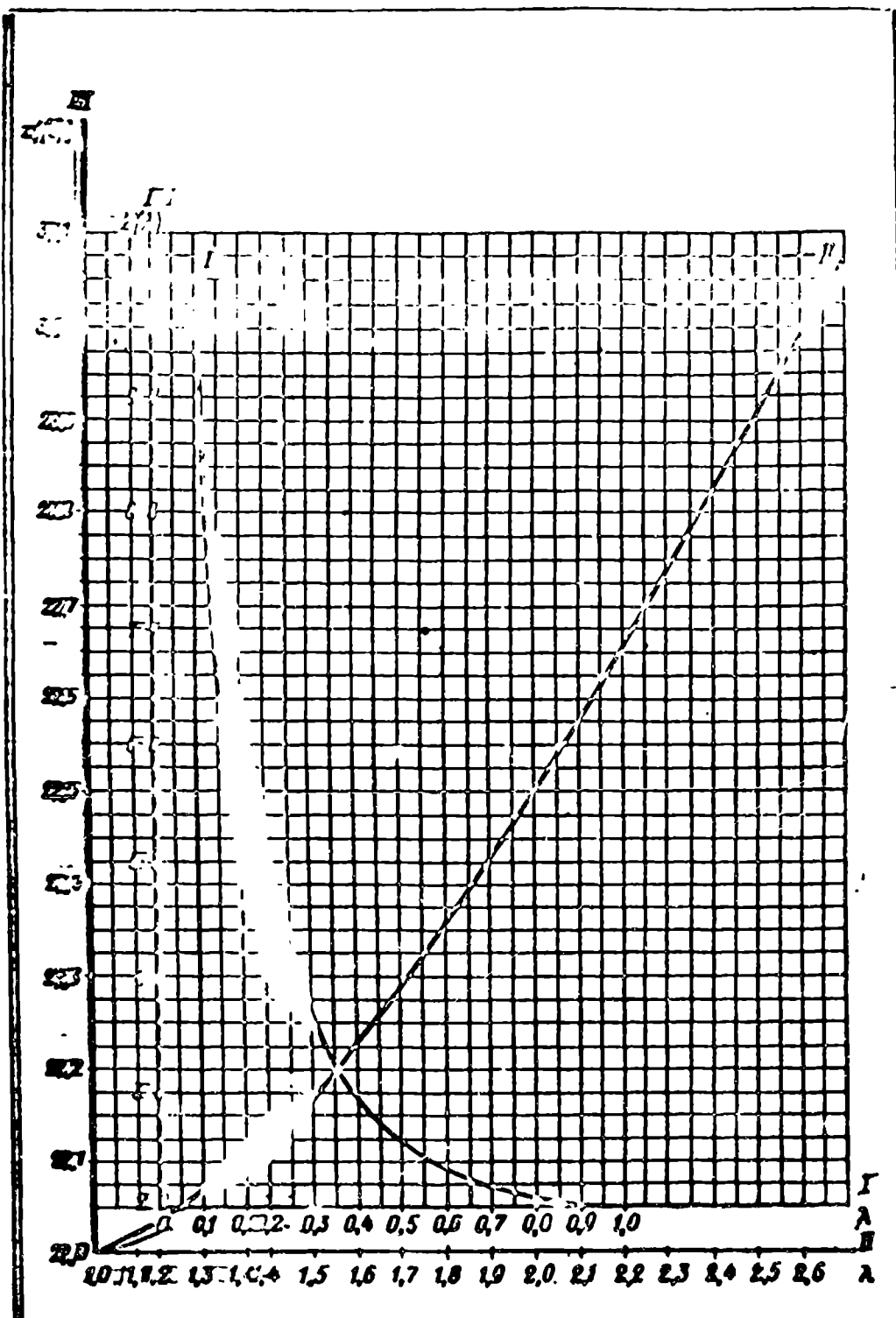
Fig. 208. A graph if the gaæs dynamic function $z(\lambda) = \lambda + \dfrac{1}{\lambda}$.